

**Phytochemical investigation of some selected medicinal plants and
synthetic transformations of an abundant natural product zerumbone
from *Zingiber zerumbet* (L.) Roscoe ex Sm.**

**Thesis Submitted to AcSIR for the Award of the Degree of
DOCTOR OF PHILOSOPHY
in Chemical Sciences**



**By
Greeshma Gopalan
Registration Number: 10CC13A39006**

Under the Combined Guidance of

Dr. K. V. Radhakrishnan and Dr. Mangalam S. Nair



**Organic Chemistry Section
Chemical Sciences and Technology Division
CSIR-National Institute for Interdisciplinary Science and Technology (CSIR-NIIST)
Thiruvananthapuram - 695019, Kerala**

August 2018

To My Family and Teachers

DECLARATION

I hereby declare that the Ph.D. thesis entitled “**Phytochemical investigation of some selected medicinal plants and synthetic transformations of an abundant natural product zerumbone from *Zingiber zerumbet* (L.) Roscoe ex Sm.**” is an independent work carried out by me under the combined supervision of Dr. K. V. Radhakrishnan and Dr. Mangalam S. Nair at the Organic Chemistry Section, Chemical Sciences and Technology Division, CSIR-NIIST, Thiruvananthapuram and it has not been submitted anywhere else for any other degree or diploma.

In keeping the general practice of reporting scientific observations, due acknowledgment has been made wherever the work described is based on the findings of other investigators.


Greeshma Gopalan

Thiruvananthapuram
August 2018

National Institute for Interdisciplinary Science and Technology (CSIR-NIIST)



Council of Scientific & Industrial Research
(CSIR)

AcSIR

Industrial Estate P. O., Trivandrum - 695 019
Kerala, India

CERTIFICATE

*This is to certify that the work incorporated in this Ph.D. thesis entitled "Phytochemical investigation of some selected medicinal plants and synthetic transformations of an abundant natural product zerumbone from *Zingiber zerumbet* (L.) Roscoe ex Sm." submitted by Ms. Greeshma Gopalan to Academy of Scientific and Innovative Research (AcSIR), New Delhi, in fulfillment of the requirements for the award of the Degree of Doctor of Philosophy in Chemical Sciences, embodies original research work under our combined supervision, at the Chemical Sciences and Technology Division, CSIR-National Institute for Interdisciplinary Science and Technology (CSIR-NIIST), Thiruvananthapuram. We further certify that this work has not been submitted to any other University or Institution in part or full for the award of any degree or diploma. Research material obtained from other sources has been duly acknowledged in the thesis. Any text, illustration, table etc., used in the thesis from other sources, have been duly cited and acknowledged.*

Dr. K. V. Radhakrishnan

(Thesis Supervisor)

Thiruvananthapuram

August 2018

Dr. Mangalam S. Nair

(Co-Supervisor)

Greeshma Gopalan

(Student)

ACKNOWLEDGEMENTS

When I look back at my career, the highlights will never be the awards and appreciations, but the 'people' with whom I've worked with.

With delightful happiness and great respect, I would like to convey my sincere and deep sense of gratitude to my research supervisor Dr. K. V. Radhakrishnan for introducing me to the fascinating area of Natural products and also for his excellent guidance, persistent motivation, sustained encouragement, wholehearted help, patience and constructive criticism throughout my research work.

I am grateful to Dr. Mangalam S. Nair, for her timely help and advice given to me, as my co-supervisor and as former AcSIR programme coordinator at CSIR-NIIST, which helped me in the successful completion of my research work.

I like to thank the present and former directors of CSIR-NIIST, Dr. A. Ajayaghosh, Dr. Suresh Das and Dr. Gangan Prathap for allowing me to avail the laboratory facilities to carry out the research work.

I would like to acknowledge Dr. R. Luxmi Varma, AcSIR programme coordinator at CSIR-NIIST for her timely help and advice for the academic procedures of AcSIR.

My honest gratitude to Dr. R. Luxmi Varma, Dr. Kaustabh Kumar Maiti and Dr. K. G. Raghu (my Doctoral Advisory Committee members) for their help, support and inspiration throughout my Ph. D. period.

I like to state kind regards to Dr. R. Luxmi Varma, Head and, Dr. K. R. Gopidas and Dr. D. Ramaiah, Former Heads, Chemical Sciences and Technology Division for their endless support.

With a lot of pleasure, I remember Dr. G. Vijay Nair, Emeritus Scientist, Organic Chemistry Section for his inspiring presence.

I also would like to state credits respectively to Dr. Kaustabh Kumar Maiti, Dr. B. S. Sasidhar, Dr. L. Ravi Shankar and Dr. Sunil Varughese, Scientists of Organic Chemistry Section, for the stimulation and assistance. I am indebted to Dr. Jubi John for his constant help, support and motivation and also extend my sincere thanks to Dr. Ganesh Chandra Nandi, for the worthwhile discussions.

My sincere thanks and respect are also due to : Dr. P Nisha, Agroprocessing and Technology Division, CSIR-NIIST, Thiruvananthapuram for antidiabetic studies; Dr. S. Priya, Agroprocessing and Technology Division, CSIR-NIIST, Thiruvananthapuram for

antiproliferative studies; Dr. M. Sabu, Department of Botany, University of Calicut, Thenjipalam for the collection and authentication of plant materials; Dr. I. G. Shibi, Sree Narayana College, Kollam for the pharmacophore and QSAR studies; Dr. Dr. Ajaikumar B. Kunnumakkara, IIT-G, Assam for anticancer studies; Dr. T. K. Manojkumar, IIIM-T, Thiruvananthapuram for molecular docking studies.

I would like to thank Dr. Sunil Varughese for single crystal-X ray analysis. Mrs. Saumini Mathew, Mr. Saran P. Raveendran, Mr. Syam and Mr. Rakesh Gokul are acknowledged for recording NMR spectra. Thanks are also due to Mrs. S. Viji and Ms. S. Aathira for mass spectral analysis.

I am utilizing this occasion to convey my kind regards to Dr. Sarath Chand S and Dr. B. P. Dhanya, for their emphatic help and fabulous support during all stages of my doctoral studies. Also stating special thanks to Ms. B. Prabha, Ms. J. Saranya, Ms. T. R. Reshmitha, Ms. M. T. Meenu, Ms. J. S. Arya, Ms. K. Varsha and Ms. Biji for their contribution in conducting some of the experiments presented in this thesis.

I am appreciating Mr. M. Madhukrishnan, Mr. Firoz Khan and Mrs. Mehjabin Sachariah for their esteemed help in the completion of AcSIR-800 course work.

I would like to thank from bottom of my heart to: My seniors- Dr. Praveen Prakash, Dr. E. Jiji, Dr. K. R. Ajish, Dr. T. V. Baiju, Dr. P. Preethanuj, Dr. S. Saranya, Dr. P. S. Aparna, Dr. Ajesh Vijayan, Dr. M. Shimi, Dr. P. V. Santhini, Dr. R. J. Maya, Dr. Nayana Joseph, V. S. Suchithra and Dr. S. Anu Priya; and my colleagues- Mr. P. Sasikumar, Mrs. Athira Krishna, Mrs. C. T. Fathimath Salfeena, Mr. K. K. Rajeev, Mr. K. Jayakrishnan, Ms. Remya Raj, Ms. P. Sreedevi, Ms. S. Santhi, Ms. P. Sharathna, Ms. P. R. Nitha, Ms. K. T. Ashitha, Ms. S. Neethu, Ms. M. Aswathy, Ms. V. Jiitha, Mr. V. Praveen Kumar, Ms. Irfana Jesim, Mr. Vishnu K. Omanakkuttan, Ms. P. R. Rajimol, Ms. C. P. Ummu Jumaila and Mrs. Jyothi B. Nair; for their assistances, considerations, companionship and massive support.

I wish to thank Dr. C. R. Cinu, Dr. Rony Rajan Paul, Dr. K. Sajin Francis, Dr. S. R. Dhanya, Dr. K. C. Seetha Lakshmi, Mr. K. Jagadeesh, Ms. Mayadevi and all other present and former members of Organic Chemistry Section, for their friendship and creative inspirations. I am penning and remembering with lot of thanks some of our internship fellows, Ms. Rajalekshmi, Dr. R. Karthika, Ms. K. B. Sobhini, Ms. S. R. Devika, Ms. Kavya Krishnamoorthy, Ms. Krishna S. nair, Ms. K. Rincy K, Ms. M. K. Kavyasree, Ms. S. Smrithy and V. Dhrishya for their togetherness and intimacy. I acknowledge Ms. M. Dhanya and Ms. Anju Alphonsa for making my stay at Thiruvananthapuram, a memorable one.

I sincerely acknowledge all my teachers, especially Dr. D Bahulayan, for encouraging me to take up a career in chemistry. I also would like to extend my sincere thanks to all my friends at CSIR-NIIST.

I am grateful to Council of Scientific and Industrial Research (CSIR) and Department of Science and Technology (DST) New Delhi, for the financial assistance.

I would never have completed the dissertation without the support, encouragement and unconditional love from my family. I am deeply and forever indebted to my parents, brothers, sister-in-law, niece, Sangeeth and Jithu who made it possible for me to reach up to here.

Above all, I thank Almighty for bestowing his blessings upon me and giving all these people to help and encourage me, for the successful completion of the work.

Greeshma Gopalan

CONTENTS

Declaration	i
Certificate	ii
Acknowledgements	iii
Abbreviations	xii
Preface	xiv

CHAPTER 1

An Overview of Natural Products in Drug Discovery	1-26
1.1 Introduction	1
1.2 Classification of Natural Products	6
1.2.1. Based on source/origin	6
1.2.1.1. Plant derived natural products	7
1.2.1.2. Microbial world derived natural products	9
1.2.1.3. Marine world derived natural products	10
1.2.1.4. Animal world derived natural products	10
1.2.2. Based on biosynthetic pathways	11
1.2.3. Based on chemical structures	13
1.2.3.1. Flavanoids	14
1.2.3.2. Terpenoids	15
1.2.3.3. Phenylpropanoids	16
1.2.3.4. Alkaloids	17
1.3 Role of Natural products in Drug Discovery	19
1.4 Nutraceuticals and Dietary Supplements	20
1.5 Conclusion and Present Work	21
1.6 References	24

CHAPTER 2

Part A: Screening of <i>Musa balbisiana</i> Colla. Seeds for Antidiabetic Properties and Isolation of Apiforol, a Potential Lead, with Antidiabetic Activity	27-62
2A.1 Introduction	27

2A.2	Phytoconstituents and Pharmacological Activities of <i>Musa</i>	29
2A.3	Aim and Scope of the Present Work	35
2A.4	Proximate Composition Analysis and Extraction of <i>Musa</i> balbiana	36
	2A.4.1. Collection of plant material	36
	2A.4.2. Proximate composition analysis	37
	2A.4.2.1. Total moisture content	37
	2A.4.2.2. Dry ashing	37
	2A.4.2.3. Lipid content	37
	2A.4.2.4. Protein content	37
	2A.4.2.5. Total carbohydrate content	38
	2A.4.3. Extraction and isolation procedures	38
2A.5	GCMS Analysis of Seed Oil	39
2A.6	In vitro Antidiabetic Potentials of the Extracts	40
	2A.6.1. α -Amylase and α -glucosidase inhibitory activity of the extracts	41
	2A.6.2. Antiglycation property of the extracts	42
2A.7	Isolation and Characterization of Apiforol	43
2A.8	<i>In vitro</i> Antidiabetic Studies of Apiforol	45
2A.9	Molecular Docking Studies	47
2A.10	Glucose Uptake in L6 Myoblasts	48
2A.11	In vitro Antioxidant Studies	50
2A.12	Conclusion	52
2A.13	Experimental Section	52
	2A.13.1. GCMS profiling	52
	2A.13.2. α -Amylase inhibitory activity	53
	2A.13.3. α -Glucosidase inhibitory activity	53
	2A.13.4. Antiglycation property	53
	2A.13.5. Cell culture and treatment conditions	54
	2A.13.6. Cell viability assay	54
	2A.13.7. Glucose uptake assay	54
	2A.13.8. Statistical analysis	55
2A.14	<i>In vitro</i> antioxidant studies	

2A.14.1. Evaluation of DPPH scavenging activity	55
2A.14.2. Evaluation of ABTS scavenging activity	55
2A.14.3. Evaluation of NO scavenging activity	56
2A.15 Spectral Data	56
2A.16 References	59
CHAPTER 2	
Part B: Isolation of Phytoalexins from Rhizome and Fruit Peels of	63-86
<i>Musa balbisiana</i> Colla.	
2B.1 Introduction	63
2B.2 Aim and Scope of the Present Study	63
2B.3 Isolation and Characterization of Compounds from the	64
Rhizome of <i>Musa balbisiana</i> Colla.	
2B.3.1. Extraction	64
2B.3.2. Isolation and characterization of compounds	64
2B.4 Extraction, Isolation and Characterization of Phytochemicals	
from the Peels of <i>Musa balbisiana</i> fruits	
2B.5 Conclusion	80
2B.6 Experimental Section	80
2B.7 Spectral Data	80
2B.8 References	86
CHAPTER 3	
Part A : Phytochemical Investigation of <i>Anethum graveolens</i> Linn	87-144
3A.1 Introduction	87
3A.2 Aim and Scope of the Present Study	91
3A.3 Isolation and Characterization of Phytochemicals from the	92
Seeds of <i>Anethum graveolens</i> L.	
3A.3.1. Collection of plant material	92
3A.3.2. Isolation of essential oils	92
3A.3.4. Extraction and isolation of phytochemicals	93
3A.4 Extract and Molecular Level in vitro Antioxidant Studies	126
3A.5 In silico Antidiabetic and Anticancer Studies	127
3A.6 Conclusion	131
3A.7 Experimental Section	131

3A.8	Spectral Data	131
3A.9	References	142

CHAPTER 3

Part B: Investigation on Phytochemical Constituents and 145-172

Antioxidant Properties of *Zingiber nimmonii* (J. Graham) Dalzell

3B.1	Introduction	145
3B.2	Aim and Scope of the Present Stud	146
3B.3	Isolation and Characterization of Phytochemicals from the Rhizomes of <i>Zingiber nimmonii</i> (J. Graham) Dalzell	147
	3B.3.1. Collection of plant material	147
	3B.3.2 Extraction and Isolation	147
3B.4	<i>In vitro</i> Antioxidant Studies	161
3B.5	<i>In silico</i> Antidiabetic and Anticancer Studies	163
3B.6	Conclusion	164
3B.7	Experimental Section	165
3B.8	Spectral Data	165
3B.9	References	171

CHAPTER 4

***Rotula aquatica* Lour- Phytochemistry and *in vitro* Antiurolithiatic 173-204**

Activity against Experimental Kidney Stone

4.1	Introduction	173
4.2	Reasons and Risk Factors	176
4.3	Types of kidney stones	178
4.4	Scope of the Study	179
4.5	Extraction, Isolation and Characterization of Compounds	179
4.6	Evaluation of Antiurolithiatic Activity of Different Root Extracts of <i>R. aquatica</i> against Experimental Kidney Stones	192
	4.6.1. Synthesis of experimental kidney stones	192
	4.6.2. Synthesis of semi-permeable membrane (SPM)	193
	4.6.3. Estimation of percentage of dissolution of calcium oxalate stones	193
	4.6.4. Estimation of percentage of dissolution of calcium phosphate stones	194

4.6.5. Comparison of antiurolithiatic activities of three different medicinal plants	197
4.7 Conclusion	197
4.8 Experimental Section	199
4.9 Spectral Data	199
4.10 References	203
CHAPTER 5	
Synthesis and Biological Evaluation of Novel Zerumbone Pendant and [11.3] Fused Zerumbone Derivatives	205-290
5.1 Introduction	205
5.2 Attractive Reactivity of Zerumbone	207
5.2.1. Conjugate addition reactions	207
5.2.2. Transannular reactions	208
5.2.3. Ring cleavage reactions	209
5.2.4. Ring expansion reactions	209
5.2.5. Epoxidation reactions	210
5.2.6. Reduction reactions	210
5.2.7. Photochemical reactions	211
5.2.8. Our expertise in the field of zerumbone	211
5.3 Sulfonamides	213
5.4 Aim and Scope of the Present Work	215
5.5 Results and Discussion	216
5.5.1. Optimization studies	218
5.5.2. Evaluation of in silico and in vitro antidiabetic and antiproliferative potential of synthesized derivatives	225
5.6 Aziridines	230
5.7 Aim and Scope of the Present Study	232
5.8 Results and discussion	233
5.9 Evaluation of in vitro Antiproliferative, Antidiabetic and Anti- hypertensive Potential of Synthesized Derivatives	238
5.10 Pharmacophore Modeling and QSAR Studies	242
5.10.1. Pharmacophore modeling	242
5.10.2. Quantitative structure-activity relationships (QSAR)	243

5.11	Conclusion	251
5.12	Experimental Section	251
	5.12.1. General methods	251
	5.12.2. General procedures	252
5.13	Spectral Data	255
5.14	References	287
CHAPTER 6		
Lewis Acid Catalyzed Functionalization of Zerumbone; Synthesis of Novel [5.8.3] and [5.8] Fused Sesquiterpenoid Derivatives		291-328
6.1	Introduction	291
6.2	Aim and Scope of the Present Study	291
6.3	Results and Discussion	292
6.4	Molecular Docking Studies	301
6.5	Conclusion	303
6.6	Experimental section	304
6.7	Spectral Data	304
6.8	References	328
	Summary	329
	List of Publications	337
	Academic Contributions	338

ABBREVIATIONS

Ac	: Acetyl	EWG	: Electron withdrawing group
Ar	: Argon	FT-IR	: Fourier transform infrared
Ar-	: Aryl	h	: Hour
Aq.	: Aqueous	H	: proton
brs	: Broad singlet	HCl	: Hydrochloric acid
BSA	: Bovine serum albumin	HMBC	: Heteronuclear multiple bond correlation
calcd.	: Calculated	HMQC	: Heteronuclear multiple quantum correlation
CCDC	: Cambridge crystallographic data center	H ₂ SO ₄	: Sulfuric acid
COSY	: Correlation Spectroscopy	HRMS	: High-resolution mass spectrometry
d	: Doublet, Day (reactions)	Hz	: Hertz
DCE	: Dichloroethane	IR	: Infrared
DCM	: Dichloromethane	In(OTf) ₃	: Indium (III) triflate
dd	: Doublet of doublets	<i>J</i>	: Coupling constant
ddd	: Doublet of doublets of doublets	KI	: Potassium iodide
DEPT	: Distortionless enhancement by polarization transfer	LA	: Lewis acid
DMF	: Dimethylformamide	m	: Multiplet
DMSO	: Dimethyl sulfoxide	mCPBA	: <i>m</i> -Chloroperbenzoic acid
DPPH	: 2,2-diphenyl-1-picrylhydrazyl.	Me	: Methyl
dppf	: 1,1-Bis(diphenylphosphino) ferrocene	MeOH	: Methanol
dt	: Doublet of triplet	mg	: Milligram
EDG	: Electron donating group	min	: Minute
<i>ee</i>	: Enantiomeric excess	MTT	: MTT 3-(4,5-dimethylthiazol-2-yl)-2,5-phenyltetrazolium bromide
ESI	: Electron Spray Ionisation	mL	: Milliliter
Et	: Ethyl	mol	: Mole
EtOAc	: Ethyl acetate	mmol	: Millimolar
Equiv.	: Equivalent	mol %	: Mole percent

Mp	: Melting point	PIDA	: Pentyliododiacetate
MW	: Molecular weight	RT	: Room temperature
NBS	: N-bromosuccinimide	s	: Singlet
<i>n</i> -Bu	: Normal butyl	SD	: Standard deviation
NMR	: Nuclear magnetic resonance	t	: Triplet
NO	: Nitric oxide	<i>t</i> -Bu	: Tertiary butyl
NOE	: Nuclear Overhauser effect	TBAI	: Tetrabutylammoniumiodide
Nu	: Nucleophile	<i>tert</i>	: Tertiary
<i>o</i>	: Ortho	THF	: Tetrahydrofuran
<i>p</i>	: Para	TLC	: Thin layer chromatography
PBS	: Phosphate buffered saline	TMS	: Tetramethylsilane
Ph	: Phenyl	UV	: Ultraviolet
<i>rac</i>	: racemic	ZER	: Zerumbone
R_f	: Retention factor	δ ppm	: NMR chemical shift in parts per million

PREFACE

Nature has created virtually an inexhaustible array of molecular entities of enormous structural and chemical diversity and, have made undeniable contributions to the development of the pharma industry and research. Since time immemorial, natural products have been the backbone of the traditional medicinal system throughout the globe, and have also been an integral part of history and culture. Natural products, such as plants extract, have provided unlimited breaks for the synthesis of the world's most commonly used drugs. The use of herbal medicines, especially in Asian countries represents the resilient interaction between man and nature. Plants carry a number of phytochemicals that can be used to treat chronic as well as infectious diseases. Herbs have been prized for their medicinal, aromatic and flavoring potentials for centuries, and today they are being considered as the safer remedies compared to modern synthetic drugs. Worldwide, studies show that common people are facing significant problems in affording the newly synthesized drug molecules. To reduce this financial burden on countries, it is obvious that increased use of plant drugs will be followed in the future. Hence it is necessary to initiate the systematic cultivation of medicinal plants to prevent their exploitation. The on-going research in our lab is mainly focusing on the identification of compounds that hold both food and drug applications. Accordingly, in the present work, we have carried out a systematic evaluation of some of the medicinally important plants that are present in our country; *Musa balbisiana* from Musaceae, *Anethum graveolens* from Apiaceae, *Rotula aquatica* from Boraginaceae and, *Zingiber nimmonii* and *Zingiber zerumbet* from Zingiberaceae.

Chapter 1 gives an overview of the importance of natural products in drug discovery. The scope of the present research work is also discussed in this chapter.

Chapter 2 discusses about *Musa balbiaiana* (banana family), one of the famous plant species, belonging to the family Musaceae and order Zingiberales. From the ancient time itself, all parts of banana plants were used by mankind for medicinal as well as ornamental purposes. In these aspects, we chose one of the less explored wild banana species, *Musa balbisiana* for our studies. This chapter comprises of two parts, in which Part A deals with the isolation and evaluation of antidiabetic properties of a phytochemical, apiforol from the seeds of *M. balbisiana*, while Part B discusses the isolation and characterization of phytochemicals from the rhizome and peels (fruit) of the same plant.

Chapter 3 focuses on the exploration of phytomolecules that are present in *Anethum graveolens* and *Zingiber nimmonii*. Herbs and spices have been used for both culinary and medicinal purposes for centuries. *Anethum graveolens* is a species from Apiaceae, has been used in Ayurvedic medicines since ancient times, and it is a popular herb widely used as a spice and also yields essential oil. Owing to the great biological significance of *Anethum graveolens*, a detailed phytochemical investigation of seeds of this plant has been undertaken and our investigations are presented in the first part of chapter three. In the second part, the chemo-profiling of molecules present in the rhizomes of the plant species *Zingiber nimmonii* are described.

Chapter 4 deals with the phytochemical evaluation of whole parts of *Rotula aquatica*, belonging to the family Boraginaceae. *R. aquatica* is one of the most extensively used medicinal plants in the Ayurvedic system to dissolve urinary calculi and kidney stones. We could successfully isolate and characterize a number of molecules from different parts of this plants. We also carried out the antiurolithiatic studies of various root extracts of this plant and these results are described in this chapter.

Chapter five and six are collectively describe our efforts in the functionalization of one of the abundant natural product, zerumbone from *Zingiber zerumbet*. We could successfully synthesize different classes of zerumbone derivatives, such as zerumbone-pendant, zerumbone-aziridine, [5.8.3] fused and [5.8] fused ring systems, using simple and efficient reaction strategies. Most of these derivatives exhibited significant *in silico* and *in vitro*, antidiabetic and antiproliferative activities.

An Overview of Natural Products in Drug Discovery

1.1. Introduction

The field of organic chemistry is an art executed science in which the isolation of bioactive compounds or molecules from natural resources makes it one of the most interesting and finest areas of modern chemistry. Natural products (NPs) are the molecules of nature, and in a better way, we can define them as, chemical compounds or substances produced by living organisms. They possess enormous structural and chemical diversity that cannot be harmonized by any synthetic libraries and continue to inspire novel discoveries in chemistry, biology, and medicine. The history of medicines date back practically to the existence of human civilization. From the time immemorial, humans have relied on nature to furnish their basic needs and, nature has been a source of medicinal products for millennia, with many useful drugs for the treatment of numerous diseases and illnesses. Natural products (secondary metabolites) and their derivatives have been the single most productive source of leads in the development of drugs with structural diversity.¹⁻⁵

Before the 19th century, the crude and semi-pure extracts of plants, animals, microbes and minerals represented the only medication for the treatment of illness of human and domestic animals. Natural products chemistry actually began with the work of Serturmer who isolated morphine for the first time from opium poppy (*Papaver somniferum*) in 1803. Subsequently, a more potent diacetylated derivative diamorphine (heroin) was synthesized in 1874 by Wright. Without the discussion of aspirin (acetylsalicylic acid), no historical perspective of natural products derived drugs would be complete. Mac Lagan in 1876 introduced the salicin (an alcoholic β -glucoside) from the extract of willow bark and which led to the synthesis of aspirin. The first antibiotic, derived from natural sources is the serendipitous discovery of penicillin from *Penicillium notatum* (fungus) by Alexander Fleming in 1928. The first antiviral nucleosides spongouridine and spongothymidine were isolated by Bergmann in 1950 from the Caribbean sponge *Tethya crypta*. Hence, without doubt we can say that nature is a priceless treasure chest for the humankind. We are also a part of the natural world; a species amongst millions and have emerged to be a part of nature, not apart from it.^{6,7}

Natural products provide unlimited breaks for the synthesis and development of new class of drugs because of their supreme chemical diversity as well as availability. Hence it is not a coincidence that natural products serve as lead molecules in the field of drug discovery and the corresponding pharmaceutical world. The structural diversity of natural products support their ability to undergo selective synthetic transformations, and this makes out directly into their profound biological properties. The use of herbal medicines, especially in Asian countries represent the resilient interaction between man and nature. Plants carry a number of phytochemicals that can be used to treat chronic as well as infectious diseases. Herbs have been priced for their medicinal, aromatic and flavouring potentials for centuries and today they are considered as safer remedies compared to modern synthetic drugs. Studies worldwide show that common people are facing problems in affording the newly synthesised drug molecules. In order to reduce this financial burden on countries, it is obvious that an increased use of plant drugs will be followed in the future. Even today most of the medicinal plants are collected from wild. This continued exploitation results in a decline in the population of many plant species. Hence it is necessary to initiate systematic cultivation of medicinal plants to prevent their exploitation. Medicinal values that are present in different parts of the plant like root, bark, stem, heartwood, leaf, flower, fruit or plant exudates are different. Hence they have been classified in a number of ways.^{8,9}

Structures of natural products span a range from very simple to extremely complex architectures. Another important attraction of natural products is that the Lipinski rules of five do not apply to them. These rules were developed to drive synthetic chemists towards the synthesis of compounds with better biophysical properties and are thus well orally active drug candidates. According to this, the compounds should have molecular weight less than 500 Da, possess <5 hydrogen bond donors, <10 hydrogen bond acceptors, and have $\log P < 5$. The modern mode of drug discovery from natural sources has mainly relied on bio-guided isolation methods which have led to the discovery of important drugs.¹⁰

The therapeutic areas of infectious diseases and oncology have benefited from the abundant scaffold diversity in natural products and indeed for many years, natural products acted as a source of inspiration for the majority of FDA approved drugs.¹¹ Some of FDA approved unmodified NP drugs launched in 2005-2016 are given in figure 1.1.⁹

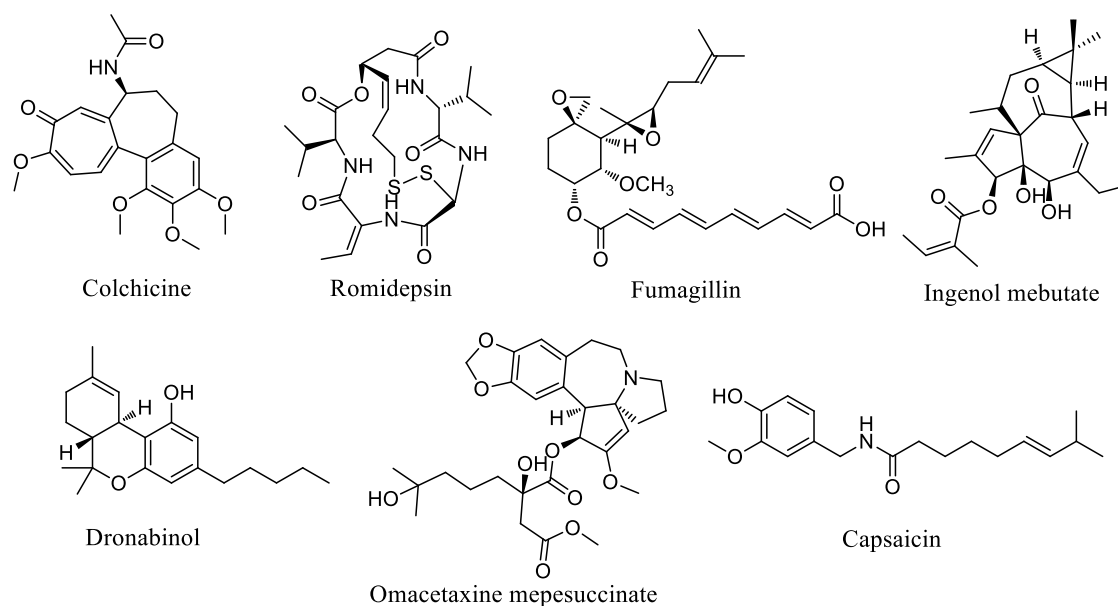


Figure 1.1. FDA approved unmodified NP drugs

The significance of natural products in drug discovery can be easily understood from a very recent paper by Newman and Cragg. In that paper, the authors have clearly said that from a total of 1562 new drugs approved in between 1985-2014, only 27 % were found to be purely synthetic drugs. Around 6 % drugs were vaccines and 21 % were NP mimics and synthetic drugs inspired/mimicked from NPs. Approximately 42 % drugs were either NPs or NPs derived compounds. It is to be noted that among all these drugs, 67 % were unaltered natural products.⁹ A statistical data prepared by them have been redrawn in figure 1.2.

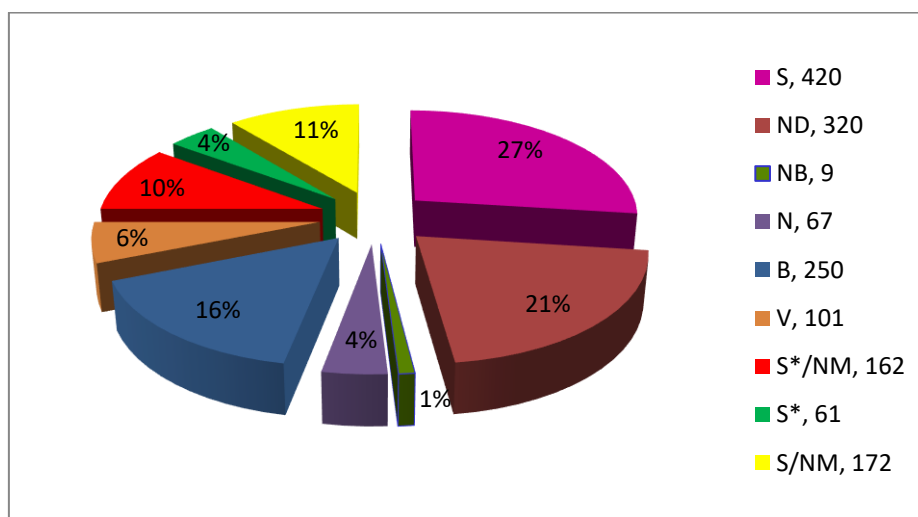


Figure 1.2. B Biological macromolecule, N Unaltered natural product, NB Botanical drug (defined mixture), ND Natural product derivative, S Synthetic drug, S* Synthetic drug (NP pharmacophore), V Vaccine, S/NM Mimic of natural product.

The past few years, however, have seen a renewed interest in the use of natural compounds and, more importantly, their role as a basis for drug development. The modern tools of chemistry and biology-in particular, the various '-omics' technologies-now allow scientists to detail the exact nature of the biological effects of natural compounds on human body, as well as to uncover possible synergies, which holds much promise for the development of new therapies against many devastating diseases, including dementia and cancer.

The properties of natural product leads are frequently improved through structural modification to achieve the final candidate. Whether within or outside of the Lipinski's rule-of-5 chemical space, natural product structures possess some unique characteristics which differentiate them from the world of synthetic drugs or chemical leads.^{12,13} Starting from the smallest natural product nitric oxide (NO- which control penile erection in male) to the largest polyketide *Brevetoxin* (algal product in red tides), NPs show structural diversity and are readily accessible by chemical synthesis and their synthetic transformation will provide improved activities. So they are often used as starting points in many important drugs. Since they are produced biosynthetically, options for the modification of their chemical structures are limited to either total synthesis, or semi-synthesis. Some of the FDA approved NP inspired/derived drugs launched in between 2005-2015 are given in table 1.1.

Table 1.1. FDA approved NP inspired/derived drugs launched in between 2005-2015

No	Year	Generic name	Lead compound	Source	Disease area/Use
1	2005	Doripenem	Thienamycin	Microbial	Antibacterial
2	2005	Tigecycline	Tetracycline	Microbial	Antibacterial
3	2005	Zotarolimus	Sirolimus	Microbial	Cardiovascular surgery
4	2005	Tamibarotene	Retinoic acid	Plant	Myelogenous leukemia
5	2005	Abraxane	Paclitaxel	Plant	Breast cancer
6	2005	Exenatide	Exenadin-4	Animal	Diabetes
7	2006	Anidulafungin	Echinocandin B	Microbial	Antifungal

8	2006	Hycamtin	Camptothecin	Plant	Cervical cancer
9	2006	Varenicline	Cytisine	Plant	Nicotine dependence
10	2006	Cesamet	Tetrahydrocannabinol	Plant	Chemotherapy and nausea
11	2007	Lisdexamfetamine	Amphetamine	Plant	ADHD
12	2007	Retapamulin	Pleuromutilin	Microbial	Antibacterial
13	2007	Ixabepilone	Epothilone B	Microbial	Cancer
14	2008	Ceftobiprole medocaril	Cephalosporin C	Microbial	Antibacterial
15	2008	Umirolimus	Sirolimus	Microbial	Cardiovascular Surgery
16	2008	Methylnaltrexone	Morphine	Plant	Opioid-induced constipation
17	2009	Tebipenem pivoxil	Thienamycin	Microbial	Antibacterial
18	2009	Telavancin	Vancomycin	Microbial	Antibacterial
19	2009	Vinflunine	vinblastine	Plant	Cancer
20	2009	Nalfurafine	Morphine	Plant	Pruritus
21	2010	Cabazitaxel	Paclitaxel	Plant	Cancer
22	2010	Fingolimod	Myriocin	Microbial	Multiple sclerosis
23	2010	Ceftaroline fosamil	Cephalosporin	Microbial	Antibacterial
24	2010	Eribulin	Halichondrin B	Marine	Cancer
25	2010	Mifamurtide	Muramyl dipeptide	Microbial	Cancer
26	2010	Zucapsaicin	Capsaicin	Plant	Pain
27	2011	Brentuximab vedotin	Dolastatin 10	Marine	Cancer
28	2012	Arterolane	Artemisinin	Plant	Antimalarial
29	2012	Dapagliflozin	Phlorizin	Plant	Diabetes
30	2012	Carfilzomib	Epoxomicin	Microbial	Cancer
31	2012	Novolimus	Sirolimus	Microbial	Cardiovascular surgery
32	2013	Canagliflozin	Phlorizin	Plant	Diabetes

33	2013	Trastuzumab emtansine	Maytansine	Plant	Cancer
34	2014	Naloxigol	Thebaine (paramorphine)	Plant	Opioid-induced constipation
35	2014	Empagliflozin	Phlorizin	Plant	Diabetes
36	2014	Oritavancin	Vancomycin	Microbial	Skin infection
37	2014	Vorapaxar	Himbacine	Plant	To reduce the risk of heart attack
38	2015	Ceftazidime/ avibactam	Cephalosporin	Microbial	Intra- abdominal infections

The above table clearly suggests that bio-actives from terrestrial plants, animals, microbes and marine organisms play a pivotal role in the development of new drugs and drug leads. Thousands of simple and complex molecules with natural origin are being reported in literature, which in turn make it difficult to classify them in a systematic manner.

1.2. Classification of Natural Products

Following Albrecht Kossel's original proposal in 1891, NPs are divided into two major classes. They are primary and secondary metabolites. A primary metabolite is directly involved in normal growth, development and reproduction of living organisms while secondary metabolites are not directly involved in the normal growth, development or reproduction of an organism or a plant. They often play a vital role in plant defence. In the field of organic chemistry, the definition of natural products is usually restricted to secondary metabolites and are the active components of most of the traditional medicines. Before going to the detailed study, their classification based on source/origin, biosynthetic pathway and chemical structure are described below.

1.2.1. Based on source/origin

Based on origin, natural products are broadly divided into four;

- Plant derived NPs
- Microbial world derived NPs
- Marine world derived NPs
- Animal world derived NPs

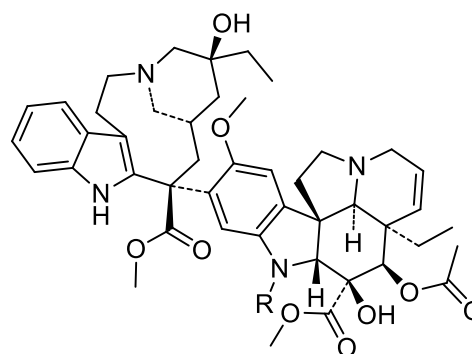
1.2.1.1. Plant derived natural products

Plants are a major source of complex and structurally varied chemical compounds (phytochemicals) that include phenols, poly phenols, tannins, terpenes and alkaloids. Many of plant species have been well studied and most of their biological importance have already been recognized. According to World Health Organization (WHO) majority of world population still depend on plant derived traditional medicines (WHO, 2002). Due to the unending and unexplored medicinal values of plants, the research on NPs is mainly focusing on them. They remain as an essential source of new drugs, new drug leads and new chemical entities. They have been an integral part of the ancient culture of India, China and Egypt as medicine and their importance even date back to the Neanderthal period.¹⁴ Ayurveda is a traditional Indian medicinal system which is exclusively attributed to the culture that utilizes the medicinal values of plant metabolites. The literal meaning of Ayurveda is “science of life”, since ancient Indian health system focused mainly on man and his illnesses. It should be pointed out that positive health means metabolically well balanced human systems. Ayurveda is preserved as a supplement of the Vedas, in particular the ‘Rig Veda’ and the ‘Atharva Veda’. The three principal texts in Ayurveda are ‘Charaka Samhita’ (1000-800 BC) ‘Sushruta Samhita’ (800-700 BC) and Vagbhatta’s ‘Astanga Hridaya’ which mention the use of several plants as medicine.¹⁵ India is one of the world’s 12 biodiversity centres, consisting of more than 45,000 different plant species, growing in varying agro-climatic and soil conditions. India is therefore rightly called the ‘emporium of medicinal plants’. The mountain ranges of Himalayas have been known to be a source of rare and important medicinal plants from the ancient time itself. The forests in India are the principal repository of a large number of medicinal and aromatic plants, which are mainly being collected as raw materials for the manufacture of drugs and perfumery products.¹⁶ Some of the important plant species possessing drug candidates/molecules are given below.

(i) *Catharanthus roseus*

Catharanthus roseus, commonly known as the Madagascar periwinkle, is a traditional herbal medicine used for the treatment of diabetes, malaria and Hodgkin's lymphoma. Vincristine and vinblastine (commonly known as vinca alkaloids; figure 1.3), isolated from *Catharanthus roseus*, by Canadian scientists Robert Noble and Charles Beer in 1950's, have proven to be effective against childhood leukaemia, breast cancer, Hodgkin's disease (cancer of the lymph nodes) and choriocarcinoma. They are naturally extracted from the pink periwinkle plant and exert their anticancer properties by inhibiting

mitosis by binding to tubulin, thus preventing the cell from making spindles. *C. roseus* can be extremely toxic if consumed orally by human beings, and is cited under its synonym *Vinca rosea* in the Louisiana State Act 159.¹⁷

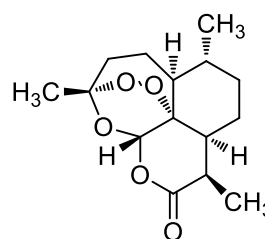


Vinblastine; R=CH₃
Vincristine; R=CHO

Figure 1.3. Some of the important vinca alkaloids

(ii) *Artemisia annua*

The research to develop antimalarial drugs from plant resources led to the discovery of artemisinin by Tu You You, a Chinese scientist, who shared the Nobel Prize in Physiology in 2015 for her discovery. Artemisinin was isolated from the plant *Artemisia annua*, sweet wormwood, a herb employed in Chinese traditional medicine. The treatment with an artemisinin derivative (artemisinin-combination therapies, ACTs) is now considered as a standard treatment against *Plasmodium falciparum* malaria worldwide and is recommended by WHO as the first-and second-line treatment for uncomplicated *P. falciparum* malaria as well as for chloroquine-resistant *P. vivax* malaria. Chemically this molecule is a sesquiterpene lactone containing an unusual peroxide bridge, which is considered to be responsible for its biological properties (figure 1.4).¹⁸



Artemisinin

Figure 1.4. Structure of artemisinin

Some other examples for plant derived drug molecules include, Morphine (a potent opiate analgesic) from *Papaver somniferum*, Quinine (antipyretic, antimalarial, analgesic,

and anti-inflammatory properties) from *Cinchona officinalis*, Podophyllotoxin (anticancer properties) from *Podophyllum peltatum* and Camptothecin (anticancer properties) from *Camptotheca acuminata* (figure 1.5).

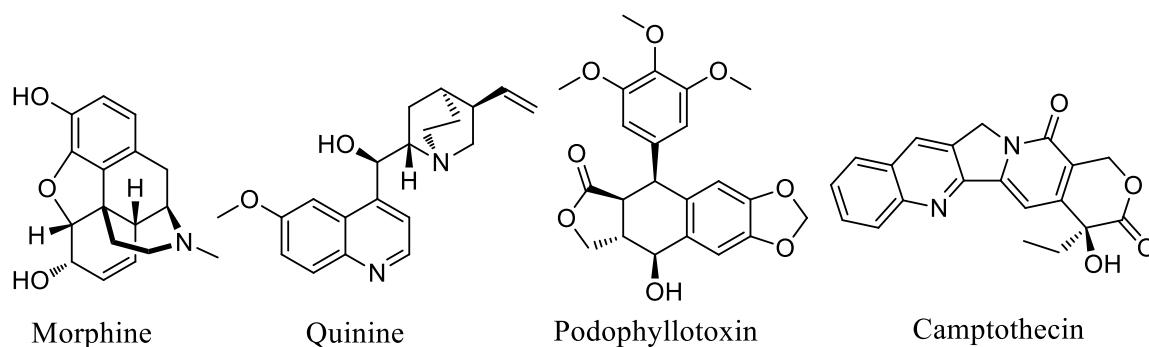


Figure 1.5. Some of the plant derived drug molecules

1.2.1.2. Microbial world derived natural products

Large varieties of microorganisms including bacteria, fungi *etc.* contribute to a significant number of medicinally important compounds. But their importance was explored only after the discovery of Penicillin, accidentally derived from a fungi *Penicillium chrysogenum* by Alexander Fleming in the year 1928. Other medicinally important fungal metabolites include cyclosporin (*Tolipocladium inflatum*), which is used to suppress the immune response after organ transplant operations. The discovery of Streptomycin (from *Streptomyces griseus*) led to the realization that not only fungi but also bacteria can contribute to the discovery of drugs. After the success of penicillin, many antibacterial compounds belonging to different classes *viz.*, β -lactams (doripenem and tebipenem), amino-glycosides, cephalosporins, tetracyclines (doxorubicin), and polyketides were developed from microorganisms.¹⁹ Some of the antibiotics isolated from microorganism are given in figure 1.6.

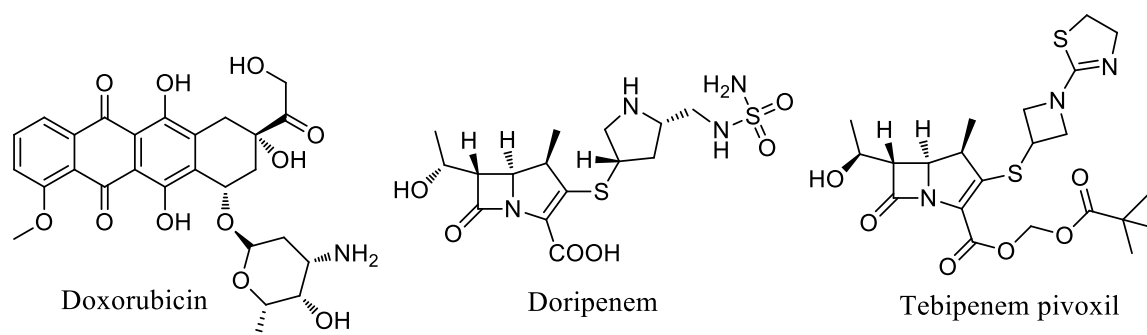


Figure 1.6. Examples for microbial world derived drug molecules

1.2.1.3. Marine world derived natural products

Oceans are an endless source of organisms wherein many of them are yet to be identified. They cover more than 70 % of earth's surface and are the interminable reservoir of structurally unique natural products. It points to the fact that the marine world comprises of unexploited, synthetically and medicinally important molecules. The number of bioactive compounds from marine animals such as sponges, tunicates, molluscs *etc.*, exceed fresh water plants (algae) by a large margin. In past few years many molecules from marine organisms were reported to have anticancer, antiviral, antibacterial, antifungal, antiprotozoal, anthelmintic, anti-inflammatory, immunosuppressive, neurosuppressive, neuroprotective and antifouling activities. Era of marine derived natural products chemistry started with the discovery of unusual nucleoside derivatives (spongouridine and spongothymidine) from the sponge *Tethya crypta* in the 1950s by Bergmann and Feeny. These two compounds further led to the synthesis of important anticancer drugs cytarabine and the antiviral drug vidarabine which are in clinical use since 1974 (figure 1.7). Among all the marine organisms investigated, marine sponges (Porifera) are recognized as the richest source of secondary metabolites, with about 4851 compounds to date, contributing nearly 30 % to all marine natural products discovered so far. It should be emphasised that, out of these, 1499 new compounds were isolated in the five years from 2008 to 2012. In short, in the present decade marine sponges continue to be the most promising source of marine natural products with vibrant biological activities.^{20,21}

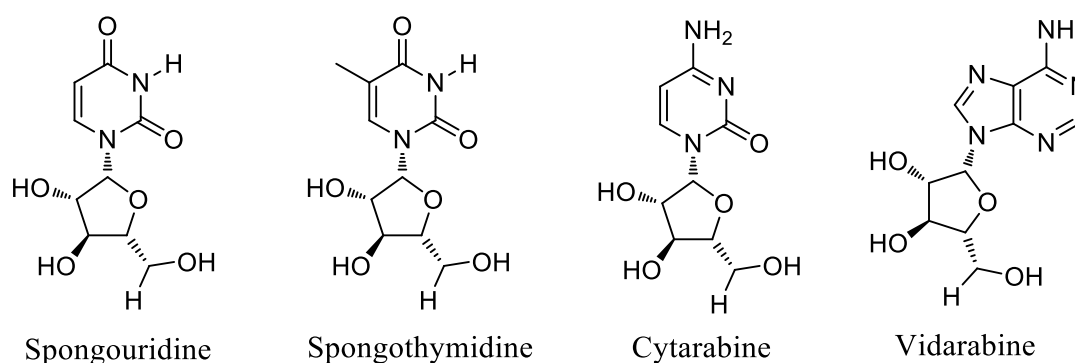


Figure 1.7. Marine derived natural products

1.2.1.4. Animal world derived natural products

In traditional systems of medicine, animal parts form the basis for many treatment regimens. Out of 252 essential therapeutic agents recognised by the World Health Organisation (WHO), 8.7 % are derived from animals and, even in the Indian Ayurvedic medicinal system, about 15–20 % of the formulations contain animal products. There are many important drug molecules in current market that are derived from animal kingdom.

A number of medicines (including tablets, creams, injections, capsules, mixtures and vaccines) contain animal products or are animal derived. For example, gelatine (used in making capsule shells) is a partially hydrolysed collagen which is usually bovine (beef) or porcine (pig) in origin and is one of many types of stabilisers added to pharmaceutical products such as vaccines. Heparin, an injectable anticoagulant, was first isolated from canine liver cells and is pharmaceutically prepared from porcine or bovine sources. Venomous organisms such as snakes, scorpions, spiders, caterpillars and frogs have also got much attention. Examples include teprotide, a peptide isolated from the venom of the Brazilian pit viper *Bothrops jararaca*, which led to the development of the anti-hypertensive agents; cilazapril and captopril. Another example is a series of antibiotic peptides extracted from the skin of the African clawed frog, and epibatidine is another drug molecule obtained from the skin of an Ecuadorian frog which is ten times powerful than morphine. Some of the naturally occurring animal derived secondary metabolites as well as their synthetic analogues are shown in figure 1.8.²²⁻²⁴

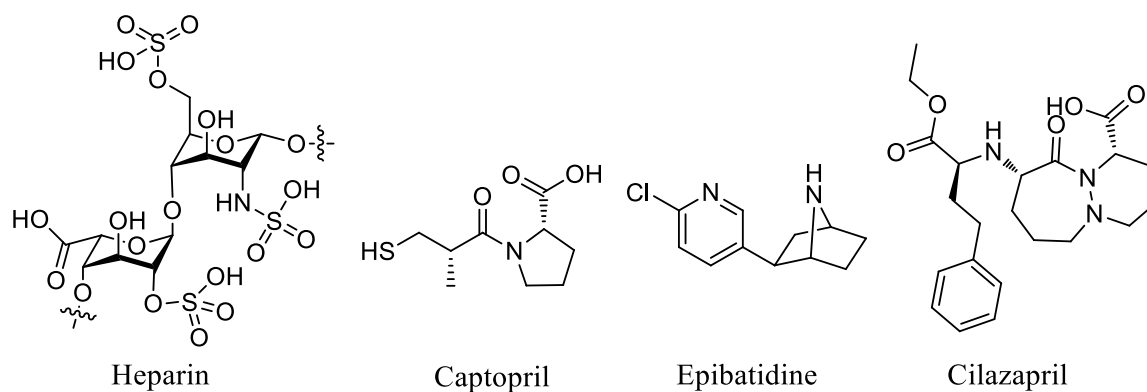
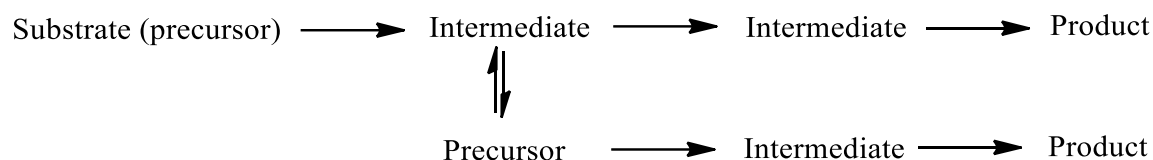


Figure 1.8. Some animal derived natural products

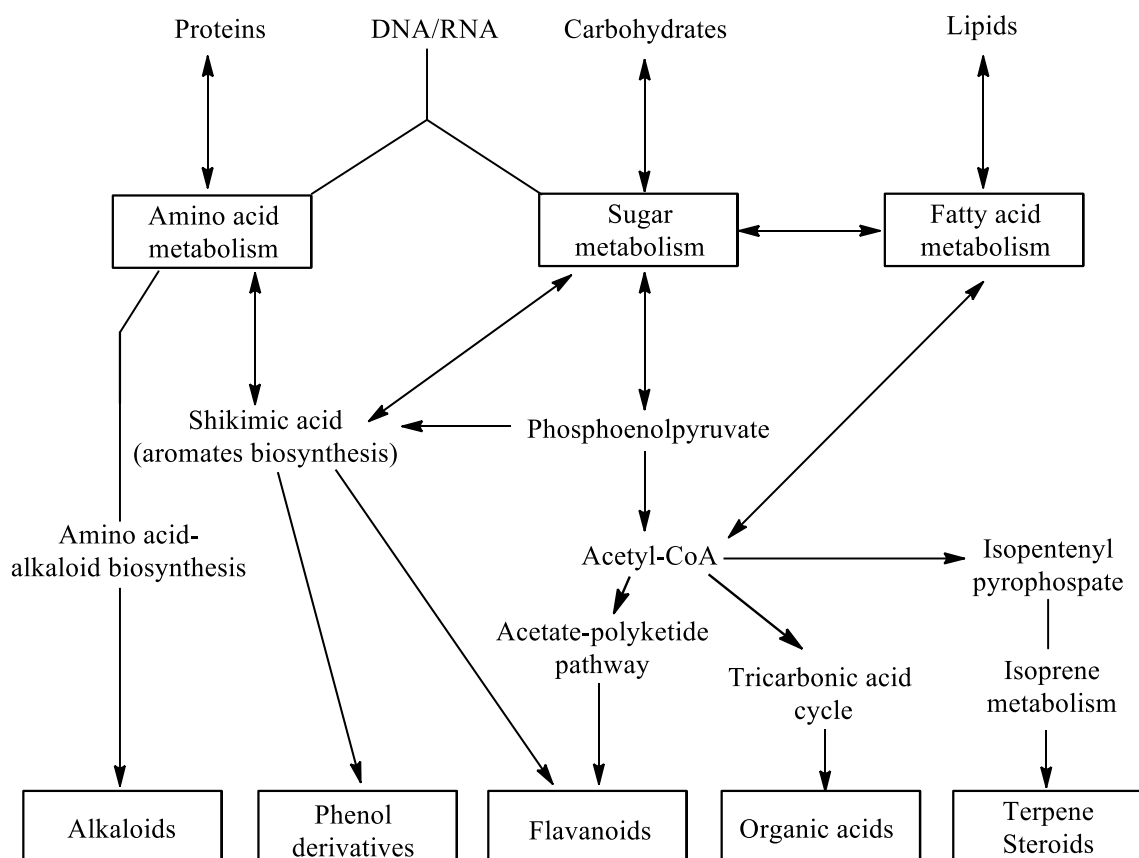
1.2.2. Based on biosynthetic pathways

The biosynthetic pathways derive from various precursors of primary metabolism. Or in a better way they can be defined as, the chemistry and metabolism of the four major classes of biomolecules- proteins, carbohydrates, lipids, and nucleic acids. These precursors are the small molecules used by a biosynthetic enzyme as a substrate and are converted to products. The product can either be an intermediate in the pathway, and in that case it is used as a precursor by the next biosynthetic enzyme, or it is the final product of the reaction chain. In a complex reaction with many reaction junctions, an intermediate simultaneously acts as a precursor for another part of the pathway. So, knowing the biosynthetic pathways of natural compounds is essential for the targeted manipulation of these pathways in biotechnology.



Most of these metabolisms are, multi-step, enzyme-catalysed processes where simple substrates are converted into more complex products or joined together to form macromolecules. In the case of natural resources, the metabolites constantly interact with a multitude of variable and potentially damaging factors of their habitats, and the metabolic plasticity evolves and exploits a range of inherent systems to create a rich repertoire of complex metabolites that hold adaptive significance for survival in various ecological niches. These phytochemical derivatives of secondary metabolism confer a multitude of adaptive and evolutionary advantages to the productive plants or any organisms. As a strategy for survival and for the generation of diversity at the organismic level, the ability to synthesize certain classes of secondary metabolites is often restricted to the selected taxonomic groups and this often impart a species-specific chemical “monogram” for the specific habitat.

Some of the major biosynthetic pathways include shikimate pathway, acetate-polyketide pathway, pyruvate pathway *etc.* and are given in scheme 1.1. The major primary precursors are derived from protein (amino acids), carbohydrate (sugars) and lipid (fatty acid) metabolism. The shikimate pathway provides the precursors for benzoic acid derivatives and phenylpropanoid compounds in plants. Shikimate is biosynthesized from *D*-erythrose-4-phosphate and phosphoenolpyruvate, two metabolites derived from the pentose phosphate cycle and glycolysis, respectively. Shikimate is further converted to chorismate by addition of a C₃ unit from phosphoenolpyruvate; and chorismate serves as the precursor of the aromatic amino acids L-phenylalanine, L-tyrosine, and L-tryptophan. The biosynthetic pathway of aromatic amino acids is one of the major sources of compounds such as flavonoids, phenols and some alkaloids. Acetyl-CoA is a central metabolite formed by glycolysis and also *via* the β -oxidation of fatty acids, and is used in the tricarboxylic acid cycle for the synthesis of organic acids, which act as the precursors of secondary metabolites. In addition, acetyl-CoA is involved in the synthesis of terpenes, which form a distinct class of metabolites. The general chemical reactions involved in these include oxidations, hydroxylations, reductions, methylations, acylations, prenylations and glycosylations.^{25,26}



Scheme 1.1. General scheme of biosynthetic pathways and precursors for the major classes of secondary metabolites.

1.2.3. Based on chemical structures

Natural products show large diversity in their chemical structures. Some contain heteroatoms, some others possess several chiral centres, cyclic structures, more than five H-bond donors, more than ten H-bond acceptors, and also some have large polar surface area. Secondary metabolites often possess fascinating pharmacological properties, and therefore their characterization is very important. There should not be any failure in recalling that plants synthesize these compounds as a part of their own survival strategies, typically as defence compounds or as signals for pollinators or symbionts. The terpenes, or terpenoids, that are present in plants, constitute the largest class of secondary metabolites. Most of the molecules belonging to this class are water insoluble. The list given below shows major classes of natural products based on their chemical structure.

- Aliphatic NPs
- Polypeptides
- Oxygen heterocycles
- Phenylpropanoids
- Tannins
- Benzofuranoids
- Flavanoids
- Polyphenols
- Poly cyclic aromatic NPs
- Terpenoids
- Steroids
- Alkaloids
- Specialized amino acids and peptides
- Glycosides
- Polypyrolles
- Lignans

Among the various classes of compounds, a detailed account of flavonoids, terpenoids, phenylpropanoids and alkaloids are given in the following sections.

1.2.3.1. Flavanoids

Flavanoids are considered as the polyketides of phenylpropanoids with more than 6,000 known compounds. They occur mostly in glycosylated form and are often accumulated in the vacuole. They fulfil several physiological functions in plants. The key intermediates in flavonoid biosynthesis are chalcones which serve as precursors of all other subgroups namely; flavones, flavonols, flavan-3,4-diols (leucoanthocyanidins), anthocyanins, and proanthocyanidins (polymerized flavan-3-ols, condensed tannins). Some other subgroups of flavonoids are restricted to certain taxa. Isoflavonoids are produced mainly in leguminous plants (Fabaceae). Aurones are yellow pigments with pervasive existence in plants like snapdragon (*Antirrhinum majus*), dahlia (*Dahlia variabilis*), and tickseed (*Coreopsis* species). Flavan-4-ols or 3-deoxyanthocyanidins are precursors of the phlobaphene polymers, which are red pigments and occur in some Poaceae (*Sorghum bicolor*, *Zea mays*) and gloxinia (*Sinningia cardinalis*) species. Anthocyanins serve as pigments to attract pollinators and seed dispersers. They are responsible for the red, pink, purple, and blue coloration of many flowers, fruits, and leaves. Flavonoids have two absorption maxima in the ultraviolet (UV) range and therefore protect the plant tissues from damage by UV radiation. Anthocyanins absorb light in the visible range also and may provide protection for chlorophyll in senescing leaves from photooxidative damage. Flavonoids are a part of the human diet, and it is suggested that dietary intake of flavonoids have beneficial health effects due to their antioxidant and radical-scavenging properties. Some of the naturally occurring flavonoids are listed in figure 1.9.²⁷⁻²⁹

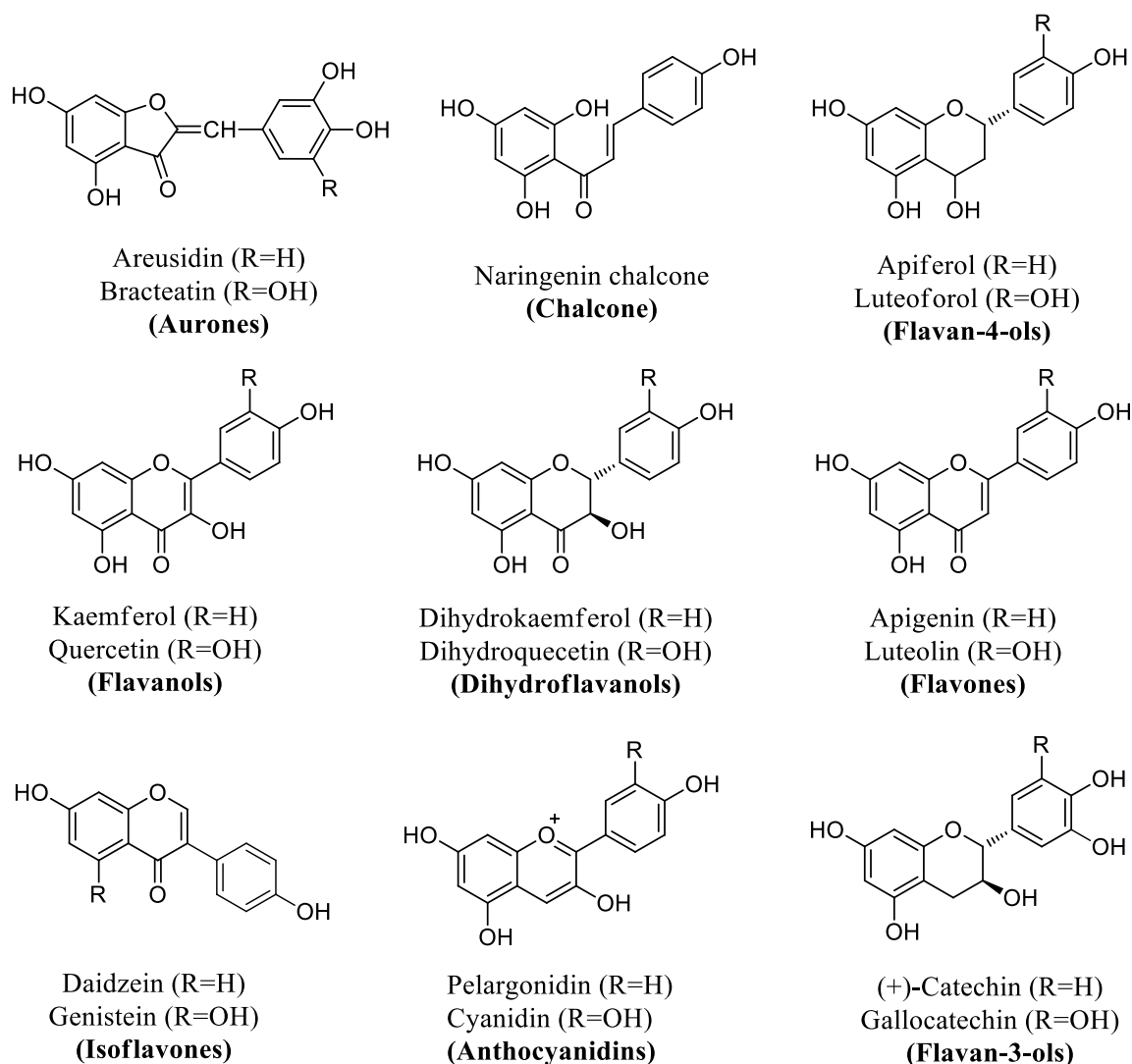


Figure 1.9. Diverse classes of flavonoids

1.2.3.2. Terpenoids

Terpenoids, also named isoprenoids, are the largest class of natural products present in plants and comprise more than 40,000 different structures. They are derived from a five-carbon monomer called isoprene unit, and according to the number of isoprene molecules that are incorporated, they can be classified into hemiterpenes (C₅), monoterpenes (C₁₀), sesquiterpenes (C₁₅), diterpenes (C₂₀), triterpenes (C₃₀), tetraterpenes (C₄₀), and polyterpenes. In plants, terpenoids originate from two different biosynthetic routes: the cytosolic mevalonic acid (MVA) pathway and the plastid-located deoxyxylulose phosphate (DXP) pathway (also called methylerythritol phosphate or MEP pathway). The odour of a freshly crushed mint leaf, orange peels, lemon grass and similar plant odours, are due to the presence of volatile C₁₀ and C₁₅ compounds existing in them. These are widely used in perfumery, as food flavourings and medicines, and as solvents. The essential oils

extracted from cloves, roses, lavender, eucalyptus, citronella, peppermint, camphor, sandalwood, cedar, and turpentine are some typical examples for terpenes with great interest in the scientific as well as in the industrial field. They also play a vital role in traditional herbal remedies and are under investigation for their anti-bacterial, anti-neoplastic, and other pharmaceutical functions. Structures of different terpenoids are given in figure 1.10.^{27,30}

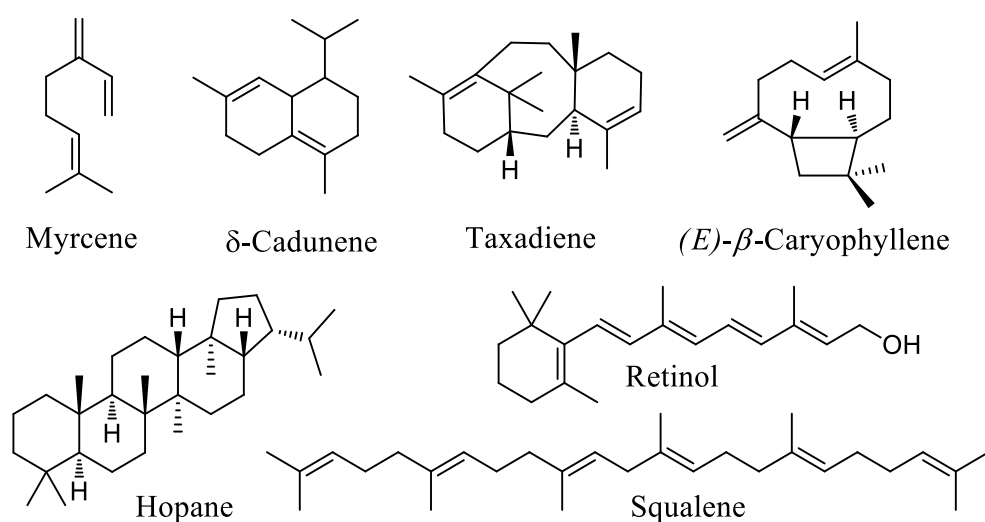


Figure 1.10. Structures of different terpenoids

1.2.3.3. Phenylpropenoids

Phenylpropenes are derived from cinnamic acid and are involved in the first few steps of lignin/lignan biosynthesis. They originate from the amino acid phenylalanine, which is shortened by one carbon. Other volatile phenylpropanoid-related compounds are phenylacetaldehyde and 2-phenylethanol. They are lipophilic in nature with a characteristic scent. They constitute the second largest group of plant volatiles after terpenoids. In many plants, phenylpropanoid and terpenoid volatiles occur as a mixture, while usually one group hoards predominantly. Essential oils with phenylpropenes are found in the Apiaceae, Lauraceae and Myrtaceae families. Many of these phenylpropene-containing plants have been employed by humans since ancient times as condiments and herbal remedies. Cloves, the unopened flower buds of the evergreen clove tree (*Syzygium aromaticum*, Myrtaceae) are not only used as spice, but also as anaesthetic and antiseptic in dentistry. The active ingredient and major component of essential oil from cloves is the phenylpropene, eugenol. Another evergreen tree of the tropics, *Cinnamomum ceylanicum* (Lauraceae) is the source of cinnamon bark with *trans*-cinnamaldehyde as main flavour component. Cinnamon was highly priced in the antique world. Some phenylpropenes are potentially carcinogenic, when some bio-activations like hydroxylation and sulphation occur at the side chain. The

examples include safrole, methyleugenol, and apiole. Some of the phenylpropenoid volatiles are given in figure 1.11.^{27,31}

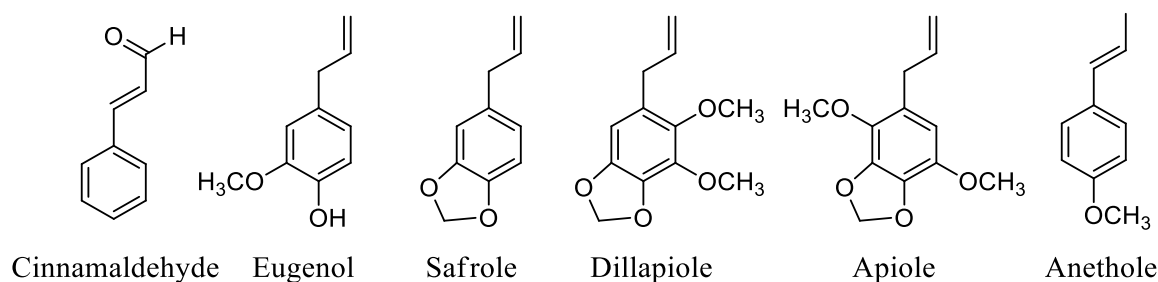


Figure 1.11. Structure of some phenylpropenoids

Lignans are a type of polyphenols, derived from phenylpropenes and are found in seeds of sesame, berries, fruits, vegetables, and whole grains. When we consume lignan precursors, bacteria in our gut will convert the “plant” lignans into “human” lignans including enterodiol and enterolactone, which have weak estrogenic activity.

1.2.3.4. Alkaloids

The term alkaloids generally refer to nitrogen-containing compounds biosynthesized from amino acids. The name "alkaloids" was introduced in 1819 by Carl Friedrich Wilhelm Meitner, and is derived from Latin root *alkali* (ashes of plants) and the *Greek*-suffix "like". They are biosynthesised *via* complex pathways, which may comprise 20 or more enzymatic steps. They possess diverse and important physiological effects on humans and other living organisms. Several alkaloids have provided lead structures for the synthesis of novel drug molecules. Some of the well-known alkaloids include morphine, strychnine, reserpine, coniine, quinine, ephedrine, and nicotine. Many other substances, however, that do not exactly match this rule are also classified under alkaloids, either for historical reasons or due to their bioactivities. Molecules bearing benzoxazinoids, glucosinolates, and cyanogenic glucoside cores are some examples for such bioactives. At present with more than 12,000 known structures, alkaloids represent one of the major groups of natural products. They are known to occur in more than 15 % in all the land plants and in more than 150 families. Interestingly, they exhibit a broad range of very specific pharmacological characteristics such as; analgesics, dilation of pupil of eye, cardiovascular drugs, mydriatics, CNS-stimulants and depressants, anticholinergics, sympathomimetics, antimalarials and purgatives. Due to their large number and the high structural diversity, a comprehensive summarisation of all different types of alkaloids are impossible and no single taxonomic principle exist that would allow consistent

classification of all alkaloids. However, some of the important class of alkaloids are given below.^{27,32}

- Purine Alkaloids
- Tropane Alkaloids
- Pyrrolizidine Alkaloids
- Indole Alkaloids
- Phenylalkylamines
- Quinolizidine Alkaloids
- Benzyloisoquinoline Alkaloids
- Ipecac Alkaloids
- Amaryllidaceae Alkaloids

Purine alkaloids are derived from nucleoside metabolism and are produced in a variety of taxonomically unrelated plant species like coffee (*Coffea arabica* and other *Coffea* species, Rubiaceae), tea (*Camellia sinensis*, Theaceae), cacao (*Theobroma cacao*, Sterculiaceae), and cola (*Cola nitida*, Sterculiaceae). The most abundant purine alkaloid is caffeine, followed by theobromine. Tropane alkaloids originate from the amino acids ornithine and/or arginine and all bear a common bicyclic tropane skeleton that consists of a seven-membered ring with an N-bridge between C-1 and C-5, the nitrogen being methylated. Hyoscamine, atropine and hyoscine are examples for tropanes. The backbone of pyrrolizidine alkaloids is composed of a hydroxymethylpyrrolizidine that is mostly esterified with branched aliphatic mono- or dicarboxylic acids. Quinolizidine alkaloids are biosynthesized from lysine *via* cadaverine. Apart from the bicyclic lupinine, most other compounds of this group are tri- or tetracyclic. Over 2,000 structurally diverse indole alkaloids are known and most of them show significant pharmacological properties. Some representative structures for alkaloids are shown in figure 1.12.²⁷

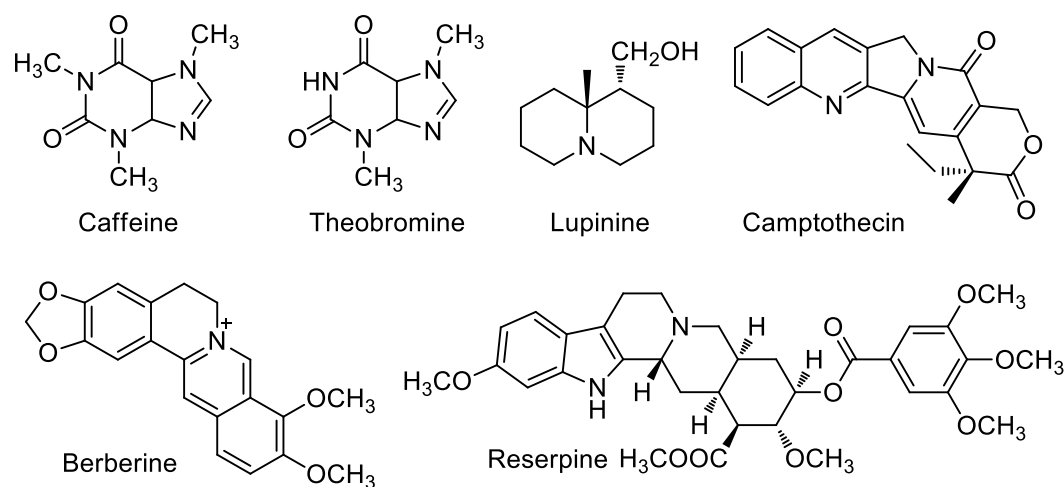


Figure 1.12. Some representative structures of alkaloids

1.3. Role of Natural products in Drug Discovery

Drug innovation is a painstaking procedure, which involve molecular-level syntheses and modifications. Moreover, most of the synthesised drugs are costly and possess many side effects including nausea, vomiting, abdominal problems *etc.* As described above, due to the broad chemical diversity and interesting biological activities, natural products have made significant contributions in biomedical sciences for the development of efficient drugs. Also, they are the chemically tailored molecules for various biological properties. Hence, the synthetic modifications of natural products have acquired much attention during the past few years. But, to some extent, the modification of natural products is quite different from *de novo* structure-based drug discovery. Some of the important contributions from nature that led to the development of drugs include; khellin, from *Ammi visnaga* (L) Lamk., which led to the development of chromolyn (in the form of sodium chromoglycate) as a bronchodilator; papaverine from *Papaver somniferum* which formed the basis for verapamil used in the treatment of hypertension and galegine, from *Galega officinalis* L., which was the model for the synthesis of metformin and other bisguanidine-type antidiabetic drugs (figure 1.13).¹

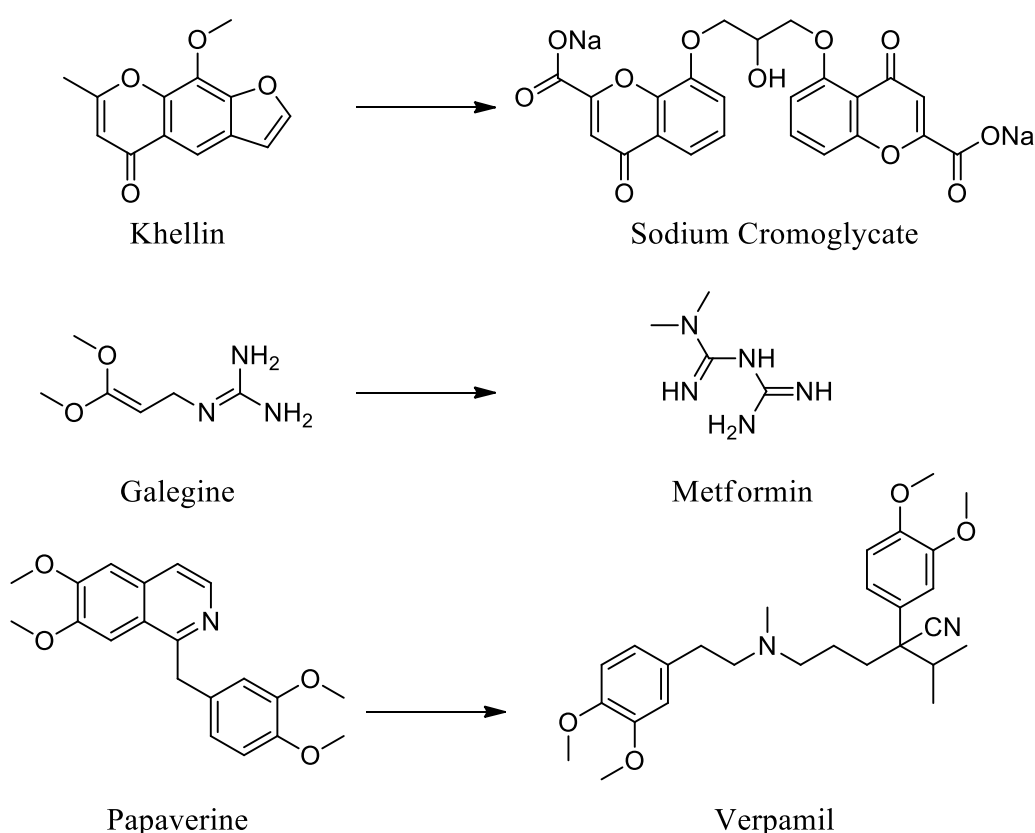


Figure 1.13. Drugs based on traditional medicine leads

1.4. Nutraceuticals and Dietary Supplements

The term “nutraceutical” was coined in 1989 by Stephen De Felice, founder and chairman of the Foundation for Innovation in Medicine, an American organization which encourages medical health research. According to him, a nutraceutical is a “food, or parts of a food, that provide medical or health benefits, including the prevention and treatment of disease”. These products range from vitamins, proteins, minerals, naturally isolated pure compounds and natural based stuffs used in capsules, tablets to foods that contain fortified bioactive ingredients. Everything from vitamins, dairy products, snacks, supplements to sports drinks, pre-prepared diet meals could be considered as nutraceutical.^{33,34} Globally, nutraceuticals are garnering much attention and has become an inevitable part of an average consumer's daily diet. The fundamental reasons for these are an increase in life expectancy and inadequate nutrition due to current lifestyle choices of people.

Nutraceuticals, have also been called medical foods, designer foods, phytochemicals, functional foods and nutritional supplements which include everyday products such as “bio” yoghurts and fortified breakfast cereals, as well as vitamins, herbal remedies and even genetically modified foods and supplements.³⁵ Over the past few years, an amassed number of dietary supplements have become available in supermarkets and health food shops and they are also available for purchase in pharmacies. In many chronic disease cases, even doctors are advising to take nutrition rich foods instead of drugs. Many different terms and definitions are used for nutraceuticals in different countries, which can result in confusion. An important class of nutraceuticals is represented by the polyunsaturated fatty acids (PUFAs), especially those of the omega n-3 and n-6 fatty acid (FA) families. Currently, the interest is highly devoted to the so-called fish-oils covering a high share of n-3 FA [eicosapentaenoic (EPA) and docosahexaenoic acids (DHA)]. It is claimed that these particular fatty acids exert a protective effect on the cardiovascular and inflammatory diseases and it is advocated that gradually this beneficial effects also cover other chronic diseases.^{34,36,37}

In fact natural food bioactives in the aetiology prevents chronic and infectious diseases to a great extent. Multiple phytochemicals and food ingredients are known for positive effects on human physiology, including interactions with the human microbiome. Special attention has always been given to phytochemistry, molecular structure and pharmacological effects of bioactive ingredients in food materials. Bioactives from a wide range of foods are investigated, including pro- and prebiotics, fungi, yeasts, herbs, spices,

fruits, vegetables, seafood and many more. Certainly, many of the nutraceutical products possess pertinent physiological functions and valuable biological activities. The on-going research will lead to a new generation of foods, which will certainly cause the interface between food and drug to become increasingly permeable. The present accumulated knowledge about nutraceuticals represent indisputably a great challenge for nutritionists, physicians, food technologists and food chemists. Public health authorities consider prevention and treatment with nutraceuticals as a powerful instrument in maintaining health and to act against nutritionally induced acute and chronic diseases, thereby promoting optimal health, longevity and quality of life.^{38,39}

In short, nutraceuticals are natural substances and, unlike drugs, are not synthesized for a certain purpose. They usually include; minerals, vitamins, herbal products (garlic, ginger, ginseng, onion, turmeric, *etc.*), dietary fibers, phytonutrients like resveratrols, saponins, carotenoids, prebiotics and probiotics.⁴⁰

1.5. Conclusion and Present Work

From the above discussions it is clear that the identification of molecules that fall within the biologically relevant sub-fraction of vast chemical space is of utmost importance to chemical biology and medicinal chemistry research. Though a number of new synthetic approaches have emerged, natural products still play a vital role in the development of new drugs. Moreover, they form the basis of many drugs that are currently in commercial use or in development. There is always an urgent need for identifying novel, active chemotypes as leads for effective drug development, and nature is the prime source of such lead discoveries. It has been estimated that only 10-20 % of species of higher plants have been systematically investigated for the presence of bioactive compounds, while the potential of the marine environment has barely been tapped.

Inspired by these observations, we selected some important plant species, used in traditional practices for our investigations. They include *Musa balbisiana* from Musaceae, *Anethum graveolens* from Apiaceae, *Rotula aquatica* from Boraginaceae and, *Zingiber nimmonii* and *Zingiber zerumbet* from Zingiberaceae family. Among these, *Musa* (banana family) is one of the famous plant species, belonging to the family Musaceae and order Zingiberales. From the ancient times, all the parts of a banana plant has been used by mankind for medicinal as well as ornamental purposes. The crude extracts of species of the Musaceae family have been investigated for their biological activities with special emphasis on the antimicrobial activity, antioxidant activity, hemagglutination and so on.

In these aspects, we chose one of the less explored species, *Musa balbisiana* for our further studies. The second chapter comprises of two parts, in which Part A deals with the isolation and evaluation of antidiabetic properties of a phytochemical, apiforol from the seeds of *Musa balbisiana* while Part B discusses the isolation and characterisation of phytochemicals from the rhizome and peels (fruit) of *Musa balbisiana*.

Herbs and spices have been used for both culinary and medicinal purposes for centuries. With their unique aroma, colour, and flavour they are inevitable in 21st century cuisine and medicine. They are also very good sources of antioxidants and other biologically active compounds. In this category, the plants from Apiacea always bear a decorative position. *Anethum graveolens* a species from Apiaceae, has been used in Ayurvedic medicines since ancient times and it is a popular herb widely used as a spice and also yields essential oil. Owing to the great biological significance of *Anethum graveolens*, a detailed phytochemical investigation of seeds of this plant has been undertaken and our investigations are presented in the first part of chapter three. In the second part we focussed on another important plant family, Zingiberaceae. They are an important natural resource that provides many useful products for food, spices, medicines, dyes, perfume and aesthetics. It constitute a vital group of rhizomatous medicinal and aromatic plants characterized by the presence of volatile oils and oleoresins of export value, as well as are widely distributed in India, and in tropical and subtropical regions of Asia (especially in Thailand, Indonesia and Malaysia). Hence, in this section, we made a phytochemical profiling of molecules present in the rhizomes of the plant species *Zingiber nimmonnii*, one of the less explored species of Zingiberaceae, via isolation and characterisation techniques.

Rotula aquatica Lour. belongs to the family Boraginaceae, is a branched shrub growing in the sandy and rocky beds of streams throughout India. Traditionally the roots of the plant are used as a laxative and diuretic, especially in the treatment of kidney stones, piles and venereal diseases. *R. aquatica* is one of the most extensively used medicinal plants in the Ayurvedic system of medicine to dissolve urinary calculi and kidney stones. In this regard, we carried out a detailed phytochemical evaluation of whole parts *R. aquatica* and we could successfully isolate and characterise a number of molecules from different parts of this plant and are described in the fourth chapter of this thesis.

Encouraged from the previous literature reports on zerumbone, a highly potent 11-membered sesquiterpenoid natural product from the rhizomes of medicinal plant *Zingiber zerumbet* Smith. we decided to isolate this bio-active from *Zingiber zerumbet* with an aim

to synthesize novel derivatives for biological evaluation. In the first part of chapter five, we describe our efforts in the synthesis of zerumbone pendant derivatives as well as zerumbone-aziridine derivatives under metal free conditions. Some biological screenings of the synthesised derivatives are also incorporated in this section. Besides, the Lewis acid catalysed activation of zerumbone-aziridine derivatives towards the synthesis of novel [5.8.3] and [5.8] fused structurally diverse sesquiterpenoid-ring systems are described in the final chapter of this thesis. Here, starting from zerumbone, we could efficiently design and execute a Lewis acid catalysed annulation processes for the inception of [5.8.3] and [5,8] fused ring systems. It was demonstrated that by selectively functionalizing zerumbone and thereby controlling the conformation of the 11-membered ring, the ring-closing processes could be tuned to fused-ring systems of choice. The highlight of the novel methodology is the utilization of renewable resources to generate complex fused skeletons.

1.6. References

1. G. M. Cragg and D. J. Newman, *Biochim. Biophys. Acta.*, **2013**, 1830(6), 3670-3695.
2. (a) D. A. Dias, S. Urban and U. Roessner, *Metabolites*, **2012**, 2, 303-336. (b) J. W. Li and J. C. Vederas, *Science*, **2009**, 325, 161-165. (c) J. D. McChesney, S. K. Venkataraman and J. T. Henri, *Phytochemistry*, **2007**, 68, 2015-2022. (d) G. M. Rishton, *Am. J. Cardiol.*, **2008**, 22, 43D-49D. (e) C. Gupta, D. Prakash and S. Gupta, Relationships between bioactive food components and their health benefits, 2013, DM. Martirosyan (ed.), Introduction to functional food science textbook, 1st ed. USA: Create Space Independent Publishing platform, pp 66-85. (f) C. S. Ramaa, A. R. Shirode, A. S. Mundada and V. J. Kadam, *Curr. Pharm. Biotechnol.*, **2006**, 7, 15-23
3. (a) A. L. Harvey, *Drug Discov. Today*, **2008**, 13, 894-901. (b) A. Ganesan, *Curr. Opin. Chem. Biol.*, **2008**, 12, 306-317.
4. M. Lahlou, *Pharmacol. Pharm.*, **2013**, 4, 17-31.
5. B. Shen, *Cell*, **2015**, 163(6), 1297-1300.
6. A. L. Harvey, R. Edrada-Ebel and R. J. Quinn, *Nat. Rev. Drug Discov.*, **2015**, 14(2), 111-129.
7. A. A. Siddiqui, S. Siddiqui and K. Sahu, *Int. J. Drug Dev. & Res.*, **2014**, 6(2), 172-204.
8. C. Katiyar, A. Gupta, S. Kanjilal and S. Katiya, *Ayu.*, **2012**, 33(1), 10-19.
9. D. J. Newman and G. M. Cragg, *J. Nat. Prod.*, **2016**, 79, 629-661.
10. J. A. Beutler, *Curr. Protoc. Pharmacol.*, **2009**, 46, 1-9.
11. B. B. Mishra and T. K. Tiwari, *Eur. J. Med. Chem.*, **2011**, 46, 4769-4807.
12. F. E. Koehn, *Med. Chem. Commun.*, **2012**, 3, 854-865.
13. F. E. Koehn and G. T. Carter, *Nat. Rev. Drug Discov.*, **2005**, 4, 206-220.
14. A. Saklani and S. K. Kutty, *Drug Discov., Today*, **2008**, 13, 161-171.
15. V. Subhose, P. Srinivas, and A. Narayana, *Bull Indian Inst. Hist. Med. Hyderabad*, **2005**, 35(2):83-92.
16. B. Ravishankar and V. J. Shukla, *Afr. J. Trad. CAM*, **2007**, 4(3), 319-337.
17. G. M. Cragg and D. J. Newman, *J. Ethnopharmacol.*, **2005**, 100, 72-79.
18. YY. Tu, MY. Ni, YR Zhong, LN. Li, SL, Cui, MQ. Zhang, XZ. Wang and XT. Liang, *Yao Xue Xue Bao*, **1981**, 16(5), 366-370.
19. M. S. Butler and M. A. Cooper, *J. Antibiot.*, **2011**, 64, 413-425

20. M. F. Mehbub, J. Lei, C. Franco and W. Zhang, *Mar. Drugs*, **2014**, *12*, 4539-4577.
21. R. Montaser and H. Luesch, *Future Med. Chem.*, **2011**, *3*(12), 1475-1489.
22. M.S. Kinch, A. Haynesworth and D. Hoyer, *Drug Discov. Today*, **2014**, *19*(8), 1033-1039.
23. M. Patlak, *The FASEB Journal*, **2016**, *18*, 421-422.
24. C. Y. Koh and R. M. Kini, *Toxicol.*, **2012**, *59*, 497-506.
25. H. O. Gutzeit and J. Ludwig-Muller, *Plant Natural Products: Synthesis, Biological Functions and Practical Applications*, First Edition. **2014**, Wiley-VCH Verlag GmbH & Co. KGaA.
26. (a) B. Jones and R. Kazlauskas, *Nat. chem.*, **2015**, *7*(1), 11-12. (b) https://www.cengage.com/resource_uploads/downloads/0495015253_60174.pdf
27. K. M Springob and T. M. Kutchan, *Plant-derived Natural Products*, **2009**, A. E. Osbourn and V. Lanzotti (eds.), Springer Science, Business Media, LLC, 975 North Warson Road, St. Louis, MO 63132, USA.
28. C. T Walsh, Y. Tang, *Natural Product Biosynthesis: Chemical Logic and Enzymatic Machinery*, **2017**, The Royal Society of Chemistry.
29. W. Heller and G. Forkmann, *Flavonoids: Advances in Research*, **1988**, J. B. Harborne (ed.), pp-399, Chapman & Hall, London.
30. D. J. McGarvey and R. Croteau, *The Plant Cell*, **1995**, *7*, 1015-1026.
31. E. Pichersky and N. Dudareva, *Trends. Biotechnol.*, **2007**, *25*, 105-110.
32. T. P. Cushnie, B. Kushnie and A. J. Lamb, *Int. J. Antimicrob. Agents*, **2014**, *44*(5), 377-386.
33. W. Andlauer and P. Furst, *Food Res. Int.*, **2002**, *35*, 171-176.
34. W. H. S. Jones (Tr.), *Nutrimet.* **1923**, Hippokrates (ed.), Heinnemann, London; Plutnam, New York, 351.
35. C.K.B. Ferrari and E.A.F.S. Torres, *Biomedicine & Pharma.*, **2003**, *57*, 251-260.
36. D. D. Rio, A. Rodriguez-Mateos, J. P. E. Spencer, M. Tognolini, G. Borges and A. Crozier, *Antioxid. redox signal*, **2013**, *18*(14), 1819-1872.
37. A. W. Boots, G. R. M. M. Haenen and A. Bast, *Eur. J. Pharmacol.*, **2008**, *585*, 325-337.
38. A. Cencic and W. Chingwaru, *Nutrients*, **2010**, *2*, 611-625.
39. L. Chen, G. E. Remendetto and M. Subirade, *Trends Food Sci. Technol.*, **2006**, *17*, 272-283.

40. H. Nazri, A. Baradaran, H. Shirzad and M. R. Rafieian-Koapei, *Int. J. Prev. Med.*, **2014**, 5(12), 1487–1499.

Part A: Screening of *Musa balbisiana* Colla. Seeds for Antidiabetic Properties and Isolation of Apiforol, a Potential Lead, with Antidiabetic Activity

2A.1. Introduction

Food plays a vital role in maintaining normal functions of human body. With recent advances in therapeutic and nutritional sciences, natural products have garnered extensive attention from both scientific and health professionals as health-promoting foodstuffs. Bioactive diets have emerged as potential supplements in various diseases, and nutrients present in them play an important role in maintaining the normal functions of the human body. The major nutrients present in food include proteins, carbohydrates, lipids, vitamins, and minerals. Besides these, there are some bioactive food components known as “phytonutrients” that play an important role in human health. They have an incredible impact on the health care system and offer medical health benefits including the prevention or treatment of the disease and various physiological disorders. Being natural products, they hold a great promise in clinical therapy as they possess no side effects that are usually associated with chemotherapy or radiotherapy. They are comparatively cheap and hence, significantly reduce health care cost.¹ Some of the important phytonutrients include polyphenols, terpenoids, limonoids, resveratrol, flavonoids, isoflavonoids, carotenoids, phytoestrogens, glucosinolates, phytosterols, anthocyanins, ω -3 fatty acids, and probiotics. Fruits and vegetables are important components of a healthy diet. This is partly because they aid in the body's retention of calcium, nitrogen, and phosphorus, all of which work to build healthy and rejuvenated tissues. Some fruits like bananas offer great medical benefits.²⁻⁵

Musaceae, an edible plant family (banana family) comprises of three genera and 120 taxa, native to tropics of Africa and Asia; however, the cultivars are spread all over the world. They have been considered as one of the most ancient families within the order zingiberales and provide most affordable and relished nutritious fruit. The family has a long history of being widely used as a food crop enriched with vitamins, carbohydrates, dietary fibres *etc.* and currently, it occupies the fourth position in the world after rice, wheat and

maize. Traditionally, the usage of different parts of Musaceae plants have proved successful in the treatment of various ailments. The parts used for curing various diseases include the flowers (bronchitis, dysentery, ulcers and diabetics), the astringent plant sap (hysteria, epilepsy, leprosy, fevers, haemorrhages, acute dysentery, diarrhoea, haemorrhoids, insects and other stings and bites), young leaves (burns and other skin afflictions), unripe peel and leaves (dysentery, diarrhoea and also for treating malignant ulcers).⁶⁻¹¹

India is the largest producer of banana (botanically they belong to genus *Musa*) in the world with about 25 million tons (18 % of total global production) and cultivates bananas of different shapes, colors and taste. Though the order zingiberales consists of three genera (*Musa* L., *Ensete* Horan. and *Musella*), only two genera- *Musa* and *Ensete*- are mainly distributed in India. *Musa* is the largest and most economically important genus in the family with evidence of cultivation dating back to 4000 BC in New Guinea. In India, bananas are highly interwoven with the national history, culture and heritage of different civilisations and encompass a great socio-economic significance. *Sushruta Samhita*, the first Sanskrit medical treatise of the 4th century and *Hortus Malabaricus* written by Hendrik van Rheede in 1678 also mention various medicinal usages of bananas. The domestication of bananas strongly indicate that edible bananas are one of the oldest tamed crops.¹²

Original bananas are seeded and in nonedible form, grow in soggy and humid forests. And it is believed that *Musa acuminata* Colla. and *Musa balbisiana* Colla. are the two wild species from which almost all of today's edible bananas have originated. The genus *Musa* was created by Carl Linnaeus in 1753, and he classified them into two species which he called *Musa paradisiaca* for those used as cooking bananas (plantains), and *M. sapientum* for those used as dessert bananas. It was later discovered that both of his "species" were cultivated varieties of the hybrid between two wild species, *M. acuminata* and *M. balbisiana*, which is now called *M. × paradisiaca* L. There are some significant phytochemical differences between various groups of bananas. *Musa acuminata* is a diverse species and consists of at least nine subspecies while *Musa balbisiana* is less diverse and no subspecies have been suggested so far. All the edible cultivars originating from these two species belong to various genome groups. They differ from each other depending on whether the clones are pure *acuminata* and *balbisiana*, otherwise diploid, triploid or tetraploid hybrids of these two wild species. Hence, a classification system was developed by Simmonds and Shepherd to organise all the edible banana cultivars systematically. On the basis of 15 vegetative morphological characteristics, the differences between *M. acuminata* and *M. balbisiana* could clearly be determined. The fruits of *M.*

balbisiana are starchier, more acidic and less aromatic to that of *M. acuminata*. Bananas are known in different names. In Malayalam, they are generally known as *Vazha* or *Bala* and most of the cultivar varieties growing in different places are known by their local names.¹³⁻¹⁵

2A.2. Phytoconstituents and Pharmacological Activities of *Musa*

The members of Musaceae have been popular since long due to their attractive culinary uses and pharmaceutical properties. The presence of anthocyanins in the bracts of banana have been reviewed by various researchers in the early nineteen hundred's, which as well gave good support to the taxonomical ordering of different genus. The presence of leucoanthocyanidin which gave rise to perlargonidin glycosides on acid treatment, has been reported by Robinson *et al.* in 1937 from the seeds of *M. sapientum*¹⁶ and Seshadri *et al.* reported the presence of proanthocyanidin glycosides, which gave rise to delphinidin in 1962 from the seeds of *M. acuminata*.¹⁷ Catecholamines such as norepinephrine, serotonin and dopamine were reported by groups of Waalkes (1958)¹⁸ and Vettorazz (1974).¹⁹ Also indole compounds like tryptophan, were identified by Shanmugavelu and Rangaswami in 1962.²⁰ Cellulose, hemicelluloses, arginine, aspartic acid, glutamic acid, leucine, valine, phenylalanine and threonine were isolated from the pulp and peel of *M. paradisiaca* by Ketiku *et al.* in 1973.²¹ Besides the Acyl steryl glycosides such as sitoindoside-I, sitoindoside-II, sitoindoside-III, sitoindoside-IV and steryl glycosides such as sitosterol gentiobioside, sitosterol myo-inositol- β -D-glucoside were isolated from fruits of *M. paradisiaca* by Ghoshal in 1985.²² figure 2A.1 shows the structure of some compounds isolated from Musaceae.

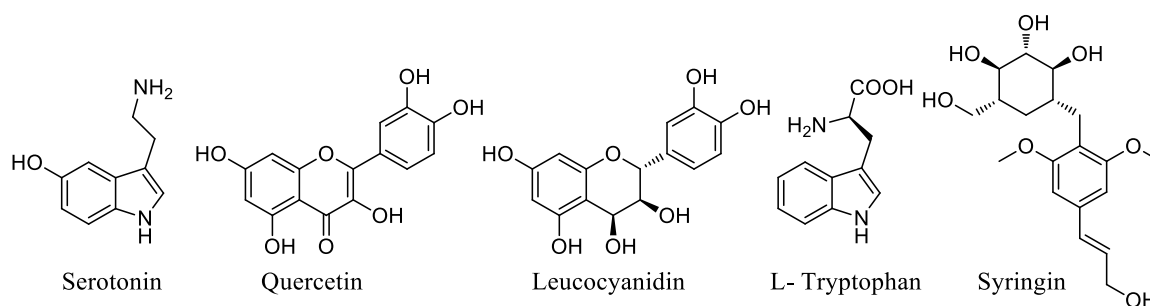


Figure 2A.1. Structure of some compounds isolated from Musaceae family.

Later in 1992, Ali reported the structures of three new neo-clerodane diterpenoids namely musabalbisianes A, B and C from the dense seeds of *Musa balbisiana* for the first time. The structure of the same is given below (figure 2A.2).²³

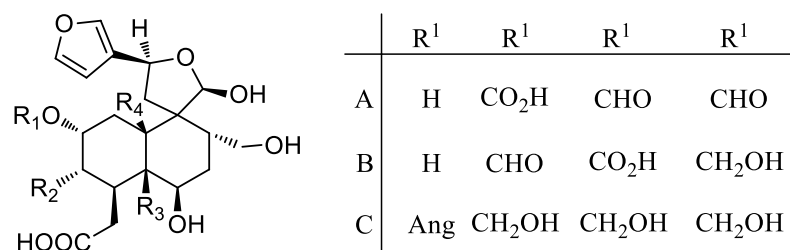


Figure 2A.2. Structure of neo-clerodane diterpenoids

Phenylphenalenones are the major bio-actives isolated from the rhizome, leaves and peels of these plants. In 1993, Javier *et al.* isolated two phenalenone type phytoalexins; irenolone and emenolone, for the first time from the infected leaves and green fruits *Musa paradisiaca* (figure 2A.3).²⁴

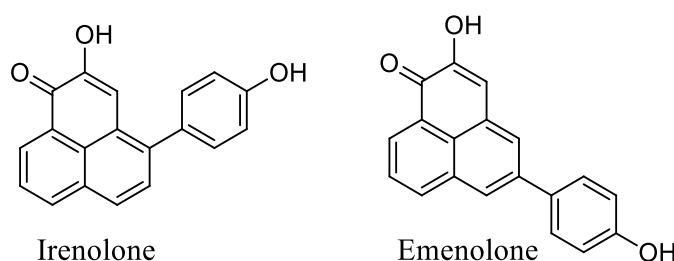


Figure 2A.3. Structure of irenolone and emenolone

Though the presence of phenalenone-type phytoalexins in bananas are reported here for the first time, other classes of phytoalexins had been isolated previously, which include flavonoids, diterpenes *etc.* In 1998 Kamo *et al.* isolated fourteen phenylphenalenone-type phytoalexins including three new compounds from the peel of unripe *Musa acuminata* (AAA), bungulam fruit. The isolated phenylphenalenones were classified by them into four classes; 4-phenylphenalenone, 9-phenylphenalenone, 2-phenyl-1,8-naphthalene dicarboxylic acid and an intermediate type (figure 2A.4). An anti-fungal study on these phytoalexin showed that a phenolic hydroxyl group is necessary for the activity.²⁵

The same group also did a comparative study on phytoalexin compounds of unripe fruits of *M. balbisiana* [BBB] with those of *M. acuminata* [AAA] in the same year which showed that species *balbisiana* mainly produces 9-phenylphenalenones and no compounds were detected that were specific to either *M. balbisiana* or *M. acuminata*. This result was in agreement with the observation that plants in the same family accumulate chemically similar phytoalexin compounds, and also their HPLC analysis showed that fruits of hybrid cultivars of *M. acuminata* and *M. balbisiana* such as Latundan and Katali whose genome types are [AAB] and [ABB] respectively, would produce the same phytoalexins as those

of [AAA] and [BBB] fruits. Also, they recounted the isolation and identification of two naphthalic anhydrides and a cyclic diarylheptanoid that is supposed to be a biosynthetic intermediate of phenylphenalenones (figure 2A.5).²⁶

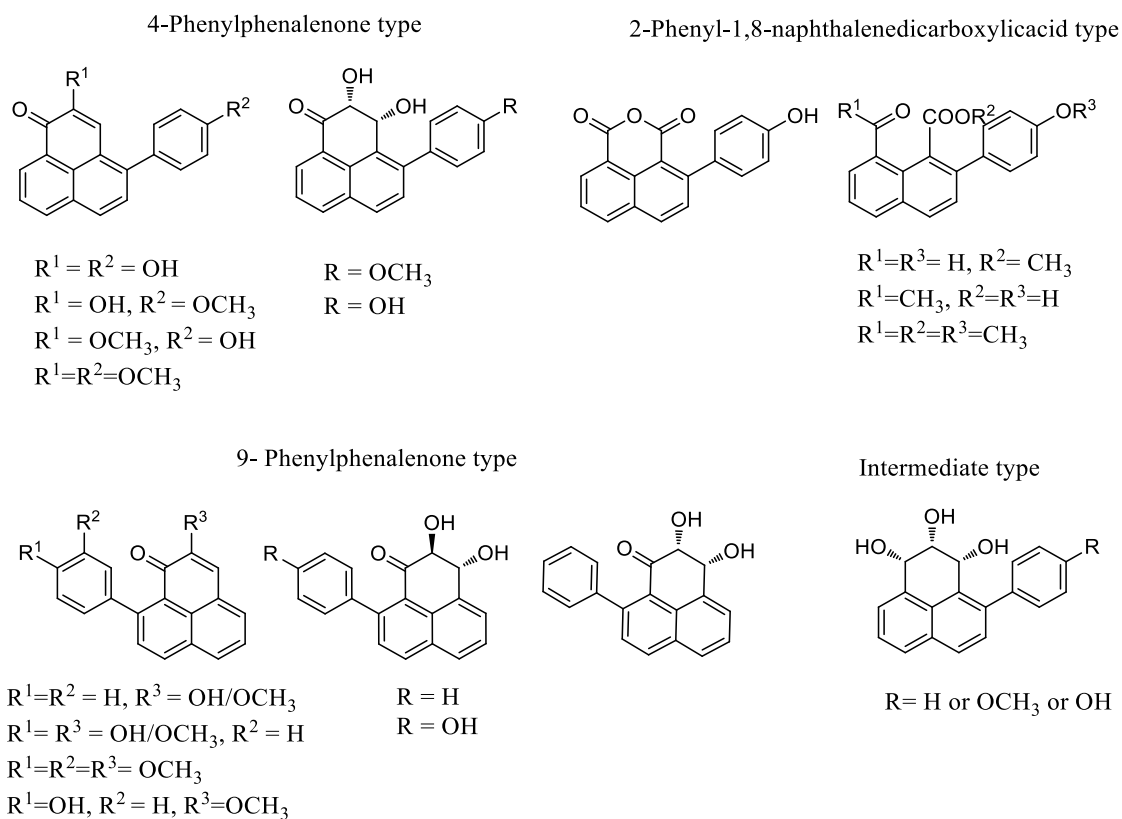


Figure 2A.4. Phenylphenalenones isolated by the group of Kamo

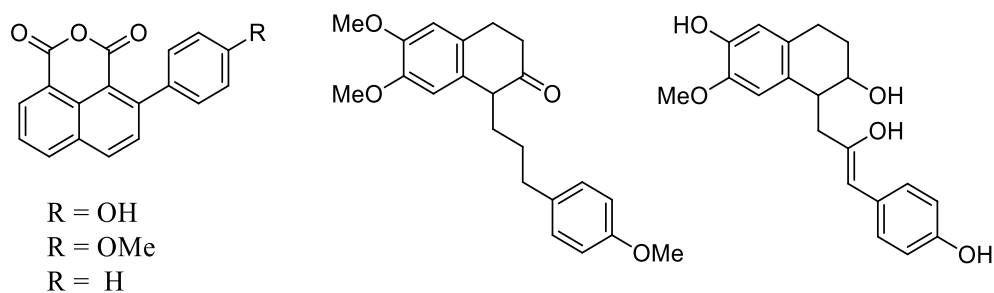


Figure 2A.5. Biosynthetic intermediate of phenylphenalenones

In 2002, Schneider *et al.* isolated three fused octacyclic phenylphenalenone dimers from *Musa acuminata*. Anigorootin, which was previously isolated from *Anigozanthos flavidus*, was isolated from *Musa acuminata* for the first time and the structure was confirmed by X-ray crystallography. 3,3'-Bis-hydroxyanigorufone, a dimer of the conventional type known from *Anigozanthos preissii*, was also found to present in *Musa*

acuminata. The occurrence of same compounds in Musaceae and Haemodoraceae, prompted them to conclude that both families show close chemotaxonomic relationships. The structures of dimeric phenylphenalenones from *Musa acuminata* and various species of the Haemodoraceae family are given below (figure 2A.6).²⁷

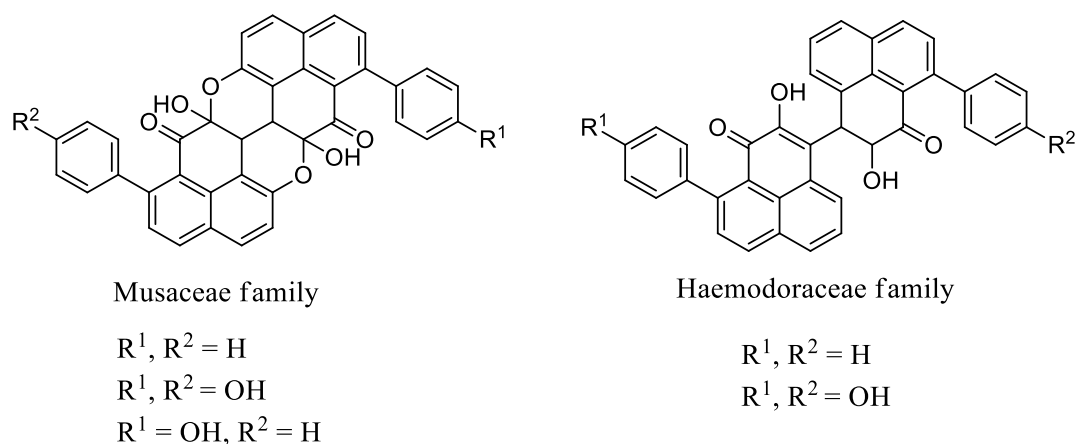


Figure 2A.6. The structures of dimeric phenylphenalenones

Later in 2004, the presence of intact long chain *p*-hydroxycinnamate esters in leaf fibers of abaca (*Musa textilis*) was identified by Rio *et al.* using gas chromatography/mass spectrometry studies. They clearly observed several peaks corresponding to esters of ferulic acid with long-chain fatty alcohols and ω -hydroxy fatty acids in the high-temperature region of the chromatogram. *p*-coumarate esters of fatty alcohols and *o*-hydroxyfatty acids could also be detected by them, although in minor amounts. These types of phenolic compounds in abaca were reported for the first time and it is also the first time report of isolation of *p*-coumarates and ω -hydroxyfatty acids from plants. The ferulates of fatty alcohols (a), ferulates of ω -hydroxyfatty acids (b), *p*-coumarates of fatty alcohols (c), and *p*-coumarates ω -hydroxyfatty acids (d) are given below (figure 2A.7).²⁸

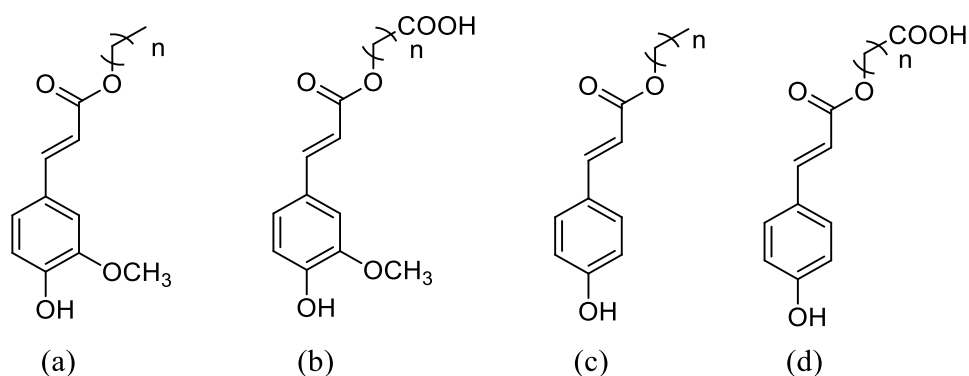


Figure 2A.7. Ferulates of fatty alcohols

The unrelenting studies on abaca by Rio *et al.* resulted in the identification of a series of phenylphenalenone type phytoalexins from the leaf fibers of abaca (*Musa textilis*). In their studies, they isolated a novel compound [(1*R*)-2,3-dihydro-4,9-dihydroxy-8-methoxy-1-phenylphenalene], along with some previously reported phenylphenalenones (figure 2A.8 (a)).²⁹ In 2010, Schneider *et al.* investigated 'Thepanom' (BBB) or 'praying hands' banana (Musaceae) using chromatographic techniques. A new natural product of the phenylphenalenone type, 3-hydroxy-4-phenyl-1*H*,3*H*-benzo[de]isochromen-1-one (figure 2A.8 (b)), and two known natural products, methoxyanigorufone and isoanigorufone, were isolated and identified by NMR spectroscopy and mass spectrometry studies. Additionally by HPLC analysis, the three condensed dimeric phenylphenalenones, namely anigorootin, 4'-hydroxyanigorootin and 4',4''-dihydroxyanigorootin were also identified by them.³⁰

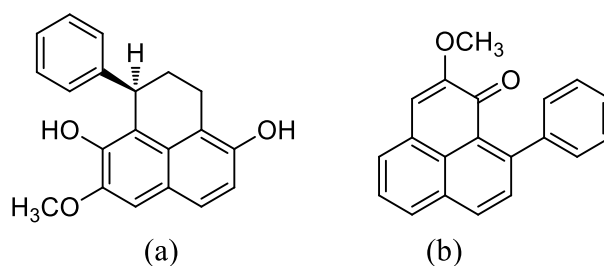


Figure 2A.8.

Phytochemical compositions of banana sap were done by Somana *et al.* in 2010 with some species that are found in Thailand. The analysis of banana saps were done using high-performance liquid chromatography-electrospray ionization mass spectrometry (HPLC-ESI-MS) and the results indicated the presence of phenolic and aromatic amino compounds. The possible structures of specific compounds were determined from the fragmentation patterns of each particular ion appearing in the mass spectra. The results indicated that there were a variety of phenolic and aromatic amino contents in many banana species. Apigenin glycosides, myricetin glycoside, myricetin-3-*O*-rutinoside, naringenin glycosides, kaempferol-3-*O*-rutinoside, quercetin-3-*O*-rutinoside, dopamine, and *N*-acetylserotonin were the major compounds that were revealed from the sap of banana accessions, namely, *Musa balbisiana*, *Musa laterita*, *Musa ornata*, and *Musa acuminata*.³¹

The production and presence of phytoprotectants in plants were studied by Rodregues *et al.* on healthy plant leaves of *Musa acuminata* in 2010. The bioassay-guided VLC-purification of the lyophilized infusion of the leaves of 4-month old healthy banana (*M. acuminata* cv. Grande Naine) plants resulted in the purification of a phytoanticipin with

strong antifungal activity against *M. fijiensis* Morelet, the causal agent of black Sigatoka, the most destructive and devastating disease of bananas and plantains in the world. The LC-MS analysis of the purified phytoanticipin suggested a steroidal saponin structure with four sugar units attached to the C-3 position of a diosgenin-like aglycone. These studies represent the first report of phytoanticipins occurring in *M. acuminata*.³²

In the same year Markovitz *et al.* reported the isolation of a jacalin-related lectin (BanLec) from the fruit of *Musa acuminata*. They determined that BanLec inhibits primary and laboratory-adapted HIV-1 isolates of different tropisms and subtypes. In their studies, BanLec possessed potent anti-HIV activity, with IC₅₀ values in the low nanomolar to picomolar range. The relative anti-HIV activity of BanLec was favourable compared to other anti-HIV lectins, such as snowdrop lectin and Griffithsin, and to T-20 and maraviroc, two anti-HIV drugs currently in clinical use.³³

Recently in 2014, Liu *et al.* isolated two diarylheptanoids, musaitinerins A and B, one novel heterodimeric phenylphenalenone musaitinerone and four known phenylphenalenones; 4-hydroxy-2-methoxy-9-phenyl-1H-phenalen-1-one, musanolone E, hydroxyanigorufone and irenolone from the fruits of *Musa itinerans* Cheesm. Their structures were elucidated using various spectroscopic analyses and the antimicrobial activity of these compounds were evaluated against *Escherichia coli*, *Staphylococcus aureus* and *Candida albicans*. Also the studies were carried out on the cytotoxic activity of these compounds against human erythromyeloblastoid leukemia (K562) and human alveolar carcinoma epithelial (A549) cell lines. Their studies showed that Musaitinerone and musanolone E exhibit weak effects against the A549 cell line, as compared with adriamycin. However, these two compounds did not exhibit any growth inhibition against K562 cells, *S. aureus*, *E. coli* or *C. albicans* and the other compounds were inactive against all of the tested cell lines and microorganisms, even at concentrations as high as 50 μ M. The structures of isolated compounds are given below (figure 2A.9). To determine the absolute configuration of musaitinerin A, the molecule was converted into its methyl derivative and the Mosher esters of that compound were synthesised.³⁴

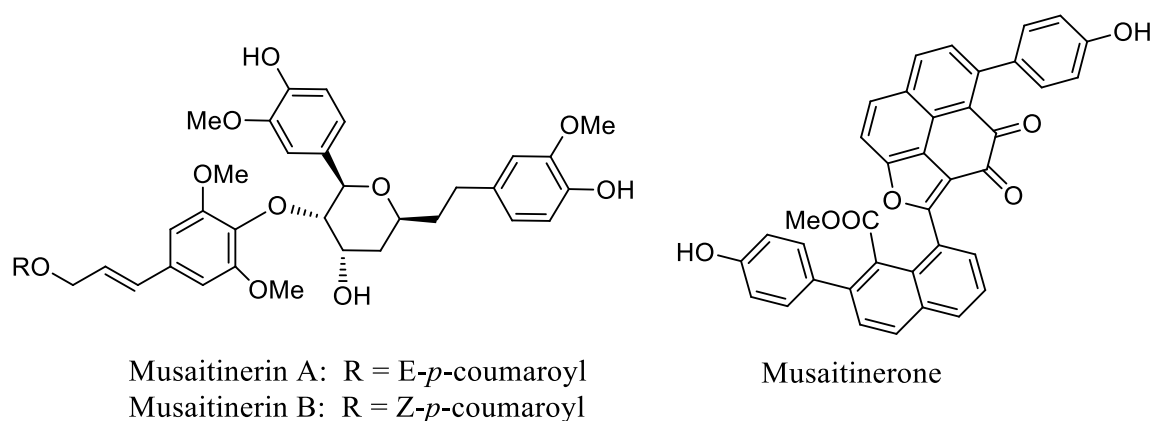


Figure 2A.9.

2A.3. Aim and Scope of the Present Work

Musaceae is an important medicinal plant family, which is extensively used in the preparation of many Ayurvedic formulations. Among various banana species, the wild species are generally distributed in the North-eastern parts of India. A property that distinguishes these wild species from the normal cultivar is the presence of large number of seeds in them. Another interesting property of these wild species is that, the fruit burst off soon after it is ripe, which facilitate the seed dispersal. Among the wild species, *Musa balbisiana* is known to produce large number of seeds, compared to others and this is the reason why we focussed mainly on this plant species. Even though the preliminary phytochemical analysis of Musaceae revealed the presence of phenylphenalenones as the major component in them, there has been no detailed report on the phytochemical investigation on the seeds of *Musa balbisiana*. Therefore as part of this PhD program, a detailed study of the seeds of *M. balbisiana* has been undertaken. The evaluation of preliminary *in vitro* antidiabetic potentials of the extracts and the isolated flavan-4-ol have been carried out, and the results are described in this chapter.

Musa balbisiana Colla.(clone cultivar B) is native to Southeast Asia, where it typically grows in gorges in tropical evergreen forests and is largely cultivated for their fruits and saps. The raw fruits are bluish green in colour, with dense seeds (figure 2A.10). This species is the commonest and widely distributed of all *Musa* species in India. *Musa balbisiana* have high medicinal properties like antilipidemic, antiulcer, antiarthritis *etc.* and the fruits are generally used in baby foods because of its superior nutritional value.³⁵ The antidiabetic potential of root extracts of *Musa balbisiana* were extensively studied by Himadri *et al.* in 2016 and the results indicated that the methanolic extract is capable of

substantial antihyperglycemic activities in STZ induced diabetic rats.³⁶ Phenylphenalenones are the major bio-actives isolated from the rhizome, leaves and peels of this plant. In 1992, Ali reported neo-clerodanes namely musabalbisianes A, B and C from the dense seeds of *Musa balbisiana* for the first time and three new triterpenes were recently reported from inflorescence of *Musa balbisiana* cv Saba.²³⁻²⁷ Apart from these, there are no decorative reports on the isolation and pharmacological evaluation of the seeds of this plant. Hence we decided to undertake a detailed phytochemical analysis of *Musa balbisiana* seeds to explore its pharmacological properties.



Figure 2A.10. Different parts of *Musa balbisiana*

2A.4. Proximate Composition Analysis and Extraction of *Musa balbisiana*

2A.4.1. Collection of plant material

The fresh mature fruits of *Musa balbisiana* were collected from Botanical Garden of University of Calicut, Malappuram District, Kerala, India during the month of May 2015. The specimen was identified by Dr. M Sabu, Associate professor, Department of Botany, University of Calicut and voucher specimen (Voucher Specimen: collected from India, Tripura, way to Ambassa from Agartala, N23° 53.344' E091° 46.240' m, on 21 May 2011, by A. Joe & P.E. Sreejith with voucher No. 116142 at Calicut university) was submitted to herbarium of Department of Botany, University of Calicut, Kerala, India.

The seeds of *M. balbisiana* were separated from the ripened fruit, dried and grounded. This powdered plant material was further subjected to proximate composition analysis, extraction and phytochemical isolation.

2A.4.2. Proximate composition analysis

The moisture, ash, crude fat and protein contents of the seeds were estimated using the standard procedures of AOAC. Triplicate samples of the seeds were oven-dried at 100 °C transferred to a desiccator and allowed to cool at room temperature for moisture content. The ash content was determined by heating a known amount of seeds in a muffle furnace at 550 °C for 12 h. Protein content was estimated by Micro-Kjeldahl method with nitrogen to protein conversion factor of 6.25 and fat content was determined using Soxhlet extraction. Total carbohydrate was calculated using the difference method. The proximate composition of seeds of *Musa balbisiana* was found out in the following order;³⁷

2A.4.2.1. Total moisture content

Moisture content or water content is one of the important and most commonly measured property of food materials. The oven drying methods are generally used for the determination of moisture content and in our study exact 4 g of *Musa balbisiana* (Triplicate samples of the seeds were oven-dried) seeds were dried in a 100 °C hot air vacuum oven, continuously for 48 hours. Then we reweighted the sample and the percentage of moisture content present in the sample was calculated using the formula given below.

Moisture content (%) of material = [(Weight of the sample - Weight of the sample after drying)/ Weight of the sample] x 100

$$\text{Moisture content (\%)} = [(4.000-3.818)/4.000] \times 100 = 4.55 \%$$

2A.4.2.2. Dry ashing

Dry ashing was carried out using a high-temperature muffle furnace maintained at a temperature of 550 °C for 12 hours attained *via* gradual increase of temperature at a rate of 5 °C per minute. Water and other volatile materials are vaporized, and organic substances are burned in the presence of the oxygen in air to CO₂, H₂O and N₂. The food sample is weighed before and after ashing to determine the amount of ash present. The results of ash test in the dry weight percentage are calculated as follows.

$$\% \text{ Ash (dry basis)} = (\text{Mass of ash/Mass of dry sample}) \times 100 = 8.19 \%$$

2A.4.2.3. Lipid content

Lipids are one of the fundamental components that are present in every organism. The plant matrixes are mainly composed of lipids and their composition differs depending on the types and parts of the plant. Generally the storage lipids are nonpolar in nature, however the functional lipids mainly consist of polar lipids. Usually, lipids are insoluble in water and are soluble in organic solvents such as hexane, chloroform, *etc.* So the selection

of most appropriate solvent for the extraction is crucial. There are many methods for lipid extraction and in our work, we used conventional Soxhlet extractor. The main advantage of this method is the continuous contact between the sample and fresh solvent, so filtration and other steps are not needed. We started our investigations with 35 g of dried and ground seeds of *Musa balbisiana*, and were placed in a 250 mL thimble of Soxhlet extractor. Here we used hexane (1L) as the solvent for lipid extraction. The extraction was carried out to a total of 18 hours and after the extraction the solvent in the extraction chamber was evaporated and the mass of the remaining lipid was calculated. The percentage of the crude lipid was calculated as follows.

$$\text{Lipid content (\%)} = [\text{mass of lipid extracted (g)}/\text{sample weight (g)}] \times 100$$

$$\text{Lipid content (\%)} = (0.382/35) \times 100 = 1.091 \%$$

2A.4.2.4. Protein content

The protein content was calculated from the concentration of nitrogen, that present in the seeds, by Kjeldahl method. A conversion factor of 6.25 (equivalent to 0.16 g nitrogen per gram of protein) is used in the calculation; however, this is only an average value.

$$\begin{aligned} \% \text{ N} &= \frac{1000 \text{ cm}^3 \times \text{mg} \times \text{moles}}{\text{X moles} \times (\text{v}_s - \text{v}_b) \text{ cm}^3 \times 14\text{g}} \times 100 \\ &= 8.60 \% \end{aligned}$$

Where, v_s and v_b are the titration volumes of the sample and blank, and 14g is the molecular weight of nitrogen N.

2A.4.2.5. Total carbohydrate content

Carbohydrates are one of the important component of food items and currently, we have many analytical methods for their quantification. In the present study, total carbohydrate content was evaluated by different method, in the form of percentage, as given below.

$$\text{By difference} = 100 - [\% \text{ of (protein + fat + water + ash) in 100 g of food}] = 77.569 \%$$

2A.4.3. Extraction and isolation procedures

800 g of the dried and powdered seeds of *M. balbisiana* were subjected to extraction (3L x 3 times) by intermittent vigorous stirring using a mechanical stirrer in one by one with hexane, acetone, ethanol and water at room temperature for 48 h. The crude extracts were concentrated at 50 °C under reduced pressure till complete dryness (removal of solvent under reduced pressure gave 5.1 g of crude hexane extract, 18.5 g of acetone

extract, 4 g of methanol extract and finally the water extract). An aliquot of acetone extract (90 % of total acetone extract) was subjected to column chromatographic separation on 100-200 mesh sized silica gel and eluted with the increasing order of hexane-ethyl acetate and ethyl acetate-methanol polarity mixtures. The entire fractions obtained were again pooled into 8 fractions by analysing the TLC (analytical thin layer chromatography was performed with Merck TLC Silica gel F254 coated on aluminium sheets). All the fraction pools were again subjected to column chromatographic separation using 100-200 mesh sized silica gel with hexane-ethyl acetate polarities and also by precipitation with suitable solvents.

2A.5. GCMS Analysis of Seed Oil

As the hexane extract mainly consists of plant oils, we carried out a GCMS profiling of the extract (as described under experimental section), and the studies revealed that the oil is a rich source of long chain fatty acids. The analysed oil contained 34 % n-hexadecanoic acid (palmitic acid) and 28.67 % oleic acid as the major constituents with a retention time of, 31.445 and 35.981 minutes respectively. Out of the thirteen detected constituents, these two comprise about 62.67 % and other constituents were present in minor amounts (table 2A.1).

Table 2A.1. GCMS profile of seed oil

Peak	Ret. Time	Area	Area %	Height %	A/H	Name
1	30.22	283400	0.33	0.64	2.49	Hexadecatetraene
2	30.495	678977	0.8	1.51	2.54	Hexadecanoic acid, methyl ester
3	31.445	29016363	34	24.49	6.71	n-Hexadecanoic acid
4	32.08	3969621	4.65	7.25	3.10	Hexadecanoic acid, ethyl ester
5	35.981	24460961	28.67	21.77	6.36	Oleic Acid
6	36.356	1570092	1.84	2.72	3.27	Ethyl (9Z,12Z)-9,12-octadecadienoate
7	36.542	3860999	4.52	5.22	4.19	9-Octadecenoic acid (Z)-, ethyl ester
8	37.072	5745633	6.73	9.62	3.38	Hexadecanoic acid, butyl ester
9	40.198	1158388	1.36	1.87	3.51	Eicosane

10	40.401	1174463	1.38	1.97	3.37	<i>n</i> -Propyl 9,12-octadecadienoate
11	40.579	2602949	3.05	4.24	3.47	14-Beta-H-pregna
12	41.468	3522775	4.13	6.17	3.23	Butyl 9,12-octadecadienoate
13	41.625	7287790	8.54	12.53	3.29	Butyl 9-octadecenoate or 9-18:1

2A.6. *In vitro* Antidiabetic Potentials of the Extracts

Diabetes is a growing health problem in which the body does not produce or does not respond properly to the hormone insulin. There are three major types of diabetes; type I, type II and gestational diabetes. Diabetes mellitus (type II) is such a serious chronic metabolic disease, characterized by hyperglycemia which in turn is caused by insulin resistance or its impaired synthesis in peripheral tissues of the pancreas.^{38,39} Rendering the 2016 WHO reports, nearly 422 million people suffer from diabetes globally and it is ranked in the top 10 causes of mortality (WHO, 2016).⁴⁰ To ameliorate diabetes or related complications, many medicines have been investigated, and many of these are found to stimulate or enhance the glucose uptake by activating the insulin receptors. However, most of the drugs which are currently in use for the management of diabetes are reported to have many side effects like cerebrovascular disease, renal failure, diarrhoea, flatulence, hepatotoxicity and so on.^{41,42} In these aspects, the daily food ingredients that can fuel insulin action to ameliorate diabetes are highly desirable. Many medicinal plants have aided in the development of new antidiabetic drugs, and the consumption of natural compounds is known to exhibit lesser side effects compared to synthetic derivatives.⁴³⁻⁴⁵ The on-going research in our lab focuses on the identification of compounds that hold both nutrition and drug applications.^{46,47} Accordingly in the present work, we emphasis on the identification of compounds from our daily life with integrated antidiabetic potentials. As bananas are very common and very much associated with the everyday life of men since the time immemorial, we took a challenge to explore the antidiabetic properties of the major phytochemical constituents present in the seeds of *Musa balbisiana*.

Inhibition of digestive enzymes, α -glucosidase and α -amylases, are the important therapeutic targets for the modulation of postprandial hyperglycaemia which is the earliest metabolic abnormality to occur in type 2 diabetes. α -amylase catalyses the digestion of carbohydrates by hydrolysing α -(1,4)-glycosidic linkages and produce maltose and glucose from starch. Also, α -glucosidase enzyme, situated in the epithelium of the small intestine,

catalyses the breakdown of disaccharides at the final step of carbohydrate digestion and releases glucose from oligosaccharides. Thus, α -glucosidase and α -amylase dual inhibitors slow the release of glucose from starch and oligosaccharides, delaying the increase of blood glucose level. Also, hyperglycemic condition causes to form excess advanced glycated end products (AGEs), which further trigger diabetes associated complications. So the consumption of foods that comprise potential α -glucosidase and α -amylase inhibitors can effectively control the postprandial blood sugar level and thus customs a dietary solution for the management of type II diabetes.^{48,49} In this context, plant extracts and their active components have always been given much attention, as a natural alternative over synthetic medicines, for more effective and safe inhibition of digestive enzymes.^{50,51} Therefore, inhibitory activities of *Musa balbisiana* seed extracts with various solvents - hexane (0.66 % of material weight), acetone (3.87 %), ethanol (0.55 %) and aqueous extracts (1 %), - were checked for the *in vitro* antidiabetic activities on digestive enzymes along with their antiglycation properties.

2A.6.1. α -Amylase and α -glucosidase inhibitory activity of the extracts

These enzymes generally hydrolyse the α -glucosidase linkages in polysaccharides that result in the increased blood sugar levels which in turn lead to hyperglycemia, one of the major impediments in diabetic mellitus.^{52,53} Therefore, in the present study, hexane, acetone, ethanol and water extracts of the seeds of *Musa balbisiana* (as described under experimental section) were evaluated for their ability to inhibit to α -amylase and α -glucosidase enzymes. The inhibitory activity of the extracts against α -amylase and α -glucosidase enzymes are shown in figure 2A.11. As can be seen, the extracts followed a dose-dependent inhibitory activity on both the enzymes. It was found that the acetone extract exhibited maximum inhibition of α -amylase and α -glucosidase enzyme with an IC_{50} value of $36.67 \pm 0.367 \mu\text{g/mL}$ and $100.61 \pm 0.707 \mu\text{g/mL}$ respectively (table 2A.2). On the basis of the IC_{50} values, it was found that the sequence of α -amylase inhibitory activity of the extracts followed the order; acetone ($36.67 \pm 0.367 \mu\text{g/mL}$) > ethanol ($102.89 \pm 0.403 \mu\text{g/mL}$) > hexane ($105.43 \pm 0.367 \mu\text{g/mL}$) > water ($567.45 \pm 0.642 \mu\text{g/mL}$) with a value of $5.72 \pm 0.231 \mu\text{g/mL}$ for the standard drug, acarbose. Whereas, in the case of α -glucosidase enzyme inhibitory activity, the order was acetone ($100.61 \pm 0.707 \mu\text{g/mL}$) > ethanol ($177.38 \pm 1.266 \mu\text{g/mL}$) > water ($398.85 \pm 1.102 \mu\text{g/mL}$) > hexane ($923.03 \pm 1.56 \mu\text{g/mL}$). Here the standard drug acarbose showed an IC_{50} value of $50.035 \pm 0.461 \mu\text{g/mL}$.

2A.6.2. Antiglycation property of the extracts

The increased protein glycation followed by the build-up of glycated end products results in the formation of reactive oxygen, and the auto-oxidation of these glycated end products contribute towards diabetics. Therefore, identifying the natural compounds having antiglycation properties always offer an economical remedy for the management of diabetic mellitus with minimal side effects. With this background, we have studied the effects of extracts on glycation process (as described under experimental section) and found that they inhibited *in vitro* glycation in a concentration-dependent manner (figure 2A.11). Among various extracts as given in table 2A.2, the acetone extract exhibited significant glycation inhibition property with an IC_{50} value of $86.48 \pm 0.751 \mu\text{g/mL}$ followed by hexane ($797.35 \pm 0.989 \mu\text{g/mL}$), ethanol ($927.26 \pm 1.462 \mu\text{g/mL}$) and water ($946.44 \pm 1.146 \mu\text{g/mL}$). Here the standard ascorbic acid showed an IC_{50} value of $115.51 \pm 0.876 \mu\text{g/mL}$.

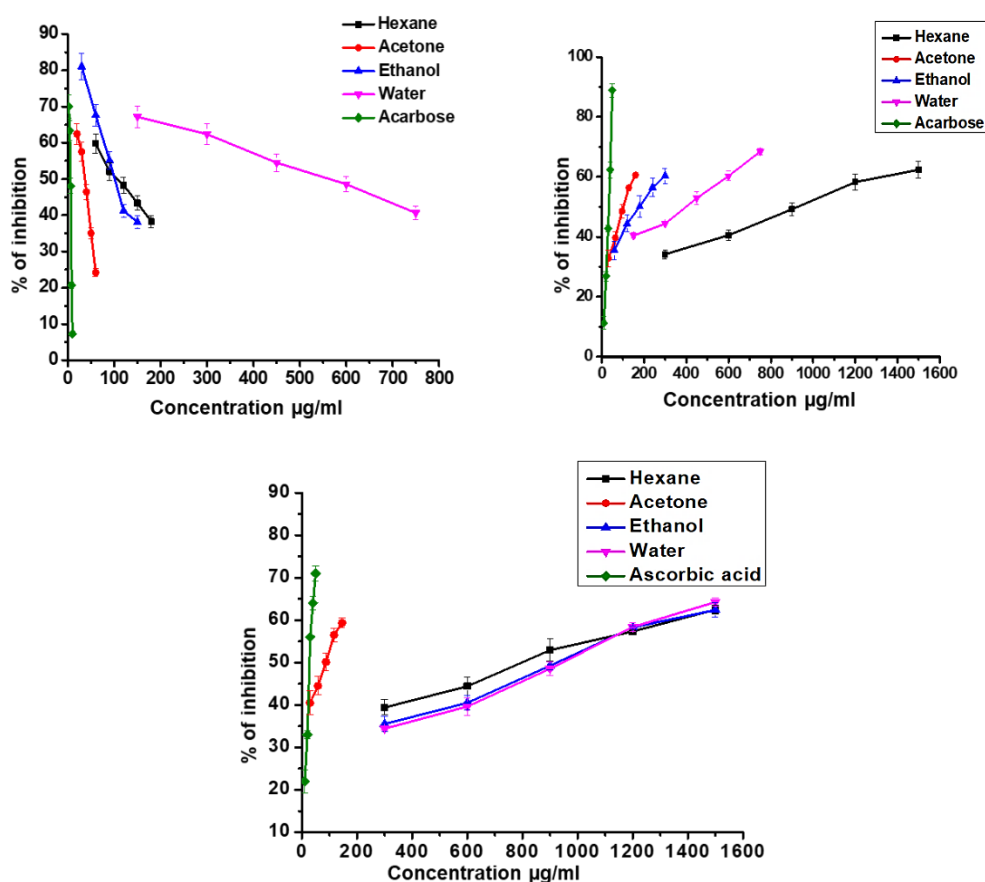


Figure 2A.11 A. Extract level α -amylase inhibitory activities, B : extract level α -glucosidase inhibitory activities, C : extract level antiglycation properties of *Musa balbisiana*

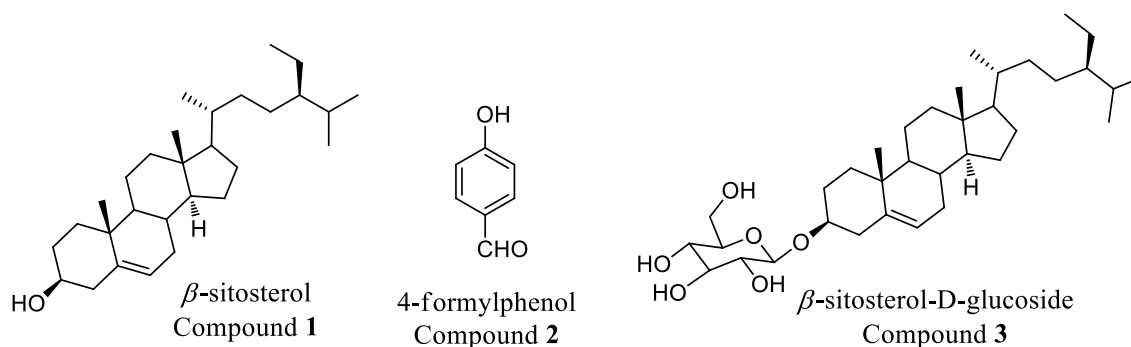
Table 2A.2. Extract level *in vitro* antidiabetic assay of extracts

Extracts	IC ₅₀ values		
	α -amylase inhibition ($\mu\text{g/mL}$)	α -glucosidase inhibition ($\mu\text{g/mL}$)	Antiglycation property ($\mu\text{g/mL}$)
Hexane	105.43 \pm 0.367	923.03 \pm 1.56	797.35 \pm 0.989
Acetone	36.67 \pm 0.367	100.61 \pm 0.707	86.48 \pm 0.751
Ethanol	102.89 \pm 0.403	177.38 \pm 1.266	927.26 \pm 1.462
Water	567.45 \pm 0.642	398.85 \pm 1.102	946.44 \pm 1.146
Acarbose	5.72 \pm 0.231	50.035 \pm 0.461	-
Ascorbic acid	-	-	115.51 \pm 0.876

2A.7. Isolation and Characterization of Apiforol

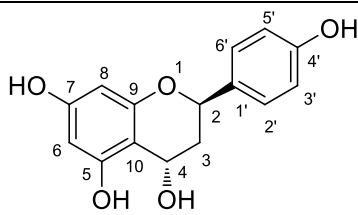
It was obvious from the above studies that, among the four extracts, acetone extract of *Musa balbisiana* exhibited the highest activity in terms of *in vitro* α -amylase, α -glucosidase and advanced glycated end products inhibition activities; hence, we further focused on the isolation and purification of compounds from the acetone extract.

An aliquot of acetone extract was subdivided by column chromatographic separation into eight fraction pools by analysing the TLC. All the fraction pools were again subjected to column chromatographic separation with hexane-ethyl acetate polarities for the isolation of active components. The fraction pools 1-3 mainly delivered phytosterols, long chain fatty acids and their triglycerides, while fraction pools 5-8 constituted the glucoside derivative of the phytosterols (figure 2A.12). The structure of all these compounds were well confirmed by analysing various spectral data with that of reported values.

**Figure 2A.12.**

From the fraction pool 4, the silica gel column chromatography with ethyl acetate, followed by precipitation with 9:11, hexane:ethyl acetate mixture resulted in the isolation of the marker compound, apiforol (compound **4**, 0.7 % of the extract).⁵⁴ This is the first report of isolation of apiforol from this genus and, the structure and NMR data of the compound are illustrated in table 2A.3.

The compound **4** was obtained as pale brown solid. Its molecular formula was determined to be C₁₅H₁₄O₅ on the basis of HR-ESI-MS: *m/z* 297.0738 [M+Na]⁺. In proton NMR, the signals displayed at δ 7.23 (d, *J* = 8 Hz, 2H) and δ 6.69 (d, *J* = 8.5 Hz, 2H) ppm respectively corresponding to four *ortho*-coupled aromatic protons at positions 2', 6' and 3', 5' of the disubstituted aromatic ring while the two *meta* coupled aromatic protons were resonated at δ 6.01 (d, *J* = 2 Hz, 1H) and δ 5.97 (d, *J* = 2 Hz, 1H) ppm as doublets respectively. The -CH₂- protons at position 3 were showed signals at δ 2.91 (dd, *J*₁ = 16.5 Hz, *J*₂ = 4.5 Hz, 1H) and δ 2.79 (dd, *J*₁ = 16.5 Hz, *J*₂ = 3 Hz, 1H) ppm as a doublet of doublets respectively. The protons resonated at δ 4.94 (brs) ppm and δ 4.24 (t, *J* = 2 Hz, 1H) ppm are corresponds to protons at position C-2 and C-4 respectively. Furthermore, the four hydroxyl groups were resonated at δ 8.40, 8.26, 8.12 and 3.85 ppm (figure 2A.13). Also, ¹³C and the DEPT-135 NMR demonstrate the nature of each carbon atoms very well. The COSY spectrum establishes the vicinity of -CH₂- protons at position 3 with protons at C-2 and C-4 positions. As well the connectivity of these fragments was well established from HMQC and HMBC analysis. The purity of the molecule was 96.84 %, checked with analytical HPLC (ESI Figure S8). The absolute configuration was established on the basis of optical activity [α]_D²⁵ = + 60.56° (c 0.1 MeOH) and the UV spectrum of the compound in MeOH showed absorption maxima at 274 and 329 nm.

Table 2A.3. ^1H and ^{13}C NMR details of apiforol


Position	^1H	^{13}C
1	-	-
2	4.94 (brs)	79.5
3	2.91(dd, $J_1 = 16.5$ Hz, $J_2 = 4.5$ Hz, 1H) & 2.79,(dd, $J_1 = 16.5$ Hz, $J_2 = 3$ Hz, 1H)	29.1
4	4.24 (t, $J = 2$ Hz, 1H)	67.0
5	-	157.5
6	5.97 (d, $J = 2$ Hz, 1H)	95.8
7	-	157.2
8	6.01 (d, $J = 2$ Hz, 1H)	96.3
9	-	157.6
10	-	99.8
1'	-	131.4
2', 6'	7.23 (d, $J = 8$ Hz, 2H)	129.1
3',5'	6.69 (d, $J = 8.5$ Hz, 2H)	115.6
4'	-	157.6
OH	8.40, 8.26, 8.12, 3.85	-

NMR- 500 MHz, Solvent : CD_3COCD_3 (in ppm).

2A.8. *In vitro* Antidiabetic Studies of Apiforol

Several flavonoids such as, quercetin, naringenin, kaempferol, hyperin and apigenin are reported to possess significant antidiabetic activities.^{55,56} Inspired from this, the flavanol apiforol which was isolated from the acetone fraction was analysed for its hypoglycaemic potential, as the acetone extract demonstrated promising hypoglycaemic activity in the preliminary extract level screening. Moreover, the only available study on apiforol is the antifungal studies, in which it gave negative results.⁵⁴

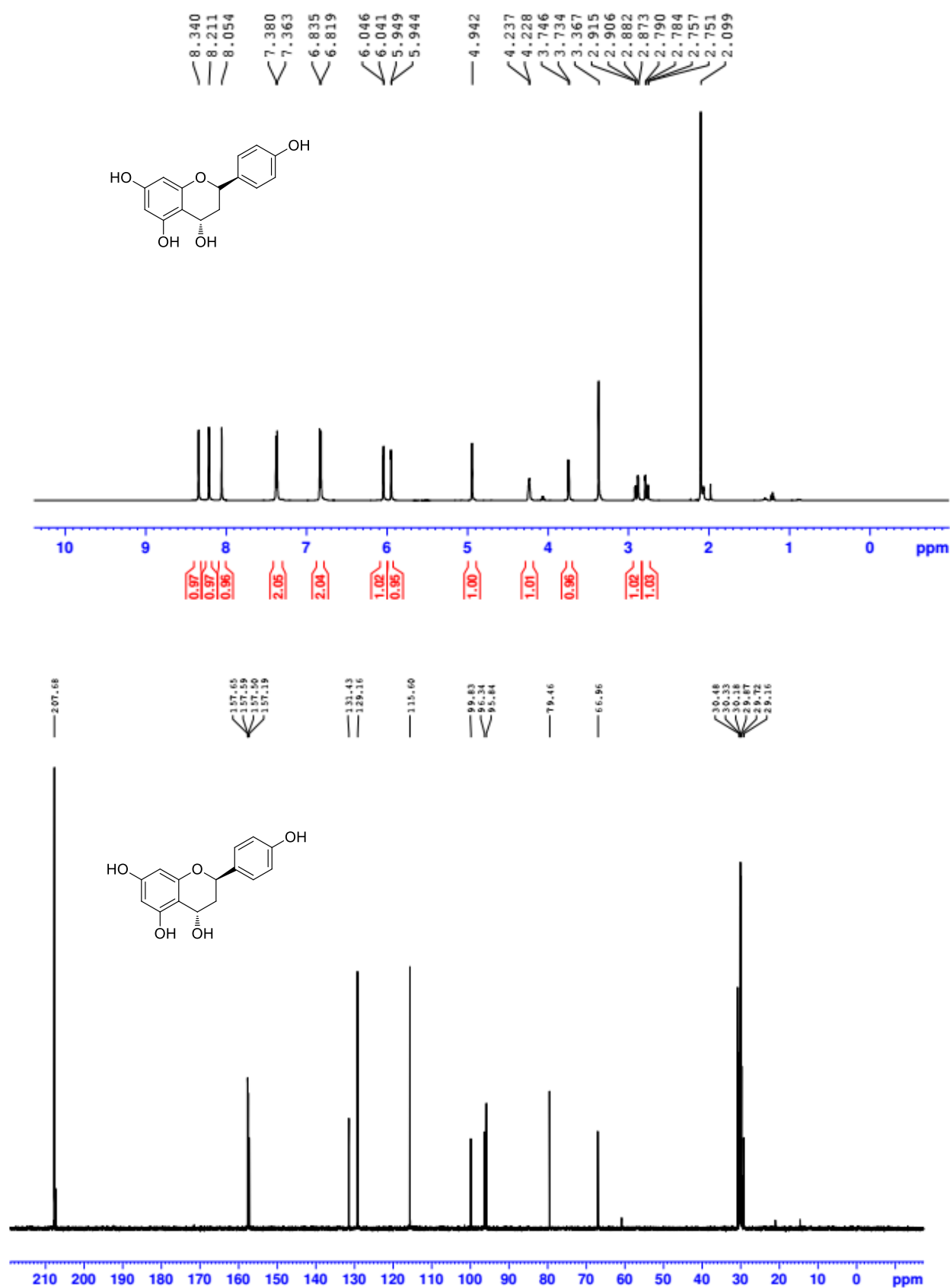


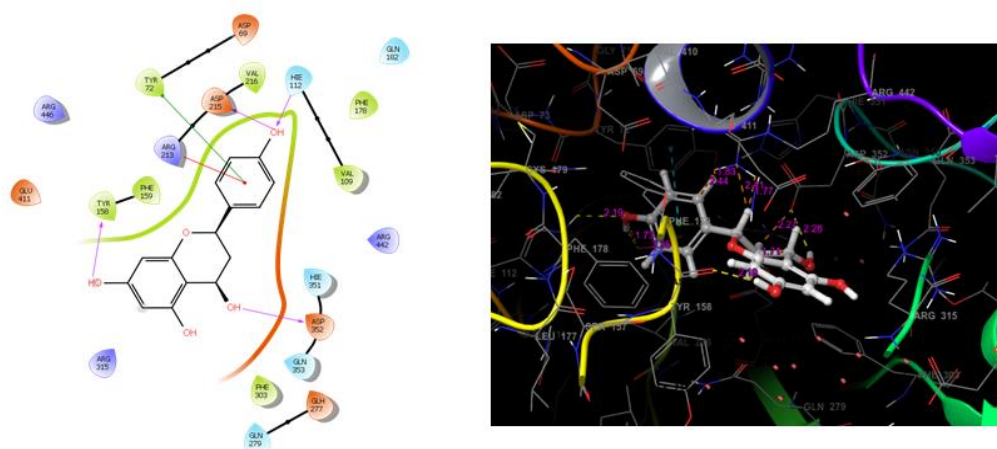
Figure 2A.13. Proton and carbon NMR of apiforol in CD₃COCD₃

In our antidiabetic studies, with the α -amylase enzyme, it was observed that the inhibitory activity was decreased for apiforol (IC₅₀ of $83.54 \pm 0.332 \mu\text{M}$) as compared to the acetone extract (standard acarbose showed an IC₅₀ of $8.93 \pm 0.480 \mu\text{M}$). However, the compound showed a significant α -glucosidase inhibitory activity with an IC₅₀ value of $48.25 \pm 0.255 \mu\text{M}$, which was better than the positive control acarbose ($52.87 \pm 0.224 \mu\text{M}$). Also it was found that the molecule effectively inhibited the formation of AGEs with a value of $114.23 \pm 0.567 \mu\text{M}$, which is promising than the positive control ascorbic acid ($154.63 \pm 0.497 \mu\text{M}$). However, the antiglycation property was less than the crude acetone extract ($86.48 \pm 0.751 \mu\text{M}$). This may be because of the synergistic effects of other compounds in the extract. Previous studies have reported better activity for crude extracts than the compounds isolated which was correlated with the synergistic effects of mixture of compounds in the extract.⁵⁷

2A.9. Molecular Docking Studies

The results of preliminary antidiabetic screening studies indicated that apiforol has significant α -glucosidase inhibition, however, the α -amylase enzyme inhibition was not promising. To predict the presumed binding mode of compound apiforol and the standard α -glucosidase inhibitor acarbose, docking analyses were carried out using the crystallized structure of isomaltase from *Saccharomyces cerevisiae* (PDB Code: **3A4A**). The docking protocol was validated by reproducing the binding mode of interaction with acarbose at the catalytic domain. The molecular docking study of apiforol was carried out using glide program of Schrodinger suite 2017.^{58,59} The ligand, apiforol was built and screened by ligprep and the pharmacokinetics parameters were analyzed using qikprop data. The results envisaged that apiforol binds in a site different from the catalytic domain [G-Score/D-Score of 6.4 kcal/mol]. The 2D and 3D interaction diagrams are shown in figure 2A.14. Results from molecular docking studies revealed that apiforol has good interactions with **3A4A** and the compound-protein interaction sites were mainly composed by hydrogen bonding and arene interactions. The hydroxyl protons at position 4, 7 and 4' formed a strong hydrogen bond donor interaction with ASP352, TYR158 and ASP215 residues. The hydroxyl oxygen at position 4' also forms a strong hydrogen bond acceptor interaction with HIE112 residue. The ring C shows Π - Π stacking interaction with TYR72 residue. Along with Π - Π stack interaction, the ring C also shows a Π - cation interaction with ARG213 residue (figure 2A.14). In detailed pharmacokinetic studies, apiforol shows promising ADME properties (table 2A.4). The compound is nontoxic to central nervous system with a CNS value of -2.

The octanol-water partition coefficient, hydrophilicity and hydrophobicity of apiforol is 1.158, -2.927 and -2.268 respectively; which proves that this phytonutrient can act as a promising candidate for the treatment of T2DM.



Compound	Targeting residues
Apiforol	TYR158, ARG213, TYR72, ASP215, HIE112, ASP352
Acarbose	ASP352, GLU277, GLU411, ASP242, SER240, TYR158

Figure 2A.14. 2D and 3D interaction diagram of apiforol with 3A4A; targeting amino acid residues in 3A4A are tabulated.

Table 2A.4. Pharmacokinetics parameters of Apiforol

Parameters	Values	Parameters	Values
G-Score	-6.42	QPlogKhsa	-0.268
D-Score	-6.42	Ro5	0
M.W.	274.273	QPlogPo/w	1.158
#stars	0	QPlogS	-2.927
CNS	-2	HBA	4.7
Dipole	2.518	HBD	4

2A.10. Glucose Uptake in L6 Myoblasts

In the case of type 2 diabetes, cells become resistant to insulin and fail to uptake glucose from blood stream, creating an imbalance in the glucose homeostasis, and resulting in hyperglycemia. Increasing the uptake of glucose by the cells is one of the important targets for diabetic therapy. Natural products have been shown to exhibit enhanced uptake of glucose by the cells.⁴⁴ As apiforol exhibited significant preliminary antidiabetic properties, it prompted us to carry out further studies in its efficacy in inducing glucose

uptake in L6 myoblasts. Therefore, apiforol was investigated for its effect on glucose uptake using L6 myoblasts.

In order to find out the working concentrations of apiforol, the cytotoxicity was examined in L6 myoblasts by MTT assay. From figure 2A.15, it is clear that cell viability decreased significantly in a dose-dependent manner. A concentration of 15 μM caused cell viability to decrease by about 58 %. Therefore, 5 μM and 10 μM concentrations of apiforol were selected for cellular glucose uptake experiments. It was monitored using the glucose fluorescent analogue, 2-NBDG (10 μM) after the pre-treatment of the differentiated L6 myoblasts with apiforol. The results indicated that the uptake of glucose analogue 2-NBDG in the cells was increased by 16.9 and 39 %, when treated with 5 μM and 10 μM concentrations of apiforol respectively (figure 2A.16). Rosiglitazone, standard drug used as positive control showed 38 % of glucose uptake at 100 nM under identical experimental condition. As can be seen, treatment of cells with apiforol induced the cellular uptake of 2-NBDG, indicating its potential in the management of diabetes.

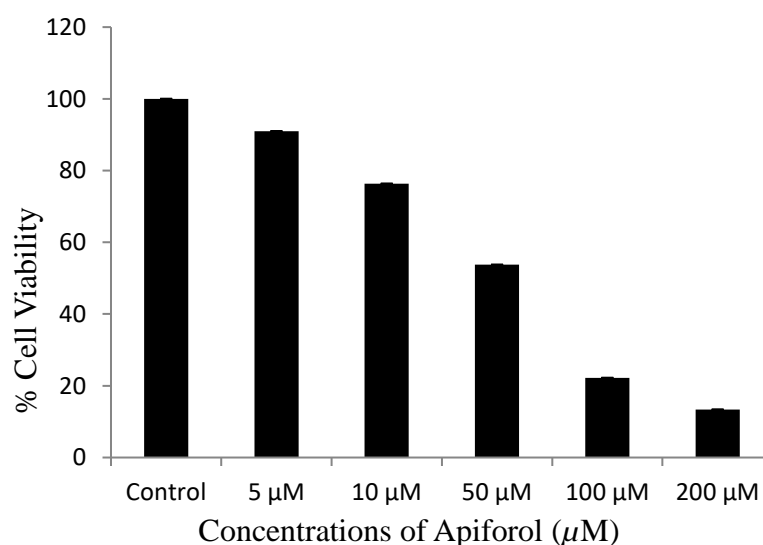


Figure 2A.15. Cell viability assay by MTT

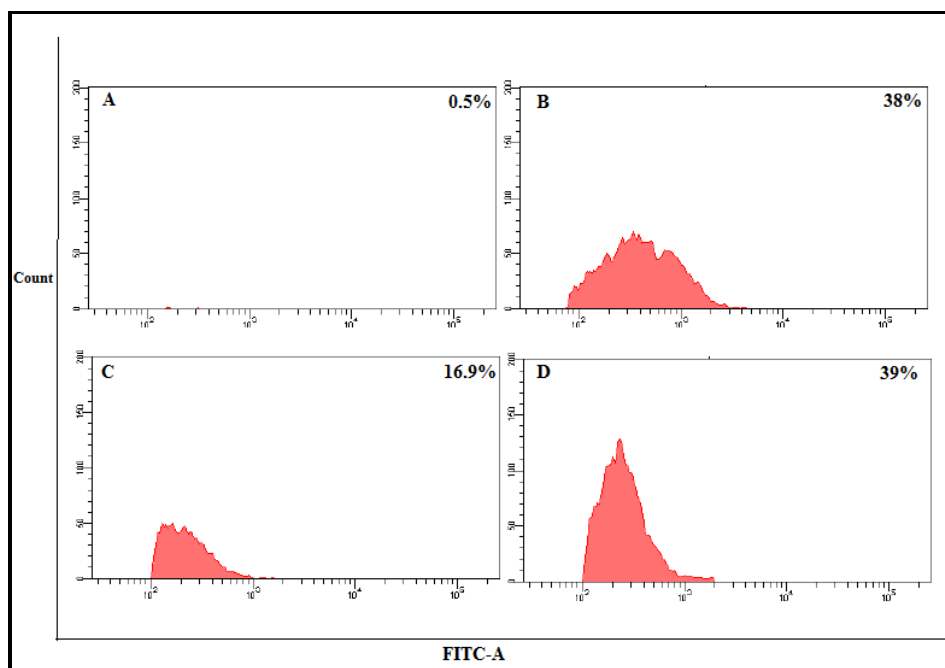


Figure 2A.16. Glucose transport in differentiated myotubes was assessed by the uptake of (A) control cells (B) 100 nM Rosiglitazone treated cells (C,D) 5 and 10 μ M of apiforol treated with cells.

2A.11. *In vitro* Antioxidant Studies

Antioxidants are vital substances which protect the body from the damage caused by free radical induced oxidative stress. Reactive oxygen species (ROS) are formed continuously in human body through usual metabolic actions and often have damaging effects on living cells such as proteins, lipids, nucleic acids or DNA. They also result in the development of several chronic diseases such as heart disease, ageing, cancer, immunosuppression, neurodegenerative *etc.* and the environmental pollutants such as cigarette smoke, automobile exhaust, radiation, and pesticides are also contributing to this. The epidemiological studies have specified that intake of more fruits and vegetables in diet can inhibit the damaging behaviour of free radicals in the human body and play an important role as a health protecting factor.⁶⁰ Therefore, the investigations of antioxidants are mainly focused on naturally occurring substances, especially the plant phytochemicals. In this point of view, a comparative study of the antioxidant potential of various extracts of *Musa balbisiana* seeds with that of the standard antioxidant reagents were also carried out. The results of our studies are given in table 2A.5.

Table 2A.5. IC₅₀ values of different extracts towards various radical generators

Extracts	IC ₅₀ values ($\mu\text{g/mL}$)		
	DPPH radical scavenging activity	ABTS radical scavenging activity	NO radical scavenging activity
Hexane	3.43 \pm 0.367	5.03 \pm 1.56	64.41 \pm 0.989
Acetone	<1	62.05 \pm 0.707	>500
Ethanol	<1	8.05 \pm 1.266	>500
Water	17.06 \pm 0.633	>500	364.89
Ascorbic acid	6.878 \pm 0.231	14.1254 \pm 0.461	-
Gallic acid	-	-	55.84 \pm 0.876

The IC₅₀ values (the concentration of the sample required to scavenge 50 % of free radicals) of each sample were calculated from the graph plotted with concentration of the samples against percentage inhibition of the free radical. The results indicate that, the hexane, acetone and ethanol extracts show higher radical scavenging activity than the water extracts and the values are much more promising than the standard drugs Ascorbic acid and Gallic acid. Inspired by these results, we also examined the antioxidant potential of apiforol (table 2A.6). The results showed that apiforol has higher DPPH, ABTS and NO radical scavenging activity than the standard drugs. These data support the fact that, *Musa balbisiana* seeds possess the potentialities of a natural antioxidant reagent and can be considered as a safe alternative to synthetic antioxidant drugs.

Table 2A.6. *In vitro* antioxidant potential of apiforol

Extracts	IC ₅₀ values (μM)		
	DPPH radical scavenging activity	ABTS radical scavenging activity	NO radical scavenging activity
Apiforol	5.62 \pm 0.112	64.48 \pm 0.31	303.93 \pm 0.751
Ascorbic acid	39.01 \pm 0.12	80.17 \pm 0.61	-
Gallic acid	-	-	320.0 \pm 0.27

2A.12. Conclusion

In conclusion, apiforol isolated from the acetone extracts of the seeds of *Musa balbisiana* can be considered as a potential antidiabetic agent as it exhibited a reduction in the postprandial hyperglycemia by inhibiting the digestive enzymes and enhancing the uptake of glucose by the cells. The molecular docking studies with α -glucosidase enzyme (3A4A) revealed that the enzymatic activity of α -glucosidase could be effectively blocked by apiforol. Apiforol also exhibited significant radical scavenging activities in the antioxidant studies. Further studies are on-going in our lab to establish the therapeutic safety and efficiency of apiforol. We hope, that apiforol, from the seeds of *Musa balbisiana* would be a promising phytochemical in the development of nutraceutical and functional food products.

2A.13. Experimental Section

Different analytical techniques were used for the characterisation of compounds. The IR spectra were measured with a Bruker FT-IR spectrometer. The nuclear magnetic resonance spectra (NMR) were recorded on a Bruker AMX 500 spectrophotometer. Chemical shifts for NMR spectra are reported as δ in units of parts per million (ppm) downfield from tetramethylsilane (δ 0.0) and relative to the signal of solvent. Mass spectra were recorded under EI/HRMS at 60,000 resolution using Thermo Scientific Exactive mass spectrometer. Specific rotation and UV spectra were recorded using Jasco P-2000 polarimeter and Shimadzu UV-1800 spectrophotometer respectively. Purity of the compound was checked using Hitachi L-2000 analytical HPLC.

2A.13.1. GCMS profiling

The GCMS phytochemical profiling of seed oil of *Musa balbisiana* was performed using GCMS-TQ8030 Shimadzu instrument. The hexane extract of seeds were dissolved in acetone and 1 μ L of sample was injected to a GC, equipped with a MS and a medium polar capillary column Rxi-5Sil MS (30 m x 0.25 mm I. D, 0.25 μ m). The oven program had an initial temperature of 60 °C for 2 min, which then increased to 200 °C for 2 min at the rate of 5 °C per minute, which then increased to 220 °C for 1min at the rate of 3 °C /min. Finally temperature was increased to 250 °C at the rate of 6 °C /min for 7min. The total run time was 50 min. The detector temperature and the injection temperature were 250 °C, and helium was the carrier gas with purity 99.999 % at a flow rate of 1 mL/ min. The sample was injected in the split less mode. The ion energy used for the electron impact ionization

(EI) mode was 70 eV. The mass m/z was scanned for a range of 100 - 1000. The essential chemical constituents were identified by matching mass spectra with spectra of reference compounds in mass spectral library of NIST and WILEY. The relative amounts of individual components were expressed as percentage peak areas relative to total peak area.

2A.13.2. α -Amylase inhibitory activity

The α -amylase inhibitory activity of the extracts were assayed according to a previous method based on the starch-iodine test.⁶¹ Starch containing α -amylase solution (1U mL⁻¹) along with different concentrations of the samples were incubated at 50 °C for 30 min. After incubation, the reaction was stopped with 1 M HCl and 100 μ L of iodine reagent was added to the reaction mixture. Enzymatic activity was quantified by measuring absorbance at 580 nm using Synergy 4 Biotek multimode reader. The IC₅₀ value was defined as the concentration of α -amylase inhibitor that inhibited 50 % of enzyme activity. Acarbose, the standard α -amylase inhibitor was used as a positive control. The percentage of inhibition was calculated using following equation,

$$\% \text{ of inhibition} = \frac{\text{Absorbance of control} - \text{Absorbance of sample}}{\text{Absorbance of control}} \times 100$$

2A.13.3. α -Glucosidase inhibitory activity

The α -glucosidase inhibitory activity was also determined using a previous method with slight modification.⁶² Different concentrations of samples containing α -glucosidase solution (1U mL⁻¹) were mixed and kept at room temperature for 5 min, after incubation 250 μ L of *p*-NPG was added and incubated at 37 °C for 20 min. The reaction was terminated by adding 500 μ L of 9.4 mM Na₂CO₃. The standard α -glucosidase inhibitor drug, acarbose was used as a positive control. Enzymatic activity was quantified by measuring absorbance at 405 nm using Synergy 4 Biotek multimode reader and the percentage inhibition was calculated using the same equation mentioned above.

2A.13.4. Antiglycation property

Antiglycation property was analysed as depicted in Arom method with slight modification.⁶³ In short, 1 mg/mL of bovine serum albumin was incubated with 200 mM of α -D-glucose along with different concentrations of the sample in 0.2 M potassium phosphate buffered saline at 60 °C for 24 h. The reaction was terminated by adding 100 % trichloro acetic acid (TCA) and kept at 4 °C for 10 min, and the fluorescence of the glycated end products was measured using excitation at 370 nm and emission at 440 nm using

Synergy 4 Biotek multimode reader. The advanced glycated end products formation are calculated using the following equation

$$\text{AGEs formation} = \frac{\text{Fluorescence of control} - \text{Fluorescence of sample}}{\text{Fluorescence of control}} \times 100$$

2A.13.5. Cell culture and treatment conditions

L6 myoblast cells were obtained from NCCS, Pune, India and were cultured in DMEM supplemented with 10 % FBS and 0.5 % antibiotic-antimycotic (penicillin-streptomycin-amphotericin B mix) solution at 37 °C, in a humidified atmosphere containing 5 % CO₂. Cells at above 80 % confluence were used for all the experiments.

2A.13.6. Cell viability assay

Cytotoxicity was determined using MTT assay.⁶⁴ Cultures were maintained at 37 °C in 5 % CO₂ incubator. The cells were trypsinized and seeded in 24 well plates (1x10⁴ cells per well). Cells after attaining above 80 % of confluency, were treated with different concentrations of the apiforol for 24 h. After the incubation, cells were treated with MTT reagent (0.5 g/L) for 4 h. Mitochondrial dehydrogenase enzyme is active only in live cells that reduce the yellow dye, MTT to purple formazan crystals. The formazan crystals were dissolved in 200 μL DMSO and the absorbance was read at 570 nm using Synergy 4 Biotek multimode reader. The untreated cells were used as a control and the percentage of cell viability was calculated as,

$$\% \text{ of cell viability} = \frac{\text{Absorbance of test}}{\text{Absorbance of control}} \times 100$$

2A.13.7. Glucose uptake assay

Glucose uptake assay was performed in differentiated L6 cell lines as described by Chen *et al* procedure.⁶⁵ Glucose uptake with 5 % fetal serum was used for differentiating the L6 cells. Differentiated L6 cells were pre-treated with different concentrations of samples for 24 h. The medium was removed, and the cells were washed twice with pre-cooled phosphate buffered saline (PBS). The cells were then treated with the fluorescent analogue of glucose; 2- NBDG and incubated for 30 min. The uptake of 2-NBDG by the cells was stopped by removing the incubation medium, and the cells were washed twice with pre-cold PBS. Cells were then trypsinized and subsequently re-suspended in 1 mL buffer. For each measurement, data from 10,000 single cell events were collected using Fluorescence Activated Cell Sorting (BD FACS Aria II, BD Bioscience, USA) and BD FACS Diva software. Rosiglitazone (100 nM) was used as positive control.

2A.13.8. Statistical analysis

The experimental results were expressed as mean \pm SD (standard deviation) of triplicate measurements. The data were subjected to one-way analysis of variance (ANOVA), and the significance of differences between means was calculated by Duncan's multiple range tests using SPSS for Windows, standard version 7.5.1, SPSS (SPSS Inc., USA) and the significance accepted at $p \leq 0.05$.

2A.14. *In vitro* Antioxidant Studies

2A.14.1. Evaluation of DPPH scavenging activity

The extract was added to methanolic solution of DPPH and the reaction mixture was kept at 25 °C for one hour in an incubator. The absorbance of the residual DPPH solution was determined at 517 nm in a UV-Visible Spectrophotometer. The experiment was performed in triplicate. Vitamin C was used as positive control. The inhibition was calculated in following formula,

$$I (\%) = 100 \times (A_0 - A_1) / A_0$$

where A_0 is the absorbance of the control, A_1 is the absorbance of the extract/standard/compound, respectively. A percent inhibition versus concentration curve was plotted and the concentration of sample required for 50 % inhibition was determined and expressed as IC_{50} value. The lower the IC_{50} value indicates high antioxidant capacity.⁶⁰

2A.14.2. Evaluation of ABTS scavenging activity

The ABTS radical cation preparation: 2 mM solution of ABTS and 70 mM Potassium persulphate were prepared in distilled water. 200 μ L of potassium persulphate and 50 mL of ABTS were mixed and used after 2 hrs for the assay. To the various concentrations of extracts/standard/compound, 0.3 mL of ABTS radical cation and 1.7 mL of phosphate buffer pH 7.4 was added and the absorbance was measured at 734 nm. Vitamin C was used as positive control. The experiment was performed in triplicate. The inhibition was calculated in following way,

$$I (\%) = 100 \times (A_0 - A_1) / A_0$$

where A_0 is the absorbance of the control, A_1 is the absorbance of the extract/standard. A percent inhibition versus concentration curve was plotted and the concentration of sample required for 50 % inhibition was determined and expressed as IC_{50} value. The lower the IC_{50} value indicates high antioxidant capacity.⁶⁰

2A.14.3. Evaluation of NO scavenging activity

NO was generated from sodium nitroprusside and measured by the Greiss reaction. The sodium nitroprusside in aqueous solution at physiological pH spontaneously generates NO, which interacts with oxygen to produce nitrite ions that can be estimated by use of Greiss reagent. Sodium nitroprusside (5 mM) in phosphate-buffered saline was mixed with different concentrations of the extracts/drug/compound dissolved in suitable solvent systems and incubated at 25 °C for 150 minutes. The samples were then reacted with Greiss reagent (1 % sulfanilamide, 2 % H₃PO₄, and 0.1 % naphthylethylenediamine dihydrochloride). The absorbance of the chromophore formed during the diazotization of nitrite with sulfanilamide and its subsequent coupling with naphthylethylenediamine was read at 546 nm, relative to the absorbance of standard solutions of potassium nitrite treated in the same way with Greiss reagent. The percentage nitrite radical scavenging activity of the extracts and gallic (standard) acid were calculated using the following formula,

$$\text{nitric oxide scavenged (\%)} = (A_{\text{control}} - A_{\text{test}}) / A_{\text{control}} \times 100$$

where, A_{control} = absorbance of control sample and A_{test} = absorbance in the presence of the samples of extracts or standards.⁶⁶

2A.15. Spectral Data

Compound 1 (β - sitosterol)

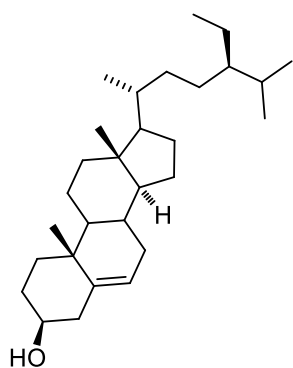
From fraction pool 2, we obtained a mixture of β - sitosterol and stigmasterol which showed blue intense spot while charring the TLC in Mc Gill solution. The fraction on column chromatography in silica gel yielded colorless needle shaped crystals. From spectroscopic analysis the compound was identified as β - sitosterol. Signals at 5.37 ppm in ¹H NMR and 121.7 ppm in ¹³C NMR indicated the presence of olefinic proton. The proton at position 3 resonated as a multiplet between δ 3.53-3.54 ppm, and it is one of the characteristic peaks. DEPT experiment reveals that the compound contains eleven -CH₂- and six -CH₃ groups. The mass spectra showed molecular ion peak at 415.1097 (M+H)⁺.

Molecular formula : C₂₉H₅₀O

Mp : 128-130 °C

FT-IR (Neat) ν_{max} : 3408, 2935, 2863, 1459, 1374, 1316, 1257, 1190, 1099, 1054, 1024, 958, 802 cm⁻¹.

¹H NMR (500 MHz, CDCl₃, TMS) : δ 5.37 (d, J = 5 Hz, 1H), 3.53-3.54 (m, 1H), 2.30-2.29 (m, 2H), 2.04-1.87 (m, 2H), 1.87-1.84 (m, 3H), 1.68-1.66 (m, 2H), 1.60-1.45 (m, 7H), 1.32-1.23 (m,



6H), 1.20-1.10 (m, 3H), 1.09-1.96 (m, 3H), 1.02 (s, 5H), 0.94-0.93 (m, 3H), 0.87-0.71 (m, 9H), 0.69 (s, 3H) ppm.

¹³C NMR (125 MHz, CDCl₃, TMS) : δ 140.8, 121.7, 71.8, 56.8, 56.0, 50.1, 45.8, 42.3, 42.3, 39.8, 37.2, 36.5, 36.2, 33.9, 31.9, 31.7, 29.1, 28.3, 26.0, 24.3, 23.0, 21.1, 19.8, 19.4, 19.0, 18.8, 11.9, 11.9 ppm.

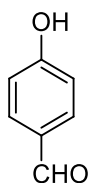
HRMS (ESI) : *m/z* Calcd for C₂₉H₅₁O : 415.3997; Found 415.3940.

Compound 2 (4-formylphenol)

On column chromatography with silica gel, the fraction pool 3 yielded an off-white colored solid in 4 mg. In the proton NMR, the molecule showed two doublets in the aromatic region along with an aldehyde peak. Further characterization of this compound showed that it is 4-hydroxybenzaldehyde (4-formylphenol).

Molecular formula : C₇H₆O₂

Mp : 128-130 °C



FT-IR (Neat) *v*_{max} : 2945, 2863, 1645, 1459, 1264, 1316, 902 cm⁻¹.

¹H NMR (500 MHz, CDCl₃, TMS) : δ 9.8 (s, 1H), 7.79 (d, *J* = 8.5 Hz, 2H), 6.96 (d, *J* = 8.5 Hz, 2H) ppm.

¹³C NMR (125 MHz, CDCl₃, TMS) : δ 191.3, 158.1, 32.0, 116.7, ppm.

HRMS (ESI) : *m/z* Calcd for C₇H₇O₂ : 122.0367; Found 121.0289.

Compound 3 (β-sitosterol-*D*-glucoside)

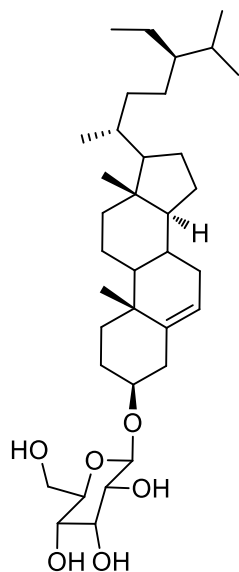
Compound 1 was isolated from fraction pool 7 in 60 mg as colourless solid. The structural characterization of this molecule showed that it is β-sitosterol-*D*-glucoside.

Molecular formula : C₃₅H₆₀O₆

Mp : 128-130 °C

FT-IR (Neat) *v*_{max} : 3409, 3266, 2995, 2863, 1257, 1190, 1090, 1054, 1029, 968, 844 cm⁻¹.

¹H NMR (500 MHz, DMSO-*d*₆, TMS) : δ 5.34 (d, *J* = 5 Hz, 1H), 4.88 (m, 3H), 4.44(m, 1H), 4.23 (d, *J* = 8 Hz, 1H), 3.65 (m, 1H), 3.46 (m, *J* = 8 Hz, 1H), 3.13 (m, 1H), 3.08 (m, 1H), 3.02 (m, 1H), 2.89 (m, 1H), 2.36 (m, 1H), 2.13 (m, 1H), 1.94 (m, 2H), 1.80 (m,



3H), 1.64 (m, 1H), 1.51-1.40 (m, 6H), 1.28-1.23 (m, 6H), 1.16 (m, 4H), 0.96 (s, 3H), 0.91 (s, 5H), 0.82 (m, 9H), 0.66 (s, 3H) ppm.

¹³C NMR (125 MHz, DMSO-d₆, TMS) : δ 140.4, 121.2, 100.7, 99.5, 76.9, 76.7, 73.4, 70.1, 61.1, 56.1, 55.4, 49.6, 45.1, 41.8, 38.3, 36.8, 36.2, 35.4, 33.3, 31.4, 31.3, 29.2, 28.7, 27.8, 25.4, 23.8, 22.6, 20.6, 19.7, 19.1, 18.9, 18.6, 11.8, 11.6 ppm.

HRMS (ESI): *m/z*. Calcd for C₃₅H₆₁O₆: 577.4468; Found 577.4013.

2A.16. References

1. C. Gupta and D. Prakash, *J. Complement Integr. Med.*, **2014**, 11(3), 151-169.
2. C. Gupta, D. Prakash and S. Gupta, *Relationships between bioactive food components and their health benefits*, **2013**, DM. Martirosyan (ed.), Introduction to functional food science textbook, 1st ed. USA: Create Space Independent Publishing platform, pp 66-85.
3. D. Bagchi D, *Toxicol.*, **2006**, 221, 1-3.
4. M. M. Berger and M. Shenkin, *Nutrition*, **2006**, 22, 952-955.
5. C. S. Ramaa, A. R. Shirode, A. S. Mundada and V. J. Kadam, *Curr. Pharm. Biotechnol.*, **2006**, 7, 15-23.
6. M. Z. Imam and S. Akter, *Journal of Applied Pharmaceutical Science*, **2011**, 1(5), 14-20.
7. S. Kumar, C.K. Mishra, A. Ahuja, A. Rani and R.K. Nema, *Asian Journal of Biochemical and Pharmaceutical Research*, **2012**, 2(4), 199-206.
8. K. P. Sampath Kumar, B. Debjit, S. Duraiavel, and M. Umadevi, *J. Pharmacogn. Phytochem.*, **2012**, 1(3), 51-63.
9. K. Lavanya, A. Beaulah, and G. Vani, *wjpmr*, **2016**, 2(6), 163-173.
10. D. Swathi, B. Jyothi and C. A. Sravanthi, *Int. j. innov. pharm. sci. res.*, **2011**, 2(2), 122-125.
11. V. Sumathy, S. Jothy Lachumy, Z. Zuraini, S. Sasidharan, *Pharmacologyonline*, **2011**, 2, 118-127.
12. P. E. Sreejith and M. Sabu, *Edible bananas of south India, Taxonomy and Phytochemistry*. **2017**, India association of Angiosperm Taxonomy, Calicut University, Kerala-673 635, India, ISBN 81-901637-4-4.
13. R. V. Valmayor, S. H. Jamluddin, B. Silayoi, S. Kusumo, L. D. Danh, O. C. Pascua and R. R. C. Espino, *Banana Cultivar Names and Synonyms in Steast Asia*. **2000**, Internationsl Network for the Improvmentation of Banana and Plantain, Asia and Pacific Office, Los Banos, Laguna, Philippines.
14. N. W. Simmonds and K. Shepherd, **1955**. *J. Linn. Soc. London (Botany)*, **1995**, 55, 302-312.
15. R. R. C. Wspino, S. H. Jamaluddin, B. Silayoi, and R. E. Nasution,. *Musa L. (edible cultivars) Pant resources of Southeast Asia No 2*, **1992**, Edible fruits and Nuts. Prosea, Bogor, Indonesia.

16. G. M. Robinson, *J. Chem. Soc.*, **1937**, 3, 1157-1160.
17. J. S. Chadha, and T. R. Seshadri, *CWT.Sci.*, 1962, *31*, 233-235.
18. T. P. Waalkes, A. Sjoerdsma, C. R. Creveling, H. Weissbach and S. Udenfriend, *Science*, **1958**, *127*(3299), 648-650.
19. G. Vettorazz, *Food Cosmet. Toxicol.*, **1974**, *12*, 107-113.
20. K. G. Shanmugavelu and G. Rangaswami, *Nature*, **1962**, *194*, 775-776.
21. A. O. Ketiku, *J. Sci. Food Agr.*, **1973**, *24*(6), 703-707.
22. S. Ghosal, *Phytochemistry*, **1985**, *24*(8), 1807-1810.
23. M. Ali, *Phytochemistry*, **1992**, *31*(6), 2173-2175.
24. G. L. Javier, E. Fernando, Q. Winston, B. Ivan, L. Matias, T. Fernando, C. Gloria, A. Zahira, P. Carlos and R. Mauricio, *J. Org. Chem.*, **1993**, *58*(16), 4306-4308.
25. T. Kamo, N. Kato, N. Hirai, M. Tsuda, D. Fujioka and H. Ohigashi, *Biosci. Biotechnol. Biochem.*, **1998**, *62*(1), 95-101.
26. T. Kamo, N. Kato, N. Hirai, M. Tsuda, D. Fujioka and H. Ohigashi, *Phytochemistry*, **1998**, *49* (6), 1617-1621.
27. O. I. Felipe, G. Helmar, H. Dirk, S. Bettina, E. Fernando, Q. Winston, and S. Bernd, *Phytochemistry*, **2002**, *60*(1), 61-66.
28. J. C. del Rio, I. M. Rodriguez and A. Gutierrez, *Rapid Commun. Mass Spectrum*, **2004**, *18*, 2691-2696
29. J. C. del Rio, J. Jimenez-Barbero, I. C. Maria, M. Polito and G. Ana, *J. Agric. Food Chem.*, **2006**, *54*(23), 8744-8748.
30. K. Jitsaeng, C. Paetz and B. Schneider, *Rec. Nat. Prod.*, **2010**, *4*(1), 26-30.
31. P. Pothavorn, K. Kitdamrongsont, S. Swangpol, S. Wongniam, K. Atawongsa, J. Svasti and J. Somana, *J. Agric. Food Chem.*, **2010**, *58*, 8782-8787.
32. C. A. Cruz-Cruz, G. Ramírez-Tec, K. García-Sosa, F. Escalante-Erosa, L. Hill, A. E. Osbourn and L. M. Peña-Rodríguez, *Eur. J. Plant Pathol.*, **2010**, *126*, 459-463.
33. M. D. Swanson, H. C. Winter, I. J. Goldstein and D. M. Markovitz, *J. Biol. Chem.*, **2010**, *12*, 8646-8655.
34. F. Liu, Y. Zhang, S. Qian-Yun, Y. Fu-Mei, W. Gu, J. Yang, N. Hong-Mei, W. Yue-Hu and L. Chun-Lin, *Phytochemistry*, **2014**, *103*, 171-177.
35. B. Kongkona, S. K. Borthakur and T. Bhaben, *Journal of Traditional Knowledge*, **2016**, *15*(1), 116-120.
36. K. Himadri, C. Dulal, D. Meetali, H. Ankita, S. Rahul, K. Sima , K. Raghuram, K. Jibon, and R. Devi, *Front Pharmacol.*, **2016**, *7*(102), 1-11.

37. Association of Official Analytical Chemistry (AOAC). Official Methods of Analysis, 15th ed.; Association of Official Analytical Chemists: Gaithersburg, MD, USA, **1990**.
38. A. R. Saltiel and C. R. Kahn, *Nature*, **2001**, *414*, 799-806.
39. P. Zimmet, K. G. M. M. Alberti, and J. Shaw, *Nature*, **2002**, *414*, 782-787.
40. Global report on diabetes, World Health Organisation. April 2016. http://apps.who.int/iris/bitstream/10665/204871/1/9789241565257_eng.pdf
41. B. K. Tripathi and A. K. Srivastava, *Med. Sci. Monit.*, **2006**, *12*, RA130-RA147.
42. M. Bodmer, C. Meier, S. Krähenbühl, S. S. Jick and C. R. Meier, *Diabetes Care*, **2008**, *31*(11), 2086-2091.
43. C. Liang, S. Peng, W. Ting, C. Kaixian, J. Qi, W. Heyao, L. Yiming, *J. Agric. Food Chem.*, **2012**, *60*, 9144-9150.
44. A. E. Patricia, M. M. Gabriela, P. M. Pedro, G. Carmen and P. B. Ana de la Rosa, *J. Agric. Food Chem.*, **2014**, *62*, 427-433.
45. Y. Yang, Y. Xiushi, T. Jing, L. Changyou, C. Xuzhen and R. Guixing, *J. Agric. Food Chem.*, **2013**, *61*, 8104–8109
46. K. B. Arun, T. Sithara, T. R. Reshmitha, G. C. Akhil and P. Nisha, *J. Funct. Foods.*, **2017**, *31*, 198-207.
47. S. Thomas, B. P. Dhanya, K. B. Arun, S. Suresh, M. Dan, K. V. Radhakrishnan and P. Nisha, *J. Agric. Food Chem.*, **2018**, *66* (3), 602-612.
48. P. S. Johnston, H. E. Lebovitz, R. F. Coniff, D. C. Simonson, P. Raskin and C. L. Munera, *J. Clin. Endocrinol. Metab.*, **1998**, *83*, 1915-1922.
49. S. Hua, W. Dong, S. Xiaotong, Z. Yazhou, D. Weina, P. Xiaolin, Z. Xiaoting, L. Yashan, M. Ying, W. Runling and Y. Peng, *J. Agric. Food Chem.*, **2017**, *65*, 1574-1581
50. R. Roman-Ramos, J. L. Flores-Saenz and F. J. Alarcon-Aguilar, *J. Ethnopharmacol.*, **1995**, *48*(1), 25-32.
51. D. K. Patel, S. K. Prasad, R. Kumar and S. Hemalatha, *Asian Pac. J. Trop. Biomed.*, **2012**, *2*(4), 320-330
52. M. Fried, S. Abramson and J. H. Meyer, *Dig. Dis. Sci.*, **1987**, *32*(10), 1097-1103.
53. P. Agaewal and R. Gupta, *Research and Reviews Journal of Medical and Health Sciences*, **2016**, *5*(4), 1-8.
54. C. Schutt and D. Netzly, *Journal of Chemical Ecology*, **1991**, *17*(11), 2261-2262.
55. W. Hui, D. Yang-Ji, and S. Hua-Can, *Food Chem.*, **2010**, *123*, 6-13.

56. T. Kenjoro, M. Yuji, T. Kouta, and M. Tomoko, *J. Nutr. Sci. Vitaminol.*, **2006**, *52*, 149-153.
57. Y. Sakina, D. Natalia, B. Frédéric, H. Max, C. Yves and L-M. Dominique, *S. Afr. J. Bot.*, **2013**, *84*, 124-127.
58. QikProp 3.5; Schroëdinger, L.L.C.: New York, NY, **2012**.
59. Schroëdinger User Manuals, Glide 5.8; Schroëdinger, L.L.C.: New York, NY, **2012**.
60. M. Raghavendra, A. M. Reddy, P. R. Yadav, A. S. Raju and L. Siva Kumar, *Asian J. Pharm. Clin. Res.*, **2013**, *6*(3), 96-99.
61. Z. Xio, R. Storms and A. A. Tsang, *Anal. Biochem.*, **2006**, *351*(1), 146-148.
62. S. Adisakwattana, O. Lerdsuwankij, U. Poputtachai, A. Minipun and C. Suparpprom, *Plant Foods Hum. Nutr.*, **2001**, *66*(2), 143-148.
63. A. Jedsadayamata, *Naresun University Journal*, **2005**, *13*(2), 35-41.
64. T. Mosmann, *J. Immunol. Methods*, **1983**, *65*(1), 55-63.
65. Q. C. Chen, W. Y. Zhang, W. Jin, L. S. Lee, B. S. Min, H. J. Jung, M. Na, S. Lee and K Bae, *Planta Medica*, **2010**, *76*(1), 79-81.
66. G. C. Jagetia and M. S. Baliga, *J. Med. Food*, **2004**, *7*(3), 343-348.

**Part B: Isolation of Phytoalexins from Rhizome and Fruit Peels of
Musa balbisiana Colla.**

2B.1. Introduction

Within the field of organic chemistry, the definition of natural product is usually restricted to purified organic compounds isolated from natural sources, that are produced by the pathways of primary or secondary metabolism, whereas, in medicinal chemistry, the definition is often further restricted to secondary metabolites. Secondary metabolites are not essential for survival, but provide evolutionary advantages to the organism. Many secondary metabolites are cytotoxic, and have been selected and optimized through evolution for use as "chemical warfare" agents against prey, predators, and competing organisms. Among these, the phytoalexins are a group of natural compounds defined by their physiological features rather than their structural frameworks. These compounds are synthesized *de novo* by some plant organs when they are provoked by physical, microbiological, or chemical agents.^{1,2} They are usually detected when the plant parts are infected with some microorganisms. As mentioned in Part A, India is a treasure trove of biodiversity that hosts a large variety of plants and animals. It is one of the major centres of origin and distribution of both wild and cultivated bananas, especially *Musa balbisiana*-derived hybrids. Due to the antiquity of bananas in India, their great diversity and the long history of domestication are often interwoven with national heritage and culture and have great socio-economic significance.

Phenylphenalenones represent the class of compounds/phytoalexins isolated from the Musaceae (genus *Musa* and *Ensete*), Haemodoraceae and Strelitziaceae families. Modified phenylphenalenones are also found to be present in Pontederiaceae species.^{3,4} Hence in the present study, we are disclosing our efforts of identifying the phytoalexins that are present in the rhizomes and the fruit peels of *Musa balbisiana*.

2B.2. Aim and Scope of the Present Study

Phytoalexins are antibiotic compounds produced by plants, and these secondary metabolites are part of the complex defense mechanisms of plants against pathogenic microorganisms. Thus, a comprehensive analysis of phytoalexin production and biogenesis regulation could contribute to the design of plants and pesticides possessing enhanced

resistance against pests. Therefore it is relevant in the present scenario to carry out the phytochemical investigation of various parts of *Musa balbisiana* Colla. So as a part of this research, we carried out a detailed phytochemical analysis of secondary metabolites, especially phytoalexins, from different parts of *Musa balbisiana*, one of the phytochemically less explored species.

2B.3. Isolation and Characterization of Compounds from the Rhizome of *Musa balbisiana* Colla.

Bananas are one of the most popular fruits in the world market. It is well known that their fruits contain various antioxidants, such as vitamin C, vitamin E, and flavonoids. But the phytoalexins are generally synthesized by the rhizomes and leaves *in situ*.⁵ In the present study, healthy rhizomes of *M. balbisiana* from the Botanical Garden of University of Calicut (voucher No. 116142 at Calicut university herbarium) were subjected to phytochemical analysis.

2B.3.1. Extraction

Freshly collected rhizomes of *Musa balbisiana* (8 kg) were washed, chopped, dried (1.15 kg), then crushed to powder and subjected to extraction with various organic solvents in the order of increasing polarity. Around 1.1 kg of rhizome was first soaked in 5 L hexane at room temperature for three days, and the solvent was then removed under reduced pressure to obtain the crude extract. The same procedure was repeated thrice, and we obtained around 5.1 g of crude hexane extract. The residue was further subjected to acetone extraction, which gave 18.5 g acetone extract. In the same way, we obtained 4 g of methanol extract and finally the water extract.

2B.3.2. Isolation and characterization of compounds

After studying the TLC, around 17.8 g of acetone extract was subjected to column chromatography on 100-200 mesh sized silica gel. Initially, the column was eluted with hexane-ethyl acetate mixtures of increasing polarities and the final elution was carried out using 10 % methanol in ethyl acetate. A total of 81 fractions of approximately 250 mL each were collected, and according to the similarity in TLC they were pooled into 13 major fraction pools. This on further purification resulted in the isolation of compounds **1, 3 & 5-10**. A pictorial representation of the entire isolation procedure is given below (figure 2B.1).

From fraction pools 1-2, we could isolate a mixture of β - sitosterol (compound **1**) and stigma sterol as a white solid substance of 80 mg weight. The fraction pools 4-5 were first subjected to column chromatography on silica gel, followed by Sephadex-LH 20 column

in hexane-diethyl ether mixture. This yielded three compounds, *ie.* **5**, **6** and **7**. Compounds **8** and **9** were isolated from fraction pools 6-7 by the same procedure; however methanol was used as the eluent for the Sephadex column. From the fraction pool eight, the compound **10** was isolated by column chromatography on silica gel. Finally 60 mg of compound **3** was isolated from ninth fraction pool by column chromatography on silica gel.

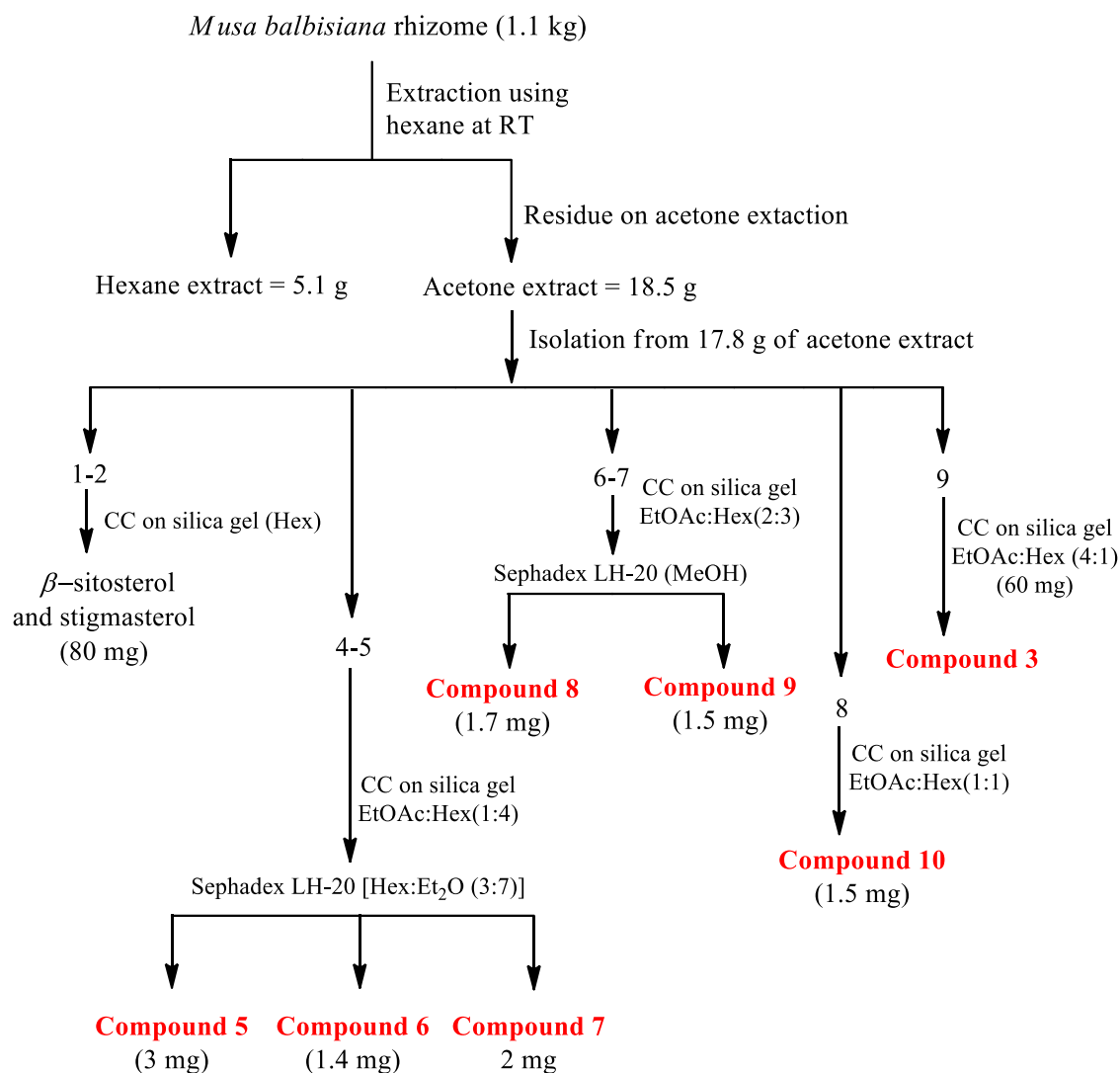


Figure 2B.1. A pictorial representation of isolation procedure

As we studied the fresh and healthy rhizomes of *Musa balbisiana*, most of the compounds or the phytoalexins (which are produced *de novo* due to external attack) were obtained only in a few milligram. It was challenging to carry out all the spectroscopic analysis for the characterization of molecules, hence in many cases, we relied heavily on the literature reports. Also, for the clarity of the peaks, the proton and carbon NMR spectra of some compounds were recorded in different solvents.

Several compounds with a phenalenone nucleus have been reported as usual metabolites/phytoalexins in plants and microorganisms. The phenalenones isolated from plant until now possess a side phenyl ring typically on C-9 or C-4, positions and have been found in species of the Musaceae and Haemodoraceae families. Also these isomers can be easily identified from the resonance field of C-9 hydrogen. The studies on phenylphenalenones show that phenalenones with a hydrogen atom at the 9th position generally show resonance at a higher downfield region of δ 8.5 ppm or more, whereas C-9 phenyl substituted systems always shows a value of δ <8.5 ppm. Also, C-9 systems often forms $(M+H-H_2O)^+$ peaks in the ESI-MS spectrometry (figure 2B.2).⁶

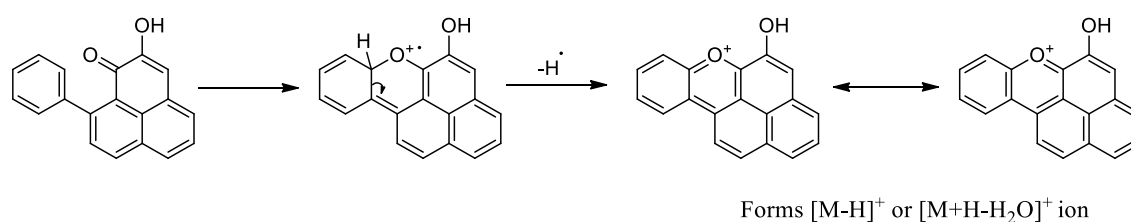
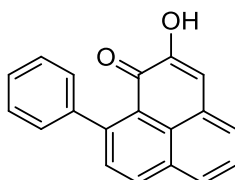


Figure 2B.2. Formation of $(M+H-H_2O)^+$ or $(M-H)^+$ peaks in the ESI-MS

Three compounds were isolated from the fraction pools 4-5. The portion of the fraction eluted with 20 % ethyl acetate in hexane was further subjected to Sephadex LH-20 column, where 30 % of hexane in diethyl ether resulted in the separation of compounds **5** (3 mg), **6** (1.4 mg) and **7** (2 mg).

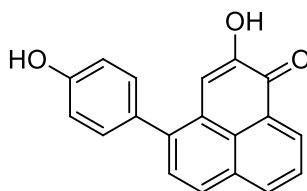
Compound **5** was obtained as a UV active bright orange colored crystalline powder with a melting point of 124-126 °C. In the UV spectroscopy analysis, the compound showed a λ_{max} at 367.12 nm. Two peaks at ν_{max} 3348 and 1657 cm^{-1} in IR spectrum clearly indicate the presence of hydroxyl as well as carbonyl groups in the molecule. In the proton NMR (figure 2B.3), peaks resonated in between δ 8.3-7.0 ppm, corresponding to twelve protons could be attributed to the aromatic protons. Also, the peak that resonated at δ 7.03 ppm, which does not possess any relation with carbon atoms in the HMQC analysis, clearly indicates the presence of an exchangeable hydrogen atom. The peak resonating at δ 180.3 ppm in the carbon NMR (figure 2B.4) obviously indicates that the compound contains one carbonyl group. Though, the proton NMR undoubtedly gives a phenylphenalenone structure, the position of the phenyl ring (either 4 or 9) was confirmed by the shifts in the proton signal values. In our compound, no proton resonated at fields lower (higher downfield) than δ 8.30 ppm, whereas phenalenones with a hydrogen atom at the 9-position generally show resonance at δ 8.5 or more. This difference in the signals indicates the absence of a proton at the ninth position. Also, the mass spectrum of the compound showed

a molecular ion peak at m/z 273.0909, which is the $[M+H]^+$ peak. While the $[M+H-H_2O]^+$ peak obtained at 255.0808 indicates the presence of 9-phenyl substituted phenalenones.⁶ From all the above spectral details and on comparison with the literature reports, the compound was confirmed as **anigorufone** (2-hydroxy-9-phenyl-1H-phenalen-1-one).⁷ It is the simplest of the natural phenalenone pigments now known. The structure of the compound is shown below.



Anigorufone
Compound **5**

Compound **6**, a deep orange-red in colored compound was also isolated from fraction pools 4-5. The molecule was highly UV active (λ_{max} at 367.12 nm) and was solid in nature. The sharp peak at ν_{max} 1634 cm^{-1} is presumed to be an α,β -unsaturated carbonyl system. The molecule also showed a molecular ion peak at 289.0864 corresponding to $[M+H]^+$ peak. Also, the absence of the $[M+H-H_2O]^+$ peak and the doublet at δ 8.58 ppm (C-9 proton) indicate the presence of C-4 phenyl substitution, rather than C-9 phenyl substitution (figure 2B.5). In the proton NMR, the peaks showed a slight difference from that compound **5**. The two doublets at δ 7.27 and 6.93 ppm corresponds to two protons each, displaying the presence of a *para* substituted benzene ring. Also, in the carbon NMR, the peak at δ 179.1 ppm is attributed to a carbonyl carbon (figure 2B.6). From all the spectral analysis and literature reports,² the structure of compound **6** was deduced as, **irenolone** (2-hydroxy-4-(4-hydroxyphenyl)-1H-phenalen-1-one), a phenylphenalenone system, with a hydroxyl group at C-4 position of the phenyl ring as shown in the figure given below.



Irenolone
Compound **6**

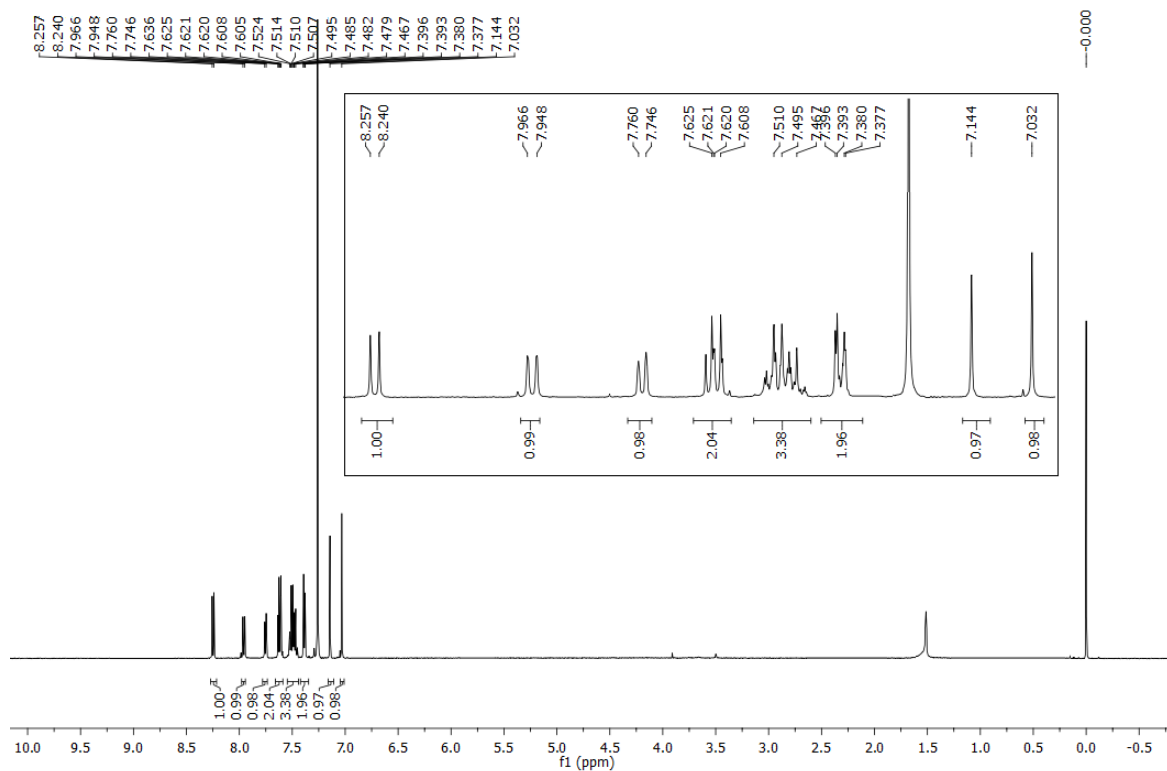


Figure 2B.3. ^1H NMR of compound **5** in CDCl_3

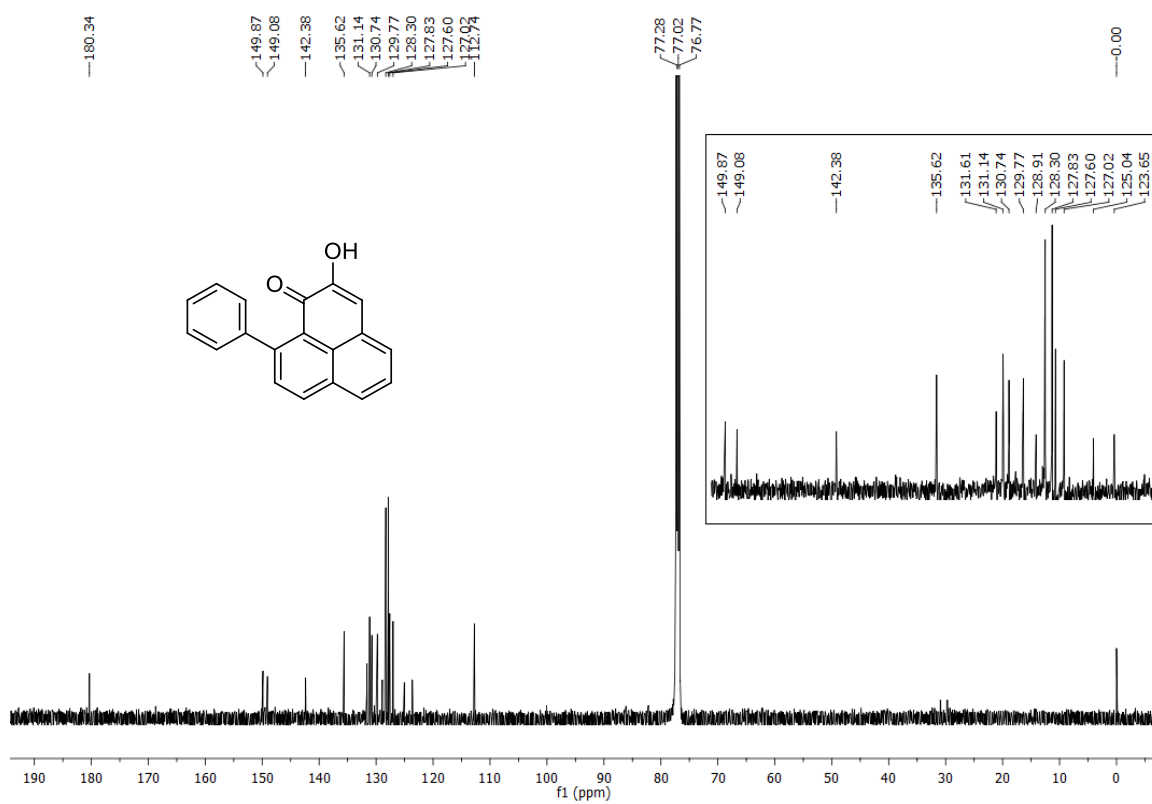


Figure 2B.4. ^{13}C NMR of compound **5** in CDCl_3

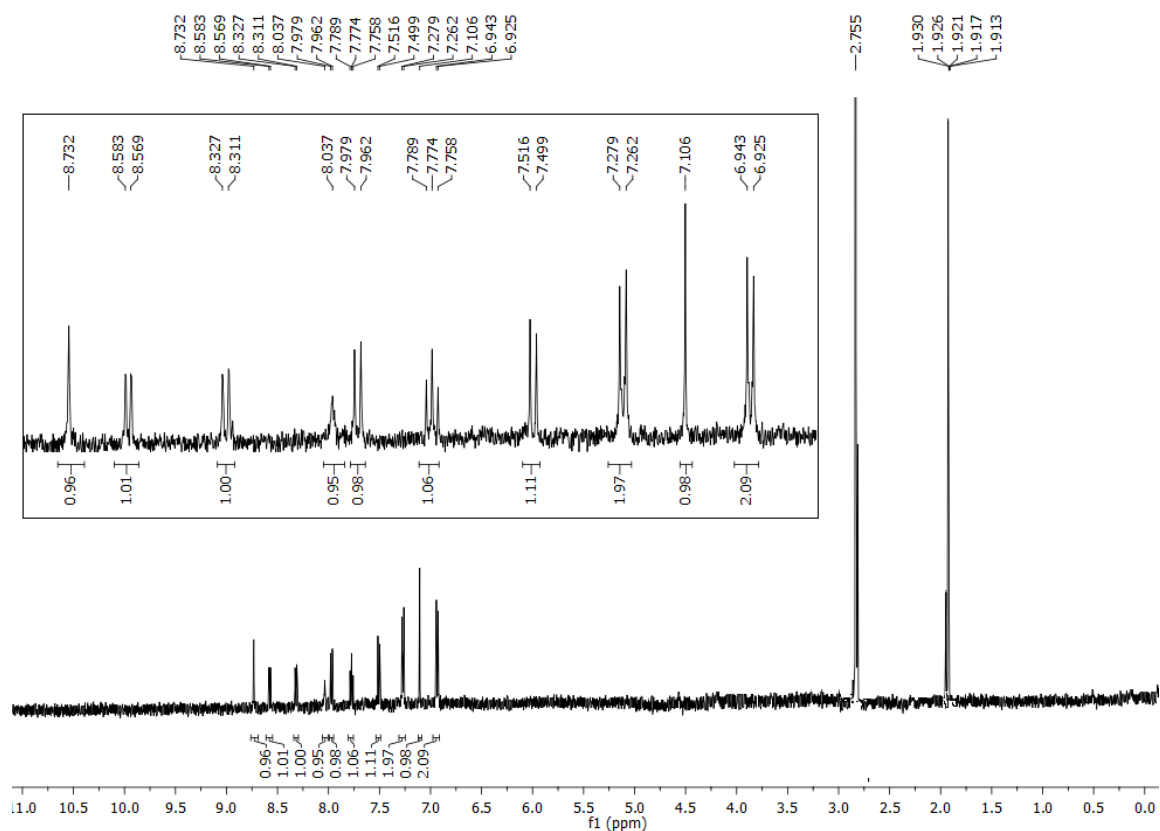


Figure 2B.5. ^1H NMR of compound **6** in CD_3COCD_3

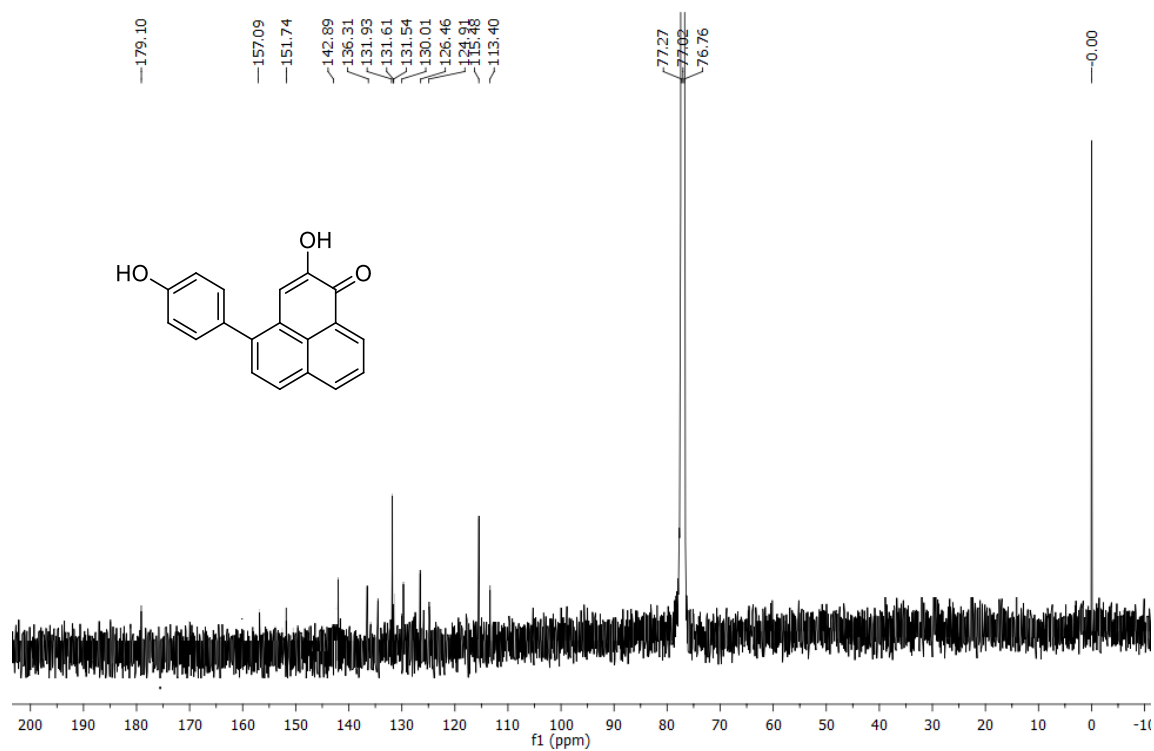
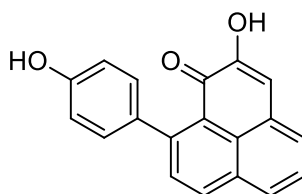


Figure 2B.6. ^{13}C NMR of compound **6** in CDCl_3

The third molecule, isolated from fraction pools 4-5, showed almost same characteristics to that of compound **5**. It was isolated as deep red UV active (λ_{\max} at 372.12 nm) crystalline solid and showed a melting point of 239-241 °C. In the HRMS analysis, the molecule gave a m/z value of 289.0859 corresponding to $[M+H]^+$ peak. The peak at 271.0754 in HRMS indicates $[M+H-H_2O]^+$ that the molecule possess the phenyl ring at ninth position. Also, in the IR spectrum, the peaks at ν_{\max} 3440 and 1640 cm^{-1} presumed to be a hydroxyl group as well as a α,β -unsaturated carbonyl system. Twelve protons were present in the proton NMR, and the peaks resonated at δ 7.29 and 6.93 ppm as two doublets indicates the presence of a *para* substituted benzene ring (figure 2B.7). Also, the carbon resonating at δ 180.7 ppm, clearly indicates the presence of a carbonyl group (figure 2B.8). Hence on comparing the structures of compounds **5** and **6**, and also the literature reports,⁸ the compound **7** was confirmed to be **4'-hydroxyanigorufone/emamolone** (2-hydroxy-9-(4'-hydroxyphenyl)-1H-phenalen-1-on). The structure of the same is given below.



Emamolone
Compound **7**

From the fraction pools 6-7, two compounds namely compound **8** (1.7 mg) and **9** (1.5 mg) were isolated *via* column chromatography initially on silica gel followed by Sephadex LH-20. For the complete structure elucidation of compound **8**, the molecular weight was determined by ESI-MS (m/z 597.1315 $[M+Na]^+$), which suggested a dimeric phenalenone structure. The signals from the aromatic rings were easily assigned by the same strategy, used for the above compounds. It was isolated as a yellow UV active solid with a λ_{\max} of 368.12 nm in dichloromethane. In the IR spectra, the peaks at ν_{\max} 3442, 2918, 1703 and 1496 indicate the presence of hydroxyl as well as carbonyl groups. In the proton NMR the singlet at δ 4.19 ppm, integrating two protons, having significant upfield shift indicate the presence of aliphatic methine protons (figure 2B.9). Also, the splitting pattern of aromatic protons highly resembled with that of anigorufone and the ^1H - ^1H COSY correlation of protons at positions δ 7.42 and δ 8.16 ppm as well as δ 7.03 and δ 7.83 ppm were in good agreement with that of reported values of **anigorootin** (6a,13a-dihydroxy-1,8-diphenyl-13a,13a,1-dihydronaphtho[8,1,2-hij]naphtha [8',1',2': 7,8,1]).^{9,10}

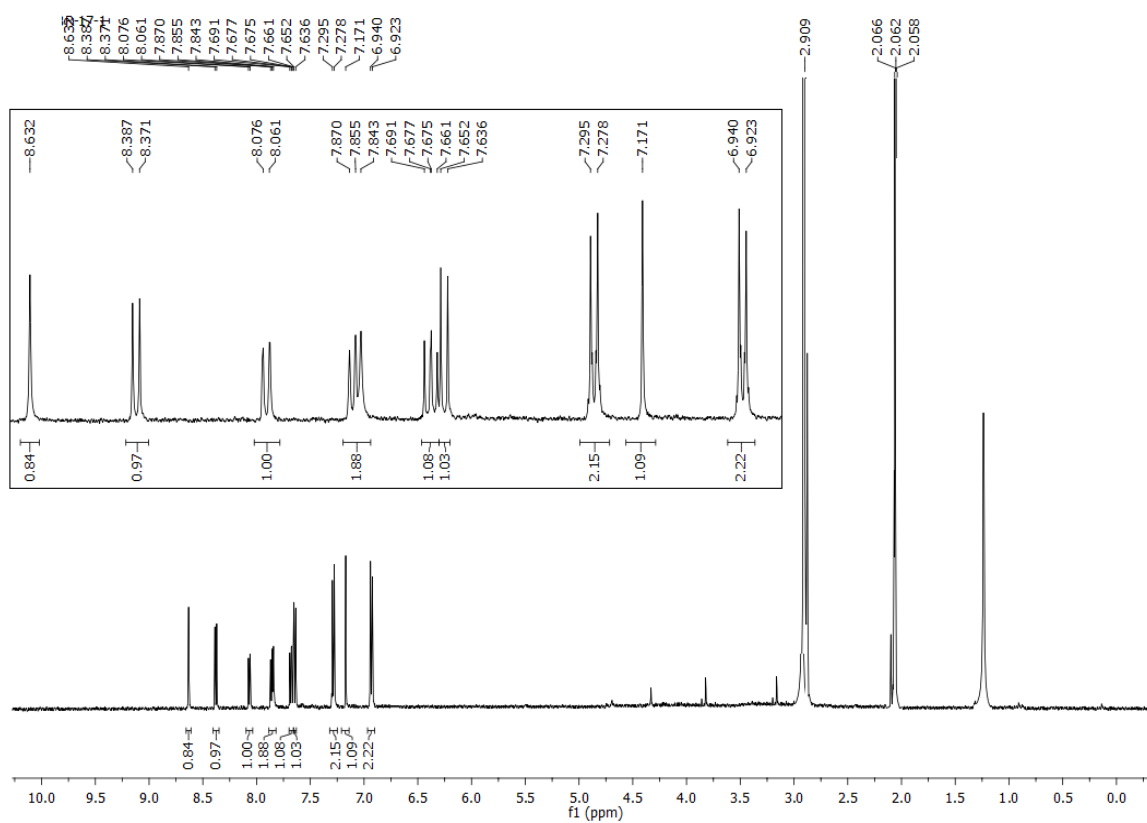


Figure 2B.7. ^1H NMR of compound 7 in CD_3COCD_3

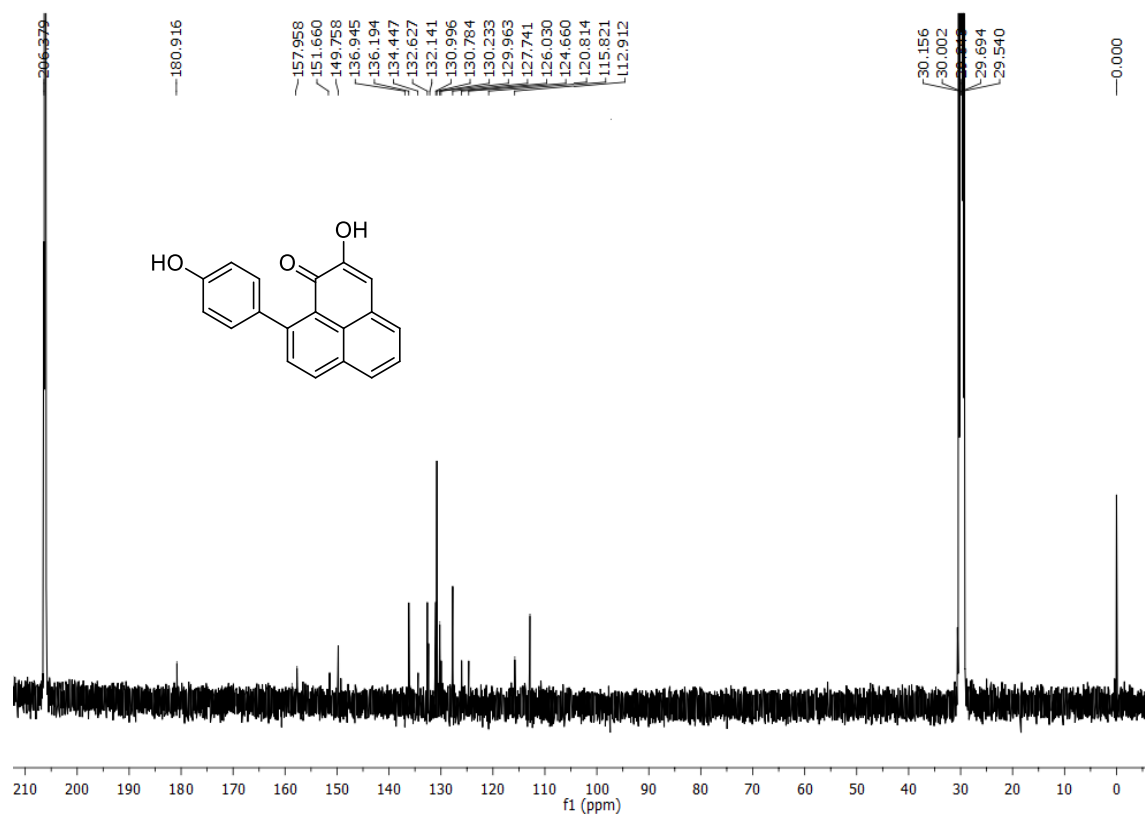
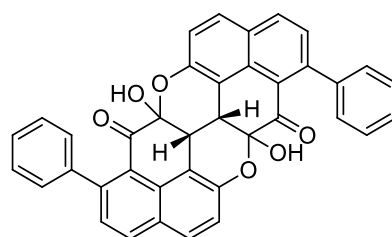


Figure 2B.8. ^{13}C NMR of compound 7 in CD_3COCD_3

In the carbon NMR, the methane carbons were clearly observed at δ 31.5 ppm, when the NMR was recorded in CDCl_3 (figure 2B.10). Also, the hydroxyl attached quaternary carbons were highly deshielded and resonated at δ 91.2 ppm. Finally, the presence of carbonyl groups were unambiguously confirmed from the signal obtained at δ 189.2 ppm. Hence from all the spectral data and literature reports, the compound was confirmed to be **anigorootin**, which is a dimeric form of anigorufone. The structure of the compound **8** is given below.



Anigorootin
Compound **8**

Compound **9** was isolated from the same fraction pool **8** by column chromatographic technique on silica gel using ethyl acetate: hexane in 2:3 ratio as the eluent, followed by Sephadex LH-20 in methanol. The molecule was pale yellow in color with a λ_{max} of 367.2 nm in dichloromethane. The molecular weight of compound **9** was determined by ESI-MS (m/z 629.1211 $[\text{M}+\text{Na}]^+$) that suggested a dimeric structure similar to compound **8**. In the proton NMR, all the protons (attached with carbon) resonated as doublets with a coupling constant around 8 Hz in a highly deshielded region, suggesting the presence of fully *ortho* coupled aromatic protons. The *p*-substituted phenyl rings were detected as intense doublets at δ 7.31 and δ 6.96 ppm; each doublet corresponding to four protons (figure 2B.11). In the carbon NMR two signals (at δ 131.3 and δ 115.7) exhibited twice the intensity as the other protonated carbon atoms (figure 2B.12), these were readily assigned as two sets of *para* substituted aromatic ring carbons. The methine protons which resonated at δ 4.16 ppm as singlet (carbon at δ 33.8 ppm), also supported the symmetrical dimeric structure of the molecule. With the aid of NMR data as well as HRMS analysis, the compound was confirmed as **4',4''-dihydroxyanigorootin** (6a,13a-dihydroxy-1,8-bis (4-hydroxyphenyl) - 13a,13a1-dihydronaphtho[8,1,2-hij]naphtha[8',1',2':7,8,1]isochromeno[5,4,3-cde]isochromene-7,14 (6aH, 6a1H)-dione).¹⁰ The structure of the compound is shown in the figure given below.

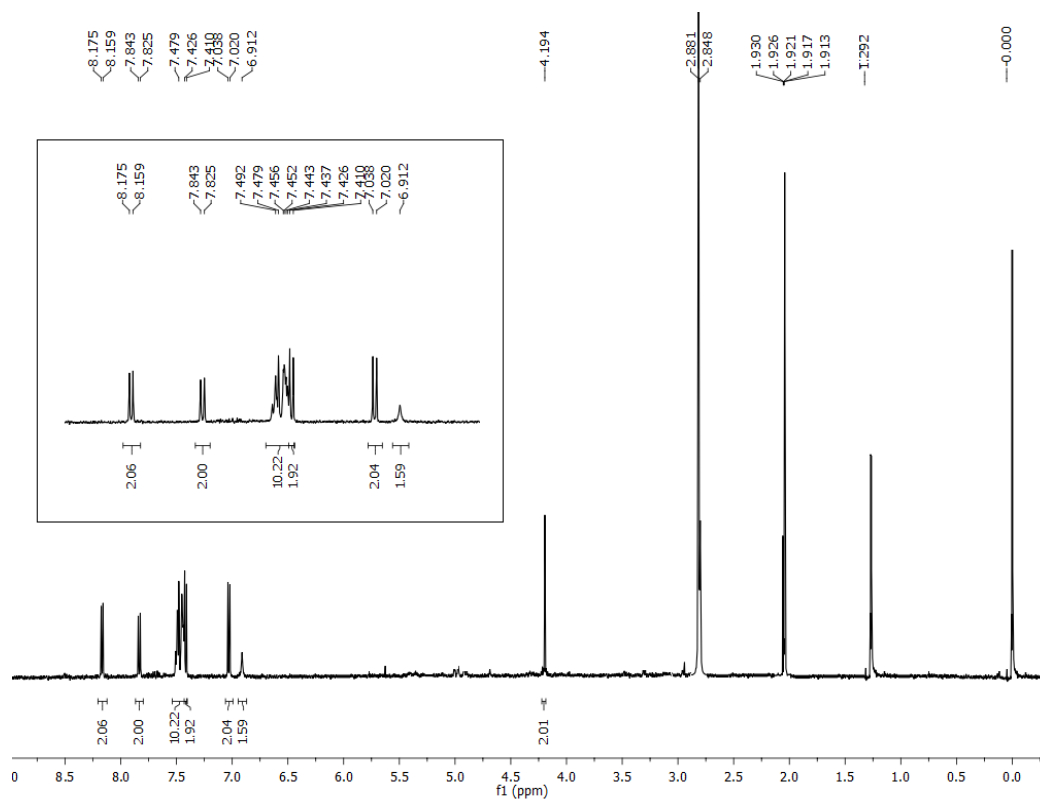


Figure 2B.9. ^1H NMR of compound **8** in CD_3COCD_3

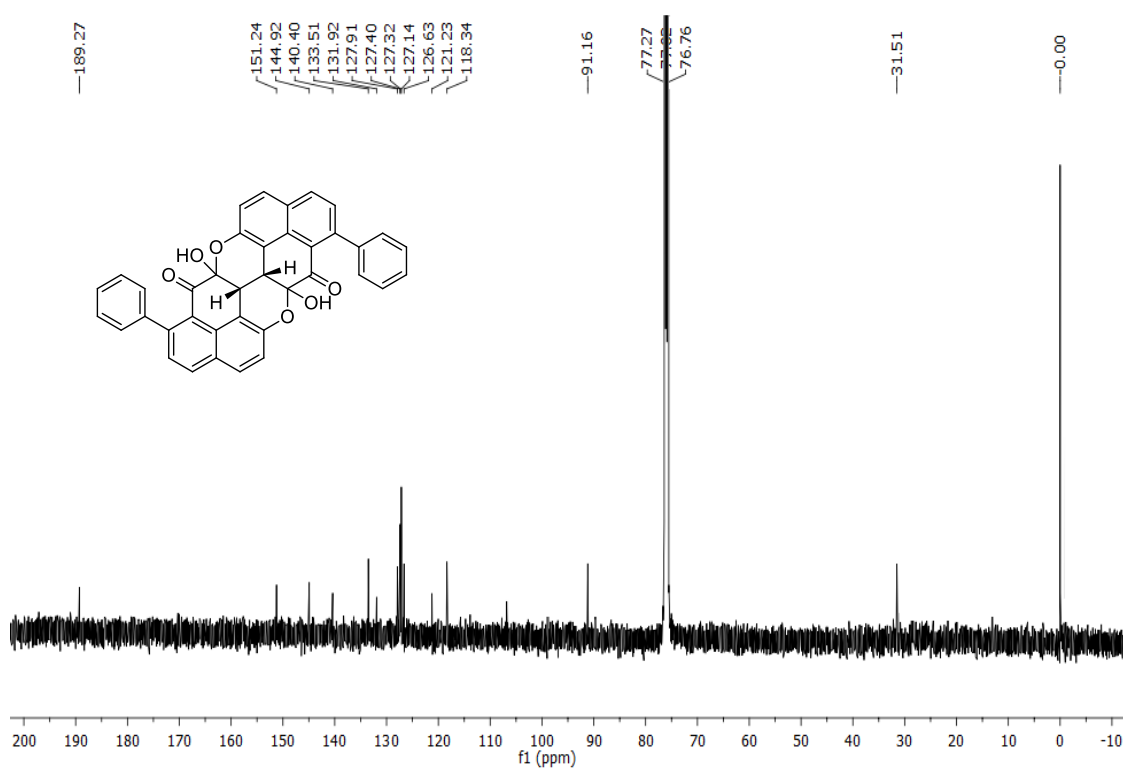
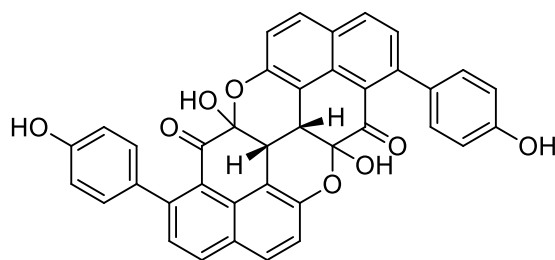
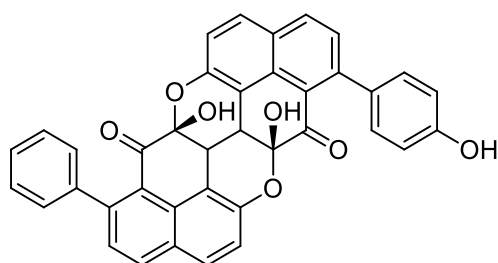


Figure 2B.10. ^{13}C NMR of compound **8** in CDCl_3



4',4''-Dihydroxyanigorootin
Compound **9**

Fraction pool eight on column chromatography with silica gel (using 1:1 hexane-ethyl acetate mixture) resulted in the isolation of compound **10** as a pale yellow solid, with a λ_{max} of 363.7 nm in dichloromethane. The HRMS mass of m/z 613.1272 ($[M+Na]^+$), suggested a dimeric structure as that of compounds **8** and **9**. In the proton NMR spectrum, the signals displayed at δ 4.03 and 4.05 ppm as doublets, indicate the characteristic chemical shift values of ring junction methane protons of fused phenylphenalenone dimers (figure 2B.13), that are asymmetric. However, this signal and further proton and resonances appeared in duplicate, indicate a nonsymmetrical dimer. A multiplet between δ 7.27 and δ 7.35, corresponding to five protons, points out to a typical mono-substituted phenyl ring. The singlet at δ 8.51 (1H) was attributed to the phenolic *p*-hydroxyl group and those at δ 6.90/6.80 indicates -OH groups at the ring junction. In the carbon NMR, the peak at δ 191.6 ppm obviously indicates the presence of carbonyl carbon (figure 2B.14). Hence with the help of literature reports and the close resemblances of aryl rings with those of compounds **8** and **9**, the structure of compound **10** was elucidated as **4'-hydroxyanigorootin**(6a,13a-dihydroxy-1-(4-hydroxyphenyl)-8-phenyl-13a,13a1-dihydronaphtho[8,1,2-hij]naphtha[8',1',2':7,8,1]isochromeno[5,4,3-cde]isochromene-7,14(6aH,6a1H)-dione). The structure of the same is given below.¹⁰



4'-Hydroxyanigorootin
Compound **10**

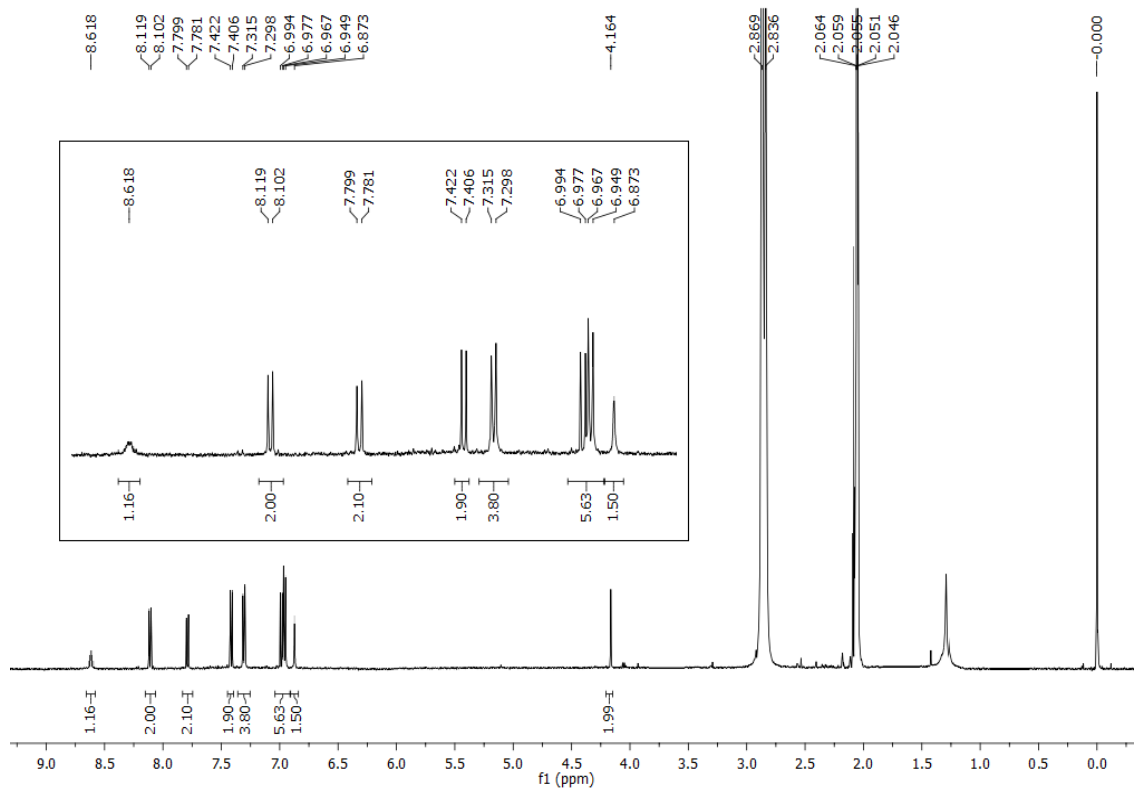


Figure 2B.11. ^1H NMR of compound **9** in CD_3COCD_3

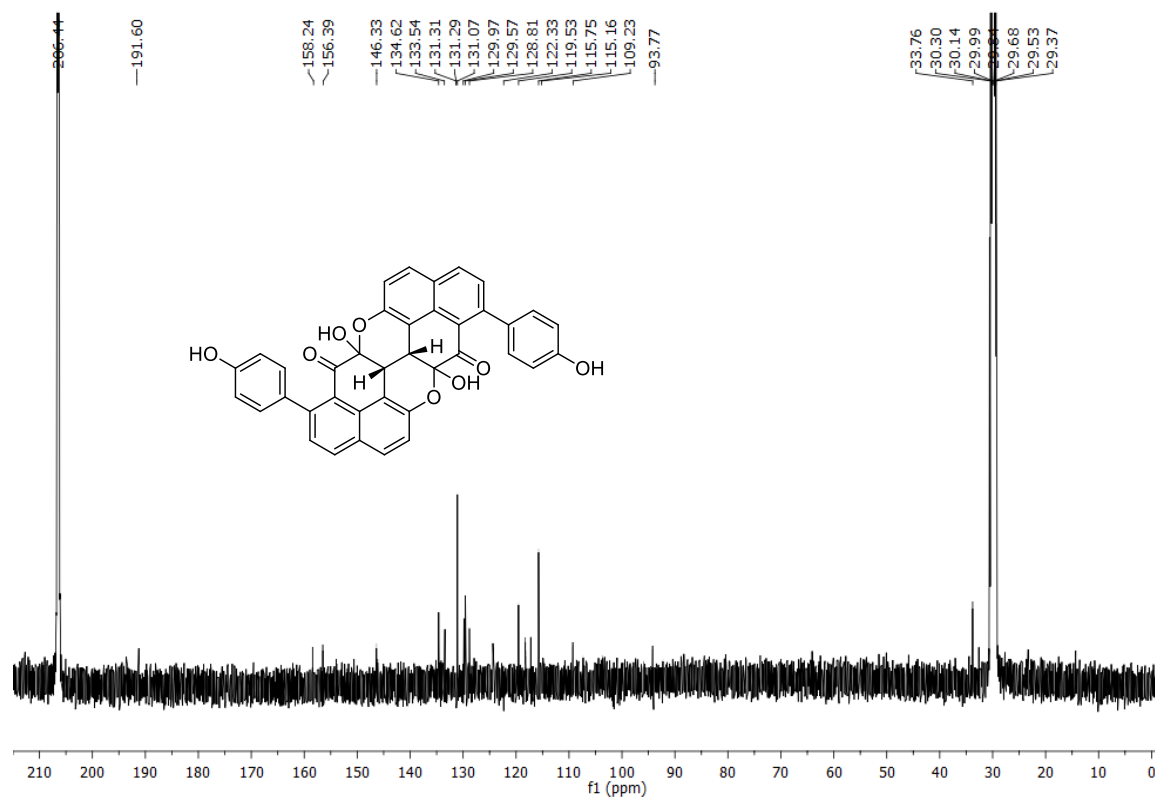


Figure 2B.12. ^{13}C NMR of compound **9** in CD_3COCD_3

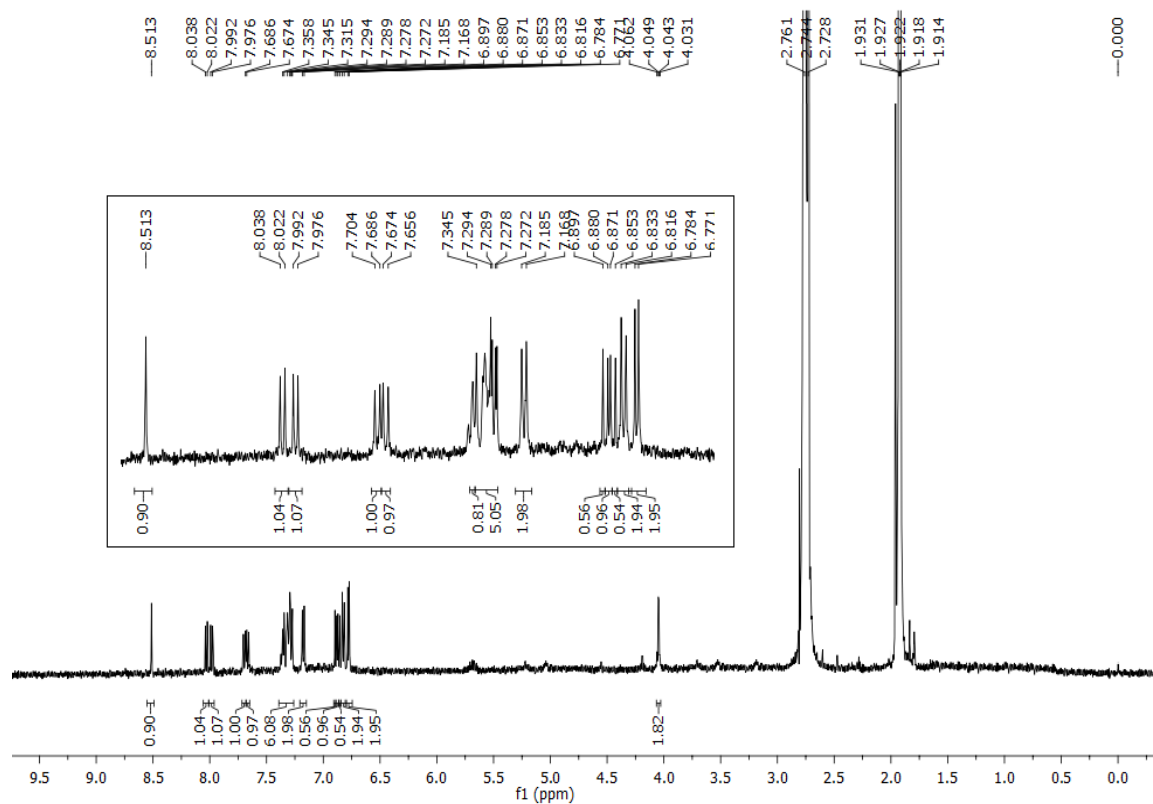


Figure 2B.13. ^1H NMR of compound **10** in CD_3COCD_3

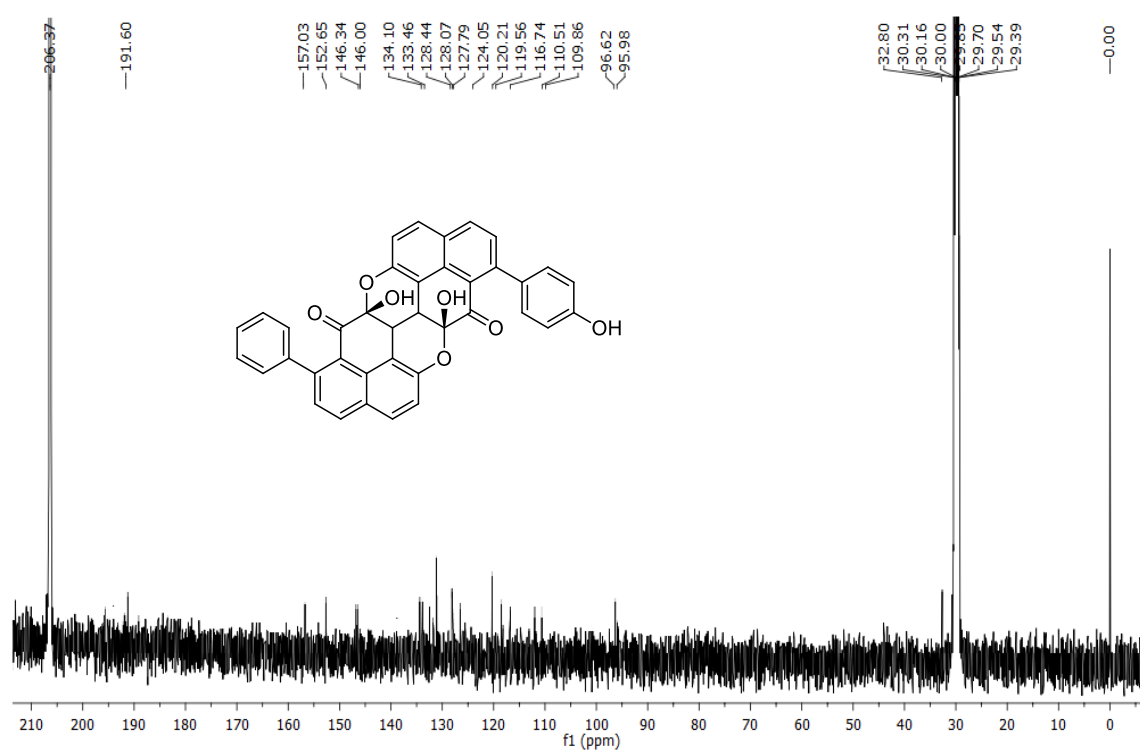


Figure 2B.14. ^{13}C NMR of compound **10** in CD_3COCD_3

From the fraction pool 9, a colorless solid compound was obtained after the column chromatographic purification with 4:1, ethyl acetate: hexane mixtures. From the detailed NMR analysis, the structure of the compound was confirmed as ***β*-sitosterol-*D*-glucoside** (same to compound **3** in part A of chapter 2).

2B.4. Extraction, Isolation and Characterization of Phytochemicals from the Peels of *Musa balbisiana* fruits

The peels of the raw fruit of *Musa balbisiana* (same plant) were dried, and were subjected to extraction with various organic solvents. Around 350 g of peel was first soaked in 3L hexane at room temperature for three days, and the same procedure was repeated twice. Removal of solvent under reduced pressure gave 2 g of crude extract. The residue was further subjected to acetone extraction, which yielded 4 g of acetone extract. In the same way, we obtained 1 g of methanol extract and finally water extract. Around 3.5 g of acetone extract was subjected to column chromatography on 100-200 mesh sized silica gel and eluted with hexane-ethyl acetate mixtures of increasing polarities to give 13 fraction pools. This on further purification resulted in the isolation of four compounds, namely **2**, **5**, **7** and **11**. A pictorial representation of the entire isolation procedure is given below (figure 15).

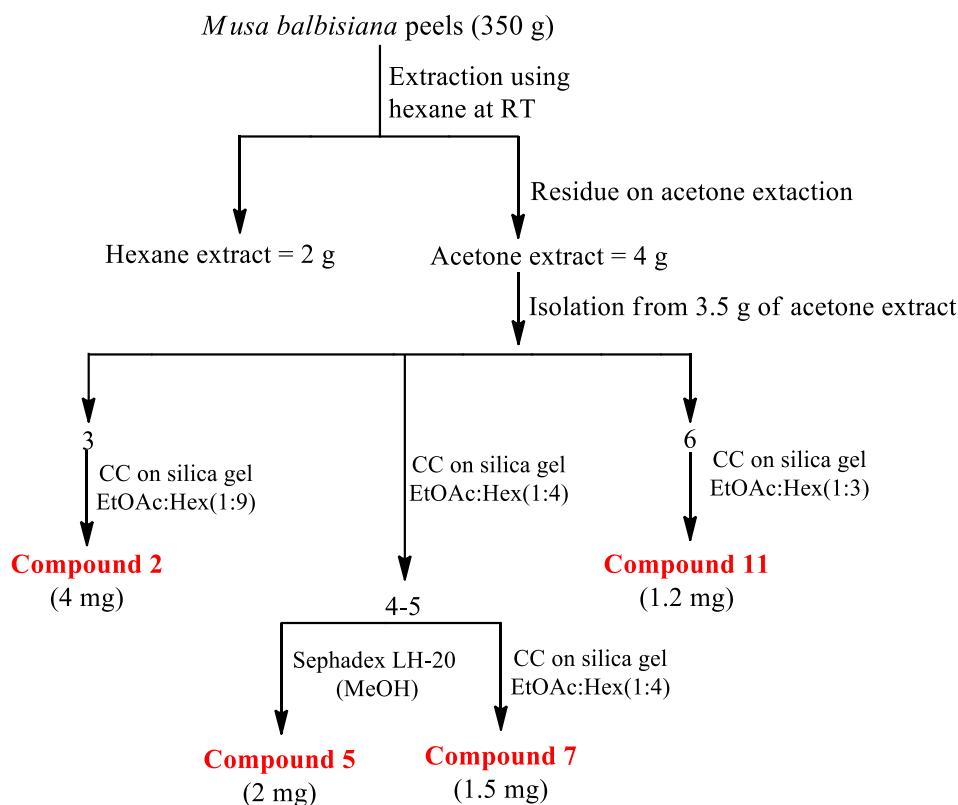
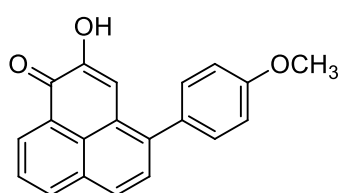


Figure 2B.15. A pictorial representation of isolation procedure

The fraction pool 3 on column chromatography with silica gel, yielded 4 mg of a colorless solid compound which on further spectral analyses was confirmed as compound **2** (**4-formylphenol**). Also the compounds isolated from fraction pools 4-7 on spectral analyses and comparison with previous reports confirmed that, they are equivalent to compounds **5** (**anigorufone**) and **7** (**4'-hydroxyanigorufone**). Here the compound **5** was isolated initially using silica gel column chromatography, followed by Sephadex column, while compound **7** was isolated with silica columns. Compound **11** was isolated from fraction pool six, as a highly UV active orange colored solid with an ESI-MS m/z mass of 303.1012 corresponding to $[M+H]^+$ peak. The molecule showed an absorption maxima at 337 and 388 nm in the UV spectrum and the bands for carbonyl as well as for phenolic groups were obtained at 1615 and 3319 cm^{-1} respectively, in the IR spectrum. In the proton NMR, the peak at δ 3.80 ppm as singlet clearly indicates the presence of one methoxy group. Also, the two proton, two doublets at δ 7.37 and δ 7.04 ppm represent a *para* substituted phenyl ring (figure 2B.16). The one proton triplet at δ 7.79 ppm and two, one proton doublet of doublet at δ 8.58 and 8.33 ppm represent three consecutive protons of a fused aromatic ring. The doublet peak at δ 8.59 ppm undoubtedly denotes a 4-phenyl phenalenone core. In the carbon NMR, the peak at δ 180.3 ppm represents the presence of one carbonyl atom (figure 2B.17). Hence, comparing with the proton as well as the carbon NMR data along with the previous reports, the compound **11** was confirmed as 2-hydroxy-4-(4-methoxyphenyl)-1H-phenalen-1-one or **4'-methoxyirenolone**.¹¹ The structure of the same is given below.



4'-Methoxyirenolone
Compound **11**

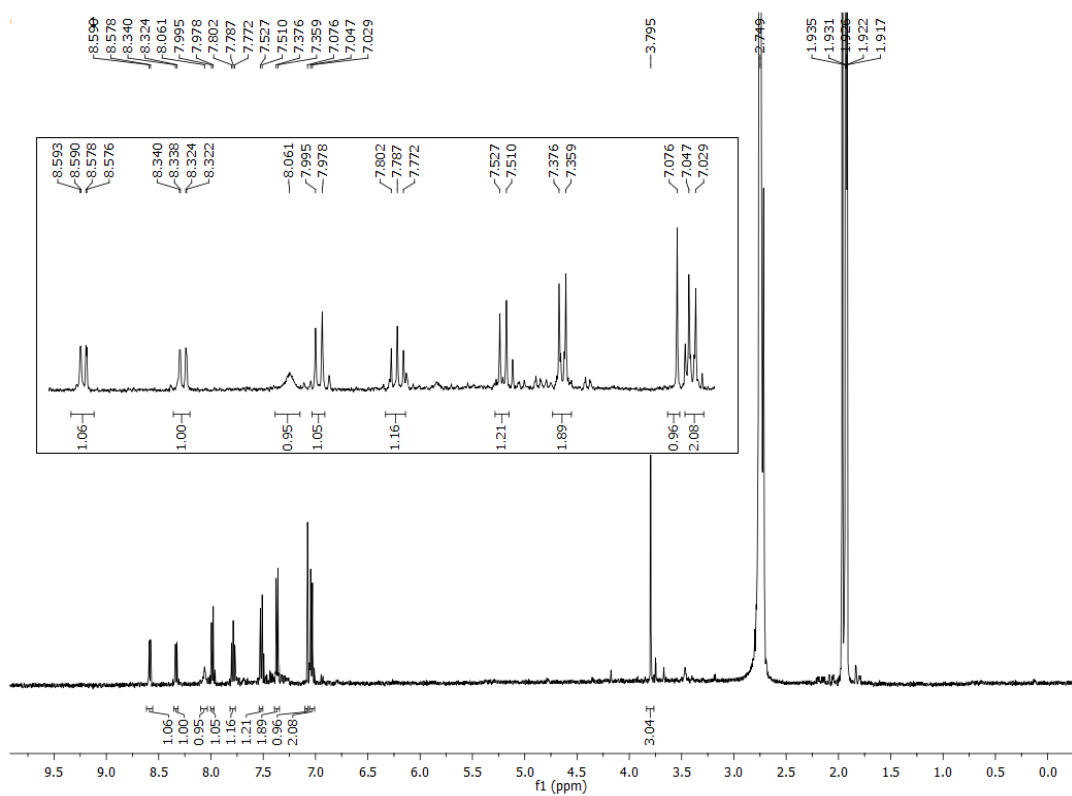


Figure 2B.16. ^1H NMR of compound 11 in CD_3COCD_3

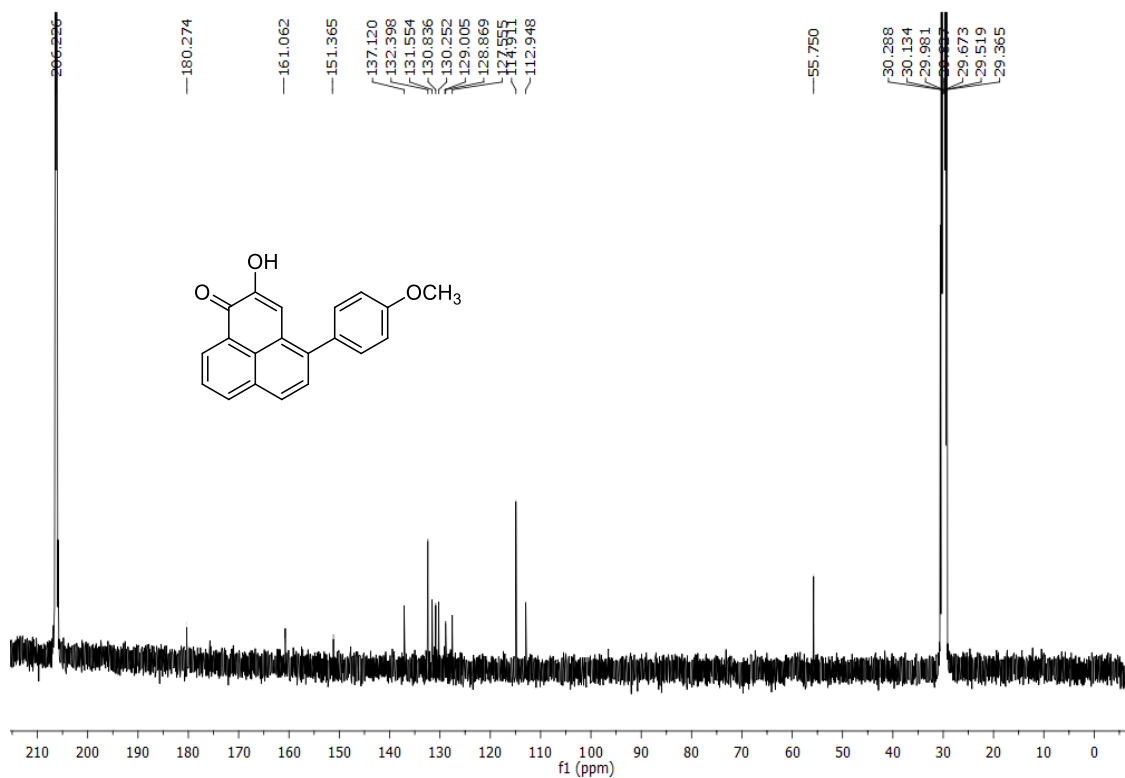


Figure 2B.17. ^{13}C NMR of compound 11 in CD_3COCD_3

2B.5. Conclusion

In conclusion, we have isolated nine phytochemicals from rhizome and fruit peels of *Musa balbisiana*. Most of the isolated molecules were phenylphenalenones, in which some were monomeric, and some others were dimeric in nature. Here we made a comprehensive analysis of phytoalexin production and biogenesis regulation in *M. balbisiana* which could contribute to the design of plants and pesticides possessing enhanced resistance against pests.

2B.6. Experimental Section

Different analytical techniques were used for the characterization of compounds. The IR spectra were recorded with a Bruker FT-IR spectrometer. The nuclear magnetic resonance spectra (NMR) were recorded on a Bruker AMX 500 spectrophotometer (CDCl_3 , CD_3COCD_3 , MeOD and DMSO-d_6 as solvents). Chemical shifts for NMR spectra are reported as δ in units of parts per million (ppm) downfield from tetramethylsilane (δ 0.0) and relative to the signal of solvent. Mass spectra were recorded under ESI/HRMS at 60,000 resolution using Thermo Scientific Exactive mass spectrometer and specific rotation was recorded using Jasco P-2000 polarimeter. Shimadzu UV-1800 spectrophotometer was used to measure the absorption maxima.

2B.7. Spectral Data

Compound 5 (anigorufone)

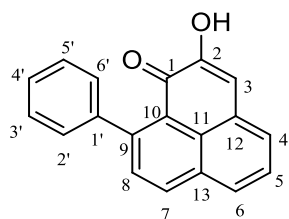
Compound 5 was obtained as an UV active orange colored powder from fraction pools 4-5 through various column chromatographic methods. The ^1H NMR, ^{13}C NMR and mass spectral studies of this compound on comparison with literature values, confirmed that the molecule is anigorufone (2-hydroxy-9-phenyl-1H-phenalen-1-one).

Molecular formula : $\text{C}_{19}\text{H}_{12}\text{O}_2$

Mp : 124-126 °C

FT-IR (Neat) ν_{max} : 3348, 1657, 1611, 1592, 1411, 1289, 1273, 1190, 1056, 865 cm^{-1} .

^1H NMR (500 MHz, CDCl_3 , TMS) : δ 8.25 (d, $J = 8$ Hz, 1H, H-7), 7.96 (d, $J = 8.5$ Hz, 1H), 7.75 (d, $J = 7$ Hz, 1H), 7.63-7.60 (m, 2H, H-2' and H-6'), 7.52-7.47 (m, 3H, H-3', H-4' and H-5'), 7.39-7.38 (m, 2H), 7.14 (s, 1H, H-3), 7.03 (s, 1H, OH) ppm.



^{13}C NMR (125 MHz, CDCl_3 , TMS) : δ 180.3 (C-1), 149.9 (C-2), 149.1 (C-7), 142.4, 135.6, 131.6, 131.1, 130.7, 129.8, 128.9, 128.3, 127.8, 127.6, 127.0, 125.0, 123.6, 112.7(C-3) ppm.

HRMS (ESI) : m/z Calcd for $\text{C}_{19}\text{H}_{13}\text{O}_2$: 273.0915; Found; 273.0909.

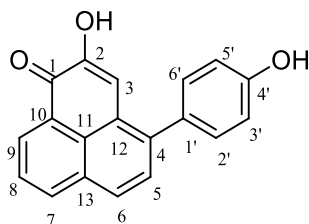
Compound 6 (ire nolone)

Compound **2**, having a deep orange-red in color was also isolated from fraction pools 4-5. The molecule is highly UV active and solid in nature. The compound **2** was confirmed as ire nolone (2-hydroxy-4-(4-hydroxyphenyl)-1H-phenalen-1-one) based on its spectral data and literature reports.

Molecular formula : $\text{C}_{19}\text{H}_{12}\text{O}_3$

FT-IR (Neat) ν_{max} : 3310, 1634, 1608, 1588, 1650, 1421, 1349, 1273 cm^{-1} .

^1H NMR (500 MHz, CD_3COCD_3 , TMS) : δ 8.73 (s, 1H), 8.58 (d, $J = 7$ Hz, 1H, H-9), 8.32 (d, $J = 8$ Hz, 1H, H-7), 8.04 (brs, 1H), 7.97 (d, $J = 8$ Hz, 1H, H-6), 7.77 (t, $J = 8$ Hz, 1H, H-8), 7.51 (d, $J = 8.5$ Hz, 1H, H-5), 7.27 (d, $J = 8.5$ Hz, 2H, H-2' and H-6'), 7.11 (s, 1H, H-3), 6.93 (d, $J = 8.5$ Hz, 2H, H-3' and H-5') ppm.



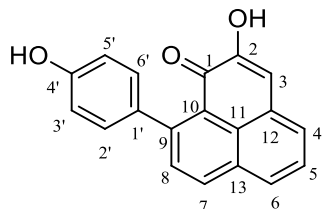
^{13}C NMR (125 MHz, CD_3Cl , TMS) : δ 179.1 (C-1), 157.1 (C-4'), 151.7 (C-2), 142.9 (C-4), 136.3, 131.9, 131.6 (C-2' and C-6'), 131.5, 130.0, 126.5, 124.9, 115.5 (C-3' and C-5'), 113.4 (C-3) ppm.

HRMS (ESI) : m/z Calcd for $\text{C}_{19}\text{H}_{13}\text{O}_3$: 289.0864; Found; 289.0865.

Compound 7 (emenolone)

Besides Compounds **5** and **6**, compound **7** was also isolated from the same fraction pools 4-5. The molecule is highly UV active and orange solid in nature. Based on the spectral data and literature reports, the molecule was confirmed as hydroxyl anigorufone/emenolone (2-hydroxy-9-(4-hydroxyphenyl)-1H-phenalen-1-one).²³

Molecular formula : $\text{C}_{19}\text{H}_{12}\text{O}_3$



FT-IR (Neat) ν_{\max} : 3440, 1640, 1608, 1680, 1541, 1477, 1355, 1280, 1231, 940 cm^{-1} .

^1H NMR (500 MHz, CD_3COCD_3 , TMS) : δ 8.63 (s, 1H), 8.37 (d, $J = 8$ Hz, 1H, H-7), 8.06 (d, $J = 8$ Hz, 1H), 7.86 (d, $J = 7$ Hz, 1H), 7.8 (brs, 1H), 7.67 (t, $J = 7.5$ Hz, 1H, H-5), 7.64 (d, $J = 8.5$ Hz, 1H), 7.28 (d, $J = 8.5$ Hz, 2H, H-2' and H-6'), 7.17 (s, 1H, H-3), 6.93 (d, $J = 8.5$ Hz, 2H, H-3' and H-5') ppm.

^{13}C NMR (125 MHz, CD_3COCD_3 , TMS) : δ 180.9 (C-1), 157.9 (C-41), 151.6 (C-2), 149.7 (C-7), 136.9, 136.2, 132.6, 131.0 (C-2' and C-6'), 130.8, 130.2, 129.9, 127.7, 126.0, 124.7, 120.8, 115.8 (C-3' and C-5'), 112.9 (C-3) ppm.

HRMS (ESI) : m/z Calcd for $\text{C}_{19}\text{H}_{13}\text{O}_3$: 289.0859; Found : 289.0864.

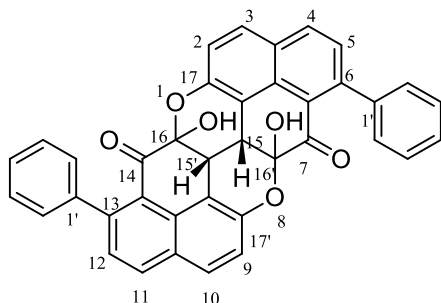
Compound 8 (anigorootin)

Compound **8** was isolated along with compound **9** from fraction pools 6-7. The compound **8** is highly UV active and yellow solid in nature. The spectral analysis of this compound showed that it's a dimeric phenylphenalenone and is matching with that of anigorootin (6a,13a-dihydroxy-1,8-diphenyl-13a,13a1-dihydronaphtho [8,1,2-hij] naphtha [8',1',2':7,8,1] isochromeno[5,4,3-cde] iso chromene-7,14(6aH,6a1H)-dione).

Molecular formula : $\text{C}_{38}\text{H}_{22}\text{O}_6$

FT-IR (Neat) ν_{\max}) : 3442, 2918, 1703, 1614, 1496 cm^{-1} .

^1H NMR (500 MHz, CD_3COCD_3 , TMS) : δ 8.17 (d, $J = 8.5$ Hz, 2H, H-4 and H-11), 7.83 (d, $J = 9$ Hz, 2H, H-3 and H-10), 7.49-7.44 (m, 10H, phenyl protons), 7.42 (d, $J = 8.5$ Hz, 2H, H-5 and H-12), 7.03 (d, $J = 9$ Hz, 2H, H-2 and H-9), 6.91 (brs, 2H, H-7 and H-14), 4.19 (s, 2H, H-15 and H-15') ppm.



^{13}C NMR (125 MHz, CDCl_3 , TMS) : δ 189.3 (C-7 and C-14), 151.2 (C-17 and C-17'), 144.9, 140.4, 133.5, 131.9, 127.9, 127.4, 127.3, 127.2, 127.1,

126.6, 121.2, 118.3, 98.9 (C-16 and C-16'), 31.5 (C-15 and C-15') ppm.

HRMS (ESI) : m/z Calcd for $C_{38}H_{22}NaO_6$; 597.1315; Found : 597.1314.

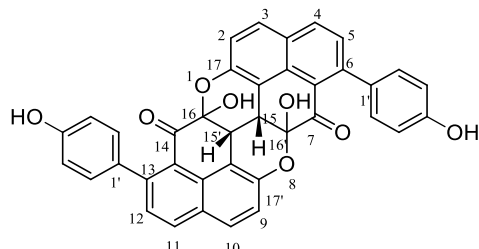
Compound 9 (4',4''-dihydroxyyanigorootin)

Compound **9** was isolated from fraction pool 6-7 by column chromatographic technique on silica gel using 2:3, ethyl acetate-hexane mixture as the eluent. The molecule was highly UV active and pale yellow in color. The spectral analysis of this molecule confirmed that this molecule has a dimeric phenylphenalenone core. Further analysis confirmed that the molecule is 4',4''-dihydroxyyanigorootin(6a,13a-dihydroxy-1,8-bis(4-hydroxyphenyl)-13a,13a1-dihydronaphtho [8,1,2-hij]naphtho[8',1',2':7,8,1] isochromeno [5,4,3-cde]isochromene-7,14(6aH,6a1H)-dione).

Molecular formula : $C_{38}H_{22}O_8$

FT-IR (Neat) ν_{max} : 3432, 2921, 1699, 1617, 1466 cm^{-1} .

1H NMR (500 MHz, CD_3COCD_3 , TMS) : δ 8.62 (s, 1H), 8.11 (d, $J = 8$ Hz, 2H), 7.79 (d, $J = 9$ Hz, 2H), 7.41 (d, $J = 8$ Hz, 2H), 7.31 (d, $J = 8.5$ Hz, 4H), 6.98 (d, $J = 9$ Hz, 2H), 6.95 (d, $J = 8.5$ Hz, 4H), 6.87 (brs, 2H, OH at 16 and 16'), 4.16 (s, 2H, H-15 and H-15') ppm.



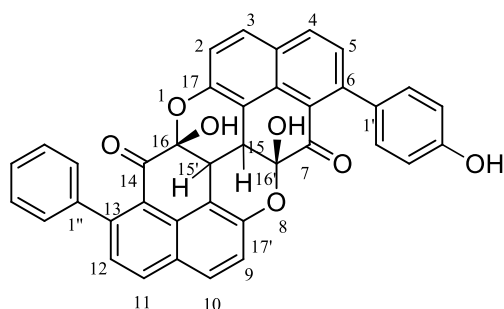
^{13}C NMR (125 MHz, CD_3COCD_3 , TMS) : δ 191.6 (C-7 and C-14), 158.2 (C-4 and C-4'), 156.4 (C-17 and C-17'), 146.3, 134.6, 133.5, 131.4, 131.3, 131.1, 130.0, 129.6, 128.8, 121.2, 119.5, 115.7, 115.2, 109.2, 93.8 (C-16 and C-16'), 33.8 (C-15 and C-15') pm.

HRMS (ESI) : m/z Calcd for $C_{38}H_{22}NaO_8$: 629.1211; Found : 629.1212.

Compound 10 (4'-hydroxyyanigorootin)

Compound **10** was highly UV active and pale yellow in colour. The spectral data showed that, likewise compounds **8** and **9**, this molecule also bears two monomeric phenylphenalenone moieties, which are asymmetrical. Further characterization studies of this molecule confirmed that, it is 4'-hydroxyyanigorootin (6a,13a-dihydroxy-1-(4-

hydroxyphenyl)-8-phenyl-13a,13a1-dihydronaphtho[8,1,2-hij]naphtha [8',1',2':7,8,1]isochromeno[5,4,3-cde]isochromene-7,14 (6aH,6a1H)-dione).



Molecular formula : $C_{38}H_{22}O_7$

FT-IR (Neat) ν_{max} : 3437, 3021, 1691, 1628, 1445, 1357 cm^{-1} .

1H NMR (500 MHz, CD_3COCD_3 , TMS) : δ 8.51 (s, 1H), 8.02 (d, $J = 8.5$ Hz, 1H), 7.98 (d, $J = 8$ Hz, 1H), 7.70-7.65 (m, 2H), 7.36-7.27 (m, 6H), 7.17 (d, $J = 8.5$ Hz, 2H), 6.89-6.85 (m, 2H), 6.83-6.81 (d, $J = 9$ Hz, 2H), 6.78-6.77 (d, $J = 8.5$ Hz, 2H), 6.52 (s, 1H), 4.05 (d, $J = 6.5$ Hz, 1H), 4.04 (d, $J = 6$ Hz, 1H) ppm.

^{13}C NMR (125 MHz, CD_3COCD_3 , TMS) : δ 191.6, 157.5, 152.6, 146.3, 146.0, 134.1, 133.5, 128.4, 128.1, 127.8, 124.0, 120.2, 119.6, 116.7, 110.5, 109.9, 96.6, 95.9, 32.8 ppm

HRMS (ESI) : m/z Calcd for $C_{38}H_{22}NaO_7$: 613.1272; Found: 613.1278.

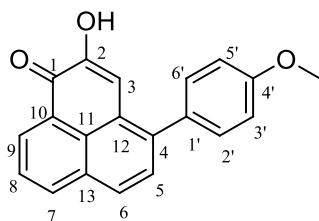
Compound 11 (4'-methoxyirenonone)

Compound **11** was isolated from fraction pool 6, through a number of silica gel column chromatography. The compound was a highly UV active. The molecule showed an intense orange-red color, and was detected in the TLC with bare eyes. On comparison of the spectral data of this molecule with literature reports, the molecule was confirmed as 2-hydroxy-4-(4-methoxyphenyl)-1H-phenalen-1-one.

Molecular formula : $C_{20}H_{14}O_3$

FT-IR (Neat) ν_{max} : 3319, 3021, 1615, 1445 cm^{-1} .

1H NMR (500 MHz, CD_3COCD_3 , TMS) : δ 8.59 (dd, $J_1 = 7.5$ Hz, $J_2 = 1.5$ Hz, 1H, H-9), 8.26 (dd, $J_1 = 8$ Hz, $J_2 = 1$ Hz, 1H, H-7), 8.86 (brs, 1H), 7.98 (d, $J = 8.5$ Hz, 1H, H-6), 7.79 (t, $J = 8$ Hz, 1H, H-8), 7.52 (d, $J = 8.5$ Hz, 1H, H5), 7.37 (d, $J = 8.5$ Hz, 2H, H-2' and H-6'), 7.08 (s, 1H,



H-3), 7.04 (d, $J = 9$ Hz, 2H, H-3' and C-5'), 3.80 (s, 3H, -OMe) ppm.

^{13}C NMR (125 MHz, CD_3COCD_3 , TMS) : δ 180.2 (C-1), 161.0 (C-4'), 151.4 (C-2), 137.1, 132.4 (C-2' and C-6'), 131.6, 130.8, 130.3, 128.9, 127.6, 114.9, 112.9, 55.7 (-OMe) ppm.

HRMS (ESI): m/z Calcd for $\text{C}_{20}\text{H}_{15}\text{O}_3$: 303.1015; Found; 303.1012.

2B.8. References

1. Editorial, *Nat. Chem. Biol.*, **2007**, 3, 351.
2. G. L. Javier, E. Fernando, Q. Winston, B. Ivan, L. Matias, T. Fernando, C. Gloria, A. Zahira, P. Carlos and R. Mauricio, *J. Org. Chem.*, **1993**, 58(16), 4306-4308.
3. F. Otálvaro, F. Echeverri, W. Quiñones, F. Torres and B. Schneider, *Molecules*, **2002**, 7, 331-340.
4. F. Otálvaro, G. Helmar, H. Dirk, S. Bettina, E. Fernando, Q. Winston and B. Schneider, *Phytochemistry*, **2002**, 60, 61-66.
5. S. Someya, Y. Yoshiki and K. Okubob, *Food Chem.*, **2002**, 79, 351-354.
6. T. Kamo, N. Kato, N. Hirai, M. Tsuda, D. Fujioka and H. Ohigashi, *Biosci. Biotechnol. Biochem.*, **1998**, 62(1), 95-101.
7. R. G. Cooke and R. L. Thomas, *Aust. J. Chem.*, **1975**, 28, 1053-1057.
8. D. Hölscher and B. Schneider, *Nat. Prod. Res.*, **2014**, 1, 171-182.
9. D. Hölscher and B. Schneider, *Phytochemistry*, **1999**, 50, 155-161.
10. F. Otálvaro, G. Helmar, H. Dirk, S. Bettina, E. Fernando, Q. Winston, and B. Schneider, *Phytochemistry*, **2002**, 60(1), 61-66.
11. J. G. Luis, Q. F. Winston, Fletcherb, F. Jkheverri and T. A. Grille, *Tetrahedron*, **1994**, 50, 10963-10970.

Part A : Phytochemical Investigation of *Anethum graveolens* Linn.

3A.1. Introduction

Medicinal plants are important in maintaining human health. Plants evolved much before than humans, and they have always acted as a rich source of food and medicines. Herbs, spices and essential oils are summarized under the terms phytobiotics or botanicals. They are well known for their pharmacological effects, and are thus extensively used in human customary and alternative medicines. Additionally, they play a pivotal role as flavors and food preservatives in human nutrition. The activities of phytobiotics are mainly due to the primary and secondary metabolites possessed by them. Many scientific experiments have been conducted to determine whether the use of aromatic plants and the addition of essential oils to the food contribute to an improvement in the health and the growth of humans.¹⁻³

Spices are one of the most inevitable ingredients in our daily life which possess medicinal properties. Apiaceae (also known as Umbelliferaceae, was first described by John Lindley in 1836) family is an important natural resource that provides many useful products like food, spices, medicines, dyes, perfumes and aesthetics. This family mostly consists of aromatic flowering plants named after the genus *Apium*, and is commonly known as the celery/carrot/parsley family. They include, over 434 genera and over 3700 species. They are widely distributed all around the world, but do not thrive in tropics or rain forests. They comprise the well-known and economically important plants such as angelica, anise, asafoetida, caraway, carrot, celery, chervil, coriander, cumin, dill, fennel, hemlock, lovage, parsley, parsnip and silphium. They produce sturdy seeds, and many of them will self-seed prolifically. Their inflorescence is fashioned like an upside down umbrella, and numerous flower stalks radiate from a single stalk which arise from a single point from the stem. These stalks again themselves offer another umbel at their tips, where the tiny flowers are formed which gradually get converted to sturdy aromatic seeds. The colors of their inflorescences are usually not very showy, and are generally white, beige or pale yellow colored. The leaves of this family are usually highly divided and have a fine feathery appearance. Both annual and perennial species occur in this family. The noteworthy character of this family is the high content of essential oils, making them an

important spice in foods. Many of the volatile oils from this family act as traditional medicines for respiratory disorders. Apparently, the plants are not highly aromatic, but the crushing or chewing of these plant materials releases the volatile oils that are held tightly in the tissues, there by releasing the aroma. These plants are fairly resistant to insects, and birds do not favor the seeds due to their dry nature. Therefore, it is necessary to evaluate these plants scientifically, to understand the composition of their essential oils and its biological activities.⁴⁻⁶

Anethum graveolens L. (dill; shatapushpa in Sanskrit and Malayalam, savaa in Hindi) is an annual herb in this family and is the sole species in the genus *Anethum* (figure 2.1). Dill has been used in Ayurvedic medicines since ancient times, and is one of the most popular culinary herb widely used throughout the world as a spice, as well as a medicinal herb which also yields essential oil. In Ayurvedic system of medicine dill seeds are used as carminative, stomachic and diuretic. Numerous volatile components are present in dill; carvone being the predominant odorant of dill seed and α -phellandrene, limonene, dill ether, myristicin are the most important odorants of dill herb. *Anethum graveolens* is believed to be the native of South-west Asia or South-east Europe. It is indigenous to Mediterranean, southern USSR and Central Asia. Since Egyptian times, *Anethum* has been used as a condiment and also in medicinal purposes. It was used by Egyptian doctors 5000 years ago, whose traces can be found in the Roman ruins in Great Britain, and Greeks used to cover their heads with dill leaves to induce sleep.^{7,8}



Figure 3A.1. Different plant parts of *Anethum graveolens*

Dill seeds are widely used to give flavor to cakes and pastries, soups, salads, potatoes, meats, and pickles. The essential oils present in Apiaceae plants stimulate the digestive enzymes and there by improve digestion. The leading producers of dill herbs are India and Pakistan, while the principal producers of the dill essential oils are USA, Canada, Hungary and Bulgaria. A number of research groups reported various pharmacological actions of *A. graveolens* such as antimicrobial, antispasmodic, antidiabetic, antihypercholesteromic, and

anti-inflammatory.⁹ On the other hand, *A. graveolens* was mentioned as “brain tonic” in 17th century in Europe.¹⁰

Its common use in Ayurvedic medicine is in abdominal discomfort, colic and for promoting digestion. Ayurvedic properties of shatapushpa are katu tikta rasa, usna virya, katu vipaka, laghu, tiksna and snigdha gunas. It cures ‘vata’, ‘kapha’, ulcers, abdominal pains, eye diseases and uterine pains. Charaka prescribed the paste of Linseed, castor seeds and shatapushpa (*A. graveolens*) pounded with milk for external applications in rheumatic and other swellings of joints. Kashyapa samhita attributed tonic, rejuvenating and intellect promoting properties to the herb (*A. graveolens*). It is used in Unani medicine in colic, digestive problems and is also an ingredient of gripe water. *A. graveolens* is used in the preparations of more than 56 ayurvedic preparations, which include Dasmoolarishtam, Dhanwantharishtam, Mrithasanjeevani, Saraswatharishtam, Gugguluthiktaquatham, Maharasnadi kashayam, Dhanwantharam quatham and so on. Seed extracts of *A. graveolens* have significant mucosal protective, antisecretory and anti-ulcer activities against HCl- and ethanol-induced stomach lesions in mice. Two flavonoids have been isolated from *A. graveolens* L. seed, quercetin and isoharmentin,^{7,11} which have antioxidant activity and can counteract free radicals. This effect may help to prevent peptic ulcer. Dill fruit hydrochloric extract is a potent relaxant of contractions induced by a variety of spasmogens in rat ileum, and hence supports the use of dill fruit in traditional medicine for gastrointestinal disorders. Besides having strong anti-hyperlipidemic effects, crude extracts of *A. graveolens* can also improve the biological antioxidant status by reducing lipid peroxidation in liver and modulating the antioxidant enzymes activity in rats fed with high fat diet. Also, the reports are saying that the aqueous and the ethanol extracts of *A. graveolens* possess a broad-spectrum antibacterial activity against gram positive and gram negative bacteria such as, *E. coli*, *S. aureus*, *S. typhimurium*, *P. aeruginosa*, *Shigella flexneri* and *Salmonella typhi*. The higher activity of these extracts can be explained on the basis of the core structure of their major constituents such as dillapiole and anethole, which have aromatic nucleus containing polar functional group, which is known to form hydrogen bonds with active sites of the target enzyme.^{7,11,12}

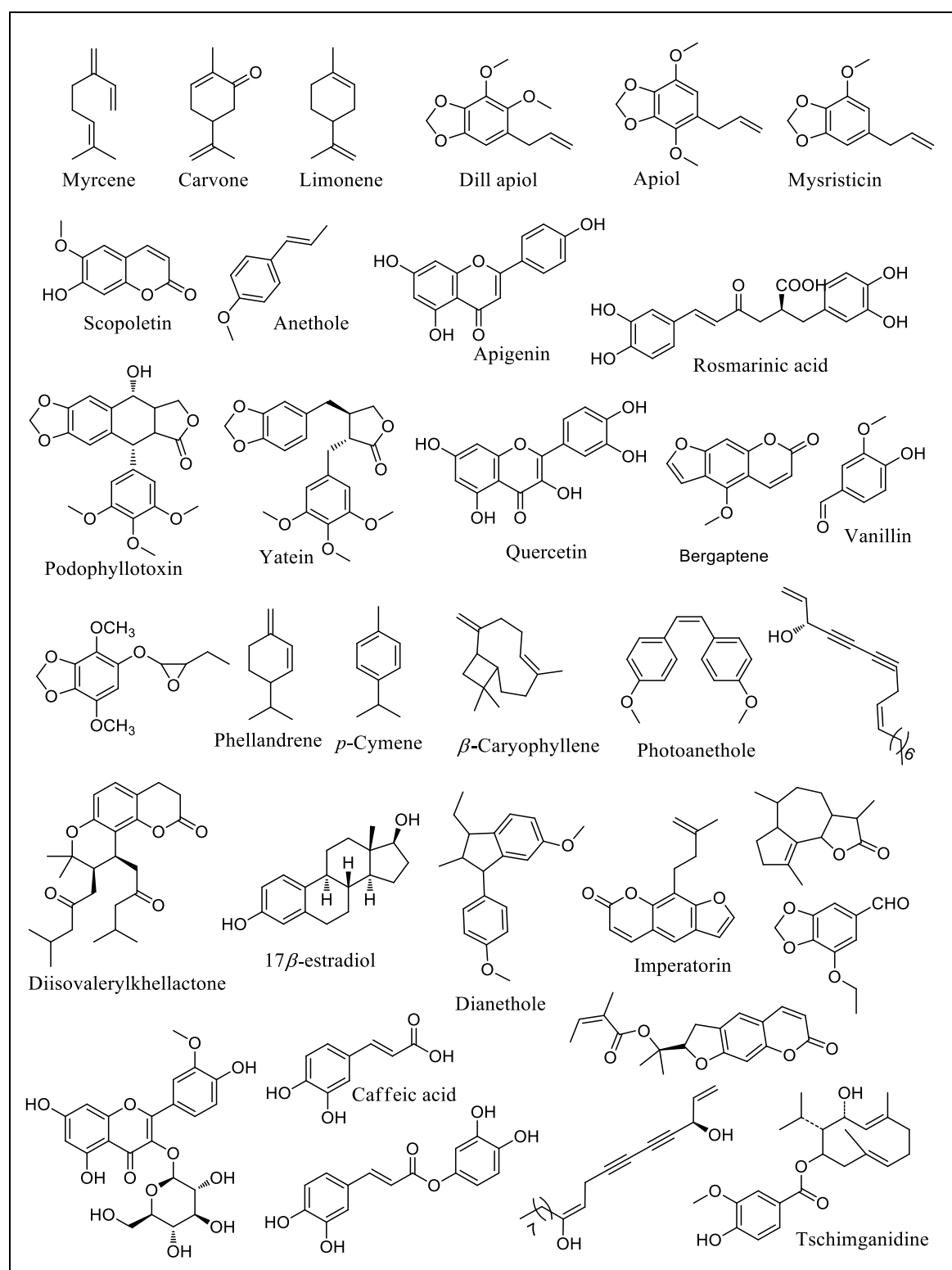
In central and eastern Europe, Baltic States, Scandinavia, Russia and Finland, dill is a common culinary herb used in the kitchen along with chives or parsley. Fresh, finely cut dill leaves are used as topping in soups, especially in the hot red borsht and the cold borsht mixed with curds, yoghurt, or sour cream. It is also common in summer to drink fermented milk (curds, kefir, yoghurt, or buttermilk) mixed with dill (and sometimes other herbs).

Fresh dill leaves are used throughout the entire year, as an ingredient in vegetable salads, the way basil leaves are used in Italy and Greece. In Anglo-Saxon England, as prescribed in Leechdoms, and Starcraft (also called Læceboc, many of whose recipes were borrowed from Greek medicinal texts), dill was used in many traditional medicines, including those against headache, boils, jaundice, lack of appetite, stomach problems, nausea, liver problems, and many other illness. Dill seeds can also be used to prepare herbal tea.^{13,14} Various names and uses of dill in Asia and Middle East are given in table 3A.1.

Table 3A.1. Various names and uses of dill

Country	Language	Name	Dish
India	Marathi,Konkani	Shepu	Shepuchi Bhaji, Shepu Pulao, Ashe Mast
India	Hindi	Soya	Soya Sabzi(with potato). Green Kheema, Kheema samosa.
India	Kannada	sabbasige soppu	-
India	Telugu	Soa-Kura	-
India	Tamil	Sadakuppi	-
India	Manipuri	Pakhon	chagem pomba
India	Punjabi	Soa	-
India	Gujarati	Suva	Suvaa ni Bhaji(with potato)
India	Malayalam	Chatapushpa	
Iran	Persian	Shevid	Aash, Baghali Polo, Shevid Polo, Mast O Khiar
Arab world	Arabic	شَبَثْ شَبَثْ، (shabat, shabath)	As flavoring in various dishes
Thailand	Thai	phak chee Lao(ผักชีลาว)	Gaeng om(แกงอ่อม)
China	Chinese	shiluo	Baozi

To date, terpenoids, saponins, flavonoids, coumarins, polyacetylenes, steroids, and essential oils have been reported in this family. Some of the major compounds isolated from Apiaceae family are listed in the table given below (table 3A.2).¹⁵

Table 3A.2. Some of the major compounds present in Apiaceae family

3A.2. Aim and Scope of the Present Study

Several species of aromatic plants or spices are used medicinally because of their volatile oils or phytochemical components. In particular, some of them have been traditionally used for a long time in folk medicinal systems. Recent studies on plant

essential oils and their main components have attracted much attention from the scientific community, and have encouraged them to screen these natural products to study their chemical and pharmacological aspects that might potentially lead to the development of new compounds having advantages over current therapeutic drugs. In these aspects, we chose one of the important spices, used worldwide, *Anethum graveolens* for our further studies. From the literature reports, though it is clear that *Anethum graveolens* is one of the promising species which shows various biological activities, a detailed isolation profile is missing for this species. Therefore, a detailed reinvestigation on the phytochemical constituents of *Anethum graveolens* seeds has been undertaken as part of the present study.

3A.3. Isolation and Characterization of Phytochemicals from the Seeds of *Anethum graveolens* L.

3A.3.1. Collection of plant material

Dried seeds of *Anethum graveolens* were purchased from a local Ayurvedic raw drug store, in Southern part of Kerala, India during the month of May 2017.

3A.3.2. Isolation of essential oils

Clevenger apparatus was used for the extraction of volatile oils present in the seeds of *Anethum graveolens*. About 250 g of *Anethum graveolens* seeds were subjected to steam distillation with 2 liters of distilled water for a period of three hours. From this, we obtained around 3 mL of colorless and aromatic essential oil (figure 2.2) which was further subjected to GCMS analysis.

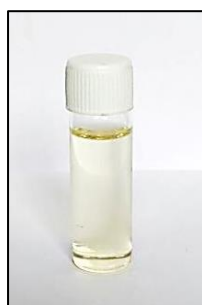


Figure 3A.2. Essential oil isolated from dill seed

From the GCMS analysis it was found that the essential oil mainly consists of limonenes, carvones and 2-methyl-5-(1-ethenyl) cyclohexanones as the major constituents (table 3A.3). Limonene together with carvone constituted almost 50 % of the total essential oil.

Table 3A.3. GCMS analysis of essential oil from dill seeds

Sl No	Ret. Time	Area %	Height %	Compound Name
1	7.894	0.07	0.13	1,6-Octadiene
2	8.473	0.16	0.21	5-Isopropenyl-2-methyl-acetate
3	9.234	5.38	9.64	D-Limonene
4	9.420	20.29	27.46	D-Limonene
5	11.859	0.34	0.56	1-Methyl-4-(1-methylethynyl) Benzene
6	16.658	36.22	23.21	Cyclohexanone
7	16.874	8.96	10.72	Cyclohexanone
8	17.546	0.31	0.29	<i>trans</i> -D-Dihydrocarveol
9	17.644	0.17	0.21	5-Isopropynyl-2- methylcyclohexene
10	18.179	0.19	0.24	<i>cis</i> -D-Dihydrocarveol
11	18.643	20.67	18.72	2-Cyclohexene-1-one
12	34.163	7.24	8.61	1,3-Benzodioxole

3A.3.4. Extraction and isolation of phytochemicals

The air dried and powdered seeds of *A. graveolens* (0.70 kg) were first soaked in 5 L hexane at room temperature for 3 days and the same procedure was repeated twice. Removal of the solvent under reduced pressure gave 22 g of crude extract. The residue was further subjected to acetone extraction, which resulted in 16 g acetone extract. In the same way, we obtained 4 g of ethanol extract and finally the water extract. After studying the TLC, all the extracts were sequentially subjected to column chromatography with 100-200 mesh sized silica gel and was eluted with hexane-ethyl acetate followed by methanol-ethyl acetate mixtures of increasing polarities. All the fraction pools were again subjected to silica gel column chromatography for the isolation of compounds.

A pictorial representation of the entire isolation procedure is given below (figure 3A.3). From the hexane extract, we could isolate five compounds, whereas, twenty molecules were isolated from acetone extract. Finally, two molecules were isolated from ethanol extract.

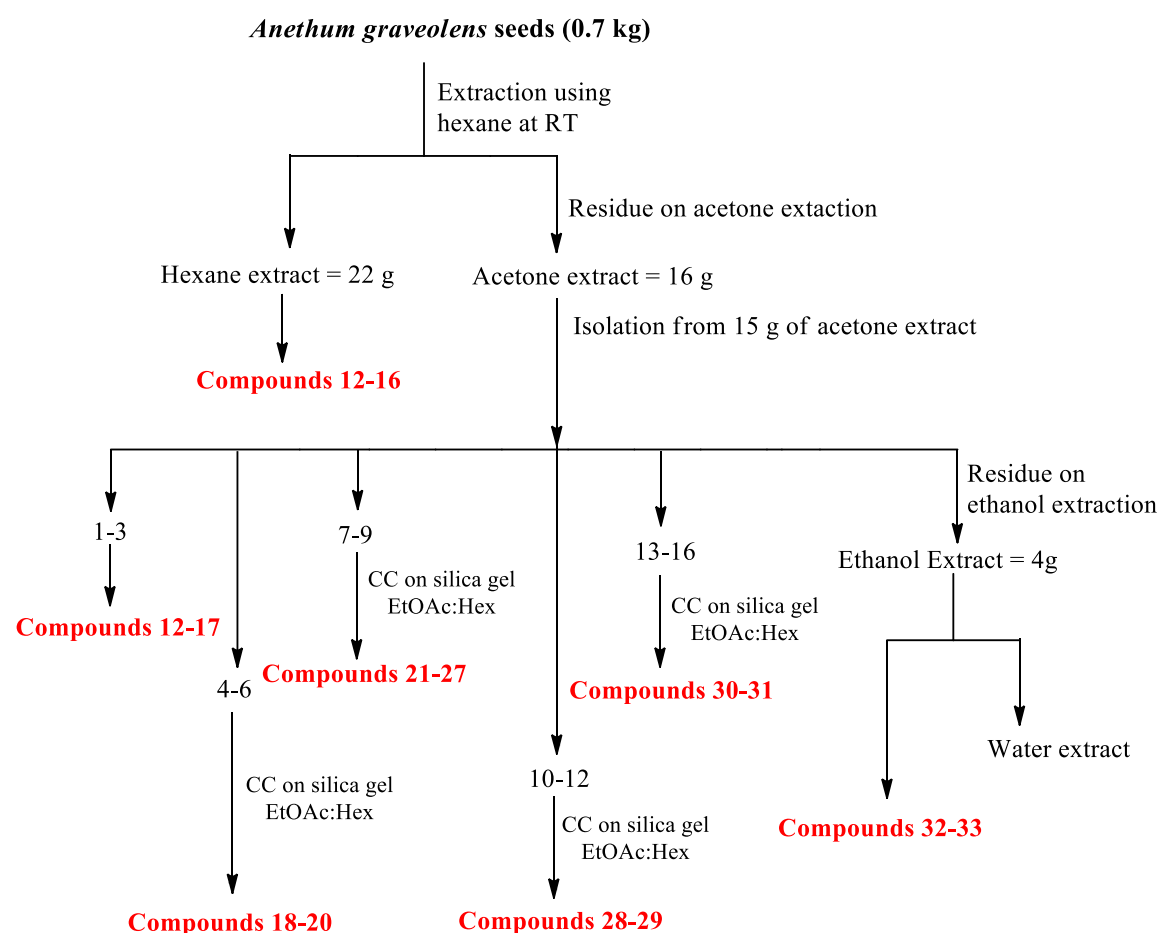
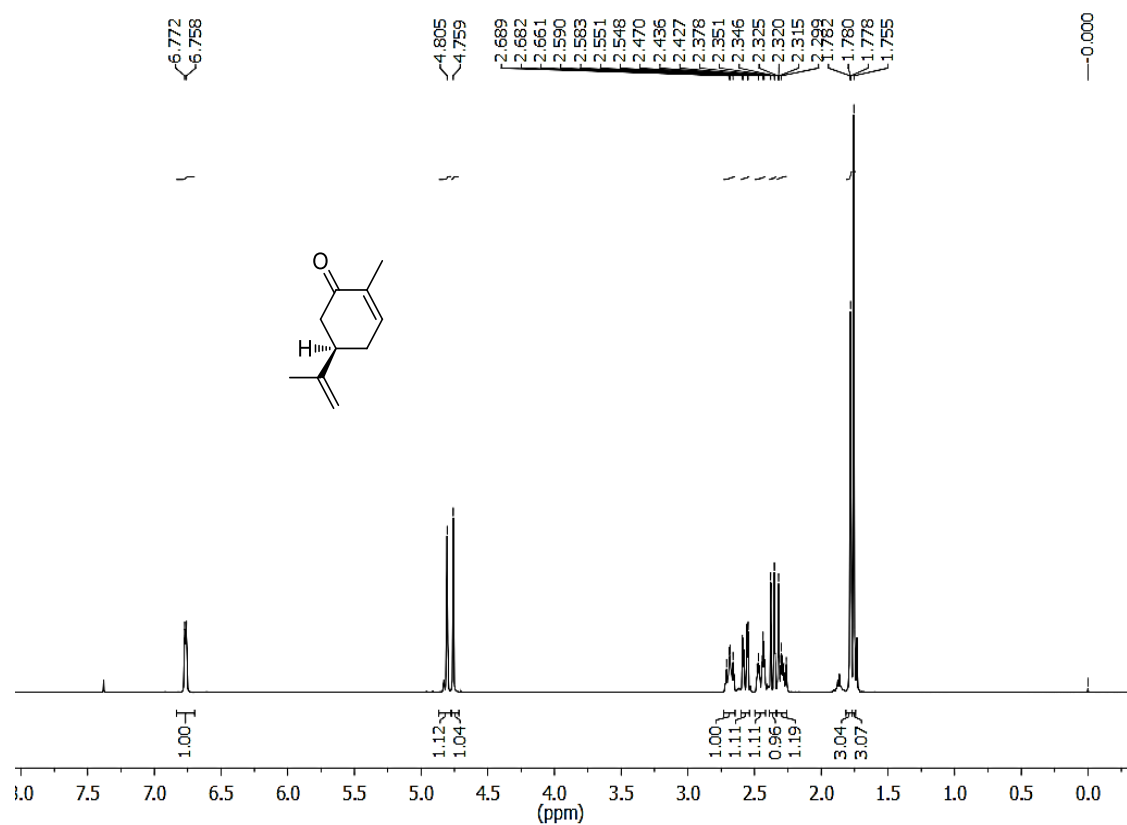
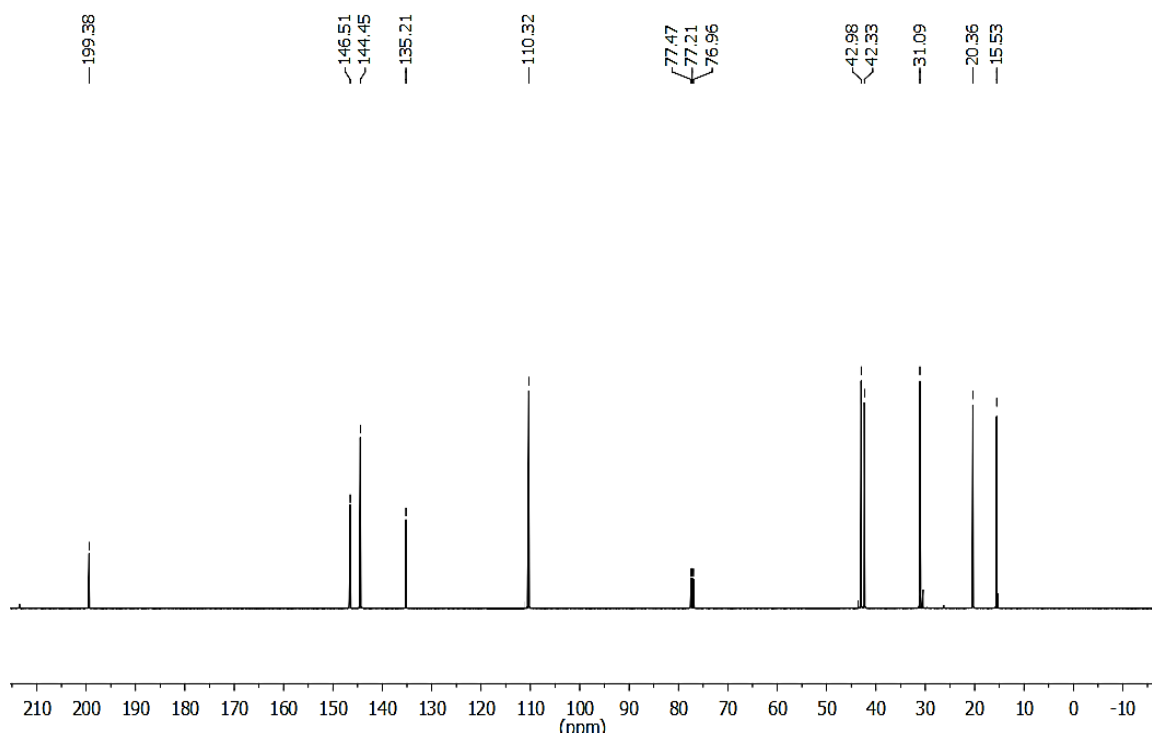
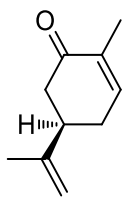


Figure 3A.3. Pictorial representation of extraction and isolation process.

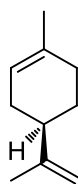
Compounds **12-17** were isolated from hexane extract through repeated column chromatography techniques. Compound **12** was obtained in 6 g as UV active colorless viscous liquid from hexane as well as from fraction pools 1-3 of acetone extract through various column chromatographic methods. The peak at 1675 cm^{-1} in the IR spectrum indicates the presence of an α,β -unsaturated carbonyl group. In the proton NMR (figure 3A.4), three olefinic protons resonated in between δ 6.8-4.7 ppm, and 2D-NMR studies showed that two of them are exocyclic protons. Also the peak resonated at δ 199.4 ppm in carbon NMR (figure 3A.5) indicates the presence of a carbonyl carbon. In addition to these, a total of ten carbons with a cyclohexane ring in the molecule suggested a monoterpene structure. By comparing the IR, ^1H NMR, ^{13}C NMR and other 2D NMR spectral data of this compound with literature reports, the compound was confirmed as (+)-*S*- **carvone** ($[\alpha]_{\text{D}}^{25} = +52.56^\circ$).¹⁶ The structure of the same is given below.

Figure 3A.4. ^1H NMR of compound **12** in CDCl_3 Figure 3A.5. ^{13}C NMR of compound **12** in CDCl_3



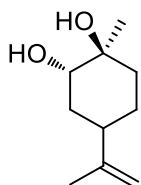
(+) *S*-Carvone
Compound **12**

Compound **13** was obtained in 4.6 g as UV inactive viscous liquid with blue charring in Mc Gill stain solution. Similar to compound **12**, here also olefinic protons resonated in between δ 5.5 and 4.5 ppm, in which two of them were confirmed as exocyclic protons (figure 3A.6). The two singlets resonated at δ 1.73 and 1.65 ppm confirmed the presence of two methyl groups. A total of ten carbons in the carbon NMR (figure 3A.7), with a cyclohexane ring supported the structure of the compound as a monoterpene. By comparing the spectral data with the literature reports, the compound was confirmed as (-) *S*-limonene ($[\alpha]_D^{25} = -81.12^\circ$).¹⁶ The structure of the compound is given below.

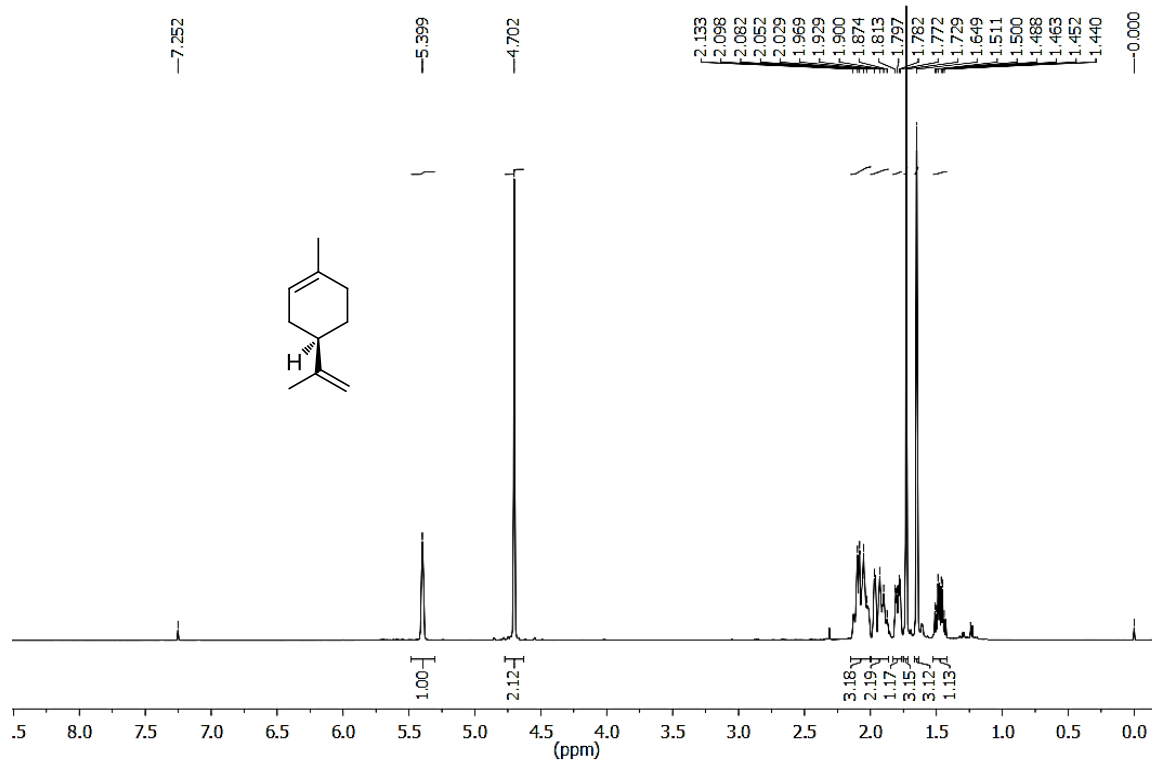
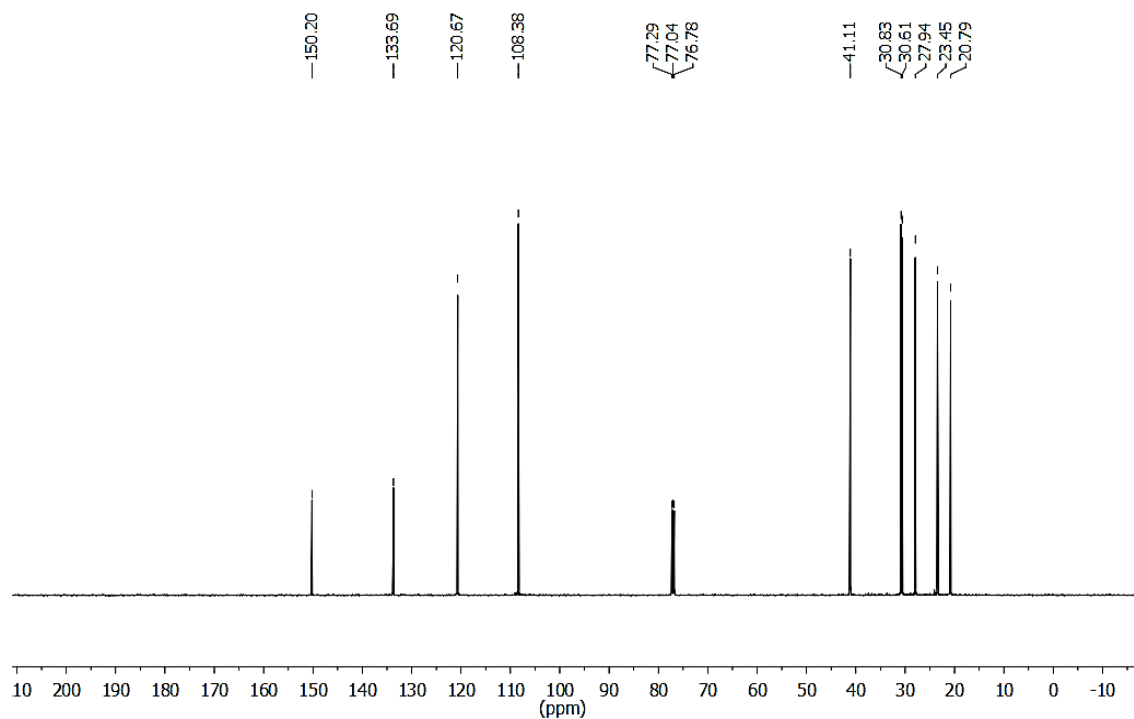


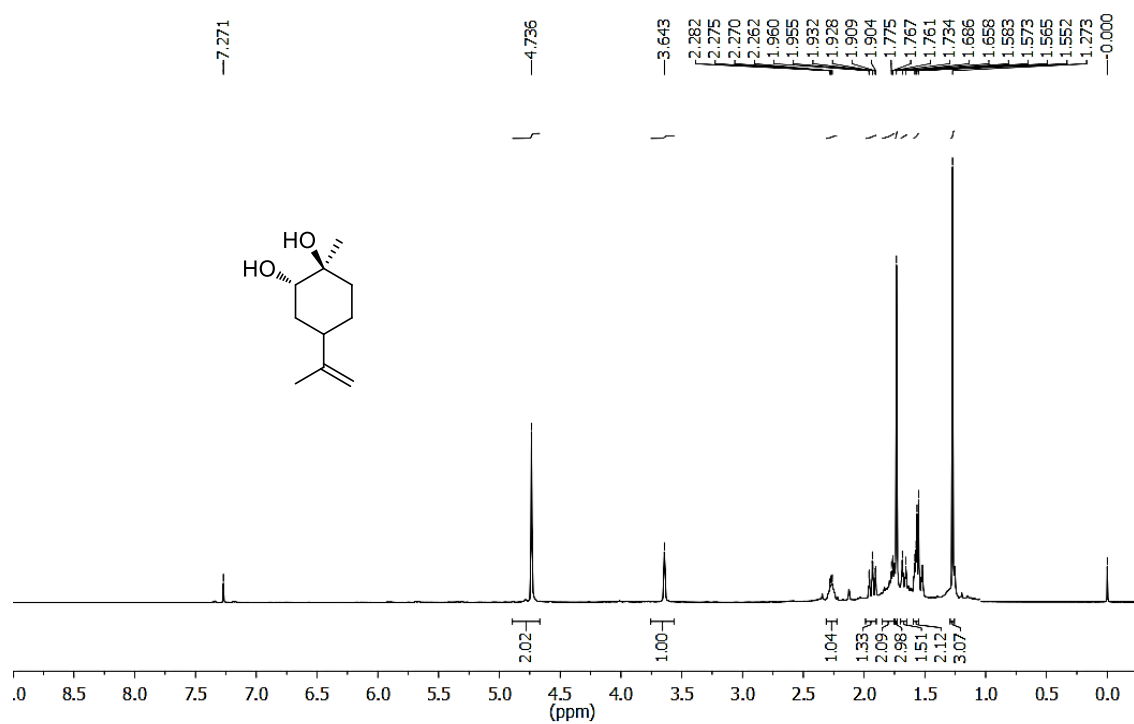
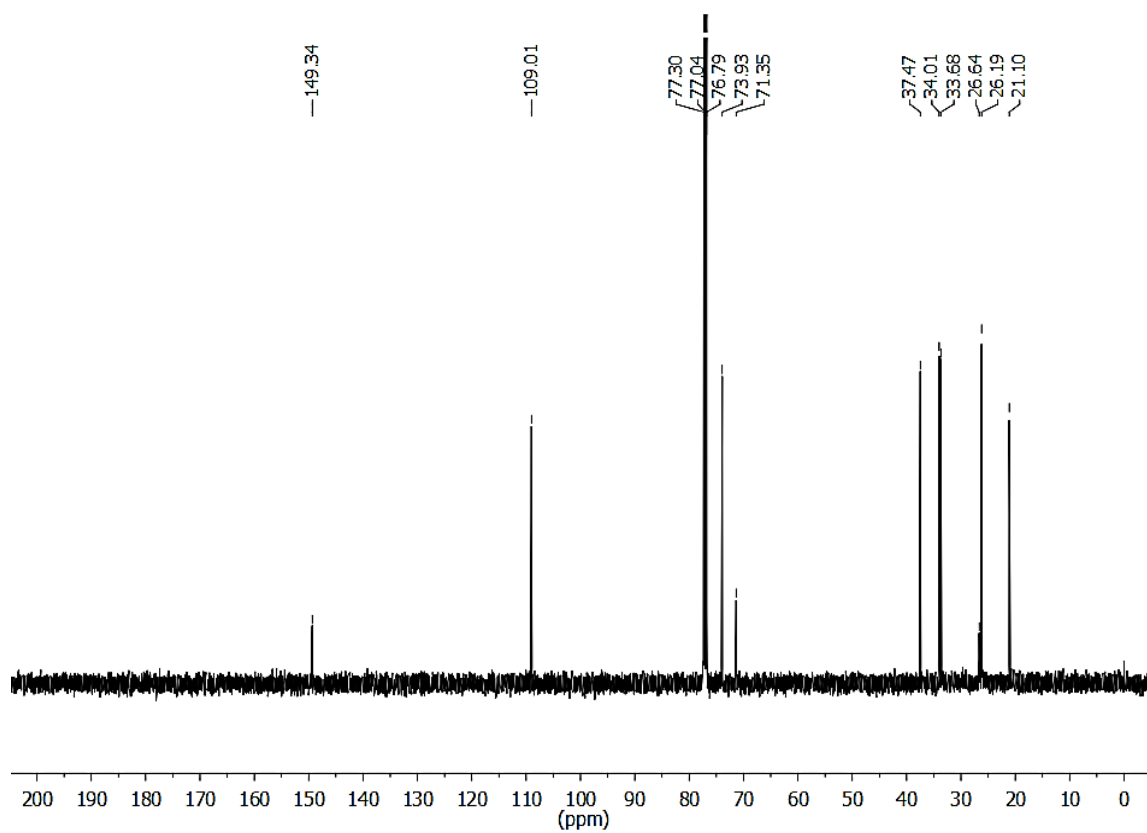
(-) *S*-Limonene
Compound **13**

Compound **14** was also UV inactive with a blue charring in Mc Gill stain solution. The exocyclic olefinic protons resonated at δ 4.75 ppm as a singlet (figure 3A.8). The proton that resonated at δ 3.64 ppm as one proton singlet along with two carbons at δ 73.9 and 71.4 confirmed presence of a diol system (figure 3A.9). Also the resemblances of the spectral data with that of compounds **12** and **13**, clearly confirm that the molecule consists a monoterpene skeleton. Finally, from the spectral data and literature reports, the molecule was confirmed as **limonene diol** (viscous liquid-27 mg).¹⁷

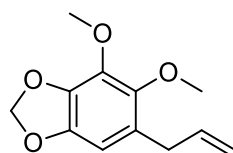


Limonene diol
Compound **14**

Figure 3A.6. ^1H NMR of compound 13 in CDCl_3 Figure 3A.7. ^{13}C NMR of compound 13 in CDCl_3

Figure 3A.8. ^1H NMR of compound **14** in CDCl_3 Figure 3A.9. ^{13}C NMR of compound **14** in CDCl_3

Compound **15** was obtained in 6.8 g as UV active viscous liquid from hexane as well as first fraction pools of acetone extract. In the proton NMR, the two singlets at δ 4.01 and 3.76 ppm confirmed that the molecule consists of two methoxy groups (figure 3A.10 and 3A.11). The two proton singlet at δ 5.88 ppm with a carbon at δ 101.1 ppm at negative region in DEPT suggests that the molecule consists of a methylenedioxy group. Also, the carbon at δ 115.5 ppm bearing two protons (as exocyclic system) having a HOMO COSY relation with an olefinic proton and a HMBC relation with an aliphatic methylene group evidently gives the presence of a propene side chain. In the HRMS spectrometry the molecule gave a peak at 223.0973, corresponding to $(M+H)^+$. By comparing these spectral data with the literature reports, the compound was confirmed as **dillapiol**.¹⁸



Dillapiol
Compound **15**

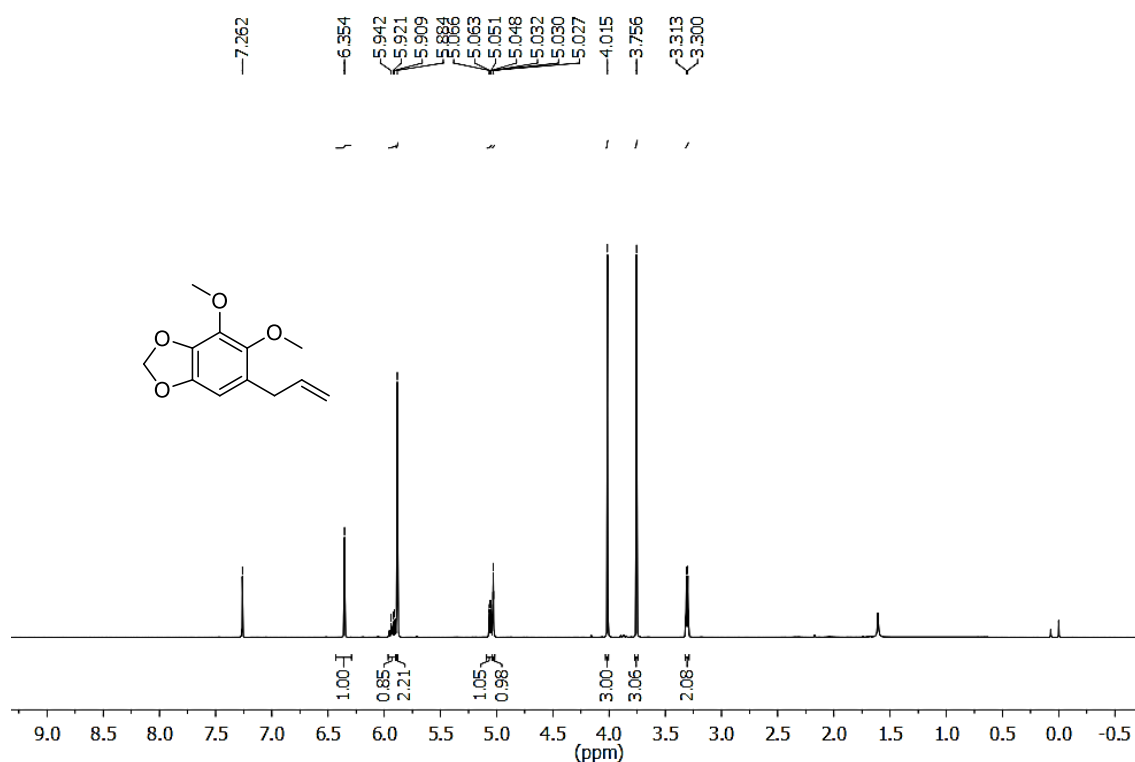


Figure 3A.10. ^1H NMR of compound **15** in CDCl_3

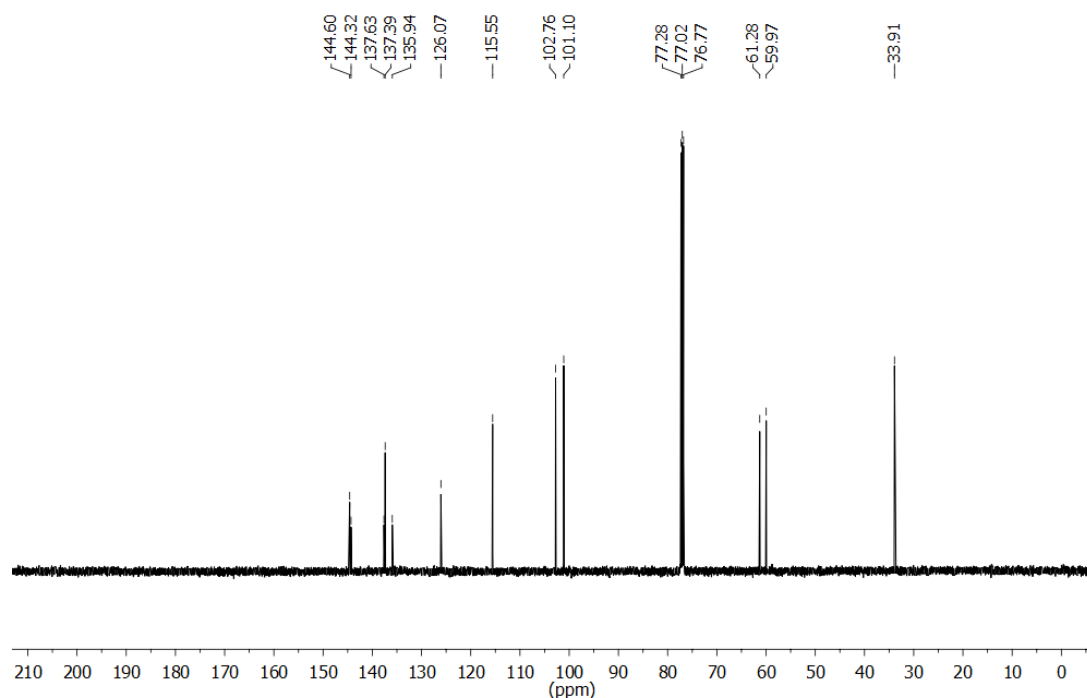
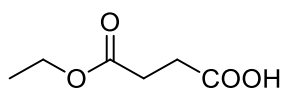


Figure 3A.11. ^{13}C NMR of compound **15** in CDCl_3

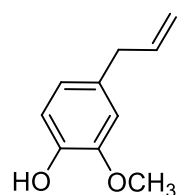
From hexane extract, we could also isolate one molecule, showing two carbonyl carbons in the carbon NMR, which was confirmed as **4-ethoxy-4-oxo butanoic acid**. The carbonyl carbon of carboxylic and ester groups resonated at δ 177.2 and 172.2 ppm respectively. In the IR spectra, the carbonyl stretching frequencies were obtained at ν_{max} 1780 and 1765 cm^{-1} . All other spectral data were in good agreement with the proposed structure (colorless waxy substance).



4-Ethoxy-4-oxobutanoic acid
Compound **16**

Compound **17** was obtained in 230 mg as a pale yellow viscous liquid with pleasant smell. The three proton singlet resonated at δ 3.85 ppm (figure 3A.12) with a carbon at δ 55.9 ppm (figure 3A.13) confirmed the presence of a methoxy group. The broad singlet without carbon which resonated at δ 5.60 ppm confirmed that the molecule possess a phenolic hydroxyl group. Also the peak at δ 3.31 ppm, resonated as doublet for two hydrogen and the HMBC relations of the molecule with an exocyclic olefinic system clearly states that the molecule bears a propylene side chain. The aromatic protons along with

olefinic protons resonated in between δ 6.84 and 5.04 ppm. Also in HRMS analysis, a peak corresponding to $(M+H)^+$ was obtained at 165.0919. From the detailed NMR studies the structure of the compound was confirmed as **eugenol** and the same is given below.¹⁹



Eugenol
Compound **17**

From fraction pools 4-6, three compounds were isolated, namely compound **18**, **19** and **20**. Compound **18** was obtained in 21 mg as a UV active colorless viscous liquid. In the proton NMR, the six proton singlet at δ 3.85 ppm and a three proton singlet at δ 3.83 ppm indicated the presence of three methoxy groups (figure 3A.14). The presence of six quaternary carbons, verified from carbon and DEPT spectra supported the presence of a fully substituted aromatic ring (figure 3A.15). Also, the two proton singlet at δ 6.41 ppm, with carbon at δ 105.4 ppm having a negative phase in the DEPT 135 indicates the presence of a methylenedioxy system. In the HRMS analysis, a peak corresponding to $(M+H)^+$ was obtained at 253.1076. Then comparing the spectral data of the molecule with dill apiol and other literature reports, the compound was confirmed as **nothoapiol**.²⁰

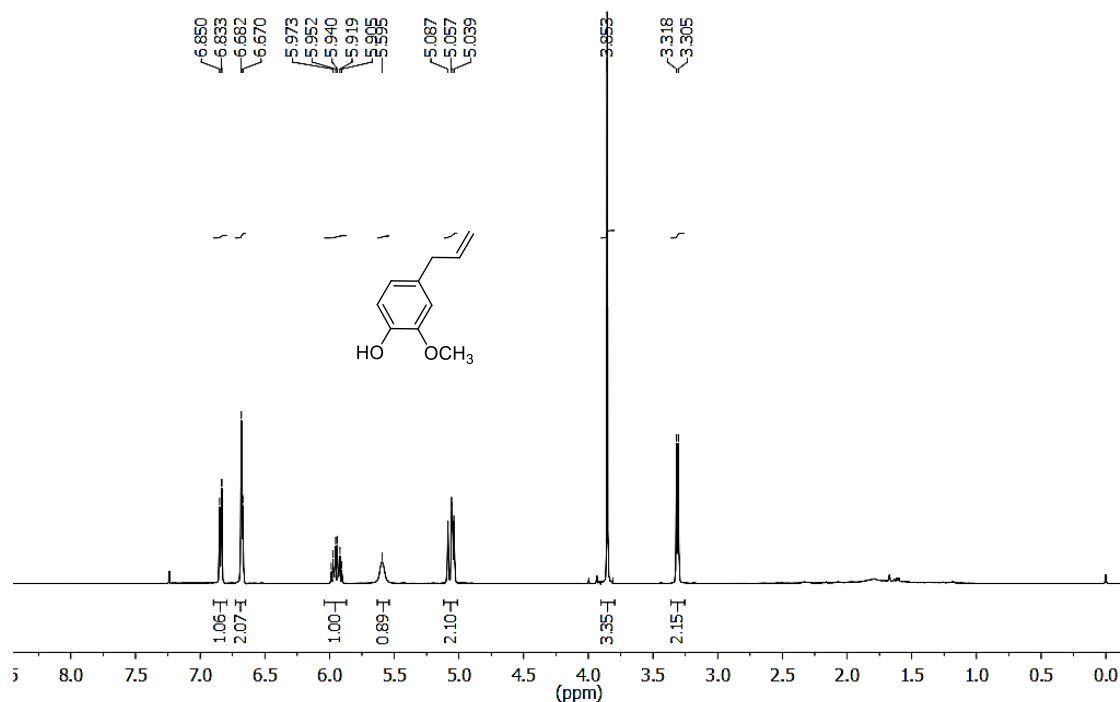


Figure 3A.12. ^1H NMR of compound **17** in CDCl_3

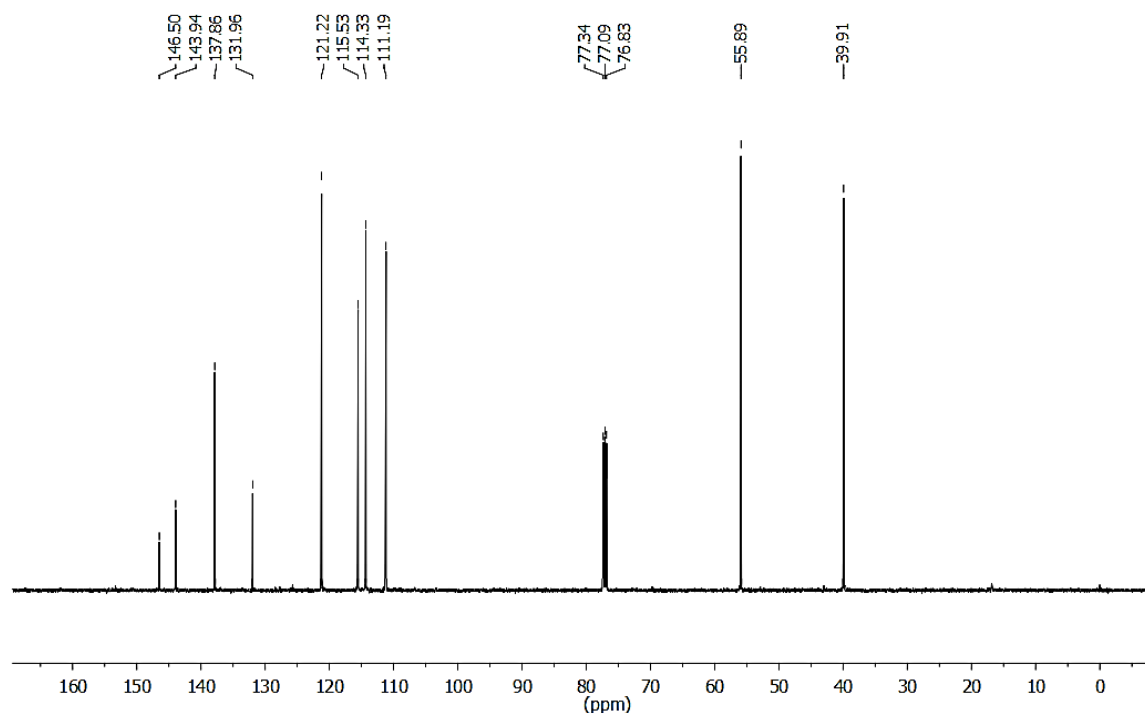
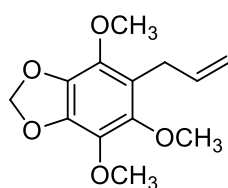


Figure 3A.13. ^{13}C NMR of compound **17** in CDCl_3



Nothoapiol
Compound **18**

Compound **19** was obtained in 16 mg as a pale yellow colored viscous liquid. It showed an intense blue color in short UV. The two 3 proton singlets resonated at δ 4.02 and 3.77 ppm clearly indicate the presence of two methoxy groups (figure 3A.16). The two proton singlet at δ 5.92 ppm in the proton NMR with a carbon δ 101.4 ppm having a negative phase in the DEPT spectra points to the presence of a methylenedioxy group (figure 3A.17). In the IR spectra, the peak at 3341cm^{-1} suggested the presence of a hydroxyl group. The one proton doublet at δ 6.83 ppm, with a coupling constant of 16 Hz could be attributed to the *trans* coupled olefinic proton. Also, the two proton doublet at δ 4.31 ppm having carbon at δ 64.1 ppm can be assigned to the protons near the hydroxyl group. The mass spectrum of the compound showed a molecular ion peak at 239.0919, which is the $(\text{M}+\text{H})^+$ peak. From all these spectral data and on comparison with the literature reports,

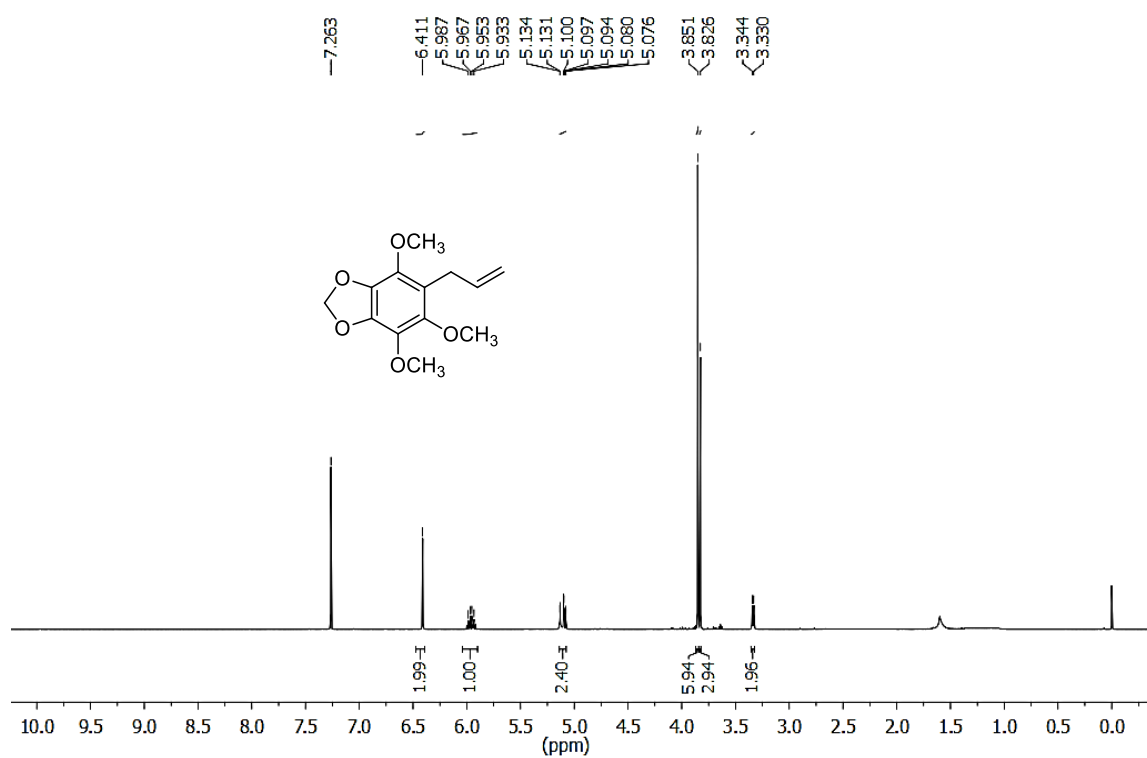


Figure 3A.14. $^1\text{H NMR}$ of compound **18** in CDCl_3

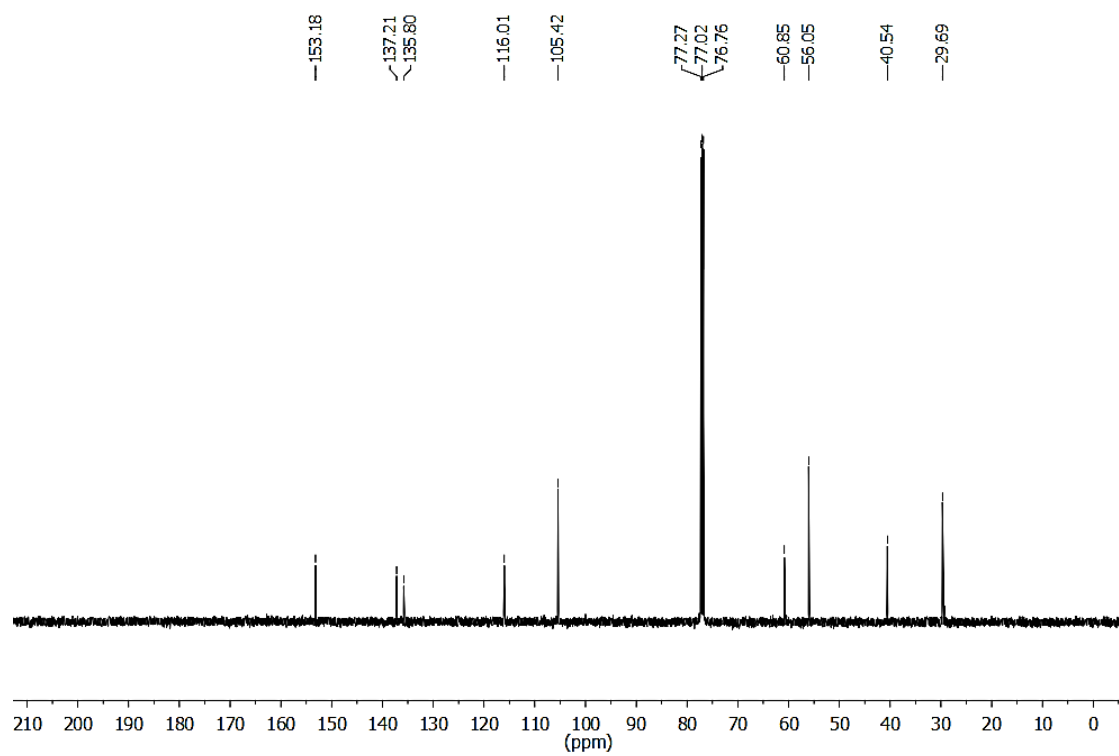
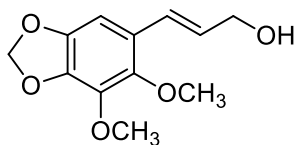


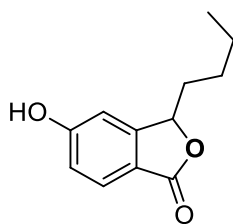
Figure 3A.15. $^{13}\text{C NMR}$ of compound **18** in CDCl_3

compound **19** was confirmed as ω -hydroxyapiol.²¹ The structure of the compound is shown below.



ω -hydroxyapiol
Compound **19**

From the fraction pools 4-6, one more molecule was obtained as colorless solid, during column chromatography with 15 % ethyl acetate in hexane polarity, which was labelled as compound **20** (16 mg). In the IR spectra, the compound gave peaks at 3112 and 1745 cm^{-1} which clearly indicate the presence of a hydroxyl as well as a carbonyl group. The peaks at δ 7.76 (d, $J = 8.5$ Hz), 6.99 (dd, $J_1 = 8.5$ Hz, $J_2 = 2$ Hz, 1H) and 6.86 (d, $J = 2$ Hz, 1H) ppm give a clear picture of an *ortho* coupled proton system along with a *meta* substituted proton (figure 3A.18 and 3A.19). The three consecutive $-\text{CH}_2-$ protons along with a methyl system in between δ 0.9 to 2 ppm with a sequential diagonal relationship in HOMO COSY confirmed the presence of a *n*-butane chain. Mass spectrum of the molecule showed molecular ion peak at m/z 207.0918 corresponding to $(\text{M}+\text{H})^+$. From these spectral data and on comparison with the literature reports, compound **20** was confirmed as an **isobenzofuranone derivative**, and is the first report from this species. Some similar type of compounds have already been reported from this family.²²



3-Butyl-5-hydroxyisobenzofuran-1(3H)-one
Compound **20**

Compounds **21-27** were isolated from fraction pools 7-9. Compound **21** was an intense UV active pale yellow solid with a molecular ion peak at 309.0763 corresponding to $(\text{M}+\text{H})^+$ (9 mg). The singlet proton resonated at δ 13.60 ppm without a carbon atom in HMQC, confirmed the presence of a phenolic hydroxyl group, having a hydrogen bond (figure 3A.20). In the proton NMR, three protons at δ 9.50 (d, $J = 2.5$ Hz), 7.80 (d, $J = 9$ Hz) and 7.24 (dd, $J_1 = 8.5$ Hz, $J_2 = 2.5$ Hz) ppm clearly attributed to an *ortho* coupled aromatic system, along with a *meta* coupled proton. The three proton singlet at δ 4.05 ppm,

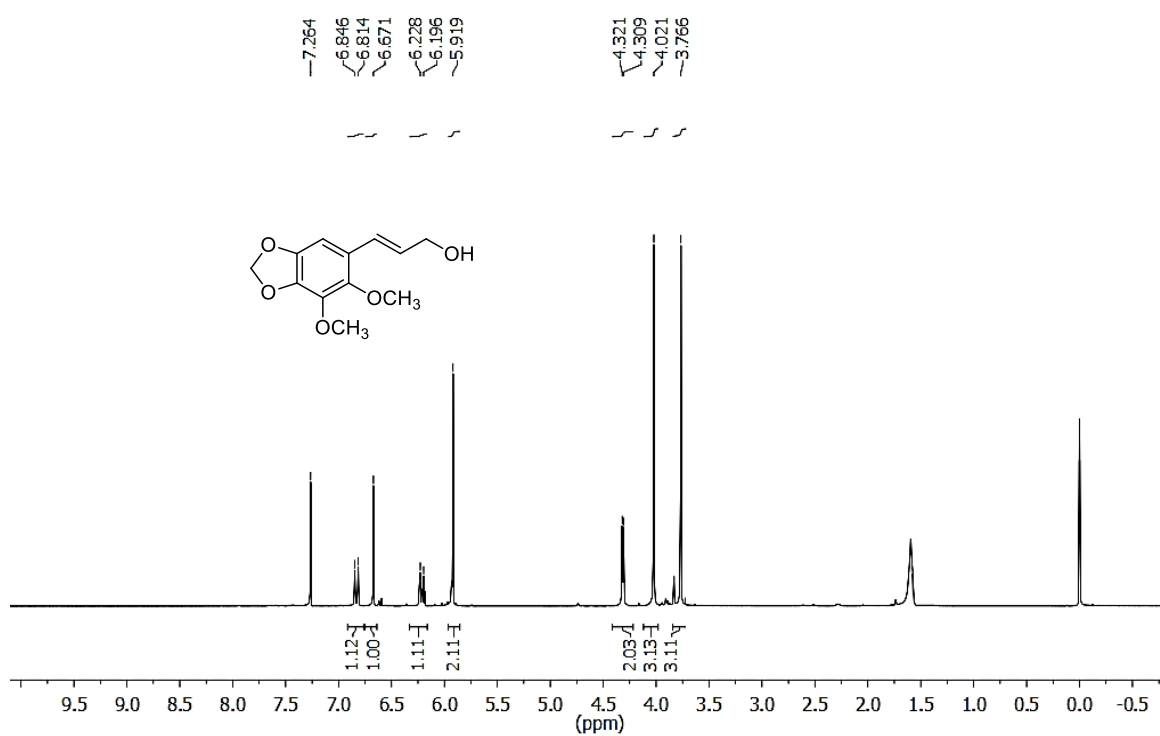


Figure 3A.16. ¹H NMR of compound **19** in CDCl₃

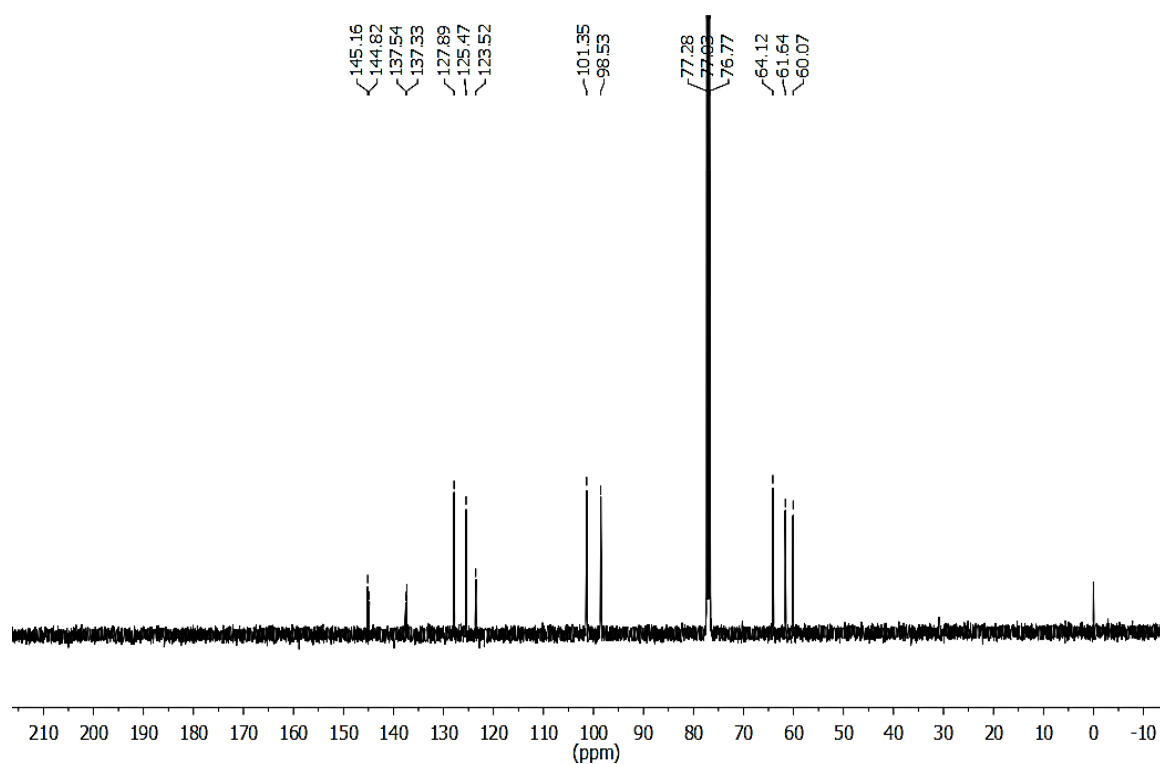


Figure 3A.17. ¹³C NMR of compound **19** in CDCl₃

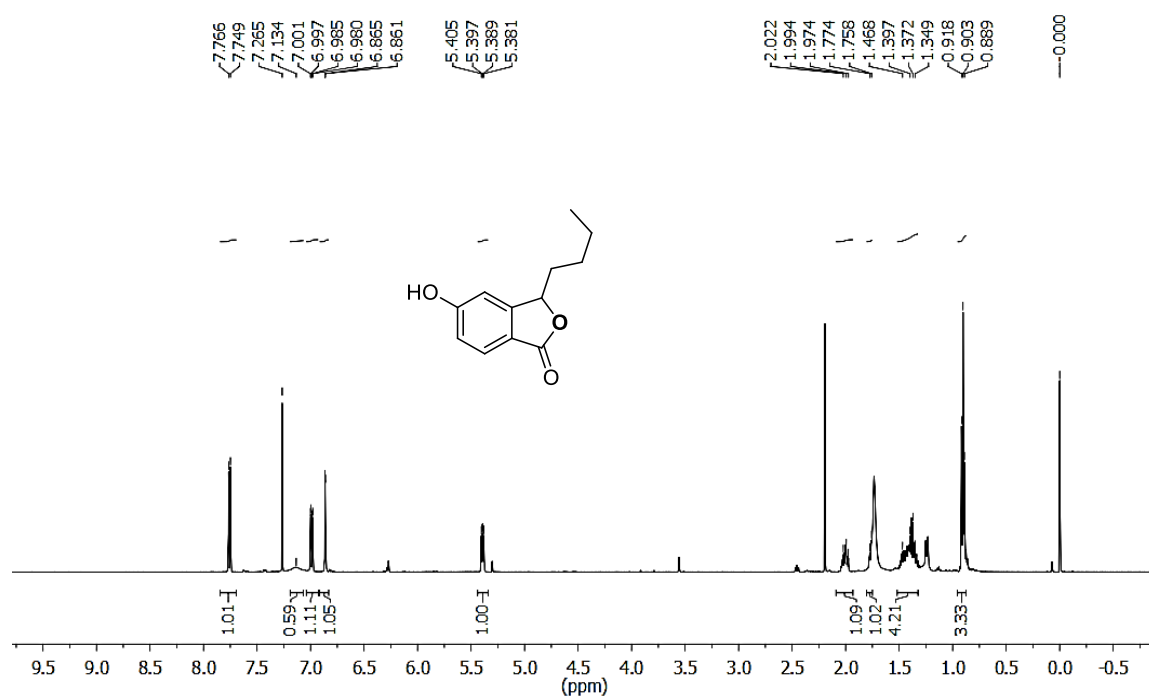


Figure 3A.18. ^1H NMR of compound 20 in CDCl_3

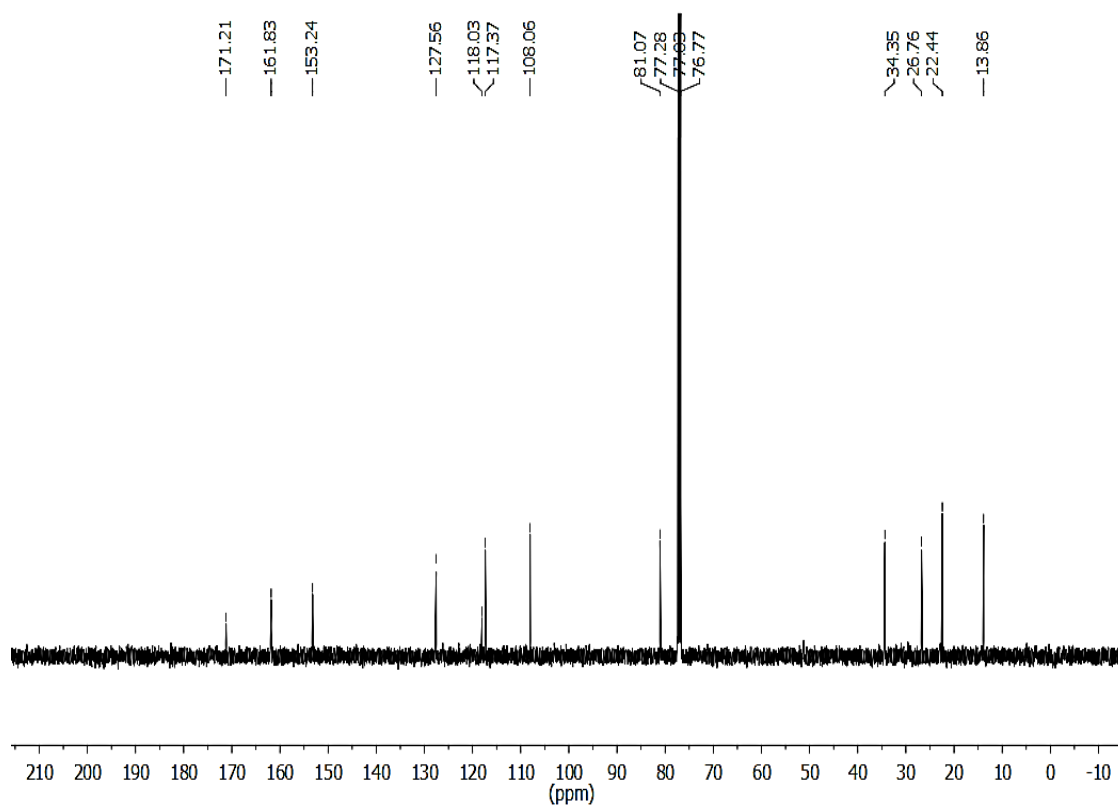
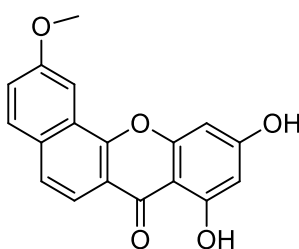


Figure 3A.19. ^{13}C NMR of compound 20 in CDCl_3

with a carbon at δ 55.6 ppm suggest the presence of a methoxy group (figure 3A.20). Carbon NMR spectrum showed sixteen peaks ranging from δ 164 - 93 ppm which confirmed the presence of sixteen aromatic carbons (figure 3A.21), among which ten were identified as quaternary from DEPT. In addition to this, a peak at δ 183.2 ppm suggested the presence of a carbonyl system. Also, two doublets at δ 6.34 ($J = 1.5$ Hz) and 6.32 ($J = 2$ Hz) could be attributed to a highly shielded *meta* coupled aromatic system. From all these data and on comparison with the literature reports, compound **21** was confirmed as a **xanthone derivative**²³ and the structure of the same is given below.



8,10-Dihydroxy-2-methoxy-7H-benzo[c]xanthen-7-one
Compound **21**

Compound **22** (6 mg) was obtained as a pale yellow colored solid from fraction pools **21-27**, while eluting the column with 10 % ethyl acetate in hexane. The IR spectrum of the compound showed absorption at 3333 and 1701 cm^{-1} suggesting the presence of hydroxyl as well as a carbonyl groups. Proton NMR (figure 3A.22) and carbon NMR spectra (figure 3A.23) of the compound was suggestive of a xanthone type compound, just like compound **21**. In the proton NMR, three protons at δ 8.32 (d, $J = 3$ Hz), 7.11 (d, $J = 8$ Hz) and 6.78 (dd, $J_1 = 8$ Hz, $J_2 = 3$ Hz) pp clearly suggest an *ortho* coupled aromatic system, along with a *meta* coupled proton. The three proton singlet at δ 3.86 ppm (corresponding to a methoxy group with carbon at δ 55.5 ppm) having HMBC correlation with these protons shows that, their sequential interactions were interrupted by this aromatic methoxy group. The one proton singlet at δ 13.32 ppm without carbon correlation in HMQC clearly indicates the presence of an enolisable hydroxyl group or a hydrogen bonded system. The two proton broad singlet between δ 6.34 and δ 6.29 ppm, having carbons at δ 93.7 and 99.5 ppm obviously indicate the presence of a *meta* coupled aromatic protons. The two multiplets at δ 2.93 and 2.87 ppm indicate the presence of two $-\text{CH}_2-$ groups, which were further confirmed from DEPT-135 (in which their respective carbons (δ 26.8 and 28.5 ppm) gave the signals at negative region). The co-relations of these two $-\text{CH}_2-$ groups with aromatic carbons at positions 4, 13, 14 and 15 in HMBC spectrum (figure 3A.24), suggest that, these protons are entrapped

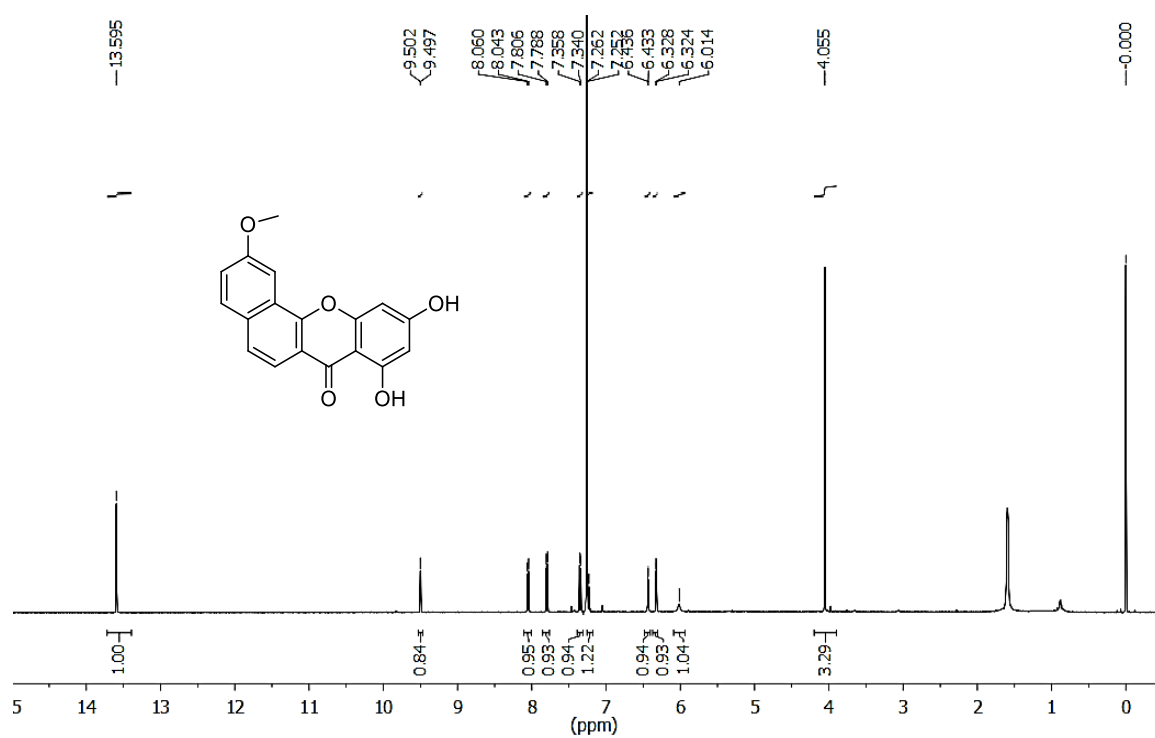


Figure 3A.20. $^1\text{H NMR}$ of compound **21** in CDCl_3

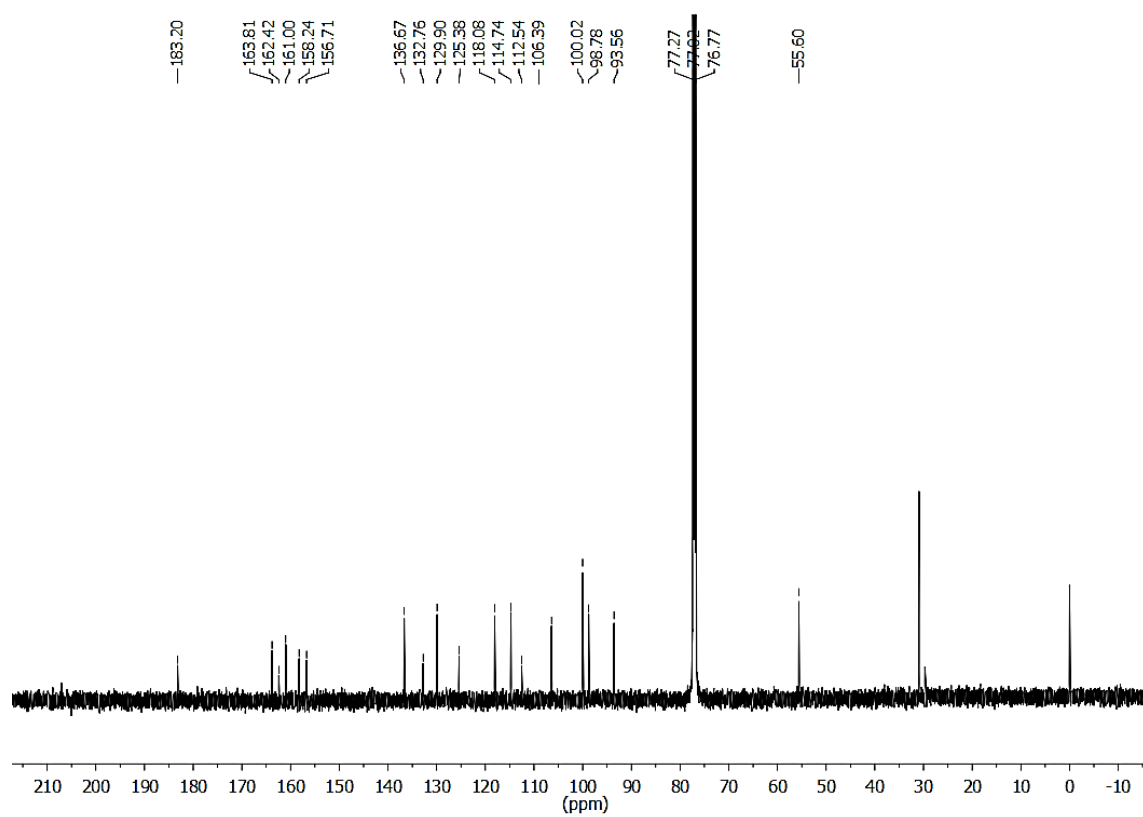
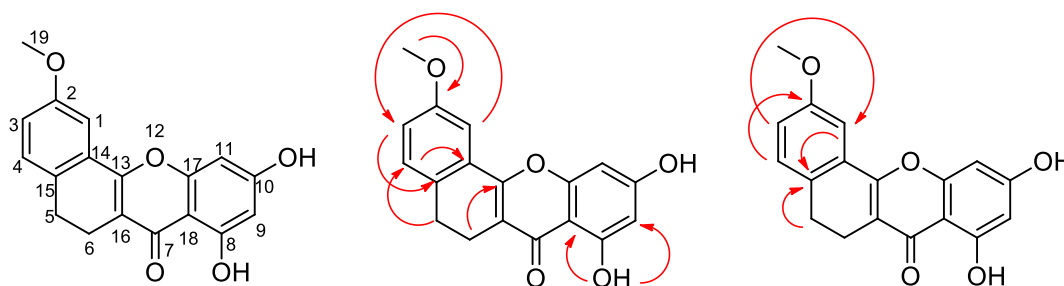


Figure 3A.21. $^{13}\text{C NMR}$ of compound **21** in CDCl_3

within the aromatic system. All the NMR data of the molecule is given in the table 3A.4. Finally, the molecular ion peak at 311.0925 corresponding to $(M+H)^+$ also given by the compound (also $(M+Na)^+$ peak at 333.0745) suggests the structure given below. To the best of our knowledge, there were no reports on the structure given below, and this molecule can be considered as a novel one.



8,10-Dihydroxy-2-methoxy-5H-benzo[c]xanthen-7(6H)-one
Compound **22**

Figure 3A.24. Some selected HMBC interactions are given in red curves

Compound **23** (4 mg) was also obtained as a pale yellow colored solid from the fraction pools **21-27**, while eluting the column with 12 % ethyl acetate in hexane. The IR spectrum of the compound showed absorptions at 3211, 1740 and 1688 cm^{-1} suggesting the presence of hydroxyl as well as carbonyl groups. Proton NMR (figure 3A.25) and carbon NMR spectra (figure 3A.26) of the compound were suggestive of a xanthone type compound just like compound **21** and **22**. The multiplet between δ 2.2 and 2.88 ppm in the proton NMR indicates the presence of two $-\text{CH}_2-$ groups and was further confirmed from DEPT-135, in which their respective carbons (δ 26.8 and 28.5 ppm) gave the signals at the negative region. In the proton NMR, three protons at δ 8.21 (d, $J = 2.5$ Hz), 7.08 (d, $J = 8$ Hz) and 6.74 (dd, $J_1 = 8$ Hz, $J_2 = 2.5$ Hz) ppm clearly attributed to an *ortho* coupled aromatic system, along with a *meta* coupled proton as in the previous cases. The one proton singlet at δ 13.42 ppm without carbon correlation in HMQC clearly indicates the presence of an enolisable hydroxyl group or a hydrogen bonded system. The one proton singlet at δ 6.32 ppm having carbon at δ 94.4 ppm obviously indicates the presence of an uncoupled aromatic proton. The co-relations of the two $-\text{CH}_2-$ groups with aromatic carbons at positions 16, 17 and 18 in HMBC spectrum (figure 3A.27), suggest that, these protons are entrapped with in the aromatic system. Also, the one proton triplet at δ 4.78 ppm, having a HOMO COSY interaction with another $-\text{CH}_2-$ group indicates the presence of a highly deshielded side chain to the aromatic system.

Table 3A.4. Proton and carbon data of compound **22**

Position	Proton NMR (¹ H NMR)	Carbon NMR (¹³ C NMR)	HMBC Correlations
1	8.32 (d, $J = 3$ Hz)	112.7	125.6, 113.1
2	-	158.5	
3	6.78 (dd, $J_1 = 8$ Hz, $J_2 = 3$ Hz)	113.1	112.7, 125.6
4	7.11 (d, $J = 8$ Hz)	128.0	130.3, 158.5, 26.3
5	2.93 (m)	26.8	128.0, 125.6
6	2.87 (m)	28.5	168.0
7	-	180.3	
8	13.32 (OH)		161.8
9	6.30	99.5	
10	OH		156.9
11	6.34	93.8	
12	-	-	
13	-	168.0	
14	-	130.5	
15	-	125.6	
16	-	114.1	
17	-	163.2	
18	-	106.1	
19	3.86 (s, 3H)	55.5	
Solvent CDCl ₃ , values are expressed as δ in ppm			

Finally, the 2 three proton singlets at δ 1.38 and 1.26 ppm, possessing HMBC and HOMO COSY interactions with the previous signals give a closed system to the side chain. All the NMR data of the molecule is given in the table 3A.5. Lastly, the molecular ion peak at 381.1338 corresponding to $(M+H)^+$ given by the compound (also $(M+Na)^+$ peak at 403.1158) suggests the structure given below. To the best of our knowledge, this molecule is being reported for the first time or can be considered as a novel molecule.

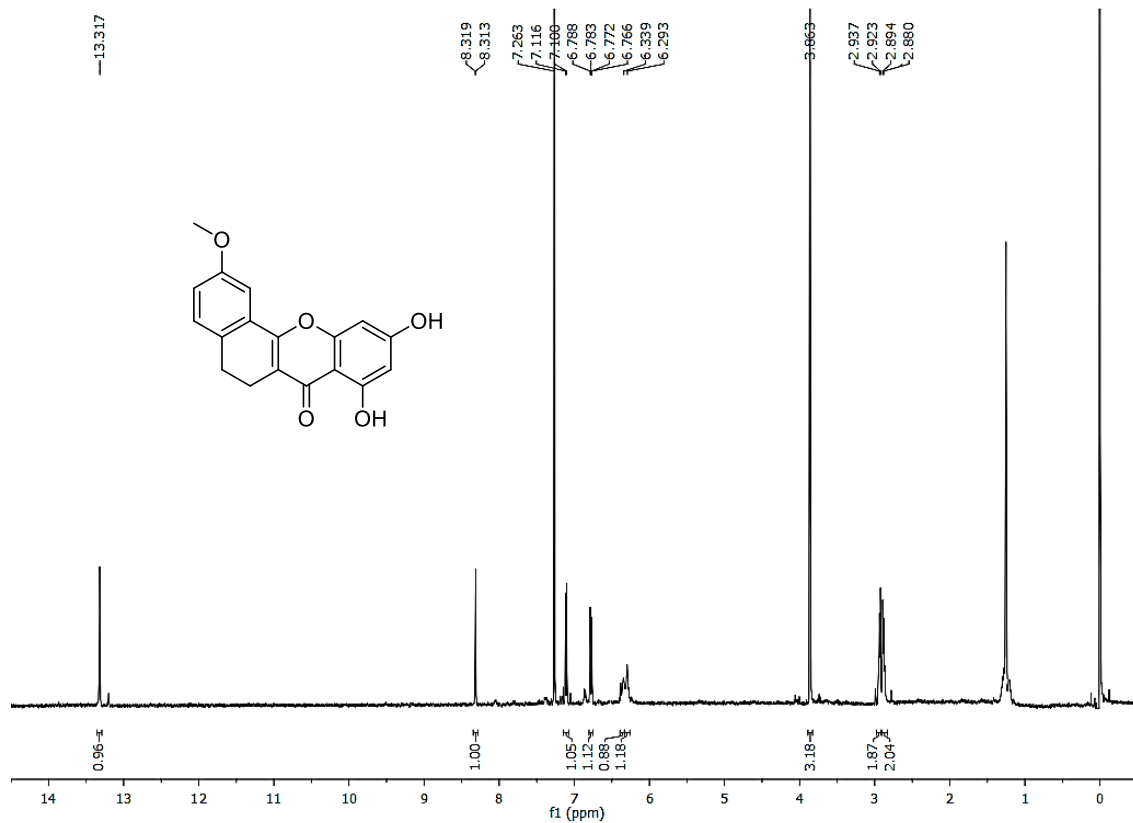
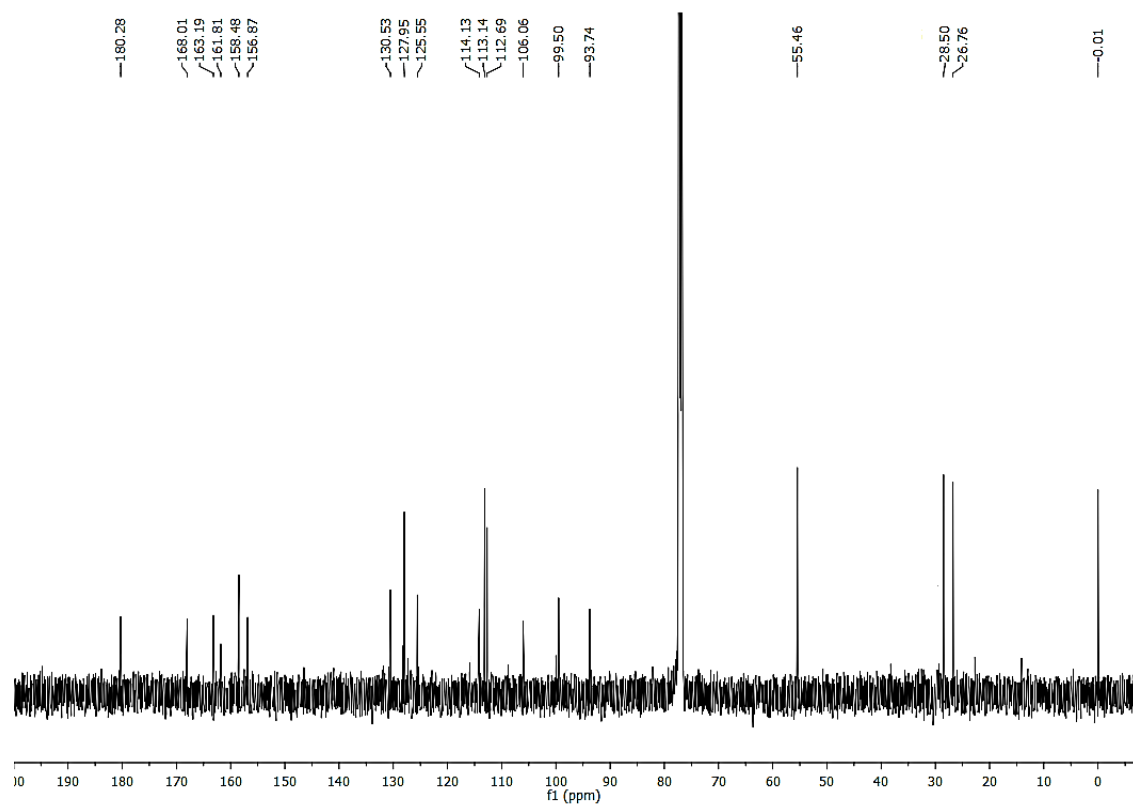
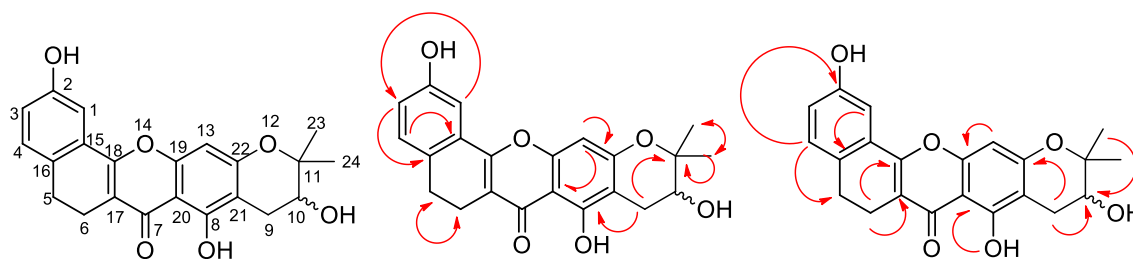
Figure 3A.22. ^1H NMR of compound 22 in CDCl_3 Figure 3A.23. ^{13}C NMR of compound 22 in CDCl_3

Table 3A.5. Proton and carbon data of compound **23**

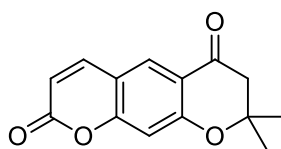
Position	Proton NMR (^1H NMR)	Carbon NMR (^{13}C NMR)	HMBC Correlations
1	8.21 (d, $J = 2.5$ Hz)	114.4	125.5, 113.9
2	OH		105.8, 163.7
3	6.74 (dd, $J_1 = 8$ Hz, $J_2 = 2.5$ Hz)	113.9	125.5
4	7.08 (d, $J = 8$ Hz)	128.3	130.6, 154.5, 26.8
5	2.92 (m)	26.8	28.5, 125.5, 167.5
6	2.88 (m)	28.5	167.5, 26.5, 125.5, 113.8
7	-	180.3	
8	13.42 (OH)		163.7, 105.8
9	3.23 (dd, $J_1 = 8.5$ Hz, $J_2 = 2$ Hz)	27.0	71.9, 91.5, 103.2, 151.6, 165.9
10	4.78 (t, $J = 9$ Hz), 4.98 (OH, brs)	91.5	
11	-	71.9	
12	-	-	
13	6.32 (s)	94.4	103.2, 105.8, 163.6, 165.9
14	-	-	
15	-	130.6	
16		125.5	
17		113.8	
18		167.5	
19		163.7	
20		105.8	
21		103.2	
22		165.9	
23	1.38 (s, 3H)	26.0	71.9, 91.5, 24.2
24	1.26 (s, 3H)	24.2	71.9, 91.5, 26.0
Solvent CDCl_3 , values are expressed as δ in ppm			



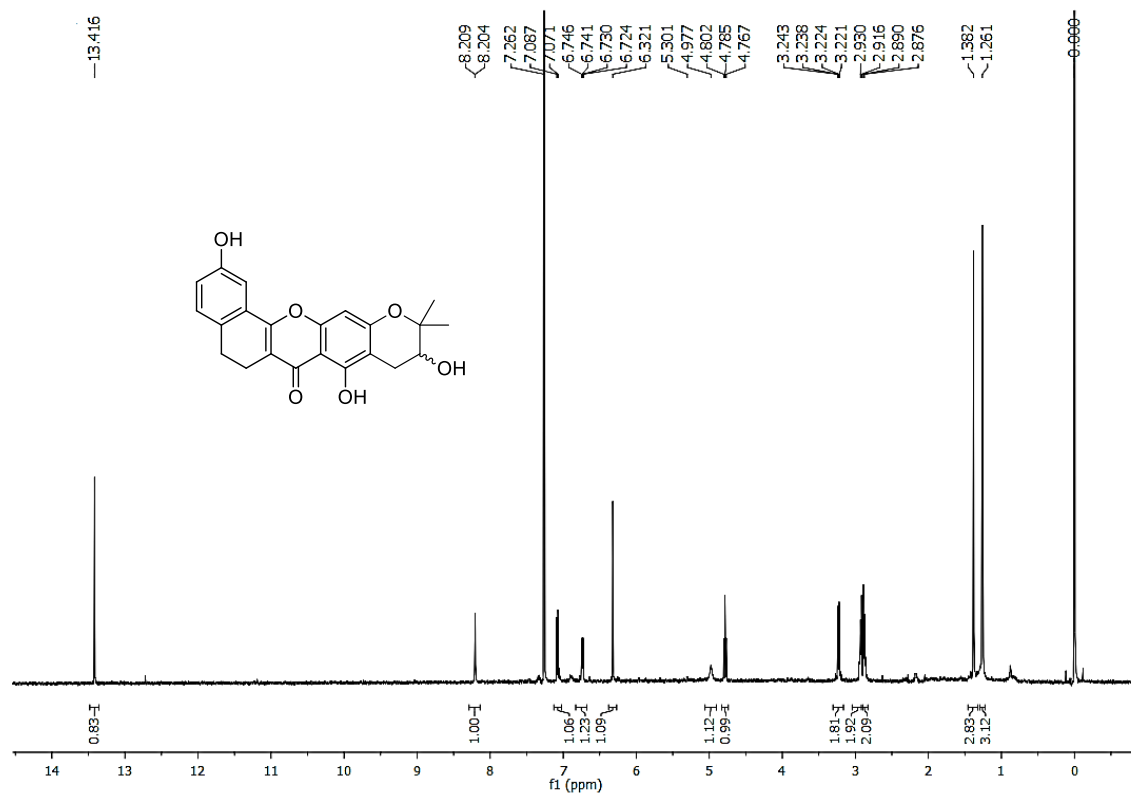
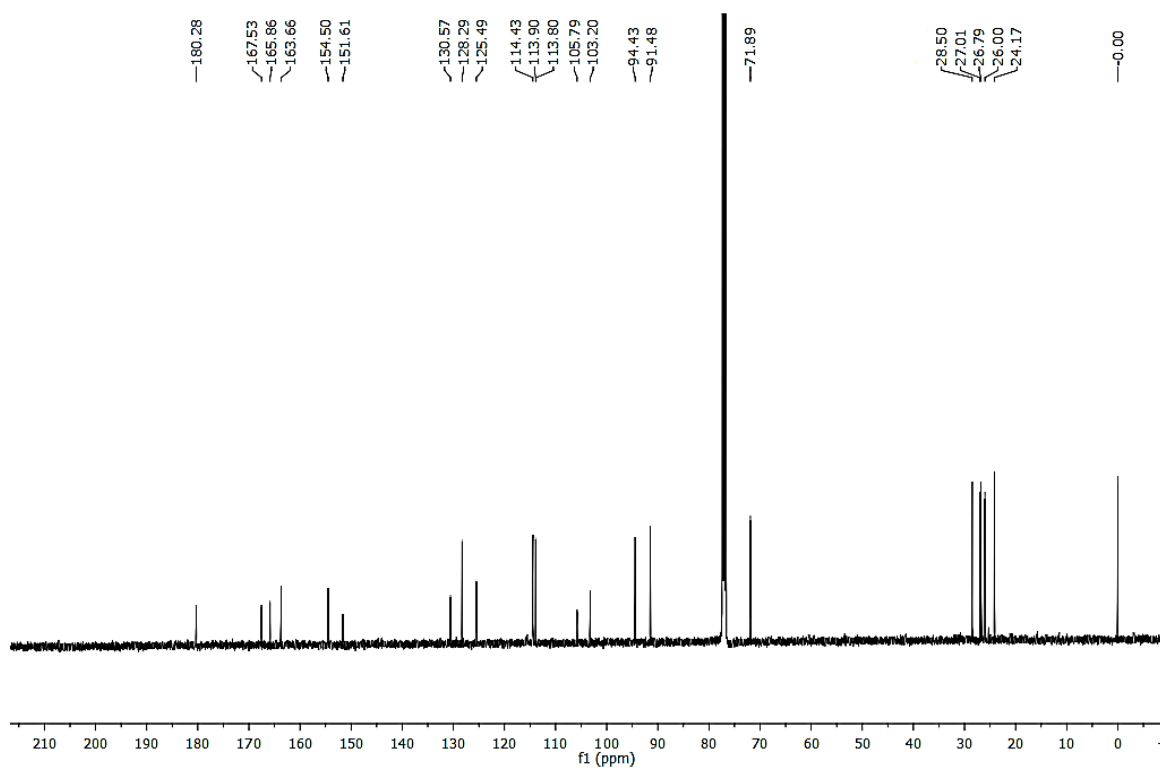
2,8,10-Trihydroxy-11,11-dimethyl-5,6,10,11-tetrahydrobenzo[*h*]pyrano[3,2-*b*]xanthen-7(9*H*)-one
Compound **23**

Figure 3A.27. Some selected HMBC interactions are given in red curves

While doing column chromatography with 20 % ethyl acetate- hexane mixture, 6 mg of compound **24** as colorless powder was obtained. The IR spectrum of the compound showed a broad absorption at 3111 cm^{-1} indicating the presence of hydroxyl group. Absorption observed at 1755 cm^{-1} suggested the presence of a carbonyl group in lactone ring. Also the peak at 1740 cm^{-1} indicates the presence of one more carbonyl group. The ^1H NMR spectrum (figure 3A.28) of the compound suggested the presence of four aromatic protons (δ 7.97 (s, 1H), 7.88 (d, $J = 9.5\text{ Hz}$, 1H), 6.70 (s, 1H) and 6.19 (d, $J = 9.5\text{ Hz}$, 1H) ppm), in which two are *ortho* coupled. Also, the six proton singlet at δ 1.37 ppm clearly indicates the presence of two methyl groups. The ^{13}C NMR spectrum (figure 3A.29) of the compound showed the presence of 13 carbons. The peak at δ 190.0 ppm, suggests the presence of carbonyl group and the peak at δ 162.1 ppm confirmed the presence of ester or lactone carbonyl moiety. Also, the DEPT-135 spectrum of the compound clearly indicated that the compound contains one $-\text{CH}_2-$ group along with a highly deshielded aliphatic quaternary carbon. Mass spectrum of the compound gave molecular ion peak at m/z 245.0712, which is the $(\text{M}+\text{H})^+$ peak. From all these spectral data and on comparison with the literatures, the compound was recognized as **graveolone**²⁴ and the structure of the same is given below.



Graveolone
Compound **24**

Figure 3A.25. ¹H NMR of compound 23 in CDCl₃Figure 3A.26. ¹³C NMR of compound 23 in CDCl₃

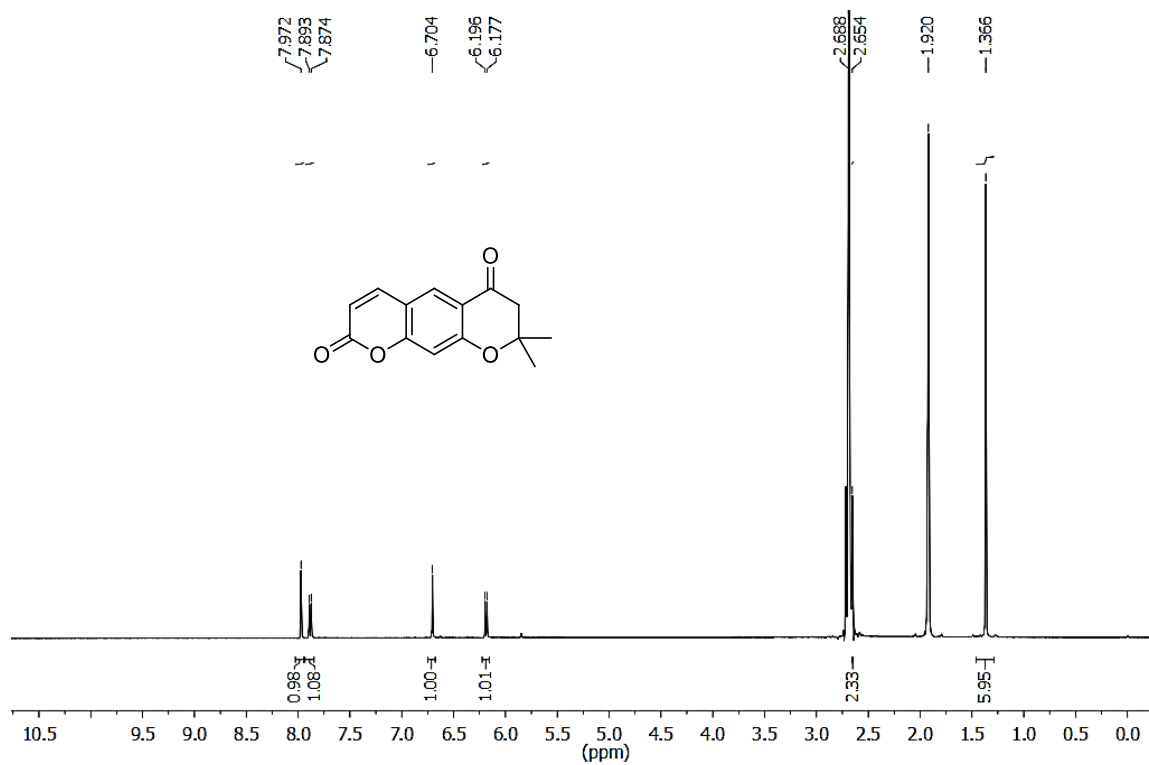


Figure 3A.28. ^1H NMR of compound **24** in CD_3COCD_3

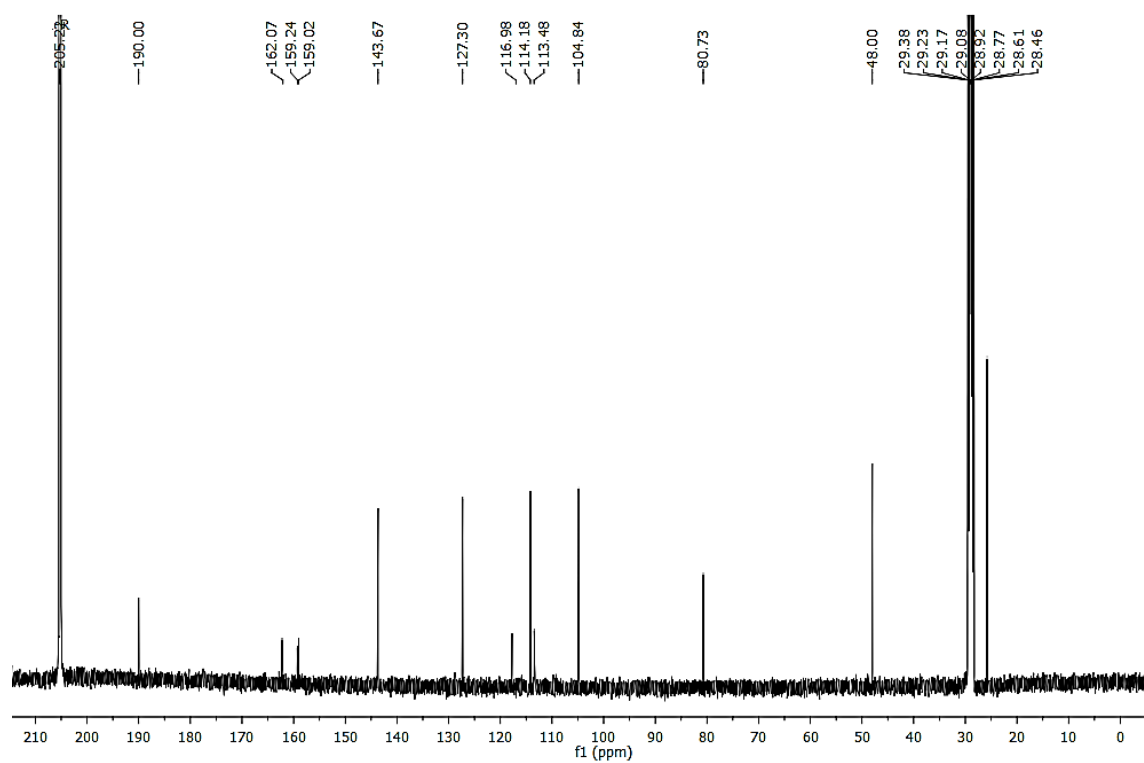
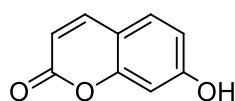


Figure 3A.29. ^{13}C NMR of compound **24** in CD_3COCD_3

Compound **25** (62 mg) was isolated as yellowish-white crystalline solid from fraction pools 7-9, obtained by eluting the column with 25 % ethyl acetate in hexane. IR spectrum of the compound showed absorption at 3293 and 1761 cm^{-1} suggesting the presence of hydroxyl and an ester/ lactone carbonyl groups respectively. In the proton NMR, three protons at δ 7.53 (d, $J = 8.5$ Hz), 6.86 (dd, $J_1 = 8.5$ Hz, $J_2 = 2.5$ Hz) and 6.76 (d, $J = 2.5$ Hz) ppm clearly indorsed to an *ortho* coupled aromatic system, along with a *meta* coupled proton as in the previous cases (figure 3A.30). Also, the two doublets at δ 7.88 and 6.18 ppm with an *ortho* coupling constant of 9.5 Hz, indicate the presence of an α,β -unsaturated carbonyl system. The broad singlet δ 9.47 ppm possessing no carbon in the HMQC NMR indicates the presence of a hydroxyl group. The ^{13}C NMR spectrum (figure 3A.31) of the compound showed the presence of nine carbon atoms in the molecule, and again the patterns of the carbon peaks suggested that the compound bears a coumarin type skeleton. From the HMQC and HMBC analysis, the ester or lactone carbonyl carbon in the molecule was found to resonate at δ 160.2 ppm. Mass spectrum of the compound showed molecular ion peak at m/z 163.0393, which is the $(\text{M}+\text{H})^+$ peak. Comparison of the ^1H and ^{13}C NMR spectral values along with DEPT-135, HOMO COSY and HMQC spectra suggested that the molecule is **7-hydroxycoumarin** or **β -umbelliferone**²⁵ and the structure of the same is given below.



Umbelliferone
Compound **25**

From the same fraction pools, compound **26** (23 mg) was obtained as a colorless viscous liquid, and the IR spectrum of the compound showed an absorption at 1748 cm^{-1} , which suggest the presence of an alkanal carbonyl group. In the proton NMR (figure 3A.32), the aldehyde group resonated as a doublet at δ 9.67 ppm with a coupling constant of 8 Hz (carbon at δ 194 ppm in figure 3A.33), proposed the presence of an α,β -unsaturated system. From the HOMO COSY relationships, the protons of the α,β -unsaturated system was assigned as δ 7.76 (d, $J = 16$ Hz), 6.56 (dd, $J_1 = 16$ Hz, $J_2 = 8$ Hz) and 9.67 (d, $J = 8$ Hz) ppm. The one proton singlet at δ 6.74 ppm, indicated the presence of an aromatic proton, while the two proton singlet at δ 6.00 ppm with a carbon at δ 102.0 ppm having negative signal in DEPT-135 is clearly attributed to a methylene group, incorporated between two oxygen atoms.

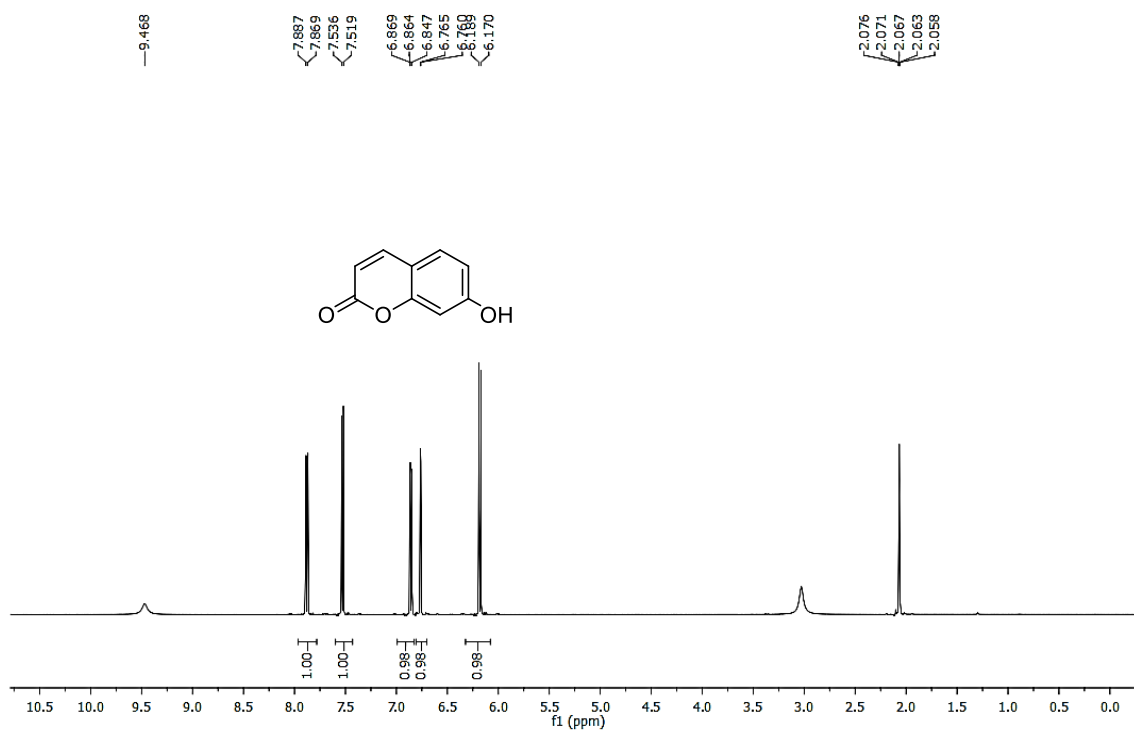


Figure 3A.30. ^1H NMR of compound 25 in CD_3COCD_3

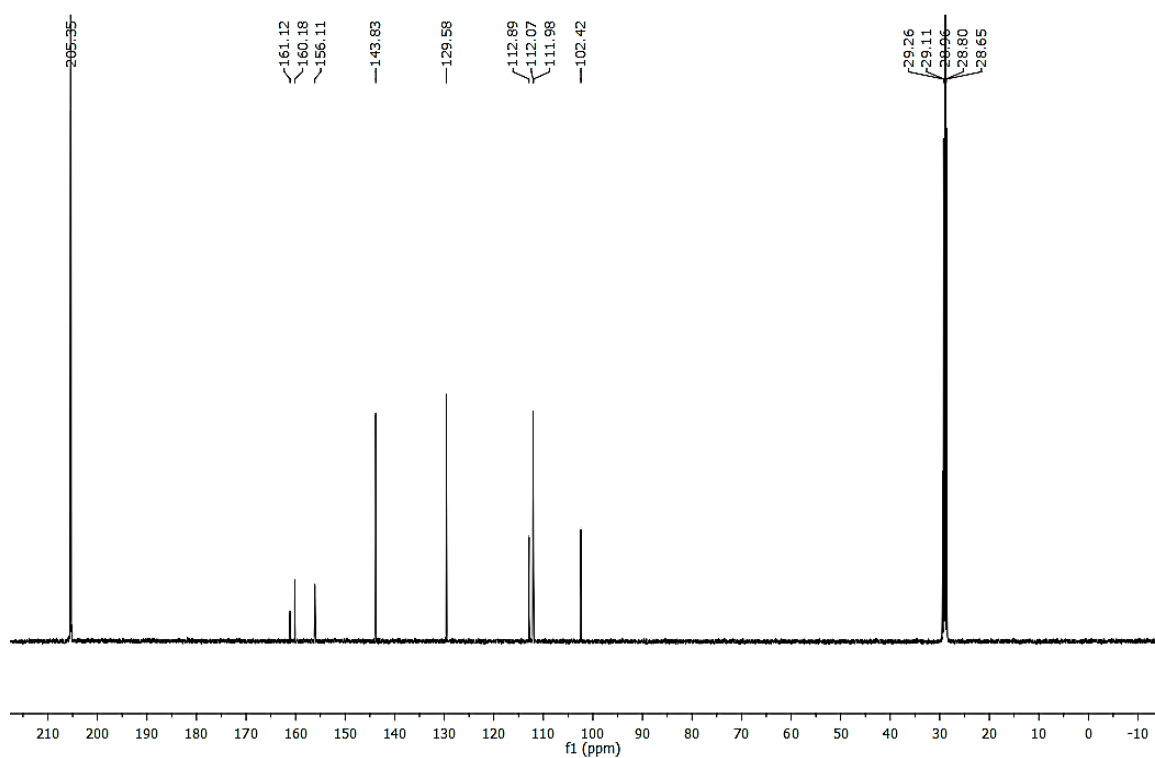
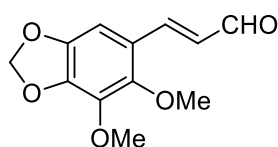


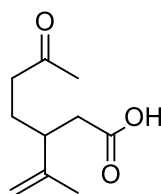
Figure 3A.31. ^{13}C NMR of compound 25 in CD_3COCD_3

The presence of two methoxy group was established from two singlets at δ 4.04 and 3.86 ppm. From detailed analysis of carbon spectra, it was found that the molecule consists of a *penta* substituted aromatic system. The molecular ion peak of the molecule was obtained at m/z 237.0760 which is the $(M+H)^+$ peak ($(M+Na)^+$ at 259.0582). From all these spectral data, and on comparison with the literature, compound **26** was identified as **dill apional**.²⁶ The structure of the compound is shown below.



Dill apional
Compound **26**

Compound **27** was isolated from same fraction pools on doing column chromatography with 35 % ethyl acetate in hexane. It was obtained as a pale yellow viscous liquid (13 mg). The IR spectrum of the molecule showed intense absorptions bands at 3311, 3050, 2980, 1748 and 1729 cm^{-1} , which clearly attribute to a ketone as well as carboxylic acid groups. In the proton NMR, the two singlets at δ 4.83 and 4.77 ppm (figure 3A.34), having same carbon at δ 113.1 ppm, having negative signal in the DEPT-135 indicate the presence of an exocyclic double bond. Also, the two quaternary carbons at δ 208.9 and 178.1 ppm confirm the presence of carbonyl as well as carboxylic groups (figure 3A.35). The presence of three $-\text{CH}_2-$ groups were confirmed from the three signals at δ 41.2, 38.9, and 26.2 ppm in the negative region of DEPT-135. The resemblances of the molecule with that of carvone and limonene led to characterize the structure as given below. Also, the m/z value of the molecule was obtained from GCMS as 184.11. This molecule is being reported for the first time from *Anethum graveolens*. Though the aldehyde derivatives have been described in other species, the acid derivative is being reported for the first time.



6-Oxo-3-(prop-1-en-2-yl)heptanoic acid
Compound **27**

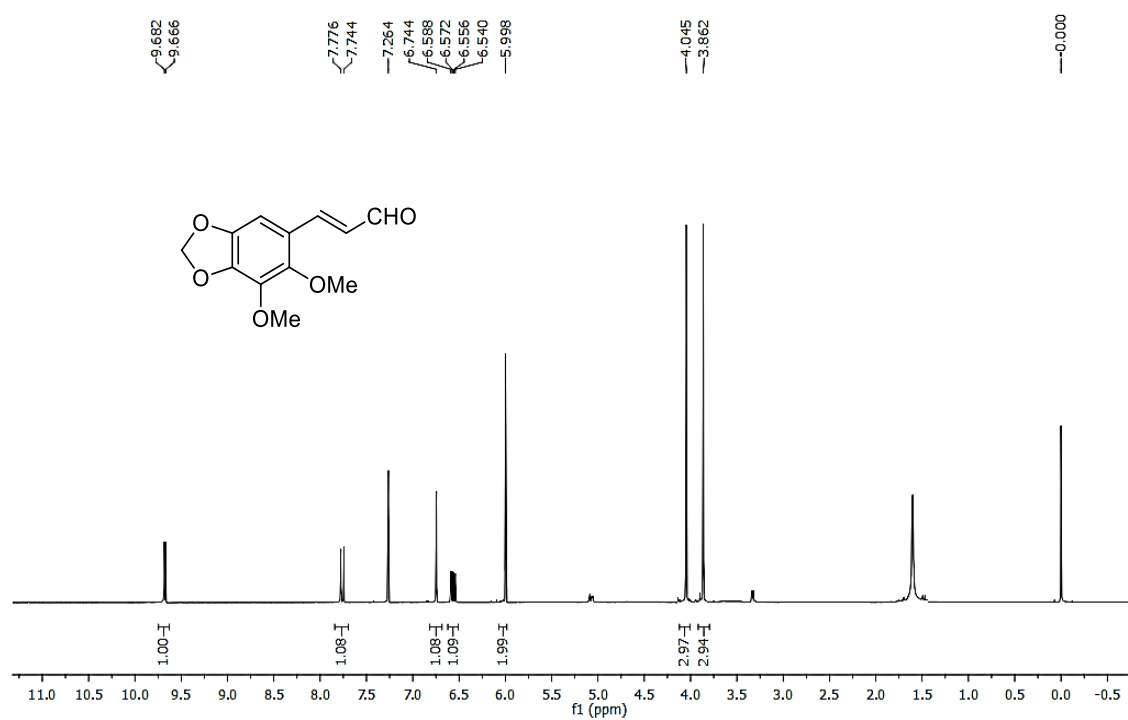


Figure 3A.32. $^1\text{H NMR}$ of compound **26** in CDCl_3

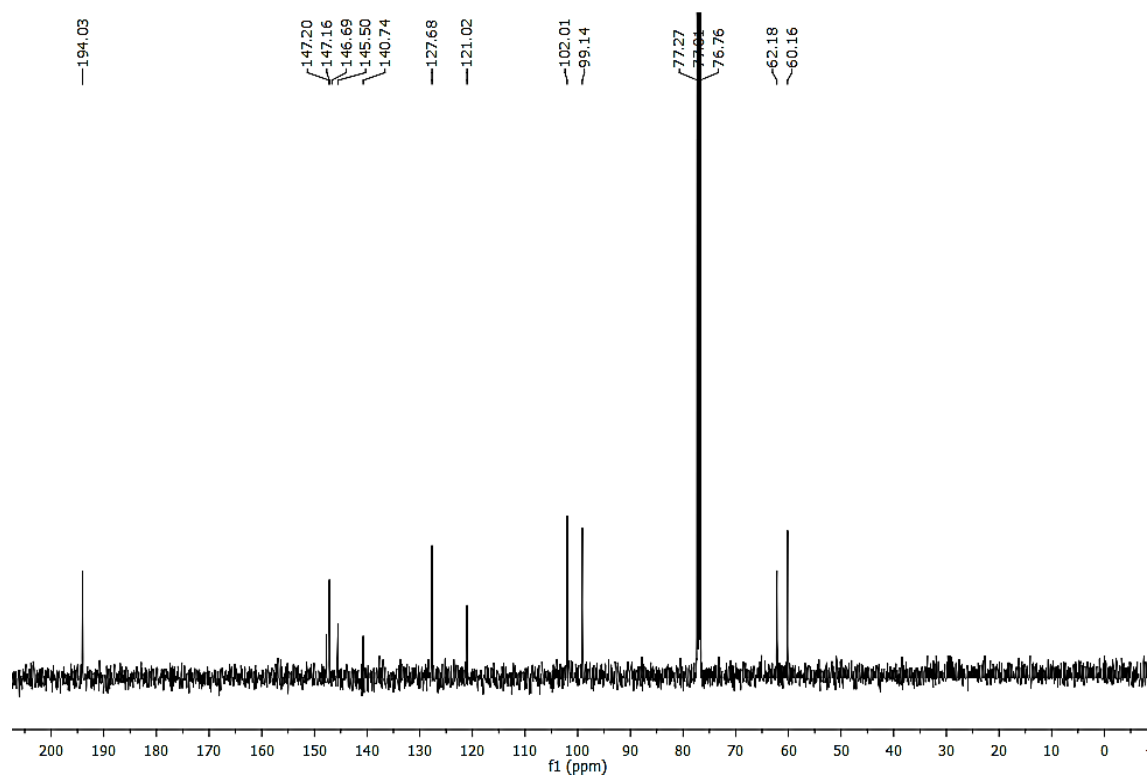
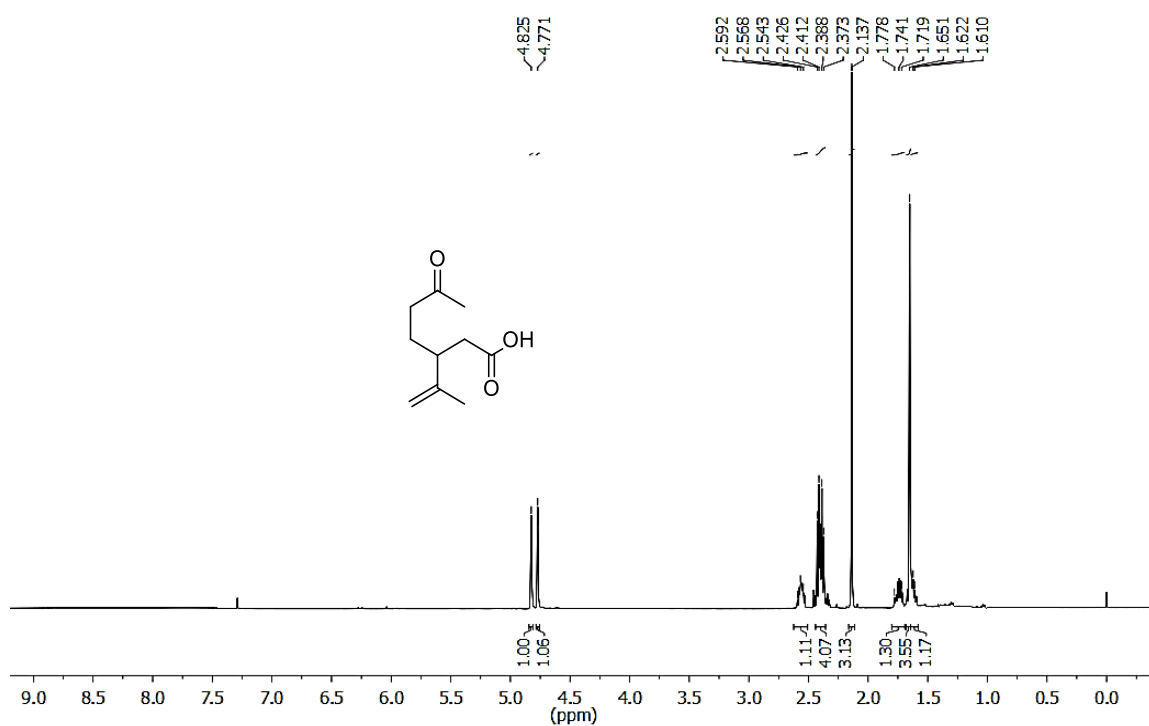
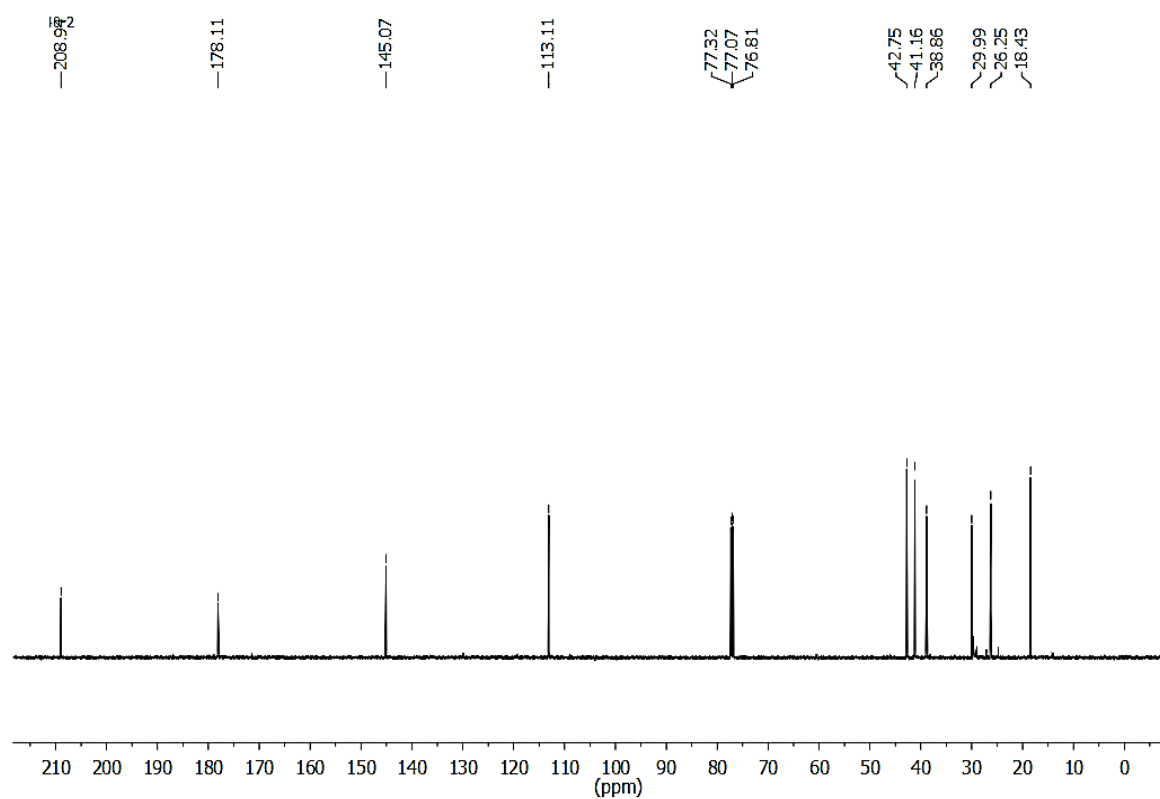
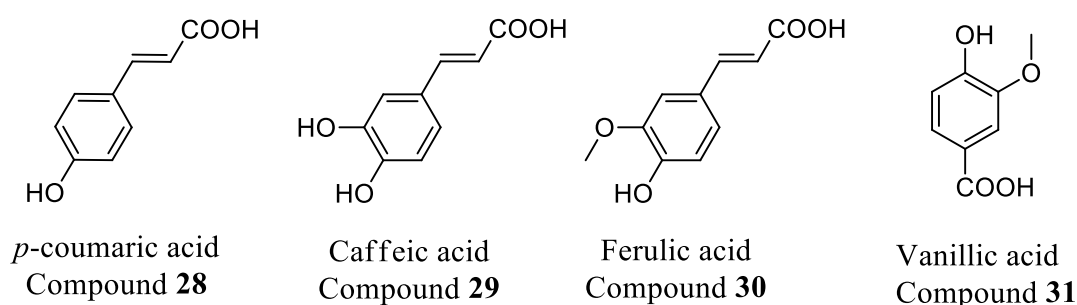
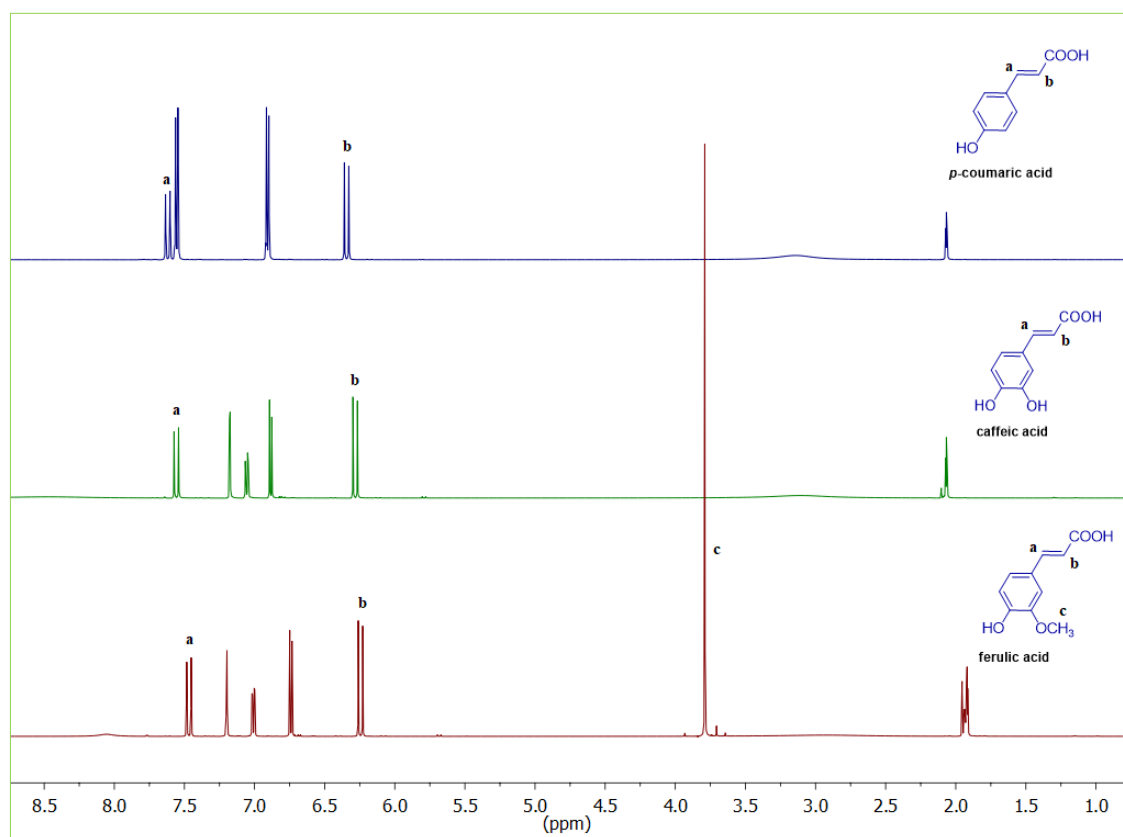


Figure 3A.33. $^{13}\text{C NMR}$ of compound **26** in CDCl_3

Figure 3A.34 ^1H NMR of compound **27** in CDCl₃Figure 3A.35. ^{13}C NMR of compound **27** in CDCl₃

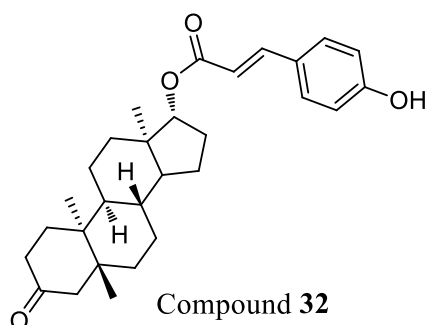
Two compounds were isolated from each of fraction pools, 10-12 and 13-16, via repeated column chromatographic techniques (compounds **28-31**). All of them were UV active and were eluted with 40-60 % of ethyl acetate in hexane, through silica gel column chromatography. Compound **28** was off-white in color, with a melting point of 209 °C. The IR absorptions at 3410, 3301, 2900, 2110 and 1738 cm^{-1} showed by the compound clearly indicate the presence of carboxyl as well as hydroxyl groups. In the proton NMR, two protons resonated as doublets (at δ 7.55 and 6.33 ppm) with a coupling constant of 16 Hz, having interactions in HOMO COSY, which indicate the presence of *trans* olefinic protons, most probably an α,β -unsaturated system. Also, two doublets (of integration 2 for each) having a coupling constant of 8.5 Hz, with interactions in HOMO COSY, with intensified carbon signals in the ^{13}C NMR attributed to a *para* substituted aromatic system. From the literature reports, the structure of the molecule was confirmed as ***p*-coumaric acid**, and it was well supported by HRMS data in which $(\text{M}+\text{H})^+$ peak was obtained at 165.0571 (figure 3A.36 and 37). The NMR characteristic of compound **29** was similar to that of compound **28**. It was obtained as a colorless solid with a melting point of 226 °C. The olefinic protons resonated at δ 7.56 and 6.28 ppm as doublets with a coupling constant of 16 Hz. Also, the splitting pattern of δ 7.18 (d, $J = 2$ Hz), 7.06 (dd, $J_1 = 8$ Hz, $J_2 = 2$ Hz) and 6.88 (d, $J = 8$ Hz) indicates the presence of a *meta* substituted aromatic system. In carbon NMR, the keto group of carboxylic acid resonated at δ 167.3 ppm. From the literature reports and further spectral analysis, the compound **29** was confirmed as **caffeic acid** (m/z was 181.0503 $(\text{M}+\text{H})^+$ in HRMS). Compound **30** (pale brown powder) also exhibited intense UV activity and had the same characteristics of *p*-coumaric and caffeic acids. In the proton NMR, the peak at δ 3.79 ppm indicates the presence of a methoxy group, instead of a hydroxyl group in caffeic acid. Also, the HRMS analysis gave an m/z value of 195.0653 corresponds to $(\text{M}+\text{H})^+$ peak. From the detailed spectroscopic analysis, the compound **30** was confirmed as **ferulic acid**. (figure 3A.36 and 37).²⁷

Compound **31** was a colorless, powder-like compound having three aromatic peaks in between δ 7.62-6.93 ppm. The presence of a three hydrogen singlet at δ 3.92 ppm confirmed that the compound bears of one methoxy group. In the HRMS data, m/z peak was obtained at 169.0522 corresponding to $(\text{M}+\text{H})^+$. From the detailed spectral analysis and in comparison with literature reports, the compound was confirmed to be vanillic acid (figure 3A.36).²⁷

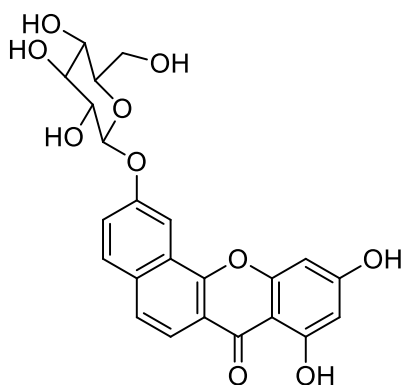
Figure 3A.36. Structures of compounds **28-31**Figure 3A.37. Proton NMR of compounds **28-30** in CD_3COCD_3

Compound **32** was isolated in 6 mg, from the ethanol extract (came in 1 % of methanol in ethyl acetate) as a colorless solid with a melting point of 165-167 °C. The IR absorptions at 3321, 3111, 2900 and 1748 cm^{-1} showed by the compound clearly indicate the presence of carboxyl as well as hydroxyl groups. In the proton NMR, two protons resonated as a doublet (at δ 7.48 and 6.23 ppm) with a coupling constant of 16 Hz, having interactions in HOMO COSY, which indicate the presence of *trans* olefinic protons. In the carbon NMR, the peaks at δ 210.2 and 166.4 ppm represents two carbonyl systems in the molecule. Also,

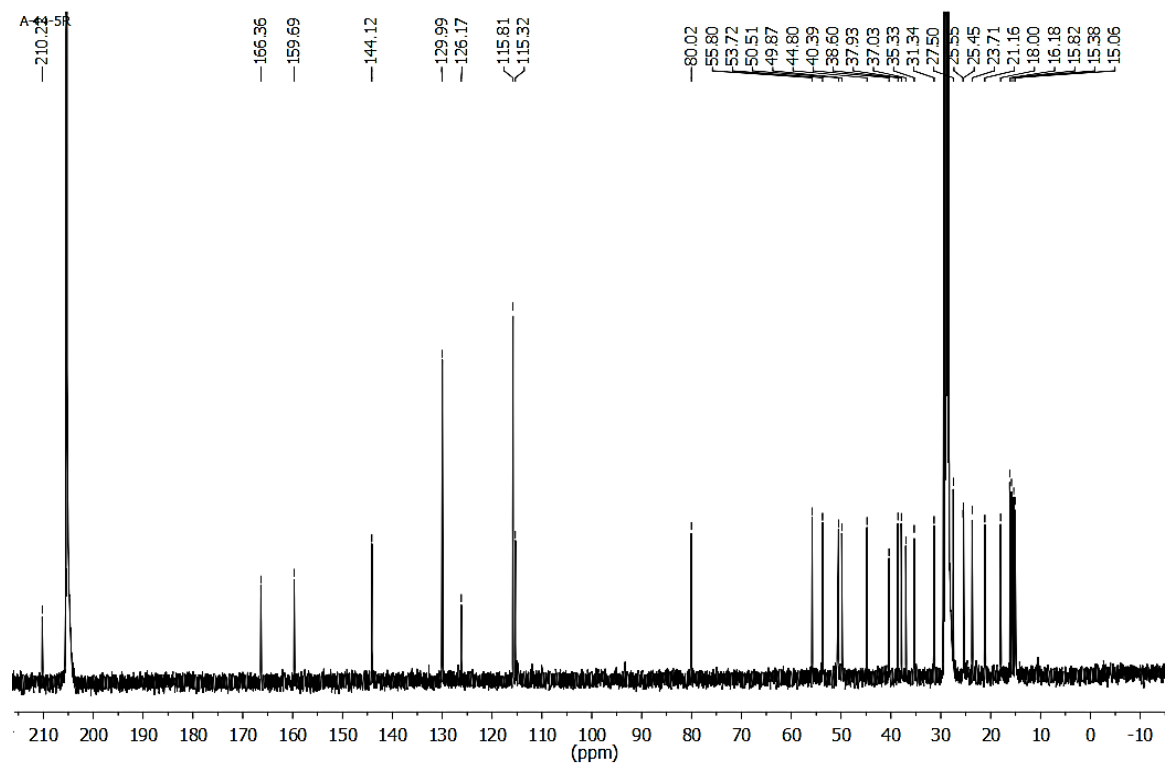
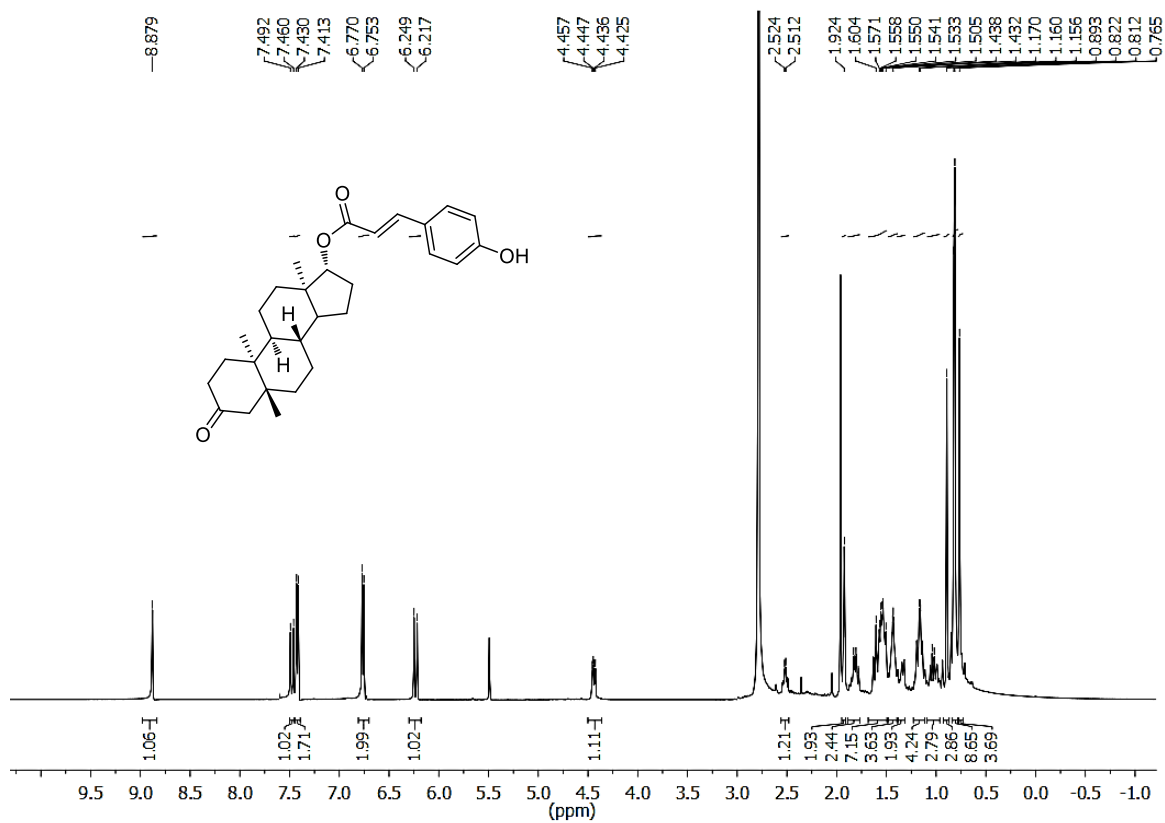
the similarity of the ^1H NMR of the compound with, compound **28** revealed that, the molecule is an ester of *p*-coumaric acid. In addition the m/z value at 451.2841 corresponds to $(\text{M}+\text{H})^+$ peak, suggested that the molecule bears a pregnane moiety. After the careful analysis of different spectroscopic data with literature reports, the structure of the compound was identified as an ester of *p*-coumaric acid (figure 3A.38 and 39).²⁸

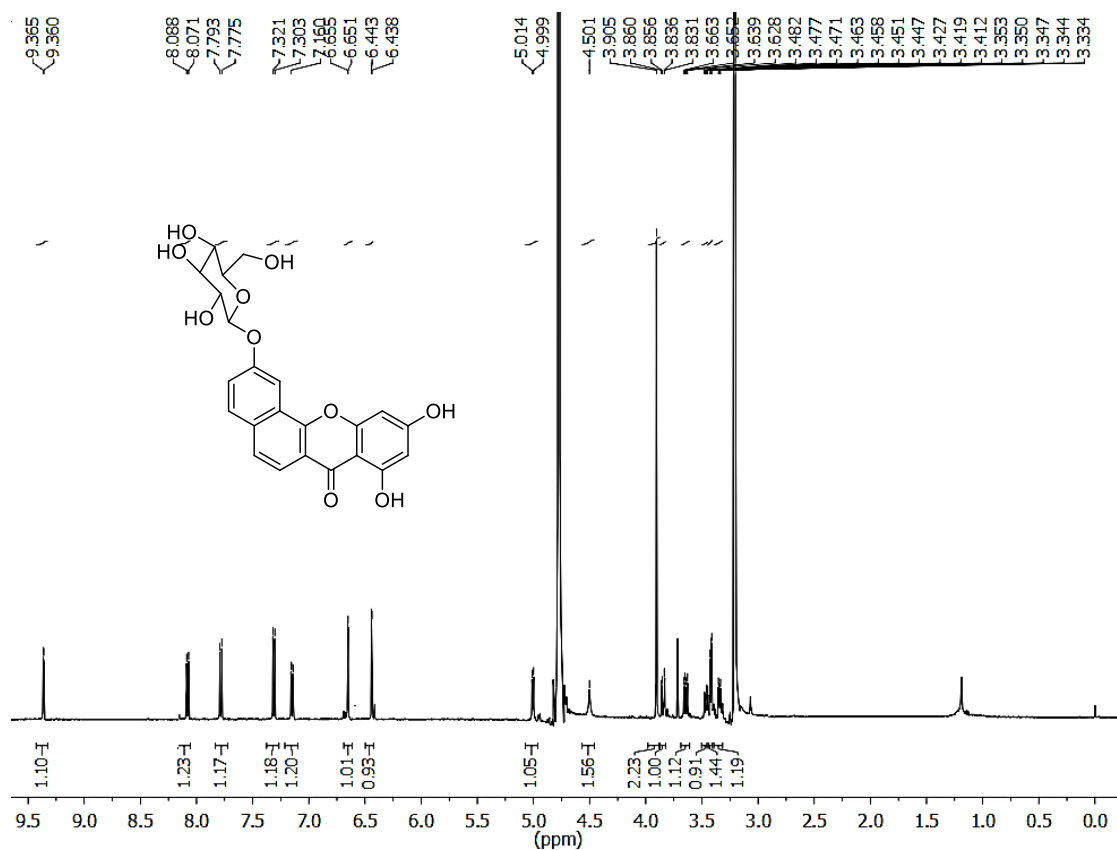
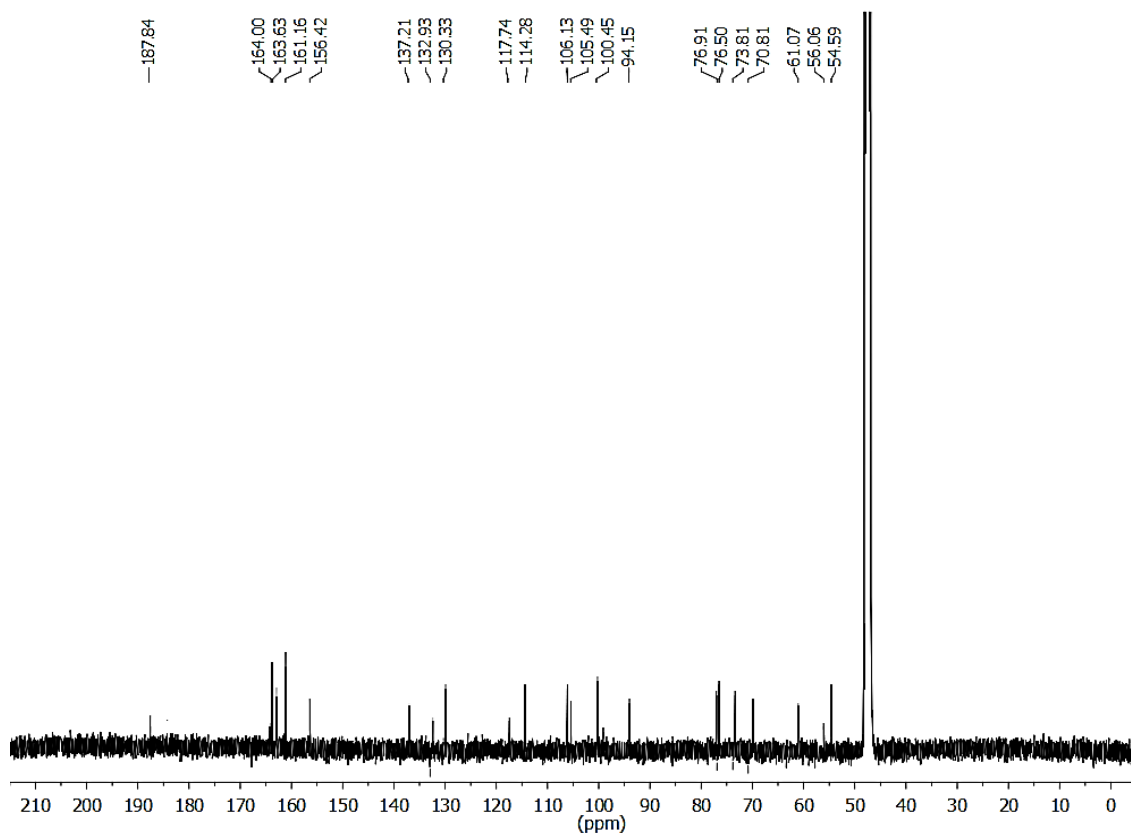


Along with **32**, compound **33** (8 mg) was also isolated from the ethanol extract, *via* silica gel column chromatography with 10 % of methanol in ethyl acetate. The compound was a colorless solid with a melting point of 210 °C and, the IR stretching frequencies at 3111, 2900 and 1698 cm^{-1} confirmed that the system consists of hydroxyl as well as carbonyl moieties. It exhibited almost similar NMR characteristics of the compound **21**, with an additional glucoside moiety and gave a molecular ion peak at m/z 479.0953 in the HRMS. The presence of a one proton doublet at δ 5.01 ppm in the proton NMR (having carbon at δ 100.4 ppm in the carbon NMR) with a coupling constant of 8 Hz, confirmed that the system consists of a β -anomeric linkage, instead of the methoxy group in compound **21**. The peak at δ 187.84 ppm in the carbon NMR, also confirmed the presence of a carbonyl moiety in the molecules (figure 3A.40 and 41). Finally, comparing the spectroscopic data of the compound with literature reports, the structure of the compound was well confirmed as a **pyranoxy-benzoxanthone** derivative.²³



Compound 33



Figure 3A.40. ^1H NMR of compound **33** in CD_3OD Figure 3A.41. ^{13}C NMR of compound **33** in CD_3OD

3A.4. Extract and Molecular Level *in vitro* Antioxidant Studies

As mentioned in Part A of Chapter 2, oxidative stress is a primary risk factor in the pathogenesis of numerous chronic diseases and are also said to be responsible for the human ageing. It is widely accepted that a plant-based diet with a high intake of vegetables, fruits, and other nutrient-rich foods may reduce the risk of oxidative stress-related diseases. In these aspects, we carried out the anti-oxidant studies of various extracts and isolated compounds of *A. graveolens*, since this plant is one of the world's all-inclusive spices. In the extract level preliminary *in vitro* antioxidant studies (table 3A.6), all the four extracts showed better DPPH scavenging activity, than ABTS and Nitric oxide. Also, the activity exhibited by these extracts were much better than the standard compound, ascorbic acid.²⁹

Table 3A.6. Extract level preliminary antioxidant studies.

Extracts	IC ₅₀ values ($\mu\text{g/mL}$)		
	DPPH scavenging activity	ABTS scavenging activity	NO scavenging activity
Hexane	9.87 ± 0.367	>500	464.41 ± 0.286
Acetone	3.65 ± 0.441	43.37 ± 0.231	>500
Ethanol	1.5 ± 0.212	95.58 ± 0.401	>500
Water	1>	>500	>500
Ascorbic acid	6.878 ± 0.231	14.1254 ± 0.461	-
Gallic acid	-	-	75.84 ± 0.876

After the effective extract level studies, we further focused on the molecular level studies and found that most of these isolated compounds effectively scavenge the DPPH and NO radicals with comparatively better IC₅₀ values than the standard compounds, ascorbic acid and gallic acid. Among the compounds studied, graveolone exhibited the better scavenging of DPPH radicals with an IC₅₀ value of $4.55 \pm 0.189 \mu\text{M}$, followed by dill apiol (IC₅₀ = $16.03 \pm 0.111 \mu\text{M}$) and compound **21** (IC₅₀ = $18.28 \pm 0.273 \mu\text{M}$). Coming to the nitic oxide radical scavenging assay, carvone demonstrated the lowest IC₅₀ ($69.4 \pm 0.762 \mu\text{M}$) followed by limonene with a value of $73.5 \pm 0.256 \mu\text{M}$. From all these studies, we can conclude that most of the antioxidant properties, exhibited by this pant are mainly attribute to the marker compound, dill apiol (table 3A.7).

Table 3A.7. Molecular level preliminary antioxidant studies.

Compounds	IC ₅₀ values (μ M)		
	DPPH scavenging activity	ABTS scavenging activity	NO scavenging activity
Dill apiol	16.03 \pm 0.111	>500	74.09 \pm 0.167
Limonene	52.35 \pm 0.76	>500	73.5 \pm 0.256
Carvone	45.93 \pm 0.102	>500	69.4 \pm 0.762
Umbeliferone	43.12 \pm 0.312	>500	131.6 \pm 0.199
Dill apional	44.44 \pm 0.112	>500	133.2 \pm 0.131
Graveolone	4.55 \pm 0.189	>500	229.77 \pm 0.188
Compound 20	49.01 \pm 0.152	>500	135.98 \pm 0.862
Compound 21	18.28 \pm 0.273	>500	170.23 \pm 0.07
Ascorbic acid	39.01 \pm 0.12	80.17 \pm 0.61	-
Gallic acid	-	-	320.0 \pm 0.27

3A.5. *In silico* Antidiabetic and Anticancer Studies

Molecular docking has become an important tool in the field of drug discovery, because the advances in the field of computational strategies allow to permeate all aspects of drug discovery today; such as the virtual screening techniques for the identification of lead molecules. This approach can be used to model the interaction between an enzyme and a small molecule at the atomic level, which allows us to illustrate the performance of these small molecules in the binding site of target proteins as well as to elucidate the fundamental biochemical processes. The docking process mainly involves two basic steps: prediction of the ligand conformation (its position and orientation within the active sites of the protein) and the assessment of its binding affinity. Knowing the location of the binding site can significantly increase the docking efficiency.³⁰ Having a set of compounds in hand, we carried out a detailed molecular docking study, in order to predict presumed binding mode of these molecules against two target proteins 3A4A (antidiabetic) and 2ITW (anticancer and anti-inflammatory). The studies were carried out using the software, MOE 2009.10. The default 'Site Finder' tool was used to identify the active site of the proteins. Using LigPlot analysis the binding interactions of the ligands to the proteins were studied and the docking results are shown in the table given below (table 3A.8)

Table 3A.8. Results of molecular docking studies

Compounds	E-score (kcal/mol)	
	2ITW	3A4A
Compound 15	-10.3687	-10.1703
Compound 17	-11.0467	-11.0468
Compound 18	-8.13521	-11.0569
Compound 19	-9.67271	-11.3126
Compound 20	-11.4141	-10.3876
Compound 21	-14.1255	-13.3802
Compound 22	-17.5201	-12.7616
Compound 23	-14.4856	-13.3384
Compound 24	-8.63177	-10.0712
Compound 25	-9.03425	-9.72151
Compound 26	-8.69118	-11.5158
Compound 28	-14.2053	-12.7881
Compound 29	-13.4413	-12.9068
Compound 30	-12.0409	-12.1101
Compound 33	-14.8727	-13.8934

Among fifteen compounds studied, the xanthone derivative exhibited higher binding scores with the protein 2ITW, compared to other compounds. The novel compound **22** displayed moderately very high docking score (-17.5201 kcal/mole), due to the large number of indirect hydrogen bonding interactions. Four prominent interactions were observed for this compound. It expressed a side chain acceptor interaction with the basic amino acid residues LysA745 (2.76 Å, 73 %) and LysB745 (2.76 Å, 73 %). Similarly it also exhibited a side chain donor interaction with the acidic amino acid residue AspA855 (1.21 Å, 27 %) and AspB855 (1.21 Å, 27 %) (figure 3A.42). The blue smudges that are drawn behind some of the atoms represent the solvent exposure. The molecular docking score of the compound **33** is -14.8727 kcal/mole. It gave eight prominent interactions, out of which four are backbone donor interactions respectively with the basic amino acid residues ArgA841 & Arg B841 (1.41 Å, 47 %), and greasy amino acid residues ProA794 & ProB794 (1.5 Å, 45 %). It also showed two side chain donor interactions with the acidic amino acid residues AspA855 & AspB855 (1.27 Å, 55 %), and side chain acceptor interactions with basic amino acid residues LysA716 & LysB716 (2.65 Å, 93 %). The

unbroken proximity contour (dotted line) shows the closeness of the group to the active site. Compound **23** demonstrated a molecular docking score of -14.4856 kcal/mole. Four prominent interactions were observed here. The binding modes of this compound consist of sidechain donor interactions with the acidic amino acid residues AspA855 & AspB855 (1.24 Å, 43 %) and two side chain acceptor interactions with the basic amino acid residues LysA745 & LysB745 (2.56 Å, 48 %). Compound **21** gave a molecular docking score of -14.1255 kcal/mole, mainly through four arene-cation interactions with the basic amino acid residues LysA860 & LysB860. It also exhibited two side chain donor interactions with the acidic amino acid residues GluA758 & GluB758 (1.33 Å, 45 %), and two backbone donor interactions with polar amino acid residues GlyA857 & GlyB857 (1.43 Å, 34 %) (figure 3A.42).

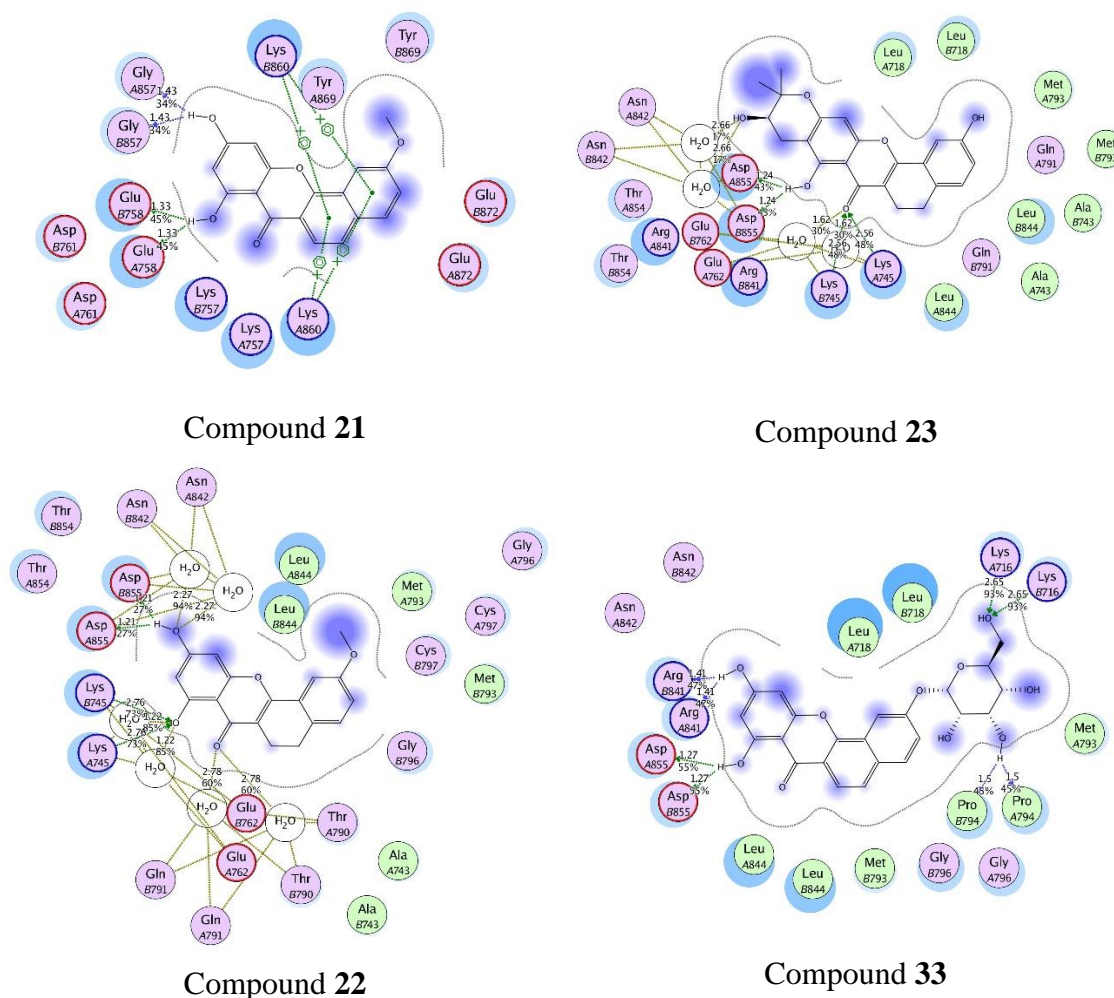


Figure 3A.42. Binding modes of compounds **21**, **22**, **23** and **33** with the protein 2ITW

In the case of antidiabetic protein 3A4A, compound **33** exhibited the highest docking score through two prominent sidechain interactions (-13.8934 kcal/mol). It showed

a side chain donor interaction with an acidic amino acid residue Asp242 (1.33 Å, 46 %), and a side chain acceptor binding interaction with a basic amino acid residue Lys156 (2.38 Å, 20 %). The molecular docking score of compound **23** was 13.3384 kcal/mol, with five prominent interactions. One of which is an arene-cation interaction with the basic amino acid residue Arg315 and other is a backbone donor interaction with the -OH group of the polar amino acid residue Tyr158 (3.77 Å, 19 %). This -OH group also exhibited a sidechain donor interaction with an acidic amino acid residue Glu411 (1.31 Å, 75 %). The molecular docking score of the compound **21** was -13.3802 kcal/mole; the binding interaction showed five prominent interactions with various amino acid residues. The greasy amino acid residue Phe303 gave two different arene-arene interactions with the benzene rings. Other interactions include, arene-cation interaction with a basic amino acid residue Arg442 and two side chain acceptor binding interaction respectively with polar amino acid residue Asn350 (3 Å, 17 %) and basic amino acid residue Arg213 (3.05 Å, 34 %) (figure 3A.43).

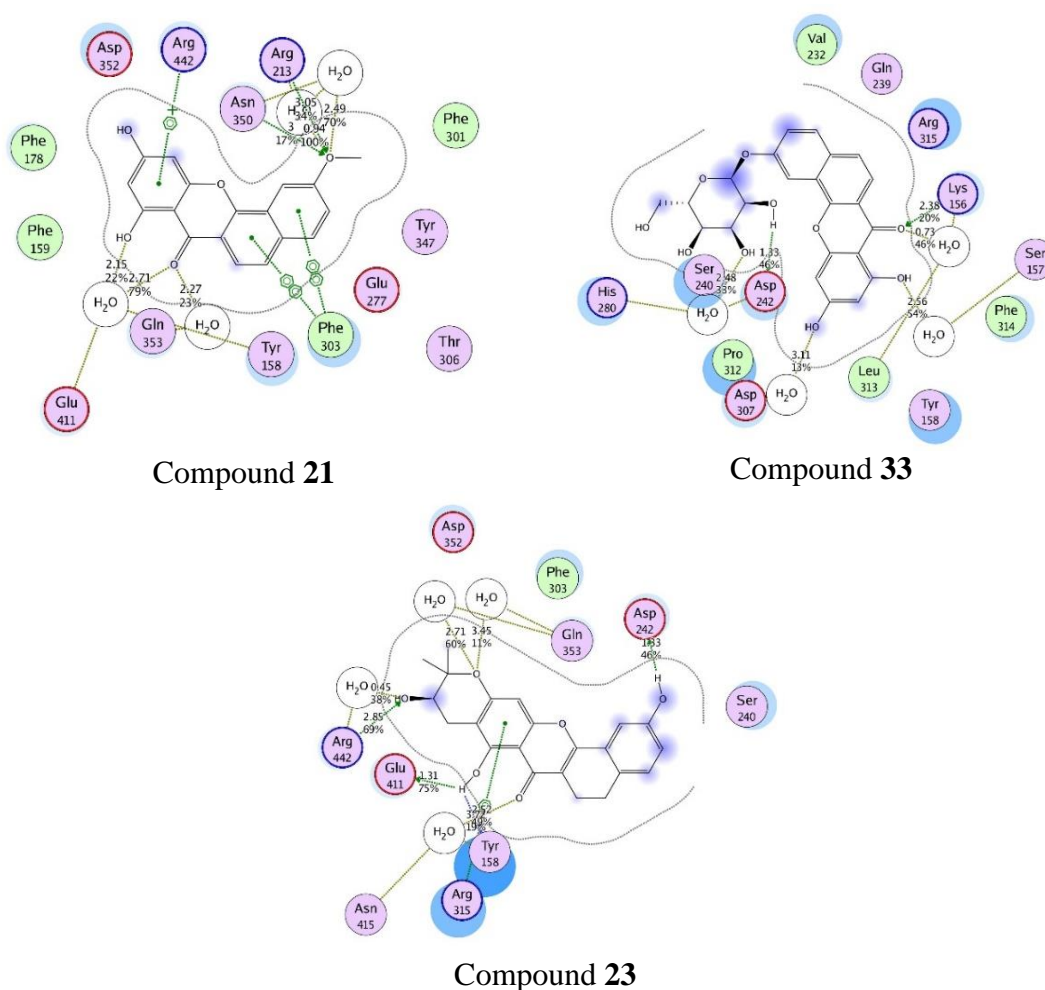


Figure 3A.43. Binding modes of compounds **21**, **23** and **33** with the protein 3A4A

3A.6. Conclusion

In summary, the phytochemical reinvestigation of seeds of *Anethum graveolens* led to the successful isolation of twenty-three compounds, among which two are novel, and five are reported for the first time from this species. We also explored the anti-oxidant and molecular docking studies of these isolated compounds. The antioxidant studies inferred that, consumption of this spice can effectively scavenge the undesirable free radicals produced through various metabolic pathways and thereby can reduce the related complications. Whereas, in the molecular docking studies, the xanthone derivatives exhibited better docking interactions with the target proteins 2ITW and 3A4A, hence they could effectively modulate the metabolism of these proteins.

3A.7. Experimental Section

Different analytical techniques were used for the characterization of compounds. The IR spectra were recorded with a Bruker FT-IR spectrometer. The nuclear magnetic resonance spectra (NMR) were recorded on a Bruker AMX 500 spectrophotometer (CDCl₃, CD₃COCD₃, MeOD and DMSO-d₆ as solvents). Chemical shifts for NMR spectra are reported as δ in units of parts per million (ppm) downfield from tetramethylsilane (δ 0.0) and relative to the signal of solvent. Mass spectra were recorded under ESI/HRMS at 60,000 resolution using Thermo Scientific Exactive mass spectrometer and specific rotation was recorded using Jasco P-2000 polarimeter. Shimadzu UV-1800 spectrophotometer was used to measure the absorption maxima. Antioxidant studies were carried out as described in section 2A.14 of Chapter 2 Part B.

3A.8. Spectral Data

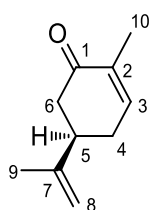
Compound 12 ((+)-*S*- carvone)

Compound 12 was obtained in 6 g as UV active colorless viscous liquid from hexane as well as from fraction pools 1-3 of acetone extract through various column chromatographic methods. The peak at 1675 cm⁻¹ in the IR spectrum indicates the presence of an α , β -unsaturated carbonyl group. By comparing the IR, ¹H NMR, ¹³C NMR and other 2D NMR spectral data of this compound with literature reports, the compound was confirmed as (+)-*S*- carvone ($[\alpha]_D^{25} = +52.56^\circ$).

Molecular formula : C₁₀H₁₄O

FT-IR (Neat) ν_{\max} : 3111, 1675 cm⁻¹

Optical activity $[\alpha]_D^{25} = +52.56^\circ$ (c 0.1 EtOH)



^1H NMR (500 MHz, CDCl_3 , TMS) : δ 6.77-6.76 (m, 1H, H-3), 4.81 (s, 1H, H-8), 4.76 (s, 1H, H-8), 2.71-2.66 (m, 1H), 2.59-2.55 (m, 1H), 2.48-2.43 (m, 1H), 2.38-2.35 (m, 1H), 2.32-2.26 (m, 1H), 1.78 (t, $J = 1$ Hz, 3H), 1.76 (9s, 3H) ppm.

^{13}C NMR (125 MHz, CDCl_3 , TMS) : δ 199.4 (C-1), 146.5 (C-7), 144.4 (C-3), 135.2 (C-2), 110.3 (C-8), 43.0, 42.3, 31.1, 20.4, 15.5 ppm.

Mass from GCMS : 150.10

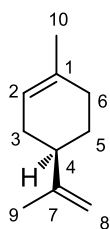
Compound 13 ((-) S-limonene)

Compound **13** was obtained in 4.6 g as UV inactive viscous liquid with blue charring in Mc Gill stain solution. By comparing with the literature reports, the compound was confirmed as (-) S-limonene.

Molecular formula : $\text{C}_{10}\text{H}_{16}$

FT-IR (Neat) ν_{max} : 2915, 2848 cm^{-1}

Optical activity $[\alpha]_{\text{D}}^{25} = -81.12^\circ$ (c 0.1 EtOH)



^1H NMR (500 MHz, CDCl_3 , TMS) : δ 5.40 (s, 1H, H-2), 4.70 (s, 2H, H-8), 2.13-2.03 (m, 3H), 1.97-1.87 (m, 2H), 1.81-1.77 (m, 1H), 1.73 (s, 3H), 1.65 (s, 3H), 1.51-1.44 (m, 1H) ppm.

^{13}C NMR (125 MHz, CDCl_3 , TMS): δ 150.2 (C-7), 133.7 (C-1), 120.7 (C-2), 108.4 (C-6), 41.1, 30.8, 30.6, 27.9, 23.4, 20.8 ppm.

Mass from GCMS : 136.13

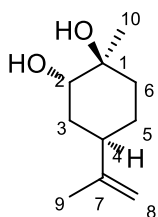
Compound 14 (limonene diol)

Compound **14** was also UV inactive with a blue charring in Mc Gill stain solution. The exocyclic olefinic protons resonated at δ 4.75 ppm as a singlet. The proton that resonated at δ 3.64 ppm as one proton singlet along with two carbons at δ 73.9 and 71.4 confirmed presence of a diol system. . Finally, from the spectral data and literature reports, the molecule was confirmed as **limonene diol** (viscous liquid-27 mg).

Molecular formula : $\text{C}_{10}\text{H}_{18}\text{O}_2$

FT-IR (Neat) ν_{max} : 2900, 1588 cm^{-1}

^1H NMR (500 MHz, CDCl_3 , TMS) : δ 4.75 (s, 2H, H-8), 3.64 (s, 1H, H-2), 2.28-2.26 (m, 1H), 1.95-1.90 (m, 1H), 1.78-1.76



(m, 2H), 1.73 (s, 3H), 1.68-1.66 (m, 1H), 1.58-1.55 (m, 2H), 1.27 (s, 3H) ppm.

^{13}C NMR (125 MHz, CDCl_3 , TMS): δ 149.34 (C-7), 109.0 (C-8), 73.9, 71.4, 37.5, 34.0, 33.7, 26.6, 26.2, 21.1 ppm.

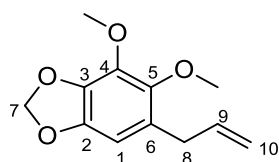
Mass from GCMS : 170.13

Compound 15 (dillapiol)

Compound **15** was obtained in 6.8 g as UV active viscous liquid from hexane as well as first fraction pools of acetone extract. In the HRMS spectrometry the molecule gave a peak at 223.0973, corresponding to $(\text{M}+\text{H})^+$. By comparing these spectral data with the literature reports, the compound was confirmed as dillapiol.

Molecular formula : $\text{C}_{12}\text{H}_{14}\text{O}_4$

FT-IR (Neat) ν_{max} : 3110, 2100, 2050, 1066 cm^{-1}



^1H NMR (500 MHz, CDCl_3 , TMS) : δ 6.35 (s, 1H, H-1), 5.94-5.90 (m, 1H, H-9), 5.88 (s, 2H, H-7), 5.07-5.05 (m, 1H, H-10), 5.03-5.02 (m, 1H, H-10), 4.01 (s, 3H), 3.76 (s, 3H), 3.31 (d, $J = 6.5$ Hz, 1H, H-8) ppm.

^{13}C NMR (125 MHz, CDCl_3 , TMS): δ 144.6 (C-4), 144.3 (C-5), 137.6 (C-2), 137.4 (C-3), 135.9, 126.1, 115.6, 102.8, 101.1 (C-7), 61.3, 60.0, 33.9 (C-8) ppm.

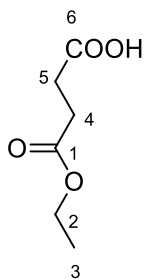
HRMS (ESI): m/z Calcd for $\text{C}_{12}\text{H}_{15}\text{O}_4$: 223.0970; Found : 223.0973.

Compound 16 (4-ethoxy-4-oxo butanoic acid)

From hexane extract, we could also isolate one molecule, showing two carbonyl carbons in the carbon NMR, which was confirmed as 4-ethoxy-4-oxo butanoic acid.

Molecular formula : $\text{C}_6\text{H}_{10}\text{O}_4$

FT-IR (Neat) ν_{max} : 3347, 2110, 1780, 1765 cm^{-1}

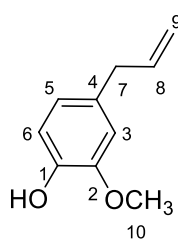


^1H NMR (500 MHz, CDCl_3 , TMS) : δ 4.17-4.16 (m, 2H, H-2), 2.69-2.67 (m, 2H, H-4), 2.63-2.62 (m, 2H, H-5), 1.26 (t, $J = 7$ Hz, 3H, H-3) ppm.

^{13}C NMR (125 MHz, CDCl_3 , TMS): δ 177.2 (C-6), 172.2 (C-1), 60.8 (C-2), 28.9, 28.8, 14.1 (C-3) ppm.

Compound 17 (eugenol)

Compound **17** was obtained in 230 mg as a pale yellow viscous liquid with pleasant smell. From the detailed NMR studies the structure of the compound was confirmed as eugenol.



Molecular formula : C₁₀H₁₂O₂

FT-IR (Neat) ν_{\max} : 3211, 2910 cm⁻¹

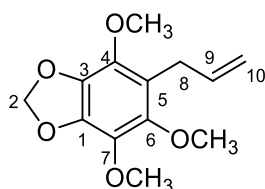
¹H NMR (500 MHz, CDCl₃, TMS) : δ 6.84 (d, J = 8.5 Hz, 1H, H-6), 6.68-6.67 (m, 2H, H-8 and H-5), 5.97-5.90 (m, 1H, H-9), 5.60 (brs, 1H, H-3), 5.09-5.04 (m, 2H), 3.85 (s, 3H, H-10), 3.31 (d, J = 6.5 Hz, 2H, H-7) ppm.

¹³C NMR (125 MHz, CDCl₃, TMS): δ 146.5 (C-2), 143.9 (C-1), 137.9 (C-8), 132.0 (C-4), 121.2 (C-7), 115.5 (C-3), 114.3, 111.2, 55.9 (C-10), 39.9 (C-7) ppm.

HRMS (ESI): m/z Calcd for C₁₀H₁₂O₂ : 165.0916; Found : 165.0573.

Compound 18 (nothoapiol)

Compound **18** was obtained in 21 mg as a UV active colorless viscous liquid. In the proton NMR, the six proton singlet at δ 3.85 ppm and a three proton singlet at δ 3.83 ppm indicated the presence of three methoxy groups. In the HRMS analysis, a peak corresponding to (M+H)⁺ was obtained at 253.1076. Then comparing the spectral data of the molecule with dill apiol and other literature reports, the compound was confirmed as nothoapiol.



Molecular formula : C₁₃H₁₆O₅

FT-IR (Neat) ν_{\max} : 3100, 2150, 2100, 1050 cm⁻¹

¹H NMR (500 MHz, CDCl₃, TMS) : δ 6.41 (s, 2H, H-2), 5.96 (dd, J_1 = 17 Hz, J_2 = 10 Hz, 1H, H-9), 5.13-5.08 (m, 2H, H-10), 3.85 (s, 6H), 3.83 (s, 3H) 3.34 (d, J = 7 Hz, 2H, H-8) ppm.

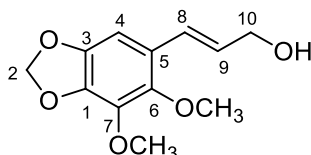
¹³C NMR (125 MHz, CDCl₃, TMS): δ 153.2 (C-6), 137.2 (C-7), 135.8, 116.0, 105.4 (C-2), 60.8, 56.1, 40.5 (C-8) ppm.

HRMS (ESI): m/z Calcd for C₁₃H₁₇O₅ : 253.1076; Found : 253.1075.

Compound 19 (ω -hydroxyapiol)

Compound **19** was obtained in 16 mg as a pale yellow colored viscous liquid. It showed an intense blue color in short UV. The two 3 proton singlets resonated at δ 4.02

and 3.77 ppm clearly indicate the presence of two methoxy groups. The mass spectrum of the compound showed a molecular ion peak at 239.0919, which is the $(M+H)^+$ peak. From all these spectral data and on comparison with the literature reports, compound **19** was confirmed as ω -hydroxyapiol.



Molecular formula : $C_{12}H_{14}O_5$

FT-IR (Neat) ν_{\max} : 3341, 3111, 2900, 1610 cm^{-1}

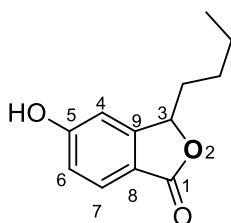
1H NMR (500 MHz, $CDCl_3$, TMS) : δ 6.83 (d, $J = 16$ Hz, 1H, H-8), 6.67 (s, 1H, H-4), 6.28-6.20 (m, 1H, H-19), 5.92 (s, 2H, H-2), 4.31 (d, $J = 6$ Hz, 1H, H-10), 4.02 (s, 3H), 3.77 (s, 3H) ppm.

^{13}C NMR (125 MHz, $CDCl_3$, TMS): δ 145.2 (C-7), 144.8 (C-6), 137.5, 137.3, 127.9, 125.5, 123.5, 101.4, 98.5, 64.1 (C-10), 61.6, 60.1 ppm

HRMS (ESI): m/z Calcd for $C_{12}H_{15}O_5$: 239.0919; Found : 239.0921.

Compound 20 (3-butyl-5-hydroxyisobenzofuran-1(3H)-one)

From the fraction pools 4-6, compound **20** (16 mg) was obtained as colorless solid, during column chromatography with 15 % ethyl acetate in hexane polarity. In the IR spectra, the compound gave peaks at 3112 and 1745 cm^{-1} which clearly indicate the presence of a hydroxyl as well as a carbonyl group. Mass spectrum of the molecule showed molecular ion peak at m/z 207.0918 corresponding to $(M+H)^+$. From these spectral data and on comparison with the literature reports, compound **20** was confirmed as an isobenzofuranone derivative.



Molecular formula : $C_{12}H_{14}O_3$

FT-IR (Neat) ν_{\max} : 3112, 2900, 1745 cm^{-1}

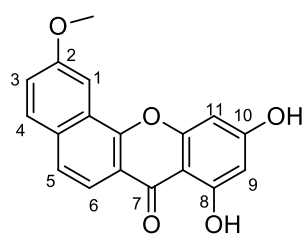
1H NMR (500 MHz, $CDCl_3$, TMS) : δ 7.76 (d, $J = 8.5$ Hz, 1H, H-7), 7.13 (brs, 1H, OH at C-5), 6.99 (dd, $J_1 = 8.5$ Hz, $J_2 = 2$ Hz, 1H, H-6), 6.86 (d, $J = 2$ Hz, 1H, H-4), 5.40-5.38 (m, 1H, H-3), 2.02-1.97 (m, 1H), 1.77-1.76 (m, 1H), 1.47-1.35 (m, 4H), 0.90 (t, $J = 7$ Hz, 3H) ppm.

^{13}C NMR (125 MHz, $CDCl_3$, TMS): δ 171.2 (C-1), 161.8 (C-5), 153.2 (C-9), 127.6 (C-8), 118.0, 117.4, 108.1 (C-3), 34.3, 26.8, 22.4, 13.9 ppm.

HRMS (ESI): m/z Calcd for $C_{12}H_{15}O_3$: 207.1021; Found : 207.1024.

Compound 21 (8,10-dihydroxy-2-methoxy-7H-benzo[c]xanthen-7-one)

Compound **21** was an intense UV active pale yellow solid with a molecular ion peak at 309.0763 corresponding to $(M+H)^+$ (9 mg). From detailed analysis of spectroscopic data and on comparison with the literature reports, compound **21** was confirmed as a xanthone derivative.



Molecular formula : $C_{18}H_{12}O_5$

FT-IR (Neat) ν_{max} : 3220, 2151, 2070, 1151 cm^{-1}

1H NMR (500 MHz, $CDCl_3$, TMS) : δ 13.60 (s, 1H, OH at C-8), 9.50 (d, $J = 2.5$ Hz, 1H, H-1), 8.05 (d, $J = 8.5$ Hz, 1H, H-4), 7.80 (d, $J = 9$ Hz, 1H, H-6), 7.35 (d, $J = 9$ Hz, 1H, H-5), 7.24 (dd, $J_1 = 8.5$ Hz, $J_2 = 2.5$ Hz, 1H, H-3), 6.34 (d, $J = 1.5$ Hz, 1H, H-9), 6.32 (d, $J = 2$ Hz, 1H, H-11), 6.01 (brs, 1H), 4.05 (s, 3H) ppm.

^{13}C NMR (125 MHz, $CDCl_3$, TMS): δ 183.2 (C-7), 163.8 (C-2), 162.4 (C-10), 161.0 (C-8), 158.2, 156.7, 136.7, 132.8, 129.9, 125.4, 118.1, 114.7, 112.5, 106.4, 105.2, 100.0, 98.8, 93.6, 55.6 ppm.

HRMS (ESI): m/z Calcd for $C_{18}H_{13}O_5$: 309.0764; Found : 309.0763.

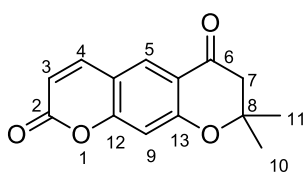
Compound 24 (graveolone)

While doing column chromatography with 20 % ethyl acetate- hexane mixture, 6 mg of compound **24** as colorless powder was obtained. The IR spectrum of the compound showed a broad absorption at 3111 cm^{-1} indicating the presence of hydroxyl group. Mass spectrum of the compound gave molecular ion peak at m/z 245.0712, which is the $(M+H)^+$ peak. From all these spectral data and on comparison with the literatures, the compound was recognized as graveolone.

Molecular formula : $C_{14}H_{12}O_4$

FT-IR (Neat) ν_{max} : 3111, 2900, 1755, 1746 cm^{-1}

1H NMR (500 MHz, CD_3COCD_3 , TMS) : δ 7.97 (s, 1H, H-5), 7.88 (d, $J = 9.5$ Hz, 1H, H-4), 6.70 (s, 1H, H-9), 6.19



(d, $J = 9.5$ Hz, 1H, H-3), 2.69-2.65 (m, 2H, H-7), 1.37 (s, 6H, H-10 and H-11) ppm.

^{13}C NMR (125 MHz, CD_3COCD_3 , TMS): δ 173.5 (C-6), 159.7 (C-2), 159.2 (C-12), 154.7 (C-13), 143.7, 127.3, 117.0, 114.2, 114.1, 104.8, 80.7, 58.2, 48.0, 25.8 (C-10 and C-11) ppm.

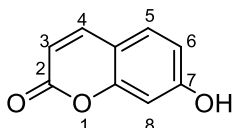
HRMS (ESI): m/z Calcd for $\text{C}_{14}\text{H}_{13}\text{O}_4$: 245.0714; Found : 245.0712.

Compound 25 (β -umbelliferone)

Compound **25** (62 mg) was isolated as yellowish-white crystalline solid from fraction pools 7-9, obtained by eluting the column with 25 % ethyl acetate in hexane. IR spectrum of the compound showed absorption at 3293 and 1761 cm^{-1} suggesting the presence of hydroxyl and an ester/ lactone carbonyl groups respectively. Mass spectrum of the compound showed molecular ion peak at m/z 163.0393, which is the $(\text{M}+\text{H})^+$ peak. Comparison of the ^1H and ^{13}C NMR spectral values along with DEPT-135, HOMO COSY and HMQC spectra suggested that the molecule is 7-hydroxycoumarin or β -umbelliferone.

Molecular formula : $\text{C}_9\text{H}_6\text{O}_3$

FT-IR (Neat) ν_{max} : 3293, 3087, 2749, 2233, 1761, 1257 cm^{-1}



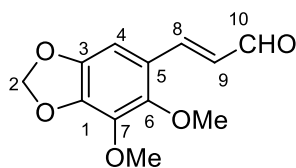
^1H NMR (500 MHz, CD_3COCD_3 , TMS) : δ 7.98 (d, $J = 9$ Hz, 1H, H-4), 7.53 (d, $J = 8.5$ Hz, 1H, H-5), 6.86 (dd, $J_1 = 10$ Hz, $J_2 = 2.5$ Hz, 1H, H-8), 6.76 (d, $J = 2$ Hz, 1H, H-3), 6.18 (d, $J = 9.5$ Hz, 1H, H-6) ppm.

^{13}C NMR (125 MHz, CD_3COCD_3 , TMS): δ 161.1, 160.2, 156.1, 143.8, 129.6, 112.9, 112.1, 112.0, 102.4 ppm.

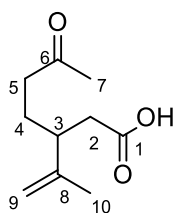
HRMS (ESI): m/z Calcd for $\text{C}_9\text{H}_7\text{O}_3$: 163.0395; Found : 163.0393.

Compound 26 (dill apional)

From the same fraction pools, compound **26** (23 mg) was obtained as a colorless viscous liquid, and the IR spectrum of the compound showed an absorption at 1748 cm^{-1} , which suggest the presence of an alkanal carbonyl group. The molecular ion peak of the molecule was obtained at m/z 237.07609 which is the $(\text{M}+\text{H})^+$ peak ($(\text{M}+\text{Na})^+$ at 259.0582). From all these spectral data, and on comparison with the literature, compound **26** was identified as dill apional.

Molecular formula : C₁₂H₁₂O₅**FT-IR** (Neat) ν_{\max} : 3067, 2711, 2243, 1748, 1253 cm⁻¹**¹H NMR** (500 MHz, CDCl₃, TMS) : δ 9.67 (d, J = 8 Hz, 1H, H-10), 7.76 (d, J = 16 Hz, 1H, H-8), 6.74 (s, 1H, H-4), 5.56 (dd, J_1 = 16 Hz, J_2 = 3Hz, 1H, H-9), 6.00 (s, 2H, H-2), 4.04 (s, 3H), 3.86 (s, 3H) ppm.**¹³C NMR** (125 MHz, CDCl₃, TMS): δ 194.0 (C-10), 147.2 (C-8), 147.1 (C-7), 146.7 (C-6), 145.5 (C-3), 140.7 (C-1), 127.7 (C-5), 121.0 (C-4), 102.0, 99.1 (C-2), 62.2, 60.2 ppm.**HRMS (ESI)**: m/z Calcd for C₁₂H₁₃O₅ : 237.0760; Found : 237.0763.**Compound 27** (6-oxo-3-(prop-1-en-2-yl)heptanoic acid)

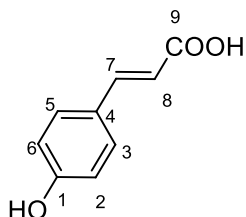
Compound **27** was isolated from same fraction pools on doing column chromatography with 35 % ethyl acetate in hexane. It was obtained as a pale yellow viscous liquid (13 mg). The IR spectrum of the molecule showed intense absorptions bands at 3311, 3050, 2980, 1748 and 1729 cm⁻¹, which clearly attribute to a ketone as well as carboxylic acid groups. The resemblances of the molecule with that of carvone and limonene led to characterize the structure as given below. Also, the m/z value of the molecule was obtained from GCMS as 184.11.

Molecular formula : C₁₀H₁₆O₃**FT-IR** (Neat) ν_{\max} : 3311, 3050, 2980, 1748, 1729 cm⁻¹**¹H NMR** (500 MHz, CDCl₃, TMS) : δ 4.83 (s, 1H, H-9), 4.77 (s, 1H, H-9), 2.59-2.57 (m, 1H), 2.54-2.37 (m, 4H), 2.14 (s, 3H), 1.78-1.74 (m, 1H), 1.72 (s, 3H), 1.65-1.61 (m, 1H) ppm.**¹³C NMR** (125 MHz, CDCl₃, TMS): δ 208.9 (C-6), 178.1 (C-1), 145.1 (C-8), 113.1 (C-9), 42.7, 41.1, 38.9, 30.0, 26.2, 18.4 ppm.

Mass from GCMS : 184.11.

Compound 28 (*p*-coumaric acid)

Compound **28** was off-white in color, with a melting point of 209 °C. The IR absorptions at 3410, 3301, 2900, 2110 and 1738 cm⁻¹ showed by the compound clearly indicate the presence of carboxyl as well as hydroxyl groups. From the literature reports, the structure of the molecule was confirmed as *p*-coumaric acid, and it was well supported by HRMS data in which (M+H)⁺ peak was obtained at 165.0571.



Molecular formula : C₉H₈O₃

Mp : 209-211 °C

FT-IR (Neat) ν_{\max} : 3301, 2900, 2110, 1738 cm⁻¹

¹H NMR (500 MHz, CD₃COCD₃, TMS) : δ 7.62 (d, J = 16 Hz, 1H, H-7), 7.55 (d, J = 8.5 Hz, 2H, H-3 and H-5), 6.91 (d, J = 8.5 Hz, 2H, H-2 and H-6), 6.33 (d, J = 16 Hz, 1H, H-8) ppm

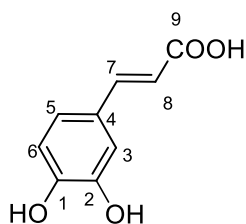
¹³C NMR (125 MHz, CD₃COCD₃, TMS): δ 166.7 (C-9), 151.2 (C-7), 147.2 (C-1), 124.0, 121.9, 114.6, 112.5 ppm.

HRMS (ESI): m/z Calcd for C₉H₉O₃ : 165.0552; Found : 165.0571.

Compound 29 (caffeic acid)

Molecular formula : C₉H₈O₄

Mp : 226-228 °C



FT-IR (Neat) ν_{\max} : 3410, 3111, 3050, 1731 cm⁻¹

¹H NMR (500 MHz, CD₃COCD₃, TMS) : δ 8.55 (brs, 1H), 7.56 (d, J = 16 Hz, 1H, H-7), 7.18 (d, J = 2 Hz, (d, J = 8 Hz, 1H, H-6), 6.28 (d, J = 16 Hz, 1H, H-8) ppm. 1H, H-5 and H-3), 7.06 (dd, J_1 = 8 Hz, J_2 = 2 Hz, 1H, H-5), 6.88

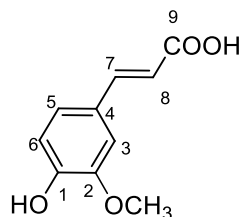
¹³C NMR (125 MHz, CD₃COCD₃, TMS): δ 167.3 (C-9), 147.8 (C-1), 145.4 (C-2), 145.1, 126.8, 121.6, 115.5, 114.9, 114.3 ppm.

HRMS (ESI): m/z Calcd for C₉H₉O₄ : 181.0501; Found : 181.0503.

Compound 30 (ferulic acid)

Molecular formula : C₁₀H₁₀O₄

Mp : 168-171 °C



FT-IR (Neat) ν_{\max} : 3317, 3070, 2900, 1718 cm⁻¹

¹H NMR (500 MHz, CD₃COCD₃, TMS) : δ 8.06 (brs, 1H, OH at C-1), 7.47 (d, J = 16 Hz, 1H, H-7), 7.20 (d, J = 1.5 Hz, 1H, H-3), 7.01 (dd, J_1 = 8.5 Hz, J_2 = 2 Hz, 1H, H-5), 6.74 (d, J = 8 Hz, 1H, H-6), 6.24 (d, J = 16 Hz, 1H, H-8), 3.79 (s, 3H) ppm.

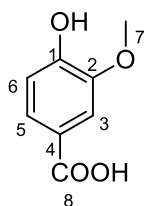
¹³C NMR (125 MHz, CD₃COCD₃, TMS): δ 167.4 (C-9), 149.1 (C-2), 147.9 (C-1), 145.1 (C-7), 126.6 (C-3), 123.0, 115.2, 115.1, 110.4, 55.4 ppm.

HRMS (ESI): *m/z*. Calcd for C₁₀H₁₁O₄ : 195.0657; Found : 195.0653.

Compound 31 (vanillic acid)

Molecular formula : C₈H₈O₄

Mp : 210-211 °C



FT-IR (Neat) ν_{\max} : 3211, 3010, 2150, 1728 cm⁻¹

¹H NMR (500 MHz, CD₃COCD₃, TMS) : δ 7.62-7.58 (m, 2H), 6.93 (d, *J* = 8.5 Hz, 1H), 3.92 (s, 3H, H-7) ppm

¹³C NMR (125 MHz, CD₃COCD₃, TMS): δ 166.7 (C-8), 151.2 (C-2), 147.2 (C-1), 124.0, 121.9, 114.6, 112.5, 55.4 (C-7) ppm.

HRMS (ESI): *m/z*. Calcd for C₈H₉O₄ : 169.0501; Found : 169.0522.

Compound 32

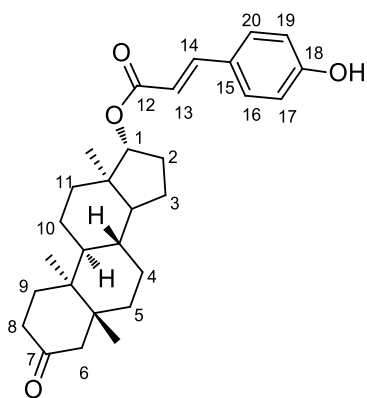
Compound **32** was isolated in 6 mg, from the ethanol extract (came in 1 % of methanol in ethyl acetate) as a colorless solid with a melting point of 165-167 °C. The IR absorptions at 3321, 3111, 2900 and 1748 cm⁻¹ showed by the compound clearly indicate the presence of carboxyl as well as hydroxyl groups. In the carbon NMR, the peaks at 210.2 and 166.4 ppm represents two carbonyl systems in the molecule. Also, the similarity of the ¹H NMR of the compound with, compound **28** revealed that, the molecule is an ester of *p*-coumaric acid.

Molecular formula : C₂₉H₃₈O₄

Mp : 165-167 °C

FT-IR (Neat) ν_{\max} : 3321, 3111, 2900, 1748 cm⁻¹

¹H NMR (500 MHz, CD₃COCD₃, TMS) : δ 8.88 (s, 1H Oh at C-18), 7.49-7.41 (m, 3H, H-14, H-16 and H-20), 6.71 (d, *J* = 8.5 Hz, 2H, H-17 and H-19), 6.23 (d, *J* = 16 Hz, 1H, H-13), 4.46-4.42 (m, 1H, H-1), 2.52-2.51 (m, 1H), 1.92-1.78 (m, 4 Hz), 1.60-1.53 (m, 7H),



1.48-1.43 (m, 2H), 1.17-1.02 (m, 4H), 1.04-1.02 (m, 3H), 0.82-0.81 (m, 9H), 0.76 (s, 3H) ppm.

^{13}C NMR (125 MHz, CD_3COCD_3 , TMS): δ 210.2 (C-7), 166.4 (C-12), 159.7 (C-18), 144.2 (C-14), 130.0 (C-16 and C-20), 126.2 (C-15), 115.8, 115.3, 80.2 (C-1), 55.8, 53.7, 50.5, 49.9, 44.8, 40.4, 38.6, 37.9, 37.0, 35.3, 31.3, 27.5, 25.6, 25.5, 23.7, 21.2, 18.0, 16.2, 15.8, 15.4, 15.1 ppm.

HRMS (ESI): m/z Calcd for $\text{C}_{29}\text{H}_{39}\text{O}_4$: 451.2848;
Found : 451.2841.

Compound 33

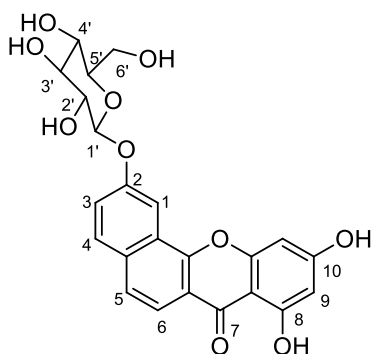
Compound **33** (8 mg) was also isolated from the ethanol extract, *via* silica gel column chromatography with 10 % of methanol in ethyl acetate. The compound was a colorless solid with a melting point of 210 °C and, the IR stretching frequencies at 3111, 2900 and 1698 cm^{-1} confirmed that the system consists of hydroxyl as well as carbonyl moieties. It exhibited almost similar NMR characteristics of the compound **21**, with an additional glucoside moiety and gave a molecular ion peak at m/z 479.0953 in the HRMS.

Molecular formula : $\text{C}_{23}\text{H}_{20}\text{O}_{10}$

Mp : 210-211 °C

FT-IR (Neat) ν_{max} : 3111, 2900, 1688 cm^{-1}

^1H NMR (500 MHz, MeOD, TMS) : δ 9.36 (d, $J = 2.5$ Hz, 1H, H-1), 8.08 (d, $J = 8.5$ Hz, 1H, H-4), 7.78 (d, $J = 8$ Hz, 1H, H-6), 7.31 (d, $J = 9$ Hz, 1H, H-5), 7.16-7.14 (m, 1H), 6.65 (d, $J = 2$ Hz, 1H, H-3), 6.44 (d, $J = 2.5$ Hz, 1H, H-8), 5.01 (d, $J = 8$ Hz, 1H, H-1'), 4.50 (brs, 1H), 3.91 (s, 2H), 3.86-3.83 (s, 1H), 3.66-3.63 (m, 1H), 3.48-3.45 (m, 1H), 3.43-3.41 (m, 1H) ppm.



^{13}C NMR (125 MHz, MeOD, TMS): δ 187.8 (C7), 164.0 (C-8), 163.6 (C-10), 161.1 (C-2), 156.4, 137.2, 132.9, 130.3, 177.7, 114.3, 106.1, 105.5 (C-1'), 100.5, 94.1, 76.9, 76.5, 73.8, 70.8, 61.1, 56.1, 54.6 ppm.

HRMS (ESI): m/z Calcd for $\text{C}_{23}\text{H}_{20}\text{O}_4\text{Na}$: 479.0954;
Found : 479.0953.

3A. 9. References

1. (a) A. R. Gohari, S. Saeidnia, A. Naseri, A. Manayi, I. Salimikia and H.R. Monsef Esfahani, *Research Journal of Pharmacognosy (RJP)*, **2014**, *1*(4), 1-5. (b) G. Lin, P. Li, S. L. Li and S. W. chan, *J. Chromatogr. A.*, **2001**, *935*, 321-328. (c) L. W. Yang, D. H. Wu, X. Tang, W. Pang, X. R. Wang, Y. Ma and W. W. Su, *J. Chromatogr. A.*, **2005**, *1070*, 35-42.
2. (a) K. Dhalwal, V. M. Shinde and K. R. Mahadik, *Chromatographia*, **2008**, *67*, 162-167. (b) The Wealth of India (Raw Materials) (1950) Council of Scientific and Industrial Research, Delhi, India, pp 313–115 5. (c) G. Singh, S. Maurya, M. P. DeLampasona and C. Catalan, *J. Food Sci.*, **2005**, *70*, 208-215.
3. (a) I. E. Orhan, F. S. Senol, N.Ozturk, S. A. Celik, A. Pulur and Y. Kan, *Food Chem. Toxicol.*, **2013**, *59*, 96-103. (b) Hemphill, *The Spice and Herb Bible: A Cook's Guide*, **2006**, sec edition, Robert Rose inc., Toronto. (c) L. Kostadinovic, N. Puvaca, S. Popovic, and J. *World Poultry Science Journal*, **2015**, *71*, 27-36. (d) N. Puvaca, L. Kostadinovic, D. Ljubojevic, D. Lukac, J. Levic, S. Popovic, N. Novakov, B. Vidovic and O. Djuragic, *European Poultry Science*, **2015**, *79*, 1-13. (e) W. Windisch, E. Rohrer and K. Schedle, (2009). Phytogetic feed additives to young piglets and poultry: mechanisms and application. In *Phytoin Animal Nutrition*. Ed. T. Steiner, Nottingham University Press, pp. 19-39.
4. (a) M. G. Aćimović, L. M. Kostadinović, N. M. Puvača, S. J. Popović and M. I. Urošević, *Food and Feed Research*, **2016**, *43*(1), 35-41. (b) M. Acimovic, L. Kostadinovic, S. Popovic, and N. Dojcinovic, *Journal of Agricultural Science (Belgrade)*, **2015**, *60*, 237-246. (c) M. Acimovic, V. Tesevic, M. Todosijevic, J. Djisalov and S. Oljaca, *Botanica Serbica*, **2015**, *39*, 9-14.
5. (a) Y. H. Gebhardt, S. W. Holger Steuber, U. Matern and S. Martens, *Plant Physiol.*, **2007** *144*(3), 1442-1454. (b) C. Zidorn, K. Jöhrer, M. Ganzera, B. Schubert, E. M. Sigmund, J. Mader, R. Greil, E. P. Ellmerer and H. Stuppner. *J Agric Food Chem.*, **2005**, *53*(7), 2518-2523. (c) <http://battlegroundhealingarts.com/articles/the-apiaceae-family-medicinal-plant-research-summary/>
6. (a) K. K. Chahal, M. A. Kumar, U. Bhardwaj and R. Kaur, *Journal of Pharmacognosy and Phytochemistry*, **2017**, *6*(2), 295-306. (b) G. S. Randhwa, S. Kau, K. L. Chadha and R. Gupta, (1995). *Dill: Medicinal and aromatic plants*. Malhotra Publication House, Delhi.

7. (a) S. Jana and G. S. Shekhawat, *Pharmacogn Rev.*, **2010**, 4(8), 179-184. (b) C. P. Khare, *Indian herbal remedies*. Berlin, New York: Springer (**2004**), Rational western therapy, ayurvedic and other traditional usages, botany; pp. 60–61. (c) P. ravindran and I. Balachandran, *Underutilized medicinal spices II*, Spice India. Vol. 17. (**2005**), India: Publisher V K Krishnan Nair; 2005. pp. 32–36. (d) J. Bailer, T. Aichinger, G. Hackl, K. D. Hauber and M. Dachler, *Indus Crops Prods.*, **2001**, 14, 229-239.
8. A. Esmail Al-Snafi, *Int. J. Pharm. Pharm. Sci.*, **2014**, 6 (4), 11-13.
9. S. Heamalatha, S. Swarnalatha, M. Divya, R. Gandhi Lakshmi, A. Ganga Devi and E. Gomathi, *Research Journal of Pharmaceutical, Biological and Chemical Sciences*, **2011**, 2(4), 565-576.
10. J. Stannard, *Wurzburg Medizinhist Forsch.*, **1982**, 24, 411-424.
11. (a) M. T. Goodarzi, I. Khodadadi, H. Tavilani and E. A. Oshaghi, *Journal of Tropical Medicine*, **2016**, 1-11. (b) M. Setorki, M. Rafieian-Kopaei and A. Merikhiatal, *International Journal of Preventive Medicine*, **2013**, 4(8), 889-895.
12. G. J. Kaur and D. S. Arora, *Journal of Medicinal Plants Research*, **2010**, 4(2), 87-94.
13. (a) Routledge, *The Cultural History of Plants* (**2005**), eds. Sir Ghillean Prance & Mark Nesbitt), pp. 102-03. (b) <https://en.wikipedia.org/wiki/Dill>
14. E. A. Oshaghi, H. Tavilani, I. Khodadadi and M. T. Goodarzi, *Asian Pac. J. Trop. Biomed.*, **2015**, 5(90) 720-727.
15. (a) M. Stavri and S. Gibbons, *Phytother. Res.*, **2005**, 19, 938-941. (b) V. Sathya and V. K. Gopalakrishnan, *Int. J. Pharm. Sci.*, **2013**, 5(2), 535-539. (c) B. Bonnländer and P. Winterhalter, *J. Agric. Food Chem.*, **2000**, 48, 4821-4825. (d) S. Goodarzi, A. Hadjiakhoondi, N. Yassa, M. Khanavi and Z. Tofighi, *Iranian Journal of Pharmaceutical Research*, **2016**, 15(4), 901-906. (e) O. T. Olaru, G. M. Nițulescu, A. Orțan and C. E. Dinu-Pîrvu. *Molecules*, **2015**, 20, 15003-15022.
16. (a) U. Ravid, M. Bassat, E. Putievsky V. Weinstein and R. Ikan, *flavour and fragrance journal*, **1987**, 2, 95-97. (b) Y. Qiao, B. J. Xie, Y. Zhang, Y. Zhang, G. Fan, X. L. Yao and S. Y. Pan, *Molecules*, **2008**, 13, 1333-1344.
17. G. K. Poon, D. Vigushin, L. J. Griggs, M. G. Rowlands, R. C. Coombes and M. Jarman, *Drug Metab. Dispos.*, **1996**, 24(5), 565-571.
18. M. Razzaghi-Abyaneh, T. Yoshinari, M. Shams-Ghahfarokhi, R. Mohammad-Bagher, H. Nagasawa, and S. Sakuda, *Biosci. Biotechnol. Biochem.*, **2007**, 71(9), 2329-2332.
19. A. A. Rahimi, A. Ashnagar and N. Hamideh, *Int. J. ChemTech Res.*, **2012**, 4(1), 105-108.

20. C. S. Mathela, R. K. Joshi, B. S. Bisht and S. C. Joshi, *Rec. Nat. Prod.*, **2015**, 9(4), 546-552.
21. V. S. Prakash Chaturvedula, S. M. Hecht, Z. Gao, S. H. Jones, X. Feng and D. G. I. Kingston, *J. Nat. Prod.*, **2004**, 67, 964-967.
22. S. E. Sajjadi Y. Shokoohinia and P. Mehramiri, *Res. Pharm. Sci.*, **2013**, 8(1), 35-41.
23. M. Kozawa, K. Baba, T. Arima and K. Hata, *Che. Pharm. Bull.*, **1976**, 24(2), 220-223.
24. J. Widelski, M. Popova, K. Graikou, K. Glowniak and I. Chinou, *Molecules*, **2009**, 14, 2729-2734.
25. Y. Tan, T. Gao, H. Wang, Zhi-Hui Zhang, Feng-Hua Yu and Meng-Meng Kan, *Chemistry of Natural Compounds*, **2017**, 53, 147-148.
26. Y. S. Kwon, W. G. Choi, W. J. Kim, W. K. Kim, M. J. Kim, W. H. Kang and C. M. Kim, *Arch. Pharm. Res.*, **2002**, 25, 154-157.
27. (a) H. Katsuragi, K. Shimoda, N. Kubota, N. Nakajima, H. Hamada and H. Hamada, *Biosci. Biotechnol. Biochem.*, **2010**, 74(9), 1920-1924. (b) S. E. Sajjadi, Y. Shokoohinia and Narjess-Sadat Moayedi, *Jundishapur J. Nat. Pharm. Prod.*, **2012**, 7(4), 159-162. (c) Y. Wei, Y. Gao, K. Zhang and Y. Ito, *J. Liq. Chromatogr. Relat. Technol.*, **2010**, 33(6), 837-845. (d) R. Cai, D. Li, Y. Yuan, Z. Wang, C. Guo, B. Liu and T. Yue, *J. Sci. Food Agric.*, **2016**, 96, 2925-2931.
28. Kuo-Hsiung Lee, Toshiro Ibuka, Sun-Hyuk Kim, Bruce R. Vestal, Iris H. Hall and Eng-Shang Huang, *J. Med. Chem.*, **1975**, 18 (8), 812-817.
29. M. Raghavendra, A. M. Reddy, P. R. Yadav, A. S. Raju and L. Siva Kumar, *Asian J. Pharm. Clin. Res.*, **2013**, 6(3), 96-99.
30. (a) Xuan-Yu Meng, Hong-Xing Zhang, Mihaly Mezei and Meng Cui, *Curr. Comput. Aided Drug Des.*, **2011**, 7(2), 146-157. (b) S. A. Muhammad and N. Fatima, *Pharmacogn Mag.*, **2015**, 11(Suppl 1), S123-S126. (c) X. Qing, X. Y. Lee, J. D. Raeymaeker, J. R. H Tame, K. Y. J Zhang, M. D. Maeyer and A. R. D Voet, *J. Recept. Ligand Channel Res.*, **2014**, 7, 81-92. (d) C. G. Wermuth, P. Lindberg, C. R. Ganellin and L. A. Mitscher, *Pure Appl. Chem.*, **1998**, 70, 1129-1143.

Part B: Investigation on Phytochemical Constituents and Antioxidant Properties of *Zingiber nimmonii* (J. Graham) Dalzell

3B.1. Introduction

The family Zingiberaceae, is an important natural resource that provides many useful products like food, spices, medicines, dyes, perfume and aesthetics. It constitutes a vital group of rhizomatous medicinal and aromatic plants, characterized by the presence of volatile oils and, oleoresins of export value. The family is made up of about 50 genera, with a total of about 1600 known species of aromatic flowering perennial herbs with horizontally creeping or tuberous rhizomes, distributed throughout tropical Africa, Asia, and the Americas. These plants are one of the inevitable components in the folklore medicines. They are widely distributed in India, and in tropical and subtropical regions of Asia (especially in Thailand, Indonesia and Malaysia). India is one of the richest and diverse regions for Zingiberaceae, having 22 genera and about 170 species. The important genera coming under Zingiberaceae are *Curcuma*, *Kaempferia*, *Hedychium*, *Amomum*, *Zingiber*, *Alpinia*, *Elettaria* and *Costus*. The plants in this family exhibit a wide spectrum of pharmacological properties. Many terpenoid compounds, with varied physiological activities - antimicrobial, antiarthritic, antioxidant, anticancer, anti-inflammatory, antidiabetic, anti-HIV, neuroprotective and larvicidal *etc.* have been identified from the essential oils of zingiberaceous plants.¹

The genus *Zingiber* has about 85 species of aromatic herbs, mostly distributed in East Asia and tropical Australia. The term '*Zingiber*' is derived from the Sanskrit word 'shringavera', owing to their 'hornshaped', sympodially branched rhizomes. These species are rich in volatile oils, and are used in traditional medicine and as spices. Classic examples for plants belonging to the genera include *Z. officinale* (ginger), *Z. zerumbet* (wild ginger), *Z. cernuum* *etc.* The rhizomes are variously colored, ranging from pale yellow, deep yellow, greenish blue, pink or combinations of these in different species. The young rhizomes and axillary buds are protected by scale leaves. Leafy shoots are generally unbranched, and true aerial stem is present in some genera and absent in others.²

Zingiber nimmonii (J. Graham) Dalzell, an endemic species of the Western Ghats in South India, grows both at high and low altitudes, in moist areas under the shades of trees. Its rhizomes are fleshy with a yellowish cross-section and an occasional purple tinge (figure 3B.1). The rhizome oil of *Z. nimmonii* is a unique natural source with 69.9 % of isomeric caryophyllenes, viz. β -caryophyllene (42.2 %) and α -caryophyllene (27.7 %), along with traces of isocaryophyllene (0.03 %) in it. The major constituents of the rhizome oil of *Z. nimmonii* vary from the rhizome oils of *Z. zerumbet* and *Z. officinale*, the most studied *Zingiber* oils. The available reports on this plants are the extract level anti-microbial as well as antioxidant studies. In these studies, the rhizome oil showed significant activities against the human pathogenic fungi, *Candida glabrata*, *C. albicans* and *Aspergillus niger*, but no action against the plant pathogen, *Fusarium oxysporum*.³



Figure 3B.1. *Zingiber nimmonii*- Flower, plant and collected rhizome

Also, in the anti-oxidant studies, on the basis of the results obtained from the evaluation of nitric oxide and super superoxide scavenging; the best IC₅₀ values were exhibited by the hexane extract, when compared to the respective standards. Very recently, Giovanni *et al.* reported that the essential oil from *Z. nimmonii* can acts as a newer and safer natural larvicide and repellent against malaria, dengue and filariasis mosquito vectors. In this regard, it becomes more evident that the isolation of the bio-actives from this species will be extremely significant, and this encouraged us to penetrate into the molecular level studies of the unexplored plant species *Zingiber nimmonii*.⁴

3B.2. Aim and Scope of the Present Study

Zingiberaceae family is well-known for its medicinal and economic significances. The pharmacological evaluation of molecules isolated from this family showed potential biological activities. Also, these herbs are widely used as a raw material for various Ayurvedic formulations. Hence, a study on the phytochemical constituents of this family

offers many opportunities, to investigate the different functions and prospects in various pharmaceutical studies, which is also evident from the work of various researchers. Therefore it appeared sensible and relevant to carry out the phytochemical investigation of *Z. nimmonii* and as a part of this Ph.D. program, a detailed study on the rhizomes of *Z. nimmonii* has been undertaken. To the best of our knowledge, this is the first report on the isolation of phytochemicals from the species *Z. nimmonii*. Also, the *in vitro* antioxidant potential of some of the isolated compounds have been carried out, and the results are described in this chapter.

3B.3. Isolation and Characterization of Phytochemicals from the Rhizomes of *Zingiber nimmonii* (J. Graham) Dalzell

3B.3.1. Collection of plant material

The fresh mature rhizomes of *Zingiber nimmonii* were collected from Botanical Garden of University of Calicut, Malappuram District, Kerala, India during December 2017. The specimen was identified by Dr. M Sabu, Associate professor, Department of Botany, University of Calicut, and voucher specimen (voucher No. 103001) was submitted to herbarium of Department of Botany, University of Calicut, Kerala, India.

3B.3.2. Extraction and Isolation

Fresh rhizomes of *Zingiber nimmonii* were washed, dried, then crushed into powder and subjected to extraction with various organic solvents. Around 650 g of dried rhizome was first soaked in 5L hexane at room temperature for 3 days, and the same procedure was repeated twice. Removal of solvent under reduced pressure gave 1.4 g of crude hexane extract. The residue was further subjected to acetone extraction, which gave 16 g of acetone extract. In the same way we obtained 2 g of ethanol extract and finally the water extract. Around 14 g of acetone extract was subjected to column chromatography on 100-200 mesh sized silica gel and eluted with hexane-ethyl acetate mixtures of increasing polarities to give twelve fraction pools. This on further purification resulted in the isolation of compounds **1, 3, 34-42**. A pictorial representation of entire isolation procedure is given below (figure 3B.2).

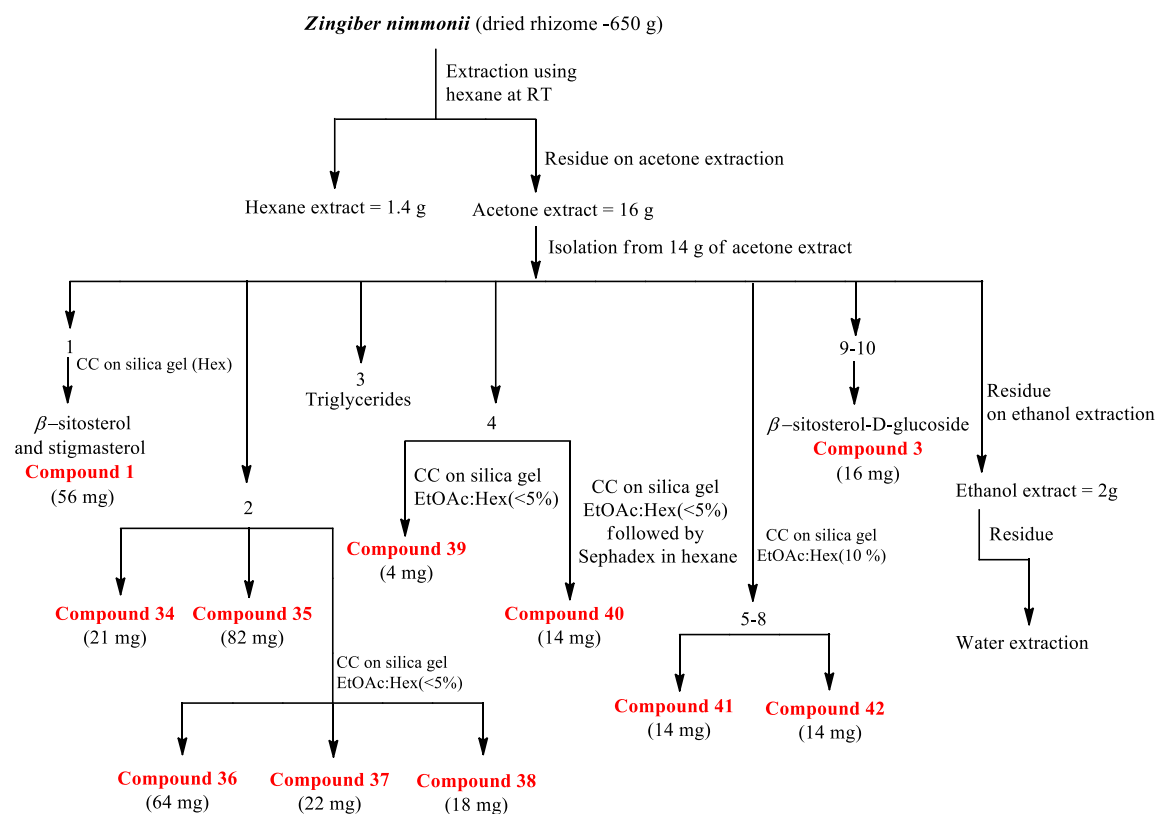
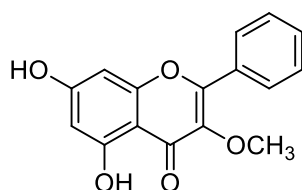


Figure 3B.2. Pictorial representation of extraction/ isolation procedure

From fraction pool 1, we could isolate a mixture of β - sitosterol and stigmaterol as a colorless crystalline solid in 56 mg, from this 10 mg of pure β - sitosterol was isolated (compound 1) after repeated column chromatography on silica gel. Compounds 34 and 35 were directly obtained from the main column and were recrystallized from hexane. Fraction pool 2 was further subjected to column chromatography on silica gel yielded compounds 36, 37 and 38. Similarly, compounds 39 and 40 were isolated from fraction pool 4 *via* silica gel and Sephadex column chromatography techniques, respectively. Finally, compounds 41 and 42 were isolated from fraction pools 5-8.

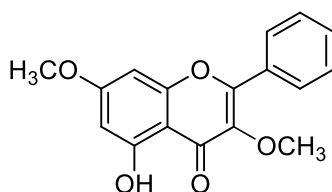
Compound 34 was isolated as a yellow solid, and is highly UV active. It showed a pink color which turned to blue while charring the TLC in Enholm yellow solution. IR spectrum of the compound showed a broad and a sharp peak at 3316 and 1660 cm^{-1} corresponding to the hydroxyl and carbonyl groups respectively. One proton singlet at δ 11.66 ppm in ^1H NMR (figure 3B.3) indicates the presence of phenolic-OH with intramolecular H- bonding. The five aromatic protons, resonating in between δ 7.5-8.3 ppm, with interactions in HOMO COSY, can be attributed to a phenyl side chain. The two doublets at δ 6.38 and 6.50 ppm of coupling constant 2 Hz, can be considered as a *meta*

coupled aromatic protons and they do not show any interactions with the methoxy carbon in HMBC. The peak at δ 175.4 ppm suggests the carbonyl group (figure 3B.4). Three proton singlet at δ 3.89 ppm indicates the presence of $-\text{OCH}_3$ group. DEPT-135 experiment revealed that the compound contains seven CH and one $-\text{CH}_3$ group. The mass spectrum of the molecule showed the molecular ion peak at m/z 285.0767, as $(\text{M}+\text{H})^+$ peak. From all the above spectral details, and on comparison with the literature reports compound **34** was confirmed as 5,7-dihydroxy-3-methoxy-2-phenyl-4H-chromen-4-one or **galangin-3-*O*-methyl ether**.⁵ The structure of the same is given below.

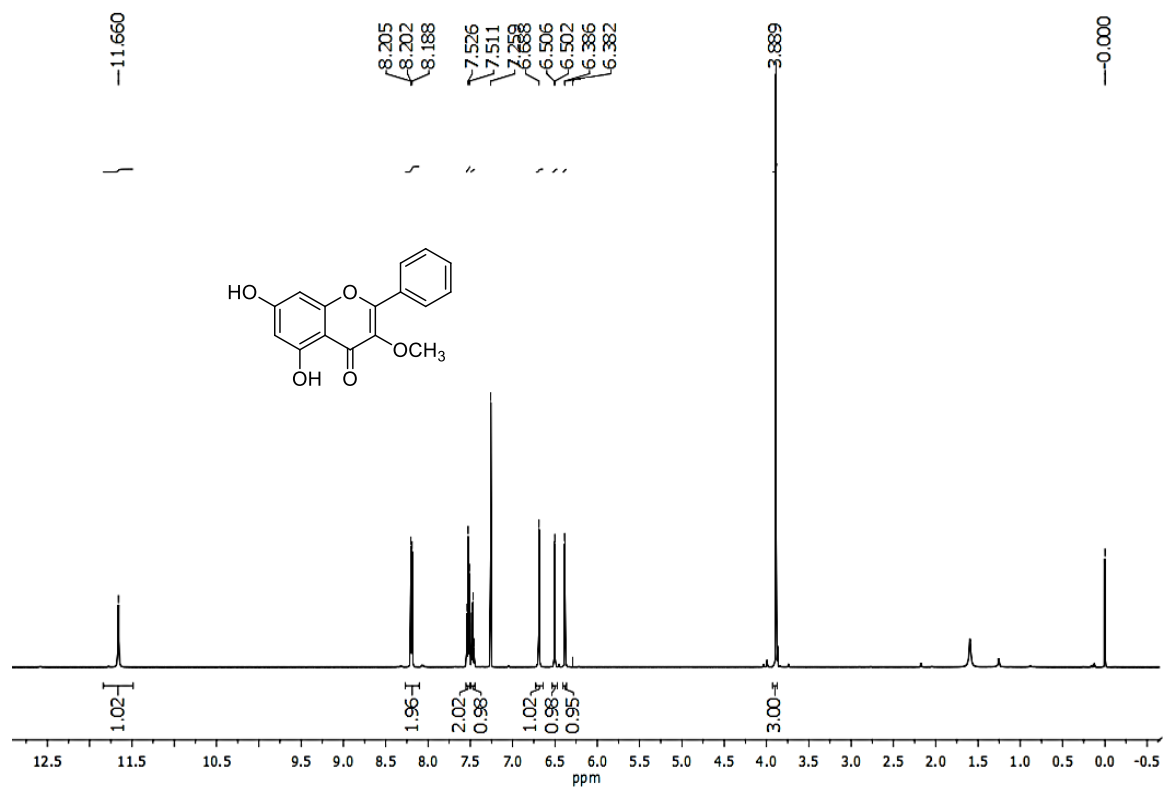
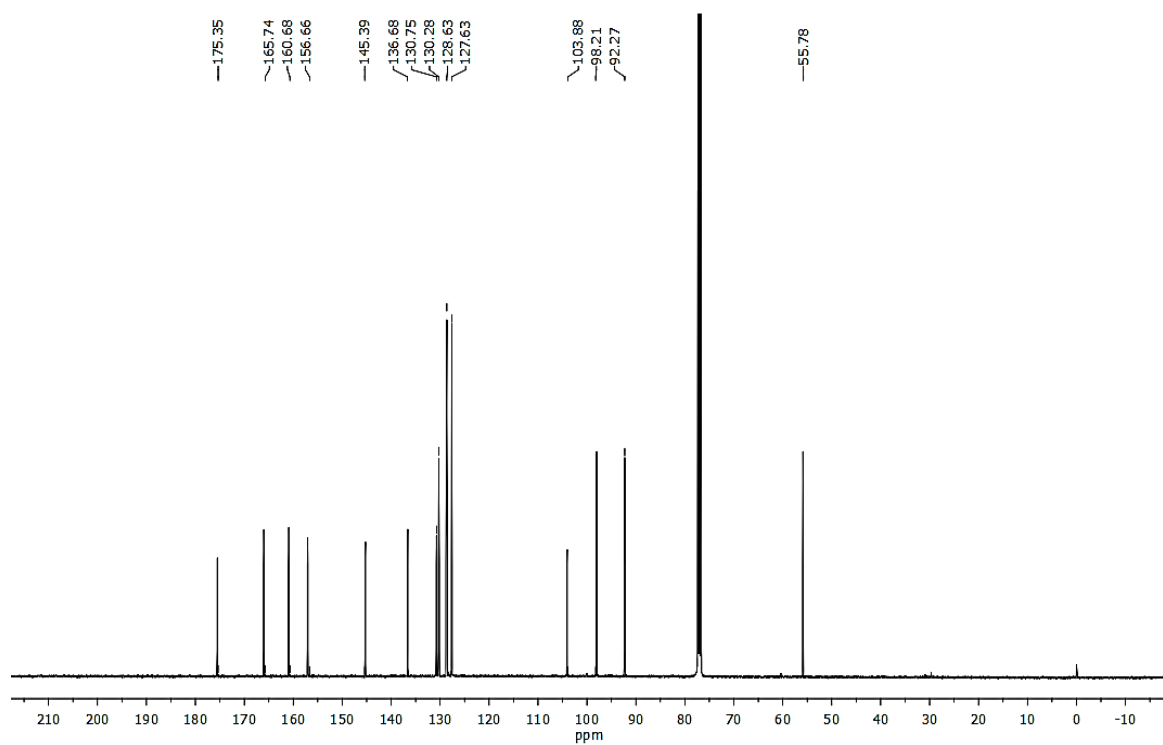


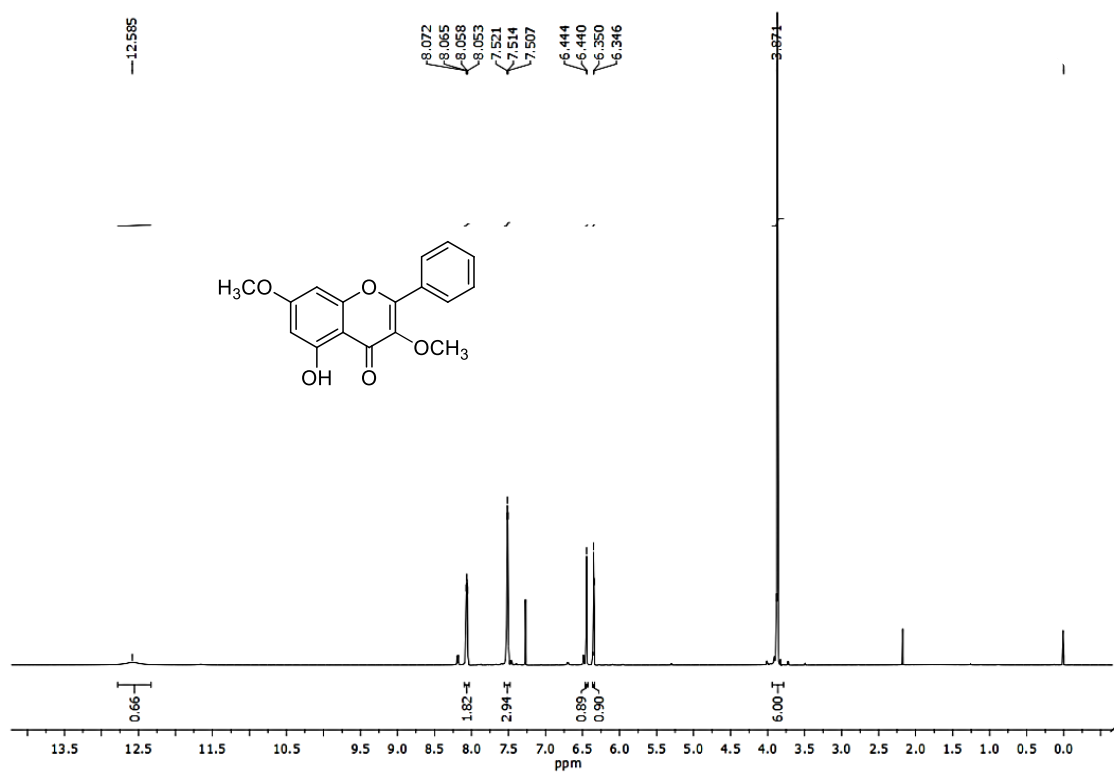
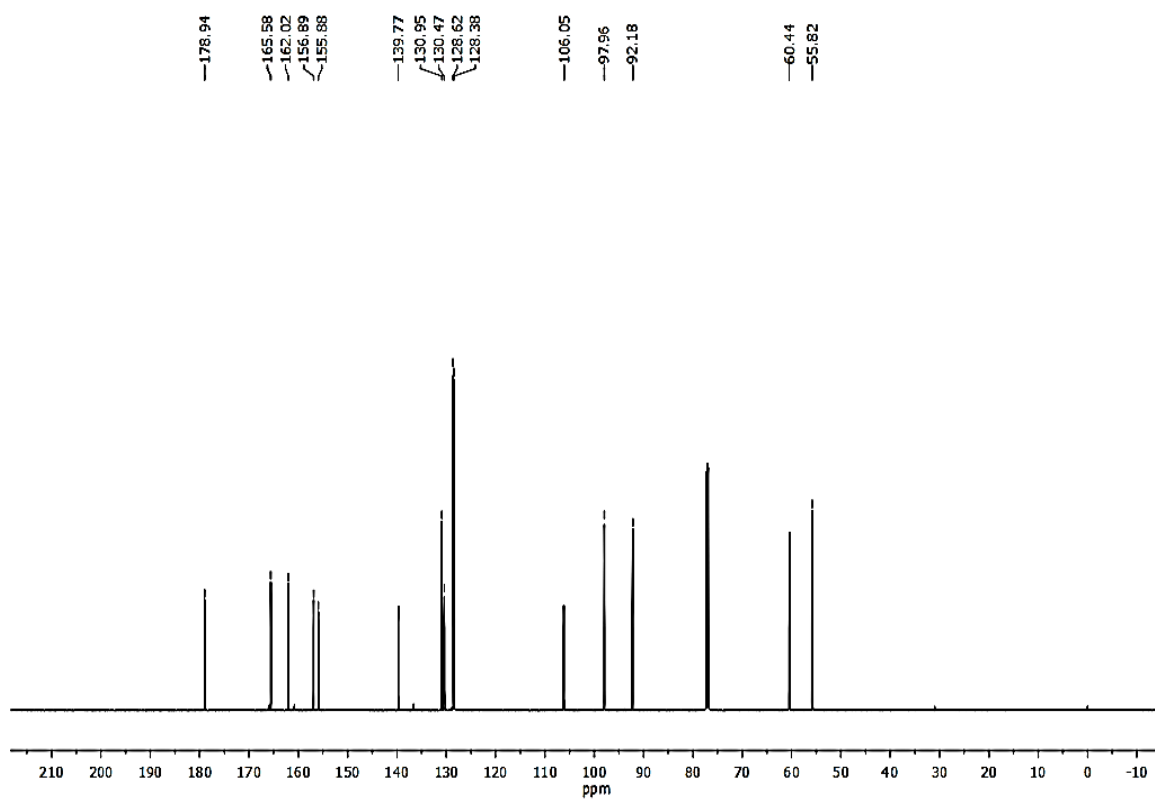
Galangin 3-methyl ether
Compound **34**

Compound **35** was isolated from the same fraction pool as a yellow solid, and is highly UV active. Like compound **34**, this compound also showed a pink color on TLC which is turned to blue, after charring in Enholm yellow solution. The one proton singlet at δ 12.58 ppm in ^1H NMR (figure 3B.5) indicates the presence of a phenolic $-\text{OH}$ with intramolecular H-bonding. 6 proton singlet at δ 3.87 ppm indicate the presence of two $-\text{OCH}_3$ groups. DEPT experiment reveals that the compound contains six CH and two $-\text{CH}_3$ groups. Also, in the carbon NMR (figure 3B.6), the peak at δ 178.9 ppm indicates the presence of a carbonyl group. While comparing the spectral features of compound **35** with that of compound **34**, it was found that, they differ only in the presence of an excess methoxy group. Hence, based on its spectral data and literature reports, the structure of compound **35** was confirmed as 5-hydroxy-3, 7-dimethoxy-2-phenyl-4H-chromen-4-one or **galangin-3,7-di-*O*-methyl ether**.⁵ Finally, the mass spectrum of the molecule well supported the structure with $(\text{M}+\text{H})^+$ ion peak at m/z 299.0917. The structure of the compound **35** is given below.

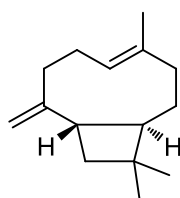


Galangin-3,7-di-*o*-methyl ether
Compound **35**

Figure 3B.3. $^1\text{H NMR}$ of compound 34 in CDCl_3 Figure 3B.4. $^{13}\text{C NMR}$ of compound 34 in CDCl_3

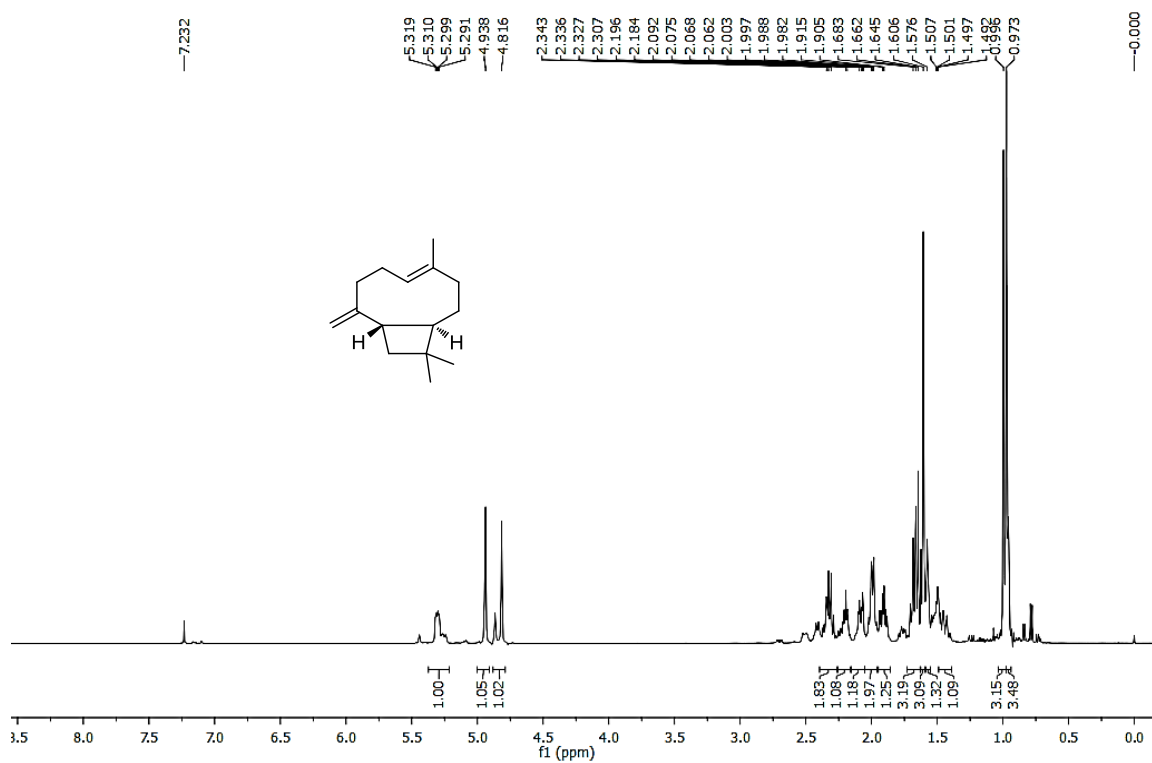
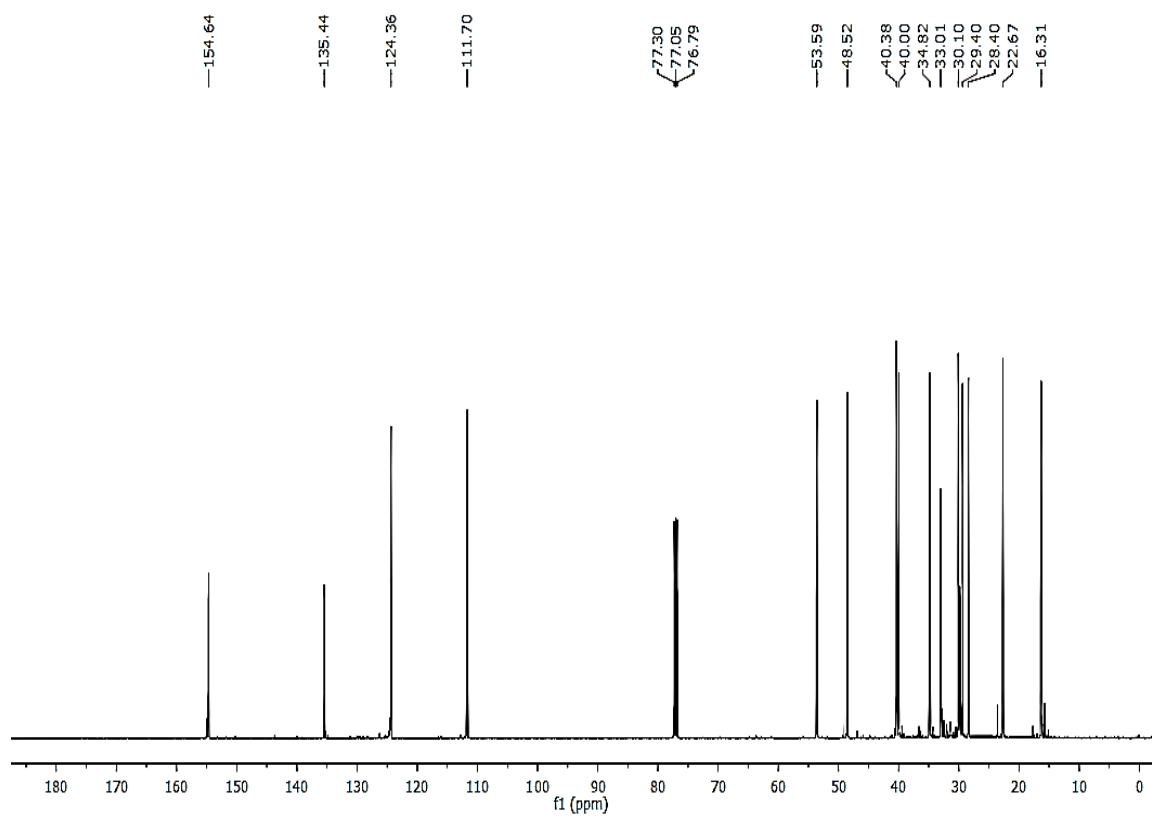
Figure 3B.5. $^1\text{H NMR}$ of compound 35 in CDCl_3 Figure 3B.6. $^{13}\text{C NMR}$ of compound 35 in CDCl_3

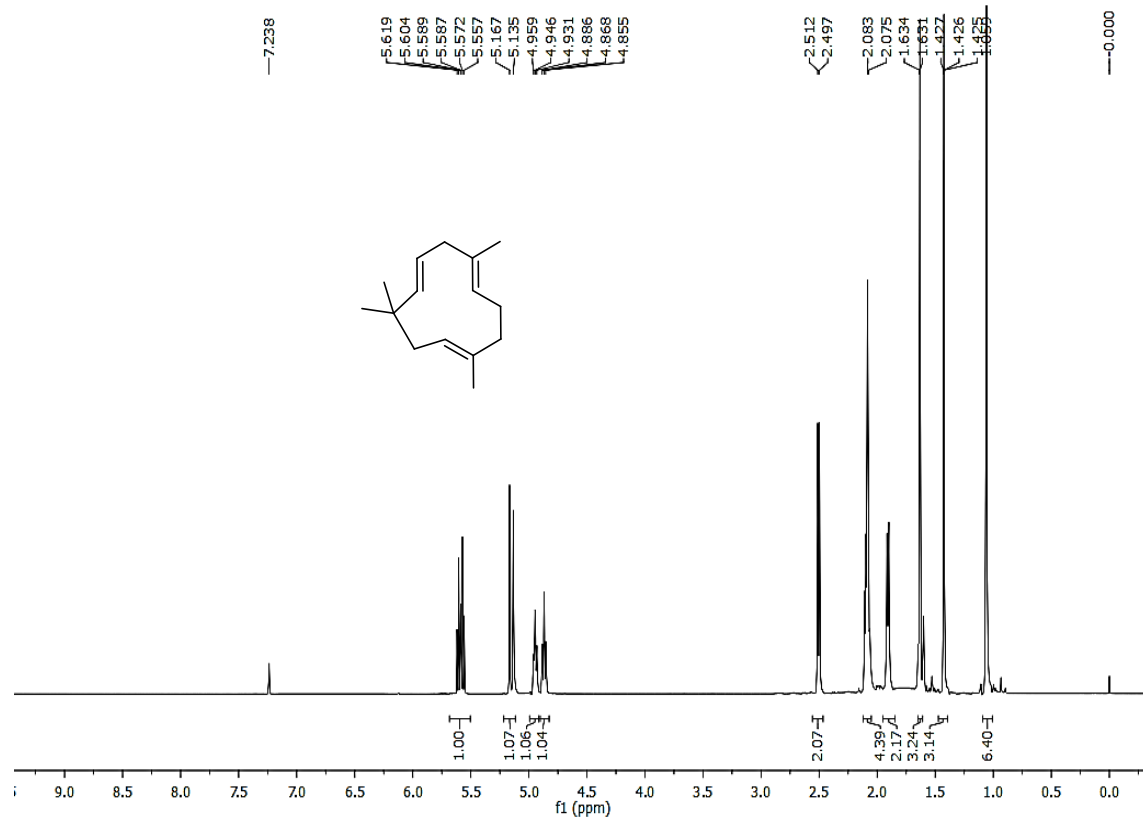
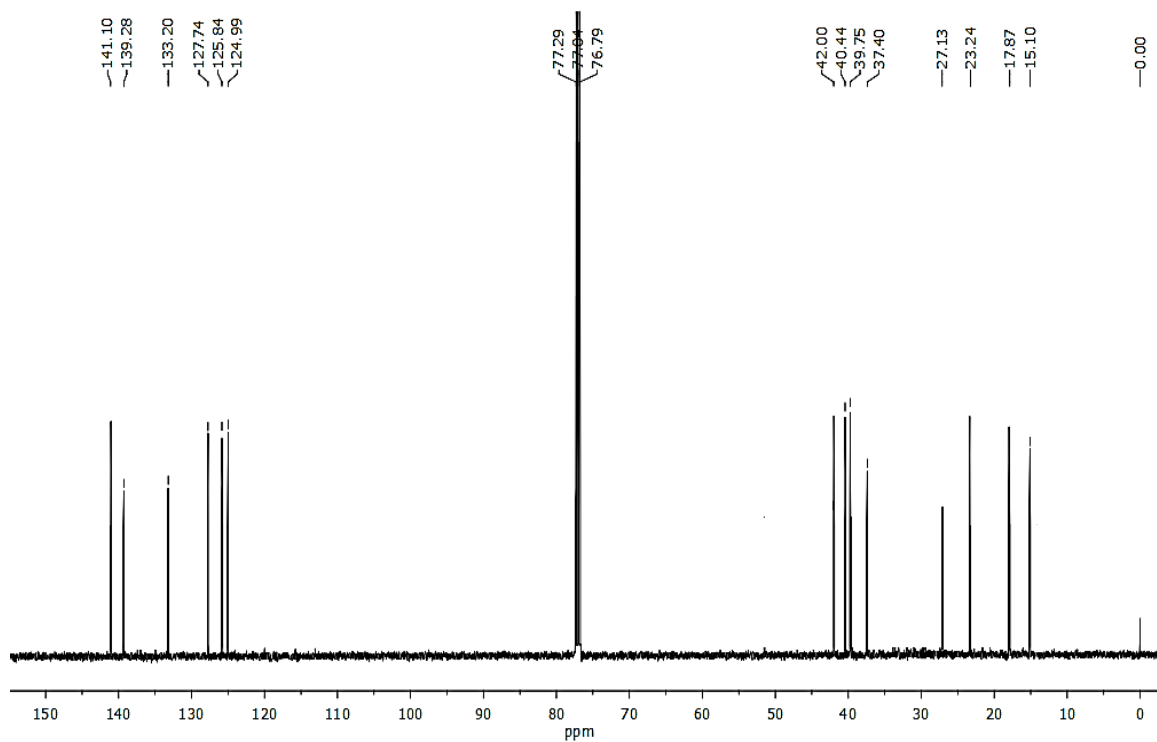
Compound **36** was obtained as a viscous oil, with pleasant smell. In the proton NMR (figure 3B.7), the molecule showed three methyl groups, along with twelve more aliphatic protons. The spectrum seemed to be an isomeric mixture, due to the repetition of almost all the peaks in less than 10 % of the major compound (64 mg). In the carbon NMR (figure 3B.8), the molecule showed a total of fifteen carbons, in which six are $-\text{CH}_2-$ in nature. Also, the detailed studies of various NMR spectra showed that the molecule possess one exocyclic double bond and is bicyclic. From the detailed analysis, the compound was confirmed as **β -caryophyllene**, a natural bicyclic sesquiterpene which is a constituent of many essential oils. The isomeric mixture may be probably isocaryophyllene (the *cis* double bond isomer), which is usually found as a mixture with β -caryophyllene. Caryophyllene is notable for having a cyclobutane ring, as well as a *trans*-double bond in a 9-membered ring, both rarities in nature.⁶ The structure of the same is given below.

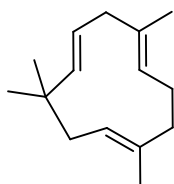


β -Caryophyllene
Compound **36**

Compound **37** was also isolated from the same fraction pool. It was a colorless viscous liquid with intense UV activity (22 mg). The IR spectrum of the compound showed signals in between $1660\text{-}1700\text{ cm}^{-1}$, corresponding to the $\text{C}=\text{C}$ stretching frequency. In the proton NMR spectrum, the signals due to the olefinic protons were noticeable as a multiplet in between δ 5.62-5.56 ppm and as a doublet resonating at δ 5.15 ppm with coupling constant of 16 Hz. The two triplets at δ 4.95 and 4.87 ppm are also represent olefinic protons (figure 3B.9). The singlets at δ 1.64, 1.43 and 1.06 ppm were attributed to four methyl groups. In ^{13}C NMR spectrum (figure 3B.10), the carbons that resonated at 141.1, 139.3, 133.2, 127.7, 125.8 and 125.0 ppm are correspond to olefinic carbons, and among them four are protonated. The presence of four CH, four $-\text{CH}_2-$ and four $-\text{CH}_3$ were confirmed using the DEPT-135. From various spectral analyses, the structure of the compound was confirmed as α -caryophyllene or **humulene**, and the spectral data were in good agreement with the literature reports.⁶ Furthermore, the structure was well supported by HRMS data, in which the molecular ion peak was obtained at m/z 205.1949 corresponding to $(\text{M}+\text{H})^+$. The structure of the compound is given below.

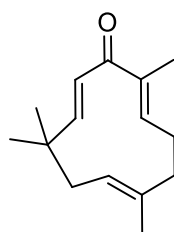
Figure 3B.7. $^1\text{H NMR}$ of compound 36 in CDCl_3 Figure 3B.8. $^{13}\text{C NMR}$ of compound 36 in CDCl_3

Figure 3B.9. ^1H NMR of compound 37 in CDCl_3 Figure 3B.10. ^{13}C NMR of compound 37 in CDCl_3



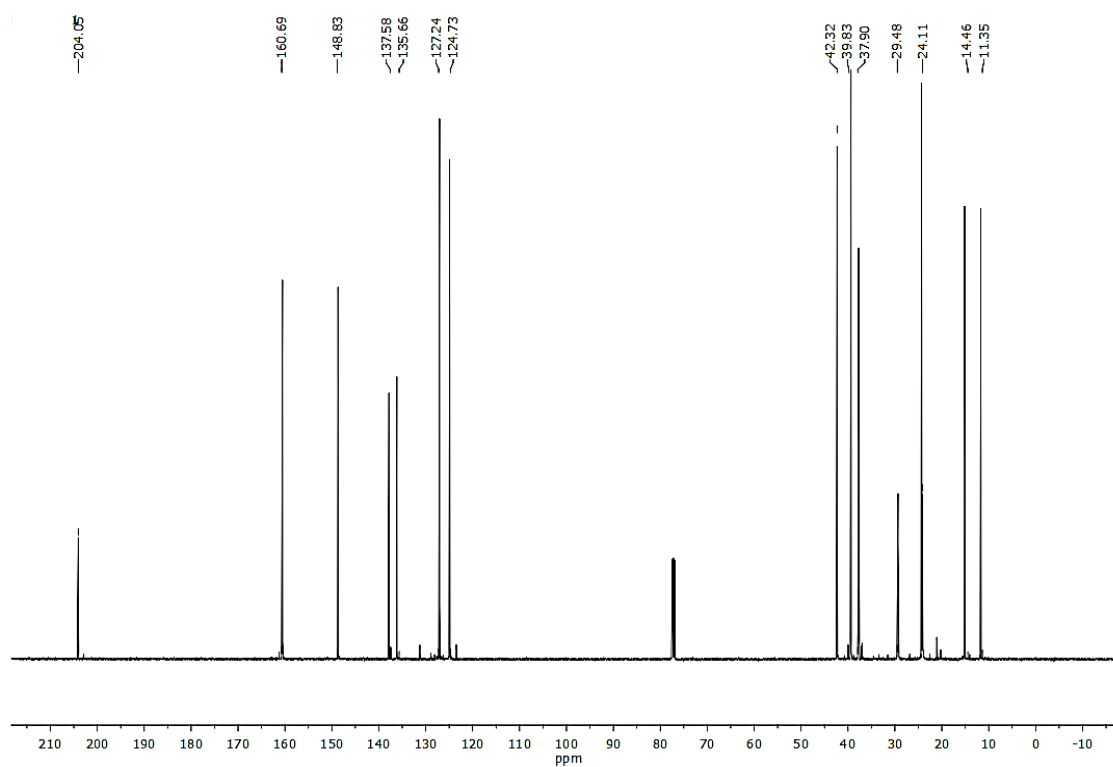
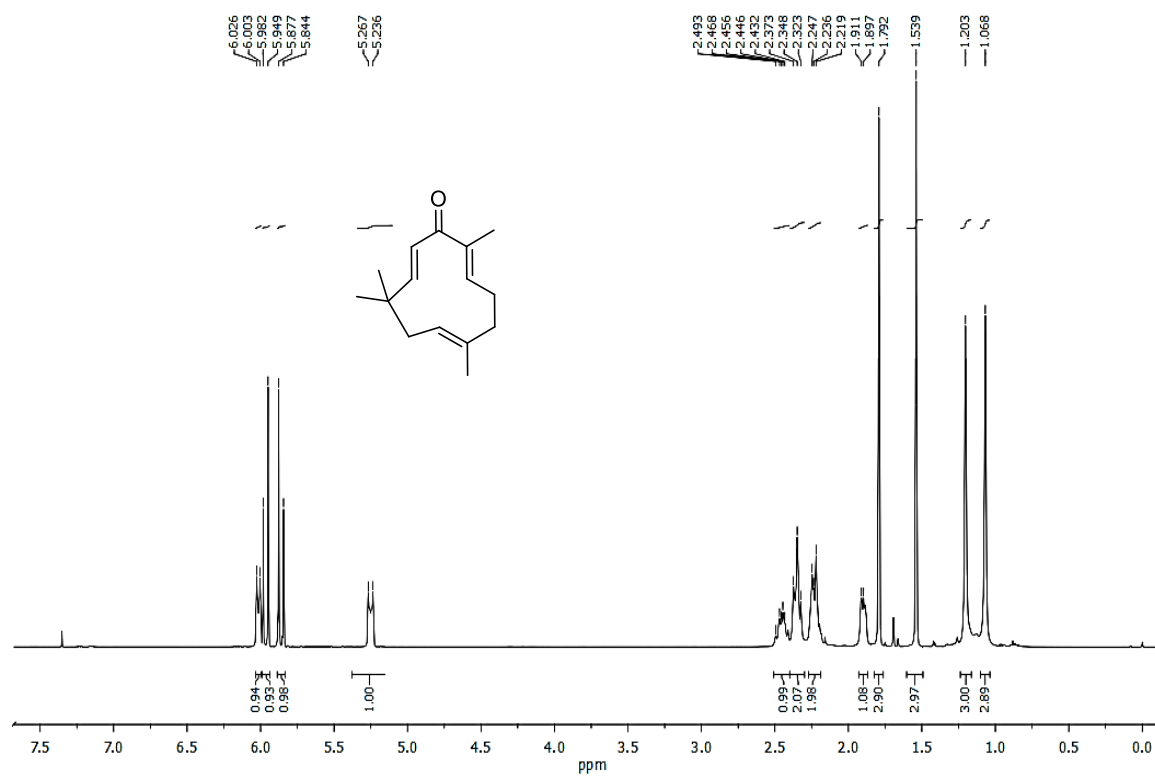
Humulene
Compound **37**

Compound **38** was isolated as a colorless crystalline solid with intense UV activity. The IR spectrum showed a strong absorption at 1657 cm^{-1} indicating the presence of a dienone/amide moiety (18 mg). The ^1H NMR spectrum showed the presence of four olefinic protons as two doublets at δ 5.96 and 5.86 ppm with a coupling constant of 16 Hz and two multiplets between δ 5.50- 6.50 ppm (figure 3B.11). Four singlets at δ 1.08, 1.21, 1.54 and 1.79 ppm, each accounting for three protons could be readily identified as four methyl groups. The presence of fifteen carbons in the ^{13}C spectrum (figure 3B.12), along with the resemblances with previous compounds, the molecule was confirmed as a sesquiterpene. DEPT-135 experiment revealed that the compound contains three $-\text{CH}_2-$ and four $-\text{CH}_3$ groups. The key feature of the spectrum was the signal at δ 204.0 ppm indicating the carbonyl group. Also, the mass spectrum showed a molecular ion peak at m/z 241.1567 corresponding to $[\text{M}+\text{Na}]^+$. From the detailed spectral analysis and on comparison with literature reports, the compound was identified as **zerumbone**/ (2*E*,6*E*,10*E*)-2,6,9,9-tetramethylcycloundeca-2,6,10-trienone.⁷ The structure of the same is given below.

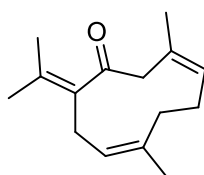


Zerumbone
Compound **38**

Compound **39** was isolated as a colorless solid, with a molecular ion peak at m/z 219.1740 corresponding to $[\text{M}+\text{H}]^+$. The strong absorption at 1688 cm^{-1} in the IR spectrum, indicates the presence of a α,β -unsaturated carbonyl moiety. In the proton NMR (figure 3B.13), the molecule showed two multiplets in between δ 4.50-5.00 ppm, which indicate the presence of two olefinic protons. Also, comparing with the carbon and other 2D NMR techniques, it was found that the molecule possess four methyl (at δ 1.78, 1.73, 1.63 and 1.44 ppm) and four $-\text{CH}_2-$ groups (carbon at δ 55.9, 38.11, 29.2 and 16.7 ppm), which are

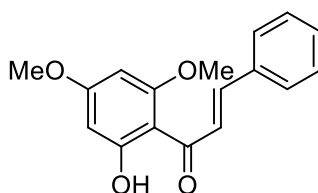


aliphatic in nature. The peak at δ 207.9 ppm in the carbon NMR (figure 3B.14) indicates the presence of a carbonyl group as in the case of zerumbone. The presence of three double bonds were also confirmed from the four quaternary carbons in the olefinic region (by comparing the DEPT-135 NMR with ^{13}C NMR). A total of fifteen carbons in the carbon NMR, is suggestive for a sesquiterpenoid moiety. From detailed spectral analysis, and comparison with previous literature reports, the compound **39** was identified as **germacrone**/ (3Z,7Z)-3,7-dimethyl-10-(propan-2-ylidene)cyclodeca-3,7-dienone (4 mg).⁸ The structure of the compound is given below.

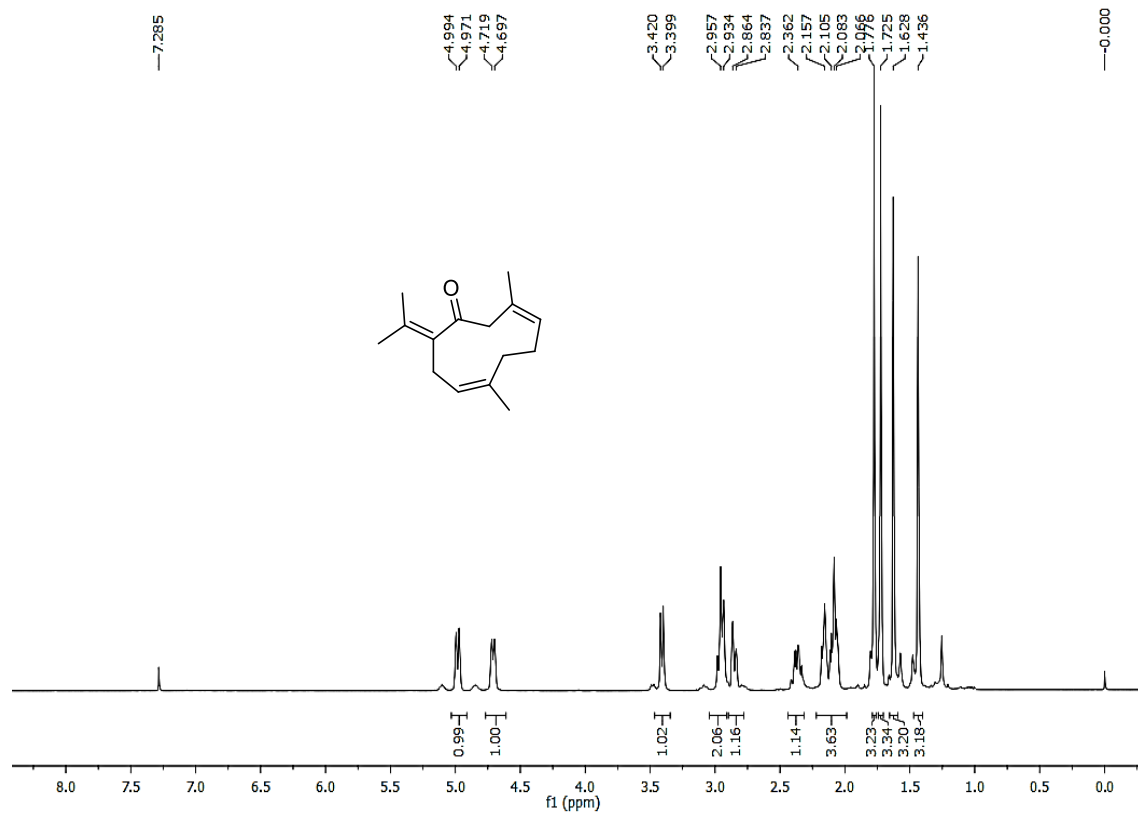
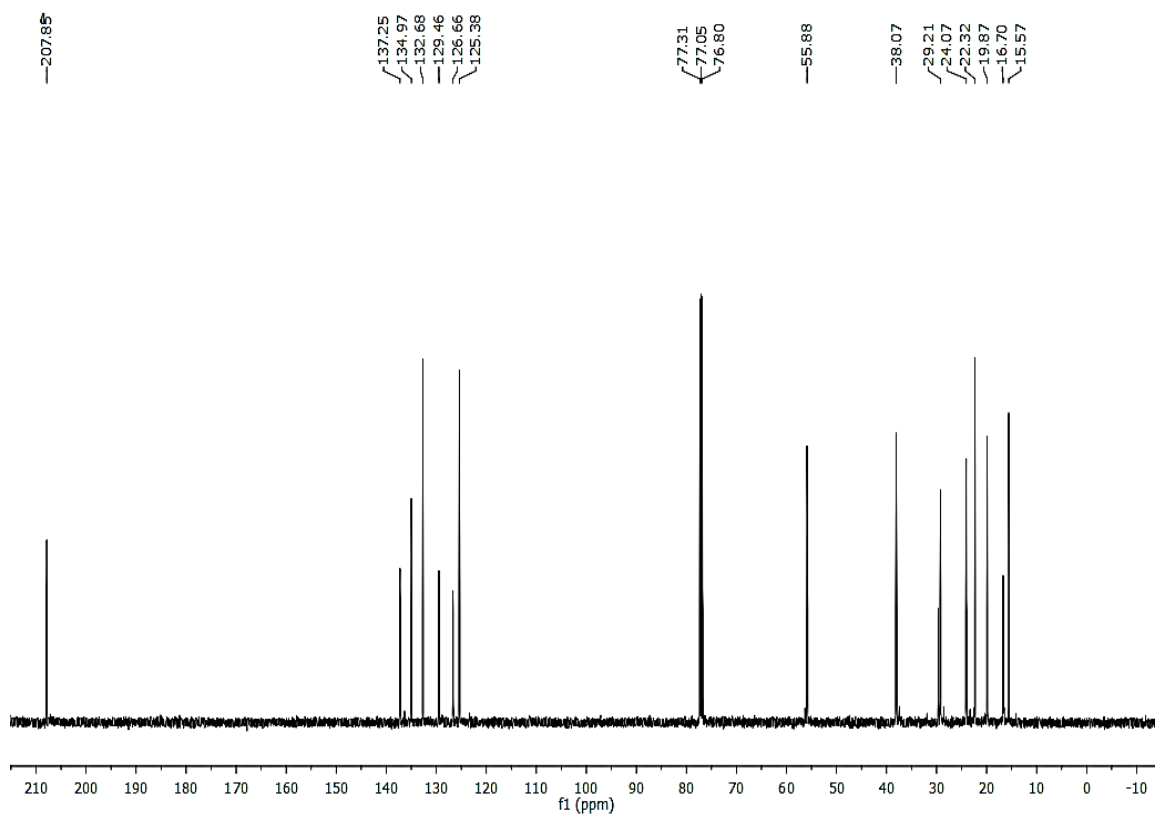


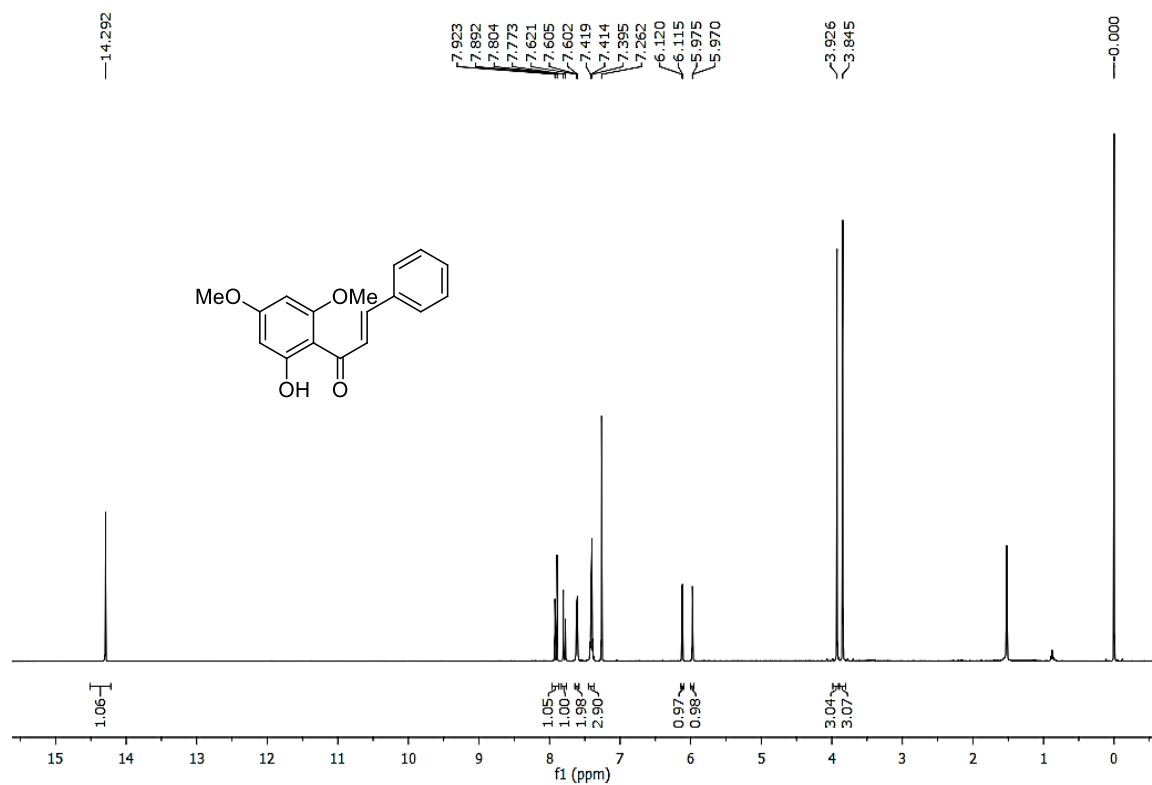
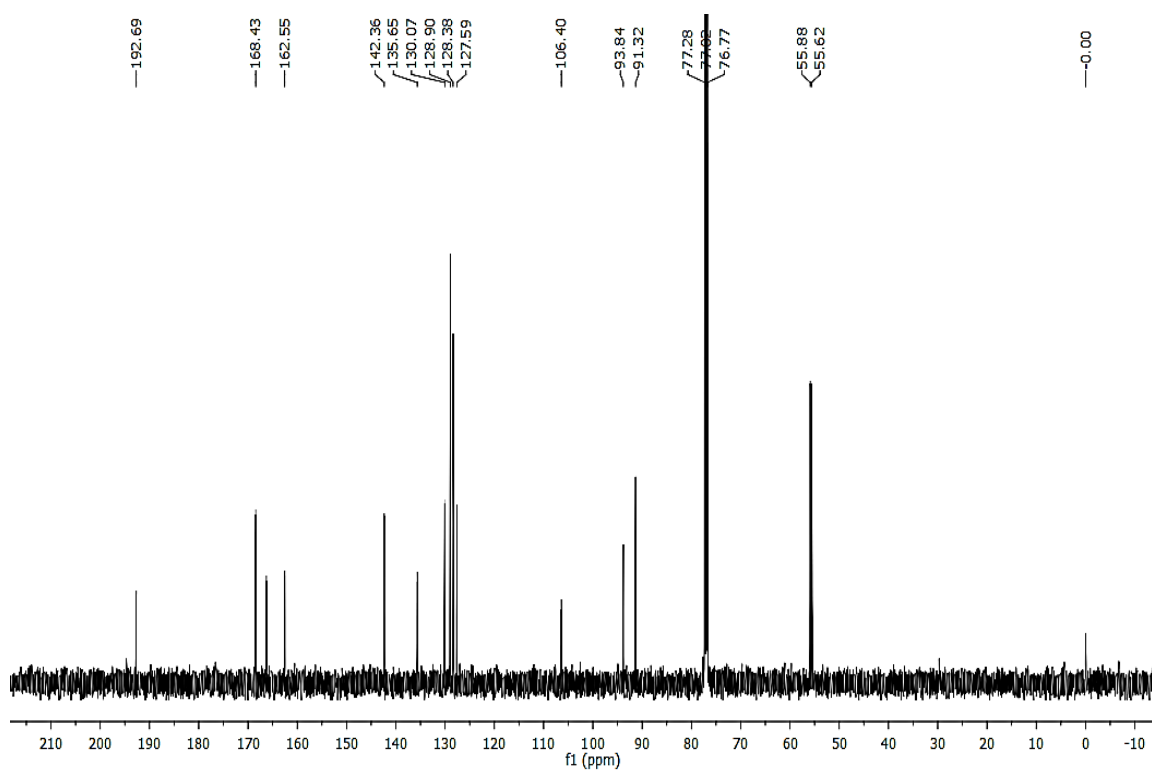
Germacrone
Compound **39**

Compound **40** was isolated from the same fraction pool 4, as a pale yellow colored solid (14 mg). In the IR spectra, the molecule showed an intense absorption at 1691 cm^{-1} , which indicates the presence of an α,β -unsaturated carbonyl or an amide moiety. The proton, as well as carbon NMR of the molecule showed (figure 3B.15 and 16) much resemblance with the spectral data of compounds **34** and **35**. Unlike compound **35**, this molecule carried two distinct methoxy groups at δ 3.93 and 3.85 ppm. The two doublets at δ 7.91 and 7.79 ppm with a coupling constant of 15.5 Hz, clearly indicate the presence of a *trans* olefinic protons. Also, the singlet proton at δ 14.29 ppm is clearly attributed to a hydroxyl group, with hydrogen bonding interactions. In the carbon NMR, the peak at δ 192.7 ppm supports the presence of a flavone carbonyl group. Finally, by the comparison of spectral data of the compound with that of literature reports, the structure of the molecule was confirmed as **flavokavain B** [(*E*)-1-(2-hydroxy-4,6-dimethoxyphenyl)-3-phenylprop-2-en-1-one].⁹ Also, the structure of the compound **40** was well supported by HRMS data, in which the molecular ion peak was obtained at m/z 285.1086, corresponding to $[\text{M}+\text{H}]^+$ peak. The structure of the same is given below.

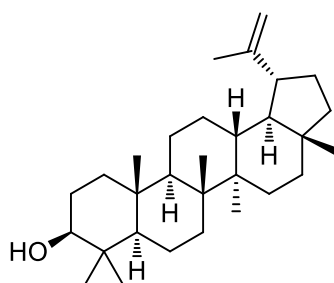


Flavokavain B
Compound **40**

Figure 3B.13. ^1H NMR of compound 39 in CDCl_3 Figure 3B.14. ^{13}C NMR of compound 39 in CDCl_3

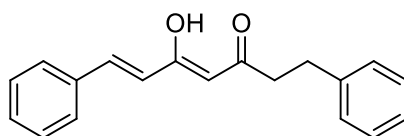
Figure 3B.15. $^1\text{H NMR}$ of compound **40** in CDCl_3 Figure 3B.16. $^{13}\text{C NMR}$ of compound **40** in CDCl_3

Compound **41**, was isolated from the fraction pools 5-8, as white crystalline needles with a melting point of 119-121 °C (14 mg). In the infrared spectrum, the intense absorptions at 3449, 2931, 2311, 1587, 1258 and 899 cm^{-1} displayed by the compound clearly indicated that, it consists of hydroxyl and olefin functionalities. The presence of an exocyclic olefinic system in the molecules was confirmed from two singlets at δ 4.70 and 4.57 ppm with carbon at δ 109.3 ppm. The ^1H NMR spectrum also revealed the presence of seven tertiary methyl protons in between δ 0.77 and 1.65 ppm. Finally, the structure of the compound **41** was accomplished as the plant sterol, **lupeol**, through various 2D NMR experiments (COSY, HMQC and HMBC).¹⁰ The mass spectrum of the compound also well supported the structure, with a m/z value at 427.3943 corresponding to $(\text{M}+\text{H})^+$ peak. The structure of the compound is given below.

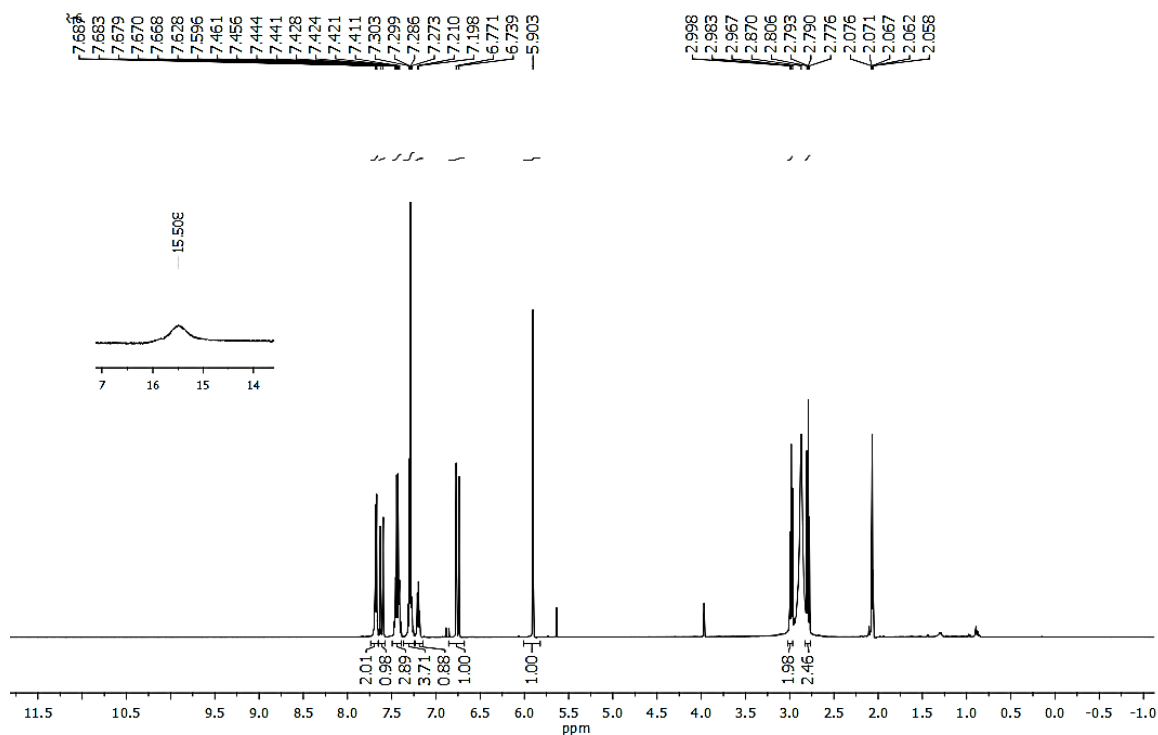
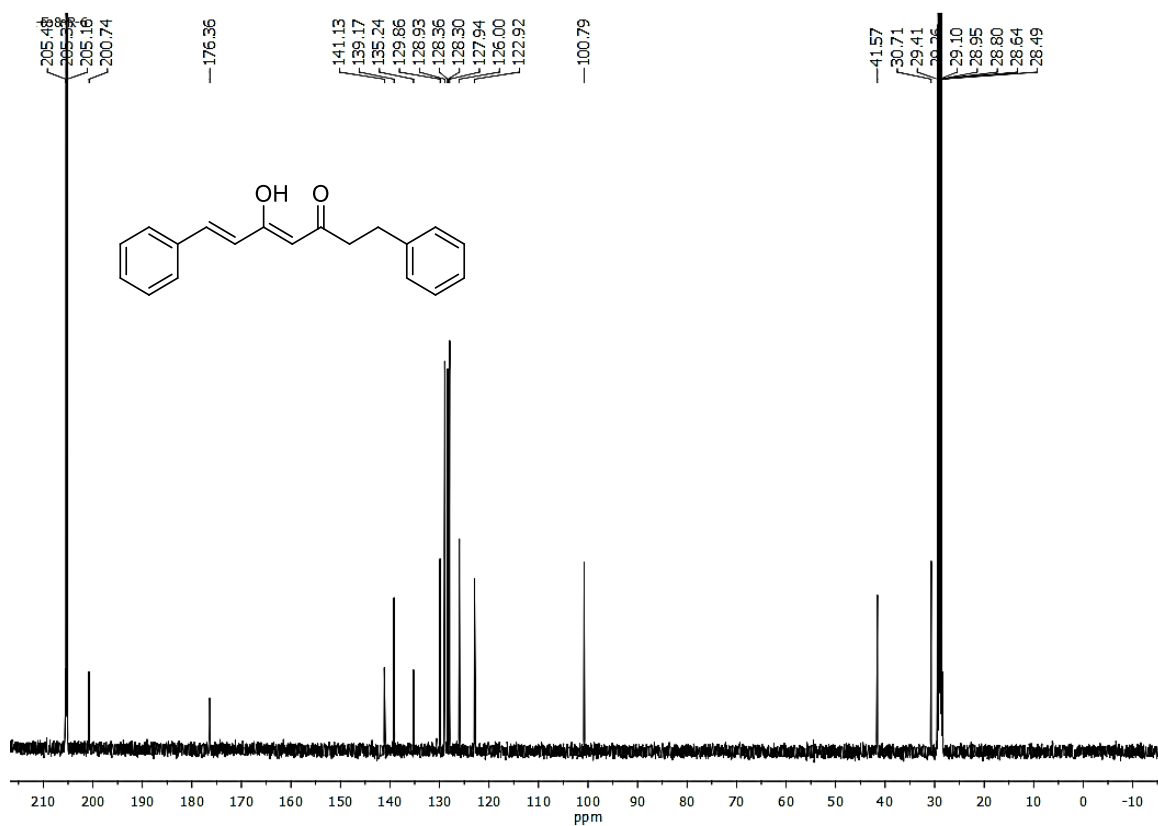


Lupeol
Compound **41**

Compound **42** was also isolated from the same fraction pool, as a pale yellow crystalline solid (melting point between 58-60 °C) with intense UV activity. The peaks at 3261 and 1645 cm^{-1} in the IR spectrum, confirmed the presence of a hydroxyl and a carbonyl moiety in the compound. The one proton broad singlet at δ 15.51 ppm in the ^1H NMR also confirmed the presence of hydroxyl group, with an intramolecular H-bonding. Two doublets at δ 6.75 and 5.90 ppm with a coupling constant of 16 Hz clearly indicate the presence of *trans* olefinic protons (figure 3B.17 and 18). The presence of two triplets at δ 2.98 and 2.81 ppm, also confirmed the presence of two $-\text{CH}_2$ groups. Also, the mass spectrum showed a molecular ion peak at m/z 279.1377 corresponding to $(\text{M}+\text{H})^+$. Finally, by the comparison of spectral data with that of literature reports, the structure of the compound **42** was confirmed as **(4Z,6E)-5-hydroxy-1,7-diphenylhepta-4,6-dien-3-one**.¹¹



(4Z,6E)-5-hydroxy-1,7-diphenylhepta-4,6-dien-3-one
Compound **42**

Figure 3B.17. ^1H NMR of compound **42** in CD_3COCD_3 Figure 3B.18. ^{13}C NMR of compound **42** in CD_3COCD_3

3B.4. *In vitro* Antioxidant Studies

In the preliminary extract level antioxidant studies,¹² the hexane extract exhibited the lowest IC₅₀ against all the three radicals (IC₅₀ = 1.987 ± 0.201 μg/mL for DPPH, 60.6493 ± 0.76 μg/mL for ABTS and 90.010 ± 0.332 μg/mL for NO radicals), followed by acetone, ethanol and water extracts (table 3B.1). Though the extracts demonstrated significant scavenging of DPPH radicals, their activity against ABTS and NO radicals were comparatively poor.

Table 3B.1. IC₅₀ values of different extracts towards various radical generators

Extracts	IC ₅₀ values (μg/mL)		
	DPPH radical scavenging activity	ABTS radical scavenging activity	NO radical scavenging activity
Hexane	1.987 ± 0.201	60.6493 ± 0.76	90.01 ± 0.332
Acetone	9.0043 ± 0.546	117.386 ± 0.943	91.0 ± 0.831
Ethanol	2.01 ± 0.112	110.386 ± 0.221	119 ± 0.563
Water	3.12 ± 0.887	117.413 ± 0.269	110 ± 0.731
Ascorbic acid	6.878 ± 0.231	14.1254 ± 0.461	-
Gallic acid	-	-	55.84 ± 0.876

After the successful extract level antioxidant studies, we further focussed on the molecular level studies and found that most of these isolated compounds effectively scavenge the DPPH and NO radicals with comparatively better IC₅₀ values than the standard compounds, ascorbic acid and gallic acid. Among the compounds studied, compound **35** and flavokavain B displayed the better scavenging of DPPH radicals with IC₅₀ values of 33.76 ± 0.651 μM and 30.21 ± 0.111 μM respectively. Coming to the ABTS, germacrone and compound **34** demonstrated the lowest IC₅₀ values (51.7189 ± 0.688 μM and 53.506 ± 0.811 μM respectively) followed by zerumbone (57.8181 ± 0.751 μM) and compound **35** (69.0536 ± 0.713 μM). While the compound zerumbone exhibited the lowest IC₅₀ value against the nitric oxide radicals (with an IC₅₀ value of 97.876 ± 0.853 μM). From the table given below (table 3B.2), it is clear that, most of the isolated compounds exhibit better antioxidant properties, especially against the nitric oxide radicals, for which the standard gallic acid demonstrated an IC₅₀ value of 320.0 ± 0.27 μM

Table 3B.2. *In vitro* antioxidant potential of isolated compounds

Compounds	IC ₅₀ values (μ M)		
	DPPH radical scavenging activity	ABTS radical scavenging activity	NO radical scavenging activity
Compound 34	35.08 \pm 0.54	53.506 \pm 0.811	114.29 \pm 0.12
Compound 35	33.76 \pm 0.651	69.0536 \pm 0.713	111.8743 \pm 0.87
Caryophyllene	46.77 \pm 0.813	189.0842 \pm 0.251	226.87 \pm 0.93
Humulene	44.87 \pm 0.366	250.2597 \pm 0.912	262.81 \pm 0.331
Zerumbone	40.08 \pm 0.951	57.8181 \pm 0.751	97.876 \pm 0.853
Germacrone	41.88 \pm 0.776	51.7189 \pm 0.688	213.05 \pm 0.571
Flavokavain B	30.21 \pm 0.111	77.8321 \pm 0.03	189.01 \pm 0.616
Ascorbic acid	39.01 \pm 0.12	80.17 \pm 0.61	-
Gallic acid	-	-	320.0 \pm 0.27

3B.5. *In silico* Antidiabetic and Anticancer Studies

In the next step, we carried out a virtual screening of these isolated compounds, for their antidiabetic and anticancer activities. The purpose of this study was to analyse the inhibitory action of these compounds by computational docking studies. The molecular docking studies of all the compounds were carried out, with an antidiabetic protein 3A4A and an anticancer protein 2ITW using MOE 2009.10. The default 'Site Finder' tool was used to identify the active site of the proteins. Using LigPlot analysis the binding interactions of the ligands to the proteins were studied and the docking results are given in table 3B.3.¹³

In our studies, the compounds subjected to docking studies exhibited better antidiabetic properties, than anticancer effects. Among these, the compounds **34** and **35** were effectively binded to the active sites of the enzymes with a docking score of -11.2018 kcal/mol and -11.2703 kcal/mol respectively for the enzyme 2ITW and, -13.1593 kcal/mol and -11.9667 kcal/mol respectively for the enzyme 3A4A. Three prominent interactions were observed for the compound **34** with the antidiabetic enzyme 3A4A, which include two arene-cation interactions between the benzene ring and the basic amino acid residues Arg315 and His280, and one hydrogen bond acceptor interaction between the hydroxyl

group at the seventh position with the hydrophilic amino acid residue Thr310 (figure 3B.19).

Table 3B.3. Results of molecular docking studies

Compounds	E-score kcal/mol	
	2ITW	3A4A
Compound 34	-11.2018	-13.1593
Compound 35	-11.2703	-11.9667
Caryophyllene	-6.36811	-8.03946
Humulene	-6.5089	-9.08878
Zerumbone	-5.97459	-8.35367
Germacrone	-6.75311	-9.23364
Flavokavain B	-9.84695	-11.4503
Compound 42	-9.08736	-10.7358

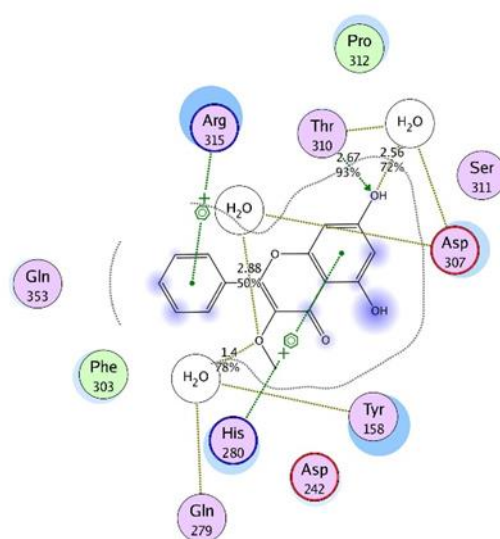


Figure 3B.19. Interactions observed for the compound **34** with the protein 3A4A

3B.6. Conclusion

In summary, we have successfully carried out the chemo-profiling of the rhizomes of one of the newly identified plant species *Zingiber nimmonii*, and led to the isolation of ten different compounds. In addition to these, we also carried out the preliminary extract and molecular level antioxidant studies and, came to an inference that, consumption of this herb can effectively scavenge the undesirable free radicals produced in our body through various metabolic pathways. Also, the docking studies of the isolated compounds showed

that most of these molecules could dock well with the antidiabetic protein 3A4A and anticancer protein 2ITW. Hence most of these molecules can play a vital role in modulating the antidiabetic and anticancer enzymes.

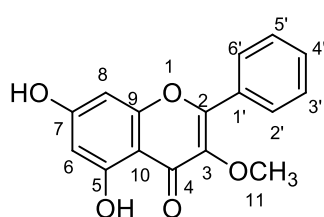
3B.7. Experimental Section

Different analytical techniques were used for the characterization of compounds. The IR spectra were recorded with a Bruker FT-IR spectrometer. The nuclear magnetic resonance spectra (NMR) were recorded on a Bruker AMX 500 spectrophotometer (CDCl_3 , CD_3COCD_3 , MeOD and DMSO- d_6 as solvents). Chemical shifts for NMR spectra are reported as δ in units of parts per million (ppm) downfield from tetramethylsilane (δ 0.0) and relative to the signal of solvent. Mass spectra were recorded under ESI/HRMS at 60,000 resolution using Thermo Scientific Exactive mass spectrometer and specific rotation was recorded using Jasco P-2000 polarimeter. Shimadzu UV-1800 spectrophotometer was used to measure the absorption maxima. Antioxidant studies were carried out as described in section 2A.14 of Chapter 2 Part B.

3B.8. Spectral Data

Compound 34 (5,7-dihydroxy-3-methoxy-2-phenyl-4H-chromen-4-one)

Compound 34 was isolated as a yellow solid, and is highly UV active. It showed a pink color which turned to blue while charring the TLC in Enholm yellow solution. Based on its spectral data and literature reports, the compound was confirmed as 5,7-dihydroxy-3-methoxy-2-phenyl-4H-chromen-4-one.



Molecular formula : $\text{C}_{16}\text{H}_{12}\text{O}_5$

FT-IR (Neat) ν_{max} : 3316, 1660, 1615, 1322, 1166 cm^{-1}

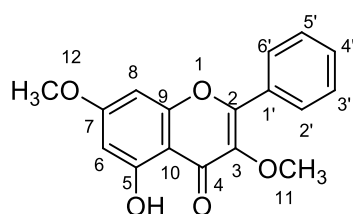
^1H NMR (500 MHz, CDCl_3 , TMS) : δ 11.55 (s, 1H, OH at C5), 8.20-8.19 (m, 2H, H-2' and C6'), 7.54-7.51 (m, 2H, H-3' and H-5'), 7.48-7.46 (m, 1H, H-C4'), 6.69 (s, 1H, H-7), 6.50 (d, $J = 4$ Hz, 1H, H-6), 6.38 (d, $J = 4$ Hz, 1H, H-8), 3.89 (s, 3H, H-11) ppm.

^{13}C NMR (125 MHz, CDCl_3 , TMS) : δ 175.4 (C-4), 165.7 (C-7), 160.7 (C-5), 156.7 (C-9), 145.4 (C-1'), 136.7 (C-11), 130.7 (C-10), 130.3, 128.6, 127.6, 103.3 (C-10), 98.2 (C-6), 92.7 (C-8), 55.8 (C-11) ppm.

HRMS (ESI): m/z Calcd for $\text{C}_{16}\text{H}_{13}\text{O}_5$: 285.0765; Found : 285.0767.

Compound 35 (5-hydroxy-3, 7-dimethoxy-2-phenyl-4H-chromen-4-one)

Compound **35** was isolated from the same fraction pool as a yellow solid (82 mg), and is highly UV active. Like compound **34**, this compound also showed a pink color on TLC which is turned to blue, after charring in Enholm yellow solution. From the detailed spectral analysis and literature survey, the compound was confirmed as 5-hydroxy-3, 7-dimethoxy-2-phenyl-4H-chromen-4-one.



Molecular formula : C₁₇H₁₅O₅

FT-IR (Neat) ν_{\max} : 3268, 1647, 1611, 1162 cm⁻¹.

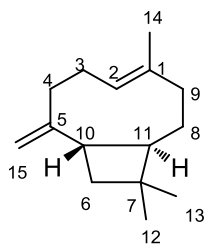
¹H NMR (500 MHz, CDCl₃, TMS) : δ 12.58 (s, 1H, OH at C5), 8.07-8.05 (m, 2H, H-2' and H-6'), 7.52-7.51 (m, 3H, H-3' and H-5'), 6.44 (d, $J = 4$ Hz, 1H, H-6), 6.35 (d, $J = 4$ Hz, 1H, H-8), 3.87 (s, 6H, H-11 and H-12) ppm

¹³C NMR (125 MHz, CDCl₃, TMS) : δ 178.9 (C-4), 165.6 (C-7), 162.0 (C-5), 156.9 (C-9), 155.9 (C-1'), 139.8 (C-11), 130.9 (C-10), 130.5, 128.6, 128.4, 106.0, 97.9 (C-6), 92.2 (C-8), 60.4 (C-11 or C-12), 55.8 (C-11 or C-12) ppm.

HRMS (ESI): m/z . Calcd for C₁₇H₁₆O₅ : 299.0916; Found : 299.0917.

Compound 36 (β -caryophyllene)

Compound **36** was also obtained from the same fraction pool, as a viscous oil, with pleasant smell (64 mg). The spectrum seemed to be an isomeric mixture, due to the repetition of almost all the peaks in less than 10 % of the major compound. From the detailed analysis, the compound was confirmed as **β -caryophyllene**, a natural bicyclic sesquiterpene, which is a constituent of many essential oils.



Molecular formula : C₁₅H₂₄

FT-IR (Neat) ν_{\max} : 3066, 2917, 1124 cm⁻¹.

¹H NMR (500 MHz, CDCl₃, TMS) : δ 5.32-5.29 (m, 1H, H-2), 4.94 (s, 1H, H-15), 4.82 (s, 1H, H-15), 2.34-2.22 (m, 2H), 2.25-2.22 (m, 1H), 2.15-2.13 (m, 1H), 2.01-1.88 (m, 2H), 1.83-1.78 (m, 1H), 1.75-1.60 (m, 3H), 1.59-1.55 (m, 3H), 1.52-1.40 (m, 2H), 1.00 (s, 3H), 0.97 (s, 3H) ppm.

^{13}C NMR (125 MHz, CDCl_3 , TMS) : δ 154.6 (C-2), 135.4 (C-5), 124.5 (C-1), 111.7 (C-5), 53.6, 48.5, 40.4, 40.0, 34.8, 33.0, 30.1, 29.4, 28.4, 22.7, 16.3 ppm.

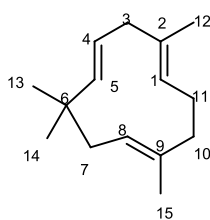
HRMS (ESI): m/z . Calcd for $\text{C}_{15}\text{H}_{25}$: 205.1956; Found : 205.1960.

Compound 37 (humulene)

Compound **37** was isolated in 22 mg from the same fraction pool. It was a colorless viscous liquid with intense UV activity. The structure of the compound was established by various spectroscopic analyses and confirmed as α - humulene.

Molecular formula : $\text{C}_{15}\text{H}_{24}$

FT-IR (Neat) ν_{max} : 2711, 1662, 1443, 1354, 1178, 969, 824 cm^{-1} .



^1H NMR (500 MHz, CDCl_3 , TMS) : δ 5.64-5.61 (m, 1H, H-4), 5.17 (d, $J = 16$ Hz, 1H, H-C5), 4.96-4.94 (m, 1H, H-1), 4.88-4.86 (m, 1H, H-8), 2.51 (d, $J = 7.5$ Hz, 2H, H-3), 2.11-2.07 (m, 4H, H-10 and H-11), 1.91 (d, $J = 7.5$ Hz, 2H, H-7), 1.64 (s, 3H, H-12), 1.06 (s, 6H, H-13 and H-14) ppm.

^{13}C NMR (125 MHz, CDCl_3 , TMS) : δ 141.1 (C-5), 139.3 (C-2), 133.2 (C-9), 127.7 (C-4), 125.8 (C-1), 125.0 (C-8), 42.0 (C-7), 40.4 (C-3), 39.7 (C-10), 37.4 (C-6), 27.1 (C-14 or C-15), 23.2 (C-14 or C-15), 17.9 (C-12), 15.1 (C-15) ppm.

HRMS (ESI): m/z . Calcd for $\text{C}_{15}\text{H}_{25}$: 205.1956; Found : 205.1959.

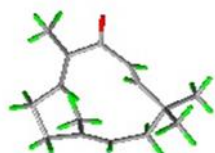
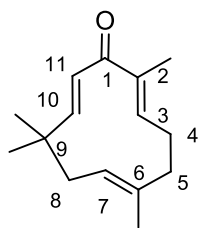
Compound 38 (zerumbone)

Compound **38** was isolated as a colorless crystalline solid with intense UV activity. The IR spectrum showed a strong absorption at 1657 cm^{-1} indicating the presence of a dienone/amide moiety (18 mg). Using various spectroscopic analyses, including single crystal X-ray analysis, the structure of the compound was identified as zerumbone.

Molecular formula : $\text{C}_{15}\text{H}_{22}\text{O}$

Mp : 52-54 $^{\circ}\text{C}$

FT-IR (Neat) ν_{max} : 3026, 2964, 2924, 2856, 1656 (dienone), 1455 cm^{-1} .



¹H NMR (500 MHz, CDCl₃, TMS) : δ 6.03-6.00 (m, 1H, H-3), 5.96 (d, *J* = 16 Hz, 1H, H-10), 5.86 (d, *J* = 16 Hz, 1H, H-10), 5.24 (m, 1H, H-7), 2.47-2.43 (m, 1H, H-3), 2.35-2.32 (m, 2H), 2.25-2.22 (m, 2H), 1.91-1.89 (m, 1H, H-8), 1.79 (s, 3H), 1.54 (s, 3H), 1.20 (s, 3H), 1.07 (s, 3H) ppm.

¹³C NMR (125 MHz, CDCl₃, TMS) : δ 204.0 (C-1), 160.7 (C-10), 148.8 (C-3), 137.6 (C-2), 127.2 (C-11), 124.7 (C-7), 42.3 (C-8), 39.8 (C-5), 37.9 (C-9), 29.5 (C-14 or C-15), 24.3 (C-4), 24.1 (C-14 or C-15), 15.2 (C-12), 11.3 (C-13) ppm.

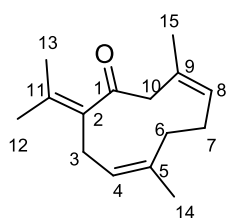
HRMS (ESI): *m/z* Calcd for C₁₅H₂₃O : 219.1749; Found : 219.1748.

Compound 39 (germacrone)

Compound **39** was isolated from fraction pool 4 in 4 mg as a colorless solid with intense UV activity. The IR spectrum showed a strong absorption at 1688 cm⁻¹ indicating the presence of a enone/amide moiety. Using various spectroscopic analyses, the structure of the compound was identified as germacrone.

Molecular formula : C₁₅H₂₂O

FT-IR (Neat) *v*_{max} : 2962, 2933, 1688 (enone), 1466 cm⁻¹.



¹H NMR (500 MHz, CDCl₃, TMS) : δ 4.99-4.97 (m, 1H, H-8), 4.72-4.70 (m, 1H, H-4), 3.42-3.40 (m, 1H), 2.96-2.93 (m, 2H), 2.86-2.84 (m, 1H), 2.36-2.28 (m, 1H), 2.24-2.06 (m, 3H), 1.78 (s, 3H), 1.72 (s, 3H), 1.63 (s, 3H), 1.44 (s, 3H) ppm.

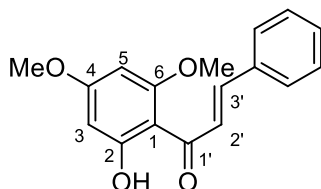
¹³C NMR (125 MHz, CDCl₃, TMS) : δ 207.8 (C-1), 137.2 (C-2), 135.0 (C-11), 132.7 (C-4), 129.5 (C-8), 126.7 (C-9), 125.4 (C-5), 55.9, 38.1, 29.2, 24.1, 22.3, 19.9, 16.7, 15.6 ppm.

HRMS (ESI): *m/z* Calcd for C₁₅H₂₃O : 219.1749; Found : 219.1740.

Compound 40 (flavokavain B)

Compound **40** was isolated from the same fraction pool 4, as a pale yellow colored solid (14 mg). In the IR spectra, the molecule showed an intense absorption at 1691 cm⁻¹, which indicates the presence of an α,β- unsaturated carbonyl or an amide moiety. The proton, as well as carbon NMR of the molecule showed much resemblance with the spectral

data of compounds **34** and **35**. From the detailed spectral analysis, the compound was confirmed as flavokavain B.



Molecular formula : C₁₇H₁₆O₄

FT-IR (Neat) ν_{\max} : 3341, 2962, 2997, 2935, 1691(enone), 1466 cm⁻¹.

¹H NMR (500 MHz, CDCl₃, TMS) : δ 14.29 (s, 1H, OH at C-2), 7.91 (d, J = 15.5 Hz, 1H, H-3'), 7.79 (d, J = 15.5 Hz, 1H, H-2'), 7.62-7.60 (m, 2H), 7.42-7.40 (m, 3H), 6.12 (d, J = 2.5 Hz, 1H, H-3), 5.97 (d, J = 2.5 Hz, 1H, H-5), 3.92 (s, 3H, 3.84 (s, 3H) ppm.

¹³C NMR (125 MHz, CDCl₃, TMS) : δ 192.7 (C-1'), 168.4 (C-4), 162.5 (C-6), 142.4, 135.6 (C-3'), 130.1, 128.9, 128.4, 127.6 (C-2'), 106.4 (C-1), 93.8, 91.3, 55.9, 55.6 ppm.

HRMS (ESI): m/z Calcd for C₁₇H₁₇O₄ : 285.1107; Found : 285.1086.

Compound **41** (lupeol)

Compound **41**, was isolated from the fraction pools 5-8, as white crystalline needles with a melting point of 119-121 °C (14 mg). In the infrared spectrum, the intense absorptions at 3449, 2931, 2311, 1587, 1258 and 899 cm⁻¹ displayed by the compound clearly indicated that, it consists of hydroxyl and olefin functionalities. Finally, the structure of the compound **41** was accomplished as the plant sterol, **lupeol**, through various 2D NMR experiments (COSY, HMQC and HMBC).

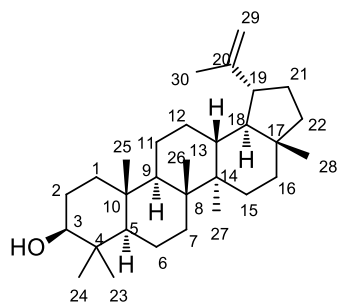
Molecular formula : C₃₀H₅₀O

Mp : 119-121 °C

FT-IR (Neat) ν_{\max} : 3449, 2931, 2311, 2117, 1587, 1433, 1258, 899 cm⁻¹.

¹H NMR (500 MHz, CDCl₃, TMS) : δ 4.68 (s, 1H, H-29), 4.57 (s, 1H, H-29), 3.24-3.18 (m, 1H, H-3), 2.38-2.32 (m, 1H), 2.33-1.75 (m, 8H), 1.69-1.25 (m, 11H), 1.40-1.25 (m, 7H), 1.66 (s, 3H), 1.01 (s, 6H), 0.93 (s, 3H), 0.87 (s, 3H), 0.85(s, 3H), 0.78 (s, 3H) ppm.

¹³C NMR (125 MHz, CDCl₃, TMS) : δ 151.1 (C-20), 108.8 (C-29), 78.9 (C-3), 54.3 (C-5), 50.7 (C-9), 47.9 (C-18), 48.3



(C-19), 43.1 (C-17), 42.9 (C-14), 40.7 (C-8), 39.9 (C-22), 38.9 (C-4), 38.6 (C-1), 38.4, 37.1 (C-10), 35.4, 29.9 (C-21), 28.1 (C-23), 27.3 (C-2), 27.2 (C-15), 25.1 (C-12), 21.0 (C-11), 19.5, 18.3, 18.0, 16.1, 15.9, 14.6 ppm.

HRMS (ESI): m/z Calcd for $C_{30}H_{51}O$: 427.3940; Found : 427.3941.

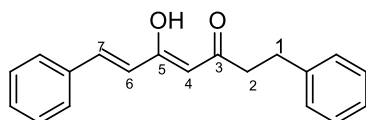
Compound 42 (4*Z*,6*E*)-5-hydroxy-1,7-diphenylhepta-4,6-dien-3-one

Compound **42** was also isolated from the same fraction pool, as a pale yellow crystalline solid (melting point between 58-60 °C) with intense UV activity. The peaks at 3261 and 1645 cm^{-1} in the IR spectrum, confirmed the presence of a hydroxyl and a carbonyl moiety in the compound. From the detailed spectral analysis, the compound was confirmed as 4*Z*,6*E*)-5-hydroxy-1,7-diphenylhepta-4,6-dien-3-one.

Molecular formula : $C_{19}H_{18}O_2$

Mp : 58-60 °C

FT-IR (Neat) ν_{max} : 3261, 2841, 1645, 1561, 1159 cm^{-1}



1H NMR (500 MHz, CD_3COCD_3 , TMS) : δ 15.51 (brs, 1H, OH at C-5), 7.69-7.67 (m, 2H), 7.61 (d, $J = 16$ Hz, 1H, H-7), 7.46-7.41 (m, 3H), 7.31-7.27 (m, 4H), 7.22-7.19 (m, 1H), 6.75 (d, $J = 16$ Hz, 1H, H-6), 5.90 (s, 1H, H-4), 2.98 (t, $J = 8$ Hz, 2H, C-2), 2.81 (t, $J = 8$ Hz, 2H, H-1) ppm.

^{13}C NMR (125 MHz, CD_3COCD_3 , TMS) : δ 200.7 (C-3), 176.3 (C-5), 141.2, 140.9, 135.4, 129.9, 128.4, 128.3, 127.9, 126.0, 125.9, 122.9, 100.7 (C-4), 41.7 (C-2), 30.8 (C-1) ppm.

HRMS (ESI): m/z Calcd for $C_{19}H_{19}O_2$: 279.1385; Found : 279.1377.

3B.9. References

1. (a) K. M. Kumar, G. R. Asish, M. Sabu and I. Balachandran, *Anc. Sci. Life*, **2013**, 32(4), 253-261. (b) S. A. Jathoi, A. Kikuchi and K. N. Watnable, *Genes, Genomes and Genomics*, **2007**, 1(1), 56-72. (c) S. E. Lakhan, C. T. Ford and D. Tepper, *Nutrition Journal*, **2015**, 14, 50-53. (d) T. S. Basaka, G. C. Sarma and L. Rangana, *Journal of Ethnopharmacology*, **2010**, 132 (1) 286-296. (e) P. Sirirugsa, *Pure Appl. Chem.*, **1998**, 70(11), 2111-2117. (f) I. B. Jantan, M. S. M. Yassin, C. B. Chin, L. L. Chen, N. L. Sim, *Pharm. Bio.*, **2003**, 41, 392-397.
2. (a) Medicinal V, S. P, A. of 500 Species, vol. 5. Orient Longman, Madras; p.431. *Arch Surg* **1996**. (b) A. Finose and V. K. Gopalakrishnan, *Int. J. Pharm. Pharm. Sci.*, **2014**, 6 (6), 50-52.
3. (a) B. Sabulal, M. Dan, R. Kurup, N. Sukumaran, R. Krishna and V. George, *Phytochemistry*, **2006**, 67, 2469-2473.
4. M. Govindarajan, M. Rajeswary, S. Arivoli, S. Tennyson and B. Giovanni, *Parasitology Research*, **2016**, 115(5), 1807-1816.
5. (a) D. S. Jang, Ah-Reum Han, G. Park, GiI-Ja Jhon and Eun-Kyoung Seo, *Arch. Pharm. Res.*, **2004**, 27 (4), 386-389. (b) H. Dong, Yu-Lin Gou, Shu-Geng Cao, Shao-Xing Chen, Keng-Yeow Sim, Swee-Hock Goh and R. M. Kini, *Phytochemistry*, **1999**, 50, 899-902.
6. (a) K. Fidy, A. Fiedorowicz, L. Strza and A. Szumny, *Cancer Medicine*, **2016**, 5 (10), 3007–3017. (b) <https://en.wikipedia.org/wiki/Caryophyllene>.
7. (a) S. Dev, *Tetrahedron*, **1960**, 8, 171-180. (b) N. P. Damodaran and S. Dev, *Tetrahedron*, **1965**, 13, 1977-1981. (c) N. P. Damodaran, and S. Dev, *Tetrahedron Lett.*, **1968**, 24, 4113-4122. (d) N. P. Damodaran and S. Dev, *Tetrahedron Lett.*, 1968, 24, 4123-4132.
8. O. A. Ahmed Hamdi, Lo Jia Ye, M. N. Alfarizal, M. Kamarudin, H. Hazni, M. Paydar, C. Y. Looi, J. A. Shilpi, H. A. Kadir and K. Awang, *Rec. Nat. Prod.*, **2015**, 9(3), 349-355.
9. D. F. Rodrigues, D. A. Maniscalco, F. A. J. Silva, B. G. Chiari, M. V. Castelli, V. L. B. Isaac, R. M. B. Cicarelli and S. N. López, *Planta. Med.*, **2016**, 83(3), 239-244.
10. S. M. Abdullahi, A. M. Musa, M. Abdullahi, M. Sule and Y. M. Sani, *Sch. Acad. J. Biosci.*, **2013**, 1(1), 18-19.

11. K.B. Rameshkumar, D.B. Alan Sheeja, Mangalam S. Nair and V. George, *Nat. Prod. Research*, **2015**, 29(13), 1276-1279.
12. M. H Carlsen, B. L Halvorsen, K. Holte, S. K Bøhn, S. Dragland, L. Sampson, C. Willey, H. Senoo, Y. Umezono, C. Sanada, I. Barikmo, N. Berhe1, W. C. Willett, K. M. Phillips, D. R. Jacobs Jr and R. Blomhoff, *Nutrition Journal*, **2010**, 9, 2-11.
13. (a) X. Qing, X. Y. Lee, J. D. Raeymaeker, J. R. H Tame, K.Y. J Zhang, M. D. Maeyer and A. R. D Voet, *J. Recept. Ligand Channel Res.*, **2014**, 7, 81-92. (b) C. G. Wermuth, P. Lindberg, C. R. Ganellin and L. A. Mitscher, *Pure Appl. Chem.*, **1998**, 70, 1129-1143.(c) O. F. Güner, *Curr. Top. Med. Chem.*, **2002**, 2, 1321-1332. (d) A. R. Voet, A. Kumar and K. Y. Zhang, *J. Comput. Aided Mol. Des.*, **2014**, 28(4), 363-373.

Rotula aquatica Lour- Phytochemistry and *in vitro* Antiurolithiatic Activity against Experimental Kidney Stones

4.1. Introduction

The herbal system of medicine has been maneuvered since historical times, and several ancient civilizations, such as Indians, Chinese, and North Africans have provided written evidence for the use of natural sources for curing various ailments. Also, it is noteworthy to mention that before the advancement of synthetic drugs, plant based remedies formed the basis of the primary healthcare system, and decoction and tinctures were house-hold remedies for many ailments. The plant extracts have always provided unlimited breakthroughs for new drugs because of their vast availability and chemical diversity.¹ *Rotula aquatica* Lour. is one among them, and has been used for the treatment of various ailments such as diabetes, cancer, piles and urinary calculi. The plant, belongs to the family Boraginaceae, is a branched shrub, growing in the sandy and rocky beds of streams throughout India, especially in the states of Kerala and Karnataka.

Rotula aquatica (Pashanabheda) is one of the most extensively used medicinal plants in the Ayurvedic system to dissolve urinary calculi or kidney stones; a condition, which is considered as one of the painful disorders of urinary tract, and still remain a common problem worldwide. During their growth, *R. aquatica* extensively absorb the minerals and nutrients from the rocks and gradually weather it down. This is the reason why they are highly recommended for the treatment of urinary stones in Ayurveda.^{2a-d} Pashanabheda/Asmabheda (Pashana/Asma=stone; Bheda=break) is a term used in Ayurveda for a group of plants with diuretic and antiurolithiatic activities and about 40 plants including *R. aquatica* are attributed to this class in different Ayurvedic texts. *Bergenia ligulata*, *Aerva lanata*, *Tribulus terrestris*, *Ammania baccifera*, *Coleus aromaticus* etc. are some among them, being used either as a genuine or as a substitute drug, across India. The plant *R. aquatica* has also demonstrated potential antimitotic and antibacterial properties. Though the plants is known for centuries, a systematic evaluation or a detailed phytochemical investigation for the active components is missing in many cases. In this aspect, the current study aims to investigate the anti-urolithiatic effect of

various extracts, and phytomolecules that are present in *R. aquatica*, against the experimental kidney stones.²

The development of calculi characterizes the stone formation or lithiasis. There are two main types of calculi formation, such as urolithiasis and nephrolithiasis. Urolithiasis is the calculi formation in urinary bladder, ureter or any part of urinary tract rather than kidneys, while the calculi formation in kidneys characterizes nephrolithiasis. Generally, calcification for the formation of teeth and bone take place in a controlled biological situations. But, when the solvent becomes so saturated with certain undissolved minerals, an uncontrolled pathological crystallization occurs and thus leading to the development of precipitates in the body called as kidney stones.³



Figure 4.1. Habitation and different parts of the plant, *R. aquatica*

The incidence of urinary stones has been increasing over the past few years while the age of onset is decreasing. This affect 10–12 % of the world's population, especially in industrialized countries and there are only a few geographical areas in which stone disease is rare (in Greenland and the coastal areas of Japan). With a prevalence of > 10 % and an expected recurrence rate of ~ 50 %, stone disease has an important effect on the healthcare system. Features associated with recurrence, include a young age of onset, positive family history and infection. The Epidemiological studies revealed that nephrolithiasis is more common in men (12 %) than in women (6 %) and is more prevalent between the ages of 20 to 40 in both sex.⁴

The etiology of this disorder is multifactorial, and is strongly related to the luxurious lifestyle habits or practices which have made remarkable changes in the food habit of people all over the world with an increased reliance on soft drinks and junk foods. The increased rates of hypertension and obesity, which are linked to nephrolithiasis, also contribute to an increase in stone formation. Management of stone removal depends on the size and location of the stones. Stones that fail to pass through or stones larger than 5 mm, should be treated by some interventional procedures such as extracorporeal shock

ureteroscopy (URS), wave lithotripsy (ESWL) or percutaneous nephrolithotomy (PNL). Unfortunately, the propensity for stone recurrence is not altered by removal of stones with ESWL and stone recurrence is still about 50 %. In addition, ESWL might show some significant side effects such as renal damage, ESWL induced hypertension or renal impairment.⁵

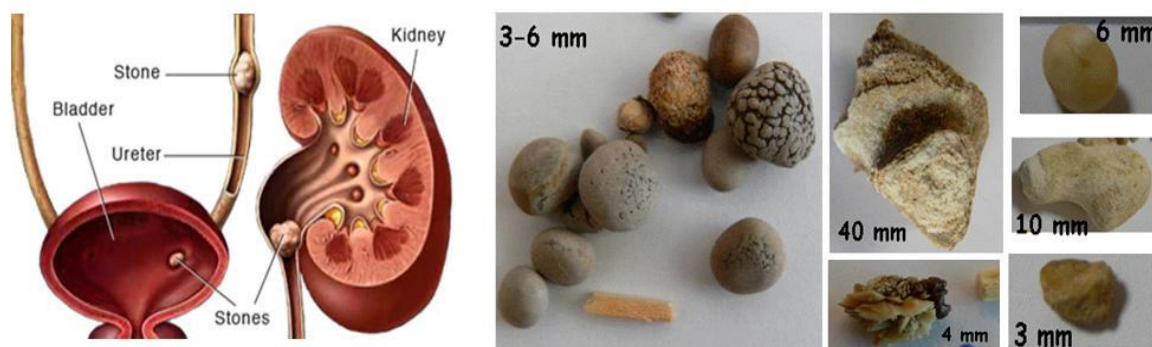


Figure 4.2. Urolithiasis and different types of kidney stones

Kidney stones can be traced back to the primitive records in human civilizations. Prehistoric documents and archaeological evidence revealed that stone formation had distressed the mankind since the earliest known civilizations. The presence of urinary calculi had been found in the kidneys of several Egyptian Mummies. The most ancient of these calculi was discovered from the pelvic remains of an Egyptian boy Mummy dated back to 4800 BC, in a prehistoric tomb at el-Amrah near Abydos. It was discovered by G. Elliot Smith in 1901 and was presented to the Museum of the Royal College of Surgeons of England. The yellow stone weighed 12 g, with a uric acid nucleus and concentric laminations of calcium oxalate and magnesium ammonium phosphate.⁶

Though there are a few recent reports of favorable effects of medical treatments in enhancing the clearance of stones from the distal ureters, in reality, still there is no satisfactory drug to use in clinical therapy, especially for the prevention or the recurrence of stones. In this regard, many plants have been traditionally used to treat kidney stones and have shown to be effective. Various therapies including thiazide diuretics and alkali-citrate are being used in the attempt to prevent recurrence of hypercalciuria and hyperoxaluria induced calculi, but scientific evidence for their efficacy is less convincing. Even if minimally invasive surgery has revolutionized acute and complex stone management, it has not reduced recurrence rates because less invasive therapies, including extracorporeal shockwave lithotripsy (ESWL), often result in incomplete stone clearance.⁷

Nearly about 80 % of these calculi are composed of calcium oxalate and phosphate. The recurrence rate of urolithiasis without any preventive treatment is approximately 10 % per year. It is a multifarious process which includes crystal nucleation, aggregation, and growth of undissolved particles. It is assumed that when the urine becomes saturated with insoluble materials, as a result of their excessive rate of excretions, crystals are formed which aggregate to form a stone. Urolithiasis needs both preventive and curative therapy because of having a higher rate of reoccurrences of kidney stone. At present, no suitable drugs in modern medicine are available for the management of urolithiasis. Several therapies which include thiazide diuretic and alkali citrate are used for the preventive therapy but no allopathic medicine available which can dissolve the stone. Currently, treatments such as percutaneous nephrolithotomy (PCNL), extracorporeal shock wave lithotripsy (ESWL) and surgical removal of stones are being used for the management of stones. Moreover, these are less convincing, and cause side effects such as hemorrhage, hypertension, tubular necrosis, and subsequently fibrosis of the kidney.^{7,8}

4.2. Reasons and Risk Factors

It is assumed that the stone usually begins as tiny sand like speck of material (nidus) in the kidney. Minerals in the urine especially calcium, build on the speck in a similar way to that in which a pearl grows in an oyster shell. The formation of the nidus may be analogous to the first stage in the physiologic calcification of bone in which a nucleus of calcium phosphate emerges in controlled biological situations. The present medical management of urinary stone includes lithotripsy and surgical procedures which are prohibitively expensive for the common man. Also, with these, the recurrence is quite common and the patient has to be examined through careful follow up for several years. Various factors such as size of calculi, the severity of symptoms, kidney function, location of the stone and associated infections, influence the choice of one type of intervention over the other. Stones which are smaller than 5 mm have a high probability of spontaneous passage, which can take up to 40 days. During this watchful waiting period, patients can be treated with hydration and pain relieving medication. However, stones larger than 5 mm or stones that fail to pass through urine are treated by interventional procedures. ESWL is a noninvasive practice which uses shock waves to fragment calculi. This technique is the most extensively used method for managing renal and ureteral stones. However, success of treatment rates depends on stone composition, size, properties and location of the stone as well as the instrumentation type and shock frequency. It also needs to be considered that

the forces that are directed at the stones also have deleterious effects on surrounding tissues. Damage to almost every abdominal organ systems have been reported, but by far the most common injury is acute renal hemorrhage although its true incidence is unclear and poorly defined. Most often renal hemorrhage can be managed predictably; however, in rare instances the complications are fatal. Reports of post-ESWL perirenal hematoma range from less than 1 % to greater than 30 %. Besides, ESWL has been associated with long-term medical effects such as diabetes mellitus and hypertension.^{8,9}

- Dehydration
- Obesity
- A diet with high levels of glucose, protein or salt
- Hyperparathyroidism condition
- Inflammatory bowel diseases that increase calcium absorption
- Taking medications such antiseizure drugs, and calcium-based antacids
- Gastric bypass surgery

Risk factors

Many factors increase your risk of developing kidney stones, and some of the major reasons include:¹⁰

- Family or personal history: If someone in your family has kidney stones, you're more vulnerable to develop the same. Also, if you've already had one or more kidney stones, you're at increased risk of recurrence of the stones.
- Certain diets: Diet that is high in protein, sugar and sodium (salt) may increase your risk of some types of kidney stones. Too much salt in your daily diet increases the amount of calcium which your kidneys must filter off, and this significantly enhances the risk of kidney stones.
- Dehydration: Avoiding enough drinking water can increase your risk of kidney stones and, people who sweat a lot and those who live in warm climates may be at higher risk than others.
- Being obese: High body mass index (BMI), weight gain and large waist size have been linked to an increased risk of kidney stones.
- Digestive diseases and surgery: Digestive diseases like chronic diarrhea or inflammatory bowel disease, and gastric bypass surgery can cause changes in the digestive system that affect your absorption of calcium and water. This gradually leads to the formation of stones in your urine. Certain other diseases, like cystinuria, renal tubular acidosis, hyperparathyroidism are also known to cause the same.

Symptoms

Usually, a kidney stone remains symptomless until it moves into the ureter - the tube connecting the kidney and bladder. When symptoms of kidney stones become apparent, they cause,¹⁰

- Severe pain in the groin and/or side
- Reduced amount of urine excreted
- Pain that radiates to the lower abdomen and groin
- Blood in urine, vomiting and nausea
- Burning sensation during urination
- Persistent urge to urinate and white blood cells or pus in the urine
- Fever and chills if there is an infection

4.3. Types of kidney stones

Not all kidney stones are made up of the same crystals. They differ in composition, size and shape. Knowing the type of kidney stones, help to determine the cause and may give clues on how to reduce the risk of getting more stones. The different types of kidney stones include:^{3,7,10}

i. Calcium stones (~ 80 %): Calcium stones are the most common and are often made of calcium oxalate. They can also consist of calcium phosphate or maleate. Oxalates occur in many edible plants and is also synthesized by our liver. So, eating fewer oxalate-rich foods can reduce the risk of developing this type of stones. Some of the common foods having high-oxalate content include;

- | | |
|----------------|-------------------|
| • Potato chips | • Beets |
| • Peanuts | • Spinach |
| • Chocolate | • Milk and Cheese |
| • Wheat bran | • Sweet potato |

Dietary factors, high doses of vitamin D, intestinal bypass surgery, and several metabolic disorders often increase the concentration of calcium or oxalate in urine. Despite of calcium oxalates, these stones may also occur in the form of calcium phosphate. The phosphate stones are more common in metabolic conditions, such as renal tubular acidosis or with certain migraine headaches. It may also be associated with taking some seizure medications such as topiramate (Topamax).

-
- ii. Uric acid stones (~ 5-15 %):** Uric acid stones are more common in men than in women. This can form in people who don't drink enough fluids or who lose too much fluid. This can also occur in people with gout or those going through chemotherapy and those who eat a high-protein diet. Certain genetic factors also may increase the risk of uric acid stones. This type of stone develops when urine is too acidic because of a diet, rich in purines (purine is a colorless substance that present in animal proteins, such as fish, shellfish, and meats).
- iii. Struvite stones (~ 5-10 %):** This type of stone is found mostly in women in response to urinary tract infections (UTIs). These stones grow quickly, and become large with little warning. Treating an underlying infection can prevent the development of struvite stones
- iv. Cystine stones (~ 3 %):** These are hereditary in nature. It causes the kidneys to excrete too much of certain naturally occurring amino acids (cystine) and results in the accumulation of these in the wall of nephrons.

4.4. Scope of the Study

Natural products remain the finest sources of novel drugs and drug leads, and is true today, despite the fact that many pharmaceutical firms have deemphasized natural products research in favor of HTP screening, during the past few decades. But, while taking the statistical data from 1940's to date, 131 (74.8 %) out of 175 small molecule anticancer drugs are natural product-based/inspired, with 85 (48.6 %) being either natural products or derived molecules. *R. aquatica* is one amongst those plants, which are used in the treatment of urolithiasis. Though this plant is native to India and used in many decoctions, there is no reports on the detailed phytochemical profiling of this plant. Hence in the present study, we carried out a detailed phytochemical analysis of *Rotula aquatica* and also carried out an *in vitro* antiurolithiatic studies of various extracts towards the experimental kidney stones.

4.5. Extraction, Isolation and Characterization of Compounds

The dried roots of *Rotula aquatica*, were collected from Kannur District of Kerala, India during the month of March 2018. The roots were thoroughly washed 2-3 times in running water then with distilled water and dried in an air oven maintained at 40 °C. The air dried roots were coarsely grounded and subjected to extraction procedures. 900 g of the dried and powdered roots of *R. aquatica* were extracted (3 L x 3 times) by intermittent vigorous stirring using a mechanical stirrer in one by one with hexane, acetone, ethanol, ethanol:water and water at room temperature for 48 h. The crude extracts were then concentrated at 50 °C under reduced pressure till complete dryness (Removal of solvent

under reduced pressure which gave 17 g of crude hexane extract, 14 g acetone extract, 4 g of ethanol extract, 2 g of ethanol:water extract and finally the water extract (4 g).

After studying the TLC, each extracts (17 g of hexane extract, 13.5 g of acetone extract and 4 g of ethanol extract) were fractionated according to the increasing polarity of molecules *via* silica gel column chromatography using 100-200 mesh-sized silica gel. Initially, the column was eluted with hexane-ethyl acetate mixtures of increasing polarities and the final elution was carried out using 10 % methanol in ethyl acetate. The hexane extract mainly afforded a mixture of two compounds (**43** and **44**) in an inseparable form. Along with these molecules, compounds **30** and **45-51** were isolated from the acetone extract. From the ethanol extract, we could successfully isolate compounds **7**, **50** and **51**. A pictorial representation of the entire isolation procedure is given below (figure 4.3).

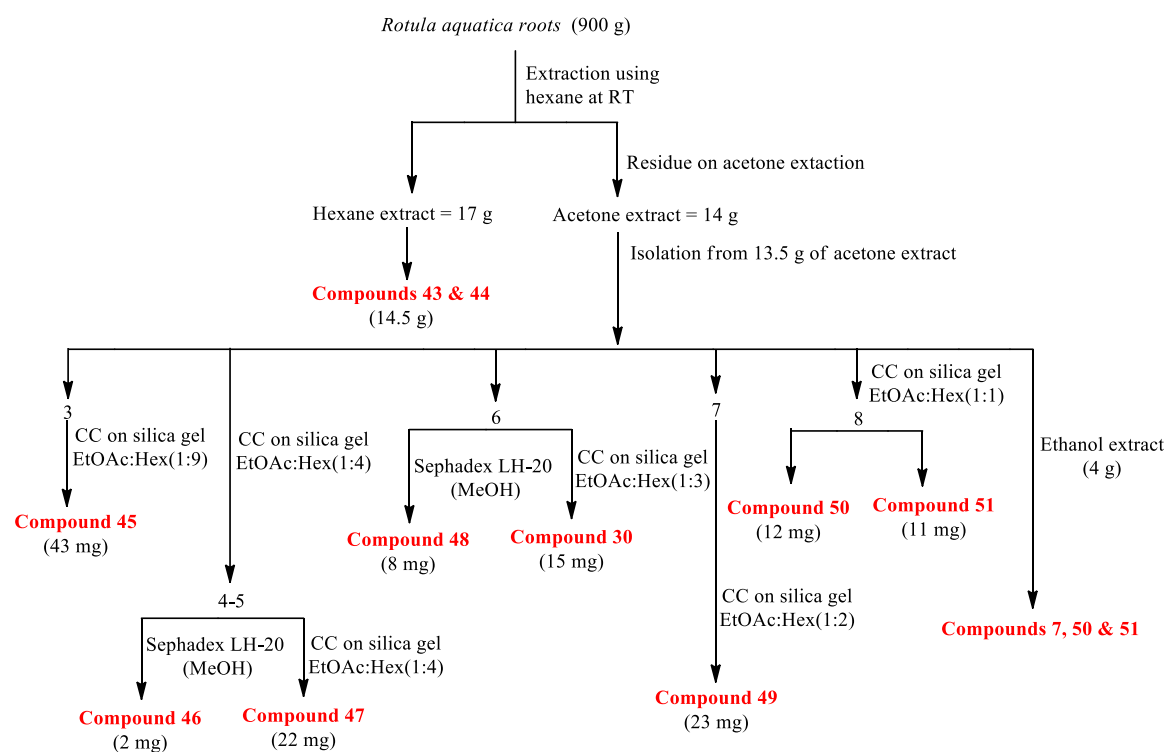
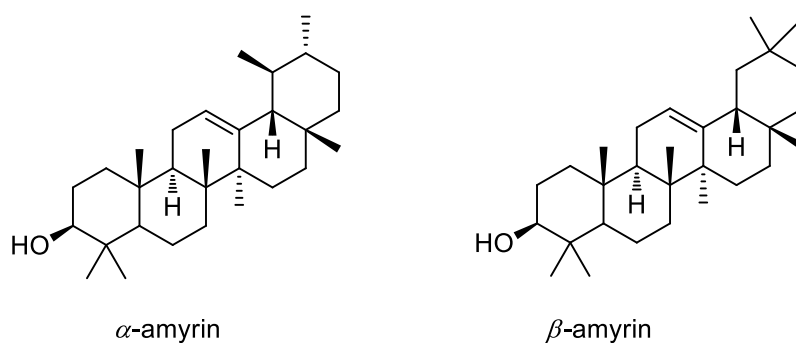


Figure 4.3. A schematic representation of isolation procedure

Compounds **43** and **44** were obtained as a white waxy substance (14.5 g), in an inseparable form. From the TLC analysis, it was assumed to be a single compound, but when we carried out a detailed NMR studies, we found that it's a mixture of two. Around hundred protons and sixty carbons were present in the ^1H NMR and ^{13}C NMR respectively.

Due to the difficulty in the characterization of these compounds (because of the crowded NMR), we went with the GCMS analysis, to get some information about the fragmentation pattern of these molecules in the mass spectra. From the GCMS analysis, we obtained two sharp signals, which on comparison with the library (NIST Wiley library) of the instrument, confirmed the structures of the molecules as α and β -amyryns (figures 4.4, 4.5 & 4.6).¹¹

The infra-red spectrum of the compounds showed, peaks at 3453, 3367 at 2894, 1650 cm^{-1} confirmed the presence of hydroxyl and olefinic functionalities. The olefinic protons of α -amyryn resonated at δ 5.12 ppm as a triplet, while that of β -amyryn resonated as a triplet at δ 5.19 ppm. Also the protons attached with the carbon, bearing hydroxyl group, resonated together as a doublet of doublet (with a integral of two) at δ 3.22 ppm with a coupling constant of $J = 10.5$ and $J = 5.5$ Hz (figure 4.4). In the carbon NMR, the olefinic carbons of α -amyryn resonated at δ 124.4 and 139.6 ppm while that of β -amyryn resonated at δ 121.7 and 145.1 ppm (figure 4.5). The structure of the compounds were also well supported with HRMS data, in which $(M+Na)^+$ peak was obtained at 449.3755.



Structures of compounds **43** and **44**

Apart from these, the hexane fraction also provided some long chain fatty acids and triglycerides. These compounds were identified as the esters of oleic acid and octadecanoic acid *via* GC-MS analysis.

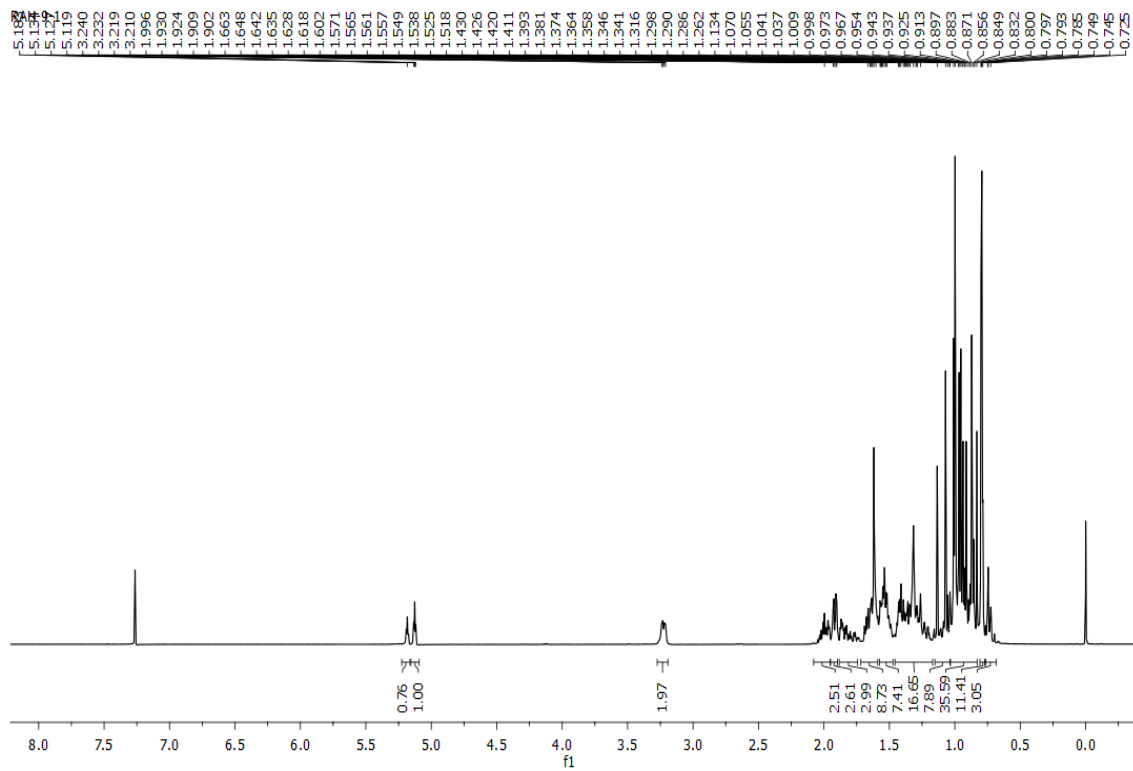


Figure 4.4. ^1H NMR of compounds **43** and **44** in CDCl_3

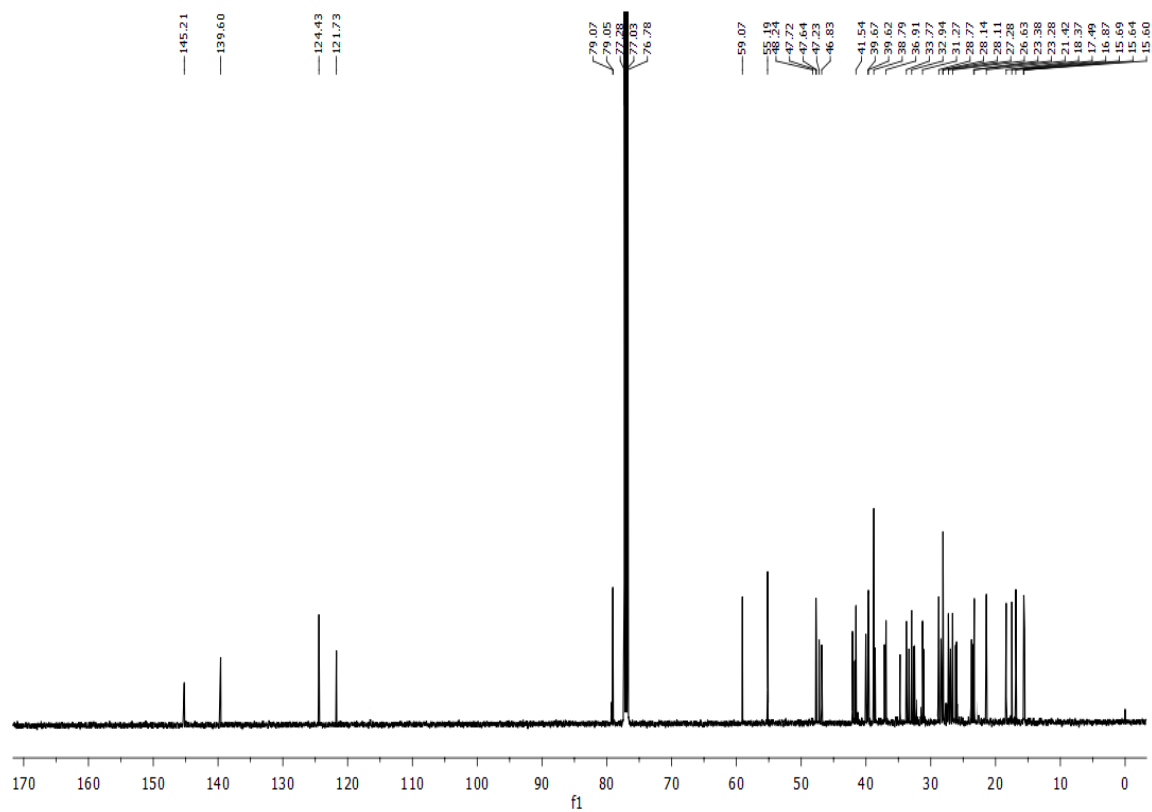


Figure 4.5. ^{13}C NMR of compounds **43** and **44** in CDCl_3

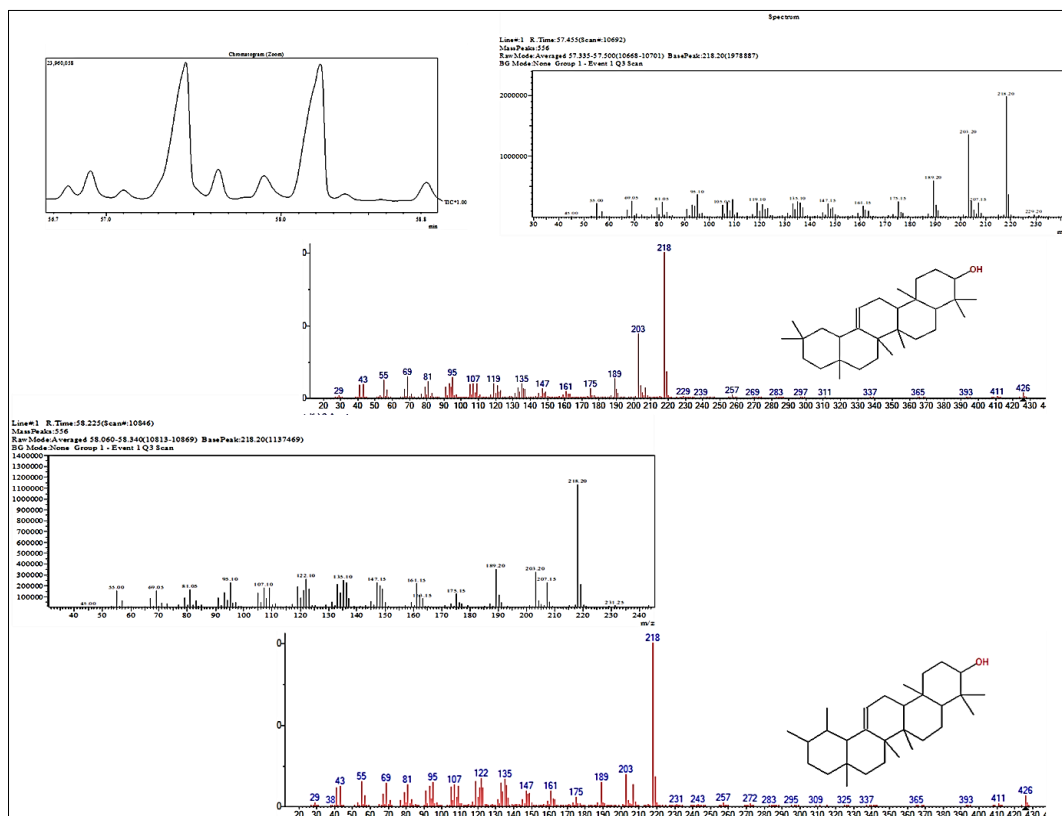
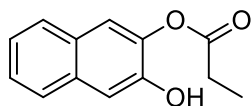


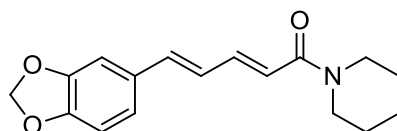
Figure 4.6. Comparison of GCMS data with NIST Wiley library

Compound **45** (42 mg) was isolated from fraction pools 4-5. The molecule was pale white solid in nature and highly UV active. It showed a pink charring which turned to blue in Enholm yellow solution. The peak at 1868 cm^{-1} in the IR spectra suggests the presence of an ester carbonyl group. Also the peak at 3415 cm^{-1} represents the presence of a hydroxyl group. In the proton spectra, the two proton quartet at $\delta 2.42$ ppm and three proton triplet at $\delta 1.23$ ppm with a co-relation in HOMO COSY represents the presence of an ethyl side chain. Also the peaks that resonated beyond $\delta 7$ ppm in the proton NMR represent the presence of six aromatic protons (figure 4.7). Besides, the peak that resonated at $\delta 170.2$ ppm in the carbon NMR indicates the presence of an ester carbonyl system ((figure 4.8)). From these data and other 2-D NMR techniques, the structure of the compound **4** was confirmed to be **3-hydroxynaphthalen-2-yl propionate**. Further, the peak at $m/z = 217.0856$ ($[M+H]^+$ peak) in ESI spectra well supported the structure of the molecule. Moreover, this is the first report on the isolation of 3-hydroxynaphthalen-2-yl propionate from natural resource.¹²



3-Hydroxynaphthalen-2-yl propionate
Compound **45**

Compound **46** was an UV inactive compound, isolated from fraction pools 4-5 in 2 mg. After the detailed spectroscopic analysis, the structure of the compound was confirmed to be the phytosterol, **stigma sterol**. From the same fraction pools, while doing column chromatography with 25 % of ethyl acetate in hexane mixture, a pale yellow colored solid was obtained in 22 mg. While checking various staining reagents to know the core structure of the compound, it showed a deep orange red color with Dragendorff reagent, confirmed the presence of an alkaloid moiety. The impure compound was again purified by column chromatography with Sephadex LH-20 in methanol yielded a colorless crystalline solid, compound **47**, with a melting point between 127-372 °C. In the IR spectrum, the peak vibrated in a region of 1690 cm^{-1} , represented the presence of an amide moiety. The presence of doublets and doublets of doublets having coupling constants above 13 Hz, indicate the presence of *trans* olefinic protons. The two proton singlet at δ 5.99 ppm suggests the presence of a methylenedene group (figure 4.9). The peaks at aliphatic region corresponding to ten protons clearly indicate the presence of a cyclic system of ten protons. Also, the peak which resonated at δ 165.5 ppm in the carbon NMR confirmed the presence of an amide moiety (figure 4.10). Finally, the peak at m/z 286.1433, corresponds to $(M+H)^+$ in the HRMS data, along with the literature reports, the structure of the compound was confirmed to be **piperine**. Though the presence of pyrazolidine and piperidine alkaloids have already been reported from this family, this is the first report on the isolation of piperine alkaloid from this family.¹³



Piperine
Compound **47**

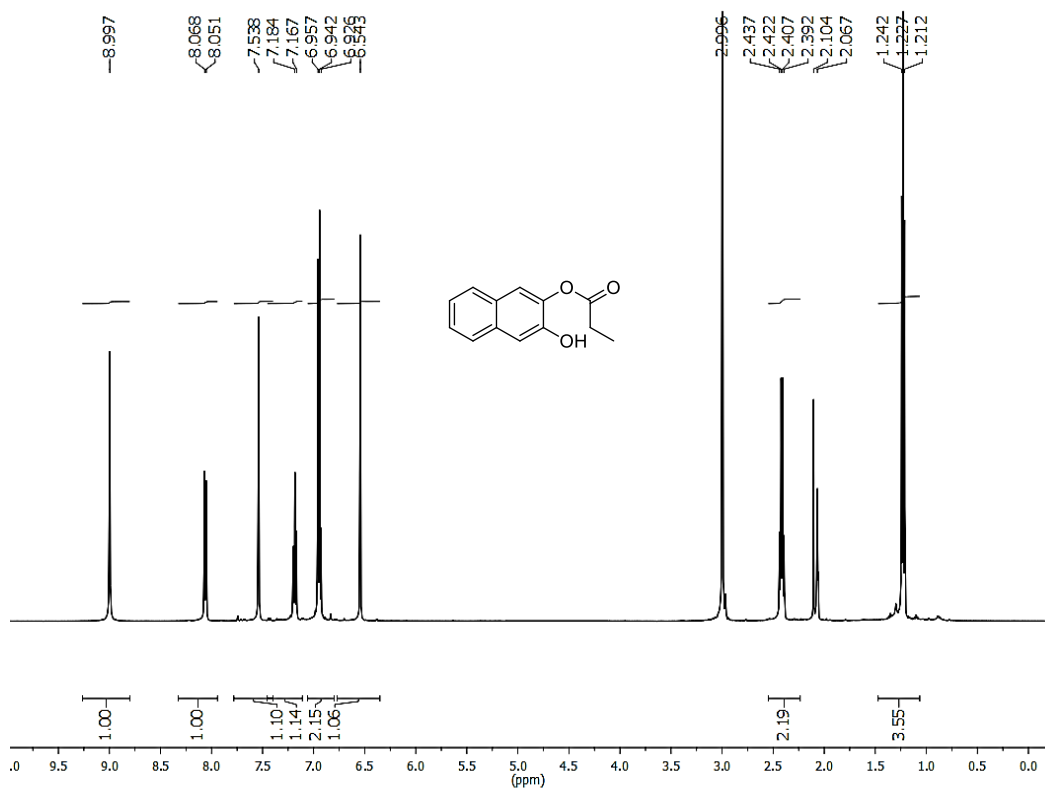


Figure 4.7. ^1H NMR of compound **45** in CD_3COCD_3

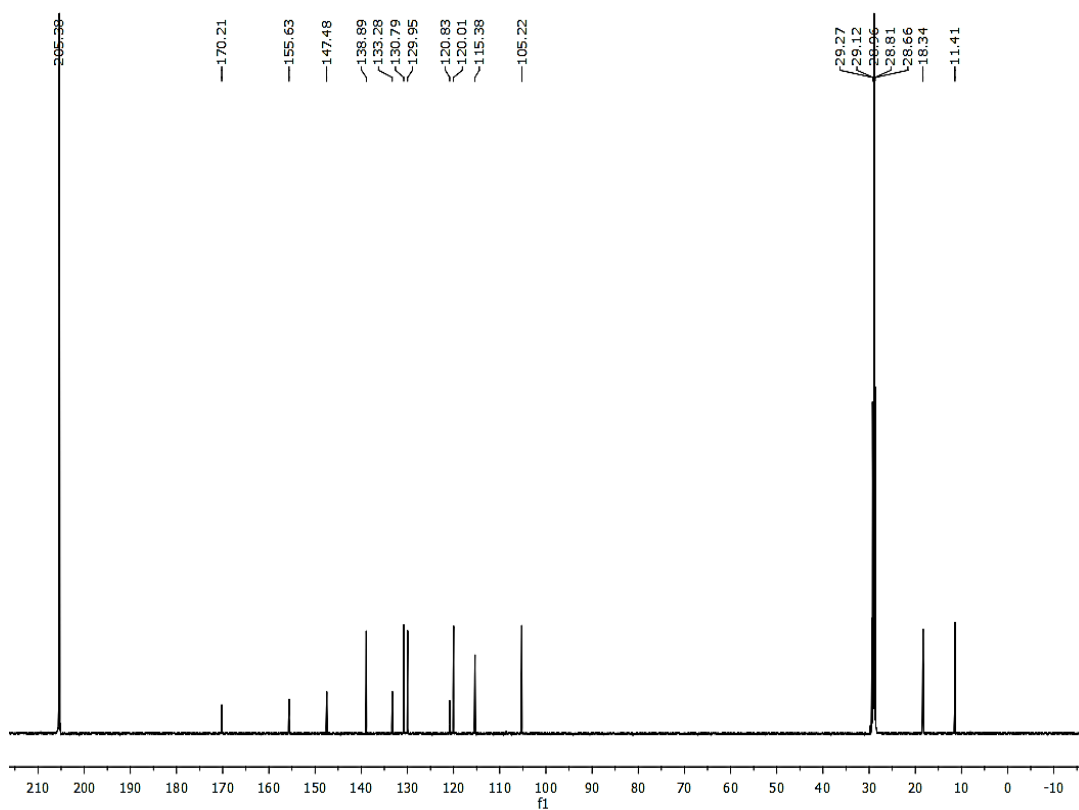


Figure 4.8. ^{13}C NMR of compound **45** in CD_3COCD_3

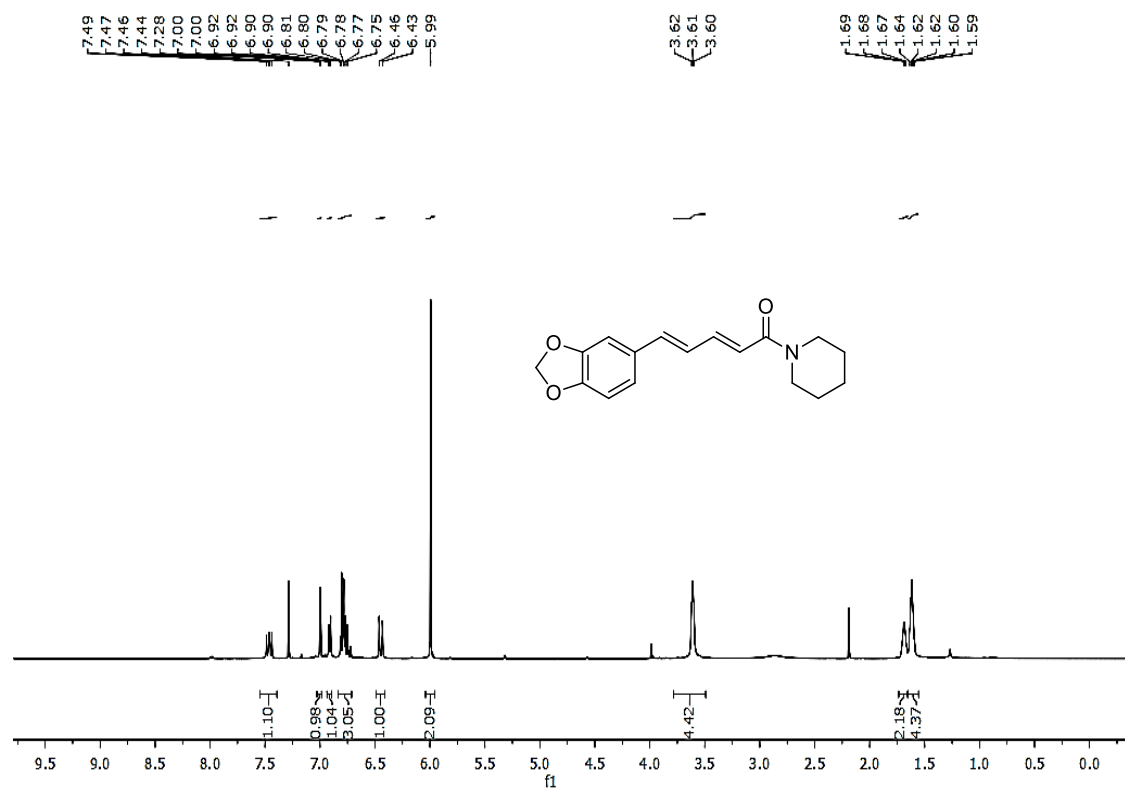


Figure 4.9. ^1H NMR of compound **47** in CDCl_3

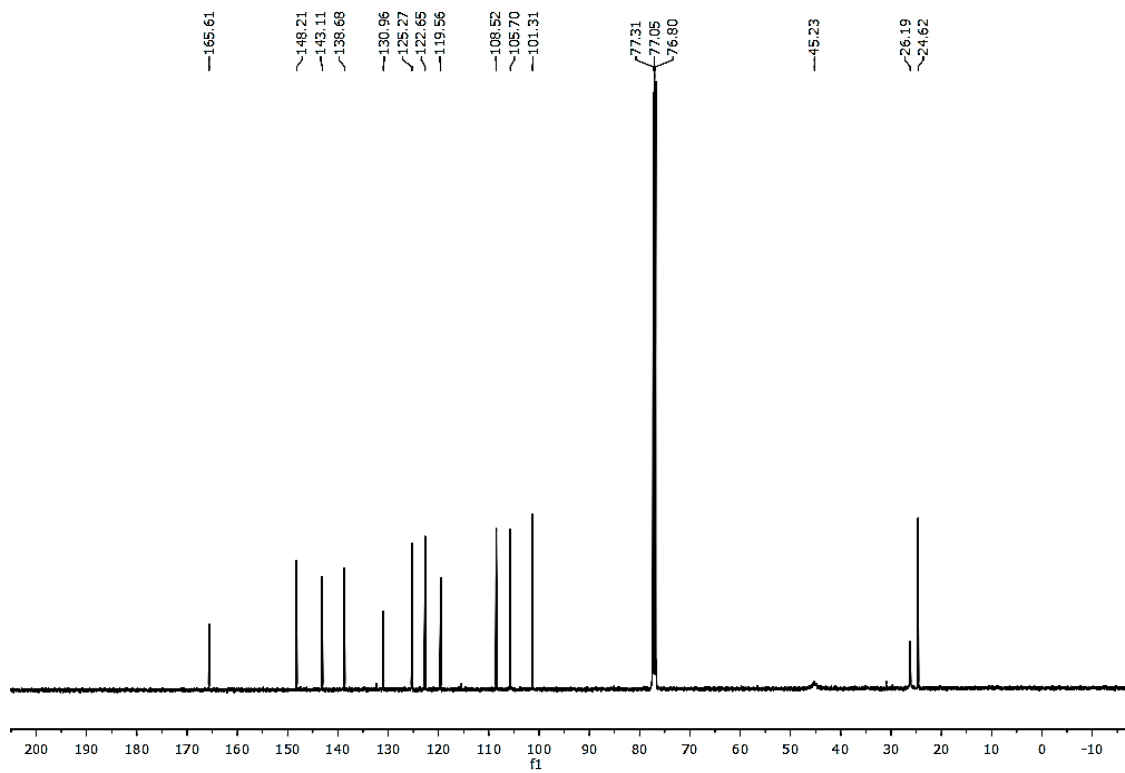
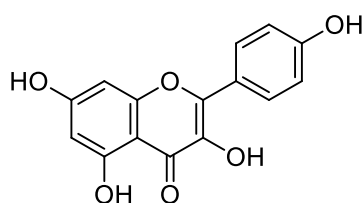


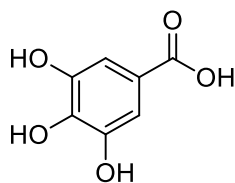
Figure 4.10. ^{13}C NMR of compound **47** in CDCl_3

Compound **48** was isolated from fraction pool 6 as a yellow solid (8 mg), through Sephadex LH-20 column in methanol. Using various spectroscopic techniques and literature reports, compound **48** was identified as a flavonol, named **kaempferol**. IR spectrum of the compound showed a broad and a sharp peaks at 3327 and 1669 cm^{-1} corresponding to the hydroxyl and carbonyl groups respectively. Two similar aromatic protons resonated at δ 8.19 ppm as a doublet with a coupling constant of 8.5 Hz and another doublet seen at δ 7.10 ppm represents the *para*-substituted phenyl system. The aromatic protons that resonated at δ 6.53 and δ 6.34 ppm with a coupling constant of 2 Hz, indicates the presence of *meta* coupled aromatic protons (figure 4.11). ^{13}C NMR spectrum of kaempferol displayed a peak at δ 181.6 corresponding to the carbonyl carbon of the enone moiety (figure 4.12). All other signals in the ^1H and ^{13}C NMR spectra were in agreement with the literature report. Also, the HRMS spectrum well supported the structure of the compound with a peak at m/z 309.0371 $[\text{M}+\text{Na}]^+$.¹⁴



Kaempferol
Compound **48**

Compound **49** was isolated from fraction pool 7, in 23 mg as a colorless solid with a melting point of 258-260 $^{\circ}\text{C}$. which displayed a broad singlet at δ 6.32 (brs, 2H) ppm in the proton NMR. From the carbon NMR, it was found that it is a symmetric aromatic system with five distinct carbons. Also, in the IR spectrum, the peaks at 3459, 3345 and 1751 cm^{-1} indicate the presence of hydroxyl and carbonyl groups. After the careful analysis and in comparison with literature reports, the structure of the molecule was confirmed as **gallic acid**.¹⁵



Gallic acid
Compound **49**

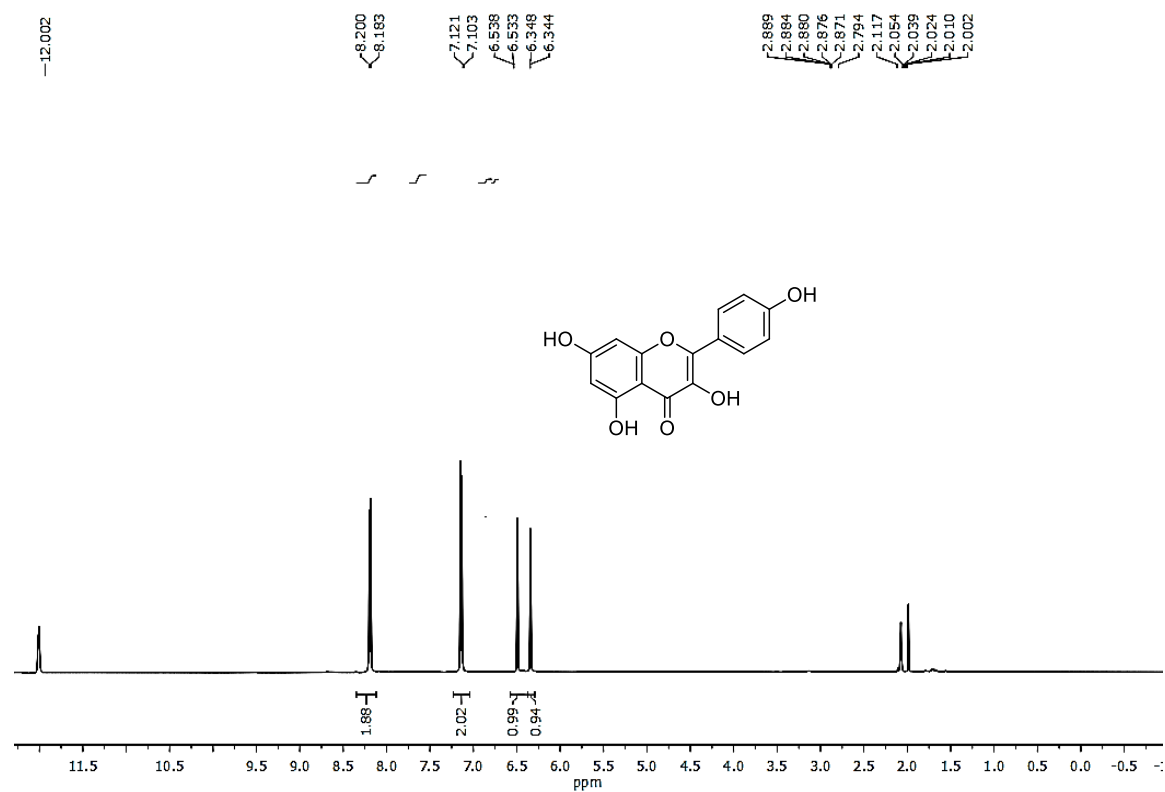


Figure 4.11. ^1H NMR of compound **48** in CD_3COCD_3

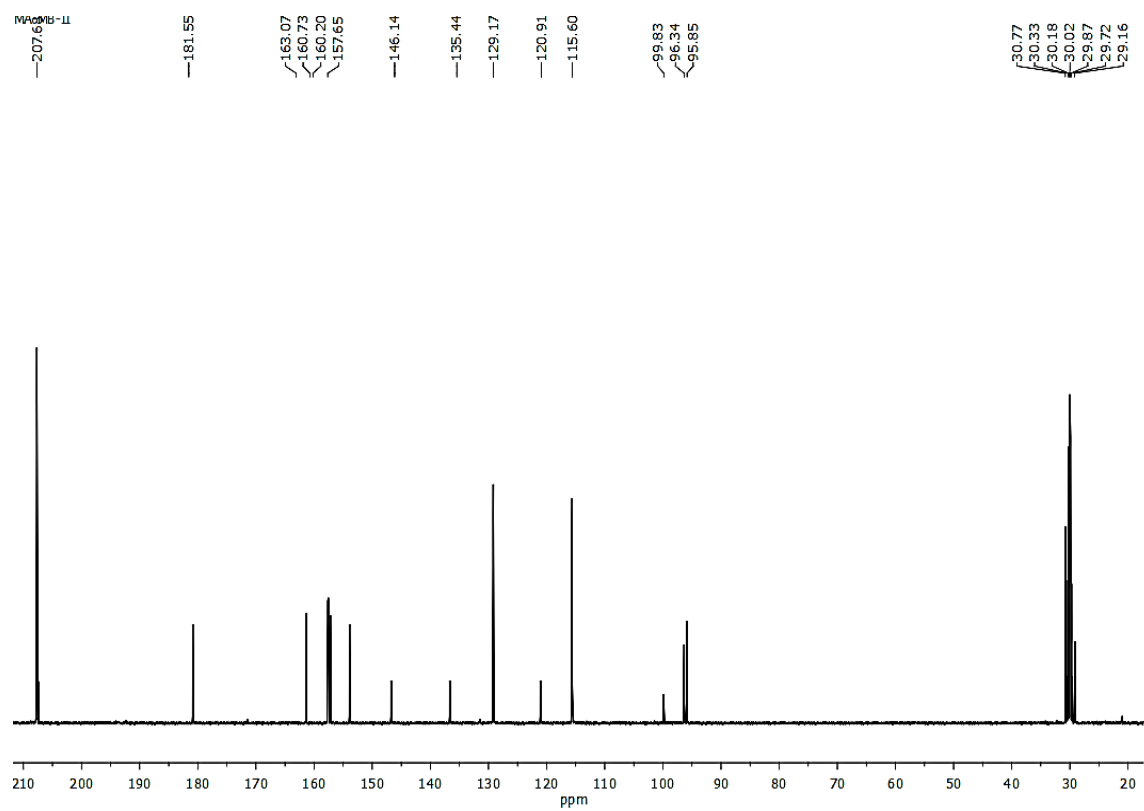
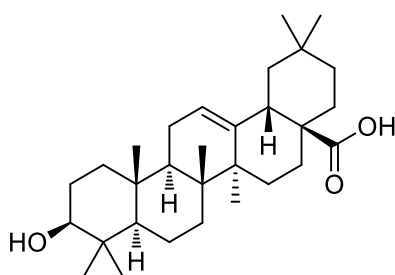


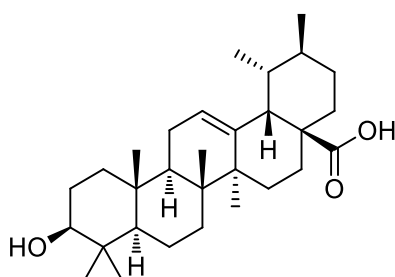
Figure 4.12. ^{13}C NMR of compound **48** in CD_3COCD_3

Compound **50** was isolated from the fraction pool 8 as colorless powder (12 mg), with UV activity. The compound was confirmed as **oleanolic acid** based on its spectral data and literature reports. In the ^1H NMR spectrum, one proton triplet at δ 5.28 ppm indicates the presence of an olefinic proton. One proton, doublet of doublet at δ 3.22 ppm indicates the presence of a methine proton attached to a hydroxyl group. Again one proton, doublet of doublet at δ 2.82 ppm indicates the presence of a methine group adjacent to $-\text{COOH}$ group (figure 4.13). The peak at δ 183.2 ppm in the ^{13}C experiment revealed that the compound contains a $-\text{COOH}$ group (figure 4.14). Finally the mass spectrum of the molecule well supported the structure with $(\text{M}+\text{Na})^+$ ion peak at m/z 479.3603.¹⁶



Oleanolic acid
Compound **50**

Compound **51** was also isolated from the same fraction pool as a colorless solid (11 mg), having almost same characteristics with that of compound **50**. This molecule also showed a one proton triplet peak at δ 5.19 ppm, corresponding to an olefinic proton. Likewise, the one proton doublet of doublet at δ 3.14 ppm indicates the presence of a methine proton attached to a hydroxyl group (figure 4.15). Also, the carbonyl carbon was resonated at δ 180.65 ppm (figure 4.16). Finally the mass spectrum of the molecule ($(\text{M}+\text{Na})^+$ ion peak at m/z 479.3603) well supported the fact that, the molecule is the **ursolic acid**, the α -isomer of oleanolic acid.¹⁶



Ursolic acid
Compound **51**

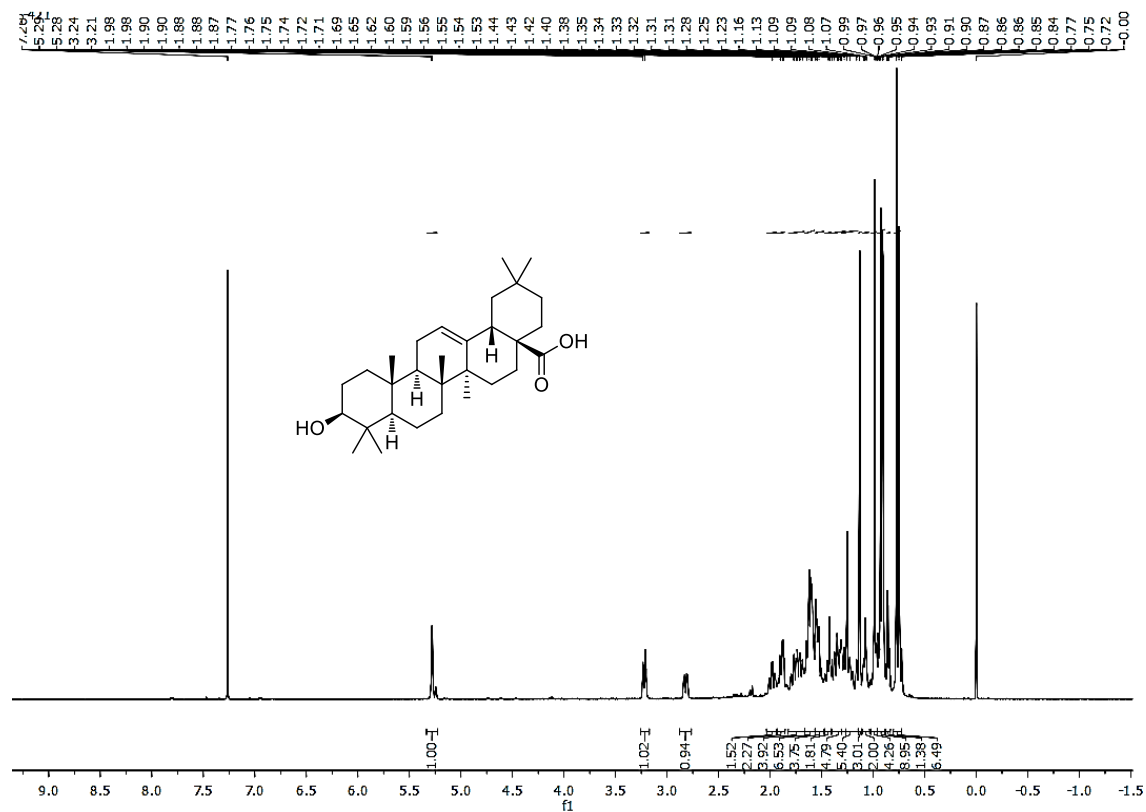


Figure 4.13. ¹H NMR of compound 50 in CDCl₃

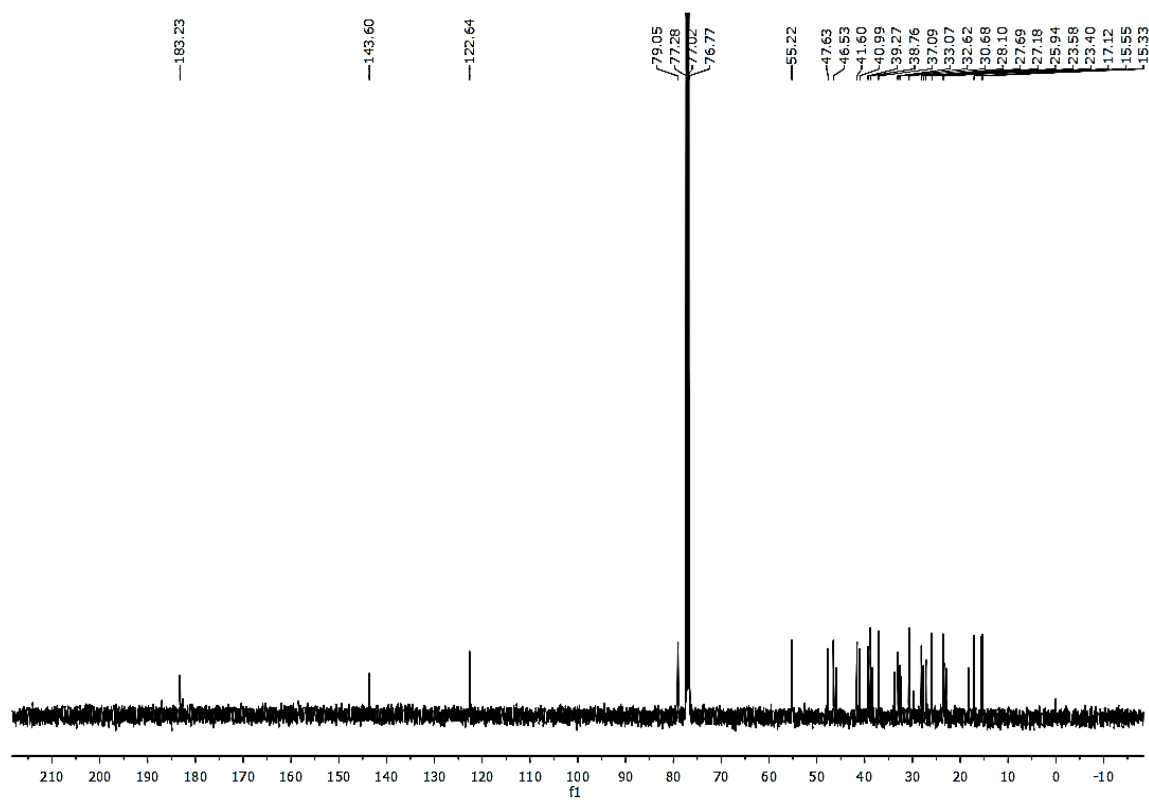


Figure 4.14. ¹³C NMR of compound 50 in CDCl₃

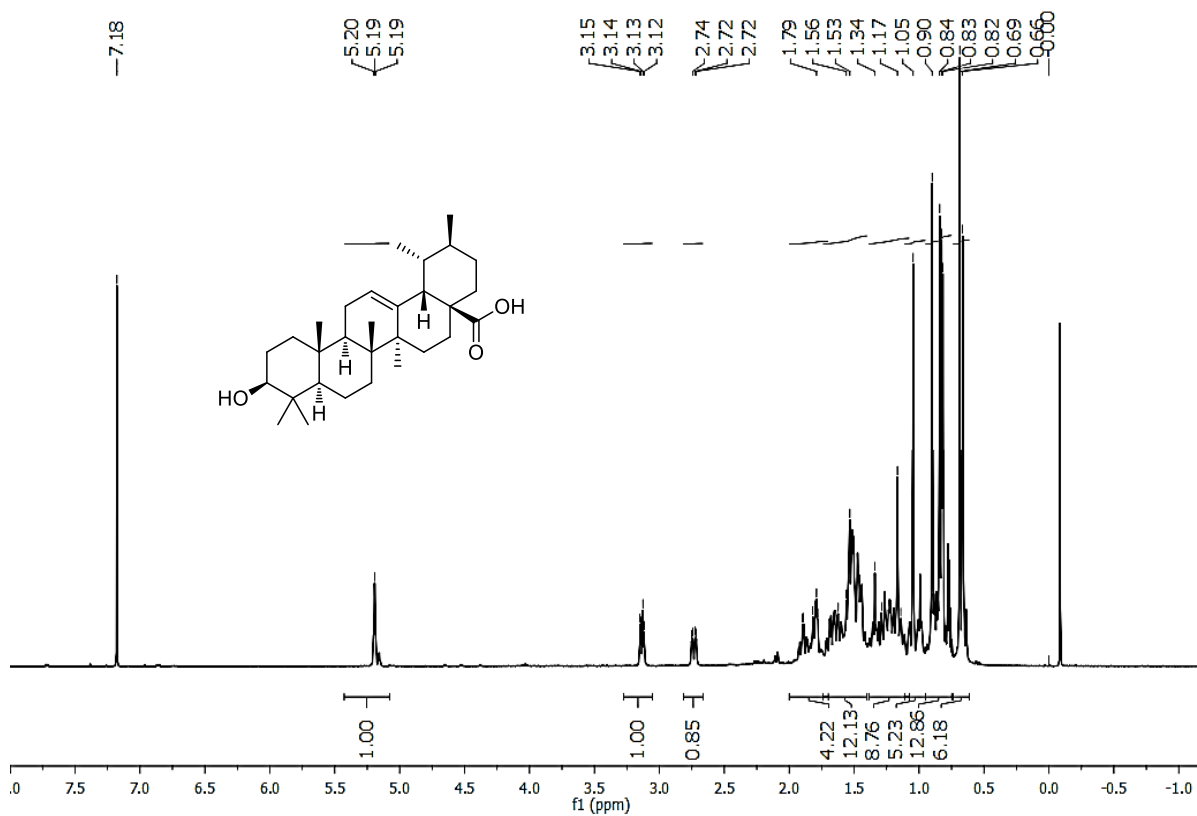


Figure 4.15. ^1H NMR of compound **51** in CDCl_3

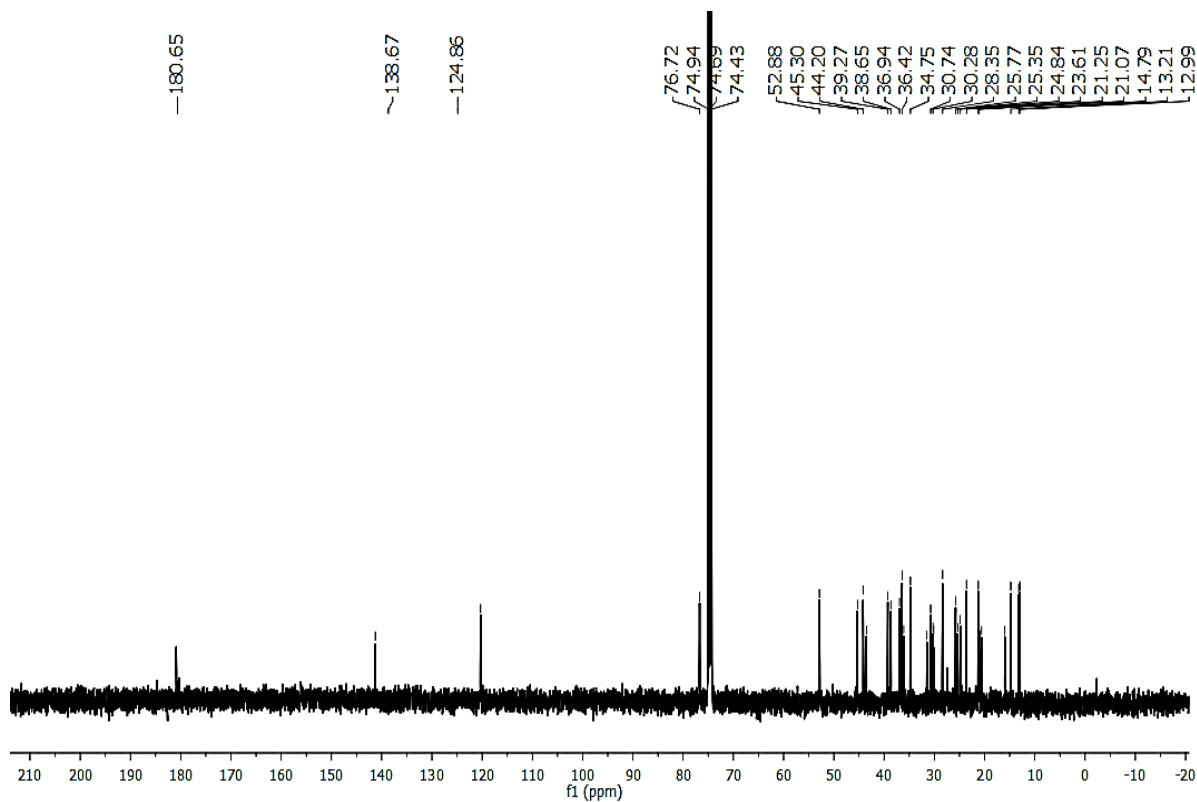


Figure 4.16. ^{13}C NMR of compound **51** in CDCl_3

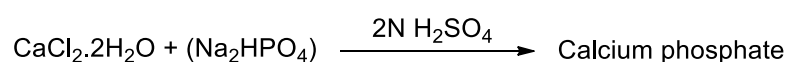
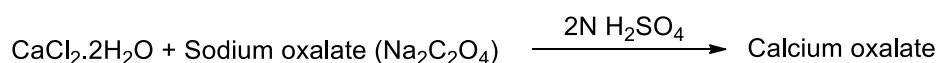
After the successful isolation of compounds from the roots of *R. aquatica*, we further focused on the isolation of molecules from the aerial parts of the same plant. Fortunately, we could isolate almost all the molecules that are obtained from roots, except the gallic acid and piperine. Subsequently, we carried out the *in vitro* antiurolithiatic activity of root extracts of *R. aquatica* against the experimental kidney stones using reported procedures. The results of our studies are explained in the following sections.

4.6. Evaluation of Antiurolithiatic Activity of Different Root Extracts of *R. aquatica* against Experimental Kidney Stones

The present study started with the synthesis of experimental kidney stones, mainly the calcium oxalate and calcium phosphate crystals, which were prepared using reported procedures. These are the two most common types of kidney stones and these minerals are a part of person's normal diet, which improves the normal body metabolisms. But an excessive intake of these minerals saturates the urine and results in the formation of stones.

4.6.1. Synthesis of experimental kidney stones

For the preparation of calcium oxalate crystals, an equimolar solution of calcium chloride dihydrate (AR, 1.47 g) in 100 mL distilled water and sodium oxalate (AR, 1.34 g) in 100 mL of 2N sulfuric acid were allowed to react for five minutes, in a 500 mL round bottom flask. The reaction resulted in the formation of calcium oxalate, as a precipitate. This precipitate was then washed with ammonia solution, to make it free from the traces of sulfuric acid; later the precipitate was washed with distilled water and dried at 60 °C for 4 hours (scheme 6.1, figure 4.17). In the case of calcium phosphate crystals, as in the previous case, equimolar solution of calcium chloride dihydrate (1.47 g) in 100 mL of distilled water and disodium hydrogen phosphate (AR, 1.42 g) in 100 mL of 2N sulfuric acid were allowed to react in sufficient quantity of distilled water in a round bottom flask. The resulting precipitate then freed from traces of sulfuric acid, by ammonia wash, followed by water wash. Then, it was dried at 60 °C for 4 hours (scheme 6.1, figure 4.18).¹⁷



Scheme 6.1. Synthesis of experimental kidney stones

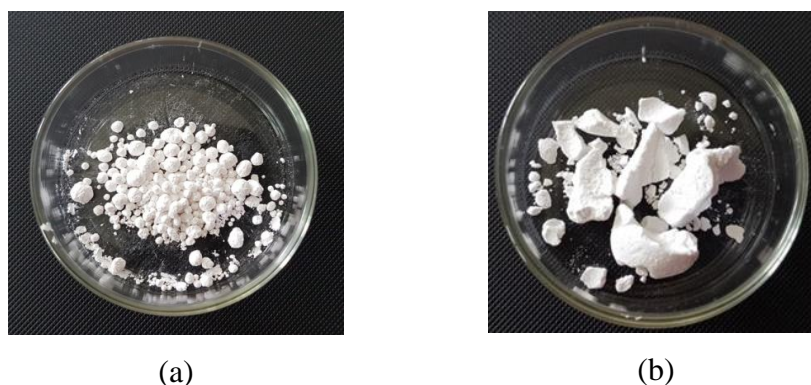


Figure 4.18. (a) calcium oxalate stones, (b) calcium phosphate stones

4.6.2. Synthesis of semi-permeable membrane (SPM)

The semi-permeable membrane was prepared by decalcification of farm chicken eggs. These membranes lie in between the outer calcified shell and the inner contents like albumin and yolk. Shell was removed (decalcification) chemically by placing the eggs in 2 M hydrochloric acid for a period of eight hours. After the complete decalcification, the eggs were washed thoroughly with distilled water, and carefully with a sharp knife a hole is made at the apex of eggs and the contents were squeezed out completely from the egg. Then, the egg membrane washed thoroughly with distilled water and placed in ammonia solution for a while, and rinsed it with distilled water. These membranes were kept in a refrigerator at a pH of 7-7.4, in the moistened condition.¹⁷

4.6.3. Estimation of percentage of dissolution of calcium oxalate stones

Exactly 1 mg of calcium oxalate and 10 mg of the extract/compound/standard were packed together in an egg shell semi-permeable membrane by suturing with a thread as shown in figure 4.19. These were suspended in a conical flask containing 100 mL of 0.1 M TRIS buffer and covered with an aluminum foil. One group served as negative control (contained only 1 mg of calcium oxalate) while other as positive control (1 mg of calcium oxalate and 10 mg of 500 mg tablet of Cystone). All conical flasks were kept in an incubator, preheated to 37 °C for 2 hours, for about 7-8 hours. The entire contents of semi-permeable membrane from each group were then removed into test tubes, individually. Then 4 mL of 1 N sulfuric acid (heated to 60 °C) was added and titrated against 0.9494 N KMnO₄ till a light pink color end point was obtained. A conversion factor of 1 mL of 0.9494 N KMnO₄ equivalent to 0.1898 mg of calcium, was used for further calculation. Then, the amount of undissolved calcium oxalate was determined by subtracting the obtained value from the total, which used in the beginning of the experiment. Triplicate experiments were carried out to get concordant values.¹⁷



Figure 4.19. *In vitro* experimental model set-up to evaluate antiurolithiatic activity

$$\% \text{ of dissolution} = \frac{\text{Weight of Ca}^{2+} \text{ reduced}}{\text{Weight of Ca}^{2+} \text{ estimated (control)}} \times 100$$

The amount of undissolved calcium oxalate is then subtracted from the total quantity used initially, to know the amount of calcium oxalate dissolved by the extracts. From the experimental studies, it was revealed that among these five different extracts, the aqueous exhibits highest dissolution of calcium oxalate compared to other extracts. The percentage of dissolution of calcium oxalate by the successive solvent extracts were found to be 2.25 %, 26.48 %, 29.8 %, 21.6 % and 30.58 %, for hexane, acetone, ethanol, ethanol:water and aqueous extracts respectively. Higher percentage indicates more potency in dissolution of calcium oxalate crystals. Under the same experimental conditions, the standard drug Cystone has shown better demineralization (37.67 %) of calcium oxalate, compared to the extracts of *R. aquatica* (figure 4.20).

4.6.4. Estimation of percentage of dissolution of calcium phosphate stones

The percentage of dissolution of calcium phosphate crystals were analyzed by measuring the optical density of phosphomolybdic acid. Here also, the same experimental procedures were followed as mentioned in the previous section.¹⁷

i. Preparation of molybdate-sulphuric acid reagent

Molybdate-sulphuric acid reagent was prepared by 5 % w/v of sodium molybdate solution in H₂SO₄ (prepared by mixing 13 mL of concentrated acid with 80 mL distilled water), and finally, the volume was adjusted to 100 mL with distilled water.

ii. Preparation of reducing solution

1 gm of *p*-phenylene diamine was dissolved in, 3 % w/v of sodium meta-bisulfite solution and the entire system was made up to 100 mL with distilled water.

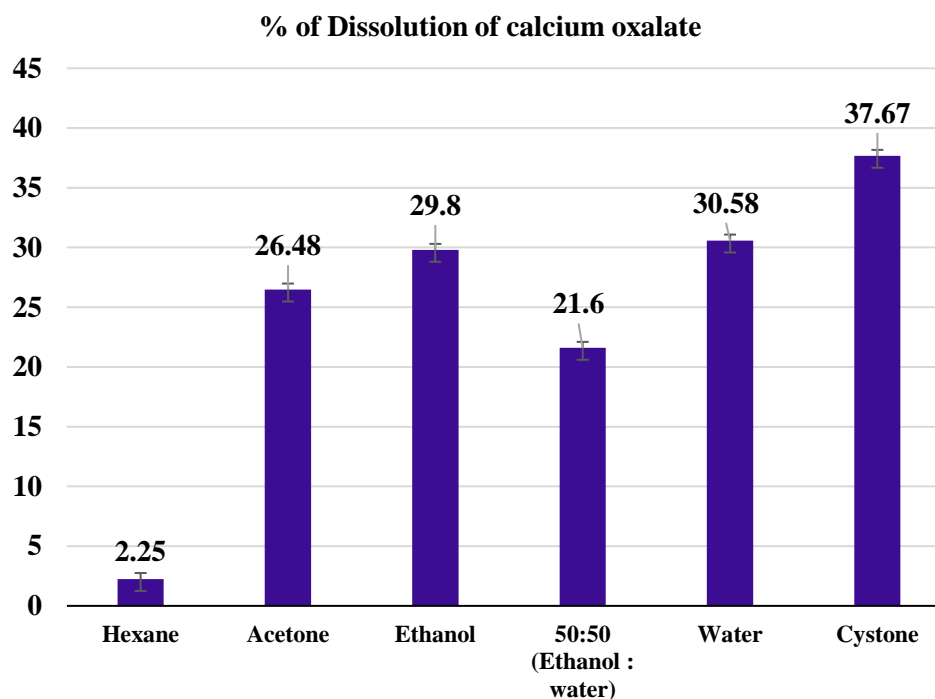


Figure 4.20. % of dissolution of calcium oxalate crystal by extracts

Then, exact 1 mg of calcium phosphate and 10 mg of the extract/compound/standard were packed together in an egg shell semi-permeable membrane by suturing with a thread. All of these were suspended in a conical flask containing 100 mL of 0.1 M TRIS buffer and covered with an aluminum foil. One group served as negative control while other as positive control (1 mg of calcium phosphate and 10 mg of 500 mg tablet of Cystone). All conical flasks were kept in an incubator, preheated to 37 °C for 2 hours, for about 7-8 hours. The entire contents of semi-permeable membrane from each group were then removed into test tubes, individually. Then 4 mL of 1 N H₂SO₄, 3 mL of molybdate-sulphuric acid reagent and 1 mL of reducing solution were added and kept aside for 2 hours. A color change from pinkish violet to colorless was observed after 2 hours. The color change was measured spectrophotometrically at 650 and 700 nm wavelengths. All experiments were performed in triplicates. Concentration of undissolved calcium was determined by the extrapolation of standard calibration curve of calcium phosphate, which is prepared by mixing 200, 400, 600, 800 and 1000 μg of calcium phosphate with 4 mL of 1 N H₂SO₄, 3 mL of molybdate-sulphuric acid reagent and 1 mL of reducing solution. The results of our investigations are given in figure 4.21.

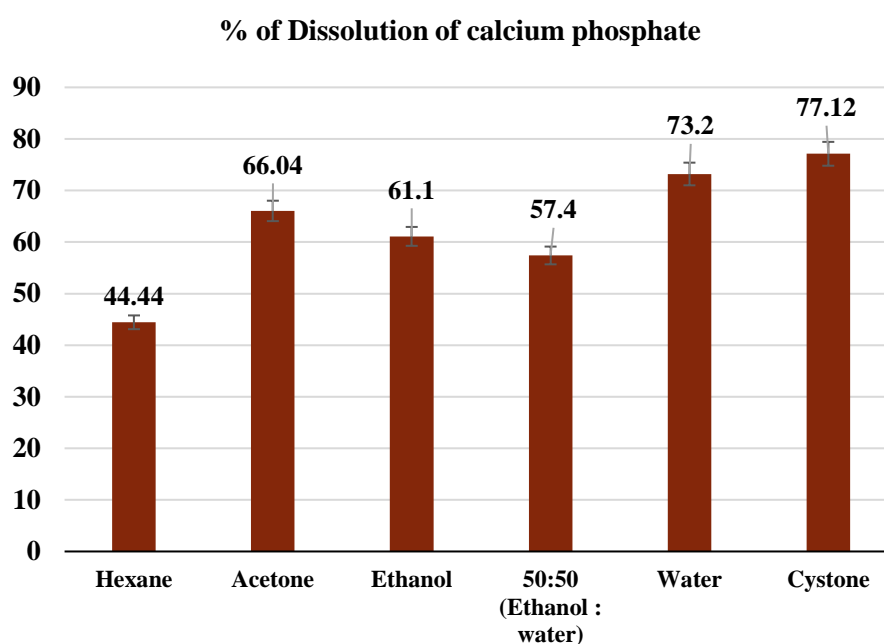


Figure 4.21. % of dissolution of calcium phosphate crystal by extracts

In our studies, the aqueous extract at 10 mg concentration exhibited a higher dissolution of calcium phosphate stones (73.2 %) as compared to other extracts. Here also, as in the previous case, the standard drug Cystone showed the highest dissolution (77.12 %) compared to others. Hence, from our studies, we found that the aqueous extract of *R. aquatica* exhibited the better demineralization property with the calcium stones, compared to others and among these stones, the extract easily dissolves calcium phosphate stones rather than oxalates.

Apart from *R. aquatica*, several other medicinal plant extracts have also been traditionally used for the dissolution of kidney stones till date, which include *Bergenia ligulata*, *Abutilon indicum*, *Biophytum reinwardtii*, *Bryophyllum pinnatum*, *Ocimum tenuiflorum*, *Scoparia dulcis*, *Apium graveolens* and so on (figure 4.22).¹ Among these, *Bryophyllum pinnatum* and *Scoparia dulcis* are the two common plants that used preferably in Kerala, for the management of kidneys stones. The Ayurveda system of medicines also describes the potency of these plants in the breaking up of kidney stones. In this regard we planned to carry out a comparison study of these two plants with *R. aquatica*, to understand their efficiency in dissolving kidney stones.

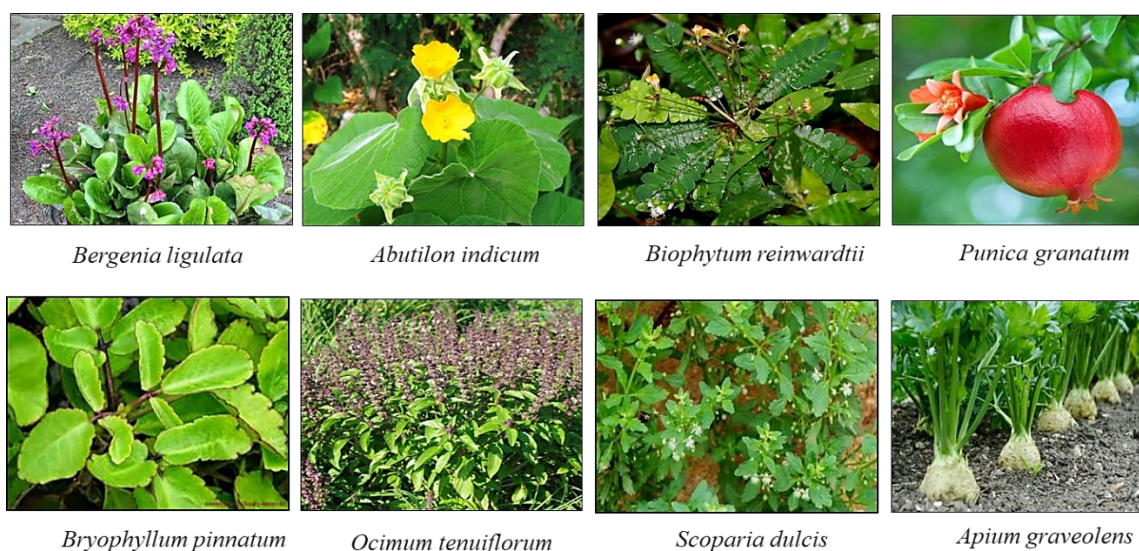


Figure 4.22. Traditionally used antiurolithiatic medicinal plants

4.6.5. Comparison of antiurolithiatic activities of three different medicinal plants

The plant *Bryophyllum pinnatum* belongs to the family Crassulaceae, while *Scoparia dulcis* belongs to Plantaginaceae and, both of them are widely seen in Kerala. In the present study, we mainly focused on the ethanol and water extracts, since these two showed better dissolution properties, in the previous cases. The leaves of *B. pinnatum* were chosen for the present study, while entire plant parts were chosen for *S. dulcis*. In our study we analyzed that, in the case of calcium oxalate stones, the ethanol and aqueous extracts of *S. dulcis* exhibited the highest dissolution (38.48 % and 40.28 %), followed by the aqueous extracts of *B. pinnatum* (31.21 %) and *R. aquatica* (30.56 %) respectively. Here the efficiency of the standard drug (37.33 %) was comparably lesser than *Scoparia dulcis* (figure 4.23). Moving to calcium phosphate studies, here we could see that, among these three plants, the ethanol and water extracts of *R. aquatica* exhibited better dissolution property followed by *Scoparia dulcis* and *Bryophyllum pinnatum* (figure 4.24). Since, the main intention of this work is the exploration of antiurolithiatic properties of medicinal plants, this study revealed the efficacy of three different medicinal plants in the management of kidney stones.

4.7. Conclusion

In the present study, we could successfully isolate and characterize twelve compounds from the roots of *Rotula aquatica* for the first time. In addition to these, we carried out a detailed study on the antiurolithiatic properties of various root extracts the

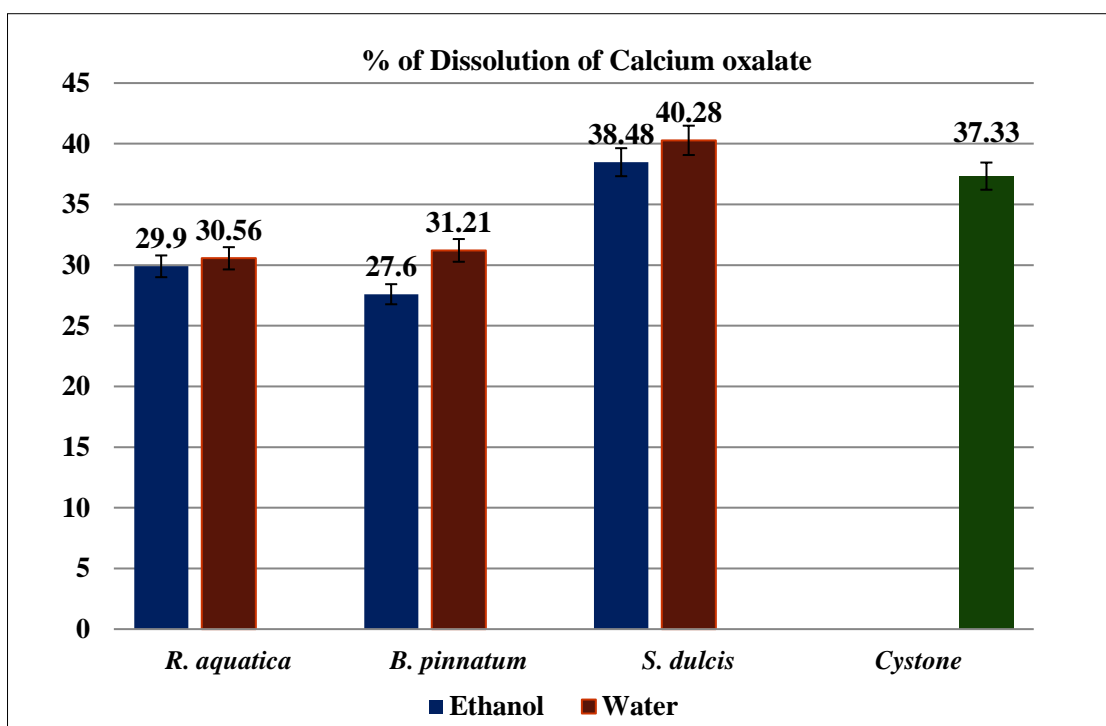


Figure 4.23. Comparison of antiurolithiatic activity of three different plant species against calcium oxalate stones

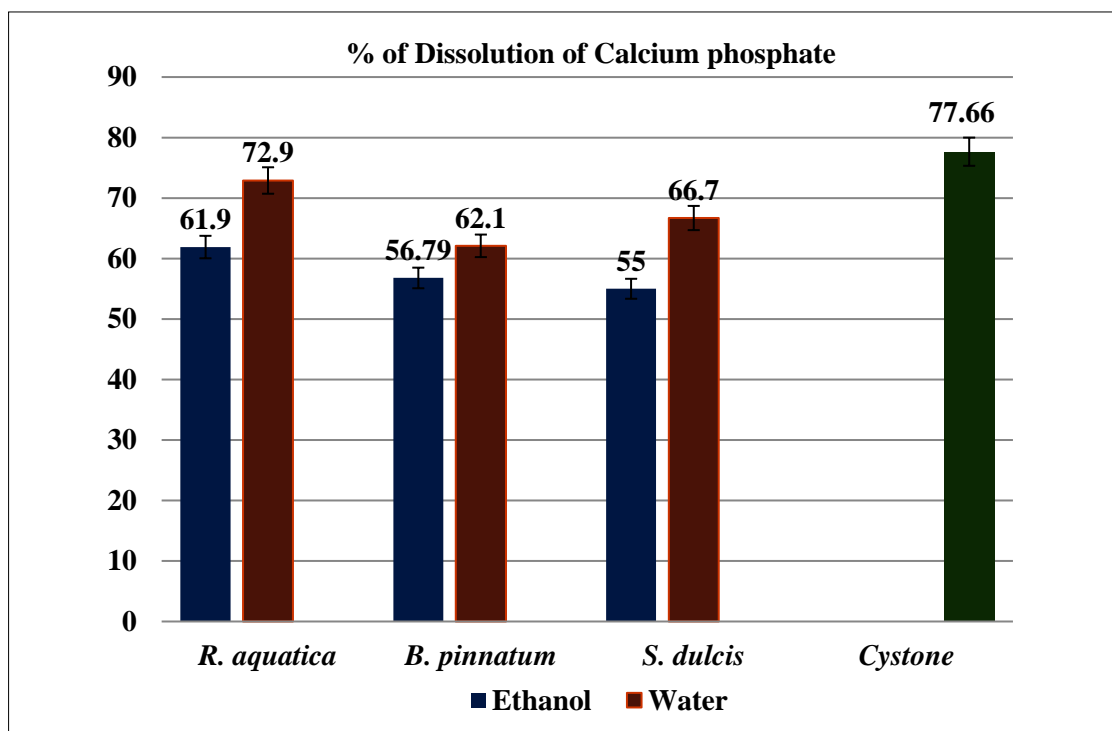


Figure 4.23. Comparison of antiurolithiatic activity of three different plant species against calcium phosphate stones.

same plant and found that the aqueous extract is efficiently dissolved the calcium phosphate stones. Also, we carried out a comparative study between three different plant species and

our results interpreted that among these three species; *Rotula aquatica*, *Bryophyllum pinnatum* and *Scoparia dulcis*, the aqueous extract of *S dulcis* has the highest calcium oxalate dissolution property, while *R. aquatica* exhibited the better activity against calcium phosphate stones. Hence, we can conclude as, a combination of these plants can effectively be used in the treatment of kidney stones.

4.8. Experimental Section

Different analytical techniques were used for the characterization of compounds. The IR spectra were recorded with a Bruker FT-IR spectrometer. The nuclear magnetic resonance spectra (NMR) were recorded on a Bruker AMX 500 spectrophotometer (CDCl₃, CD₃COCD₃, MeOD and DMSO-d₆ as solvents). Chemical shifts for NMR spectra are reported as δ in units of parts per million (ppm) downfield from tetramethylsilane (δ 0.0) and relative to the signal of solvent. Mass spectra were recorded under ESI/HRMS at 60,000 resolution using Thermo Scientific Exactive mass spectrometer and specific rotation was recorded using Jasco P-2000 polarimeter. Shimadzu UV-1800 spectrophotometer was used to measure the absorption maxima.

4.9. Spectral Data

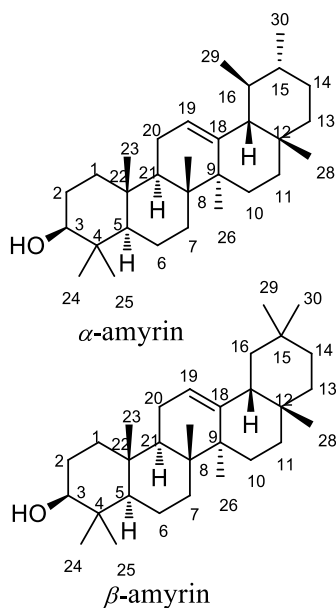
Compounds 43 and 44 (α - and β - amyryns)

Compounds 43 and 44 were obtained as a white waxy substance (14.5 g), in an inseparable form. From the TLC analysis, it was assumed to be a single compound, but when we carried out a detailed NMR studies, we found that it's a mixture of two. Due to the difficulty in the characterization of these compounds (because of the crowded NMR), we went with the GCMS analysis, to get some information about the fragmentation pattern of this molecules in the mass spectra. From the GCMS analysis, we obtained two sharp signals, which on comparison with the library (NIST Wiley library) of the instrument, confirmed the structures of the molecules as α and β -amyryns. The literature reports also well supported the proposed structures.

Molecular formula : C₃₀H₅₀O

FT-IR (Neat) ν_{\max} : 3453, 3367, 2894, 1650 cm⁻¹.

¹H NMR (500 MHz, CDCl₃, TMS) : δ 5.19 (t, J = 3.5 Hz, 1H, β H-19), 5.12 (t, J = 3.5 Hz, 1H, α H-19), 3.22 (dd, J_1 = 10.5 Hz, J_2 = 5.5 Hz, 2H, β H-3 and α H-3), 2.1-1.75 (m, 5H), 1.7-1.40 (m, 19H), 1.39-1.25 (m, 24H), 1.22-0.75 (m, 50H) ppm..



^{13}C NMR (125 MHz, CDCl_3 , TMS) : δ 145.1 (β C-18), 139.6 (α C-18), 124.4 (β C-19), 121.7 (α C-19), 79.1 (β C-3), 79.0 (α C-3), 59.1, 55.2, 48.2, 48.1, 47.7, 47.6, 46.8, 46.3, 41.7, 41.5, 39.7, 39.6, 38.8, 38.5, 36.9, 36.8, 33.8, 32.9, 31.3, 28.8, 28.1, 28.1, 27.3, 26.6, 23.4, 23.3, 21.4, 21.1, 18.4, 17.5, 16.9, 15.7, 15.5, 15.6 ppm.

HRMS (ESI) : m/z Calcd for $\text{C}_{30}\text{H}_{50}\text{ONa}$: 449.3755;
Found: 449.3759.

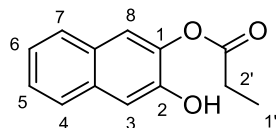
Compound 45 (4 (3-hydroxynaphthalen-2-yl) propionate)

The molecule was pale white solid in nature and is highly UV active. It showed a pink charring which turned to blue while charring the TLC in Enholm yellow staining solution. Detailed analyses of spectral data as well on comparison with literature reports, the molecule was confirmed as 2-hydroxy-4-(4-methoxyphenyl)-1H-phenalen-1-one.

Molecular formula : $\text{C}_{13}\text{H}_{12}\text{O}_3$

FT-IR (Neat) ν_{max} : 3415, 2791, 2111, 1868, 1312 cm^{-1}

^1H NMR (500 MHz, CDCl_3 , TMS) : δ 8.99 (s, 1H), 8.06 (d, $J = 8.5$ Hz, 1H, H-7), 7.54 (s, 1H, H-6), 7.20-7.17 (m, 1H), 6.96-6.93 (m, 2H), 6.54 (s, 1H, H-3), 2.42 (q, $J = 7.5$ Hz, 2H, H-2'), 1.23 (t, $J = 7.5$ Hz, 3H, H-1') ppm.



^{13}C NMR (125 MHz, CDCl_3 , TMS) : δ 170.2 (CO), 155.6 (C-2), 138.9 (C-1), 130.8, 130.0, 120.8, 120.0, 115.4, 105.2, 18.3 (C-2'), 11.4 (C-1') ppm

HRMS (ESI) : m/z Calcd for $\text{C}_{13}\text{H}_{12}\text{O}_3$: 217.0856;
Found : 217.0865.

Compound 47 (piperine)

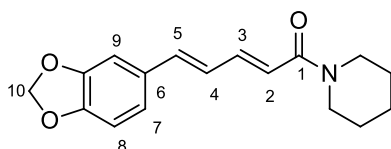
Compound 47 was a pale yellow colored solid, which showed deep orange red color with Dragendorff reagent, confirmed the presence of an alkaloid moiety. On comparison of the spectral data of this molecule with literature reports, the molecule was confirmed as piperine.

Molecular formula : C₁₇H₁₉NO₃

Mp: 127-372 °C

FT-IR (Neat) ν_{\max} : 3334, 3070, 2900, 1690 cm⁻¹

¹H NMR (500 MHz, CDCl₃, TMS) : δ 7.46 (dd, $J_1 = 14.5$ Hz, $J_2 = 10$ Hz, 1H), 7.00 (d, $J = 1.5$ Hz, 1H), 6.91 (dd, $J_1 = 8$ Hz, $J_2 = 1.5$ Hz, 1H), δ 6.81-6.75 (m, 3H), 6.44 (d, $J = 14.5$ Hz, 1H), 5.99 (s, 2H C-10), 3.61 (t, $J = 5$ Hz, 4H), 1.69-1.68 (m, 2H), 1.62-1.60 (m, 4H) ppm.



¹³C NMR (125 MHz, CDCl₃, TMS) : δ 165.6 (C-1), 148.2, 143.2, 143.1, 138.1, 131, 125.3, 125.6, 119.6, 108.5, 105.7, 105.7, 101.3, 45.2, 26.2, 24.6 ppm.

HRMS (ESI): m/z Calcd for C₁₇H₂₀NO₃; Found: 286.1433.

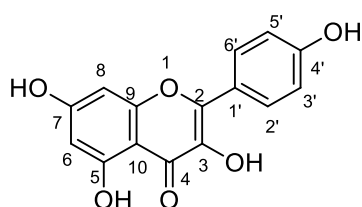
Compound 48 (kaempferol)

Compound **48** was isolated as a yellow solid. Using various spectroscopic techniques and literature reports, the compound was identified as the flavanone, kaempferol.

Molecular formula : C₁₅H₁₀O₆

FT-IR (Neat) ν_{\max} : 3326, 1668 cm⁻¹

¹H NMR (500 MHz, CD₃COCD₃, TMS) : δ 12.0 (s, 1H, C-5 OH), 8.19 (d, $J = 8.5$ Hz, 2H, H-2' and H-6'), 7.10 (d, $J = 9$ Hz, 2H, H-3' and H-5'), 6.53 (d, $J = 2$ Hz, 1H, H-8), 6.34 (d, $J = 2$ Hz, 1H, H-6) ppm.



¹³C NMR (125 MHz, CD₃COCD₃, TMS) : δ 181.5 (C-4), 163.1, 160.7, 160.2, 157.6, 146.1, 135.4, 129.2, 120.9, 115.6, 99.8, 96.3, 95.8 ppm.

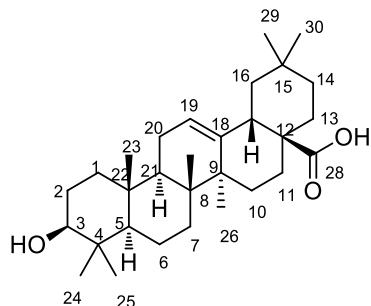
HRMS (ESI): m/z Calcd for C₁₅H₁₀O₆Na: 309.0371; Found : 309.0375.

Compound 50 (oleanolic acid)

Compound **50** was isolated from fraction pool 8 as colorless powder (12 mg), with UV activity. The compound was confirmed as **oleanolic acid** based on its spectral data and literature reports.

Molecular formula : C₃₀H₄₈O₃

Mp : 300-310 °C



FT-IR (Neat) ν_{\max} : 3449, 2945, 2866, 1701, 1460 cm^{-1}

^1H NMR (500 MHz, CDCl_3 , TMS) : δ 5.28 (t, $J = 3$ Hz, 1H, H-19), 3.22 (dd, $J_1 = 11$ Hz, $J_2 = 5$ Hz, 1H, H-5), 2.83-2.80 (dd, $J_1 = 10$ Hz, $J_2 = 4$ Hz, 1H 1H) 2.01-1.86, 1.79-1.59, 1.53-1.35, 1.34-1.20, 1.16-.06 (as multiplets, 30H), 0.98 (s, 3H), 0.92 (s, 3H), 0.91-0.90 (m, 6H), 0.77-0.72 (m, 6H) ppm.

^{13}C NMR (125 MHz, CDCl_3 , TMS) : δ 183.1 (C-28), 143.5 (C-18), 122.6 (C-19), 79.0 (C-3), 55.2, 47.6, 46.5, 45.8, 41.6, 41.0, 39.2, 38.7, 38.4, 37.1, 33.8, 33.1, 32.6, 32.4, 30.7, 28.7, 28.1, 27.6, 27.2, 25.9, 23.5, 23.4, 22.9, 18.3, 17.1, 15.5, 15.3 ppm.

HRMS (ESI) : m/z Calcd for $\text{C}_{30}\text{H}_{48}\text{O}_3\text{Na}$: 479.3503; Found : 479.3501.

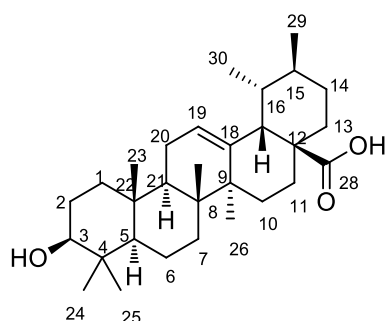
Compound 51 (ursolic acid)

Compound **51** was also isolated from fraction pool 8 as a colorless solid (11 mg), having almost same characteristics with that of compound **50**. After the careful analysis and in comparison with literature reports, the compound was confirmed as ursolic acid.

Molecular formula : $\text{C}_{30}\text{H}_{48}\text{O}_3$

Mp : 195-198 $^\circ\text{C}$

FT-IR (Neat) ν_{\max} : 3437, 3240, 3021, 2555, 1646, 1623 cm^{-1}



^1H NMR (500 MHz, CDCl_3 , TMS) : δ 5.19 (t, $J = 3$ Hz, 1H, H-19), 3.14 (dd, $J_1 = 11$ Hz, $J_2 = 5$ Hz, 1H, H-3), 2.73 (dd, $J_1 = 10$ Hz, $J_2 = 4$ Hz, 1H) 1.79-1.53, 1.52- 1.37, 1.22-1.13, 1.07-1.06 (as multiplets, 30 H), 0.98 (s, 3H), 0.90(s, 6H), 0.82 (s, 3H), 0.69-0.66 (m, 6H) ppm

^{13}C NMR (125 MHz, CDCl_3 , TMS) : δ 180.65 (C-28), 138.67 (C-18), 124.86 (C-19), 76.7 (C-3), 52.88, 45.3, 44.2, 39.3, 38.6, 36.9, 36.4, 34.7, 30.7, 30.3, 28.3, 25.8, 23.6, 21.3, 21.1, 14.8, 13.2, 13.0 ppm.

HRMS (ESI): m/z Calcd for $\text{C}_{30}\text{H}_{48}\text{O}_3\text{Na}$: 479.3506; Found: 479.3501.

4.10. References

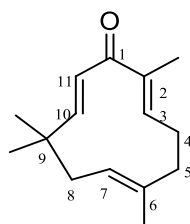
1. (a) R. E. Schultes, **1992**. Ethnobotany and Technology in Northwest Amazon: A partnership in Sustainable harvest and marketing of rain forest products. Edited by M. J. Plotkin & L. M. Famolare. Island Press, Washington, DC, pp 7-13, 45-76. (b) M. J. Balick, **1996**. Annals of the Missouri botanical garden. Volume 4. Missouri Botanical garden, pp 57-65. (c) M. R. Robinson and Zhang, **2011**. World Health Organization, Geneva. (d) P. A. Cox and J. B. Michael, *Scientific American*, **1994**, 270 (6), 82-87.
2. (a) B. Abhishek and S. Avinash, *Indian Journal of Pharmaceutical & Biological Research*. **2013**, 1(1), 63-68. (b) A. R. Ashwini, S. Sudha, S. Subrata, S. P. Nancy and D. B. V. Ashok, *Fitoterapia*, **2008**, 79, 544 -547. (c) C. K. Chauhan, M. J. Joshi and A. D. B. Vaidya, *Indian J. Biochem. Biophys.*, **2011**, 48, 202-207. (d) A J. Christina, M. M. Priya and P. Moorthy, *Methods find. Exp. Clin. pharmacol.*, **2002**, 24(6), 357-359. (e) U. K. Gilhotra and A. J. M. Christina, *Int. J. drug dev. Res.*, **2011**, 3(1): 273-280. (f) K. Mamta, B. Abhishek and Rohit, *International Journal of Pharma and Biosciences*, **2010**, 1(2), 1-4. (g) S. Patil, C. I. Jolly and S. Narayanan, *Indian J. Exp. Biol.*, **2004**, 42, 893-899. (h) G. Mukhopadhyaya, **1929**. History of Indian Medicine. Calcutta University Press, Calcutta: p. 32. (i) G. Pandey, **2001**. Dravyaguna vijana. (Materia medica, Vegetable drugs). Krishnadas academy. Oriental publishers and distributors. Varanasi. Vol. I, II & III. (j) S. N. Venugopal, **2009**. Herbal stone Crushers: The Pashanabheda. ENVIS Newsletter on Medicinal plants. 1 (2 & 3), 7.
3. (a) J. E. Howard, W. C. Thomas, L. M. Barker, L. H. Smith and C. L. Wadkins, *Johns Hopkins Med. J.*, **1967**, 120, 119-126. (b) W. H. Boyce and J. S. King, Jr. *Ann. N. Y. Acad. Sci.*, **1963**, 104, 563-572. (c) C. W. Vermeulenand and E. S. Lyon, *Amer. J. Med.*, **1963**, 45, 684-689.
4. (a) R. Bartoletti, T. Cai, N. Mondaini, F. Melone, F. Travaglini and M. Carini, *Urol Int.*, **2007**, 79 (suppl 1), 3-7. (b) Tribuneindia sensus, <http://www.Tribuneindia.com/2000/Nov.,2000>.
5. (a) T. C. Ngo and D. G. Assimios, *Rev Urol.*, **2007**, 9, 17-27. (b) D. M. Coll, M. J. Varanelli and R. C. Smith, *Am. J. Roentgenol.*, **2002**, 178, 101-103.
6. G. Eknayan, *Clin. Rev. Bone Min. Metab.*, **2004**, 2, 177-185.
7. (a) D. Mattle and B. Hess, *Urol Res.*, **2005**, 33, 73-79. (b) O. W. Moe, *Lancet*, **2006**, 367, 333-344.
8. T. Knoll, *Eur Urol Suppl.*, **2007**, 6, 717-722.

9. J. Silberstein, C. M. Lakin and P. J. Kellogg, *Rev Urol.*, **2008**, *10*, 236-241.
10. (a) S. Park and M. S. Pearle, *Urol. Clin. North Am.*, **2007**, *34*, 323-334. (b) <https://www.mayoclinic.org/diseases-conditions/kidney-stones/symptoms-causes/syc-20355755>.
11. (a) J. L Powers and W. E. Powers, *J. Am. Pharm. Assoc.*, **1940**, *29*, 175-178. (b) N. N. Okoye, D. L. Ajaghaku, H. N. Okeke, E. E. Ilodigwe, C. S. Nworu and F. B. Okoye, *Pharm Biol.*, **2014**, *52*(11), 1478-1486.
12. K. Takahiro, K. Noriyuki, K. Kenichi, K. Takeshi, I. Hiroshi, T. Kazunori, **2000** JP 2000-372088, Sony Corp., Japan.
13. K. C. Saha, H. P. Seal and M. A. Noor, *J. Bangladesh Agril. Univ.*, **2013**, *11*(1), 11-16.
14. B. L. Williams and S. H. Wender, *J. Am. Chem. Soc.*, **1952**, *74* (23), 5919-5920.
15. S. Kamatham, N. Kumar and P. Gudipalli, *Toxicology Reports*, **2015**, *2*, 520-529.
16. M. A. Hossain and Z. Ismail, *Arabian Journal of Chemistry*, **2013**, *6*(3), 295-298.
17. (a) A. B. Shukla, D. R. Mandavi, M. J. Barvaliya, S. Baxi and C. R. Tripathi, *AJP*, **2014**, *4*, 151-159. (b) U. Atodariya, R. Barad, S. Upadhyay and U. Upadhyay, *Journal of Pharmacognosy and Phytochemistry*, **2013**, *2*, 209-213. (c) V. V. Byahatti, K. V. Pai and Marina G. D'Souza, *Ancient Science of Life*, **2010**, *3*, 14-17. (d) P. Prashanthi, S. Anitha and S. Shashidhara, *International Journal of Pharmacognosy and Phytochemical Research*, **2015**, *7*(6), 1142-1146. (e) R. S. Phatak and A. S. Hendre, *International Journal of Pharmacognosy and Phytochemical Research*, **2015**, *7*(2), 275-279.

Synthesis and Biological Evaluation of Novel Zerumbone Pendant and [11.3] Fused Zerumbone Derivatives

5.1. Introduction

Natural products, especially plant-derived compounds occupy a proficient position in the development of numerous useful drugs. Diversity-oriented synthesis has been used successfully for the generation of biologically relevant or drug-like molecules *via* simple chemical transformation of readily available natural products.¹ For the past few decades, there has been a surge in the development of new plant-derived medicines² and in this line, the family *Zingiberaceae* has attained much attention from the scientific community, because of its unusual biological properties.³ While considering the molecules isolated from *Z. nimmonii*, we were highly fascinated by the compound **38** from fraction pool 2, called zerumbone. It is a monocyclic sesquiterpene, having three double bonds; two are as part of a cross conjugated dienone moiety and one as an isolated double bond. This molecule is considered as the major constituent of rhizome extract of *Zingiber zerumbet* Smith, another species belonging to the same genera *Zingiber*. This ginger plant is widespread in Southeast Asia, India and Okinawa and is used as a spice, and also used in ethnomedicines. From the literature survey, it was revealed that the molecule zerumbone shows potent pharmacological activities, and the rhizome oils of *Z. zerumbet* contains about eighty percent of zerumbone, which can be easily obtained by simple column chromatography, steam distillation or recrystallization techniques.⁴ So, as a continuation of our ongoing work on ‘the synthesis of bio-actives from affordable and readily available natural sources’, we were interested in the structural modification of zerumbone, the marker compound present in *Z. zerumbet*.



Zerumbone (**1**)

Numerous researches have been carried out in *Z. zerumbet* since 1944, and this plant serves as a very potent and reliable drug candidate for various diseases. They have been

explored for its prospects of effectiveness against number of activities in *in vitro* as well as *in vivo* models; and for mechanisms that may involve in chemo preventive measures and in several pharmaceutical studies. Zerumbone (**1** (2*E*,6*E*,10*E*)-2,6,9,9-tetramethylcycloundeca-2,6,10-trienone) was first isolated by Dev *et al.* in 1960, and later the structure was elucidated in 1965 using NMR and X- ray spectroscopy. The molecule can be easily isolated from the rhizome by simple steam distillation in a yield of more than 4 % of the dry rhizome.⁴

Zingiber zerumbet is used as an anti-inflammatory agent in folk medicine in Indonesia and is a potent inhibitor of 12-*O*-tetradecanoyl-13-acetate-induced Epstein Barr Virus.⁵ In 1987, Elliot and Brimacombe reported that zerumbone possesses anti-inflammatory property, and is especially useful in treating ulcerative colitis, which is an inflammatory bowel disease.⁶ The studies of zerumbone on the expression of pro-inflammatory genes in human colon adenocarcinoma cell lines, Caco-2, Colo320DM, and HT-29, with reverse transcription-polymerase chain reaction (RT-PCR) assays reported that zerumbone markedly induces the expression of interleukin (IL)-1a, IL-1b, IL-6, and tumor necrosis factor (TNF)-a in each cell line in concentration- and time-dependent manners. Recent researches on this molecule have demonstrated that zerumbone is a potential drug for the treatment of several cancers as well as leukemia.⁷ Zerumbone suppressed the activation of NF-KB and NF-KB regulated gene expression induced by carcinogens, and it is reported that this inhibition may deliver molecular basis for the prevention and treatment of cancer. The cytotoxic effect of zerumbone on leukemia cells was found to be mediated through the induction of Fas receptors and the histological examination revealed that pretreatment(s) with zerumbone suppressed leukocyte infiltration and reduced proliferating cell nuclear antigen-labeling indices. Also, zerumbone is a promising and rational agent for the prevention of skin cancers, whereas its oral activity to prevent skin cancers and issues of metabolism and absorption remain to be addressed. Zerumbone is reported to stimulate the neoplastic cell death through the mitochondrial pathway of apoptosis. Zerumbone inhibited the growth of human colon cancer (HT-29) and human leukemia cell lines (HL-60 cell) in *in vitro*. Furthermost studies pointed that, the α,β -unsaturated carbonyl group in zerumbone is the likely source of most of the effects.⁸

In 2002, Murakami *et al.* reported that zerumbone is able to suppress the formation of free radicals (superoxide anion) from NADPH oxidase xanthine oxidase, expression of iNOS (inducible nitric oxide synthase) and COX (cyclo-oxygenase)-2 as well as release of TNF- α .⁹ Later in 2009, Ibrahim *et al.* reported the defensive effect of zerumbone in

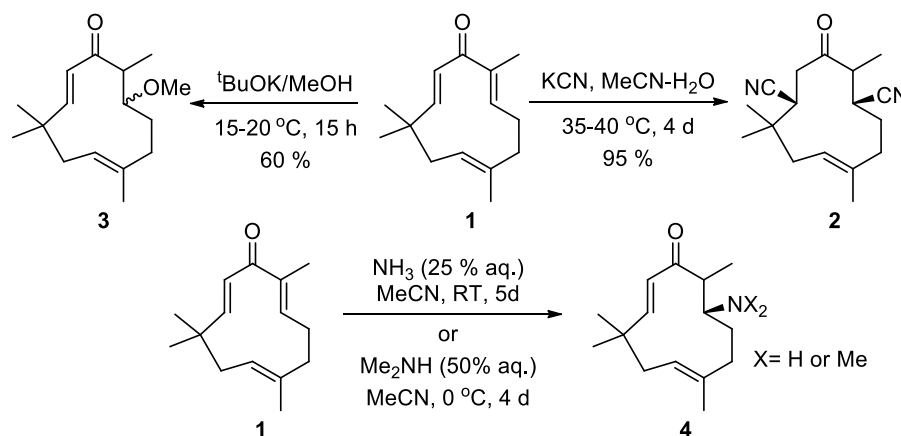
cisplatin-induced liver dysfunction and organ damage in rats *via* prevention of lipid peroxidation and preservation of the anti-oxidant glutathione.¹⁰ The curative effect of zerumbone in a dose-dependent manner on the osteoarthritic knee joints were reported in 2010 and the studies revealed that oral administration of zerumbone in a dose of 2 mL/kg. Wt. of 0.4 % w/v diluted with corn oil for a period of 4 weeks had some chondroprotective effects on the knee osteoarthritis of the Sprague–Dawley rats.^{11,12}

From above all, it becomes more evident that, zerumbone is a potential bioactive that may bring numerous opportunities and prospects in various pharmaceutical studies. Apart from these, zerumbone has powerful latent reactivity, and among the three double bonds C-2 is the most active and less hindered double bond, being farthest from the gem disubstituted methyl groups at C-9 position. Also, the X-ray structure reveals that the dienone system lies in a distorted plane, perpendicular to that of the isolated double bond. The group of Kitayama built a foundation for the extensive use of zerumbone, by establishing novel methods for the functionalization of zerumbone that include conjugate addition reaction, ring expansion and ring cleavage reactions, transannular reactions and asymmetric induction. Recently, we also succeeded in the synthesis of novel zerumbone derivatives, which showed potent antidiabetic and antiproliferative properties. Some of the important works on zerumbone has been listed below.

5.2. Attractive Reactivity of Zerumbone

5.2.1. Conjugate addition reactions

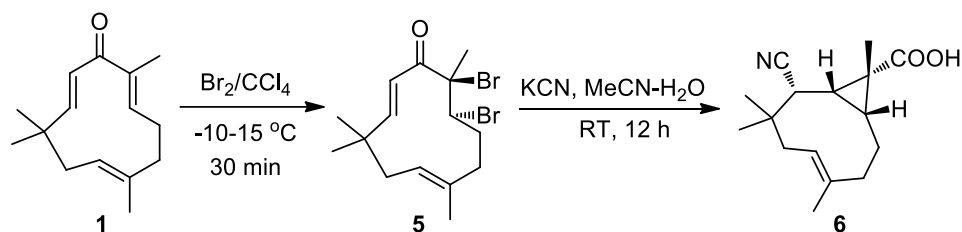
The introduction of additional functionalities on zerumbone can easily be achieved by simple conjugate addition reaction with various nucleophiles, and many such derivatives have been synthesized by Kitayama *et al.* in moderate to high yield, with regio and stereo selectivity (scheme 5.1).¹³⁻¹⁵



Scheme 5.1

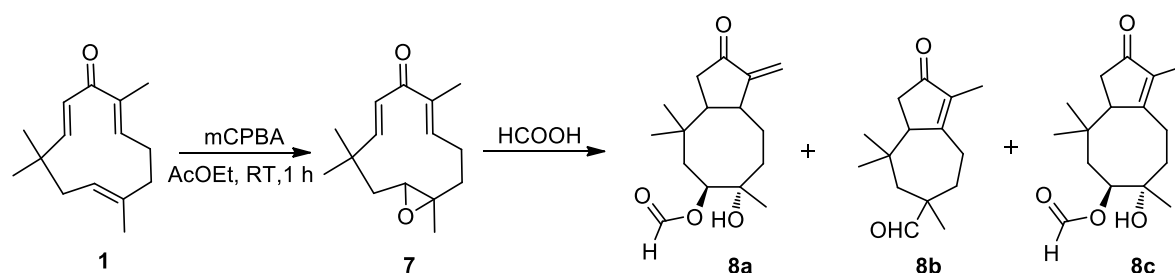
5.2.2. Transannular reactions

A double Favorskii rearrangement or a unique transannular reaction of zerumbone was also reported by the same group in 1999 (scheme 5.2). They also succeeded in the generation of two cyclopropane rings, when 6,7-epoxyzerumbone (zerumbone epoxide) is used instead of zerumbone.¹⁶



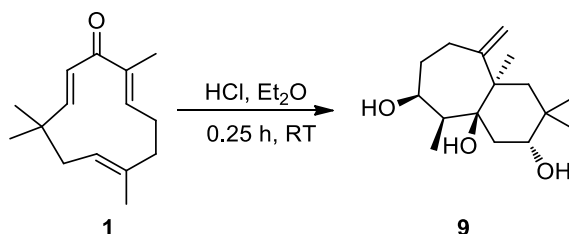
Scheme 5.2

Other reactions include, the synthesis of rare bicyclo[6.3.0] and [5.3.0] decane skeletons *via* reaction of zerumbone with formic acid (resulted in the formation of three compounds), as shown in scheme 5.3.¹⁷



Scheme 5.3

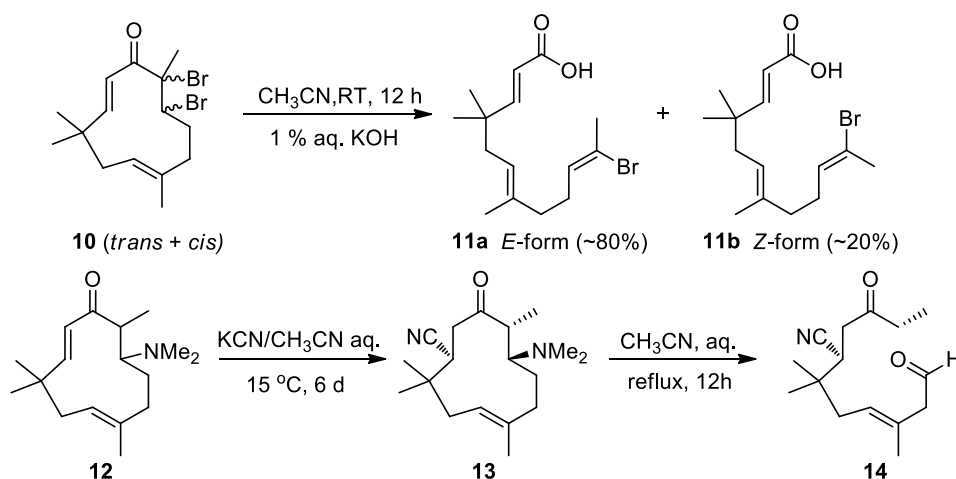
The acid catalyzed transannular cyclisation of zerumbone between C-1 and C-7 leading to bicyclo[5.4.0]undecane skeletons were reported by Chhabra and co-workers in 1985 (scheme 5.4). Followed by these, Luu *et al.* reported the Nazarov-type cyclization between C-3 and C-10 of 6,7-epoxyzerumbone **7** (zerumbone can be easily converted into its epoxide using peroxybenzoic acids) that afforded bicyclo[6.3.0]undecane and bicyclo[5.3.0]decane skeletons.¹⁸



Scheme 5.4

5.2.3. Ring cleavage reactions

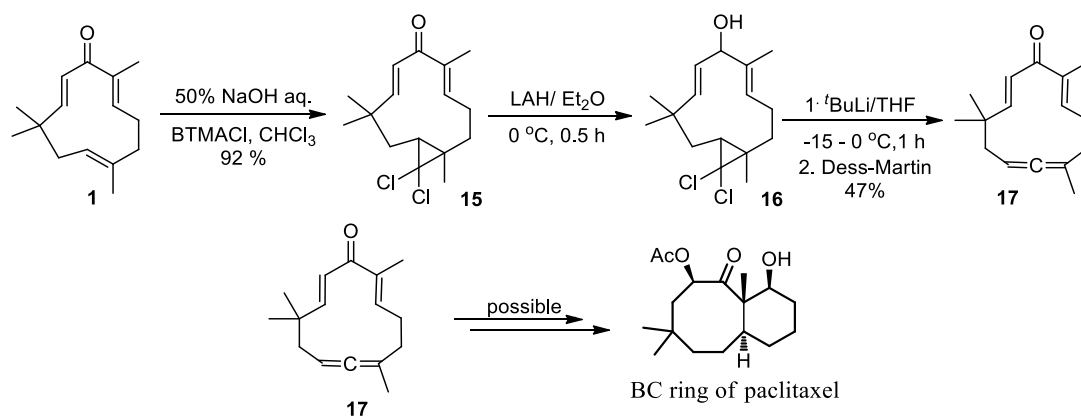
The regioselective cleavage of eleven membered zerumbone ring between the positions C1-C2 and C2-C3, were accomplished by Kitayama *et al.* in 2001 and 2003 respectively. In their studies, the reaction of zerumbone dibromide or epoxyzerumbone dibromide with aqueous KOH resulted in the cleavage of the ring at the positions C1-C2, *via* nucleophilic addition to the double bond followed by a Favorskii rearrangement. While the cleavage of the bonds at C2-C3 position was accomplished by retro-Mannich reaction, with cyanide as the nucleophile (scheme 5.5).^{15,16}



Scheme 5.5

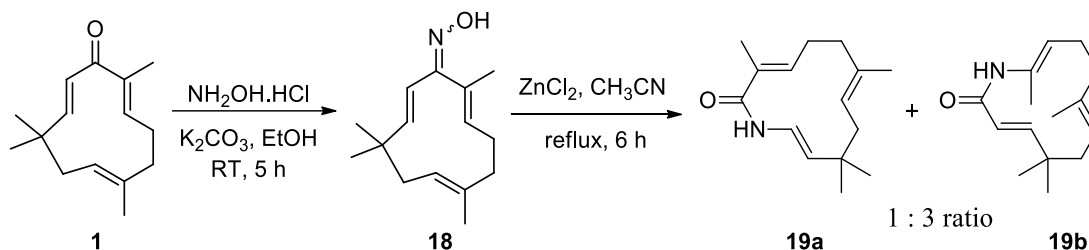
5.2.4. Ring expansion reactions

The ring expansion of zerumbone to a 12-membered ring was also studied by the group of Kitayama, in 2006. They achieved the desired product through Doering-LaFlamme allene synthesis method, with an extensive study on the ring opening or the ring closure properties of zerumbone. The work also suggests that, if the ring expansion of the 12-membered ring system is established with the maintaining of double conjugated system, then the synthesis of paclitaxel may become a reality as depicted in scheme 5.6.¹⁹



Scheme 5.6

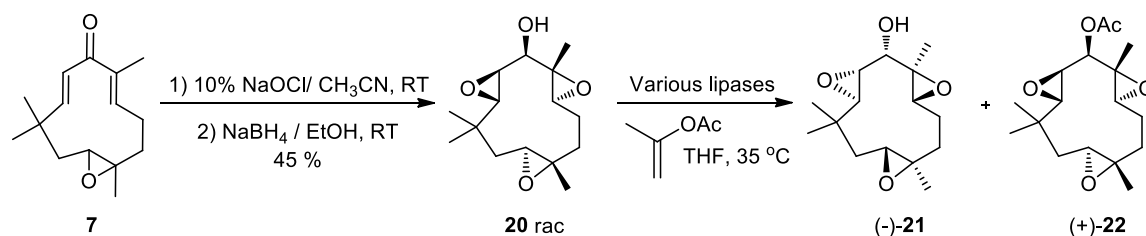
Very recently, Bettadaiah *et al.* reported a facile synthesis of two new analogues of zerumbone with an amide moiety in a 12 membered ring system (scheme 5.7). They synthesized these azazerumbones *via* Beckmann rearrangement of zerumbone-oxime, and the products exhibited better anti-bacterial and antimutagenic activity than zerumbone.²⁰



Scheme 5.7

5.2.5. Epoxidation reactions

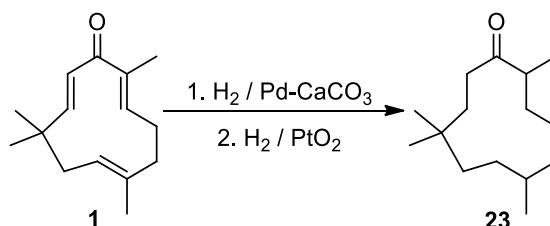
Optically active triepoxyzerumbol(-)-**21** and its acetate (+)-**22** were synthesized by lipase-catalyzed enantioselective transesterification of racemic **20** by the group of Kitayama. Under the optimized conditions, a lipase from *Alcaligenes* sp. (Meito QL) catalyzed the reaction of racemic **20** with isopropenyl acetate in THF at 35 °C to afford (1S)-**21** and (1R)-**22** with an *e*-value of 79. They also determined the absolute configuration of (1R)-**22** by single crystal X-ray diffraction techniques (scheme 5.8).²¹



Scheme 5.8

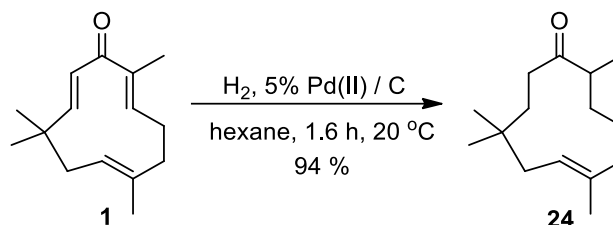
5.2.6. Reduction reactions

In 1960, Dev and co-workers reported the first reduction reaction of zerumbone, and they successfully synthesized the hexahydrozerumbone **23** in a two-step reaction pathway using hydrogen gas (as hydrogen source) and Lindlar's catalyst along with platinum(IV)oxide as the catalysts (scheme 5.9).²²



Scheme 5.9

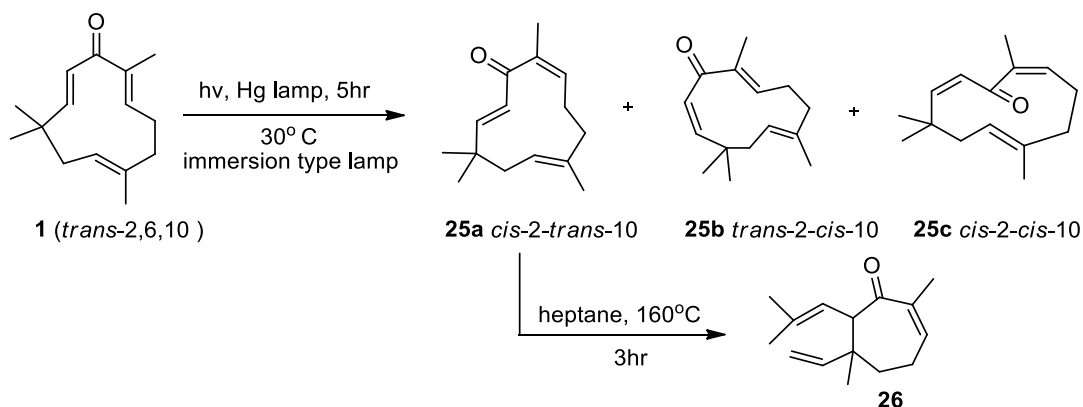
Later in 2010, Kitayama *et al.* demonstrated a regioselective reduction of zerumbone into tetrahydrozerumbone **24**, instead of hexahydrozerumbone **23**. Here, the isolated double bond remained as such, while the two double bonds of dienone moiety got reduced (scheme 5.10).²³



Scheme 5.10

5.2.7. Photochemical reactions

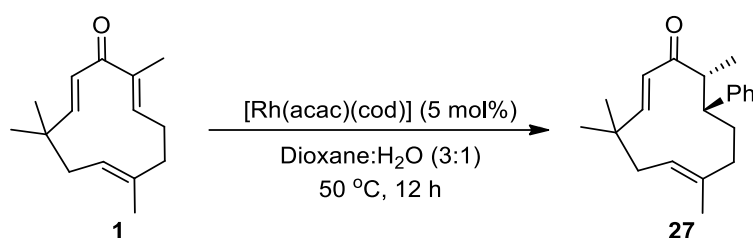
The photochemical characteristics of zerumbone ring were first described in 1967 by Dev *et al.* They also explored the thermochemical aspects of each of the products that were formed during the photochemical reaction (scheme 5.11).²⁴



Scheme 5.11

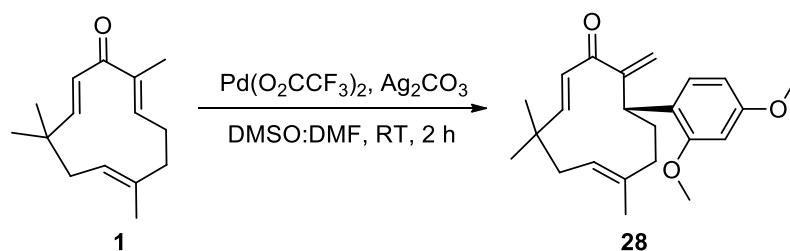
5.2.8. Our expertise in the field of zerumbone

In 2013, we have developed a straightforward, catalytic and general method for the synthesis of novel zerumbone derivatives, *via* rhodium (I)-catalyzed 1,4-conjugate addition reaction using various boronic acids (scheme 5.12). The addition across the enone moiety of zerumbone took place in a regio- and diastereoselective manner. We have evaluated the anti-microbial and α -glucosidase inhibitory potential of the newly synthesized molecules under *in vitro* conditions. Unfortunately, the derivatives did not show any promising inhibitory activity as compared to zerumbone. However, analysis of the newly synthesized molecules against other targets, as well as the exploration of its synthetic utility are under way in our laboratory.²⁵



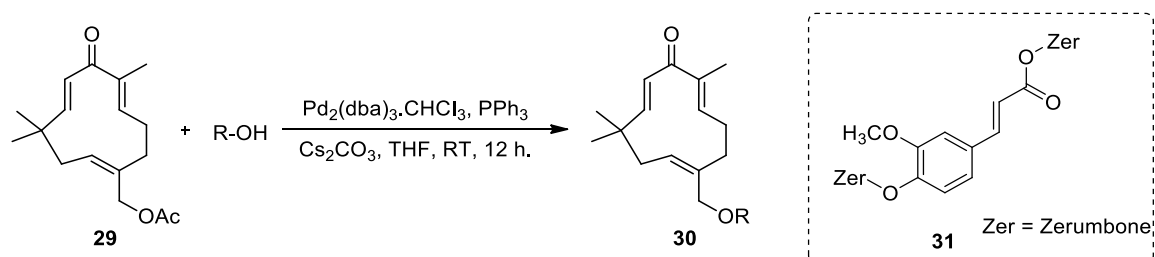
Scheme 5.12

Later in 2014, we developed a regio- and stereoselective palladium catalysed decarboxylative coupling of arene carboxylic acids with zerumbone for the first time (scheme 5.13). This straightforward synthetic route was successful in repositioning the rigid endocyclic double bond of the parent molecule, zerumbone and provided a class of molecules having an exocyclic double bond with a new dienone system. Also in the preliminary *in vitro* α -glucosidase inhibition assays, all the compounds exhibited potent inhibitory activity, compared to the zerumbone and the standard drug, acarbose.²⁶



Scheme 5.13

Very recently, we have utilized the palladium catalyzed Tsuji-Trost coupling of phenols and arene carboxylic acids with zerumbone ester **29** to provide a new class of zerumbone pendant derivatives (ZPD). The preliminary *in vitro* α -glucosidase, α -amylase and glycation inhibition studies revealed that all the compounds show potent activity than zerumbone (scheme 5.14). These zerumbone pendant derivatives were also tested for their cytotoxicity against some selected human cancer cells and among them compound **31** showed significant anti-proliferative effects.²⁷



Scheme 5.14

Hence we carried out a detailed study of **31** towards the induced morphological changes in HeLa cells. The derivative promoted DNA fragmentation, phosphatidyl serine translocation, increased activity of caspase 3, up-regulation of expression of Bax, cleaved PARP, cleaved caspase 3 and down-regulation of anti-apoptotic protein Bcl-2, which confirmed the programmed cell death in HeLa cells. **31** also suppressed cell migratory effects by decreasing migration of HeLa cells, decreasing the production of MMP-2,-9 and downregulation of expression of MMPs and VEGF. Taken together, our studies indicated that ZPD is a promising candidate, as a potent inducer of cytotoxicity, apoptosis and anti-migratory effects. Further structural modifications of zerumbone and its molecular mechanisms are still underway.²⁸

We also examined the cytotoxic potential of zerumbone in SW480 cells, and found that zerumbone could damage cell membrane integrity, DNA fragmentation, alter the mitochondrial membrane potential ($\Delta\Psi_m$), and induce extrinsic and intrinsic apoptotic pathways. It was also noticed that the antiproliferative potential of zerumbone was accompanied by a decrease in antioxidant status along with a corresponding increase in ROS level in SW480 cells. In addition, our study also demonstrated that zerumbone could arrest the cell cycle at the G2 or M phase, exert severe collapse of the cellular microfilament network, and inhibit *in vitro* cell migration.²⁹

The reports on zerumbone (**1**) show that the biological properties of this molecule are mainly due to the presence of the dienone system. Hence, we planned to improve the biological properties of this molecules by coupling with suitable bio-active cores, without making any changes to this dienone system. While checking the literature reports, we were attracted by the sulfonamide entities, the active group present in many modern drugs. They are an important class of compounds having a versatile role in the pharmaceutical industry and are widely used in the trade name sulfa drugs, for various syndromes due to their anti-viral, anti-inflammatory, carbonic anhydrase inhibitory and anti-cancer properties. They are the first chemotherapeutic agent successfully used to treat general infections, and are widespread in many naturally existing molecules having potent biological properties.

5.3. Sulfonamides

Sulfonamide drugs were the first class of antibiotics to be used systemically, and paved the way for the antibiotic revolution in medicine. Prontosil, the first sulfonamide, was a prodrug, which is metabolized to active form with in the body (figure 5.1). Today, they are widely used as antimicrobial agents, chiefly because of their low toxicity, low cost

and excellent activity against bacterial diseases. Over the course of time, the application of sulfonamides has been extended from their use as antimicrobial agents to anticancer agents, inhibitors of gamma-secretase, antiglaucoma agents, hypoglycemic agents, anticonvulsant agents, cyclooxygenase-2 and lipoxygenase. Clinical treatment with sulfonamides has regained confidence with the use of a combination of sulfamethoxazole and trimethoprim to treat urinary tract bacterial infections (figure 5.1). These drugs work by inhibiting a specific enzyme called dihydropteroate synthase (DHPS), which is critical for the synthesis of folate (vitamin B9), an essential nutrient present in every organism. Mammals get folate from their diet, but bacteria must synthesize this vitamin on their own. Since folate synthesis requires a chemical reaction between two molecules, 6-hydroxymethyl-7,8-dihydropterin-pyrophosphate (DHPP) and *p*-aminobenzoic acid PABA, that is catalyzed by DHPS; the inhibition of DHPS leads to the inhibition of bacterial growth and is the active principle in sulfa drugs.³⁰⁻³³

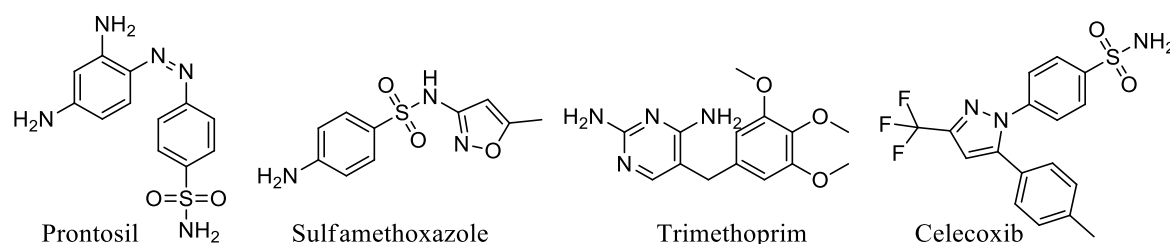


Figure 5.1. Examples for sulfa-drugs

For the last two decades, drug resistance has led to a decrease in the clinical utility of virtually all marketed antibacterial agents, and this created a challenge in the synthesis or identification of more active and specific cores in pharma industry. Apart from the antibacterial properties, sulfa drugs often show potent antitumor activities. In 2011, Suparan *et al.* reported an efficient synthesis of a new class of sulfonamide derived molecules having potent inhibitory activity on the zinc enzyme, carbonic anhydrase (CA). These types of compounds were prepared by the reaction of aromatic or heterocyclic sulfonamides having amino, imino, or hydrazino moieties with N, N-dialkyldithiocarbamates in the presence of oxidizing agents such as iodine and sodium hypochlorite. Three of these new classes of CA inhibitors were also tested for their *in vitro* antitumor activities. These sulfonamides showed a potent inhibition against the growth of several tumor cells such as colon, leukemia, ovarian, melanoma and non-small cell lung. Examples for some such active sulfonamides are given below (figure 5.2).³⁴

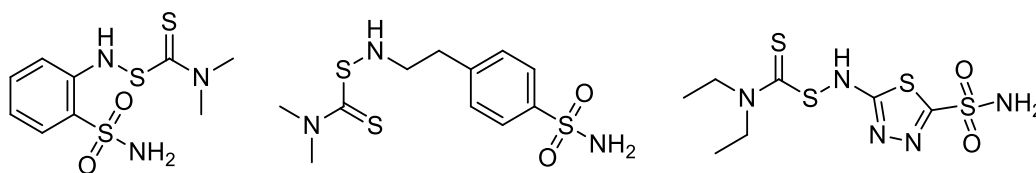
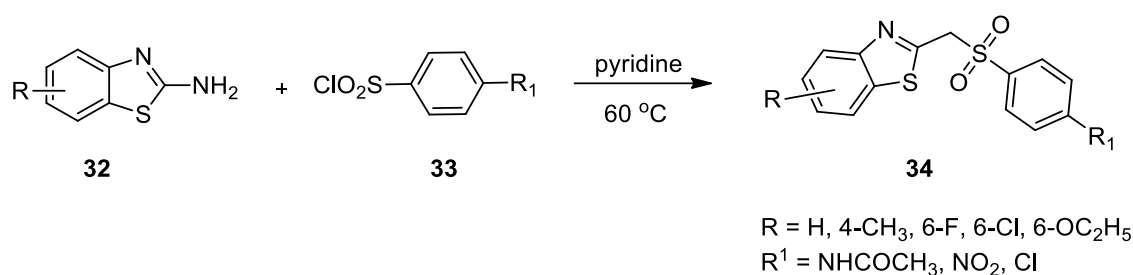


Figure 5.2: Sulfonamides showing anti-tumor activities

Another important contribution in this area is by Geronikaki *et al.* in 2009. They synthesized a new class of thiazoles and benzothiazoles carrying a benzenesulfonamide moiety at position 2 of the heterocyclic nucleus and tested them for their antimicrobial properties. Most of the synthesized products showed effective antibacterial properties against Gram-positive bacteria such as several *bacilli*, *staphylococci* and *streptococci*, including methicillin-resistant *Staphylococcus aureus* and *Staphylococcus epidermidis* strains.³⁵



Scheme 5.15. Synthesis of sulfonamides having antibacterial properties

Inspired from these results, we planned to develop some synthetic strategies for the functionalisation of zerumbone, using sulfonamides as the coupling partner, and the results of our experiments are discussed in the following chapters.

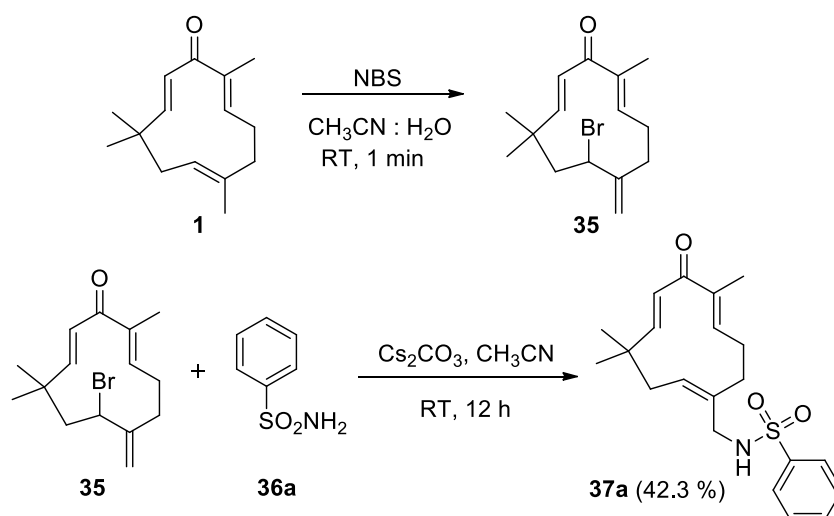
5.4. Aim and Scope of the Present Work

As mentioned in the introduction, even though zerumbone is the most abundant compound present in the rhizomes of *Zingiber zerumbet*, only a few derivatives of the compound have been synthesized. Most importantly, apart from these semi-synthetic derivatives, there have been no further reports in the area of chemical modification of zerumbone and neither zerumbone nor its derivatives have been explored in detail for their antidiabetic activities. Therefore in the present study, we have embarked upon studying the antidiabetic and antiproliferative activities of zerumbone and its derivatives, which are synthesised *via* simple chemical modifications. The reports on zerumbone show that the biological properties of zerumbone are mainly due to the presence of the dienone system.

Hence, without making any changes to this dienone system, we have functionalized zerumbone with sulfonamides, and the results of our studies are discussed in the following chapters.

5.5. Results and Discussion

The syntheses of zerumbone pendant derivatives are quite difficult due the high reactivity of the dienone system present in the ring. Hence in order to activate the isolated double bond of zerumbone, we followed the reaction strategy put forwarded by Kitayama *et al.* in 2013. In their work, the reaction of zerumbone with N-bromosuccinimide (NBS) afford a highly reactive intermediate **35** with an *exo*-methylene group (scheme 5.16) by maintaining the conjugation system.³⁶ The formation of the highly reactive intermediate (**35**) was considered to take place through a radical mechanism. The C-Br bond is located parallel to the planar surface formed by the conjugated (dienone) system, and the *exo*-olefin is located vertically to the surface. Thus regio-selective S_N2' -type reaction might be regulated in the following two ways; either the reaction at carbon binding to bromine or at the exocyclic carbon. The backside attack of nucleophiles to the carbon binding to bromine is not favorable due to steric hindrance; meanwhile, the space for the nucleophilic attack on *exo*-olefin, located vertically to the surface is very advantageous for the reaction. Utilizing this synthetic strategy we synthesized the highly reactive intermediate **35** (1 equiv.) and this on reaction with benzenesulfonamide **36a** (1 equiv.) in the presence of a base (Cs_2CO_3 , 2 equiv.) at room temperature for 12 h using acetonitrile as the solvent afforded the product, sulfonamide pendant zerumbone in 42.3 % yield.



Scheme 5.16

The structure of the product was confirmed by various spectroscopic techniques such as ^1H NMR, ^{13}C NMR, other 2D NMR techniques and HRMS experiments. In the IR spectrum, the signals at 1688 cm^{-1} and 3158 cm^{-1} represent the carbonyl group and N-H groups respectively. In the ^1H NMR, the aromatic protons resonated between δ 7.62 and 7.52 ppm, and the α and β protons of the dienone part resonated at δ 5.94 and 5.59 ppm as two doublets of coupling constant 16.5 Hz (figure 5.3). The broad peak that resonated between δ 5.37 and 5.33 ppm characterizes the proton of isolated double bond. In the ^{13}C NMR the peak at 203.1 ppm represents the carbonyl carbon of zerumbone (figure 5.4). Finally the mass spectrum of the molecule well supported the proposed structure with $[\text{M}+\text{Na}]^+$ ion peak at m/z 396.1608.

To improve the yield of the reaction, we tried different solvent and base systems. Besides, we also monitored the time dependence of the reaction by checking the TLC at constant time intervals. In the analysis; we observed that initially only one proton of the sulfonamide-amine was substituted by zerumbone, but, as the time progressed the possibility for the substitution of one more zerumbone on the sulfonamide amine increased (table 5.1).

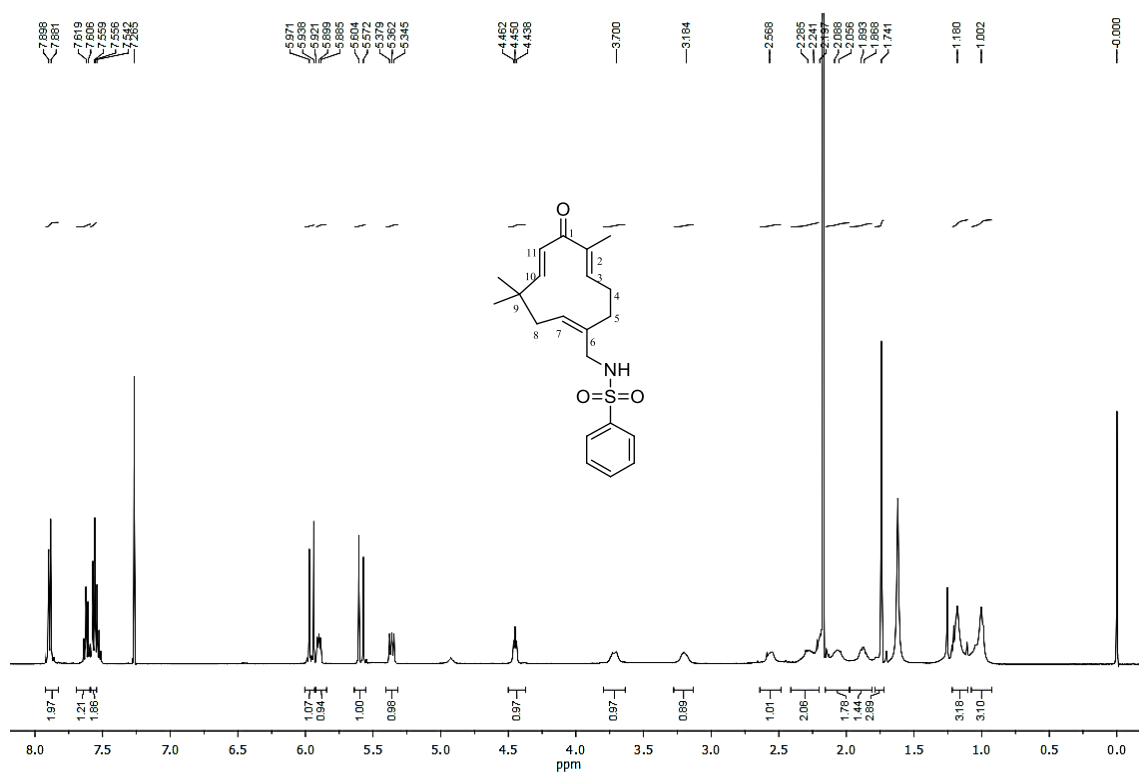


Figure 5.3. ^1H NMR of compound **37a** in CDCl_3

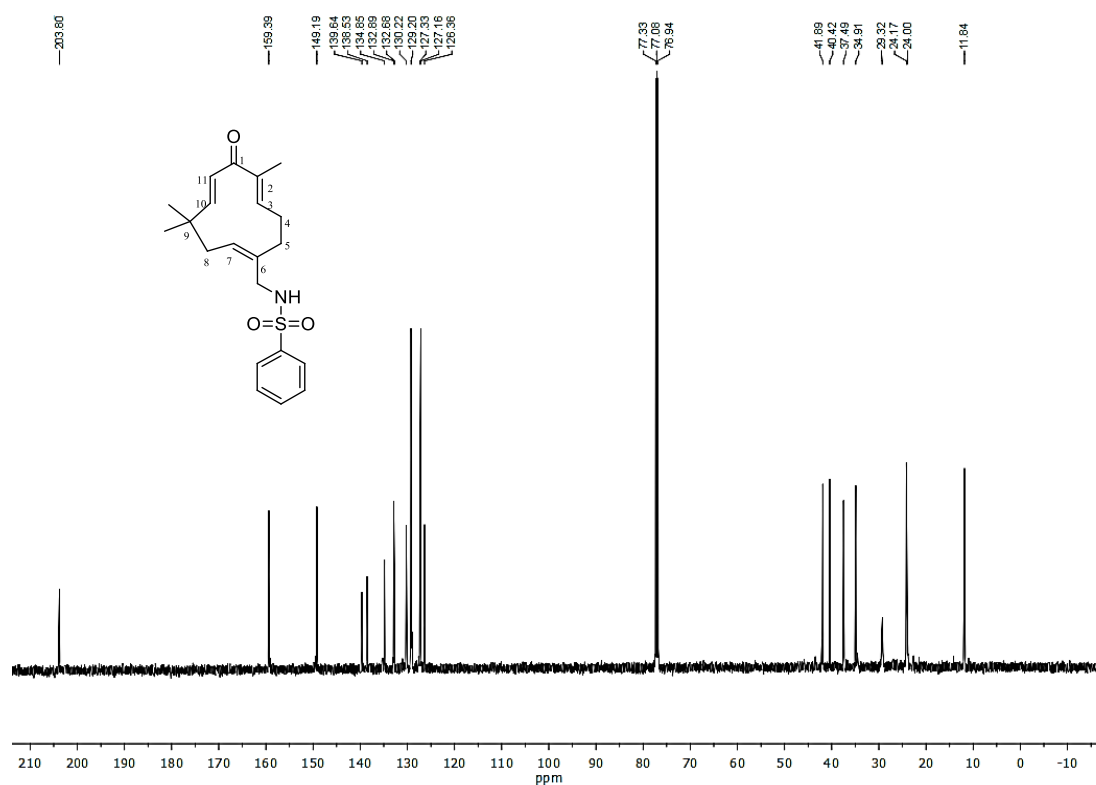


Figure 5.4. ¹³C NMR of compound 37a in CDCl₃

5.5.1. Optimization studies

From the preliminary optimisation studies, it was found that Cs₂CO₃ in acetonitrile at room temperature is the best condition for the reaction (table 5.1). In the next stage, we also evaluated the equivalence of Cs₂CO₃ needed for the maximum conversion of zerumbone to the desired product. From the optimisation table 5.2, it was found that brominated zerumbone 1 equiv., sulfonamide 2 equiv., base 3 equiv. in 2 mL of CH₃CN, at room temperature for 16 h is the best condition for the reaction mono-zerumbone substituted sulfonamides. Under this particular reaction condition, we tested the substrate scope of the reaction with various sulfonamides and the results of our observations are tabulated in table 5.3. In the case of benzene sulfonamide, after 16 hours, we obtained only the mono zerumbone substituted derivative. But, the *ortho* and *para* substituted sulfonamides gave the products despite of their electronic factor. The *para* substituted sulfonamides gave both the products while, the *ortho* substituted sulfonamides mainly yielded the mono-substituted derivatives after 16 hours.

Table 5.1. Optimization of reaction conditions

Entry	Solvent	Base(2 equi)/ additive	Catalyst/ LA (20 mol%)	Ligand (40mol%)	Temp (°C)	Yield(%)
1	CH ₃ CN	K ₂ CO ₃	Pd(OAc) ₂	PPh ₃	80	9.6
2	"	-	-	-	RT	NR
3	"	Sc(OTf) ₃	-	-	"	"
4	"	Cs ₂ CO ₃	-	-	RT	42.3
5	"	K ₂ CO ₃	-	PPh ₃	"	NR
6	DMF	Cs ₂ CO ₃	-	-	"	39.7
7	DCM	"	-	-	"	trace
8	THF	"	-	-	"	18.5
9	Toluene	"	-	-	"	NR
10	DCE	"	-	-	"	1
11	CH ₃ CN	K ^t OBu	-	-	"	34.4
12	"	NaH	-	-	"	13.2
13	"	K ₂ CO ₃	-	-	"	NR
14	"	NaOH	-	-	"	42.3
16	"	-	-	-	-	NR
17	"	Cs ₂ CO ₃	-	-	60	17
18	"	-	-	-	80	NR
19	"	KF	-	-	RT	13.2
20	"	TBAB	-	-	RT	18.5
21	"	Cs ₂ CO ₃	Pd ₂ (dba) ₃ .CHCl ₃	-	80	12
22	"	DBU	-	-	-	20.9

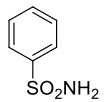
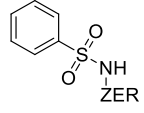

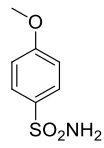
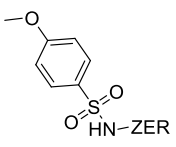
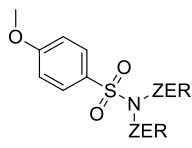
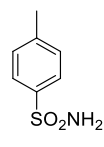
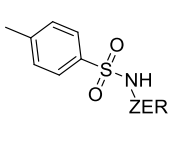
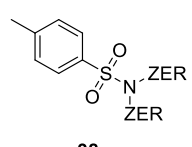
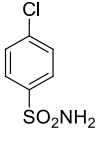
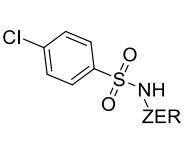
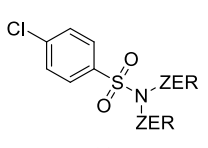
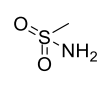
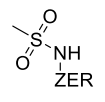
Reaction conditions: Brominated zerumbone (1 equiv.), sulfonamide (1 equiv.), base (2 equiv.)
CH₃CN (2 mL), RT for 12 h.

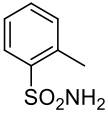
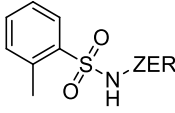
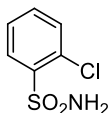
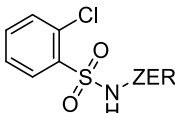
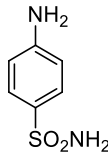
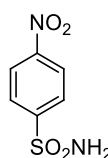
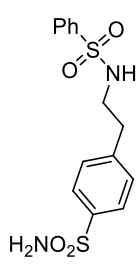
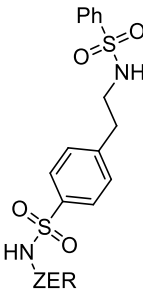
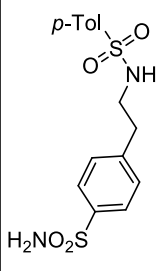
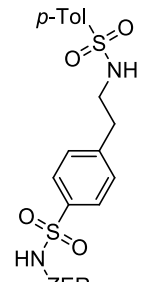
Table 5.2. Optimization of reaction conditions

Entry	Equivalents	Time (h)	Cs ₂ CO ₃ (equiv.)	Yield(%)
1	1:2	12	2	43
2	1:2	16	3	69
3	1:2	24	3	61
4	1:2	36	3	24
5	1:2.5	16	3	56
6	1:3	16	3	69

Reaction conditions: Brominated zerumbone (1 equiv.), sulfonamide (2 equiv.), base (3 equiv.), CH₃CN (2 mL), RT for 16 h.

Table 5.3. Generality of the reaction

Entry	Sulfonamides	Products		Yield (%) A : B
		37	38	
1	 36a	 37a	 38a	69
2	 36b	 37b	 38b	44 : 11
3	 36c	 37c	 38c	51 : 18
4	 36d	 37d	 38d	48 : 30
5	 36e	 37e		16

6	 36f	 37f	57
7	 36g	 37g	33
8	 36h		42
9	 36i		47
10	 36j	 37j	69
11	 36k	 37k	67

Reaction conditions: Brominated zerumbone (1 equiv.), sulfonamide (2 equiv.), base (3 equiv.) CH₃CN (2 mL), RT for 16 h.

Inspired from these results, we envisaged the scope of the reaction with some other class of molecules, and this headed us to choose oxazolidinones as the suitable coupling partner for the above reactions. Oxazolidinones are a class of azoles, in which, the carbon between the nitrogen and oxygen is oxidized to a ketone. These are a new class of synthetic drugs which have unique and specific activity against a large spectra of Gram-positive

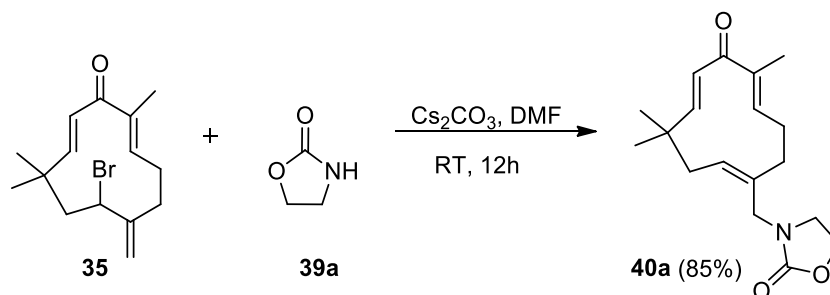
bacteria, including methicillin- and vancomycin-resistant *staphylococci*, vancomycin-resistant *enterococci*, penicillin-resistant *pneumococci* and anaerobes. Linezolid, the first oxazolidinone class of drug, has already taken its place in the clinic for the treatment of Gram-positive infections. Pharmacokinetic properties as well as, its good penetration and accumulation in bone, lung, haematoma and cerebrospinal fluid, allow its usage for surgical infections. The modes of action of these class of molecules are interesting. They inhibit the protein synthesis in the ribosomal 50S subunit of the bacteria, and this prevents the formation of the 70S initiation complex which is a prerequisite for bacterial reproduction.³⁷⁻⁴⁰ Our success in the incorporation of sulfonamides with zerumbone encouraged us to check the reactivity of zerumbone under the above optimized reaction condition. Unfortunately, the reaction did not proceed. This prompted us to carry out a detailed optimization study for this system (table 5.4) and found that brominated zerumbone (1 equiv.), oxazolidinone (1 equiv.) with Cs₂CO₃ (2 equiv.) as the base in 2 mL of DMF at room temperature for 12 hours is the best reaction condition and it afforded a yield of 85 % (scheme 5.17).

Table 5.4. Optimization of reaction conditions

Entry ^a	Base	Solvent	Temp (°C)	Yield(%)
1 ^b	Cs ₂ CO ₃	DMF	RT	68
2 ^c	Cs ₂ CO ₃	"	"	80
3	Cs₂CO₃	"	"	85
4 ^d	Cs ₂ CO ₃	"	"	85
5	Cs ₂ CO ₃	"	100	67
6	K ₂ CO ₃	"	RT	54
7	NaOH	"	RT	NR
8	NaH	"	RT	Trace
9	Cs ₂ CO ₃	Toluene	RT	Trace
10	"	Toluene	100	NR
11	"	CH ₃ CN	RT	NR
12	"	CH ₃ CN	80	10
13	"	THF	RT	NR
14	"	THF	60	NR
15	"	DCM	RT	NR
16	"	DMSO	RT	29

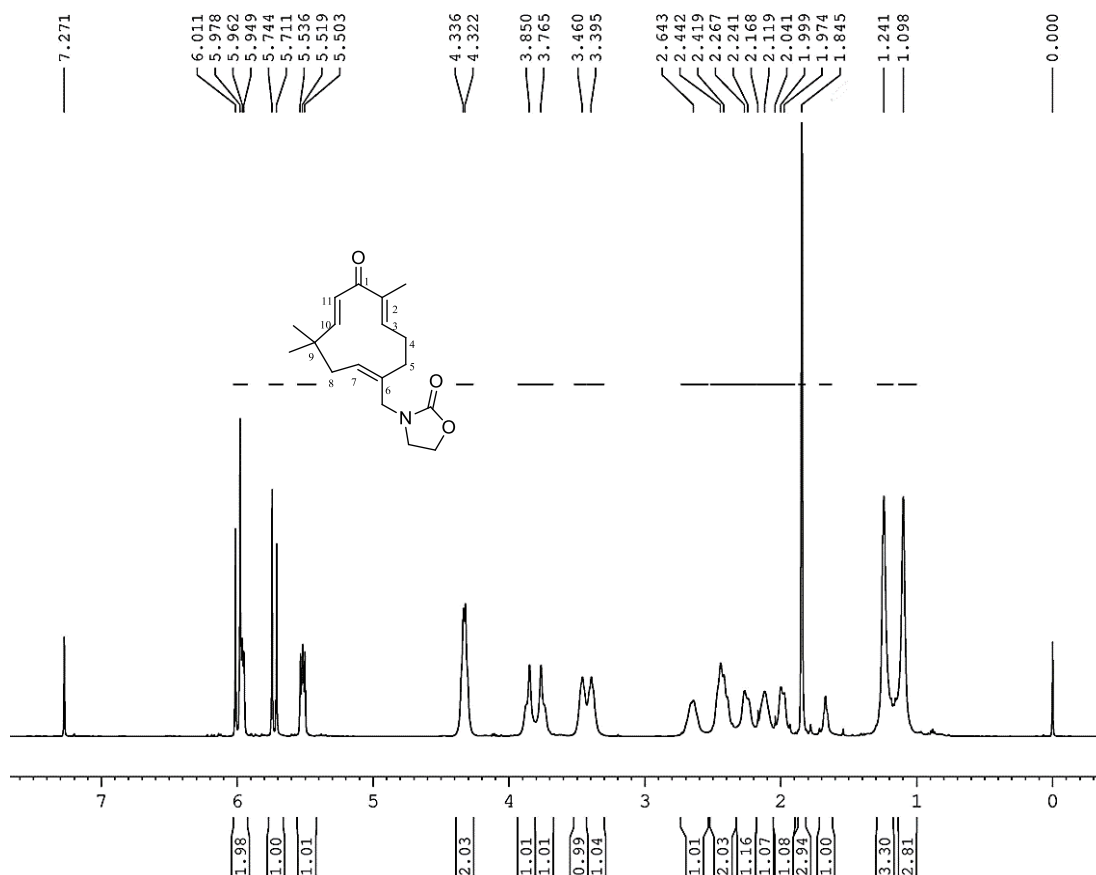
Reaction conditions: ^aOxazolidinone (1 equiv.) brominated zerumbone (1 equiv.), base (2 equiv.) DMF (2 mL), RT, 12 h, ^bbase 1 equiv., ^cbase (1.5 equiv.), ^dbase (2.5 equiv.)

The structure of the product was well established using different spectroscopic techniques such as ^1H , ^{13}C , other 2-D NMR techniques and finally by HRMS data.



Scheme 5.17.

In the IR spectrum, the two carbonyl moieties present in the molecule vibrated at frequencies of 1668 cm^{-1} and 1681 cm^{-1} and in the proton NMR, the α, β unsaturated protons of the dienone part resonated as two doublets (at δ 5.99 and 5.72 ppm) of coupling constant 16.5 Hz. The broad peak resonated between δ 5.54 and 5.50 ppm characterize the proton of isolated double bond and the three singlet peaks at δ 1.84, 1.24, and 1.09 ppm represent the methyl groups on zerumbone (figure 5.5).



In the ^{13}C NMR spectrum, the carbonyl carbon of the dienone moiety resonated at δ 203.2 ppm, while that of oxazolidinone moiety resonated at δ 158.8 ppm (figure 5.6). Finally the mass spectrum of the molecule well supported the structure with $[\text{M}+\text{Na}]^+$ ion peak at m/z 326.1731.

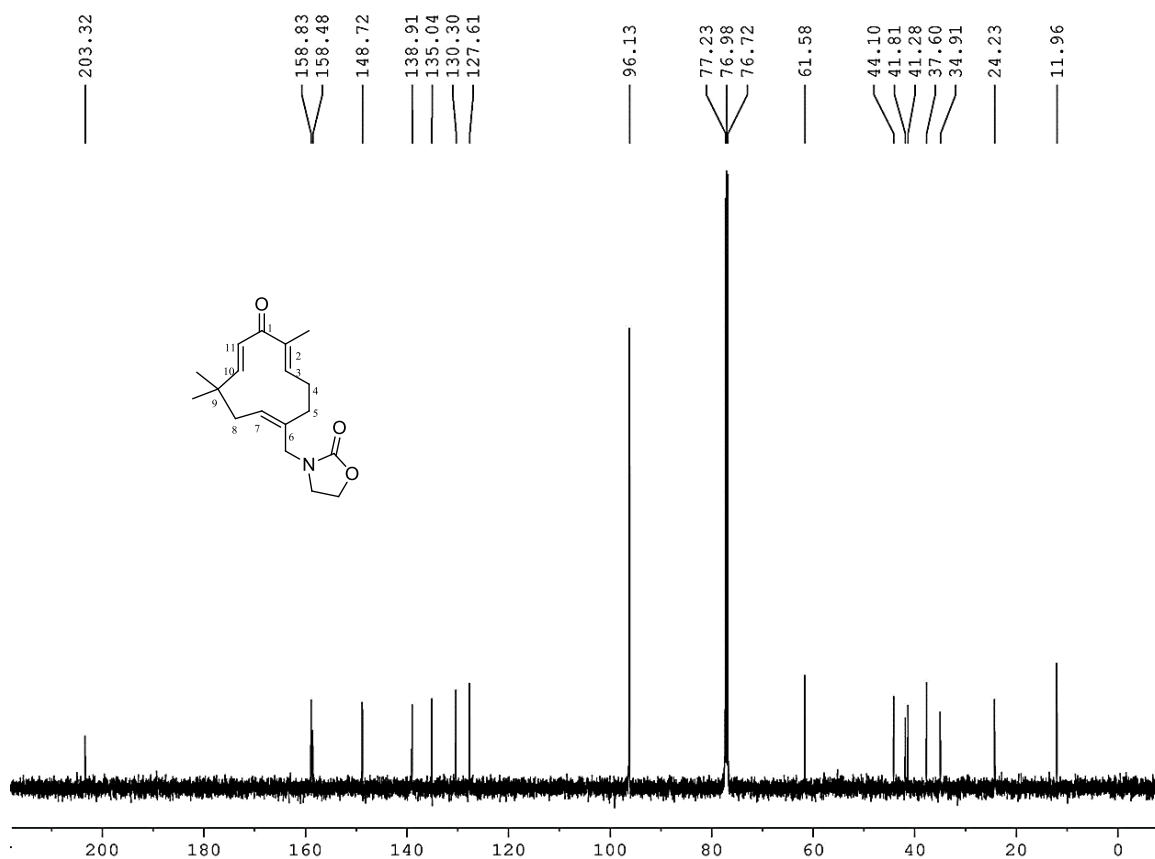
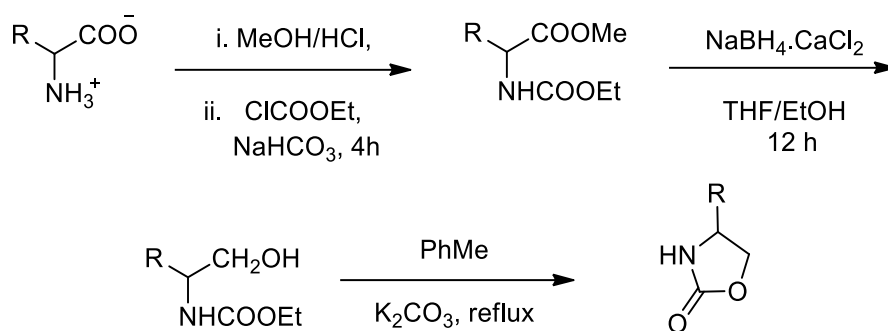


Figure 5.6. ^{13}C NMR of compound **40a** in CDCl_3

With the optimal condition in hand, the scope of the reaction was tested with various oxazolidinones (table 5.5). In all reactions the desired products were formed in excellent yields. Most of the oxazolidinones, utilized in our studies, were synthesized from their corresponding amino acids, using reported procedures. The overall reaction comprised the protection of amino acids, followed by its reduction and cyclisation (scheme 5.18).⁴¹



Scheme 5.18. Synthesis of oxazolidinones from amino acids

Table 5.5. Generality of the reaction

Entry	Oxazolidinones 39a-f	Product 40a-f	Yield(%)	Entry	Oxazolidinones 39g-l	Product 40g-l	Yield(%)
1			85	7			78
2			42	8			55
3			50	9			56
4			75	10			80
5			49	11			74
6			73	12			64

Optimized condition: Oxazolidinone (1 equiv.) brominated zerumbone (1 equiv.), Cs₂CO₃ (2 equiv.) DMF (2 mL), RT, 12 h.

5.5.2. Evaluation of *in silico* and *in vitro* antidiabetic and antiproliferative potential of synthesized derivatives

Modern drug discovery mainly focuses on target oriented syntheses of novel pharmacophores. Natural products are evolutionarily optimized as drug like molecules, and have profoundly impacted advances in biology and therapy. Many natural products and

their derivatives have been recognized for many years as sources of therapeutic agents. The increase in the cost of drug development along with a significant drop in the number of new drug approvals raises the need for innovative approaches for target identification and efficiency prediction. Molecular docking studies are considered as one among those, used to predict the preferred binding modes and affinity of molecule/drug candidates with various enzymes. Hence, we took the advantage of this study, which would help to describe the “best-fit” orientation of a ligand that binds to a particular protein of interest. Having in hand, a set of zerumbone-sulfonamide and zerumbone-oxazolidinone derivatives (*i.e.*, **37a-k**, **38b-h** and **40a-l**), we initially carried out the *in silico* studies of these molecules with the α -glucosidase enzyme 3A4A and crystal structures of EGFR enzyme 2ITW (for anticancer and anti-inflammatory properties). And in the next stage, we carried out the experimental studies (*in vitro*) of those molecules, which showed better binding scores with these enzymes, and our results are tabulated in the tables given below (table 5.6).⁴²

The *in vitro* cytotoxic studies of the derivatives were performed against five human cancer cell lines, namely, A549 (human lung adenocarcinoma), HCT116 (human colon carcinoma), HeLa (human cervix carcinoma), HT1080 (human fibrosarcoma), and MDAMB231 (human breast adenocarcinoma), using the 3-(4,5-dimethylthiazol-2-yl)-2,5-diphenyltetrazolium bromide (MTT) assay, and the results are tabulated in terms of the median inhibitory concentration (IC₅₀) values (table 5.6). Treatment of zerumbone and its synthetic derivatives on the normal cell line (H9c2: rat heart myoblast cells) showed nontoxicity relative to other cell lines.⁴³

Among the 20 derivatives screened, compounds **37b**, **37c**, **37k**, **38h**, **40a**, **40d**, **40h** and **40i** showed the highest binding scores with the EGFR enzyme, 2ITW. So, we further focused on these molecules for the *in vitro* antiproliferative activity studies. In our studies, all these compounds showed better inhibition activity towards the HCT116 cell lines. Also, the compounds, **37b**, **37c**, **37k** and **40d** exhibited significant growth inhibition, as depicted in the molecular docking studies, against the HT1080, A549, and MDAMB231 cell lines after 24 h of incubation relative to zerumbone and the other compounds. Amid these, the compound **37k** demonstrated the lowest IC₅₀ value for A549 and HT1080 cell lines with a value of 20.04 ± 0.91 and $19.02 \pm 0.03 \mu\text{M}$ respectively.

Table 5.6. *In silico* and *in vitro* antiproliferative studies of zerumbone and its pendant derivatives

Samples	2ITW (kcal/mol)	IC ₅₀ (μ M)				
		HT 1080	A549	HeLa	HCT 116	MDA-MB-231
37b	-11.4450	22.34 \pm 502	24.11 \pm 0.13	16.66 \pm .34	4.50 \pm 0.12	> 30
37c	-11.1136	> 30	20.19 \pm 0.65	> 30	4.47 \pm .17	> 30
37k	-13.1134	19.02 \pm .03	20.04 \pm 0.91	> 30	4.06 \pm .17	18.3 \pm 0.43
38h	-11.3232	> 30	26.34 \pm 0.87	> 30	4.41 \pm 0.76	> 30
40a	-11.0555	23.02 \pm 0.03	22.04 \pm 0.91	> 30	5.02 \pm 0.73	21.3 \pm 0.43
40d	12.7131	22.79 \pm 0.21	22.71 \pm 0.62	> 30	4.59 \pm 0.23	24.3 \pm 0.45
40h	-10.2243	> 30	26.77 \pm 0.43	> 30	5.12 \pm 0.54	> 30
40i	-9.9215	25.01 \pm 0.26	22.16 \pm 0.61	> 30	4.53 \pm 0.87	23.3 \pm 0.76
ZER	-	> 30	> 30	16.62 \pm 0.63	4.97 \pm 0.73	24.4 \pm 0.45
Paclitaxel	-	8.64 \pm 0.22 nM	7.31 \pm 500 nM	7.75 \pm 0.45 nM	5.5 \pm 0.76 nM	9.12 \pm 0.22 nM

Inhibition of the digestive enzymes (e.g., α -glucosidase, α -amylase, *etc.*) is one of the targets for the control and management of postprandial glycaemia in diabetic treatment. During prolonged hyperglycemia, advanced glycation end products (AGEs) are formed in the body, as a result of modifications to proteins or lipids that become non-enzymatically glycosylated and oxidized after contact with sugars. AGEs formed under hyperglycemic conditions, are reported to lead to various diabetic complications. In the search for new hyperglycemic lead compounds from the biologically relevant zerumbone molecule, we also evaluated the *in vitro* α -glucosidase, α -amylase, and antiglycation activity of those compounds (**37b**, **37c**, **37j**, **40a**, **40d**, **40h** and **40i**) which showed better binding score with the enzyme 3A4A. The results of our studies are given in table 5.7.⁴⁴

Table 5.7. *In silico* and *in vitro* antidiabetic studies of zerumbone and its pendant derivatives

Samples	3A4A (kcal/mol)	IC ₅₀ (μM)		
		α- Glucosidase inhibition assay	α- amylase inhibition assay	Antiglycation inhibition assay
37b	-11.2295	76.19 ± 0.650	284.995 ± 0.015	996.525 ± 0.455
37c	-11.9256	104.345 ± 0.525	409.575 ± 0.455	416.185 ± 0.095
37j	-15.5065	45.845 ± 1.075	30.49 ± 0.36	88.015 ± 0.053
40a	-12.287	124.04 ± 0.17	287.740 ± 0.48	109.765 ± .505
40d	-12.5425	545.795 ± 0.475	774.61 ± 0.17	98.015 ± 0.055
40h	-12.3359	55.615 ± 0.065	395.14 ± 0.03	98.015 ± 0.061
40i	-13.9608	57.45 ± 1.033	551.895 ± 0.195	98.015 ± 0.055
ZER	-	271.01 ± 0.5835	51.66 ± 0.1225	104.88 ± 0.4155
Acarbose	-	82.635 ± 0.075	8.255 ± 0.055	-
Ascorbic acid	-	-	-	149.605 ± 0.055

Among the derivatives screened, **37j**, **40a**, **40d**, **40h** and **40i** showed promising inhibition against the formation of glycated end products while **37j** demonstrated better α-glucosidase inhibition properties as depicted in molecular docking studies.

The pictorial representation for the presumed binding modes of compounds **37k** and **37j** are given in figure 5.7. In the case of compound **37k**, it showed two prominent sidechain interactions with the enzyme 2ITW. One of them is a sidechain acceptor interaction with an acidic amino acid residue Asp761 (1.75 Å, 40 %) and another one is a sidechain donor interaction with a basic amino acid residue Lys757 (2.45 Å, 98 %). Whereas, three prominent interactions were observed for the compound **37j** with the enzyme 3A4A. It showed a side chain acceptor interaction between the -S=O group and the polar amino acid residue Ser241 (2.56 Å, 48 %). Both the -NH groups present in this compound gave backbone donor interactions with the basic and greasy amino acid residue Lys156 (1.78 Å, 35 %) and Pro312 (1.44 Å, 44 %) respectively. The blue smudges that are drawn behind

some of the atoms represent the solvent exposure. The unbroken proximity contour (dotted line) shows the closeness of the group to the active site (figure 5.7).

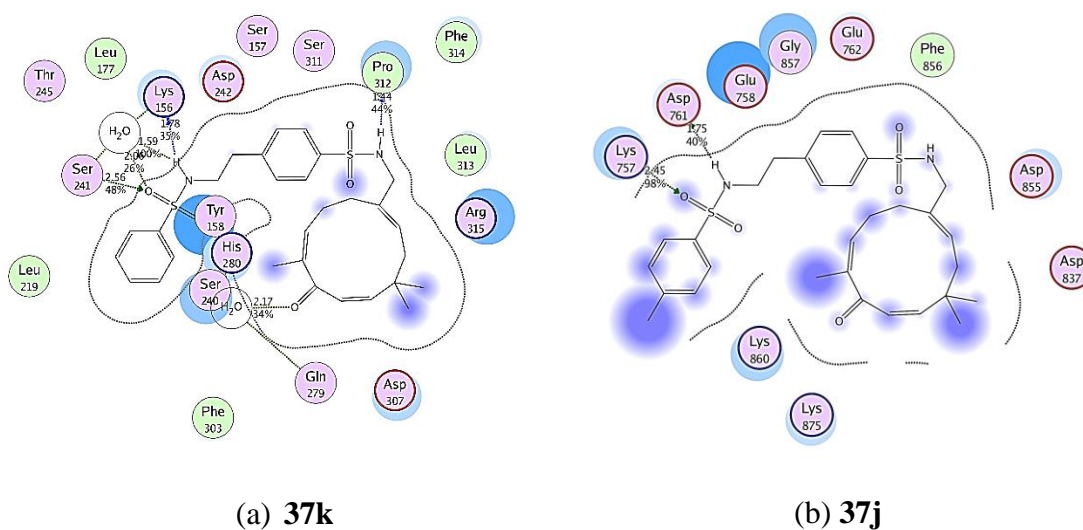
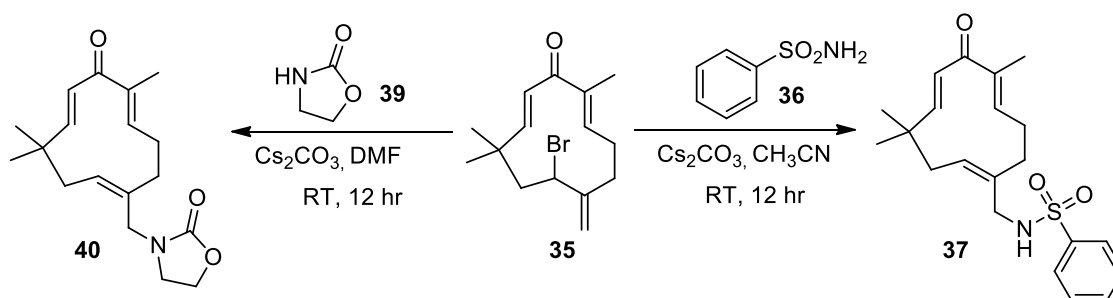


Figure 5.7. Binding modes of **37k** with the protein 2ITW and **37j** with the protein 3A4A



Scheme 5.19

After the successful incorporation of sulfonamides and oxazolidinones to the zerumbone core (scheme 5.19), we had searched a lot for the synthesis of a new class of zerumbone-derivatives. While going through the literature report we found that, though zerumbone and its analogs say humulene, zerumbol and zerumbone epoxides are known to exist either naturally or synthetically (figure 5.8), there are no reports on its aziridine derivatives.

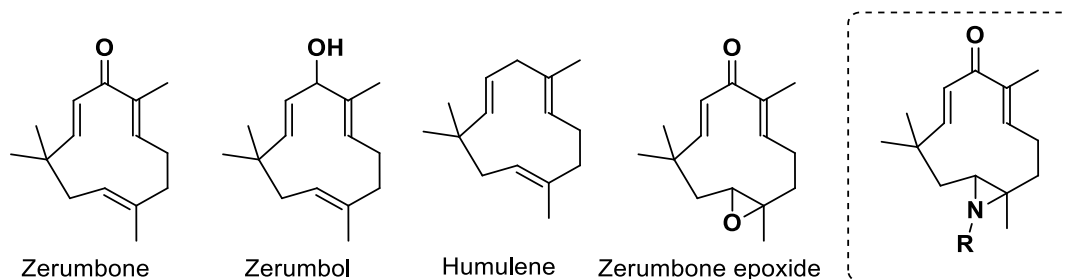


Figure 5.8.

5.6. Aziridines

Aziridines are one of the most important synthetic targets owing to their biological profile and ring strain, which make them an active and versatile intermediate for further functionalization. Therefore the interest towards synthetic methodologies for the preparation of the aziridinyl system have increased in the last few decades. Such interest for synthesizing this small heterocycle is dictated either by the biological activity, displayed by some naturally occurring compounds (figure 5.9) or by the ring strain of those spring-loaded heterocycles that make them valuable precursors of more complex molecules. Mainly, there are three synthetic routes to aziridines: (i) the dehydration of 1,2-aminoalcohols, (ii) the reaction of a carbene equivalent with an imine (protected imines) or (iii) the reaction of a nitrene equivalent with an alkene. Within the past two decades, significant advancements have been achieved in the transition-metal-catalyzed aziridination of alkenes using several nitrogen sources such as N-haloamine salts, organic azides and N-sulfonyliminophenylidodanes.⁴⁵

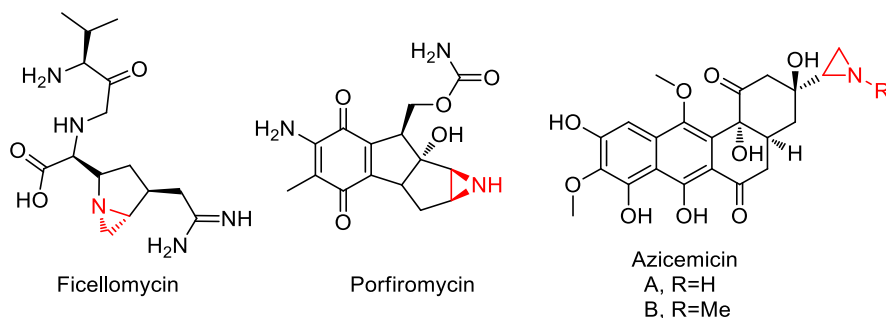
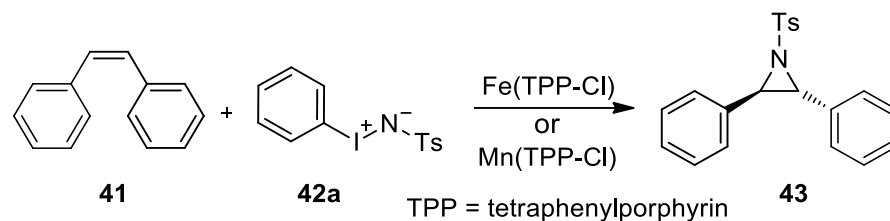


Figure 5.9. Some biologically relevant aziridine bearing molecules

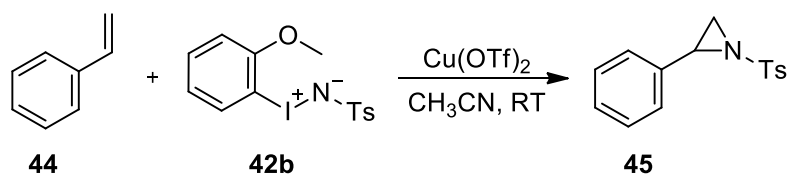
Among these reagents, iminoiodinanes (since the discovery of a practical method for the synthesis of N-tosyliminophenylidodane; $\text{PhI}=\text{NTs}$) have been extensively used as a primary nitrene source for transition metal-catalyzed aziridination reactions, including asymmetric versions. Recently, the metal-free aziridination of alkenes has attracted considerable attention from economical, practical and environmental points of view.⁴⁶ In 2006, Minakata *et al.* reported the first metal-free aziridination reaction of olefins with sulfonamides as the nitrogen source, by using *tert*-butylhypoidite. However, to the best of our knowledge, aziridination using iminoiodinanes under metal-free conditions, which would be highly desirable, has not been well developed, although the direct amidation of a C-H bond has been achieved. Some of the N-tosyliminophenylidodane mediated aziridination and halocyclisation reactions of olefins are given below.⁴⁷

In 1984 Mansuy *et al.* reported an Iron- and manganese-porphyrin catalyzed aziridination of alkenes by Tosyl- and Acyl-iminoiodobenzenes. In their studies, they successfully transferred the NR from $\text{PhI}=\text{NR}$ to alkenes and was catalyzed by metalloporphyrins (scheme 5.20).⁴⁸



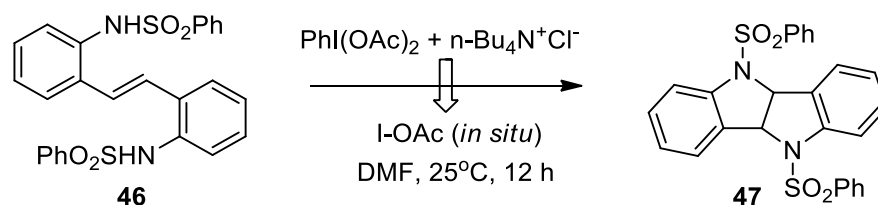
Scheme 5.20

Later in 2011, Zhdankin *et al.* described the preparation and reactivity of new, highly reactive nitrene precursors based on the ortho-alkoxyiodobenzene structural fragment (scheme 5.21). Owing to the presence of the ortho substituent on the phenyl ring, these new iminoiodanes showed excellent solubility in organic solvents, and are efficient reagents for the catalytic aziridination of alkenes or the metal free tosylation of silyl enol ethers and adamantane (products were obtained in more than 75 % yield).⁴⁹



Scheme 5.21

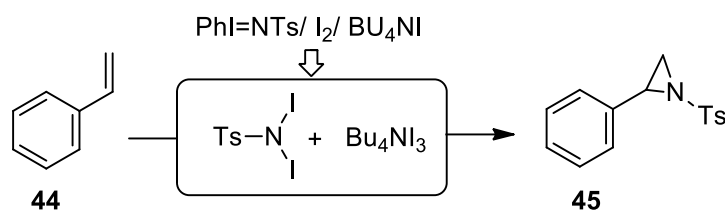
A simple metal-free procedure for the facile intramolecular oxidative diamination of olefins using an iodobenzenediacetate (PIDA) oxidant and a halide additive to furnish bisindolines at room temperature was reported by Chang *et al.* in 2012. Their reaction was convenient and they successfully extended the procedure to the aminohydroxylation reactions also (scheme 5.22).⁵⁰



Scheme 5.22. Diamination of olefins using an iodobenzenediacetate

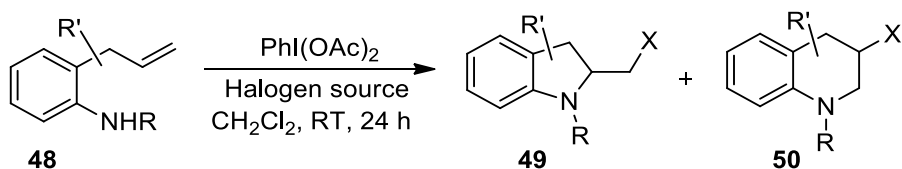
The metal-free catalytic aziridination of styrenes with N-tosyliminophenyl iodane ($\text{PhI}=\text{NTs}$) in the presence of a combination of I_2 and tetrabutylammonium iodide (TBAI) was reported by Minakata *et al.* in 2013. The *in situ* generated TBAI_3 from I_2 and TBAI

dramatically promoted the reaction of alkenes with N,N-diiodotosylamide, which is formed *in situ* (scheme 5.23).⁵¹



Scheme 5.23

After that, in 2014 Liu *et al.* reported a metal-free method for intramolecular halocyclization of non-functionalized olefins, using diacetoxiodobenzene (PIDA). In their studies, a variety of non-functionalized olefins were converted to corresponding 1,2-bifunctional cyclic skeletons in good to excellent yields (scheme 5.24).⁵²



Scheme 5.24. Halocyclisation products in the presence of PIDA

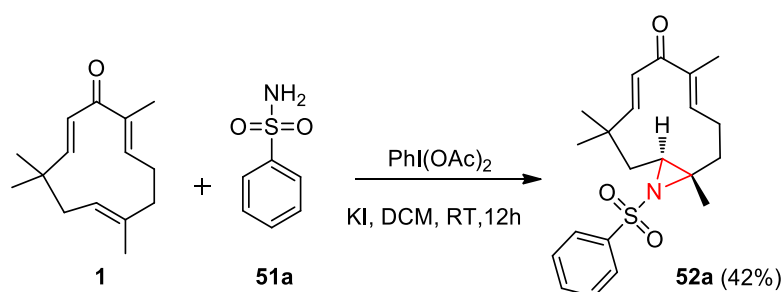
5.7. Aim and Scope of the Present Study

Aziridines are an important structural motif in natural products, and they also act as a useful building block in organic synthesis. This has resulted in the development of numerous synthetic methodologies for preparing aziridines in the past decades. The direct preparation of aziridines from sulfonamides and olefins, without the use of heavy metal catalysts would enhance the scope and synthetic value of the reaction. However, to the best of our knowledge, only one report exists on the aziridination using iminoiodinanes of sulfonamides under metal-free conditions. One of the major drawbacks of this reaction is that, it gives generality only with alkenes and not with sulfonamides, because most of the sulfonamides were unsuccessful in the ylide formation. During literature survey, we found that there are no reports on the aziridination of olefins with the direct employment of PIDA and sulfonamides, without the formation of the ylide PhI=NTs. Also, though zerumbone-epoxide is occurring naturally, there are no reports on its nitrogen counterpart. Hence, in the present study, we took the challenge of functionalizing zerumbone to its aziridines. Here we disclose our efforts in the synthesis of novel aziridine derivatives of zerumbone with the direct employment of sulfonamides and PIDA.

5.8. Results and discussion

We started our investigation by examining the reaction of zerumbone **1** (1 equiv.) with benzenesulfonamide **51a** (1 equiv.) in the presence of iodosobenzene diacetate (1.5 equiv.) as the oxidizing agent and KI (1 equiv.) as the promoter in dichloromethane at room temperature for 12 h. To our delight, we obtained the desired product **52a** in 42 % yield (scheme 5.25). The product was well characterized by using various spectroscopic techniques (figure 5.2 and 5.3) and was unambiguously confirmed by single-crystal X-ray analysis of compound **52i**; CCDC No : **1530684** (figure 5.12).

Previously we had only less number of sulfonamides in our hand. Hence we decided to synthesize or purchase some more number of them (that's why the numbering of sulfonamides were changed from **36** to **51**) to produce a vast library of derivatives.



Scheme 5.25

In the IR spectrum, the characteristic peak of carbonyl group of zerumbone was obtained at 1692 cm^{-1} . In the ^1H NMR, the five aromatic protons resonated in between δ 7.91 and 7.52 ppm as three multiples. The proton at position 3 of the dienone moiety resonated as multiplet between δ 6.21-6.18 ppm and the protons at positions 10 and 11 resonated as two doublets respectively at δ 6.06 and 6.13 ppm with a coupling constant of $J = 16.5\text{ Hz}$. The proton at position 7 was resonated in a deshielded area as a multiplet between δ 2.89-2.87 ppm. The four methyl groups resonated as singlets at δ 1.84 (3H), 1.28 (6H) and 1.01 (3H) ppm (figure 5.10). In the ^{13}C NMR the peak at δ 202.0 ppm represents the carbonyl carbon of zerumbone (figure 5.11). Finally the structure was confirmed by mass spectra in which the $[\text{M}+\text{Na}]^+$ ion peak was observed at m/z 396.1593 corresponding to $\text{C}_{21}\text{H}_{27}\text{NNaO}_3\text{S}$. The ^1H and ^{13}C NMR of the product are given below. After the detailed characterization techniques, the reaction conditions were optimized by examining various additives, solvents, and temperature (table 5.8).

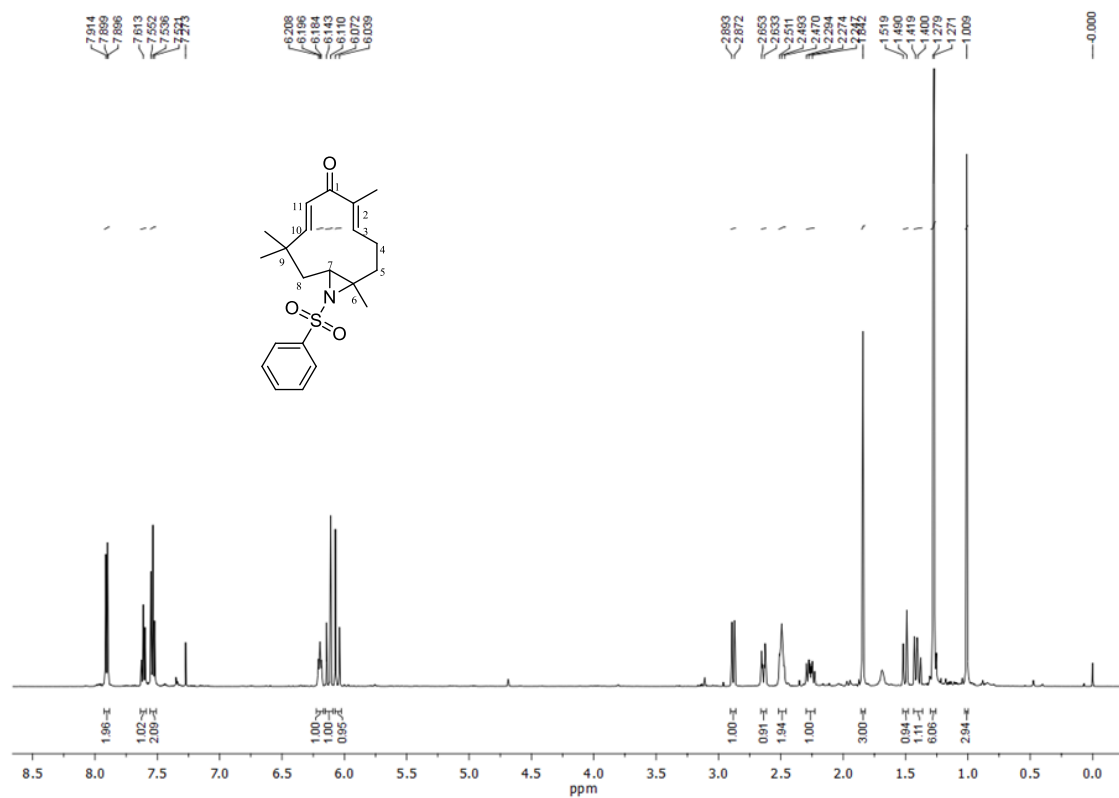


Figure 5.10. ^1H NMR of compound **52a** in CDCl_3

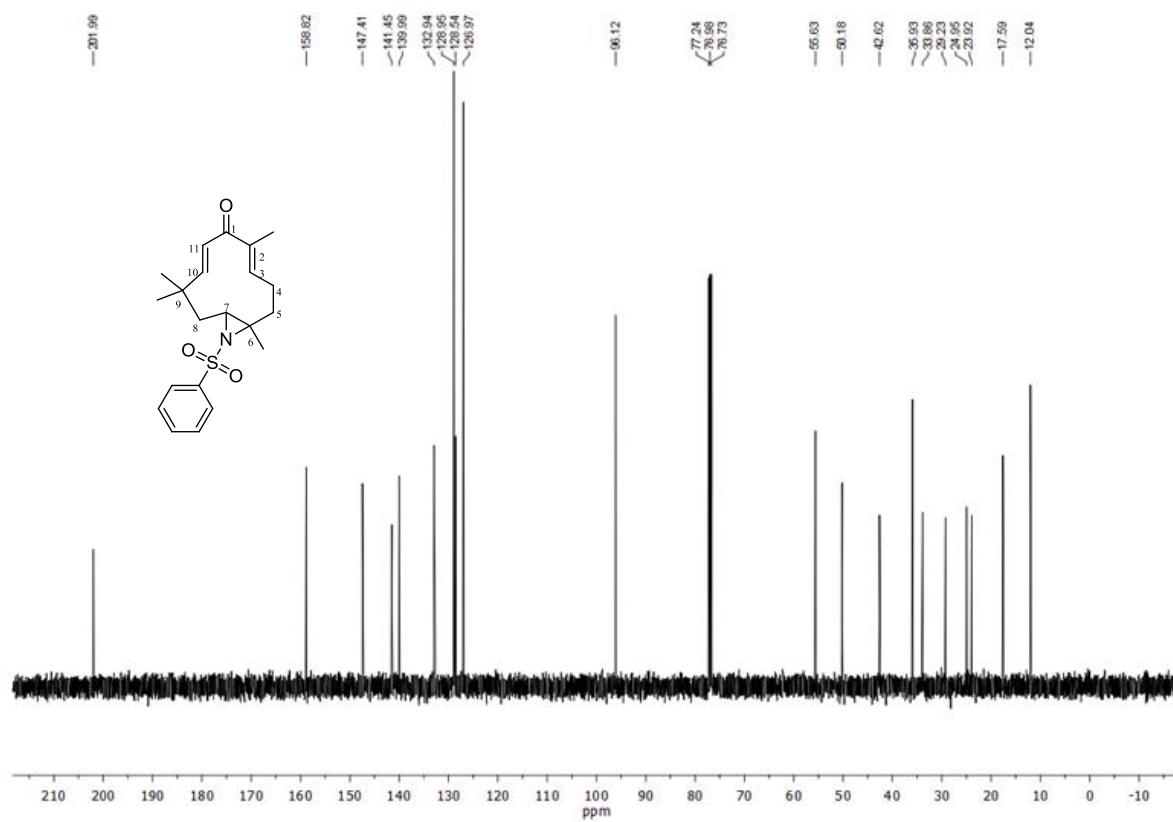
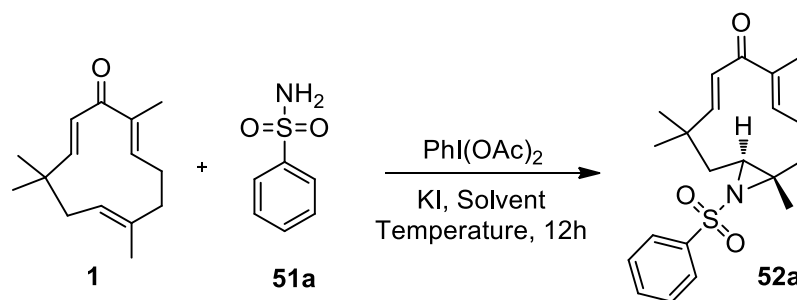


Figure 5.11. ^{13}C NMR of compound **52a** in CDCl_3

Table 5.8. Optimization studies for aziridine synthesis

Entry ^a	Additives	Solvent	Temperature(°C)	Yield(%) ^c
1	KI	DMF	RT	NR
2	KI	DMF	100	NR
3	KI	DCM	RT	42
4	KI + I ₂	DCM	40	33
5^b	KI	DCM	RT	62
6	Bu ₄ N ⁺ Cl ⁻	DCM	RT	15
7	NaI	DCM	RT	11
8	NaI	DCM	RT	NR
9	NaI	DCE	RT	20
10	KI	DCE	RT	14
11	KI	CH ₃ CN	RT	8
12	KI	TFE	RT	NR

Reaction conditions: zerumbone (1 equiv.), sulfonamide (1 equiv.), PIDA (1.5 equiv.), KI (1 equiv.), solvent (2 mL), RT, 12 h. ^[b]zerumbone (1 equiv.), sulfonamide (2 equiv.), PIDA (1.5 equiv.), KI (2 equiv.). ^[c]isolated yield.

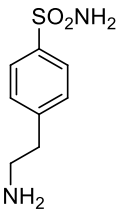
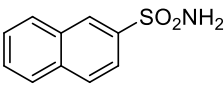
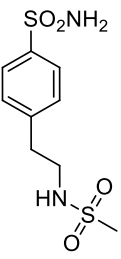
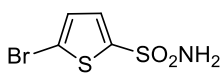
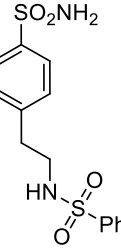
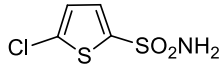
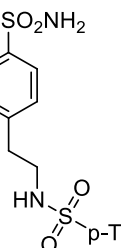
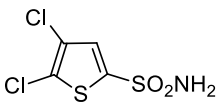
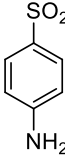
From the optimization studies, a combination of zerumbone (1 equiv.), sulfonamide (2 equiv.), PIDA (1.5 equiv.), and potassium iodide (2 equiv.) in dichloromethane (2 mL) at room temperature for 12 h was found to be the best condition under which the product was delivered in 62 % yield (table 5.1). Also, to improve the yield of the reaction, we synthesized an ylide (PhI=NTs) between iodosobenzene diacetate and benzenesulfonamide, which upon reaction with zerumbone yielded the corresponding product in 60 % yield. Aziridination through ylide formation from PIDA, followed by

reaction with zerumbone was unsuccessful with all sulfonamides except for **51a** and **51j**. The reaction worked well with zerumbone and sulfonamides in the presence of PIDA as the oxidizing agent. With the optimal conditions in hand, we investigated the scope of the reaction with functionally different sulfonamides (table 5.9).

Table 5.9. Generality of the reaction

Entry	Sulphonamide	Product	Yield(%) ^[a]	Entry	Sulphonamide	Product	Yield(%) ^[a]
1	51a 	52a	62	10	51j 	52j	53
2	51b 	52b	40	11	51k 	52k	52
3	51c 	52c	24	12	51l 	52l	50
4	51d 	52d	42	13	51m 	52m	51
5	51e 	52e	26	14	51n 	52n	33
6	51f 	52f	46	15	51o 	52o	51
7	51g 	52g	78	16	51p 	52p	35
8	51h 	52h	54				
9	51i 	52i	53				

Continued..

Entry	Sulphonamide	Product	Yield(%) ^[a]	Entry	Sulphonamide	Product	Yield(%) ^[a]
17	51q 	52q	26	21	51u 	52u	51
18	51r 	52r	87	22	51v 	52v	43
19	51s 	52s	37	23	51w 	52w	34
20	51t 	52t	40	24	51x 	52x	40
				25	51y 	52y	Trace
				26	51z CH ₃ SO ₂ NH ₂	52z	28

Reaction conditions: zerumbone (1 equiv.), sulfonamide (2 equiv.), PIDA (1.5 equiv.), KI (2 equiv.), DCM (2 mL), 12 h. ^[a]isolated yield.

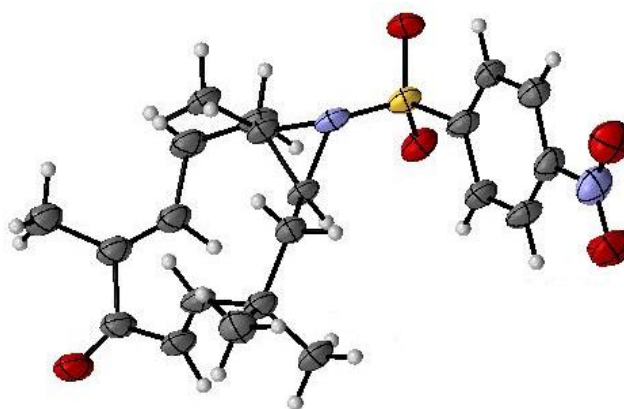
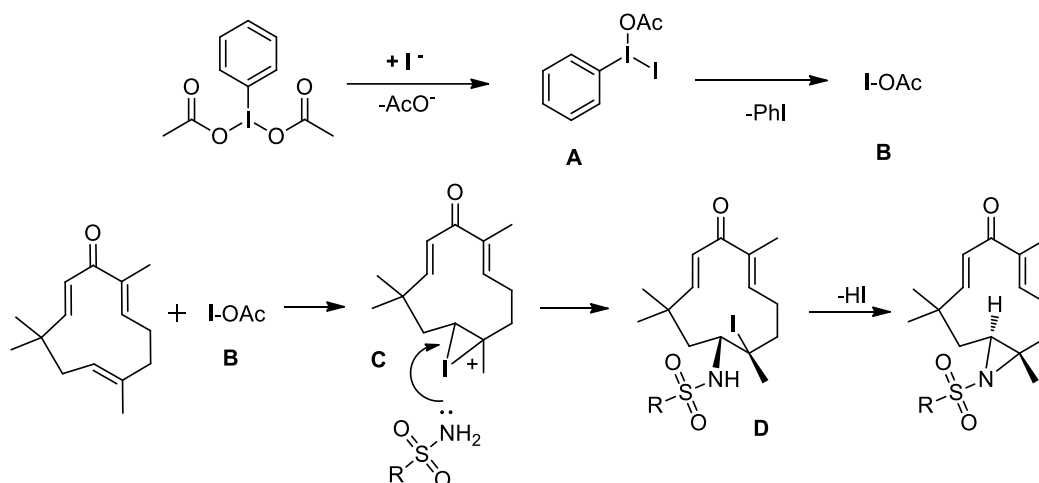


Figure 5.12. Single crystal X-ray structure (ORTEP representation) of **52i**

Sulfonamides bearing various functional groups in the *para* position were suitable substrates for this transformation. Moreover, the steric hindrance played an important role in the yield of the reaction. Unlike *ortho*-substituted sulfonamides, *para*-functionalized substrates afforded good product yields, except in the case of 2,3-dichlorobenzenesulfonamide (table 5.9, entry 7). But, in the case of sulfanilamide (**51y**; table 5.9, entry 25), because of its poor solubility in dichloromethane, we obtained only a trace amount of the product.

The sulfonamides **51r**, **51s** and **51t** were synthesized from **51q** using reported procedures.⁵³ A plausible mechanism for the *trans*-aziridination of zerumbone is shown in scheme 5.26. Initially, iodosobenzene diacetate reacts with the iodide ion to give ligand-exchanged halonium species **A**, which is subsequently converted into active hypohalite intermediate **B**. Upon reaction of intermediate **B** with zerumbone at its unactivated double bond, intermediate **C** is formed, and subsequent intermolecular addition of the sulfonamide followed by an S_N2 replacement reaction gives **D**. Elimination of hydrogen iodide from **D** leads to the *trans* product with complete selectivity.



Scheme 5.26. Proposed reaction mechanism for aziridination of zerumbone

5.9. Evaluation of *in vitro* Antiproliferative, Antidiabetic and Anti-hypertensive Potential of Synthesized Derivatives

Having in hand a set of zerumbone-aziridine derivatives (*i.e.*, **52a–z**), we undertook a study for their antiproliferative, antidiabetic and anti-hypertensive properties based on their molecular docking scores. In the virtual screening of these twenty-six derivatives with the enzyme 2ITW, sixteen gave better binding score, among which compounds **52e** (-11.1306 kcal/mol), **52m** (-11.6962 kcal/mol), **52r** (-11.4220 kcal/mol) and **52t** (-14.1247 kcal/mol) showed better binding compared to other molecules. Then we performed the *in*

in vitro cytotoxic studies of these sixteen zerumbone-aziridine derivatives against five human cancer cell lines, namely, A549 (human lung adenocarcinoma), HCT116 (human colon carcinoma), HeLa (human cervix carcinoma), HT1080 (human fibrosarcoma), and MDAMB231 (human breast adenocarcinoma), by using the 3-(4,5-dimethylthiazol-2-yl)-2,5-diphenyltetrazolium bromide (MTT) assay, and the results are tabulated in terms of the median inhibitory concentration (IC₅₀) values (table 5.3). Treatment of zerumbone and its synthetic derivatives on the normal cell line (H9c2: rat heart myoblast cells) showed nontoxicity relative to other cell lines.^{42,43}

As depicted in the molecular docking studies, the compounds **52e** and **52r** showed significant growth inhibition against the HT1080, A549, and MDAMB231 cell lines after 24 h of incubation, relative to zerumbone and the other compounds (table 5.10).

Table 5.10. Antiproliferative studies of zerumbone and its aziridine derivatives

Entry	Compounds	IC ₅₀ (μM)				
		HT 1080	A549	HeLa	HCT116	MDAMB231
1	52a	>30	24.66 ± 0.653	>30	4.62 ± 0.153	>30
2	52b	26.34 ± 0.554	24.11 ± 0.474	16.66 ± 1.205	4.50 ± 0.733	>30
3	52e	15.33 ± 0.615	17.21 ± 1.169	>30	4.5 ± 0.208	12.5 ± 1.299
4	52f	25.72 ± 0.325	23.88 ± 1.329	>30	4.6 ± 0.242	>30
5	52h	22.59 ± 0.70	22.20 ± 1.209	>30	5.3 ± 0.090	16.8 ± 0.894
6	52i	>30	28.33 ± 0.130	17.64 ± 1.216	4.85 ± 0.3955	>30
7	52j	25.95 ± 1.410	25.28 ± 1.140	>30	4.48 ± 0.219	>30
8	52k	>30	>30	>30	4.5 ± 0.251	>30
9	52l	>30	>30	>30	5.56 ± 0.283	>30
10	52m	22.36 ± 1.22	22.16 ± 1.350	>30	4.3 ± 0.150	>30
11	52n	24.17 ± 0.024	24.78 ± 1.410	>30	4.71 ± 0.327	>30
12	52o	>30	20.19 ± 0.020	>30	4.47 ± 0.183	>30
13	52r	17.52 ± 0.745	16.18 ± 0.480	18.29 ± 1.136	5.23 ± 0.115	17.8 ± 1.347
14	52t	22.12 ± .091	23.53 ± 1.410	>30	4.65 ± 0.791	20.2 ± 1.165
15	52u	>30	26.34 ± 0.912	>30	4.41 ± 0.600	>30
16	52v	>30	24.87 ± 0.207	>30	5.23 ± 0.277	>30
18	Zerumbone	>30	>30	16.62 ± 0.063	4.97 ± 0.459	24.4 ± 0.644
19	Paclitaxel	8.64 ± 0.205 nM	7.31 ± 0.102 nM	7.75 ± 0.077 nM	5.5 ± 0.208 nM	9.12 ± 1.109 nM

Diabetes mellitus is one of the severe chronic metabolic diseases, characterized by impairment in insulin secretion. Natural product has played an important role in controlling the diabetes, and rosiglitazone and metformin are some examples for it. Hence, in the search

for new hyperglycemic lead compounds from the biologically relevant zerumbone molecule, we evaluated the *in vitro* α -glucosidase, α -amylase, and antiglycation activity of some of the derivatives, based on their docking scores.⁴⁴ From the screening studies, **52j** turned out to be a more potent α -glucosidase inhibitor ($IC_{50} = 45.845 \pm 1.075 \mu\text{M}$ and docking score = -10.4995 kcal/mol) than the standard drug, acarbose ($IC_{50} = 82.635 \pm 0.075 \mu\text{M}$). In the α -amylase inhibition studies, **52g** showed better activity with an IC_{50} value of $30.49 \pm 0.36 \mu\text{M}$ (docking score -9.6395 kcal/mol), and the derivative **52k** exhibited the highest antiglycation properties with an IC_{50} value of $47.865 \pm 0.405 \mu\text{M}$ (standard ascorbic acid IC_{50} value: $149.605 \pm 0.375 \mu\text{M}$). From the results, we could infer that **52g** bearing two halogen atoms showed promising antidiabetic activity relative to the other derivatives. The results of our studies are shown in table 5.4.

Table 5.11. Antidiabetic screening studies

Entry	Product	$IC_{50} \mu\text{M}$		
		α -glucosidase	α -amylase	anti-glycation
1	52f	283.215 ± 1.215	226.805 ± 0.41	149.005 ± 0.145
2	52g	124.03 ± 0.94	30.49 ± 0.36	179.78 ± 0.26
3	52h	>1000	297.59 ± 0.41	1406.26 ± 0.13
4	52j	45.845 ± 1.075	395.14 ± 0.03	430.45 ± 0.365
5	52k	>1000	382.49 ± 0.32	47.865 ± 0.45
6	52l	147.77 ± 1.51	409.27 ± 0.16	229.685 ± 0.485
7	52m	>1000	266.3 ± 0.21	238.69 ± 0.41
8	52n	195.94 ± 0.775	355.05 ± 0.115	148.29 ± 0.08
9	52r	>1000	551.895 ± 0.195	109.765 ± 0.505
10	52u	144.355 ± 0.535	738.085 ± 0.875	128.496 ± 0.493
11	52v	587.7 ± 1.51	520.55 ± 0.46	145.695 ± 0.405
12	Zerumbone	271.053 ± 1.028	51.070 ± 1.028	104.86 ± 1.028
13	Acarbose	82.635 ± 0.075	8.255 ± 0.055	-
14	Ascorbic acid	-	-	149.605 ± 0.375

Hypertension is one of the most prevalent diseases, characterized by a persistently elevated blood pressure exceeding 140/90 mmHg or greater, and estimated to cause about 12.8 % of the total deaths in worldwide. According to World Health Organization (WHO),

about one-third of the world's population suffer from hypertension, and due to the changes in life style, its occurrence has been increasing at a rapid rate. It has been named the "silent killer," as it is asymptomatic and the major contributor or risk factor for several cardiovascular diseases such as atherosclerosis, heart failure, renal insufficiency, coronary artery disease and stroke. Nowadays, many synthetic drugs have been developed for the treatment of hypertension and most of these drugs have demonstrated better efficiency but possess a number of side effects. In this phase, herbal medicines have been regaining importance because of their ease of availability, lesser side effects and cost effectiveness. Recent researchers have been focusing on the herbal preparations as alternative agents for the treatment and prevention of cardiovascular problems. In these aspects, we evaluated the anti-hypertensive properties of our synthesized zerumbone derivatives with Captopril, a known angiotensin converting enzyme (ACE) inhibitor, as the standard compound. But to our dismay, none of the samples displayed significant inhibition of ACE. A 52 % inhibition by sample **46r** was found as the best within the group. In fact, many samples have induced the activity of enzyme, which has been documented as 0 % inhibition.⁵⁴

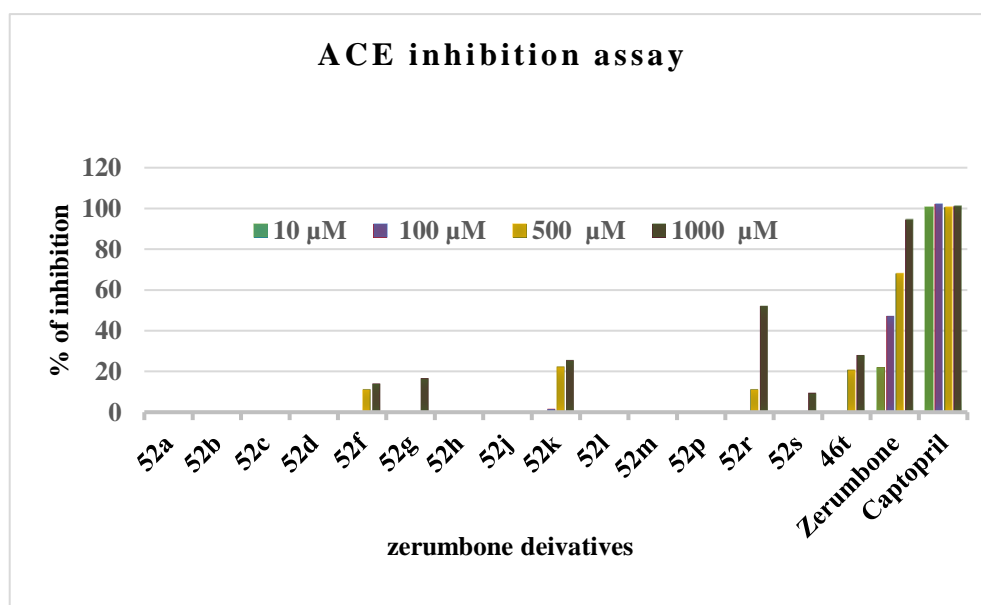


Figure 5.13. ACE inhibitory profile of zerumbone-aziridine derivatives

In general, we employed a metal-free, one-pot strategy for the *trans* aziridination of zerumbone by using sulfonamides as the reaction partners for the first time, and the derivatives were screened for their antiproliferative and antidiabetic activities. Among the zerumbone-aziridine derivatives screened, **52e** and **52r** displayed antiproliferative activities that were superior to those of the parent compound towards human colon

carcinoma and human breast adenocarcinoma cell lines. Also, in the antidiabetic screening studies, most of the derivatives exhibited promising α -glucosidase inhibition properties relative to the parent zerumbone molecule. But, none of the derivatives showed promising ACE inhibition properties.

5.10. Pharmacophore Modeling and QSAR Studies

Having many sets of zerumbone-derivatives in hand, we decided to carry out their biological evaluation. But it was difficult for us to understand which kind of activities these molecules may show or we have to carry out since their number was quite large. Hence we made pharmacophore modeling and QSAR studies of all these synthesized molecules with some cancer cell lines and diabetic enzymes to understand the presumed modes of binding.

5.10.1. Pharmacophore modeling

Some of the “chemical groups” or molecular frameworks present in a molecule carryout the important functions and cause a particular biological effect, which is termed as pharmacophores. Molecules with similar pharmacophores thus have similar biological functions. “A pharmacophore is the ensemble of steric and electronic features that is necessary to ensure the optimal supramolecular interactions with a definite biological target and to trigger (or block) its biological response”. Actually, a pharmacophore does not represent a real molecule or any set of chemical groups. The atoms or various functional groups in a molecule exhibit distinct chemical properties which can be further developed by molecular recognition to represent a unique pharmacophore feature. The important molecular patterns are hydrogen bond donors or acceptors, anionic, cationic, hydrophobic, or aromatic, and any of the combinations of the features mentioned above.

Pharmacophore modeling is extensively used in virtual screening for identifying those molecules with a desired biological effect; with a view of designing novel drugs. It is possible by computational methods to develop valid pharmacophore models. When only a single active molecule is present, the key pharmacophore features contributing to the molecule are mapped and are used for similarity searches for retrieving similar molecules. When there is a set of active molecules with known molecular structure, having similar or different scaffolds, it is possible to develop ligand-based pharmacophore modeling.⁵⁵

For pharmacophore modeling studies, PyMOL 2.1 along with its plugin LIQUID and LigFit were used as default settings. The 3D pharmacophore designing methods take into account both the three-dimensional structures and binding modes of receptors and inhibitors.⁵⁶ This is to understand whether the regions are favorable or not for a specific

receptor-inhibitor interaction. In the given figure (figure 5.14), the red contour represents H-bond acceptor and green for hydrophobic pharmacophore. In our studies, three molecules (three most active *viz.* **52m**, **52o** and **52u**) were aligned to get consensus pharmacophore model and from the figure, it is clear that the pharmacophoric pattern in the present series consists of three ellipsoidal shaped hydrophobic regions, which are arranged in a triangular manner, in addition to six spherical shaped H-bond acceptor regions. The distances in the below figure are in angstrom unit.

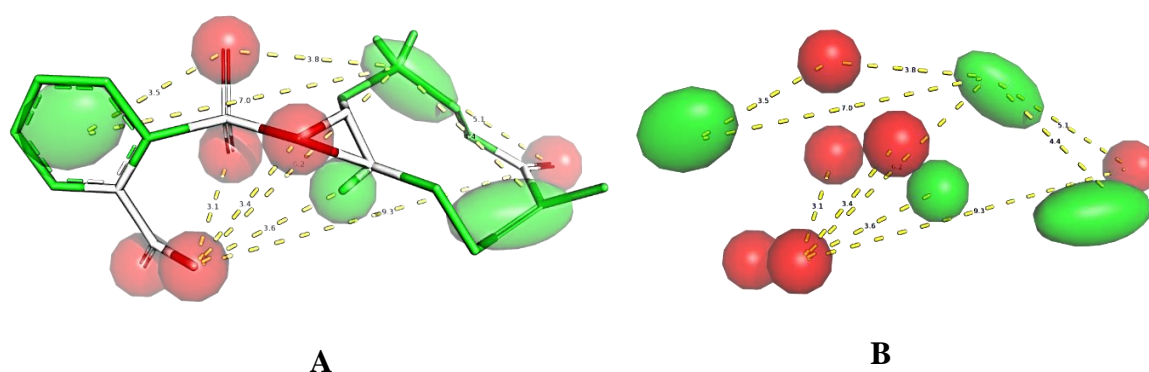


Figure 5.14. **A** Pharmacophore model with molecule; **B** Pharmacophore model without molecule display

For QSAR building, the structures were optimized using MMFF94 force field using Avogadro 1.2 default settings, followed by descriptor calculation using PyDescriptor. Chemometrics and Intelligent Laboratory Systems, 169 (2017) 12-18. This resulted in a descriptor pool of 16,299 molecular descriptors. Then, redundant (inter correlation >90 %) and constant descriptors (> 95 %) were eliminated using Phakiso. The descriptor pool was then reduced to 310 descriptors. Genetic algorithm module available in ‘QSARINS-Chem’ was used to build QSAR model.

5.10.2. Quantitative structure-activity relationships (QSAR)

In the present work, the activity values for HCT116 have been considered for QSAR analysis. As the dataset is small, all the molecules were used to build the QSAR model *viz.* Single parametric, Bi-parametric and Tri-parametric models. For QSAR, the experimental IC_{50} values were converted to pIC_{50} ($-\log_{10}IC_{50}$).⁵⁷

A central observation in chemistry is that, consequent to any structural change, a measured experimental property of a compound changes. The structural variations lead to changes in the shape and electronic distribution of the compound, which can be represented by a large number of numerical descriptors. Quantitative structure-activity relationship

(QSAR) analysis correlates the changes that happen in an observed experimental property with that of the numerical descriptors generated. This aids in developing novel compounds with desired properties. A series of molecules prepared in the laboratory are tested for the relevant biological activity by *in vivo* or *in vitro* methods and is a valuable source of information, enabling one to develop QSAR. The simplest of this procedure is 2D QSAR which is represented by mathematical equations that connect the biological activity with that of the numerical descriptors of the respective compounds.

5.10.2.1. Single parameter based model

Variable	Coeff.	(+/-) Co. int. 95 %
Intercept	5.4224	0.0690
sp ³ N_all_3Å	-0.0079	0.0058

(Fitting criteria)

R2: 0.5101	R2adj: 0.4557	R2-R2adj: 0.0544	LOF: 0.0006
Kxx: 0.0000	Delta K: 0.7142	RMSE tr: 0.0196	MAE tr: 0.0124
RSS tr: 0.0042	CCC tr: 0.6756	s: 0.0217	F: 9.3721

(Internal validation criteria)

Q2loo: 0.4001	PRESS cv: 0.0052	CCC cv: 0.6101
R2-Q2loo: 0.1100	RMSE cv: 0.0217	MAE cv: 0.0140

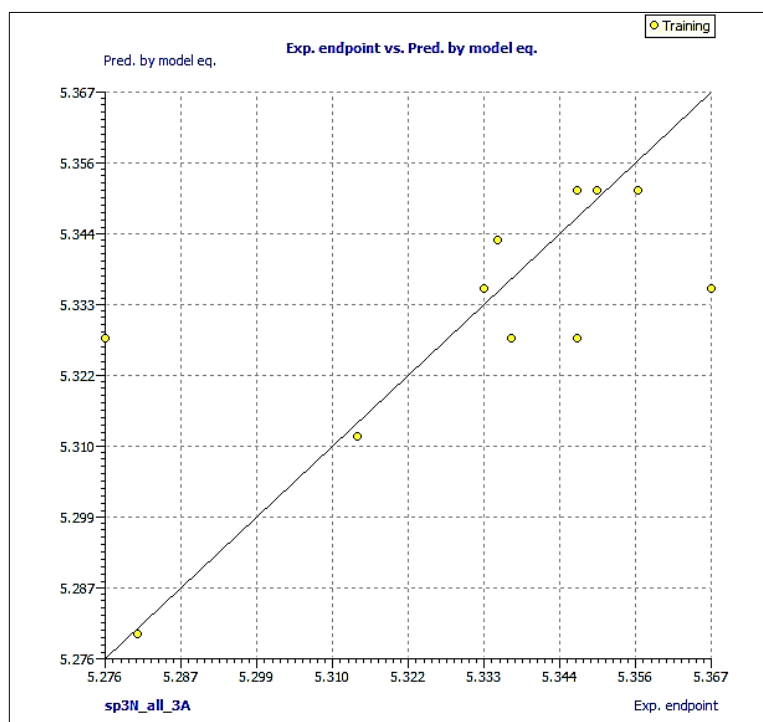
Here sp³N_all_3A means ‘all atoms which are within 3 angstroms from sp³ hybridized Nitrogen atom’. Due to its negative coefficient, it appears that lower the number of atoms in the vicinity of the sp³ hybridized Nitrogen atom, better is its activity. The graph for model 1 is as follows (graph5.1):

Table 5.12. Single parameter studies

Sample	Exp. endpoint	Pred. by model eq.	Pred.Mod. Eq.Res.	HAT i/i (h*=0.5455)
52a	5.3350	5.3434	0.0084	0.1247
52b	5.3470	5.3276	-0.0194	0.0938
52e	5.3470	5.3513	0.0043	0.1825
52f	5.3370	5.3276	-0.0094	0.0938
52h	5.2760	5.3276	0.0516	0.0938
52i	5.3140	5.3118	-0.0022	0.1761
52m	5.3670	5.3355	-0.0315	0.0951
52p	5.3500	5.3513	0.0013	0.1825
52s	5.2810	5.2802	-0.0008	0.6799
52u	5.3330	5.3355	0.0025	0.0951
52v	5.3560	5.3513	-0.0047	0.1825

5.10.2.2. Bi parameter based model studies

Variable	Coeff.	(+/-) Co. int. 95 %
Intercept	5.4638	0.1480
com_Cplus_5A	0.0209	0.0161
fSC6A	-0.0120	0.0075



Graph 5.1. Showing Predicted vs. expt pIC₅₀

Correlation matrix for above descriptors:

	com_Cplus_5A	fSC6A
com_Cplus_5A	1.0000	
fSC6A	0.1765	1.0000

(Fitting criteria)

R2: 0.7079	R2adj: 0.6349	R2-R2adj: 0.0730
LOF: 0.0006	Kxx: 0.1765	Delta K: 0.2517
RMSE tr: 0.0152	MAE tr: 0.0122	RSS tr: 0.0025
CCC tr: 0.8290	s: 0.0178	F: 9.6952

(Internal validation criteria)

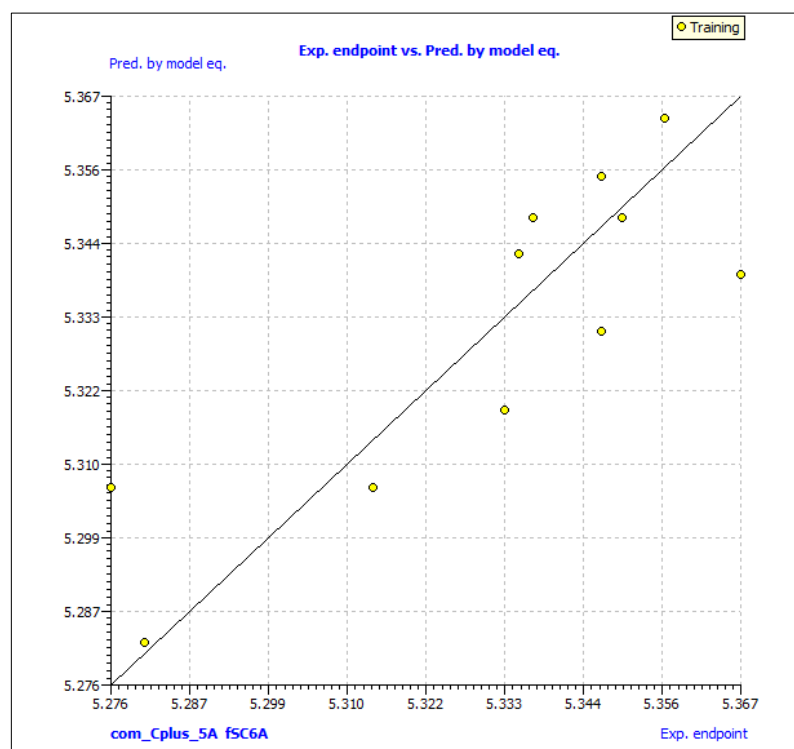
Q2loo: 0.5491	R2-Q2loo: 0.1588	RMSE cv: 0.0188
MAE cv: 0.0157	PRESS cv: 0.0039	CCC cv: 0.7440
Q2LMO:	R2Yscr:	Q2Yscr:
RMSE AV Yscr:	R2Xrnd:	Q2Xrnd:
R2Yrnd:	Q2Yrnd:	

Here com_Cplus_5A means positively charged carbon atoms which are within 5Å from the center of mass (COM) of the molecule. Its positive coefficient indicates that, increasing such carbon atoms will increase tits activity. Also, fSC6A means the frequency of occurrence of Sulphur and carbon within 6 Å from each other. Its negative coefficient indicates that such combination must be avoided for better activity profile.

Table 5.13. Bi parameter studies

Sample	Exp. endpoint	Pred. by model eq.	Pred.Mod.Eq.Res.	HAT i/i (h*=0.8182)
52a	5.3350	5.3428	0.0078	0.2319
52b	5.3470	5.3307	-0.0163	0.1516
52e	5.3470	5.3548	0.0078	0.3791
52f	5.3370	5.3484	0.0114	0.4152
52h	5.2760	5.3067	0.0307	0.1913
52i	5.3140	5.3067	-0.0073	0.1913
52m	5.3670	5.3396	-0.0274	0.1218
52p	5.3500	5.3484	-0.0016	0.4152

52s	5.2810	5.2826	0.0016	0.4982
52u	5.3330	5.3187	-0.0143	0.1381
52v	5.3560	5.3637	0.0077	0.2662



Graph 5.2. Graph for Predicted Vs. Expt. pIC₅₀

5.10.2.3. Three parametric model studies

Variable	Coeff.	(+/-) Co. int. 95 %
Intercept	5.4635	0.2223
fringNC4B	0.0432	0.0275
ringC_F_4Bc	-0.3608	0.2710
facclipo6A	-0.0218	0.0104

Correlation matrix for above descriptors:

	fringNC4B	ringC_F_4Bc	facclipo6A
fringNC4B	1.0000		
ringC_F_4Bc	0.3640	1.0000	
facclipo6A	0.3064	0.2273	1.0000

(Fitting criteria)

R2: 0.8541	R2adj: 0.7916	R2-R2adj: 0.0625
LOF: 0.0006	Kxx: 0.3009	Delta K: 0.0969
RMSE tr: 0.0107	MAE tr: 0.0078	RSS tr: 0.0013
CCC tr: 0.9213	s: 0.0134	F: 13.6587

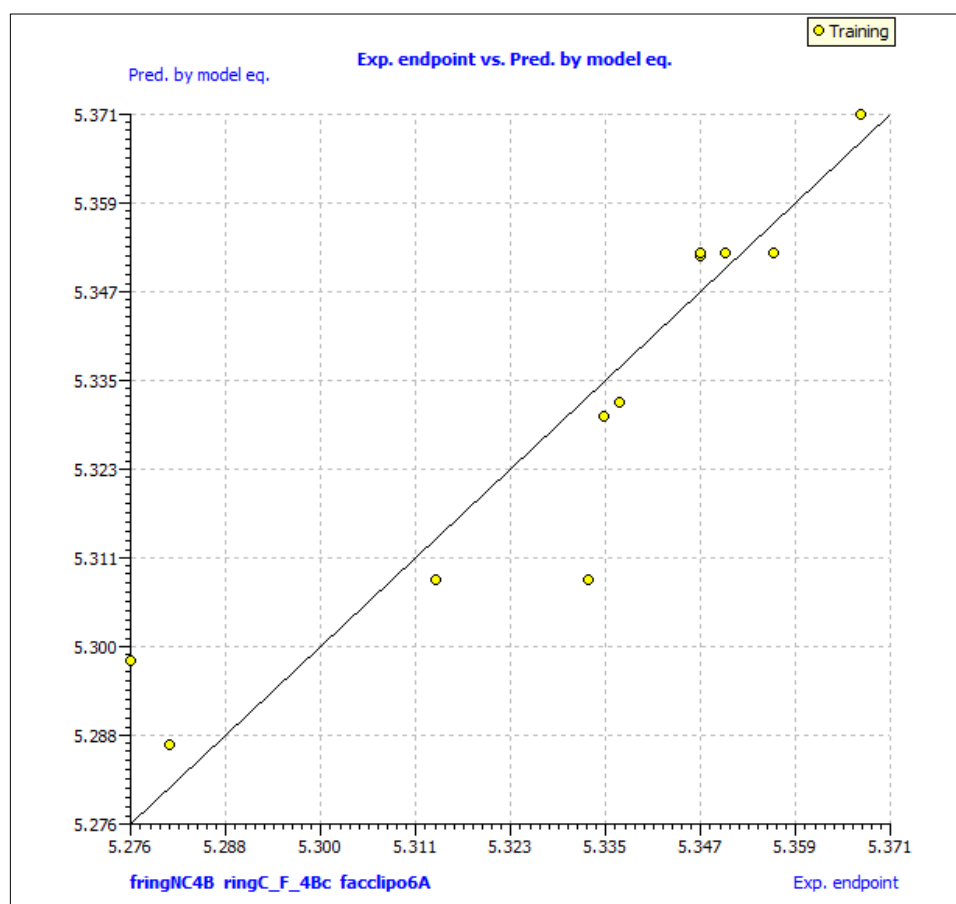
(Internal validation criteria)

Q2loo: 0.6675	R2-Q2loo: 0.1866	RMSE cv: 0.0162
MAE cv: 0.0130	PRESS cv: 0.0029	CCC cv: 0.8405
Q2LMO:	R2Yscr:	Q2Yscr:
RMSE AV Yscr:	R2Xrnd:	Q2Xrnd:
R2Yrnd:	Q2Yrnd:	

Here fringNC4B stands for the frequency of occurrence of carbon and nitrogen separated by four bonds. Its positive coefficient indicates that such a combination is useful for activity augmentation. Also, ring C_F_4Bc stands for sum of partial charges on carbon atoms which are at four bonds from fluorine, as well as part of the ring. It has negative coefficient. Hence, its value must be as low as possible. Facclipo6A means frequency of occurrence of lipophilic atoms within 6 Angstrom from H-bond acceptor atom. Its negative coefficient indicates that higher such combinations, lower will be the activity.

Table 5.14. Three parametric studies

Sample	Exp. endpoint	Pred. by model eq.	Pred.Mod.Eq.Res.	HAT i/i (h*=1.0909)
52a	5.3350	5.3303	-0.0047	0.1238
52b	5.3470	5.3518	0.0048	0.5532
52e	5.3470	5.3521	0.0051	0.2842
52f	5.3370	5.3322	-0.0048	0.5532
52h	5.2760	5.2979	0.0219	0.2625
52i	5.3140	5.3085	-0.0055	0.1764
52m	5.3670	5.3705	0.0035	0.8600
52p	5.3500	5.3521	0.0021	0.2842
52s	5.2810	5.2867	0.0057	0.4419
52u	5.3330	5.3085	-0.0245	0.1764
52v	5.3560	5.3521	-0.0039	0.2842



Graph 5.3. Graph for Predicted Vs. Expt. pIC₅₀

5.11. Conclusion

We have synthesized a new class of zerumbone appended sulfonamide or oxazolidinone derivatives under base mediated reactions, and all the products were obtained in good to excellent yields. Then we extended the reactions of sulfonamides, which resulted in the synthesis of a new class of zerumbone-aziridine derivatives. This is the first report on the *trans* aziridination of zerumbone under one-pot metal-free strategy and the reaction conditions are quite tolerable with a large number of sulfonamides. In order to explore the biological activity of these synthesized derivatives, we carried out a detailed *in silico* and *in vitro* studies. In the preliminary antidiabetic and antiproliferative studies, most of these derivatives exhibited promising activities.

5.12 Experimental Section

5.12.1. General methods

All the chemicals were of the best grade commercially available and were used without further purification. All the solvents were purified according to standard procedures and dry solvents were obtained according to the literature methods and stored

over molecular sieves. Analytical thin layer chromatography was performed with Merck TLC Silica gel F₂₅₄ coated on aluminum sheets. Gravity column chromatography was performed using 60-120 or 100-200 mesh silica gel and mixtures of hexane-ethyl acetate were used for elution. Melting points were determined on a Buchi melting point apparatus and are uncorrected. Proton nuclear magnetic resonance spectra (¹H NMR) were recorded on a Bruker AMX 500 spectrophotometer (CDCl₃ as solvent). Chemical shifts for ¹H NMR spectra are reported as δ in units of parts per million (ppm) downfield from SiMe₄ (δ 0.0) and relative to the signal of chloroform-d (δ 7.25, singlet). Multiplicities were given as: s (singlet); d (doublet); t (triplet); q (quartet); dd (double doublet); m (multiplet). Coupling constants are reported as *J* value in Hz. Carbon nuclear magnetic resonance spectra (¹³C NMR) are reported as δ in units of parts per million (ppm) downfield from SiMe₄ (δ 0.0) and relative to the signal of chloroform-d (δ 77.03, triplet). For the structural assignment, 2D NMR experiments were also conducted (¹H-¹H COSY, ¹H-¹³C HMQC, ¹H-¹³C HMBC). The peak at δ 96 ppm in ¹³C represents CCl₄. Mass spectra were recorded under EI/HRMS at 60,000 resolution using Thermo Scientific Exactive mass spectrometer. IR spectra were recorded on Bruker FT-IR spectrometer.

5.12.2. General procedures

General Procedure for the synthesis of oxazolidinones from amino acids:

Acetyl chloride (0.5 mL) was added dropwise to ice-cooled methanol (20 mL) over 20 min. Amino acid (1 equiv.) was added, and the solution was stirred overnight. Removal of the solvent in vacuo then gave the crude methyl ester hydrochloride as a colorless crystalline solid damp with methanol/HCl. The ester hydrochloride was dissolved in water (100 mL), and sodium bicarbonate (2.4 equiv.) was added portion wise. Ethyl chloroformate/methyl chloroformate (2 equiv.) was added dropwise and the solution was vigorously stirred for 4 h; a white solid separated after 2 h. Filtration and washing of the collected solid with water gave the amino and carboxyl group protected amino acid (**A**). Calcium chloride (2 equiv.) and sodium borohydride (1.1 equiv.) were added to a solution of **A** (1 equiv.) in ethanol (100 mL) and THF (50 mL) and the white suspension was stirred overnight. The mixture was then poured into a solution of citric acid (1 M, 120 mL) in water and kept for ten minutes. Followed by an ethyl acetate work-up (2 x 200 mL) and washing with brine (200 mL) gave a viscous oil which was filtered through a silica plug (50 g, EtOAc) to give an alcohol **B**. The Alcohol **B** (1 equiv.) was dissolved in toluene (100 mL) to which K₂CO₃ (1.4 equiv.) was added and the reaction mixture was boiled under

reflux in a Dean-Stark apparatus for 3 h. The hot solution was filtered and allowed to cool, and the corresponding oxazolidinones were formed as colorless crystals in the solvent.

General Procedure for the Synthesis of zerumbone pendant derivatives:

To a solution of (35) in acetonitrile or DMF, the nucleophile (sulfonamide / oxazolidinone) was added followed by base and stirred the reaction for 12 h at room temperature. After the completion of the reaction as monitored by TLC, the reaction mixture was concentrated and the crude product was purified by column chromatography on silica gel (100-200 mesh) using hexane: ethyl acetate as the eluent to afford the product.

General Procedure for the Aziridination of Zerumbone with Sulfonamides:

Zerumbone (1.0 equiv.), the sulfonamide (2.0 equiv.), iodosobenzene diacetate (1.5 equiv.), and KI (2 equiv.) were combined in a reaction tube. Dichloromethane (2 mL) was added and the mixture stirred at room temperature for 12 h. The reaction was then quenched with aqueous sodium thiosulfate solution, and the mixture was extracted with dichloromethane and dried with anhydrous sodium sulfate. The solvent was evaporated in vacuo, and the residue was purified by column chromatography (silica gel, 100–200 mesh; hexane/ethyl acetate) to yield the product.

Synthesis of Sulfonamides 51r, 51s, and 51t:

The respective sulfonyl chlorides (1.2 equiv.) were added to a solution of 51q (1 equiv.) in water (10 mL), and the mixture was stirred at room temperature until the reaction was complete. The mixture was then extracted with ethyl acetate, dried with anhydrous sodium sulfate, and concentrated under reduced pressure. The residue was purified by column chromatography (silica gel, 100–200 mesh; hexane/ethyl acetate) to yield the product.

General procedures for antidiabetic assays are given in Part A of Chapter 2.

Culture and maintenance of cells

Human cancer cell lines A549, HCT116, HeLa, HT1080, MDAMB231 and normal liver cell lines were obtained from National Center for Cell Sciences, Pune, Maharashtra. Cells were maintained at 37 °C in a 5 % CO₂ atmosphere in Dulbecco's modified Eagle's medium with 10 % fetal bovine serum. Confluent cells were passaged by treating them with 0.05 % trypsin, 0.00 2% EDTA in 0.085 % normal saline. The medium was changed every two days.

MTT assay

The MTT (3-(4,5-dimethylthiazole-2-yl)-2,5-diphenyltetrazolium bromide) assay developed by Mosmann, was used with slight modifications. In brief, the trypsinized cells from T-25 flask were seeded in each well of 96-well tissue culture plate at a density of 1×10^4 cells/well in growth medium and cultured at 37 °C in 5 % CO₂ to adhere. After 48hr incubation, the cells were treated with both, standard (Paclitaxel) and synthesized molecules to achieve a final volume of 100 μ L and then cultured for 24 h. The compound was prepared as 1.0 mg/mL concentration stock solutions in DMSO. Each well then received 20 μ L of fresh MTT (5mg/mL in PBS) followed by incubation for 4 h at 37°C. The supernatant was removed from the wells and replaced with 100 μ L of DMSO to solubilize the colored formazan product. After 30 min incubation, the absorbance (OD) of the culture plate was read at a wavelength of 570 nm on a microplate reader (Biotek Synergy 4, VT, USA). The percent cell viability was determined with respect to control, is calculated using the formula,

$$\% \text{ of viability} = \frac{\text{Corrected OD of samples}}{\text{Control OD}} * 100$$

and the percentage of inhibition was determined as,

$$\% \text{ Inhibition} = 100 - \% \text{ viability}$$

Antihypertensive analysis

The compound of interest is tested at four concentrations as mentioned in the table. The samples were dissolved in DMSO and mixed with assay buffer (10 mM HEPES buffer containing 0.3 M NaCl and 10 μ M zinc sulphate) containing 20 μ L kidney cortex plasma membranes (ACE enzyme source) and 1mM Hippuryl-His-Leu as substrate. The compounds were incubated with the enzyme for 10 minutes at 37 °C. Then 10 μ L of substrate (1 mM) was added which makes a final reaction volume of 50 μ L and incubated for 45min at 37 °C. The reaction is terminated by the addition of 1M HCl (0.1 mL). The yellow color is developed by the addition of 100 μ L of pyridine and 50 μ L of benzene sulphonyl chloride. The yellow color that formed is measured at 410 nm in an ELISA Plate Reader (iMARK, BIORAD).

5.13. Spectral Data

N-(((1Z,5E,8E)-4,4,8-trimethyl-7-oxocycloundeca-1,5,8-trien-1-yl)methyl) benzene sulfonamide (37a)

Following the general procedure as described in section 5.8.3, the reaction was carried out with 30 mg (0.1009 mmol) of brominated zerumbone **35** with 0.2018 mmol of benzenesulfonamide and the corresponding product was isolated in 26 mg (yield 69 %).

R_f = 0.61 (hexane/ethyl acetate = 2:3); Colorless crystalline solid.

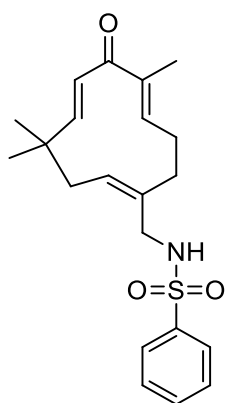
M_p = 140-144 °C.

IR (Neat) ν_{\max} : 2995, 2911, 2763, 1715, 1659 cm^{-1} .

^1H NMR (500 MHz, CDCl_3 , TMS): δ 7.90-7.88 (m, 2H), 7.56-7.54 (m, 2H), 5.95 (d, J = 16 Hz, 1H), 5.92-5.88 (m, 1H), 5.59 (d, J = 16 Hz, 1H), 5.38-5.34 (m, 1H), 4.45 (t, J = 6 Hz, 1H), 3.70 (brs, 1H), 3.18 (brs, 1H), 2.57 (brs, 1H), 2.28-2.20 (m, 2H), 2.09-2.06 (m, 2H), 1.89-1.87 (m, 1H), 1.74 (s, 3H), 1.18 (brs, 3H), 1.00 (brs, 3H) ppm.

^{13}C NMR (125 MHz, CDCl_3 , TMS): δ 203.8, 159.4, 149.2, 139.6, 138.5, 134.8, 132.9, 132.7, 130.2, 129.2, 127.3, 127.1, 126.4, 41.9, 40.4, 37.5, 34.9, 29.3, 24.2, 24.0, 11.8 ppm.

HRMS (ESI): m/z Calcd for $\text{C}_{21}\text{H}_{27}\text{NNaO}_3\text{S}$: 396.1689; Found: 396.1693.

**4-methoxy-N-(((1Z,5E,8E)-4,4,8-trimethyl-7-oxocycloundeca-1,5,8-trien-1-yl)methyl)benzenesulfonamide (37b)**

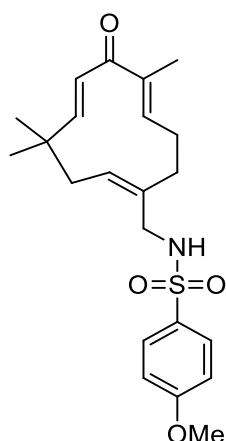
Following the general procedure as described in section 5.8.3, the reaction was carried out with 30 mg (0.1009 mmol) of brominated zerumbone **35** with 0.2018 mmol of 4-methoxybenzenesulfonamide and the corresponding products **37b** and **38b** were yielded in 18 mg and 7 mg respectively (yield 44 % and 11 %).

R_f = 0.51 (hexane/ethyl acetate = 2:3); Colorless crystalline solid.

M_p = 130-132 °C.

IR (Neat) ν_{\max} : 3195, 2921, 2883, 1711, 1349 cm^{-1} .

^1H NMR (500 MHz, CDCl_3 , TMS): δ 7.81 (d, J = 9 Hz, 2H), 6.99 (d, J = 9 Hz, 2H), 5.95 (d, J = 16.5 Hz, 1H), 5.91-5.89 (m, 1H), 5.59 (d, J = 16.5 Hz, 1H), 5.37-5.34 (m, 1H), 4.43 (brs, 1H), 3.86



(s, 3H), 3.69 (brs, 1H), 3.14 (brs, 1H), 2.59-2.53 (m, 1H), 2.32-2.27 (m, 1H), 2.19-2.12 (m, 2H), 2.09-2.00 (m, 1H), 1.94-1.86 (m, 1H), 1.73 (s, 3H), 1.18 (s, 3H), 1.01 (s, 3H) ppm.

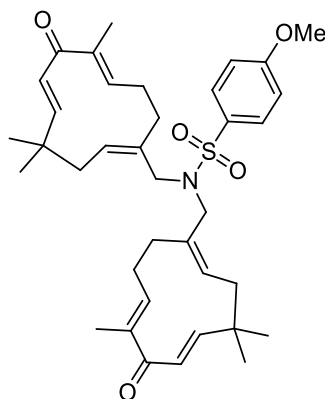
^{13}C NMR (125 MHz, CDCl_3 , TMS): δ 203.6, 159.9, 149.0, 144.5, 138.6, 135.0, 131.2, 130.2, 129.4, 128.6, 127.4, 114.3, 55.6, 41.9, 40.4, 37.5, 35.1, 29.7, 24.2, 11.9 ppm.

HRMS (ESI): m/z Calcd for $\text{C}_{22}\text{H}_{29}\text{NNaO}_4\text{S}$: 426.1715; Found: 426.1711.

4-methoxy-N,N-bis(((1Z,5E,8E)-4,4,8-trimethyl-7-oxocycloundeca-1,5,8-trien-1-yl)methyl)benzenesulfonamide (38b)

R_f = 0.64 (hexane/ethyl acetate = 2:3); Colorless crystalline solid.

Mp = 144-147 °C.



IR (Neat) ν_{max} : 3195, 2921, 2883, 1711, 1349 cm^{-1} .

^1H NMR (500 MHz, CDCl_3 , TMS): δ 7.81-7.75 (m, 2H), 7.08-6.96 (m, 2H), 5.98-5.77 (m, 3H), 5.59-5.36 (m, 5H), 3.90-3.88 (m, 3H), 3.66-3.36 (m, 4H), 2.84-2.67 (m, 3H), 2.48-2.26 (m, 6H), 2.20-1.97 (m, 3H), 1.88-1.72 (m, 6H), 1.21 (s, 6H), 1.03 (s, 6H) ppm.

^{13}C NMR (125 MHz, CDCl_3 , TMS): δ 203.5, 203.2, 160.8, 153.2, 149.1, 138.8, 129.3, 128.4, 127.5, 114.2, 56.4, 47.8, 42.2, 31.2, 24.3, 20.9, 12.4, 12.0 ppm.

HRMS (ESI): m/z Calcd for $\text{C}_{37}\text{H}_{49}\text{NNaO}_5\text{S}$: 642.3229; Found: 642.3221.

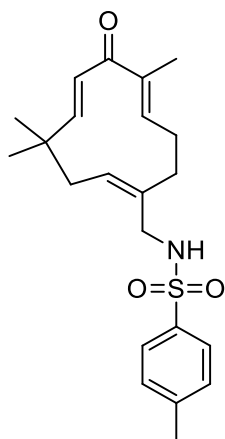
4-methyl-N-(4-(N-(((1Z,5E,8E)-4,4,8-trimethyl-7-oxocycloundeca-1,5,8-trien-1-yl)methyl)sulfamoyl)phenethyl)benzenesulfonamide (37c)

Following the general procedure as described in section 5.8.3, the reaction was carried out with 30 mg (0.1009 mmol) of brominated zerumbone **35** with 0.2018 mmol of 4-methylbenzenesulfonamide and the corresponding products **37c** and **38c** were yielded in 20 mg and 5 mg respectively (yield 51 % and 18 %).

R_f = 0.53 (hexane/ethyl acetate = 2:3); Colorless crystalline solid.

Mp = 151-153 °C.

IR (Neat) ν_{\max} : 3195, 2921, 2883, 1711, 1349 cm^{-1} .



^1H NMR (500 MHz, CDCl_3 , TMS): δ 7.74 (d, J = 8.5 Hz, 2H), 7.67 (d, J = 8.5 Hz, 2H), 7.30-7.28 (m, 4H), 5.93 (d, J = 16.5 Hz, 1H), 5.91-5.89 (m, 1H), 5.58 (d, J = 16.5 Hz, 1H), 5.36-5.32 (m, 1H), 4.91-4.88 (m, 1H), 4.77-4.74 (m, 1H), 3.67 (brs, 1H), 3.24-3.16 (m, 3H), 2.89-2.88 (m, 2H), 2.60-2.55 (m, 1H), 2.44 (s, 3H), 2.35-2.28 (m, 1H), 2.23-2.18 (m, 2H), 2.15-2.10 (m, 1H), 2.03-1.78 (m, 1H), 1.72 (s, 3H), 1.17 (s, 3H), 0.99 (s, 3H) ppm.

^{13}C NMR (125 MHz, CDCl_3 , TMS): δ 203.1, 158.9, 148.8, 143.5, 143.4, 138.6, 138.2, 136.7, 134.9, 130.1, 129.7, 129.6, 127.4, 127.2, 126.9, 126.7, 43.6, 41.9, 40.4, 37.5, 35.8, 35.0, 29.7, 24.2, 21.5, 11.8 ppm.

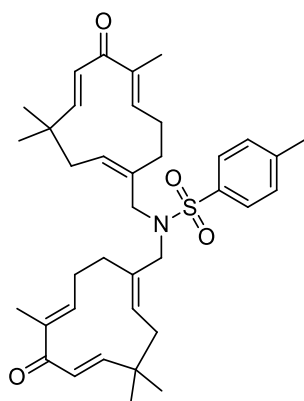
HRMS (ESI): m/z Calcd for $\text{C}_{22}\text{H}_{29}\text{NNaO}_3\text{S}$: 410.1766; Found: 410.1761.

4-methyl-N,N-bis(((1Z,5E,8E)-4,4,8-trimethyl-7-oxocycloundeca-1,5,8-trien-1-yl)methyl)benzenesulfonamide (38c)

R_f = 0.63 (hexane/ethyl acetate = 2:3); Colorless crystalline solid.

Mp = 159-163 °C.

IR (Neat) ν_{\max} : 3225, 3022, 2872, 1721, 1718, 1349 cm^{-1} .



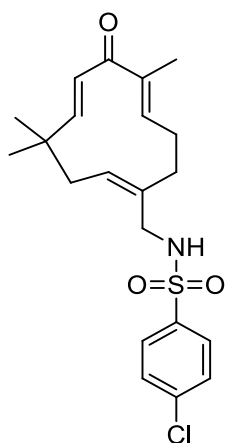
^1H NMR (500 MHz, CDCl_3 , TMS): δ 7.81-7.78 (m, 2H), 7.18-7.06 (m, 2H), 5.96-5.73 (m, 3H), 5.57-5.33 (m, 5H), 3.62-3.34 (m, 4H), 2.83-2.66 (m, 6H), 2.44-2.27 (m, 6H), 2.20-1.97 (m, 3H), 1.88-1.74 (m, 6H), 1.22 (s, 6H), 1.02 (s, 6H) ppm.

^{13}C NMR (125 MHz, CDCl_3 , TMS): δ 203.7, 203.4, 158.8, 153.1, 147.1, 136.7, 128.3, 127.4, 127.1, 114.2, 47.3, 42.2, 33.7, 31.3, 22.3, 21.9, 12.6, 11.9 ppm.

HRMS (ESI): m/z Calcd for $\text{C}_{37}\text{H}_{49}\text{NNaO}_4\text{S}$: 626.3280; Found: 626.3277.

4-chloro-N-(((1Z,5E,8E)-4,4,8-trimethyl-7-oxocycloundeca-1,5,8-trien-1-yl)methyl)benzenesulfonamide (37d)

Following the general procedure as described in section 5.8.3, the reaction was carried out with 30 mg (0.1009 mmol) of brominated zerumbone **35** with 0.2018 mmol of 4-chlorobenzenesulfonamide and the corresponding products **37d** and **38d** were yielded in 19.5 mg and 18.6 mg respectively (yield 48 % and 30 %).



R_f = 0.56 (hexane/ethyl acetate = 2:3); Colorless crystalline solid.

Mp = 155-157 °C.

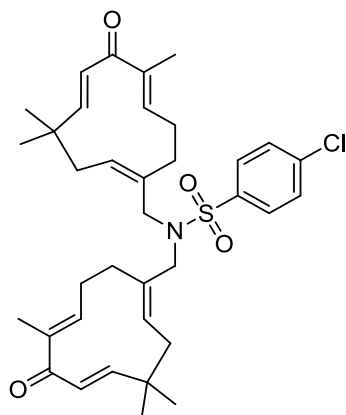
IR (Neat) ν_{\max} : 3112, 3043, 2777, 1712, 1706, 1454 cm^{-1} .

^1H NMR (500 MHz, CDCl_3 , TMS): δ 7.6 (d, J = 8.5 Hz, 2H), 7.49 (d, J = 8.5 Hz, 2H), 5.96 (d, J = 16.5 Hz, 1H), 5.93-5.89 (m, 1H), 5.59 (d, J = 16.5 Hz, 1H), 5.38-5.35 (m, 1H), 4.72-4.69 (m, 1H), 3.72 (brs, 1H), 3.20 (brs, 1H), 2.56 (brs, 1H), 2.32-2.28 (m, 1H), 2.23-2.09 (m, 3H), 2.01-1.89 (m, 1H), 1.75 (s, 3H), 1.19 (s, 3H), 1.03 (s, 3H) ppm.

^{13}C NMR (125 MHz, CDCl_3 , TMS): δ 203.3, 159.0, 148.8, 140.5, 139.3, 138.7, 138.4, 134.7, 129.5, 129.4, 128.6, 127.9, 127.4, 42.0, 40.5, 37.4, 34.9, 29.7, 24.2, 11.9 ppm.

HRMS (ESI): m/z Calcd for $\text{C}_{21}\text{H}_{26}\text{ClNNaO}_3\text{S}$: 430.1220; Found: 430.1228.

4-chloro-N,N-bis(((1Z,5E,8E)-4,4,8-trimethyl-7-oxocycloundeca-1,5,8-trien-1-yl)methyl)benzenesulfonamide (38d)



R_f = 0.62 (hexane/ethyl acetate = 2:3).

Mp = 133-136 °C.

IR (Neat) ν_{\max} : 3125, 3122, 2217, 1720, 1717, 1244 cm^{-1} .

^1H NMR (500 MHz, CDCl_3 , TMS): δ 7.85-7.79 (m, 2H), 7.19-7.03 (m, 2H), 5.97-5.75 (m, 3H), 5.59-5.36 (m, 5H), 3.66-3.39 (m, 4H), 2.84-2.67 (m, 3H), 2.48-2.29 (m, 6H), 2.22-1.97 (m, 3H), 1.89-1.76 (m, 6H), 1.26 (s, 6H), 1.01 (s, 6H) ppm.

¹³C NMR (125 MHz, CDCl₃, TMS): δ 203.3, 203.1, 156.7, 154.1, 149.1, 136.6, 128.4, 126.4, 126.1, 117.2, 42.3, 41.2, 31.3, 22.3, 21.9, 12.4, 12.1 ppm.

HRMS (ESI): m/z Calcd for C₃₆H₄₆ClNNaO₄S : 646.2734; Found: 646.2727.

N-(((1Z,5E,8E)-4,4,8-trimethyl-7-oxocycloundeca-1,5,8-trien-1-yl)methyl) methane sulfonamide (37e)

Following the general procedure as described in section 5.8.3, the reaction was carried out with 30 mg (0.1009 mmol) of brominated zerumbone **35** with 0.2018 mmol of methanesulfonamide and the corresponding product **37e** was isolated in 5 mg respectively (yield 16 %)

R_f = 0.59 (hexane/ethyl acetate = 2:3); Colorless crystalline solid.

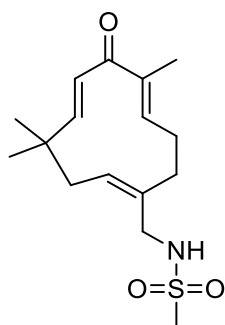
Mp = 131-134 °C.

IR (Neat) ν_{max}: 3222, 3067, 2781, 1728, 1719cm⁻¹.

¹H NMR (500 MHz, CDCl₃, TMS) : δ 5.99 (d, *J* = 16.5 Hz, 1H), 5.96-5.95 (m, 1H), 5.68 (d, *J* = 16.5 Hz, 1H), 5.48-5.45 (m, 1H), 4.18-4.15 (m, 1H), 3.98 (brs, 1H), 3.36 (brs, 1H), 2.97 (s, 3H), 2.70 (brs, 1H), 2.51-2.47 (m, 3H), 2.36-2.28 (m, 1H), 2.05 (brs, 1H), 1.82 (s, 3H), 1.25 (s, 3H), 1.16 (s, 3H) ppm.

¹³C NMR (125 MHz, CDCl₃, TMS) : δ 203.2, 159.0, 148.7, 138.8, 136.3, 130.2, 127.4, 64.4, 42.0, 40.7, 40.4, 38.0, 37.6, 34.8, 30.8, 24.3, 11.9 ppm.

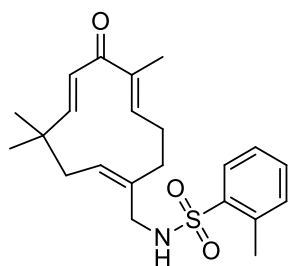
HRMS (ESI): m/z Calcd for C₁₆H₂₅NNaO₃S : 334.1453; Found: 334.1461.



2-methyl-N,N-bis(((1Z,5E,8E)-4,4,8-trimethyl-7-oxocycloundeca-1,5,8-trien-1-yl)methyl)benzenesulfonamide (37f)

Following the general procedure as described in section 5.8.3, the reaction was carried out with 30 mg (0.1009 mmol) of brominated zerumbone **35** with 0.2018 mmol of 2-methylbenzenesulfonamide and the corresponding product **37f** was isolated in 34 mg (yield 57 %).

R_f = 0.61 (hexane/ethyl acetate = 2:3); Colorless crystalline solid.



Mp = 143-146 °C.

IR (Neat) ν_{\max} : 3236, 3028, 2885, 1722, 1716, 1442 cm^{-1} .

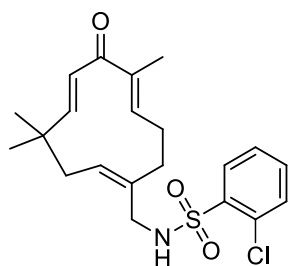
^1H NMR (500 MHz, CDCl_3 , TMS): δ 8.00-7.99 (m, 1H), 7.47-7.42 (m, 1H), 7.39- 7.37 (m, 1H), 7.32-7.30 (m, 1H), 5.94 (d, $J = 16.5$ Hz, 1H), 5.86 (brs, 1H), 5.58 (d, $J = 16.5$ Hz, 1H), 5.45-5.43 (m, 1H), 3.67-3.56 (m, 2H), 2.68 (s, 3H), 2.62 (brs, 1H), 2.46-2.40 (m, 1H), 2.32- 2.16 (m, 3H), 2.09-1.93 (m, 1H), 1.69 (s, 6H), 1.21 (s, 3H) ppm.

^{13}C NMR (125 MHz, CDCl_3 , TMS): δ 203.2, 158.7, 148.9, 140.1, 138.6, 137.8, 137.8, 136.9, 132.9, 132.7, 132.4, 42.2, 41.8, 37.3, 34.4, 30.9, 24.5, 23.5, 20.3, 11.8 ppm.

HRMS (ESI): m/z Calcd for $\text{C}_{37}\text{H}_{49}\text{NNaO}_4\text{S}$: 626.3280; Found: 626.3282.

2-chloro-N,N-bis(((1Z,5E,8E)-4,4,8-trimethyl-7-oxocycloundeca-1,5,8-trien-1-yl)methyl)benzenesulfonamide (**37g**)

Following the general procedure as described in section 5.8.3, the reaction was carried out with 30 mg (0.1009 mmol) of brominated zerumbone **35** with 0.2018 mmol of 2-chlorobenzenesulfonamide and the corresponding product **38g** was isolated in 20.6 mg (yield 33 %).



R_f = 0.615 (hexane/ethyl acetate = 2:3) ; Colorless crystalline solid.

Mp = 136-138 °C.

IR (Neat) ν_{\max} : 3143, 3166, 2232, 1721, 1709, 1452 cm^{-1} .

^1H NMR (500 MHz, CDCl_3 , TMS): δ 8.02-7.97 (m, 1H), 7.49-7.46 (m, 1H), 7.43- 7.41 (m, 1H), 7.34-7.31 (m, 1H), 6.00-5.88 (m, 2H), 5.66-5.38 (m, 1H), 3.67-3.40 (m, 2H), 2.86-2.68 (m, 1H), 2.58-2.51 (m, 2H), 2.22-1.97 (m, 1H), 1.89-1.77 (m, 2H), 1.25 (s, 6H), 1.00 (s, 3H) ppm.

^{13}C NMR (125 MHz, CDCl_3 , TMS): δ 203.3, 158.7, 155.4, 149.6, 136.5, 128.7, 125.5, 116.2, 42.3, 41.7, 31.0, 22.8, 20.6, 12.1, 12.0 ppm.

HRMS (ESI): m/z Calcd for $\text{C}_{36}\text{H}_{46}\text{ClNNaO}_4\text{S}$: 646.2734; Found: 646.2726.

4-(2-(phenylsulfonamido)ethyl)-N-(((1Z,5E,8E)-4,4,8-trimethyl-7-oxocycloundeca-1,5,8-trien-1-yl)methyl)benzenesulfonamide (37j)

Following the general procedure as described in section 5.8.3, the reaction was carried out with 30 mg (0.1009 mmol) of brominated zerumbone **35** with 0.2018 mmol of 4-aminobenzenesulfonamide derivative **36j** and the corresponding product **37j** was isolated in 36 mg (yield 69 %).

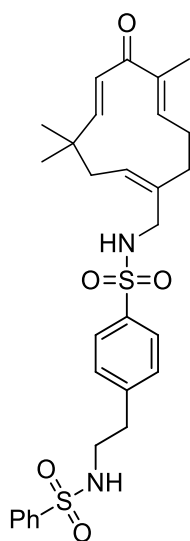
R_f = 0.45 (hexane/ethyl acetate = 2:3); Colorless amorphous solid

IR (Neat) ν_{\max} : 3077, 2921, 1594, 1417, 1317 cm^{-1} .

^1H NMR (500 MHz, CDCl_3 , TMS): δ 7.83-7.79 (m, 4H), 7.60-7.63 (m, 1H), 7.62-7.50 (m, 2H), 7.29-7.27 (m, 2H), 6.21-6.19 (m, 1H), 6.13 (d, J = 16.5 Hz, 1H), 6.05 (d, J = 16.5 Hz, 1H), 3.29-3.25 (m, 1H), 2.90-2.86 (m, 3H), 2.66-2.61 (m, 1H), 2.52-2.45 (m, 2H), 2.49-2.47 (m, 1H), 1.84 (s, 3H), 1.44-1.38 (m, 2H), 1.29-1.25 (m, 6H), 1.03 (s, 3H) ppm.

^{13}C NMR (125 MHz, CDCl_3 , TMS): δ 202.7, 157.9, 147.4, 141.2, 139.8, 132.4, 128.95, 128.6, 127.7, 127.6, 126.5, 55.5, 53.7, 50.2, 43.7, 42.4, 36.7, 36.1, 33.9, 29.4, 24.5, 23.2, 17.1, 11.3 ppm.

HRMS (ESI): m/z Calcd for $\text{C}_{29}\text{H}_{36}\text{N}_2\text{NaO}_5\text{S}_2$: 579.1963; Found: 579.1962.

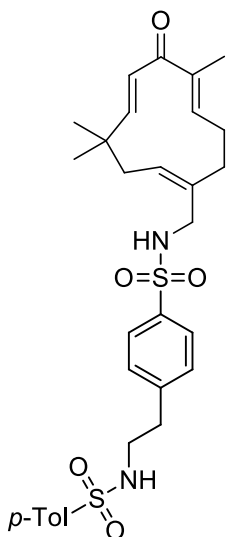


4-methyl-N-(4-(N-(((1Z,5E,8E)-4,4,8-trimethyl-7-oxocycloundeca-1,5,8-trien-1-yl)methyl)sulfamoyl)phenethyl)benzenesulfonamide (37k)

Following the general procedure as described in section 5.8.3, the reaction was carried out with 30 mg (0.1009 mmol) of brominated zerumbone **35** with 0.2018 mmol of 4-aminobenzenesulfonamide derivative **36k** and the corresponding product **37j** was isolated in 35 mg (yield 67 %).

R_f = 0.46 (hexane/ethyl acetate = 2:3); Colorless amorphous solid.

IR (Neat) ν_{\max} : 2944, 2109, 1651, 1539, 1411 cm^{-1} .



^1H NMR (500 MHz, CDCl_3 , TMS): δ 7.73-7.69 (m, 2H), 7.62-7.61 (m, 2H), 7.23-7.19 (m, 4H), 6.24-6.19 (m, 1H), 6.04 (d, $J = 16$ Hz, 1H), 5.99 (d, $J = 16$ Hz, 1H), 4.71 (brs, 1H), 3.17-3.11 (m, 2H), 2.82-2.81 (m, 3H), 2.56-2.49 (m, 1H), 2.44-2.40 (m, 1H), 2.37 (s, 3H), 2.21-2.16 (m, 1H), 1.76 (s, 3H), 1.48-1.45 (m, 1H), 1.36-1.33 (m, 1H), 1.24 (s, 3H), 1.21 (s, 3H), 0.96 (s, 3H) ppm.

^{13}C NMR (125 MHz, CDCl_3 , TMS): δ 202.2, 158.3, 147.4, 143.6, 142.7, 141.1, 139.9, 135.8, 128.9, 128.1, 127.5, 126.3, 126.1, 67.6, 54.9, 49.3, 42.7, 41.7, 34.9, 32.9, 28.2, 26.7, 23.9, 22.9, 21.1, 20.6, 16.2, 11.0 ppm.

HRMS (ESI): m/z Calcd for $\text{C}_{30}\text{H}_{38}\text{N}_2\text{NaO}_5\text{S}_2$: 593.2119; Found: 593.2116.

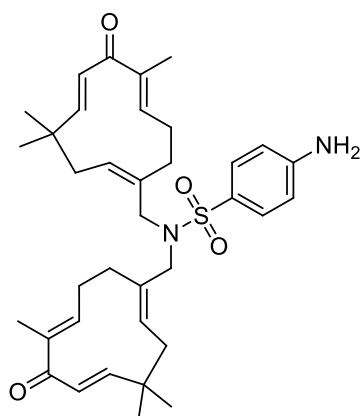
4-amino-*N,N*-bis(((1*Z*,5*E*,8*E*)-4,4,8-trimethyl-7-oxocycloundeca-1,5,8-trien-1-yl)methyl)benzenesulfonamide (**38h**)

Following the general procedure as described in section 5.8.3, the reaction was carried out with 30 mg (0.1009 mmol) of brominated zerumbone **35** with 0.2018 mmol of 4-aminobenzenesulfonamide and the corresponding product **38h** was isolated in 25.3 mg (yield 42 %).

$R_f = 0.54$ (hexane/ethyl acetate = 2:3); Colorless crystalline solid.

Mp = 161-163 °C.

IR (Neat) ν_{max} : 3433, 3146, 2231, 1718, 1716, 1242 cm^{-1} .



^1H NMR (500 MHz, CDCl_3 , TMS): δ 7.60-7.58 (m, 2H), 6.74-6.71 (m, 2H), 5.98-5.94 (m, 4H), 5.62-5.58 (m, 2H), 5.44-5.33 (m, 2H), 4.25 (s, 2H), 3.55-3.42 (m, 4H), 2.70-2.56 (m, 3H), 2.33-2.22 (m, 3H), 2.08-2.06 (m, 4H), 1.88-1.77 (m, 6H), 1.68-1.59 (m, 2H), 1.21 (s, 6H), 1.05 (s, 6H) ppm.

^{13}C NMR (125 MHz, CDCl_3 , TMS): δ 203.5, 160.6, 158.6, 150.9, 138.6, 136.9, 136.8, 130.2, 129.9, 129.0,

128.2, 127.3, 114.2, 113.9, 60.3, 43.4, 42.0, 37.5, 36.6, 30.9, 29.7, 29.4, 24.7, 24.4, 24.1, 21.0, 14.2, 11.8 ppm.

HRMS (ESI): m/z Calcd for $C_{36}H_{48}ClN_2NaO_4S$: 627.3232; Found: 627.3229.

4-nitro-N,N-bis(((1Z,5E,8E)-4,4,8-trimethyl-7-oxocycloundeca-1,5,8-trien-1-yl)methyl)benzenesulfonamide (38i)

Following the general procedure as described in section 5.8.3, the reaction was carried out with 30 mg (0.1009 mmol) of brominated zerumbone **35** with 0.2018 mmol of 4-nitrobenzenesulfonamide and the corresponding product **38i** was isolated in 29.8 mg (yield 47 %).

R_f = 0.54 (hexane/ethyl acetate = 2:3); Colorless crystalline solid.

Mp = 161-163 °C.

IR (Neat) ν_{max} : 3237, 3113, 2239, 1708, 1701 cm^{-1} .

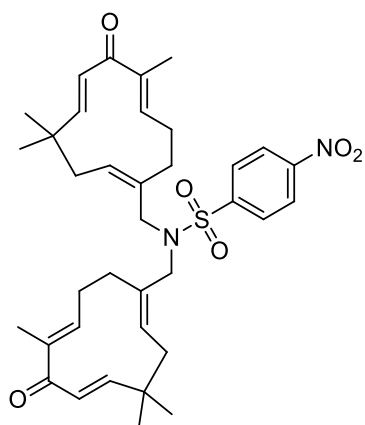
1H NMR (500 MHz, $CDCl_3$, TMS): δ 8.41-8.37 (m, 2H), 8.04-7.94 (m, 2H), 5.99 (d, J = 16.5 Hz, 2H), 5.92 (brs, 2H), 5.55 (d, J = 16.5 Hz, 2H), 5.46 (brs, 2H), 3.77-3.56 (m, 4H), 2.71 (brs, 1H), 2.64-2.62 (m, 1H), 2.53-2.48 (m, 1H), 2.41-2.26 (m, 4H), 2.13-2.02 (m, 3H), 1.94-1.88 (m, 1H), 1.81 (brs, 6H), 1.23 (brs, 6H), 1.07 (brs, 6H) ppm.

^{13}C NMR (125 MHz, $CDCl_3$, TMS): δ 203.1, 162.9, 158.4, 148.4, 145.3, 142.5, 138.8, 131.1, 130.7, 128.5, 127.6, 124.4, 111.4, 42.2, 37.5, 37.4, 36.6, 34.8, 34.7, 29.7, 29.5, 29.3, 24.2, 24.1, 24.0, 21.1, 19.8, 18.9, 11.8 ppm.

HRMS (ESI): m/z Calcd for $C_{36}H_{46}N_2NaO_6S$: 659.2974; Found: 659.2977.

3-(((1Z,5E,8E)-4,4,8-trimethyl-7-oxocycloundeca-1,5,8-trienyl)methyl)oxazolidin-2-one (40a)

Following the general procedure as described in section 5.8.3, the reaction was carried out with 30 mg (0.1009 mmol) of brominated zerumbone **35** with 0.1009 mmol of 2-oxazolidinone **39a** and the corresponding product **40a** was isolated in 26 mg (yield 85 %).



R_f = 0.59 (hexane/ethyl acetate = 1:1); Colorless crystalline solid.

Mp = 160-163 °C.

IR (Neat) ν_{\max} : 3120, 1681, 1668, 1210, 1113 cm^{-1} .

^1H NMR (500 MHz, CDCl_3 , TMS): δ .99 (d, J = 16.5 Hz, 1H), 5.96-5.95 (m, 1H), 5.73 (d, J = 16.5 Hz, 1H), 5.54-5.50 (m, 1H), 4.34-4.32 (m, 2H), 3.87-3.76 (m, 2H), 3.46-3.40 (m, 2H), 2.68 (brs, 1H), 2.64-2.40 (m, 2H), 2.29-2.22(m, 1H), 2.17-2.13 (m, 1H), 2.08-1.96 (m, 1H), 1.85 (s, 3H), 1.24 (s, 3H), 1.10 (s, 3H) ppm.

^{13}C NMR (125 MHz, CDCl_3 , TMS): δ 203.3, 158.8, 158.5, 148.7, 138.9, 135.0, 130.9, 127.6, 61.6, 44.1, 41.8, 41.3, 37.6, 34.9, 24.2, 12.0 ppm.

HRMS (ESI): m/z Calcd for $\text{C}_{18}\text{H}_{25}\text{NNaO}_3$: 326.1732; Found: 326.1731.

5-(chloromethyl)-3-(((1Z,5E,8E)-4,4,8-trimethyl-7-oxocycloundeca-1,5,8-trienyl)methyl)oxazolidin-2-one (40b)

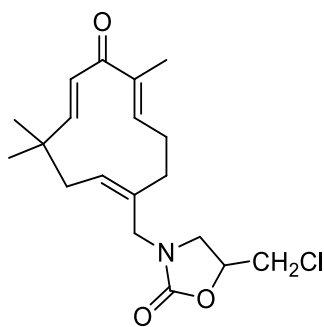
Following the general procedure as described in section 5.8.3, the reaction was carried out with 30 mg (0.1009 mmol) of brominated zerumbone **35** with 0.1009 mmol of oxazolidinone **39b** and the corresponding product **40b** was isolated in 15 mg (yield 42 %).

R_f = 0.45 (hexane/ethyl acetate = 1:2); Colorless crystalline solid.

Mp = 156-158 °C.

IR (Neat) ν_{\max} : 3218, 2997, 1673, 1665, 1188, 1122 cm^{-1} .

^1H NMR (500 MHz, CDCl_3 , TMS): δ 6.00 (d, J = 16.5 Hz, 1H), 5.96-5.91 (m, 1H), 5.71(d, J = 16.5 Hz, 1H), 5.55-5.47 (m, 1H), 4.77-5.67 (m, 1H), 3.88-3.82 (m, 1H), 3.77-3.74 (m, 1H), 3.71-3.62 (m, 2H), 3.58-3.50 (m, 1H), 3.39-3.29 (m, 1H), 2.64 (brs, 1H), 2.48-2.42 (m, 2H), 2.36-2.27 (m, 1H), 2.21 (brs, 1H), 2.13-1.96 (m, 1H), 1.85 (s, 3H), 1.25 (s, 3H), 1.11 (s, 3H) ppm.



^{13}C NMR (125 MHz, CDCl_3 , TMS): δ 203.4, 158.9, 157.2, 138.9, 134.7, 130.6, 127.6, 46.8, 44.8, 41.8, 41.1, 37.7, 34.8, 30.9, 29.4, 24.2, 12.0 ppm.

HRMS (ESI): m/z Calcd for $\text{C}_{19}\text{H}_{26}\text{NCINaO}_3$: 374.14989; Found: 374.15063.

(4*R*,5*S*)-4-methyl-5-phenyl-3-(((1*Z*,5*E*,8*E*)-4,4,8-trimethyl-7-oxocycloundeca-1,5,8-trienyl)methyl)oxazolidin-2-one (40c)

Following the general procedure as described in section 5.8.3, the reaction was carried out with 30 mg (0.1009 mmol) of brominated zerumbone **35** with 0.1009 mmol of oxazolidinone **39c** and the corresponding product **40c** was isolated in 25 mg (yield 50 %).

R_f = 0.61 (hexane/ethyl acetate = 1:2); Colorless crystalline solid.

Mp = 165-168 °C.

IR (Neat) ν_{max} : 3099, 2999, 1680, 1673, 1190, 1110 cm^{-1} .

^1H NMR (500 MHz, CDCl_3 , TMS): δ 7.40-7.33 (m, 3H), 7.27-7.26 (m, 2H), 6.02-5.96 (m, 2H), 5.74-5.71 (m, 1H), 5.57-5.53 (m, 2H), 3.96-3.90 (m, 2H), 3.77-3.73 (m, 1H), 2.75-2.73 (m, 1H), 2.54-2.52 (m, 1H), 2.40-2.38 (m, 1H), 2.28-2.26 (m, 1H), 2.16-2.14 (m, 1H), 2.00-1.98 (m, 1H), 1.88 (s, 3H), 1.24 (s, 3H), 1.08 (s, 3H), 0.721 (s, 3H) ppm.

^{13}C NMR (125 MHz, CDCl_3 , TMS): δ 203.6, 158.9, 156.8, 148.9, 139.1, 138.2, 42.2, 37.5, 29.3, 24.3, 14.6, 11.8, 7.4 ppm.

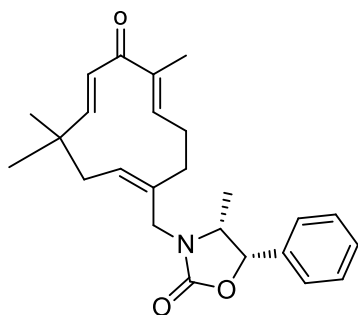
HRMS (ESI): m/z Calcd for $\text{C}_{25}\text{H}_{31}\text{NNaO}_3$: 416.2201; Found: 416.2200.

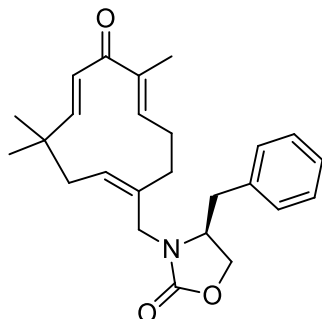
(*S*)-4-benzyl-3-(((1*Z*,5*E*,8*E*)-4,4,8-trimethyl-7-oxocycloundeca-1,5,8-trienyl)methyl)oxazolidin-2-one (40d)

Following the general procedure as described in section 5.8.3, the reaction was carried out with 30 mg (0.1009 mmol) of brominated zerumbone **35** with 0.1009 mmol of oxazolidinone **39d** and the corresponding product **40d** was isolated in 29 mg (yield 75 %).

R_f = 0.63 (hexane/ethyl acetate = 1:1); Colorless crystalline solid.

Mp = 166-168 °C.





IR (Neat) ν_{\max} : 3211, 3011, 1671, 1664, 1197, 1113 cm^{-1} .

^1H NMR (500 MHz, CDCl_3 , TMS): δ 7.33-7.30 (m, 2H), 7.27-7.26 (m, 1H), 7.12-7.09 (m, 1H), 6.02-5.94 (m, 2H), 5.71-5.68 (m, 1H), 5.59-5.57 (m, 1H), 4.19-4.16 (m, 1H), 4.03-4.01 (m, 1H), 3.93-3.90 (m, 1H), 3.83-3.80 (m, 2H), 3.06-2.91 (m, 1H), 2.72-2.70 (m, 1H), 2.64-2.60 (m, 1H), 2.40-2.36 (m, 1H), 2.29-2.24 (m, 2H), 2.22-2.20 (m, 1H), 1.99-1.97 (m, 1H), 1.86 (s, 3H), 1.25 (s, 3H), 1.08 (s, 3H) ppm.

^{13}C NMR (125 MHz, CDCl_3 , TMS): δ 203.3, 159.8, 158.6, 158.2, 149.3, 148.7, 139.0, 138.3, 135.5, 130.5, 129.0, 128.3, 127.7, 127.3, 67.0, 59.2, 54.9, 42.1, 41.9, 38.6, 37.6, 29.4, 24.2, 11.9 ppm.

HRMS (ESI): m/z Calcd for $\text{C}_{25}\text{H}_{31}\text{NNaO}_3$: 416.2201; Found: 416.2206.

4-ethyl-3-(((1Z,5E,8E)-4,4,8-trimethyl-7-oxocycloundeca-1,5,8-trienyl)methyl)oxazolidin-2-one (40e)

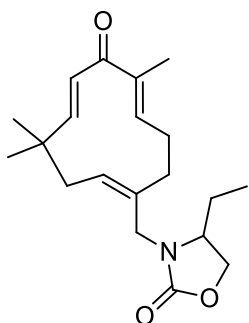
Following the general procedure as described in section 5.8.3, the reaction was carried out with 30 mg (0.1009 mmol) of brominated zerumbone **35** with 0.1009 mmol of oxazolidinone **39e** and the corresponding product **40e** was isolated in 16 mg (yield 49 %).

R_f = 0.51 (hexane/ethyl acetate = 2:1); Colorless crystalline solid.

Mp = 136-138 $^{\circ}\text{C}$.

IR (Neat) ν_{\max} : 3221, 3091, 1677, 1666, 1199, 1118 cm^{-1} .

^1H NMR (500 MHz, CDCl_3 , TMS): δ 5.99 (d, J = 16.5 Hz, 1H), 5.95-5.93 (m, 1H), 5.71 (d, J = 16.5 Hz, 1H), 5.53-5.51 (m, 1H), 4.437-4.33 (m, 1H), 3.97 (brs, 1H), 3.90-3.87 (m, 1H), 3.74-3.71 (m, 1H), 3.65-3.56 (m, 1H), 2.72 (brs, 1H), 2.39-2.37 (m, 2H), 2.24-2.22 (m, 1H), 2.08-1.98 (m, 2H), 1.86 (s, 3H), 1.65-1.62 (m, 1H), 1.49-1.46 (m, 1H), 1.25 (s, 3H), 1.10 (s, 3H), 0.89 (s, 3H) ppm.



^{13}C NMR (125 MHz, CDCl_3 , TMS): δ 203.3, 163.6, 158.6, 148.9, 139.8, 139.1, 130.3, 127.5, 59.2, 54.2, 42.2, 37.6, 30.0, 29.3, 24.3, 12.1 ppm.

HRMS (ESI): m/z Calcd for $\text{C}_{20}\text{H}_{29}\text{NNaO}_3$: 354.2045; Found: 354.2046.

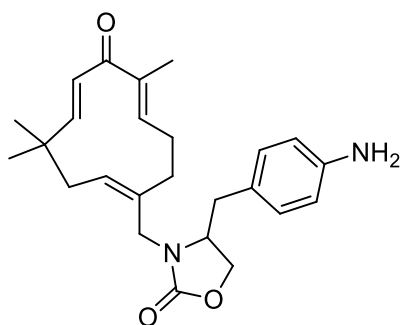
4-(4-aminobenzyl)-3-(((1Z,5E,8E)-4,4,8-trimethyl-7-oxocycloundeca-1,5,8-trienyl)methyl)oxazolidin-2-one (40f)

Following the general procedure as described in section 5.8.3, the reaction was carried out with 30 mg (0.1009 mmol) of brominated zerumbone **35** with 0.1009 mmol of oxazolidinone **39f** and the corresponding product **40f** was isolated in 30.5 mg (yield 73 %).

R_f = 0.52 (hexane/ethyl acetate = 1:3); Colorless gummy solid.

IR (Neat) ν_{max} : 3221, 3021, 1681, 1665, 1186 cm^{-1} .

^1H NMR (500 MHz, CDCl_3 , TMS): δ 6.86 (d, J = 8 Hz, 2H), 6.60 (d, J = 8.5 Hz, 2H), 6.99 (d, J = 16.5 Hz, 1H), 5.95-5.93 (m, 1H), 5.69 (d, J = 16.5 Hz, 1H), 5.57-5.55 (m, 1H), 4.17-3.99 (m, 3H), 3.91-3.74 (m, 3H), 3.70-3.65 (m, 1H), 2.92-2.90 (m, 1H), 2.74-2.67 (m, 1H), 2.52-2.47 (m, 1H), 2.39-2.35 (m, 1H), 2.32-2.21 (m, 2H), 2.21-2.20 (m, 1H), 1.99-1.96 (m, 1H), 1.86 (s, 3H), 1.25 (s, 3H), 1.09 (s, 3H) ppm.

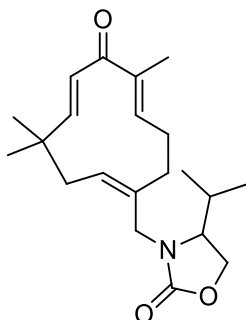


^{13}C NMR (125 MHz, CDCl_3 , TMS): δ 203.3, 163.6, 158.6, 148.9, 139.8, 139.1, 130.3, 127.5, 59.2, 54.2, 42.2, 37.6, 30.0, 29.3, 24.3, 12.1 ppm.

HRMS (ESI): m/z Calcd for $\text{C}_{25}\text{H}_{32}\text{N}_2\text{NaO}_3$: 431.2310; Found: 431.2303.

4-isopropyl-3-(((1Z,5E,8E)-4,4,8-trimethyl-7-oxocycloundeca-1,5,8-trienyl)methyl)oxazolidin-2-one (40g)

Following the general procedure as described in section 5.8.3, the reaction was carried out with 30 mg (0.1009 mmol) of brominated zerumbone **35** with 0.1009 mmol of oxazolidinone **39g** and the corresponding product **40g** was isolated in 27 mg (yield 78 %).



R_f = 0.68 (hexane/ethyl acetate = 1:1); Colorless gummy solid.

IR (Neat) ν_{\max} : 3231, 3001, 1681, 1674, 1186, 1115 cm^{-1} .

$^1\text{H NMR}$ (500 MHz, CDCl_3 , TMS): δ 6.01-5.95 (m, 2H), 5.73 (d, J = 16.5 Hz, 1H), 5.56-5.53 (m, 1H), 4.24-4.20 (m, 1H), 4.10-4.07 (m, 1H), 3.94-3.91 (m, 1H), 3.72-3.69 (m, 1H), 3.55 (brs, 1H), 2.77-2.66 (m, 1H), 2.36-2.34 (m, 2H), 2.24-2.21 (m, 1H), 2.13-2.09 (m, 1H), 2.06-2.02 (m, 1H), 1.99-1.94 (m, 1H), 1.86 (s, 3H), 1.25 (s, 3H), 1.11 (s, 3H), 0.88 (d, J = 7 Hz, 6H) ppm.

$^{13}\text{C NMR}$ (125 MHz, CDCl_3 , TMS): δ 203.4, 158.8, 158.6, 148.8, 139.0, 134.9, 130.3, 127.6, 62.5, 57.8, 41.8, 38.3, 37.6, 34.7, 29.7, 29.4, 27.4, 24.2, 17.6, 14.2, 11.9 ppm.

HRMS (ESI): m/z Calcd for $\text{C}_{21}\text{H}_{31}\text{NNaO}_3$: 368.2201; Found: 368.2200.

4-(2-(methylthio)ethyl)-3-(((1Z,5E,8E)-4,4,8-trimethyl-7-oxocycloundeca-1,5,8-trienyl)methyl)oxazolidin-2-one (**40h**)

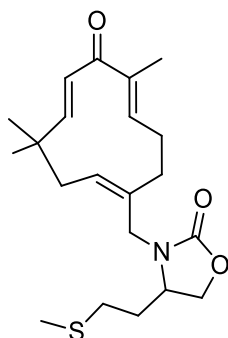
Following the general procedure as described in section 5.8.3, the reaction was carried out with 30 mg (0.1009 mmol) of brominated zerumbone **35** with 0.1009 mmol of oxazolidinone **39h** and the corresponding product **40h** was isolated in 21 mg (yield 55 %).

R_f = 0.61 (hexane/ethyl acetate = 1:1); Colorless gummy solid.

IR (Neat) ν_{\max} : 3221, 3017, 1681, 1674, 1188, 1122 cm^{-1} .

$^1\text{H NMR}$ (500 MHz, CDCl_3 , TMS): δ 6.00-5.93 (m, 2H), 5.71 (d, J = 16.5 Hz, 1H), 5.56-5.49 (m, 1H), 4.42-4.39 (m, 1H), 4.00 (brs, 1H), 3.89-3.86 (m, 1H), 3.77-3.74 (m, 2H), 2.71-2.68 (m, 1H), 2.63-2.36 (m, 4H), 2.30-2.21 (m, 2H), 2.09 (s, 3H), 2.03-1.89 (m, 2H), 1.85 (s, 3H), 1.71-1.70 (m, 1H), 1.25 (s, 3H), 1.11 (s, 3H) ppm.

$^{13}\text{C NMR}$ (125 MHz, CDCl_3 , TMS): δ 203.3, 158.9, 157.9, 139.1, 134.7, 130.6, 127.5, 57.1, 52.6, 41.9, 37.8, 34.1, 30.9, 29.7, 29.1, 24.3, 15.7, 12.1 ppm.



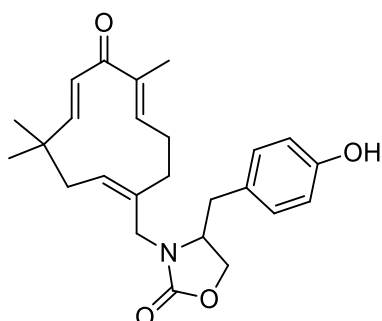
HRMS (ESI): m/z Calcd for $C_{21}H_{31}NSO_3$: 400.1922; Found: 400.1882.

4-(4-hydroxybenzyl)-3-(((1Z,5E,8E)-4,4,8-trimethyl-7-oxocycloundeca-1,5,8-trienyl)methyl)oxazolidin-2-one (40i)

Following the general procedure as described in section 5.8.3, the reaction was carried out with 30 mg (0.1009 mmol) of brominated zerumbone **35** with 0.1009 mmol of oxazolidinone **39i** and the corresponding product **40i** was isolated in 23 mg (yield 56 %).

R_f = 0.57 (hexane/ethyl acetate = 1:2); Colorless gummy solid.

IR (Neat) ν_{max} : 3223, 3008, 1672, 1669, 1199 cm^{-1} .



1H NMR (500 MHz, $CDCl_3$, TMS): δ 7.13-7.08 (m, 1H), 6.85-6.60 (m, 2H), 6.07-6.02 (m, 3H), 5.73 (s, 1H), 5.52-5.48 (m, 1H), 4.49-4.45 (m, 1H), 4.43-4.42 (m, 1H), 4.35-4.33 (m, 1H), 4.14-4.12 (m, 1H), 3.84 (s, 2H), 2.82-2.79 (m, 2H), 2.71-2.69 (m, 1H), 2.67-2.55 (m, 1H), 2.45-2.40 (m, 1H), 2.31-2.23 (m, 2H), 1.81 (s, 3H), 1.25 (s, 3H), 1.07 (s, 3H) ppm.

^{13}C NMR (125 MHz, $CDCl_3$, TMS): δ 203.7, 160.0, 158.1, 157.4, 149.2, 138.6, 136.3, 130.3, 130.0, 128.2, 127.4, 114.9, 114.6, 69.4, 65.4, 60.3, 53.8, 42.6, 40.6, 37.3, 36.1, 24.9, 14.2, 12.2 ppm.

HRMS (ESI): m/z Calcd for $C_{25}H_{31}NCINaO_3$: 400.19223; Found: 432.21507.

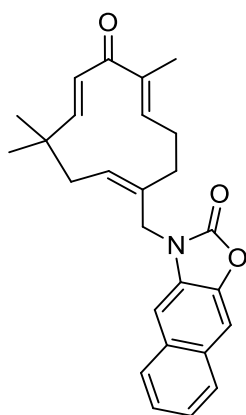
3-(((1Z,5E,8E)-4,4,8-trimethyl-7-oxocycloundeca-1,5,8-trienyl)methyl)naphtho[2,3-d]oxazol-2(3H)-one (40j)

Following the general procedure as described in section 5.8.3, the reaction was carried out with 30 mg (0.1009 mmol) of brominated zerumbone **35** with 0.1009 mmol of oxazolidinone **39j** and the corresponding product **40j** was isolated in 32 mg (yield 80 %).

R_f = 0.59 (hexane/ethyl acetate = 1:1); Colorless crystalline solid.

Mp = 127-131 $^{\circ}C$.

IR (Neat) ν_{max} : 3111, 2911, 1681, 1666, 1191 cm^{-1} .



¹H NMR (500 MHz, CDCl₃, TMS): δ 7.83-7.81 (m, 1H), 7.77-7.75 (m, 1H), 7.58 (s, 1H), 7.45-7.43 (m, 2H), 7.09 (s, 1H), 6.01(d, *J* = 16.5 Hz, 1H), 6.02-5.99 (m, 1H), 5.86 (d, *J* = 16.5 Hz, 1H), 5.88-5.65 (m, 1H), 4.48-4.42 (m, 2H), 2.69 (brs, 2H), 2.36-2.14 (m, 4H), 1.89 (s, 3H), 1.32 (s, 3H), 1.21 (s, 3H) ppm.

¹³C NMR (125 MHz, CDCl₃, TMS): δ 203.5, 158.8, 156.0, 148.6, 142.5, 134.1, 131.2, 131.0, 130.9, 130.2, 128.2, 128.1, 127.4, 126.8, 125.3, 106.7, 104.9, 42.5, 40.5, 38.1, 34.8, 24.5, 12.2 ppm.

HRMS (ESI): *m/z* Calcd for C₂₆H₂₇NNaO₃ : 424.1888; Found: 424.1882.

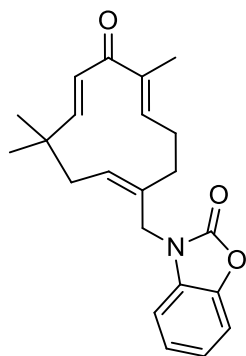
3-(((1Z,5E,8E)-4,4,8-trimethyl-7-oxocycloundeca-1,5,8-trienyl)methyl)benzo[d]oxazol-2(3H)-one (40k)

Following the general procedure as described in section 5.8.3, the reaction was carried out with 30 mg (0.1009 mmol) of brominated zerumbone **35** with 0.1009 mmol of oxazolidinone **39k** and the corresponding product **40k** was isolated in 26 mg (yield 74 %).

R_f = 0.60 (hexane/ethyl acetate = 1:1); Colorless crystalline solid.

Mp = 124-127 °C.

IR (Neat) ν_{\max} : 3221, 3002, 1677, 1662, 1201 cm⁻¹.



¹H NMR (500 MHz, CDCl₃, TMS): δ 7.26-7.21 (m, 1H), 7.13-7.11 (m, 2H), 6.85-6.84 (m, 1H), 6.04 (d, *J* = 16.5 Hz, 1H), 6.00-5.97 (m, 1H), 5.82 (d, *J* = 16.5 Hz, 1H), 5.63-5.59 (m, 1H), 4.42-4.35 (m, 2H), 2.75-2.61 (m, 2H), 2.30-2.05 (m, 4H), 1.88 (s, 3H), 1.29 (s, 3H), 1.18 (s, 3H) ppm.

¹³C NMR (125 MHz, CDCl₃, TMS): δ 203.9, 159.9, 149.8, 130.1, 127.3, 127.2, 124.0, 122.7, 121.7, 118.5, 115.3, 111.8, 110.2, 109.8, 66.1, 42.3, 37.6, 36.9, 29.4, 24.9, 142.2, 12.2 ppm.

HRMS (ESI): m/z Calcd for C₂₂H₂₅NNaO₃ : 374.1732;

Found: 374.1738.

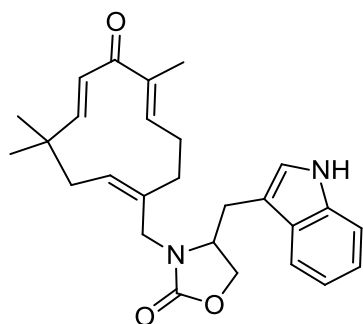
4-((1H-indol-3-yl)methyl)-3-(((1Z,5E,8E)-4,4,8-trimethyl-7-oxocycloundeca-1,5,8-trienyl)methyl)oxazolidin-2-one (40I)

Following the general procedure as described in section 5.8.3, the reaction was carried out with 30 mg (0.1009 mmol) of brominated zerumbone **35** with 0.1009 mmol of oxazolidinone **39I** and the corresponding product **40I** was isolated in 21 mg (yield 64 %).

R_f = 0.56 (hexane/ethyl acetate = 1:1); Colorless crystalline solid.

Mp = 144-147 °C.

IR (Neat) ν_{\max} : 3117, 3031, 1673, 1661, 1207, 1118 cm⁻¹.



¹H NMR (500 MHz, CDCl₃, TMS): δ 8.37 (s, 1H), 7.44-7.39 (m, 1H), 7.23-7.21 (m, 1H), 7.17-7.15 (m, 1H), 7.13-7.03 (m, 1H), 6.03-5.97 (m, 2H), 5.73-5.70 (m, 1H), 5.65-5.62 (m, 1H), 4.19-4.14 (m, 1H), 4.08-4.06 (m, 1H), 3.97-3.90 (m, 2H), 3.23-3.20 (s, 1H), 2.80-2.73 (m, 2H), 2.43-2.41 (m, 1H), 2.30-2.26 (m, 2H), 2.22-2.14 (s, 1H), 2.09-1.95 (s, 1H), 1.87 (s, 3H), 1.25 (s, 3H), 1.18-1.3 (m, 1H), 1.05 (s, 3H) ppm.

¹³C NMR (125 MHz, CDCl₃, TMS): δ 203.4, 158.6, 158.5, 149.0, 139.1, 136.4, 135.2, 130.5, 127.6, 127.1, 122.7, 122.4, 119.9, 118.0, 111.7, 109.4, 67.4, 53.6, 41.8, 37.6, 36.6, 34.5, 29.4, 28.4, 24.2, 14.2, 11.9 ppm.

HRMS (ESI): m/z Calcd for C₂₇H₃₂N₂NaO₃ : 455.2310;

Found: 455.2360.

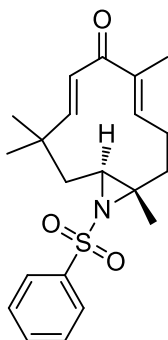
(4E,7E)-1,5,9,9-tetramethyl-12-(phenylsulfonyl)-12-azabicyclo[9.1.0]dodeca-4,7-dien-6-one (52a)

Following the general procedure as described in section 5.8.3, the reaction was carried out with 30 mg (0.1376 mmol) of zerumbone **1** with 0.2752 mmol of sulfonamide **51a** and the corresponding product **52a** was isolated in 32 mg (yield 62 %).

R_f = 0.62 (hexane/ethyl acetate = 2:3); Colorless solid.

Mp = 130-134 °C.

IR (Neat) ν_{\max} : 2935, 2908, 2863, 1725, 1649 cm^{-1} .



^1H NMR (500 MHz, CDCl_3 , TMS): δ 7.91-7.89 (m, 2H), 7.62-7.60 (m, 1H), 7.55-7.52 (m, 2H), 6.21-6.18 (m, 1H), 6.13 (d, $J = 16.5$ Hz, 1H), 6.06 (d, $J = 16.5$ Hz, 1H), 2.89-2.87 (m, 1H), 2.65-2.64 (m, 1H), 2.51-2.47 (m, 2H), 2.29-2.24 (m, 1H), 1.84 (s, 3H), 1.52-1.49 (m, 1H), 1.42-1.40 (m, 1H), 1.28 (s, 6H), 1.01 (s, 3H) ppm.

^{13}C NMR (125 MHz, CDCl_3 , TMS): δ 202.0, 158.8, 147.4, 141.4, 140.0, 132.9, 128.9, 128.5, 127.0, 56.6, 50.2, 42.6, 36.9, 33.9, 29.2, 24.9, 23.9, 17.7, 12.0 ppm.

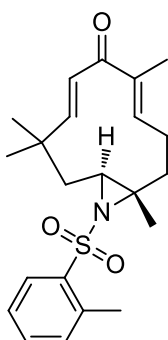
HRMS (ESI): m/z Calcd for $\text{C}_{21}\text{H}_{27}\text{NNaO}_3\text{S}$: 396.1609; Found: 396.1593.

(4E,7E)-1,5,9,9-tetramethyl-12-(*o*-tolylsulfonyl)-12-azabicyclo[9.1.0]dodeca-4,7-dien-6-one (52b)

Following the general procedure as described in section 5.8.3, the reaction was carried out with 30 mg (0.1376 mmol) of zerumbone **1** with 0.2752 mmol of sulfonamide **51b** and the corresponding product **52b** was isolated in 21 mg (yield 40 %).

$R_f = 0.67$ (hexane/ethyl acetate = 2:3); Colorless foam.

IR (Neat) ν_{\max} : 2961, 2892, 2359, 1766, 1731, 1653 cm^{-1} .



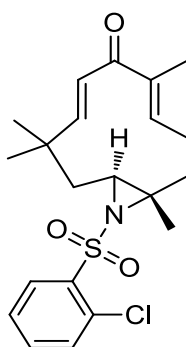
^1H NMR (500 MHz, CDCl_3 , TMS): δ 7.94-7.93 (m, 1H), 7.49-7.46 (m, 1H), 7.35-7.31 (m, 2H), 6.21-6.19 (m, 1H), 6.11 (d, $J = 16.5$ Hz, 1H), 6.05 (d, $J = 16.5$ Hz, 1H), 2.87-2.84 (m, 1H), 2.73 (s, 3H), 2.67-2.63 (m, 1H), 2.51-2.47 (m, 2H), 2.28-2.23 (m, 1H), 1.84 (s, 3H), 1.47-1.39 (m, 2H), 1.28 (s, 3H), 1.23 (s, 3H), 0.99 (s, 3H) ppm.

^{13}C NMR (125 MHz, CDCl_3 , TMS): δ 201.9, 158.6, 147.1, 140.0, 139.3, 138.1, 133.0, 132.4, 128.5, 128.4, 126.0, 56.4, 49.8, 42.7, 36.9, 34.0, 29.2, 25.0, 23.9, 20.5, 17.5, 12.1 ppm.

HRMS (ESI): m/z Calcd for $\text{C}_{22}\text{H}_{29}\text{NNaO}_3\text{S}$: 410.1765; Found: 410.1759.

**(4E,7E)-12-((2-chlorophenyl)sulfonyl)-1,5,9,9-tetramethyl-12-azabicyclo
[9.1.0]dodeca-4,7-dien-6-one (52c)**

Following the general procedure as described in section 5.8.3, the reaction was carried out with 30 mg (0.1376 mmol) of zerumbone **1** with 0.2752 mmol of sulfonamide **51c** and the corresponding product **52c** was isolated in 14 mg (yield 24 %).



R_f = 0.72 (hexane/ethyl acetate = 2:3); Colorless foam.

IR (Neat) ν_{\max} : 3066, 2484, 1645, 1704, 1570, 1489 cm^{-1} .

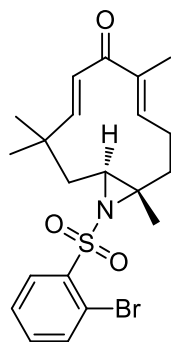
^1H NMR (500 MHz, CDCl_3 , TMS): δ 8.12-8.10 (m, 1H), 7.56-7.51 (m, 2H), 7.45-7.26 (m, 1H), 6.23-6.21 (m, 1H), 6.15 (d, J = 16.5 Hz, 1H), 6.09 (d, J = 16.5 Hz, 1H), 3.08-3.06 (m, 1H), 2.83-2.80 (m, 1H), 2.52-2.51 (m, 2H), 2.23-2.18 (m, 1H), 1.86 (s, 3H), 1.47-1.42 (m, 1H), 1.31 (s, 3H), 1.30 (s, 3H), 1.26-1.25 (m, 1H), 1.04 (s, 3H) ppm.

^{13}C NMR (125 MHz, CDCl_3 , TMS): δ 202.6, 159.4, 147.7, 140.1, 139.0, 133.9, 132.0, 131.9, 130.2, 128.5, 127.2, 56.5, 51.7, 42.8, 36.1, 34.9, 29.3, 25.1, 23.8, 17.6, 12.1 ppm.

HRMS (ESI): m/z Calcd for $\text{C}_{21}\text{H}_{26}\text{ClNNaO}_3\text{S}$: 430.1219; Found: 430.1221.

**(4E,7E)-12-((2-bromophenyl)sulfonyl)-1,5,9,9-tetramethyl-12-azabicyclo
[9.1.0]dodeca-4,7-dien-6-one (52d)**

Following the general procedure as described in section 5.8.3, the reaction was carried out with 30 mg (0.1376 mmol) of zerumbone **1** with 0.2752 mmol of sulfonamide **51d** and the corresponding product **52d** was isolated in 26 mg (yield 42 %).



R_f = 0.66 (hexane/ethyl acetate = 2:3); Colorless foam.

IR (Neat) ν_{\max} : 2963, 1650, 1450, 187, 1325 cm^{-1} .

^1H NMR (500 MHz, CDCl_3 , TMS): δ 8.15-8.13 (m, 1H), 7.76-7.75 (m, 1H), 7.48-7.47 (m, 1H), 7.44-7.42 (m, 1H), 6.23-6.20 (m, 1H), 6.15 (d, J = 16.5 Hz, 1H), 6.08 (d, J = 16.5 Hz, 1H), 3.07-3.05 (m, 1H), 2.82-2.80 (m, 1H), 2.53-2.51 (m, 2H), 2.21-2.18 (m, 1H), 1.86 (s, 3H), 1.83-1.80 (m, 1H), 1.48-1.44 (m, 1H), 1.32 (s, 3H), 1.29 (s, 3H), 1.03 (s, 3H) ppm.

¹³C NMR (125 MHz, CDCl₃, TMS): δ 202.6, 159.4, 147.7, 140.6, 140.1, 135.5, 133.9, 130.5, 128.6, 127.7, 120.3, 56.4, 51.5, 42.7, 36.2, 34.9, 29.4, 25.1, 23.9, 17.5, 12.1 ppm.

HRMS (ESI): m/z Calcd for C₂₁H₂₆BrNNaO₃S : 474.0714; Found: 474.0700 and 476.0680.

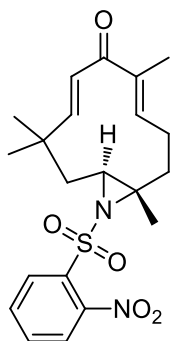
(4E,7E)-1,5,9,9-tetramethyl-12-((2-nitrophenyl)sulfonyl)-12-azabicyclo[9.1.0]dodeca-4,7-dien-6-one (52e)

Following the general procedure as described in section 5.8.3, the reaction was carried out with 30 mg (0.1376 mmol) of zerumbone **1** with 0.2752mmol of sulfonamide **51e** and the corresponding product **52e** was isolated in 25 mg (yield 42 %).

R_f = 0.67 (hexane/ethyl acetate = 2:3) ; Colorless solid.

Mp = 122-124 °C.

IR (Neat) ν_{\max} : 2925, 2856, 2357, 2154, 1648 cm⁻¹.



¹H NMR (500 MHz, CDCl₃, TMS): δ 8.21-8.18 (m, 1H), 7.75-7.74 (m, 3H), 6.21-6.16 (m, 2H), 6.09 (d, *J* = 16.5 Hz, 1H), 3.09-3.07 (m, 1H), 2.85-2.82 (m, 1H), 2.54-2.50 (m, 2H), 2.10-2.05 (m, 1H), 1.99-1.96 (m, 1H), 1.86 (s, 3H), 1.47 -1.44 (m, 1H), 1.39 (s, 3H), 1.33 (s, 3H), 1.04 (s, 3H) ppm.

¹³C NMR (125 MHz, CDCl₃, TMS): δ 202.6, 159.6, 148.1, 147.5, 140.2, 134.8, 133.9, 132.4, 130.7, 128.7, 124.2, 58.0, 52.8, 42.5, 36.1, 35.2, 29.5, 25.1, 23.8, 17.4, 12.1 ppm.

HRMS (ESI): m/z Calcd for C₂₁H₂₆N₂NaO₅S : 441.1460; Found: 441.1441.

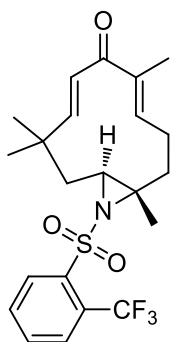
(4E,7E)-1,5,9,9-tetramethyl-12-((2-(trifluoromethyl)phenyl)sulfonyl)-12-azabicyclo[9.1.0] dodeca-4,7-dien-6-one (52f)

Following the general procedure as described in section 5.8.3, the reaction was carried out with 30 mg (0.1376 mmol) of zerumbone **1** with 0.2752mmol of sulfonamide **51f** and the corresponding product **52f** was isolated in 28 mg (yield 46 %).

R_f = 0.67 (hexane/ethyl acetate = 2:3) ; Colorless solid.

IR (Neat) ν_{\max} : 2923, 2359, 2333, 1651, 1452, 1370 cm⁻¹.

¹H NMR (500 MHz, CDCl₃, TMS): δ 8.29-8.26 (m, 1H), 7.89-7.88 (m, 1H), 7.74-7.71 (m, 2H), 6.21-6.19 (m, 1H), 6.14 (d, *J*



= 16.5 Hz, 1H), 6.05 (d, $J = 16.5$ Hz, 1H), 3.01-2.99 (m, 1H), 2.85-2.81 (m, 1H), 2.53-2.49 (m, 2H), 2.15-2.12 (m, 1H), 1.85 (s, 3H), 1.60-1.59 (m, 1H), 1.42-1.40 (m, 1H), 1.29 (s, 3H), 1.28 (s, 3H), 1.01 (s, 3H) ppm.

^{13}C NMR (125 MHz, CDCl_3 , TMS): δ 202.0, 158.9, 147.4, 140.4, 140.1, 132.8, 132.3, 131.2, 128.6, 128.1, 56.9, 51.7, 42.6, 36.9, 35.0, 30.9, 29.4, 25.0, 23.7, 17.3, 12.1 ppm.

HRMS (ESI): m/z Calcd for $\text{C}_{22}\text{H}_{26}\text{F}_3\text{NNaO}_3\text{S}$: 464.1483; Found: 464.1467.

(4E,7E)-12-((2,3-dichlorophenyl)sulfonyl)-1,5,9,9-tetramethyl-12-azabicyclo[9.1.0]dodeca-4,7-dien-6-one (52g)

Following the general procedure as described in section 5.8.3, the reaction was carried out with 30 mg (0.1376 mmol) of zerumbone **1** with 0.2752mmol of sulfonamide **51g** and the corresponding product **52g** was isolated in 47 mg (yield 78 %).

$R_f = 0.63$ (hexane/ethyl acetate = 2:3); Colorless solid.

Mp= 136-139 °C.

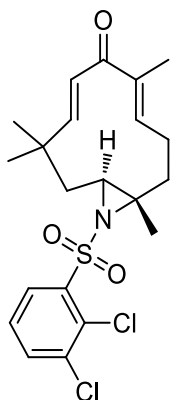
IR (Neat) ν_{max} : 2933, 1644, 1538, 1402, 1322, 1266 cm^{-1} .

^1H NMR (500 MHz, CDCl_3 , TMS): 8.04 (dd, $J_1 = 8$ Hz, $J_2 = 1.5$ Hz, 1H), 7.70 (dd, $J_1 = 8$ Hz, $J_2 = 1.5$ Hz, 1H), 7.38 (t, $J = 8$ Hz, 1H), 6.22-6.20 (m, 1H), 6.14 (d, $J = 16$ Hz, 1H), 6.08 (d, $J = 16.5$ Hz, 1H), 3.07-3.05 (m, 1H), 2.84-2.81 (m, 1H), 2.54-2.52 (m, 2H), 2.17-2.13 (m, 1H), 1.87 (s, 3H), 1.87-1.85 (m, 1H), 1.47-1.42 (m, 1H), 1.32 (s, 3H), 1.31 (s, 3H), 1.06 (s, 3H) ppm.

^{13}C NMR (125 MHz, CDCl_3 , TMS): δ 202.0, 159.0, 147.2, 141.1, 140.1, 135.6, 134.5, 130.6, 128.6, 127.4, 56.9, 51.8, 42.8, 36.1, 35.1, 29.3, 25.0, 23.8, 17.5, 12.1 ppm.

HRMS (ESI): m/z Calcd for $\text{C}_{21}\text{H}_{25}\text{Cl}_2\text{NNaO}_3\text{S}$: 464.0829; Found: 464.0820.

(4E,7E)-1,5,9,9-tetramethyl-12-((3-(trifluoromethyl)phenyl)sulfonyl)-12-azabicyclo[9.1.0]dodeca-4,7-dien-6-one (52h)



Following the general procedure as described in section 5.8.3, the reaction was carried out with 30 mg (0.1376 mmol) of zerumbone **1** with 0.2752mmol of sulfonamide **51h** and the corresponding product **52h** was isolated in 39 mg (yield 54 %).

R_f = 0.66 (hexane/ethyl acetate = 2:3) ; Colorless solid.

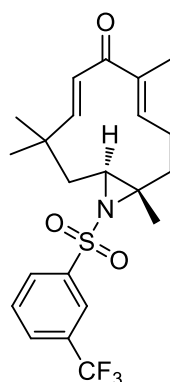
Mp=146-148 °C.

IR (Neat) ν_{\max} : 1628,1566,1523,1461 cm^{-1} .

¹H NMR (500 MHz, CDCl_3 , TMS): δ 8.18 (s, 1H), 8.13-8.11 (m, 1H), 7.89-7.88 (m, 1H), 7.72-7.69 (m, 1H), 6.20-6.19 (m, 1H), 6.16 (d, $J = 16.5$ Hz, 1H), 6.07 (d, $J = 16.5$ Hz, 1H), 2.96-2.94 (m, 1H), 2.70-2.67 (m, 1H), 2.63-2.49 (m, 2H) 2.28-2.22 (m, 1H), 1.86 (s, 3H), 1.48-1.44 (m, 2H), 1.30 (s, 3H), 1.28 (s, 3H), 1.02 (s, 3H) ppm.

¹³C NMR (125 MHz, CDCl_3 , TMS): δ 202.5, 159.0, 147.5, 142.4, 140.2, 130.1, 129.9, 129.7, 128.6, 124.1, 122.1, 56.7, 50.9, 42.5, 37.0, 34.2, 29.1, 24.9, 23.8, 17.6, 12.0 ppm.

HRMS (ESI): m/z Calcd for $\text{C}_{22}\text{H}_{26}\text{F}_3\text{NNaO}_3\text{S}$: 464.1483; Found: 464.1464.



(4E,7E)-1,5,9,9-tetramethyl-12-tosyl-12-azabicyclo[9.1.0]dodeca-4,7-dien-6-one (52i)

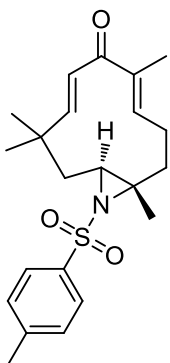
Following the general procedure as described in section 5.8.3, the reaction was carried out with 30 mg (0.1376 mmol) of zerumbone **1** with 0.2752mmol of sulfonamide **51i** and the corresponding product **52i** was isolated in 28 mg (yield 53 %).

R_f = 0.57 (hexane/ethyl acetate = 2:3) ; Colorless solid

Mp = 140-144 °C.

IR (Neat) ν_{\max} : 2350, 2340, 1641 cm^{-1} .

¹H NMR (500 MHz, CDCl_3 , TMS): δ 7.78 (d, $J = 8$ Hz, 2H), 7.32 (d, $J = 8$ Hz, 2H), 6.21-6.18 (m, 1H), 6.12 (d, $J = 16$ Hz, 1H), 6.05 (d, $J = 16.5$ Hz, 1H), 2.89-2.85 (m, 1H), 2.63-2.60 (m, 1H), 2.53-2.47 (m, 2H), 2.46 (s, 3H), 2.29-2.23 (m, 1H), 1.84 (s, 3H), 1.43-1.39 (m, 2H), 1.28 (s, 3H), 1.26 (s, 3H), 1.01 (s, 3H) ppm.



^{13}C NMR (125 MHz, CDCl_3 , TMS): δ 201.9, 158.9, 147.4, 143.8, 140.2, 138.3, 129.6, 128.3, 126.9, 55.3, 50.0, 42.6, 36.9, 33.7, 29.2, 25.0, 23.9, 21.6, 17.6, 12.1 ppm.

HRMS (ESI): m/z Calcd for $\text{C}_{22}\text{H}_{29}\text{NNaO}_3\text{S}$: 410.1765; Found: 410.1772.

(4*E*,7*E*)-12-((4-chlorophenyl)sulfonyl)-1,5,9,9-tetramethyl-12-azabicyclo [9.1.0]dodeca-4,7-dien-6-one (52j)

Following the general procedure as described in section 5.8.3, the reaction was carried out with 30 mg (0.1376 mmol) of zerumbone **1** with 0.2752mmol of sulfonamide **51j** and the corresponding product **52j** was isolated in 30 mg (yield 53 %).

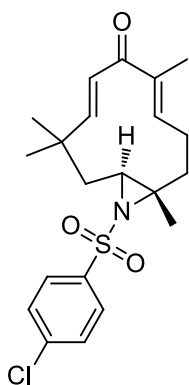
R_f = 0.66 (hexane/ethyl acetate = 2:3) ; Colorless foam.

IR (Neat) ν_{max} : 2995, 2886, 1649, 1480 cm^{-1} .

^1H NMR (500 MHz, CDCl_3 , TMS): δ 7.85 (d, J = 8.5 Hz, 2H), 7.51 (d, J = 9 Hz, 2H), 6.19-6.17 (m, 1H), 6.14 (d, J = 16.5 Hz, 1H), 6.05 (d, J = 16.5 Hz, 1H), 2.90-2.87 (m, 1H), 2.67-2.62 (m, 1H), 2.51-2.48 (m, 2H), 2.26-2.19 (m, 1H), 1.85 (s, 3H), 1.53-1.49 (m, 1H), 1.44-1.39 (m, 1H), 1.28 (s, 6H), 1.02 (s, 3H) ppm.

^{13}C NMR (125 MHz, CDCl_3 , TMS): δ 202.1, 158.8, 147.3, 140.1, 139.9, 139.6, 129.3, 128.6, 128.5, 56.0, 50.5, 42.6, 35.9, 34.0, 29.2, 24.9, 23.9, 17.6, 12.1 ppm.

HRMS (ESI): m/z Calcd for $\text{C}_{21}\text{H}_{26}\text{ClNNaO}_3\text{S}$: 430.1219; Found: 430.1221.



(4*E*,7*E*)-12-((4-bromophenyl)sulfonyl)-1,5,9,9-tetramethyl-12-azabicyclo [9.1.0]dodeca-4,7-dien-6-one (52k)

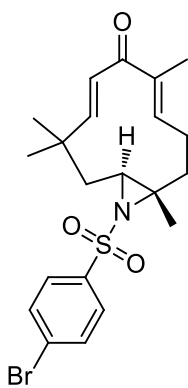
Following the general procedure as described in section 5.8.3, the reaction was carried out with 30 mg (0.1376 mmol) of zerumbone **1** with 0.2752mmol of sulfonamide **51k** and the corresponding product **52k** was isolated in 32 mg (yield 52 %).

R_f = 0.62 (hexane/ethyl acetate = 2:3) ; Colorless solid.

Mp = 154-157 $^{\circ}\text{C}$

IR (Neat) ν_{max} : 2935, 2908, 2863, 1725, 1649 cm^{-1} .

^1H NMR (500 MHz, CDCl_3 , TMS): δ 7.77 (d, J = 8.5 Hz, 2H), 7.67 (d, J = 8.5 Hz, 2H), 6.19-6.16 (m, 1H), 6.13 (d, J = 16.5 Hz,



1H), 6.04 (d, $J = 16.5$ Hz, 1H), 2.89-2.87 (m, 1H), 2.67-2.62 (m, 1H), 2.51-2.47 (m, 2H), 2.25-2.19 (m, 1H), 1.84 (s, 3H), 1.50-1.43 (m, 1H), 1.43-1.41 (m, 1H), 1.28 (s, 3H), 1.27 (s, 3H), 1.02 (s, 3H) ppm.

^{13}C NMR (125 MHz, CDCl_3 , TMS): δ 201.9, 158.7, 147.2, 140.5, 140.1, 132.3, 128.6, 128.5, 128.1, 56.0, 50.5, 42.6, 36.0, 34.0, 29.2, 24.9, 23.9, 17.6, 12.1 ppm.

HRMS (ESI): m/z Calcd for $\text{C}_{21}\text{H}_{26}\text{BrNNaO}_3\text{S}$: 474.0714; Found: 474.06943 and 476.0673.

(4E,7E)-1,5,9,9-tetramethyl-12-((4-nitrophenyl)sulfonyl)-12-azabicyclo[9.1.0]dodeca-4,7-dien-6-one (52l)

Following the general procedure as described in section 5.8.3, the reaction was carried out with 30 mg (0.1376 mmol) of zerumbone **1** with 0.2752mmol of sulfonamide **51l** and the corresponding product **52l** was isolated in 28.8 mg (yield 50 %).

$R_f = 0.61$ (hexane/ethyl acetate = 2:3) ; Colorless solid.

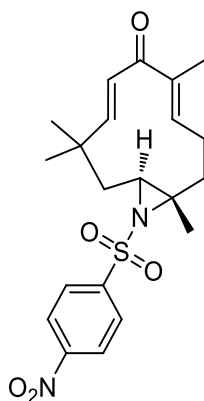
Mp = 126-129 °C.

IR (Neat) ν_{max} : 2925, 2364, 1639, 1532, 1351 cm^{-1} .

^1H NMR (500 MHz, CDCl_3 , TMS): δ 7.90 (d, $J = 8.5$ Hz, 2H), 7.62 (d, $J = 8.5$ Hz, 2H), 5.70-5.69 (m, 1H), 5.66 (d, $J = 16.5$ Hz, 1H), 5.56 (d, $J = 16.5$ Hz, 1H), 2.49-2.47 (m, 1H), 2.25-2.21 (m, 1H), 2.06-2.02 (m, 2H), 1.72-1.70 (m, 1H), 1.37 (s, 3H), 1.04-1.02 (m, 1H), 0.98-0.96 (m, 1H), 0.83 (s, 3H), 0.81 (s, 3H), 0.54 (s, 3H) ppm.

^{13}C NMR (125 MHz, CDCl_3 , TMS): δ 201.9, 158.5, 150.3, 147.0, 146.8, 140.3, 128.8, 128.3, 124.3, 57.0, 51.2, 42.6, 35.9, 34.4, 29.2, 24.9, 23.9, 17.5, 12.1 ppm.

HRMS (ESI): m/z Calcd for $\text{C}_{21}\text{H}_{26}\text{N}_2\text{NaO}_5\text{S}$: 441.1460; Found: 441.1467.



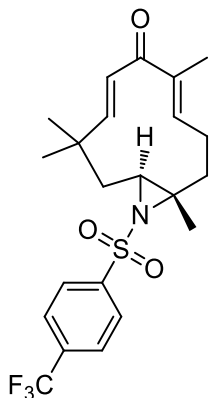
(4E,7E)-1,5,9,9-tetramethyl-12-((4-(trifluoromethyl)phenyl)sulfonyl)-12-azabicyclo[9.1.0]dodeca-4,7-dien-6-one (52m)

Following the general procedure as described in section 5.8.3, the reaction was carried out with 30 mg (0.1376 mmol) of zerumbone **1** with 0.2752mmol of sulfonamide **51m** and the corresponding product **52m** was isolated in 31 mg (yield 51 %).

$R_f = 0.67$ (hexane/ethyl acetate = 2:3); Amorphous solid.

IR (Neat) ν_{\max} : 2929, 2900, 2348, 17250, 1719, 1660 cm^{-1} .

^1H NMR (500 MHz, CDCl_3 , TMS): δ 8.05 (d, $J = 8$ Hz, 2H), 7.81 (d, $J = 8$ Hz, 2H), 6.20-6.19 (m, 1H), 6.16 (d, $J = 16.5$ Hz, 1H), 6.06 (d, $J = 16$ Hz, 1H), 2.96-2.94 (m, 1H), 2.71-2.68 (m, 1H), 2.51-2.50 (m, 2H), 2.26-2.22 (m, 1H), 1.86 (s, 3H), 1.52-1.46 (m, 1H), 1.44-1.43 (m, 1H), 1.30 (s, 3H), 1.28 (s, 3H), 1.02 (s, 3H) ppm.



^{13}C NMR (125 MHz, CDCl_3 , TMS): δ 202.4, 158.9, 147.4, 144.9, 140.2, 134.6, 134.8, 128.7, 127.5, 126.3, 126.2, 56.6, 50.9, 42.6, 36.0, 34.3, 29.2, 25.0, 23.9, 17.6, 12.1 ppm.

HRMS (ESI): m/z Calcd for $\text{C}_{22}\text{H}_{26}\text{F}_3\text{NNaO}_3\text{S}$: 464.1483; Found: 464.1466.

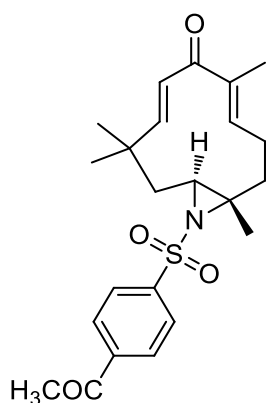
(4E,7E)-12-((4-acetylphenyl)sulfonyl)-1,5,9,9-tetramethyl-12-azabicyclo[9.1.0]dodeca-4,7-dien-6-one (52n)

Following the general procedure as described in section 5.8.3, the reaction was carried out with 30 mg (0.1376 mmol) of zerumbone **1** with 0.2752mmol of sulfonamide **51n** and the corresponding product **52n** was isolated in 19 mg (yield 33 %).

$R_f = 0.55$ (hexane/ethyl acetate = 2:3); Colorless foam.

IR (Neat) ν_{\max} : 2935, 2908, 2863, 1725, 1649 cm^{-1} .

^1H NMR (500 MHz, CDCl_3 , TMS): δ 8.03 (d, $J = 8.5$ Hz, 2H), 7.93 (d, $J = 8.5$ Hz, 2H), 6.13-6.11 (m, 1H), 6.07 (d, $J = 16.5$ Hz, 1H), 5.98 (d, $J = 16.5$ Hz, 1H), 2.86-2.84 (m, 1H), 2.63-2.62 (m, 1H), 2.60 (s, 3H), 2.46-2.43 (m, 2H), 2.19-2.12 (m, 1H), 1.78 (s, 3H), 1.45-1.42 (m, 1H), 1.37-1.35 (m, 1H), 1.22 (s, 6H), 0.95 (s, 3H) ppm.

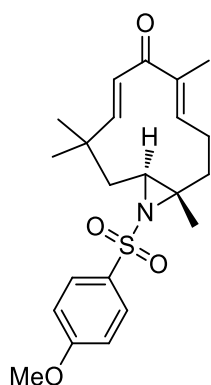


^{13}C NMR (125 MHz, CDCl_3 , TMS): δ 200.8, 195.2, 157.6, 146.1, 144.0, 139.2, 139.1, 127.8, 127.6, 126.2, 56.2, 49.6, 41.6, 34.9, 33.1, 28.2, 25.7, 23.9, 22.9, 16.5, 11.0 ppm.

HRMS (ESI): m/z Calcd for $\text{C}_{23}\text{H}_{29}\text{NNaO}_4\text{S}$: 438.1715; Found: 438.1721.

(4E,7E)-12-((4-methoxyphenyl)sulfonyl)-1,5,9,9-tetramethyl-12-azabicyclo[9.1.0]dodeca-4,7-dien-6-one (52o)

Following the general procedure as described in section 5.8.3, the reaction was carried out with 30 mg (0.1376 mmol) of zerumbone **1** with 0.2752mmol of sulfonamide **51o** and the corresponding product **52o** was isolated in 28 mg (yield 51 %).



R_f = 0.55 (hexane/ethyl acetate = 2:3); Colorless amorphous solid.

IR (Neat) ν_{\max} : 2361, 2335, 1731, 1697, 1253 cm^{-1} .

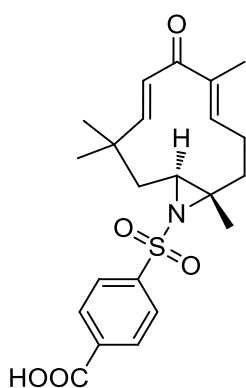
^1H NMR (500 MHz, CDCl_3 , TMS): δ 7.83 (d, J = 9 Hz, 2H), 6.98 (d, J = 9 Hz, 2H), 6.21-6.18 (m, 1H), 6.12 (d, J = 16 Hz, 1H), 6.05 (d, J = 16.5 Hz, 1H), 3.89 (s, 3H), 2.85-2.82 (m, 1H), 2.62-2.58 (m, 1H), 2.50-2.47 (m, 2H), 2.29-2.23 (m, 1H), 1.84 (s, 3H), 1.52-1.49 (m, 1H), 1.42-1.40 (m, 1H), 1.27 (s, 3H), 1.25 (s, 3H) ppm, 1.01 (s, 3H) ppm.

^{13}C NMR (125 MHz, CDCl_3 , TMS): δ 201.9, 163.1, 158.9, 147.4, 139.5, 132.9, 129.6, 128.4, 113.8, 55.5, 49.7, 42.7, 35.9, 33.6, 29.1, 24.9, 24.0, 17.6, 11.9 ppm.

HRMS (ESI): m/z Calcd for $\text{C}_{22}\text{H}_{29}\text{NNaO}_4\text{S}$: 426.1715; Found: 426.1720.

4-(((4E,7E)-1,5,9,9-tetramethyl-6-oxo-12-azabicyclo[9.1.0]dodeca-4,7-dien-12-yl)sulfonyl)benzoic acid (52p)

Following the general procedure as described in section 5.8.3, the reaction was carried out with 30 mg (0.1376 mmol) of zerumbone **1** with 0.2752mmol of sulfonamide **51p** and the corresponding product **52p** was isolated in 20 mg (yield 35 %).



R_f = 0.13 (hexane/ethyl acetate = 2:3); Colorless amorphous solid.

IR (Neat) ν_{\max} : 3556, 3472, 3185, 3065, 2361, 1700.86, 1653, 1394, 1156 cm^{-1} .

^1H NMR (500 MHz, CDCl_3 , TMS): δ 8.26 (d, J = 8.5 Hz, 2H), 8.01 (d, J = 8.5 Hz, 2H), 6.20-6.18 (m, 1H), 6.15 (d, J = 16 Hz, 1H), 6.05 (d, J = 16 Hz, 1H), 2.94-2.90 (m, 1H), 2.70-2.67 (m, 1H), 2.53-2.50 (m, 2H), 2.27-2.24 (m, 1H), 1.85 (s, 3H), 1.53-1.50 (m, 1H), 1.44-1.42 (m, 1H), 1.29 (s, 6H), 1.02 (s, 3H) ppm.

^{13}C NMR (125 MHz, CDCl_3 , TMS): δ 201.3, 168.3, 158.7, 147.1, 145.6, 140.2, 133.5, 130.8, 128.7, 127.1, 56.3, 50.6, 42.2, 37.0, 34.0, 30.7, 25.2, 23.4, 17.6, 12.1 ppm.

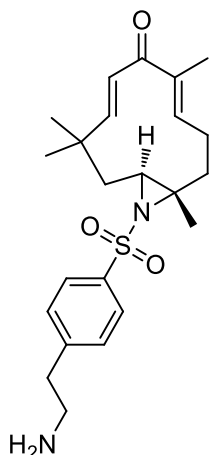
HRMS (ESI): m/z Calcd for $\text{C}_{22}\text{H}_{27}\text{NNaO}_5\text{S}$: 440.1507; Found: 440.1516.

(4E,7E)-12-((4-(2-aminoethyl)phenyl)sulfonyl)-1,5,9,9-tetramethyl-12-azabicyclo[9.1.0]dodeca-4,7-dien-6-one (52q)

Following the general procedure as described in section 5.8.3, the reaction was carried out with 30 mg (0.1376 mmol) of zerumbone **1** with 0.2752 mmol of sulfonamide **51q** and the corresponding product **52q** was isolated in 14 mg (yield 26 %).

R_f = 0.65 (hexane/ethyl acetate = 2:3); Colorless amorphous solid.

IR (Neat) ν_{max} : 3425, 2095, 1644, 1471 cm^{-1} .



^1H NMR (500 MHz, CDCl_3 , TMS): δ 7.94 (d, J = 8.5 Hz, 2H), 7.52 (d, J = 8 Hz, 2H), 6.20-6.18 (m, 1H), 6.14 (d, J = 16.5 Hz, 1H), 6.06 (d, J = 16.5 Hz, 1H), 3.86 (s, 2H), 2.92-2.67 (m, 1H), 2.66-2.63 (m, 1H), 2.62-2.48 (m, 2H), 2.27-2.22 (m, 1H), 1.65 (s, 3H), 1.60 (brs, 2H), 1.54-1.51 (m, 1H), 1.44-1.42 (m, 1H), 1.40-1.26 (m, 8H), 1.02 (s, 3H) ppm.

^{13}C NMR (125 MHz, CDCl_3 , TMS): δ 202.3, 158.9, 147.4, 141.5, 140.1, 136.2, 128.6, 127.9, 116.6, 56.1, 50.6, 42.6, 37.0, 34.0, 29.2, 25.0, 23.9, 23.6, 17.7 ppm.

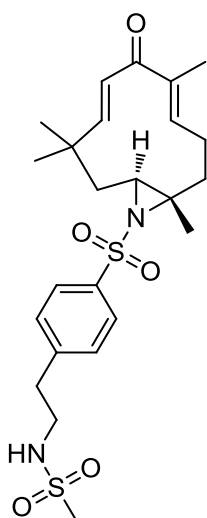
HRMS (ESI): m/z Calcd for $\text{C}_{23}\text{H}_{32}\text{N}_2\text{NaO}_3\text{S}$: 439.2031; Found: 439.2032.

N-(4-(((4E,7E)-1,5,9,9-tetramethyl-6-oxo-12-azabicyclo[9.1.0]dodeca-4,7-dien-12-yl)sulfonyl)phenethyl)methanesulfonamide (52r)

Following the general procedure as described in section 5.8.3, the reaction was carried out with 30 mg (0.1376 mmol) of zerumbone **1** with 0.2752 mmol of sulfonamide **51r** and the corresponding product **52r** was isolated in 59 mg (yield 87 %).

R_f = 0.20 (hexane/ethyl acetate = 2:3); Colorless amorphous solid.

IR (Neat) ν_{max} : 2935, 2908, 2863, 1725, 1649 cm^{-1} .



¹H NMR (500 MHz, CDCl₃, TMS): δ 7.87 (d, *J* = 9 Hz, 2H), 7.40 (d, *J* = 8 Hz, 2H), 6.21-6.19 (m, 1H), 6.15 (d, *J* = 16.5 Hz, 1H), 6.07 (d, *J* = 16.5 Hz, 1H), 4.51-4.49 (m, 1H), 3.46-3.42 (m, 2H), 3.00-2.99 (m, 2H), 2.98-2.90 (m, 4H), 2.65-2.63 (m, 1H), 2.49-2.48 (m, 2H), 2.28-2.23 (m, 1H), 1.65 (s, 3H), 1.56-1.53 (m, 1H), 1.43-1.38 (m, 1H), 1.28 (s, 6H), 1.02 (s, 3H) ppm.

¹³C NMR (125 MHz, CDCl₃, TMS): δ 202.2, 159.0, 147.6, 139.9, 137.4, 130.2, 129.6, 130.0, 128.2, 125.3, 55.8, 50.3, 43.9, 42.6, 40.3, 36.0, 33.8, 29.2, 24.9, 23.9, 21.5, 17.6, 12.0 ppm.

HRMS (ESI): *m/z* Calcd for C₂₄H₃₄N₂NaO₅S₂: 517.1806; Found: 517.1819.

N-(4-(((4E,7E)-1,5,9,9-tetramethyl-6-oxo-12-azabicyclo[9.1.0]dodeca-4,7-dien-12-yl)sulfonyl)phenethyl)benzenesulfonamide (52s)

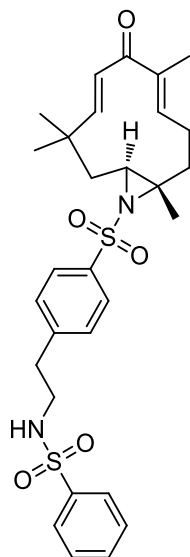
Following the general procedure as described in section 5.8.3, the reaction was carried out with 30 mg (0.1376 mmol) of zerumbone **1** with 0.2752 mmol of sulfonamide **51s** and the corresponding product **52s** was isolated in 25 mg (yield 37 %).

R_f = 0.46 (hexane/ethyl acetate = 2:3); Colorless amorphous solid
IR (Neat) *ν*_{max}: 3047, 2931, 1599, 1415, 1318 cm⁻¹.

¹H NMR (500 MHz, CDCl₃, TMS): δ 7.81-7.79 (m, 4H), 7.60-7.68 (m, 1H), 7.62-7.50 (m, 2H), 7.29-7.27 (m, 2H), 6.20-6.18 (m, 1H), 6.13 (d, *J* = 16.5 Hz, 1H), 6.05 (d, *J* = 16.5 Hz, 1H), 4.52-4.50 (m, 1H), 3.29-3.25 (m, 2H), 2.90-2.87 (m, 3H), 2.66-2.63 (m, 1H), 2.52-2.48 (m, 2H), 2.49-2.48 (m, 1H), 1.84 (s, 3H), 1.44-1.39 (m, 2H), 1.29-1.26 (m, 6H), 1.02 (s, 3H) ppm.

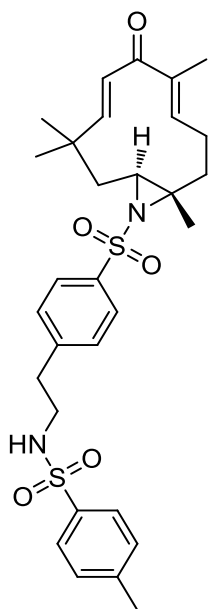
¹³C NMR (125 MHz, CDCl₃, TMS): δ 201.8, 158.9, 147.1, 143.2, 139.8, 132.6, 129.5, 128.6, 127.7, 127.1, 126.5, 55.4, 53.3, 50.2, 43.6, 42.4, 36.7, 36.0, 33.6, 29.7, 24.5, 23.8, 17.6, 11.8 ppm.

HRMS (ESI): *m/z* Calcd for C₂₉H₃₆N₂NaO₅S₂: 579.1963; Found: 579.1970.



4-methyl-N-(4-(((4E,7E)-1,5,9,9-tetramethyl-6-oxo-12-azabicyclo[9.1.0]dodeca-4,7-dien-12-yl)sulfonyl)phenethyl)benzenesulfonamide (52t)

Following the general procedure as described in section 5.8.3, the reaction was carried out with 30 mg (0.1376 mmol) of zerumbone **1** with 0.2752 mmol of sulfonamide **51t** and the corresponding product **52t** was isolated in 31 mg (yield 40 %).



$R_f = 0.47$ (hexane/ethyl acetate = 2:3); Colorless amorphous solid.

IR (Neat) ν_{\max} : 2931, 2108, 1643, 1547, 1418 cm^{-1} .

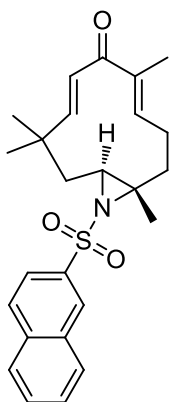
$^1\text{H NMR}$ (500 MHz, CDCl_3 , TMS): δ 7.72-7.70 (m, 2H), 7.62-7.60 (m, 2H), 7.23-7.19 (m, 4H), 6.14-6.11 (m, 1H), 6.06 (d, $J = 16$ Hz, 1H), 5.99 (d, $J = 16$ Hz, 1H), 4.71 (brs, 1H), 3.17-3.16 (m, 2H), 2.82-2.80 (m, 3H), 2.56-2.49 (m, 1H), 2.44-2.40 (m, 1H), 2.37 (s, 3H), 2.20-2.18 (m, 1H), 1.76 (s, 3H), 1.48-1.45 (m, 1H), 1.36-1.31 (m, 1H), 1.22 (s, 3H), 1.20 (s, 3H), 0.95 (s, 3H) ppm.

$^{13}\text{C NMR}$ (125 MHz, CDCl_3 , TMS): δ 201.1, 157.9, 146.4, 142.6, 142.5, 140.0, 138.9, 135.9, 128.7, 128.4, 127.5, 126.2, 126.0, 67.3, 54.7, 49.3, 42.7, 41.6, 34.9, 32.9, 28.2, 26.7, 23.9, 22.9, 21.1, 20.5, 16.5, 11.0 ppm.

HRMS (ESI): m/z Calcd for $\text{C}_{30}\text{H}_{38}\text{N}_2\text{NaO}_5\text{S}_2$: 593.2119; Found: 593.2136.

(4E,7E)-1,5,9,9-tetramethyl-12-(naphthalen-2-ylsulfonyl)-12-azabicyclo[9.1.0]dodeca-4,7-dien-6-one (52u)

Following the general procedure as described in section 5.8.3, the reaction was carried out with 30 mg (0.1376 mmol) of zerumbone **1** with 0.2752 mmol of sulfonamide **51u** and the corresponding product **52u** was isolated in 30 mg (yield 51 %).



$R_f = 0.64$ (hexane/ethyl acetate = 2:3). Colorless amorphous solid.

IR (Neat) ν_{\max} : 2928, 1648, 1312, 1269, 1154 cm^{-1} .

$^1\text{H NMR}$ (500 MHz, CDCl_3 , TMS): δ 8.44 (s, 1H), 7.99-7.97 (m, 2H), 7.92-7.89 (m, 2H), 7.88-7.61 (m, 2H), 6.22-6.19 (m, 1H), 6.13 (d, $J = 16$ Hz, 1H), 6.06 (d, $J = 16.5$ Hz, 1H), 2.95-2.70 (m, 1H), 2.69-2.52 (m, 1H), 2.51-2.48 (m, 2H), 2.35-2.28 (m, 1H), 1.85 (s, 3H), 1.52-1.47 (m, 1H), 1.42-1.39 (m, 1H), 1.29 (s, 3H), 1.28 (s, 3H), 0.98 (s, 3H) ppm.

$^{13}\text{C NMR}$ (125 MHz, CDCl_3 , TMS): δ 201.9, 158.8, 147.4, 140.0, 138.3, 135.0, 132.1, 129.4, 129.3, 128.9, 128.6, 128.2, 128.0,

127.9, 127.5, 122.5, 56.7, 50.3, 42.7, 36.9, 33.9, 30.8, 29.2, 25.0, 23.9, 17.6, 12.1 ppm.

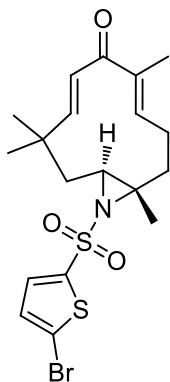
HRMS (ESI): m/z Calcd for $C_{25}H_{29}NNaO_3S$: 446.1765; Found: 446.1773.

(4E,7E)-12-((5-bromothiophen-2-yl)sulfonyl)-1,5,9,9-tetramethyl-12-azabicyclo[9.1.0]dodeca-4,7-dien-6-one (52v)

Following the general procedure as described in section 5.8.3, the reaction was carried out with 30 mg (0.1376 mmol) of zerumbone **1** with 0.2752mmol of sulfonamide **51v** and the corresponding product **52v** was isolated in 27 mg (yield 43 %).

R_f = 0.57 (hexane/ethyl acetate = 2:3); Colorless amorphous solid.

IR (Neat) ν_{max} : 2960, 2923, 2361, 1647, 1447 cm^{-1} .



1H NMR (500 MHz, $CDCl_3$, TMS): δ 7.40 (d, J = 4 Hz, 1H), 7.07 (d, J = 4.5 Hz, 1H), 6.18-6.17 (m, 1H), 6.15-6.12 (m, 1H), 6.07-6.04 (m, 1H), 2.90-2.87 (m, 1H), 2.64-2.61 (m, 1H), 2.49-2.44 (m, 2H), 2.16-2.14 (m, 1H), 1.85 (s, 3H), 1.69-1.66 (m, 1H), 1.50-1.46 (m, 1H), 1.30 (s, 3H), 1.29 (s, 3H), 1.06 (s, 3H) ppm.

^{13}C NMR (125 MHz, $CDCl_3$, TMS): δ 202.0, 158.8, 147.2, 142.9, 140.2, 132.2, 130.1, 128.6, 120.8, 56.6, 50.8, 42.6, 36.0, 34.0, 29.3, 24.9, 23.9, 17.5, 12.1 ppm.

HRMS (ESI): m/z Calcd for $C_{19}H_{24}BrNNaO_3S_2$: 480.0278; Found: 480.0286 and 482.0264.

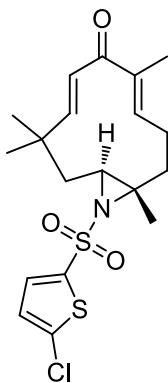
(4E,7E)-12-((5-chlorothiophen-2-yl)sulfonyl)-1,5,9,9-tetramethyl-12-azabicyclo[9.1.0]dodeca-4,7-dien-6-one (52w)

Following the general procedure as described in section 5.8.3, the reaction was carried out with 30 mg (0.1376 mmol) of zerumbone **1** with 0.2752mmol of sulfonamide **51w** and the corresponding product **52w** was isolated in 19 mg (yield 34 %).

R_f = 0.62 (hexane/ethyl acetate = 2:3); Colorless amorphous solid.

IR (Neat) ν_{max} : 2951, 2902, 2291, 1645, 1440 cm^{-1} .

1H NMR (500 MHz, $CDCl_3$, TMS): δ 7.44 (d, J = 4 Hz, 1H), 6.93 (d, J = 4 Hz, 1H), 6.17-6.12 (m, 2H), 6.05 (d, J = 16.5 Hz, 1H), 2.89-2.86 (m, 1H), 2.64-2.60 (m, 1H), 2.51-2.47 (m, 2H), 2.18-2.15



(m, 1H), 1.85 (s, 3H), 1.69-1.66 (m, 1H), 1.50-1.48 (m, 1H), 1.30 (s, 3H), 1.29 (s, 3H), 1.06 (s, 3H) ppm.

^{13}C NMR (125 MHz, CDCl_3 , TMS): δ 201.9, 158.7, 147.1, 140.2, 140.0, 138.0, 131.4, 128.7, 126.4, 56.6, 50.8, 42.5, 36.0, 33.9, 29.3, 24.9, 24.0, 17.5, 12.1 ppm.

HRMS (ESI): m/z Calcd for $\text{C}_{19}\text{H}_{24}\text{ClNNaO}_3\text{S}_2$: 436.0783; Found: 436.0794.

(4E,7E)-12-((4,5-dichlorothiophen-2-yl)sulfonyl)-1,5,9,9-tetramethyl-12-azabicyclo[9.1.0]dodeca-4,7-dien-6-one (52x)

Following the general procedure as described in section 5.8.3, the reaction was carried out with 30 mg (0.1376 mmol) of zerumbone **1** with 0.2752mmol of sulfonamide **51x** and the corresponding product **52x** was isolated in 24 mg (yield 40 %).

R_f = 0.59 (hexane/ethyl acetate = 2:3); Colorless amorphous solid.

IR (Neat) ν_{max} : 2954, 2899, 2300, 1646, 1440, 1438 cm^{-1} .

^1H NMR (500 MHz, CDCl_3 , TMS): δ 7.45 (s, 1H), 6.16-6.13 (m, 2H), 6.04 (d, J = 16.5 Hz, 1H), 2.91-2.89 (m, 1H), 2.66-2.63 (m, 1H), 2.50-2.48 (m, 2H), 2.14-2.10 (m, 1H), 1.85 (s, 3H), 1.72-1.69 (m, 1H), 1.52-1.47 (m, 1H), 1.31 (s, 6H)', 1.07 (s, 3H) ppm.

^{13}C NMR (125 MHz, CDCl_3 , TMS): δ 202.0, 158.7, 147.0, 140.2, 138.5, 132.1, 130.9, 128.7, 124.7, 57.1, 51.3, 42.5, 36.0, 34.2, 29.3, 24.9, 23.9, 17.5, 12.1 ppm.

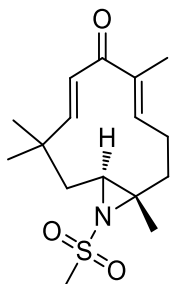
HRMS (ESI): m/z Calcd for $\text{C}_{19}\text{H}_{23}\text{Cl}_2\text{NNaO}_3\text{S}_2$: 470.0394; Found: 470.0396.

(4E,7E)-1,5,9,9-tetramethyl-12-(methylsulfonyl)-12-azabicyclo[9.1.0]dodeca-4,7-dien-6-one (52z).

Following the general procedure as described in section 5.8.3, the reaction was carried out with 30 mg (0.1376 mmol) of zerumbone **1** with 0.2752mmol of sulfonamide **51z** and the corresponding product **52z** was isolated in 12 mg (yield 28 %).

R_f = 0.56 (hexane/ethyl acetate = 2:3). Colorless amorphous solid.

IR (Neat) ν_{max} : 2888, 2820 1725, 1649, cm^{-1} .



¹H NMR (500 MHz, CDCl₃, TMS): δ 6.18-6.12 (m, 2H), 6.06 (d, *J* = 16 Hz, 1H), 3.03 (s, 3H), 2.81-2.78 (m, 1H), 2.63-2.60 (m, 1H), 2.47-2.45 (m, 2H), 2.07-2.04 (m, 1H), 1.91-1.89 (m, 1H), 1.84 (s, 3H), 1.60-1.58 (m, 1H), 1.33 (s, 3H), 1.28 (s, 3H), 1.10 (s, 3H) ppm.

¹³C NMR (125 MHz, CDCl₃, TMS): δ 202.0, 158.9, 147.4, 140.0, 128.9, 55.1, 50.2, 43.3, 43.2, 36.1, 33.9, 29.5, 25.0, 24.1, 17.57, 12.1 ppm.

HRMS (ESI): *m/z* Calcd for C₁₉H₂₃Cl₂NNaO₃S₂: 334.1452; Found: 334.1456.

5.14. References

1. G. M. Cragg and D. J. Newman, *Biochim. Biophys. Acta.*, **2013**, 1830(6), 3670-3695.
2. (a) D. A. Dias, S. Urban and U. Roessner, *Metabolites*, **2012**, 2, 303-336. (b) J. W. Li and J. C. Vederas, *Science*, 2009, 325, 161-165. (c) J. D. McChesney, S. K. Venkataraman and J. T. Henri, *Phytochemistry*, **2007**, 68, 2015-2022. (d) G. M. Rishton, *Am. J. Cardiol.* **2008**, 22, 43D-49D. (e) A. L. Harvey, *Drug Discov. Today*, **2008**, 13, 894-901. (b) A. Ganesan, *Curr. Opin. Chem. Biol.* **2008**, 12, 306-317.
3. N. J. Yob, S. M. Jofrry, M. M. R. M. M. Affandi, L. K. Teh, M. Z. Salleh, and Z. A. Zakaria, *Evidence-Based Complementary and Alternative Medicine*, **2011**, 2011, 1-12.
4. (a) S. Dev, *Tetrahedron*, **1960**, 8, 171-180. (b) N. P. Damodaran and S. Dev, *Tetrahedron*, **1965**, 13, 1977-1981. (c) N. P. Damodaran, and S. Dev, *Tetrahedron Lett.*, **1968**, 24, 4113-4122. (d) N. P. Damodaran and S. Dev, *Tetrahedron Lett.*, 1968, 24, 4123-4132. (e) N. R. Fransworth, N. Bunyapraphatsara, "Thai Medical plants" **1992**, 261, Bangkok, Thailand.
5. A. Murakami, M. Takahashi, S. Jiwajinda, K. Koshimizu and H. Ohigashi, *Biosci. Biotechnol. Biochem.*, **1999**, 63(10), 1811-1812.
6. S. Elliot and J. Brimacombe, *J. Ethnopharmacol.*, **1987**, 19, 285-317.
7. W. Wutthithamavet, *Thai traditional medicine. Odean Store Press, Bangkok*, **1997**, pp 155.
8. (a) A. Murakami, T. Tanaka, J. Y. Lee, Y. J. Surh, H. W. Kim, K. Kawabata, Y. Nakamura, S. Jiwajinda and H. Ohigashi, *Int. J. Cancer*, **2004**, 110, 481-490. (b) C. Kirana, G. H. McIntosh, I. R. Record and G. P. Jones, *Nutr. Cancer*, **2003**, 45, 218-225, (c) Y. Ozaki, N. Kawahara and M. Harada, *Chem. Pharm. Bull.*, **1991**, 39, 2353-2356.
9. A. Murakami, D. Takahashi and T. Kinoshita, *Carcinogenesis*, **2002**, 23, 795-802.
10. M. Y. Ibrahim, A. B. Abdul, W. Abdel, S. I. Elhassan, M. N. Alzubairi, A. S. Syam and M. M. Elhassan, *Res. J. Biol. Sci.*, **2009**, 4(7), 777-784.
11. F. J. Al-Saffar, S. Ganabadi, S. Fakurazi, H. Yaakub and M. Lip, *J. Appl. Sci.*, **2010**, 10(4), 248-260.
12. C. B. Singh, Kh. Nongalleima, S. Brojendrosingh, S. Ningombam, N. Lokendrajit and L. W. Singh, *Phytochem. Rev.*, **2012**, 11, 113-125.
13. T. Kitayam, *Biosci. Biotechnol. Biochem.*, **2011**, 75(2), 199-207.

14. T. Kitayama, T. Okamoto, R. K. Hill, Y. Kawai, S. Takahashi, S. Yonemori, Y. Yamamoto, K. Ohe, S. Uemura and S. Sawada, *J. Org. Chem.*, **1999**, *64*, 2667-2672.
15. T. Kitayama, T. Yokoi, Y. Kawai, R. K. Hill, M. Morita, T. Okamoto, Y. Yamamoto, V. V. Fokin, K. B. Sharpless and S. Sawada, *Tetrahedron*, **2003**, *59*, 4857-4866.
16. T. Kitayama, K. Yamamoto, R. Utsumi, M. Takatani, R. K. Hill, Y. Kawai, S. Sawada and T. Okamoto, *Biosci. Biotechnol. Biochem.*, **2001**, *65*, 2193-2199.
17. H. W. D. Matthes, G. Ourisson and B. Luu, *Tetrahedron* **1982**, *38*, 3129-3135.
18. P. S. Kalsi, B. S. Dhir, H. Shirahama, R. S. Dhillon and B. R. Chhabra, *Indian J. Chem.*, **1985**, *24B*, 499-501.
19. T. Kitayama, T. Masuda, K. Sakai, C. Imada, Y. Yonekura, Y. Kawai, *Tetrahedron* **2006**, *62*, 10859-10864.
20. S. C Santhosh Kumar, P Srinivasa, P. S. Negi and B. K. Betadaiah, *Food chemistry*, **2013**, *141*, 1097-1103.
21. (a) T. Kitayama, M. Awata, Y. Kawai, A. Tsuji and Y. Yoshida, *Tetrahedron: Asymmetry*, **2008**, *19*, 2367-2373. (b) T. Kitayama, A. Furuya, C. Moriyama, T. Masuda, S. Fushimi, Y. Yonekura, H. Kubo, Y. Kawaib and S. Sawada, *Tetrahedron: Asymmetry*, **2006**, *17*, 2311-2316. (c) T. Kitayama, R. Nagao, T. Masuda, R. K. Hill, M. Morita, M. Takatani, S. Sawada and T. Okamoto, *J. Mol. Catal. B*, **2002**, *17*, 75-79. (d) T. Kitayama, T. Masuda, Y. Kawai, R. K. Hill, M. Takatani, S. Sawada and T. Okamoto, *Tetrahedron: Asymmetry*, **2001**, *12*, 2805-2810.
22. S. Dev, *Tetrahedron*, **1960**, *8*, 171-180.
23. T. Kitayama, S. Ohta, Y. Kawai, T. Nakayama and M. Awata, *Tetrahedron: Asymmetry*, **2010**, *21*, 11-15.
24. N. Subba Rao, N. P. Damodaran and S. Dev *Tetrahedron Lett.*, **1967**, *3*, 227-233.
25. K. R. Ajish, J. Nayana, K. V. Radhakrishnan, *Synthesis*, 2013, *45*, 2316-2322
26. K. R. Ajish, B. P. Dhanya, J. Nayana, K. V. Radhakrishnan, *Tetrahedron Lett.*, 2014, *55*, 665-670.
27. B. P. Dhanya, G. Gopalan, T. R. Reshmitha, J. Saranya, P. Sharathna, I. G. Shibi, P. Nisha, K. V. Radhakrishnan, *New J. Chem.*, 2017, *41*, 6960-6964.
28. J. Saranya, B. P. Dhanya, Greeshma Gopalan, K. V. Radhakrishnan and S. Priya, *Chem.-Biol. Interact.*, **2017**, *278*, 32-39.
29. T. Sithara, B. P. Dhanya, K. B. Arun, S. Sini, Mathew Dan, K. V. Radhakrishnan and P. Nisha, *J. Agric. Food Chem.*, **2018**, *66*, 602-612.
30. A. Kołaczek, I. Fusiarcz, J. Ławecka and D. Branowska, *Chemik.*, **2014**, *7*, 625-628.

31. M. Ashfaq, S. S. Ahmad Shah, T. Najjam, S. Shaheen and G. Rivera, *Mini-Reviews in Organic Chemistry*, **2013**, *10*, 160-170.
32. I. Nishimori, T. Minakuchi and K. Morimoto K, *J. Med. Chem.*, **2006**, *49*, 2117-2126.
33. O. M. Parasca, F. Gheață, A. Pânzariu, I. Geangalău and L. Profire, *Rev. Med. Chir. Soc. Med. Nat. Iasi.*, **2013**, *117*(2), 558-564.
34. C. Supuran, F. Briganti, S. Tilli and W. Chegwiddden Scozzafava *Bioorg. Med. Chem.*, **2001**, *9*(3), 703-714.
35. I. Argyropoulou, A. Geronikaki, P. Vicini and F. Zani, *Arkivoc.*, **2009**, *6*, 89-102.
36. T. Kitayama, M. Nakahira, K. Yamasaki, I. Hiromi, C. Imada, Y. Yuji, M. Awata, H. Takya, Y. Kawai, K. Ohnishi and A. Murakami, *Tetrahedron*, **2013**, *69*, 10152-10160.
37. N. Surve and U. Bagde, *International Journal of Biology*, **2011**, *3*, 72-78.
38. J. Fernandez, P. Kumar and A. Kumar, *Int. Res. J. Pharm.*, **2013**, *4*(8), 260-264.
39. N. Pandit, K. R. Singla and B. Shrivastava, *International Journal of Medicinal Chemistry*, **2012**, *2012*, 1-25.
40. J. Vara Prasad, *Current Opinion in Microbiology*, **2007**, *10*, 454-460.
41. N. Lewis, A. McKillop, R. J. K. Taylor and R. J. Watson, *Synth. Commun.*, **1995**, *25*(4), 561-568.
42. P. Gill, W. Murray and M. Wright, *Practical Optimisation*, Academic Press, London, 1981.
43. (a) B. M. Babior, *Am. J. Med.* **2000**, *109*, 33-44. (b) D. Nipun, S. Vijay, B. Jaykumar, S. P. Kirti, and L. Richard, *Pharma Crops.*, **2011**, *2*, 1-7. (c) M. Greenwell and P. K. S. M. Rahman, *Int. J. Pharm. Sci. Res.*, **2015**, *6*, 4103-4112. (d) T. Mosmann, *J. Immunol. Methods*, **1983**, 65-63. (e) D. C. Hiss and G. A. Gabriels, *Expert Opin. Drug Discovery*, **2009**, *4*, 799-821. (f) A. Jemal, F. Bray, M. M. Center, J. Ferlay, E. Ward and D. Forman, *Cancer J. Clinic*, **2011**, *61*, 69-90. (g) G. A. Khodarahmi, P. Y. Chen, G. H. Hakimelahi and J. W. Chern, *Iran J. Pharm. Res.*, **2005**, *4*, 43-56.
44. (a) T. F. Tzeng, S. S. Liou, C. J. Chang and I. M. Liu, *Nutr. Metab.*, **2013**, *10*, 64-75. (b) T. F. Tzeng, S. S. Liou, Y. C. Tzeng and I. M. Liu, *Nutrients*, **2016**, *8*, 449-454. (c) W. Y. Liu, T. F. Tzeng and I. M. Liu, *Molecules*, **2016**, *21*, 1708-1730. (c) N. Matsuura, T. Aradate, C. Sasaki, H. Kojima, M. Ohara, J. Hasegawa and M. Ubukata, *J. Health Sci.*, **2002**, *48*, 520-526. (d) Z. Xiao, R. Storms and A. Tsang, *Anal.*

- Biochem.*, **2006**, *351*, 146-148. (e) E. Apostolidis, Y. I. Kwon and K. Shetty, *Inn. Food Sci. Emerg. Technol.*, **2007**, *8*, 46-54.
45. L. Degennaro, P. Trinchera and R. Luisi, *Chem. Rev.*, **2014**, *114*, 7881-7929.
46. R. D. Richardson, M. Desai and T. Wirth, *Chem. Eur. J.*, **2007**, *13*, 6745-6754.
47. S. Minakata, Y. Morino, Y. Oderaotoshi and M. Komatsu, *Chem. Commun.*, **2006**, *0*, 3337-3339.
48. D. Mansuy, J.-P. Maby, A. Dureault, G. Bedi and P. Battioni, *J. Chem. Soc., Chem. Commun.*, **1984**, 1161-1163.
49. A. Yoshimura, V. N. Nemykin and V. V. Zhdankin, *Chem. Eur. J.*, **2011**, *17*, 10538-10541.
50. H. J. Kim, S. H. Cho and S. Chang, *Org. Lett.*, **2012**, *14*(6), 1424-1427.
51. K. Kiyokawa, T. Kosaka and S. Minakata, *Org. Lett.*, **2013**, *15*, 4858-4861.
52. G. Q. Liu and Y. M. Li, *J. Org. Chem.*, **2014**, *79*, 10094-10109.
53. A. Kamal, J. S. Reddy, E. V. Bharathi and D. Dastagiri, *Tetrahedron Lett.*, **2008**, *49*, 348-353.
54. (a) V. K. Jimsheena, *Anal. Chem.*, **2009**, *81*, 9388-9394. (b) N. M. Hooper and A. J. Turner, *Biochem. J.*, **1987**, *241*, 625-633.
55. (a) X. Qing, X. Y. Lee, J. D. Raeymaeker, J. R. H Tame, K.Y. J Zhang, M. D. Maeyer and A. R. D Voet, *J. Recept. Ligand Channel Res.*, **2014**, *7*, 81-92. (b) C. G. Wermuth, P. Lindberg, C. R. Ganellin and L. A. Mitscher, *Pure Appl. Chem.*, **1998**, *70*, 1129-1143.
56. (a) O. F. Güner, *Curr Top Med Chem.*, **2002**, *2*, 1321-1332. (b) A. R. Voet, A. Kumar and K. Y. Zhang, *J. Comput. Aided Mol. Des.*, **2014**, *28*(4), 363-373.
57. (a) G. Jones, P. Willett and R. C. Glen, *J. Comput. Aided Mol. Des.*, **1995**, *9*(6), 532-549. (b) V. Hähnke and G. Schneider, *J. Comput. Chem.*, **2011**, *32*(8), 1635-1647.

Lewis Acid Catalyzed Functionalization of Zerumbone; Synthesis of Novel [5.8.3] and [5.8] Fused Sesquiterpenoid Derivatives

6.1. Introduction

The quest for sustainable utilisation of natural products has tempted both organic and medicinal chemists to search new and abundant resources with environmentally friendly methodologies. In this context, the generation of complex structural scaffolds from renewable resources in one or two steps are of great importance due to the utilization of natural products without adversely affecting the environment. Natural products offer a rich source of innovative therapeutic agents with enormous structural diversity. About 34 % of all the drugs approved by FDA in the past three decades, are based on natural products and in many cases, the structurally complex natural products are altered from their core structure to a distinct framework using known synthetic methodologies.

The quick remedies provided by many synthetic drugs often exploit the energy and the health of patients. Also, the shift of public preferences from synthetic to ‘natural’ products has led to a resurgence of interest in natural products from edible and non-toxic plants. The rising cost of health-care is another significant factor contributing to the same. This realization has led to search for better alternatives from natural resources, with minimum side effects. India is endowed with prolific bio-diversity, and has unique geographical advantage to cultivate varieties of plants.¹

Rapid syntheses of complex and structurally diverse molecules from natural products are of great interest to numerous researchers, specialized in drug discovery. In a quest for biologically active molecules, synthetic methodologies are often applied to natural products to generate a diverse array of scaffolds. The diversity of natural products can be further expanded, by discovering novel synthetic methodologies. In this regard, we focused on the synthetic transformations of abundantly available natural product zerumbone, using simple reaction strategies like Lewis acid catalysis.

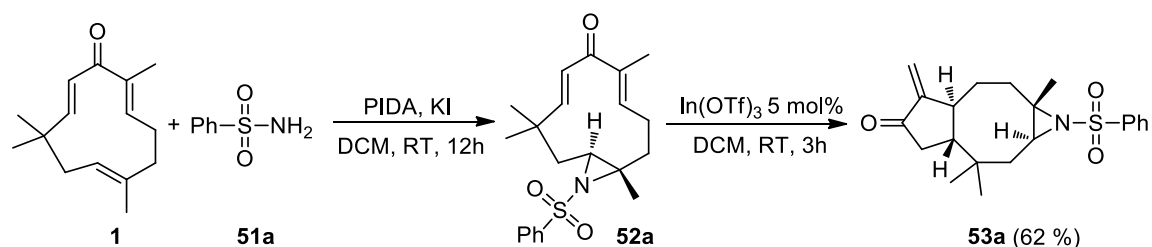
6.2. Aim and Scope of the Present Study

Lewis acid catalyzed synthetic transformations have been considered as one of the most powerful and reliable methods for the synthesis of complex molecules, from relatively simple precursors.² It is noteworthy from the previous chapter that *Zingiber zerumbet*, the

tropical wild ginger plant, can be cultivated on a large scale which yields zerumbone from the mature rhizomes after a period of growth of seven months. Since the development of a more atom- and step-economical methods for the synthesis of complex molecules have been recognized as a synthetically attractive tool, we further focused on the exploration of the synthetic utility of molecules synthesized in the previous chapter. Hence in this chapter, we disclose our efforts in the transannular cyclisation of zerumbone-aziridine derivatives in the presence as well as in the absence of an external nucleophile by Lewis acid catalysis.

6.3. Results and Discussion

A close look at the single-crystal X-ray structure of zerumbone-aziridine derivatives (**52**) led us to presume that, its strained 11-membered puckered structure could be activated with a catalyst to trigger transannular cyclization reactions, thereby leading to structurally diverse frameworks. Thus, we started to explore the synthetic utility of our zerumbone-aziridine derivatives *via* Lewis acid catalysis.³ We began our studies with the reaction of an aziridine **52a**, derived from zerumbone **1** and benzenesulfonamide **51a**, using scandium (III) triflate as the catalyst, without any external nucleophiles. However, the reaction did not proceed as expected. To our delight, after attempting the reaction with various Lewis acid and solvent combinations, a new [5.8.3] fused-ring system (**53a**) was formed *via* Nazarov cyclisation in 62 % yield by using 5 mol% In(OTf)₃, 1 equiv. phenylacetic acid in CH₂Cl₂ at room temperature as the reaction condition (scheme 6.1). After a detailed optimization study, we found that the reaction works well, even in the absence of phenylacetic acid and notably, the reaction only worked with the In(OTf)₃ and CH₂Cl₂ combination. To understand the possibilities of the reaction, different aziridinated zerumbone derivatives, prepared using our method (chapter 5) were subjected to Nazarov cyclization under the optimized reaction conditions, and in all cases, the expected [5.8.3] fused-ring systems were obtained in moderate to good yields (table 6.2).



Scheme 6.1. Nazarov cyclisation of aziridinated zerumbone

The structure of the product **53a** was well characterized using various spectroscopic analysis such as IR, ¹H NMR, ¹³C NMR and other 2-D NMR techniques. In the proton

NMR, the aromatic protons resonated as two proton doublet at δ 7.85 ppm and three proton multiplet in between δ 7.53-7.47 ppm. The exocyclic protons resonated as doublets of coupling constant 3 Hz at δ 6.13 and 5.26 ppm. The protons at the ring junction resonated at δ 2.86 and 2.10 ppm as doublets of coupling constant 19 Hz (figure 6.1). In the ^{13}C NMR, the carbonyl carbon resonated at δ 201.8 ppm (figure 6.2). All other peaks in NMR's were in good agreement with the proposed structure. The stereochemistry at the ring junction was confirmed from literature reports as well as from our own previous experimental results.³ Finally, the structure was well supported by HRMS data, in which the $[\text{M}+\text{Na}]^+$ peak was obtained at 396.1590.

Table 6.1. Generality of Nazarov cyclisation

Entry	R	Product	Yield (%)	Entry	R	Product	Yield (%)
1		53a	62	6		53k	60
2		53g	45	7		53l	65
3		53h	36	8		53o	72
4		53i	66	9		53v	45
5		53j	33				

Reaction conditions: Aziridinated zerumbone (1 equiv.), $\text{In}(\text{OTf})_3$ (5 mol%), DCM (2 mL), RT, 3 h.

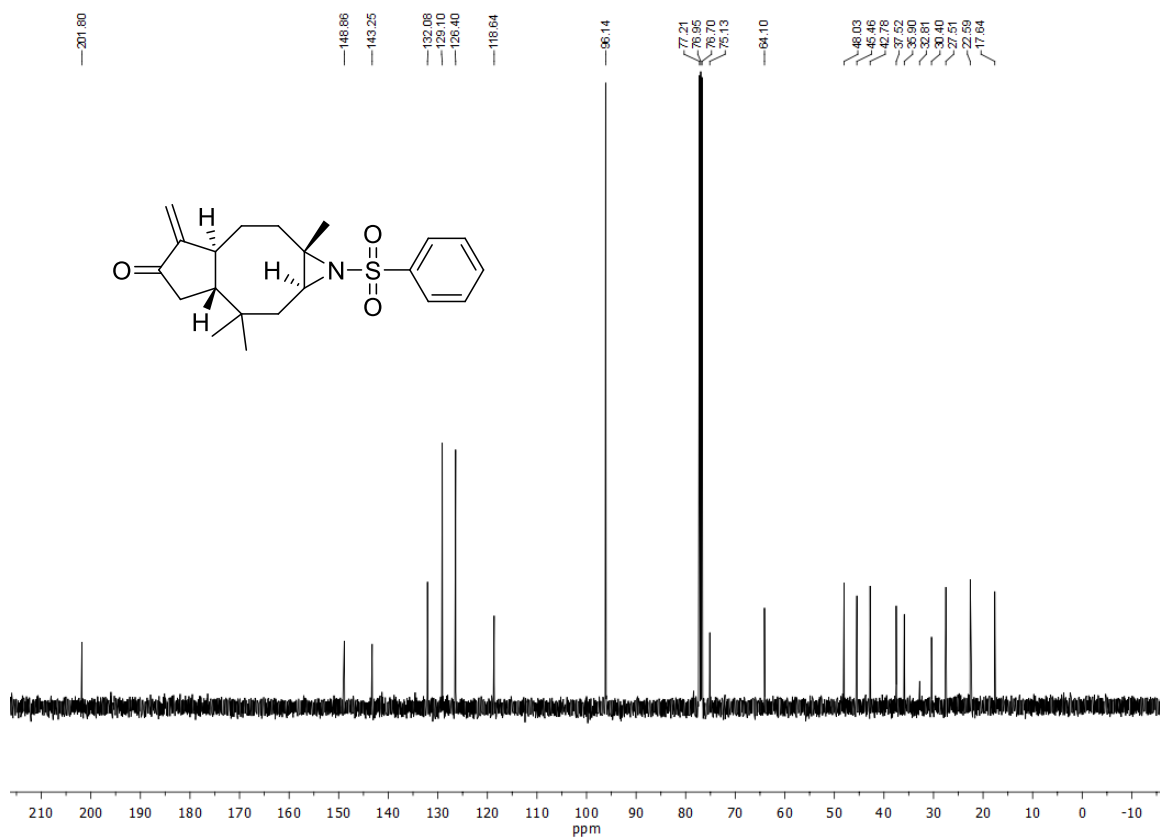
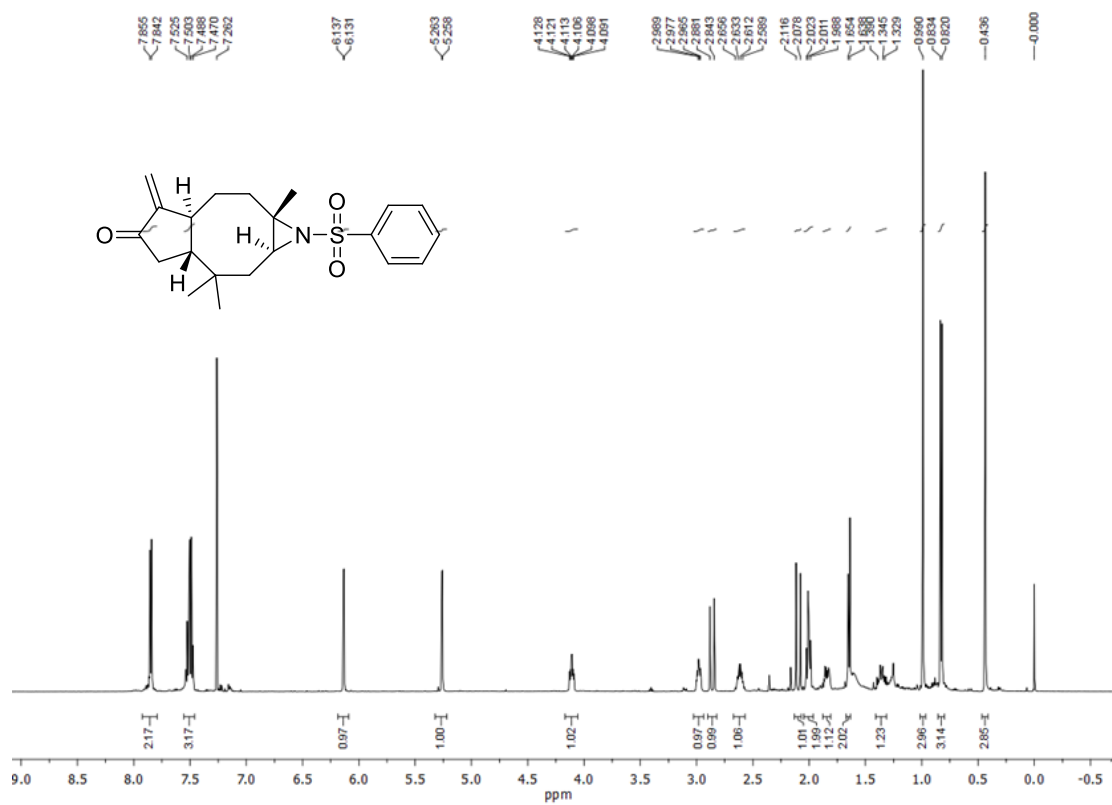
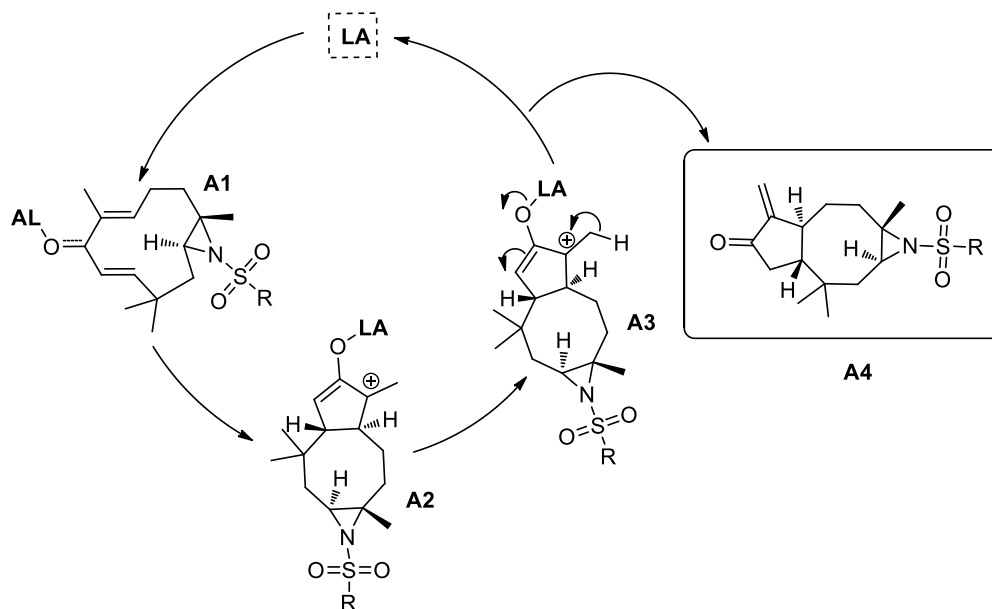


Figure 6.2. ^{13}C NMR of compound **53a** in CDCl_3

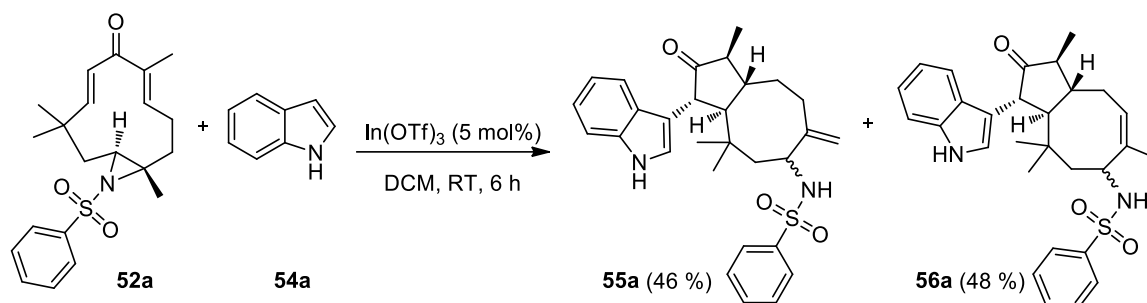
The proposed mechanism for the [5.8.3] fused products follow the Nazarov type cyclisation. Initially the Lewis acid coordinates to the carbonyl oxygen of the zerumbone, thereby creating an allyl carbocation (intermediate **A2**). Then the intermediate undergo an intramolecular cyclisation to afford the product **A4** (scheme 6.2).



Scheme 6.2. Proposed mechanisms for the cyclization reaction

The successful Nazarov cyclization of aziridinated zerumbone by Lewis acid catalysis led us to investigate the reactivity of this compound in the presence of an external nucleophile in similar reaction conditions. Though we have a number of nucleophiles having different properties, we preferably chose the indole heterocycles for our present study, since they are present in a wide variety of natural compounds with diverse physiological activities. Moreover, indoles are π -excessive heteroarenes and react much faster with electrophiles than most of the other benzene derivatives.⁴ Hence we commenced our reaction with one equivalent of each, aziridinated zerumbone **52a** and indole **54a** in the presence of 5 mol% $\text{In}(\text{OTf})_3$ in CH_2Cl_2 at room temperature. To our delight, the reaction afforded novel indole-substituted [5.8] fused-ring systems, **55a** and **56a** with a concomitant ring-opening of the aziridine (scheme 6.3). The conformational strain that was generated, owing to the formation of the [5.8] fused-ring system through an interrupted Nazarov cyclization reaction is the driving force for the aziridine ring-opening reaction. These annulated compounds were obtained in excellent yields and they only differed in the position of the double bond, and gave the maximum yield after a period of 6 hours. As

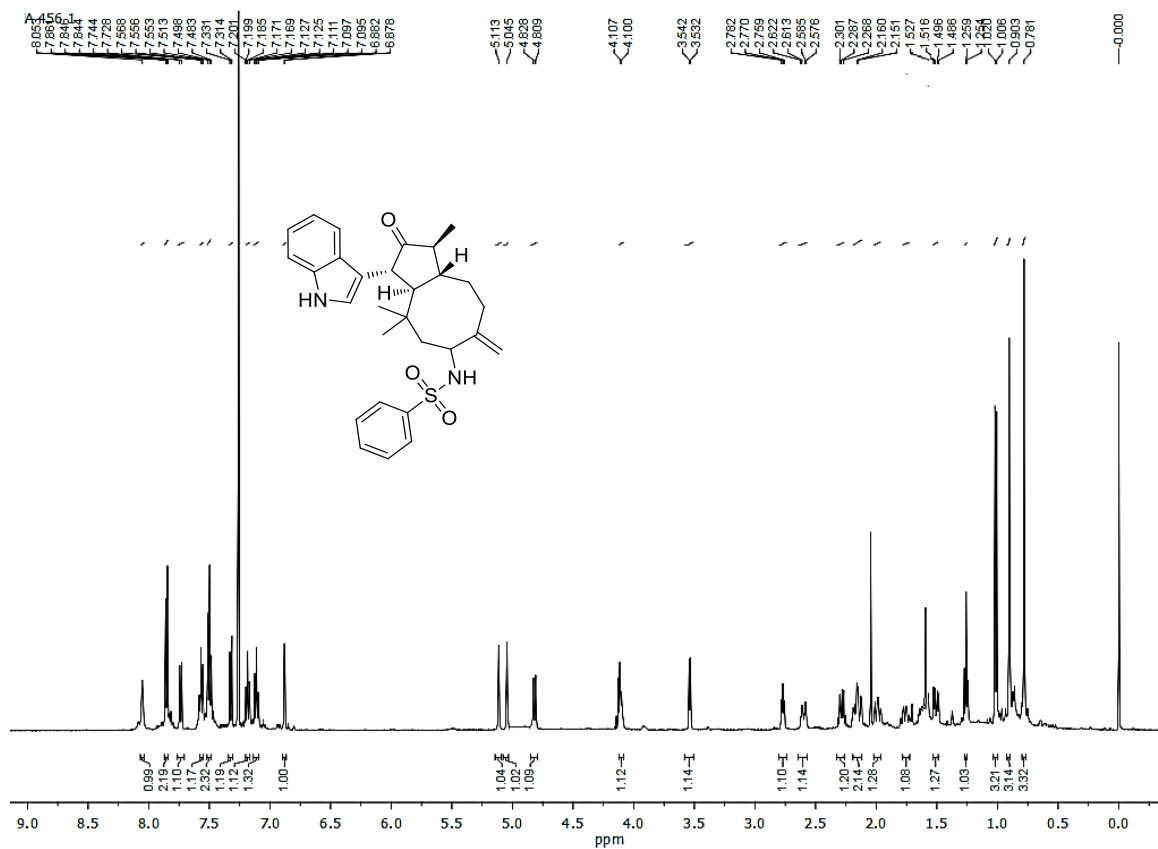
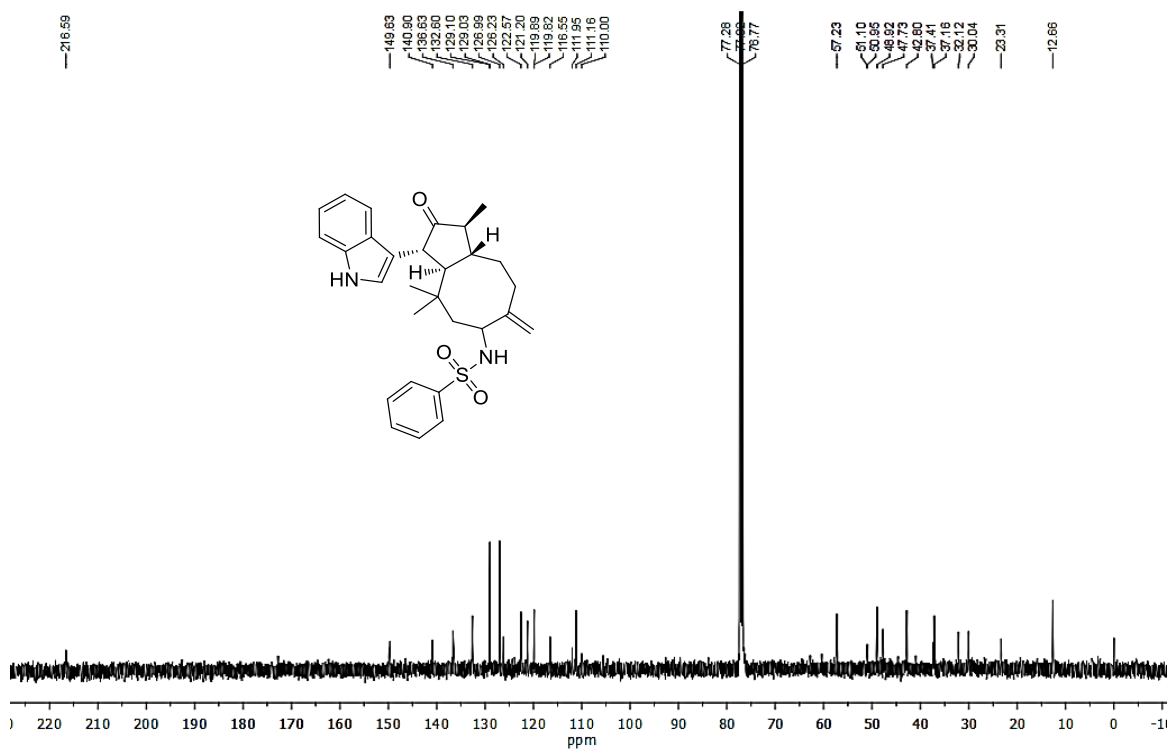
mentioned in the Nazarov cyclization reaction, the reactivity was also specific to the combination of $\text{In}(\text{OTf})_3$ and CH_2Cl_2 . These isomeric [5.8] fused-ring compounds were obtained in excellent yields, irrespective of the functional groups that were present on either the indole or the sulfonamide group.



Scheme 6.3. Interrupted Nazarov cyclisation of aziridinated zerumbone

The structure of compounds **55a** and **56a** were well characterized using various spectroscopic analyses. In the proton NMR of compound **55a**, all the eleven aromatic protons resonated in between δ 8.05 to 6.85 ppm. The protons of the exocyclic double bonds resonated as singlets at δ 5.11 and 5.04 ppm. The -NH proton of the sulfonamide group resonated as a doublet of coupling constant 9.5 Hz at δ 4.82 ppm (figure 6.3). Besides, the carbonyl carbon of the zerumbone moiety resonated at δ 216.6 ppm in the carbon NMR (figure 6.4). While, in the case of compound **56a**, the olefinic proton present in the ring resonated at δ 5.48 ppm as a triplet of coupling constant 8.5 Hz. The -NH proton resonated as a doublet of coupling constant 8 Hz at δ 4.72 ppm (figure 6.5). Also, the carbonyl carbon of the zerumbone moiety resonated at δ 217.4 ppm (figure 6.6). Besides, the formation of [5.8] fused rings were confirmed from the previous experiments of our group. Finally, the structures were well supported with HRMS data in which the $(\text{M}+\text{Na})^+$ peaks corresponding to $\text{C}_{29}\text{H}_{34}\text{N}_2\text{NaO}_3\text{S}$ were obtained at 513.2207 and 513.2201 respectively for compounds **55a** and **56a**. Also, the stereo-configuration of the molecules were confirmed from NOE experiments and from our own previous results (see supporting information).³

The scope of the reaction with various substituted indoles and sulfonamides were checked, and to our delight all these isomeric [5.8] fused-ring compounds were obtained in excellent yields of almost 1:1 ratio, and tolerable with different class of functional groups that were present on either the indole or the sulfonamide group (table 6.2).

Figure 6.3. ¹H NMR of compound 55a in CDCl₃Figure 6.4. ¹³C NMR of compound 55a in CDCl₃

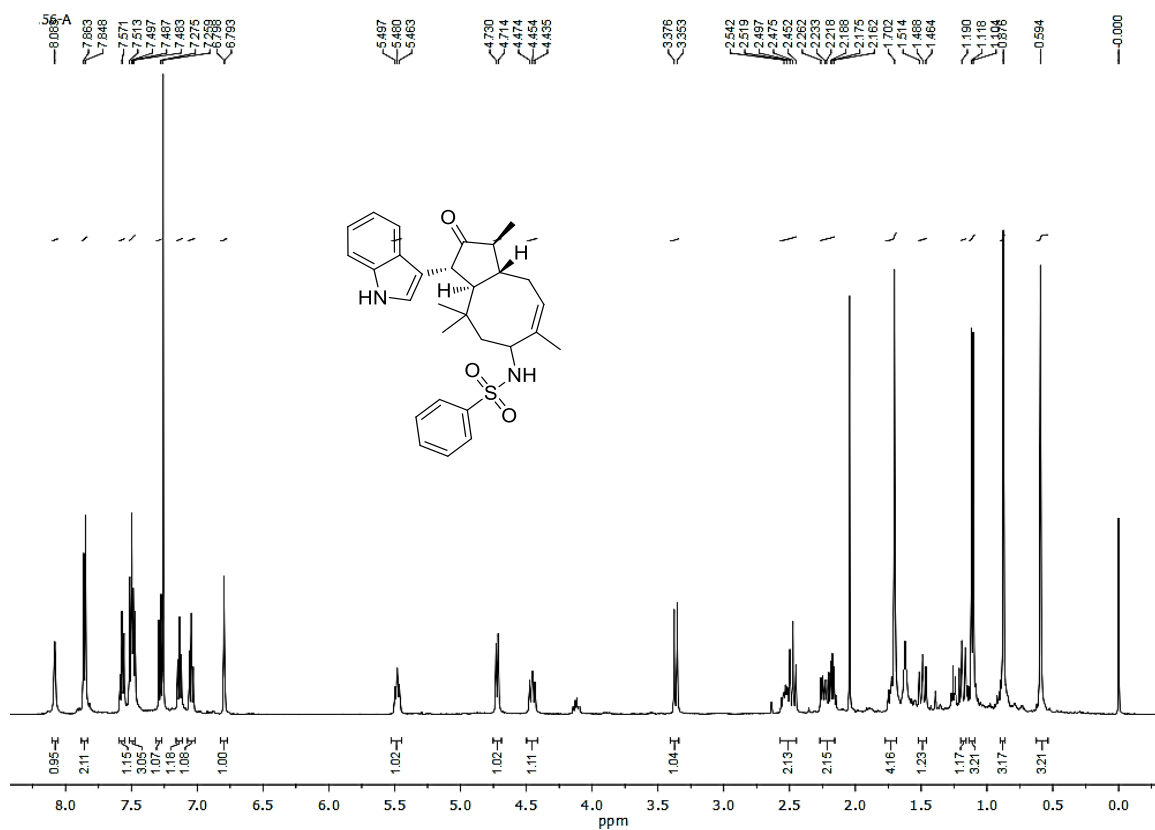


Figure 6.5. ^1H NMR of compound **56a** in CDCl_3

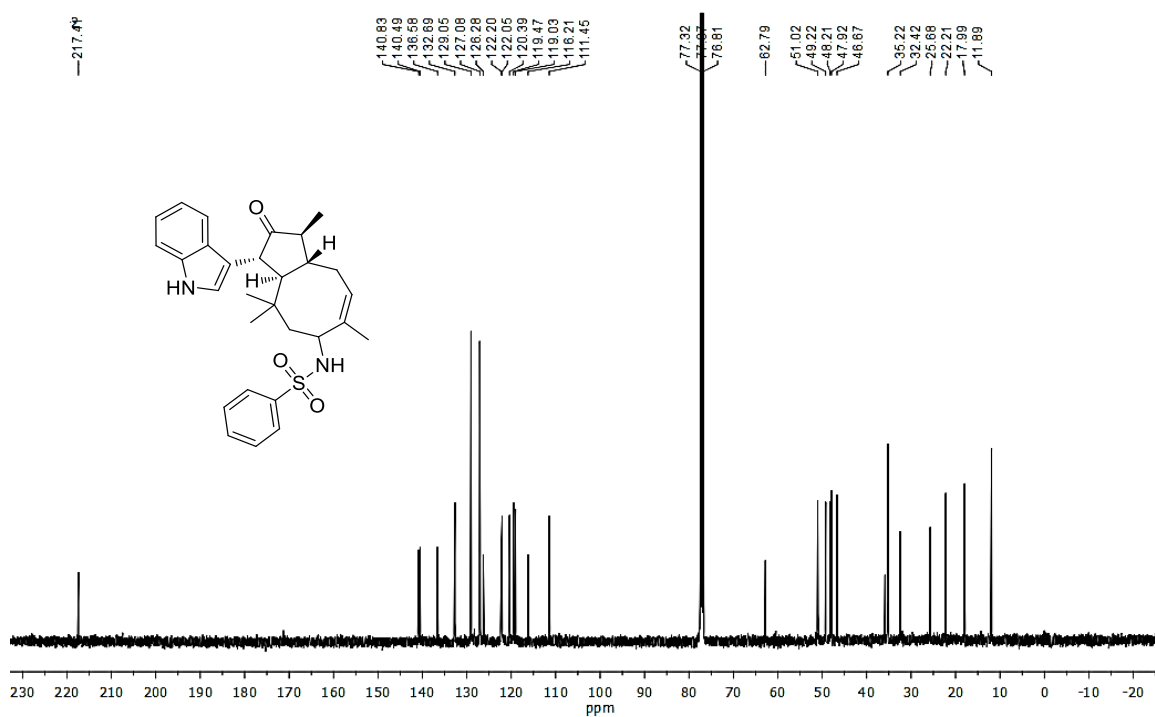


Figure 6.6. ^{13}C NMR of compound **56a** in CDCl_3

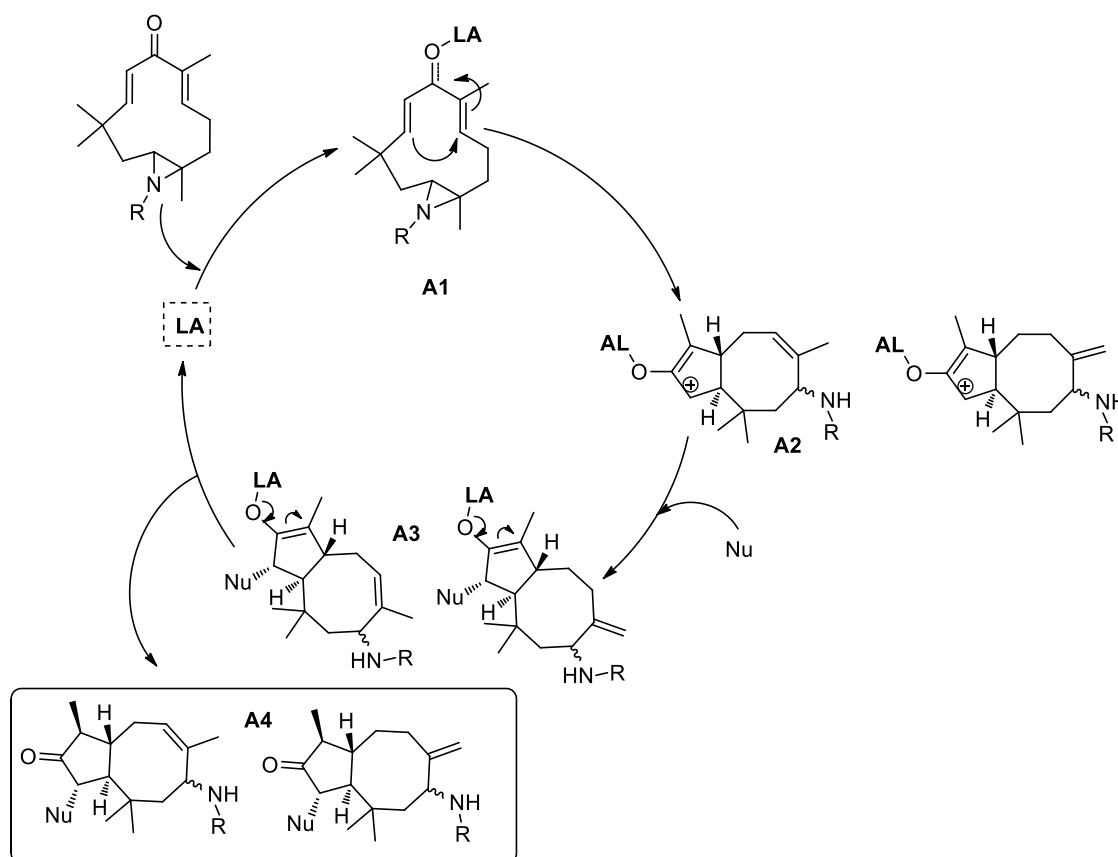
Table 6.2. Generality of interrupted Nazarov cyclisation

Entry	Sulfonamide (51)	Indole (54)	Yield(%)		Entry	Sulfonamide (51)	Indole (54)	Yield(%)	
			55	56				55	56
1			46	48	8			43	45
2			45	47	9			41	47
3			41	47	10			46	49
4			41	46	11			40	49
5			42	47	12			45	48
6			41	46	13			42	46
7			46	47					

Reaction condition: Zerumbone-Aziridine (1 equiv.), Indole (1 equiv.), In(OTf)₃ (5 mol%), DCM (2 mL), RT, 6 h.

Our proposed mechanism for the formation of the [5.8] fused-ring products follow the interrupted Nazarov-type cyclization pathway. Initially, the Lewis acid coordinates to the carbonyl oxygen atom of the zerumbone, thereby creating an allyl carbocation intermediate (**A2**). Then, the carbocation is trapped by an external nucleophile (indole),

followed by a tautomeric rearrangement to afford the product. A general mechanistic pathway for the interrupted Nazarov reaction is given in scheme 6.4.



Scheme 6.4. Proposed mechanism for the interrupted Nazarov reaction

Over-all, we have developed Lewis-acid-catalyzed cyclization reactions of zerumbone and its derivatives, to access structurally diverse polycyclic compounds. The core structures of the synthesized molecules, that is [5.8] fused-ring systems, are found in many biologically active natural products (figure 6.7). The highlight of the new method is its utilization of renewable resources to generate complicated fused skeletons. Furthermore, this reaction strategy opens new opportunities for the syntheses of chemically diverse natural product scaffolds that contain heterocyclic or carbocyclic appendages.⁵

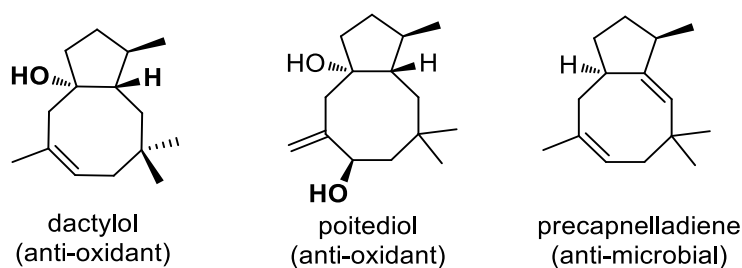


Figure 6.7. Natural products with [5.8] fused ring systems

6.4. Molecular Docking Studies

Most of our synthesized derivatives have multiple points for functionalization, and can be used as efficient scaffolds in the total syntheses of many biologically relevant molecules. Also, the compounds themselves, or their simple derivatives may show interesting biological activities. Hence we planned to explore the biological properties of these derivatives, especially for their antidiabetic and antiproliferative activities. But it was quite difficult for us to carry out the biological activities of all these molecules, consequently we focused on the virtual screening of these, with an α -glucosidase enzyme (antidiabetic protein) 3A4A and an anticancer protein (EGFR kinase domain in complex with AFN941) 2ITW using MOE 2009.10. The default 'Site Finder' tool was used to understand the active site of the proteins. The binding mode of interaction between the protein and the zerumbone derivatives were studied using LigPlot analysis, and the results of docking studies are shown in tables 6.3 and 6.4.

Table 6.3. Molecular docking study of [5.8.3] fused systems

Entry	Sample	E-score (kcal/mol)	
		3A4A	2ITW
1	53a	-11.3867	-11.5278
2	53b	-10.820	-10.7554
3	53c	-12.001	-11.8498
4	53d	-12.0105	-11.6311
5	53e	-12.6039	-11.4715
6	54f	-12.0165	-11.1329
7	54g	-12.8459	-12.0312
8	54h	-13.0765	-11.4289
9	54i	-14.5787	-12.6835

In our studies, among these nine [5.8.3] fused compounds, the compound **54i** showed the better molecular docking score of -14.5787 kcal/mol with the enzyme 3A4A. The binding interaction shows five prominent interfaces. It include, a backbone acceptor interaction with the polar amino acid residue Ser241 (2.25 Å, 30 %), and all other interactions are side chain acceptor interactions. The polar amino acid residue Tyr158 (2.13 Å, 24 %) showed a sidechain acceptor interaction with the -S=O group, while the amino acid residues Ser240 and Ser241 also showed side chain acceptor interactions with **54i**. A

pictorial representation of the binding modes of compound **54i** with the enzyme 3A4A is given in figure 6.8.

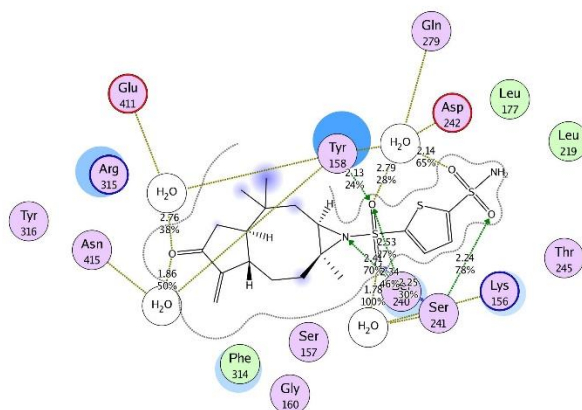


Figure 6.8. Binding modes of compound **54i** with the enzyme 3A4A

In the next stage, we extended the scope of the molecular docking studies with compounds **55a-m** and **56a-m** and the results of our studies are given in table 6.4.

Table 6.4. Molecular docking study of [5.8] fused systems

Entry	Sample	E-score (kcal/mol)		Sample	E-score (kcal/mol)	
		3A4A	2ITW		3A4A	2ITW
1	55a	-11.2955	-11.2548	56a	-12.4234	-11.6811
2	55b	-12.9279	-11.3409	56b	-12.2062	-11.3315
3	55c	-12.5751	-12.6161	56c	-13.9652	-11.4040
4	55d	-13.5343	-13.5391	56d	-13.5920	-11.5679
5	55e	-11.3683	-12.9122	56e	-13.6951	-11.5253
6	55f	-11.1548	-12.2155	56f	-13.3234	-11.4588
7	55g	-11.1466	-11.9179	56g	-12.8862	-11.6745
8	55h	-11.4320	-12.4450	56h	-13.9665	-11.4088
9	55i	-11.6598	-13.4371	56i	-13.4523	-11.6544
10	55j	-11.4483	-12.6135	56j	-13.7053	-11.8654
11	55k	-13.1925	-13.3884	56k	-14.4682	-12.9361
12	55l	-12.8854	-12.7453	56l	-13.0420	-11.6411
13	55m	-12.1283	-12.1936	56m	-13.3149	-11.1045

All these compounds showed good results in the docking studies with better binding scores. While comparing the docking scores of all the molecules, we found that, compounds with exocyclic double (**55**) bond show better affinity with the enzyme 2ITW, while

compounds with endocyclic system (**56**) gave better binding score with the enzyme 3A4A. Among these [5.8] fused derivatives, the compounds **55k** and **56k** gave the better docking scores. The compound **55k** showed a molecular docking score of -13.3884 kcal/mole with the protein 2ITW *via* an arene-cation interaction with a basic amino acid residue Lys (2.69 Å, 78 %). The molecular docking score of the compound **56k** is -14.4682 kcal/mole with the protein 3A4A through an arene-arene interaction between the benzene ring and the polar amino acid residue Tyr158 (figure 6.9).⁶

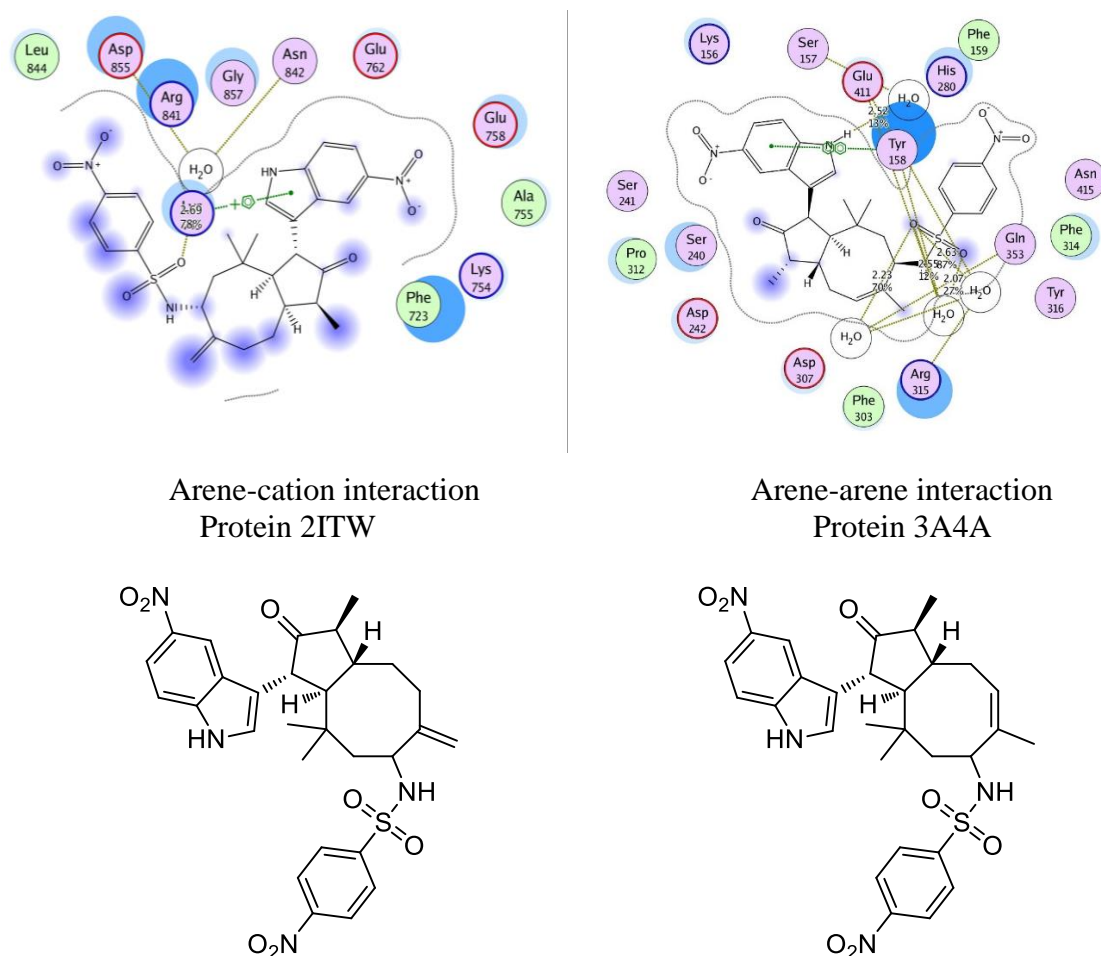


Figure 6.9. Binding modes of compounds **55k** and **56k** with the enzymes 2ITW and 3A4A

6.5. Conclusion

In conclusion, we have effectively utilized the abundant natural product, zerumbone, towards the synthesis of new classes of [5.8.3] and [5.8] fused sesquiterpenoid derivatives *via* Lewis-acid-catalyzed reactions. The synthesized derivatives have multiple points for functionalization, and can be used as an efficient scaffold in the total syntheses of many biologically relevant molecules. Also, most of these scaffolds are the core units of numerous biologically active molecules. Furthermore, this reaction strategy opens new

opportunities for the development of structurally diverse natural product scaffolds that contain heterocyclic or carbocyclic appendages. In addition to these, the preferable binding modes of these derivatives were analyzed through molecular docking studies.

6.6. Experimental section

General procedure for the synthesis of [5.8.3] fused ring system : The reaction was carried out with aziridine derived from zerumbone and benzene sulphonamide. Nazarov cyclisation on aziridine was performed in the presence of 5 mol% of $\text{In}(\text{OTf})_3$ in DCM at room temperature for 3 hours. After the completion of the reaction, as monitored by TLC, the reaction mixture was concentrated under reduced pressure, and the crude product was purified by column chromatography on silica gel (100-200 mesh) using hexane-ethyl acetate as the eluent.

Procedure for the synthesis of [5.8] fused ring system : The reaction was carried out with the aziridine derived from zerumbone and benzene sulphonamide. The reaction of one equivalent of aziridinated zerumbone with 1.0 equivalent indole in the presence of 5 mol% of $\text{In}(\text{OTf})_3$ in DCM at room temperature for 6 hours resulted in the formation of isomeric [5,8] fused ring systems. After the completion of the reaction, as monitored by TLC, the reaction mixture was concentrated under reduced pressure, and the crude product was purified by column chromatography on silica gel (100-200 mesh) using hexane-ethyl acetate as the eluent.

6.7. Spectral Data

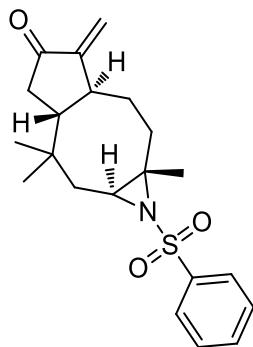
1a,7,7-trimethyl-4-methylene-1-(phenylsulfonyl)decahydrocyclopenta[5,6]cycloocta [1,2-b]azirin-5(1aH)-one (53a)

Following the general procedure as described in section, the reaction was carried out with 30 mg of aziridinated zerumbone **52a** with 5 mol% indium triflate in DCM at room temperature for 3 hours and the corresponding product was isolated in 19 mg (yield 62 %).

R_f : 0.432 (ethyl acetate : hexane = 3:2); Colorless amorphous solid.

IR (neat) ν_{max} : 3261, 2916, 2849, 1645, 1576, 1542 cm^{-1} .

^1H NMR (500 MHz, CDCl_3): δ 7.85 (d, $J = 7$ Hz, 2H), 7.53-7.47 (m, 3H), 6.13 (d, $J = 3$ Hz, 1H), 5.26 (d, $J = 2.5$ Hz, 1H), 4.13-4.09 (m, 1H), 2.99-2.96 (m, 1H), 2.86 (d, $J = 19$ Hz, 1H), 2.66-2.59 (m, 1H), 2.10 (d, $J = 19$ Hz, 1H), 2.02-1.99 (m, 2H), 1.89-1.82 (m, 1H), 1.65-1.64 (m, 2H), 1.39-



1.33 (m, 1H), 0.99 (s, 3H), 0.83 (d, $J = 7$ Hz, 3H), 0.45 (s, 3H) ppm.

^{13}C NMR (125 MHz, CDCl_3): δ 201.8, 148.8, 143.3, 132.1, 129.1, 126.4, 118.6, 75.1, 64.1, 48.0, 45.5, 42.8, 37.5, 36.9, 32.8, 30.4, 27.5, 22.6, 17.6 ppm.

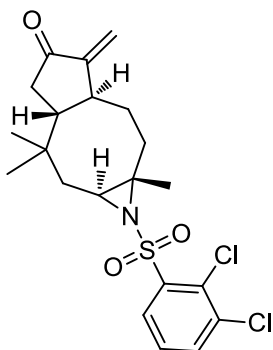
HRMS (ESI) : m/z Calcd for $\text{C}_{21}\text{H}_{27}\text{NNaO}_3\text{S}$: 396.1609; Found: 396.1590.

1-((2,3-dichlorophenyl)sulfonyl)-1a,7,7-trimethyl-4-methylenedecahydrocyclopenta[5,6]cycloocta[1,2-b]azirin-5(1aH)-one (53g)

Following the general procedure as described in section, the reaction was carried out with 30 mg of aziridinated zerumbone **52g** with 5 mol% indium triflate in DCM at room temperature for 3 hours and the corresponding product was isolated in 14 mg (yield 45 %).

R_f : 0.46 (ethyl acetate : hexane = 3:2); Colorless amorphous solid.

IR (neat) ν_{max} : 2920, 2846, 1863, 1701, 1644, 1571, 1465 cm^{-1} ;



^1H NMR (500 MHz, CDCl_3): δ 8.04 (d, $J = 8$ Hz, 1H), 7.64 (d, $J = 8$ Hz, 1H), 7.40 (t, $J = 3$ Hz, 1H), 6.12 (d, $J = 3$ Hz, 1H), 5.27 (d, $J = 2.5$ Hz, 1H), 4.69-4.66 (m, 1H), 3.09-3.06 (m, 1H), 2.52-2.46 (m, 1H), 2.38 (d, $J = 19$ Hz, 1H), 2.11-2.04 (m, 3H), 1.80-1.78 (m, 2H), 1.70-1.66 (m, 1H), 1.42-1.38 (m, 1H), 1.04 (s, 3H), 0.84 (d, $J = 7$ Hz, 3H), 0.74 (s, 3H) ppm.

^{13}C NMR (125 MHz, CDCl_3): δ 201.9, 149.1, 144.1, 135.5, 134.0, 130.0, 129.7, 128.1, 118.2, 75.0, 66.3, 47.4, 45.6, 42.9, 38.4, 36.6, 32.8, 29.9, 28.5, 23.1, 17.9 ppm.

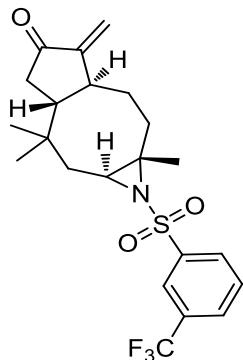
HRMS (ESI): m/z Calcd for $\text{C}_{21}\text{H}_{25}\text{Cl}_2\text{NNaO}_3\text{S}$: 464.0829; Found : 464.0826.

1a,7,7-trimethyl-4-methylene-1-((3-(trifluoromethyl)phenyl)sulfonyl) decahydrocyclopenta[5,6]cycloocta[1,2-b]azirin-5(1aH)-one (53h)

Following the general procedure as described in section, the reaction was carried out with 30 mg of aziridinated zerumbone **52h** with 5 mol% indium triflate in DCM at room temperature for 3 hours, and the corresponding product was isolated in 11 mg (yield 36 %).

R_f: 0.434 (ethyl acetate : hexane = 3:2); Colorless amorphous solid

IR (neat) ν_{\max} : 3478, 2918, 2860, 2077, 1647, 1466, 1270, 1160 cm^{-1} ; **¹H NMR** (500 MHz, CDCl_3): δ 8.07-8.05 (m, 2H), 7.81-7.79 (m, 1H), 7.68-7.65 (m, 1H), 6.14 (d, $J = 3$ Hz, 1H), 5.28 (d, $J = 2.5$ Hz, 1H), 4.11-4.08 (m, 1H), 3.03-2.99 (m, 1H), 2.75 (d, $J = 19$ Hz, 1H), 2.62-2.58 (m, 1H), 2.15 (d, $J = 19$ Hz, 1H), 2.04-1.96 (m, 2H), 1.88-1.82 (m, 1H), 1.69-1.60 (m, 2H), 1.41-1.34 (m, 1H), 1.01 (s, 3H), 0.85 (d, $J = 7$ Hz, 3H), 0.46 (s, 3H) ppm.



¹³C NMR (125 MHz, CDCl_3): δ 201.5, 148.6, 144.1, 129.9, 129.8, 128.7, 123.5, 118.9, 75.7, 64.4, 47.9, 45.5, 42.9, 37.5, 36.8, 32.9, 30.3, 27.4, 22.5, 17.6 ppm.

HRMS (ESI): m/z Calcd for $\text{C}_{22}\text{H}_{26}\text{F}_3\text{NNaO}_3\text{S}$: 464.1483; Found: 464.1479.

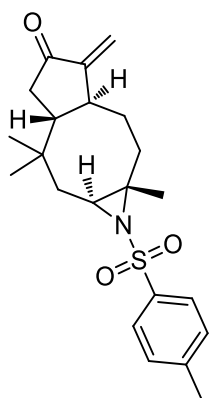
1a,7,7-trimethyl-4-methylene-1-tosyldecahydrocyclopenta[5,6]cycloocta[1,2-b]azirin-5(1aH)-one (53i)

Following the general procedure as described in section, the reaction was carried out with 30 mg of aziridinated zerumbone **52i** with 5 mol% indium triflate in DCM at room temperature for 3 hours and the corresponding product was isolated in 20 mg (yield 66 %).

R_f : 0.44 (ethyl acetate : hexane = 3:2); as colorless amorphous solid.

IR (neat) ν_{\max} : 2916, 2849, 1868, 1709, 1643, 1581, 1159 cm^{-1} .

¹H NMR (500 MHz, CDCl_3): δ 7.72 (d, $J = 7$ Hz, 2H), 7.27 (d, $J = 7$ Hz, 2H), 6.13 (d, $J = 3$ Hz, 1H), 5.26 (d, $J = 2.5$ Hz, 1H), 4.12-4.08 (m, 1H), 3.00-2.95 (m, 1H), 2.87 (d, $J = 19$ Hz, 1H), 2.63-2.55 (m, 1H), 2.41 (s, 3H), 2.09 (d, $J = 19$ Hz, 1H), 2.02-2.00 (m, 2H), 1.99-1.85 (m, 1H), 1.65-1.59 (m, 2H), 1.40-1.31 (m, 1H), 0.99 (s, 3H), 0.82 (d, $J = 7$ Hz, 3H), 0.46 (s, 3H) ppm.



^{13}C NMR (125 MHz, CDCl_3): δ 201.9, 148.9, 142.6, 140.5, 129.6, 126.4, 118.6, 75.0, 64.0, 48.1, 45.4, 42.8, 37.5, 35.9, 32.8, 30.4, 27.6, 22.6, 21.5, 17.6 ppm.

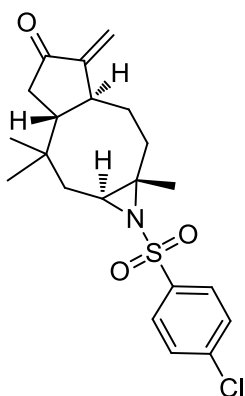
HRMS (ESI): m/z . Calcd for $\text{C}_{22}\text{H}_{29}\text{NNaO}_3\text{S}$: 410.1765; Found: 410.1759.

1-((4-chlorophenyl)sulfonyl)-1a,7,7-trimethyl-4-methylenedecahydrocyclopenta [5,6]cycloocta[1,2-b]azirin-5(1aH)-one (53j)

Following the general procedure as described in section, the reaction was carried out with 30 mg of aziridinated zerumbone **52j** with 5 mol% indium triflate in DCM at room temperature for 3 hours and the corresponding product was isolated in 23 mg (yield 72 %).

R_f : 0.464 (ethyl acetate : hexane = 3:2); colorless amorphous solid.

IR (neat) ν_{max} : 3371, 2916, 2843, 1651, 1753, 1722, 1536, 1466 cm^{-1} .



^1H NMR (500 MHz, CDCl_3): δ 7.78 (d, $J = 8.5$ Hz, 2H), 7.46 (d, $J = 9$ Hz, 2H), 6.13 (d, $J = 3$ Hz, 1H), 5.26 (d, $J = 2.5$ Hz, 1H), 4.05-4.08 (m, 1H), 3.01-2.98 (m, 1H), 2.78 (d, $J = 19$ Hz, 1H), 2.60-2.58 (m, 1H), 2.13 (d, $J = 19$ Hz, 1H), 2.02-1.99 (m, 2H), 1.97-1.83 (m, 1H), 1.67-1.65 (m, 2H), 1.38-1.25 (m, 1H), 1.01 (s, 3H), 0.82 (d, $J = 7$ Hz, 3H), 0.48 (s, 3H) ppm.

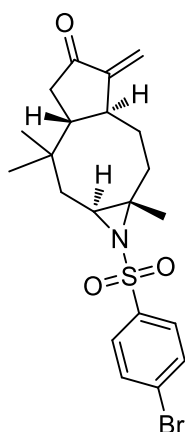
^{13}C NMR (125 MHz, CDCl_3): δ 202.7, 148.7, 141.7, 138.5, 137.4, 130.2, 129.4, 127.9, 118.8, 75.31, 64.25, 47.9, 45.5, 42.8, 37.5, 36.9, 33.2, 30.3, 27.7, 22.6, 17.6 ppm.

HRMS (ESI): m/z . Calcd for $\text{C}_{21}\text{H}_{26}\text{ClNNaO}_3\text{S}$: 430.1219; Found: 430.1218.

1-((4-bromophenyl)sulfonyl)-1a,7,7-trimethyl-4-methylenedecahydrocyclopenta [5,6]cycloocta[1,2-b]azirin-5(1aH)-one (53k)

Following the general procedure as described in section, the reaction was carried out with 30 mg of aziridinated zerumbone **52k** with 5 mol% indium triflate in DCM at room temperature for 3 hours and the corresponding product was isolated in 10 mg (yield 33 %).

R_f : 0.540 (ethyl acetate : hexane = 3:2); colorless amorphous solid.



IR (neat) ν_{\max} : 3428, 2925, 2098, 1643, 1467, 1338, 1159, 1101, 743 cm^{-1} .

$^1\text{H NMR}$ (500 MHz, CDCl_3): δ 7.71 (d, $J = 8.5$ Hz, 2H), 7.63 (d, $J = 9$ Hz, 2H), 6.15 (d, $J = 3.5$ Hz, 1H), 5.28 (d, $J = 2.5$ Hz, 1H), 4.10-4.06 (m, 1H), 3.03-3.00 (m, 1H), 2.78 (d, $J = 19.5$ Hz, 1H), 2.59-2.56 (m, 1H), 2.15 (d, $J = 19$ Hz, 1H), 2.02-1.95 (m, 2H), 1.86-1.81 (m, 1H), 1.68-1.66 (m, 2H), 1.41-1.33 (m, 1H), 1.01 (s, 3H), 0.82 (d, $J = 7$ Hz, 3H), 0.49 (s, 3H) ppm.

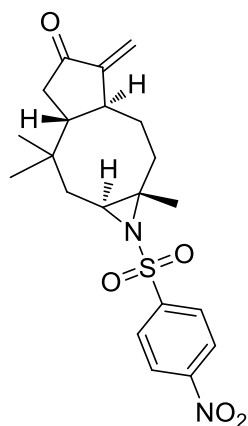
$^{13}\text{C NMR}$ (125 MHz, CDCl_3): δ 202.1, 148.8, 142.1, 132.4, 129.1, 128.2, 128.0, 127.0, 118.9, 75.5, 64.3, 47.9, 45.5, 43.0, 37.6, 36.9, 32.8, 30.2, 27.7, 22.6, 17.6 ppm.

HRMS (ESI): m/z Calcd for $\text{C}_{21}\text{H}_{26}\text{BrNNaO}_3\text{S}$: 474.0714; Found: 474.0712.

1a,7,7-trimethyl-4-methylene-1-((4-nitrophenyl)sulfonyl)decahydrocyclopenta[5,6]cycloocta[1,2-b]azirin-5(1aH)-one (53I)

Following the general procedure as described in section, the reaction was carried out with 30 mg of aziridinated zerumbone **52I** with 5 mol% indium triflate in DCM at room temperature for 3 hours and the corresponding product was isolated in 18 mg (yield 60 %).

R_f : 0.623 (ethyl acetate : hexane = 3:2); Colorless amorphous solid



IR (neat) ν_{\max} : 3369, 2917, 2851, 1643, 1759, 1724, 1532, 1467, 1349, 1161, 1105, 745 cm^{-1} ;

$^1\text{H NMR}$ (500 MHz, CDCl_3): δ 8.35 (d, $J = 9$ Hz, 2H), 8.04 (d, $J = 9$ Hz, 2H), 6.17 (d, $J = 3$ Hz, 1H), 5.31 (d, $J = 3$ Hz, 1H), 4.14-4.10 (m, 1H), 3.05-3.02 (m, 1H), 2.72 (d, $J = 19$ Hz, 1H), 2.62-2.60 (m, 1H), 2.19 (d, $J = 19$ Hz, 1H), 2.07-2.03 (m, 1H), 1.97-1.95 (m, 1H), 1.89-1.83 (m, 1H) 1.71-1.69 (m, 2H), 1.43-1.39 (m, 1H), 1.02 (s, 3H), 0.85 (d, $J = 7$ Hz, 3H), 0.46 (s, 3H) ppm.

$^{13}\text{C NMR}$ (125 MHz, CDCl_3): δ 201.6, 148.5, 148.4, 127.7, 124.5, 119.3, 75.9, 64.7, 47.8, 45.5, 43.1, 37.7, 36.8, 32.8, 30.1, 27.7, 22.5, 17.6 ppm.

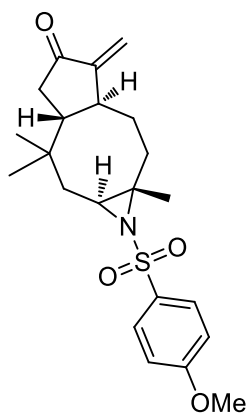
HRMS (ESI): m/z Calcd for $C_{21}H_{26}N_2NaO_5S$: 441.1460; Found : 441.1454.

1-((4-methoxyphenyl)sulfonyl)-1a,7,7-trimethyl-4-methylenedecahydrocyclopenta[5,6]cycloocta[1,2-b]azirin-5(1aH)-one (53o)

Following the general procedure as described in section, the reaction was carried out with 30 mg of aziridinated zerumbone **52o** with 5 mol% indium triflate in DCM at room temperature for 3 hours and the corresponding product was isolated in 20 mg (yield 65 %).

R_f: 0.445 (ethyl acetate : hexane = 3:2); Colorless amorphous solid.

IR (neat) ν_{\max} : 2923, 1744, 1645, 1597, 1498, 1464, 1333, 1259, 1152, 1102, 1031, 838 cm^{-1} .



¹H NMR (500 MHz, $CDCl_3$): δ 7.78 (d, $J = 9$ Hz, 2H), 6.94 (d, $J = 9$ Hz, 2H), 6.14 (d, $J = 3$ Hz, 1H), 5.26 (d, $J = 2.5$ Hz, 1H), 4.12-4.08 (m, 1H), 3.86 (s, 3H), 3.01-2.96 (m, 1H), 2.90 (d, $J = 19$ Hz, 1H), 2.61-2.58 (m, 1H), 2.12 (d, $J = 19$ Hz, 1H), 2.02-1.98 (m, 2H), 1.85-1.80 (m, 1H), 1.66-1.64 (m, 2H), 1.36-1.32 (m, 1H), 0.99 (s, 3H), 0.81 (d, $J = 7$ Hz, 3H), 0.49 (s, 3H) ppm.

¹³C NMR (125 MHz, $CDCl_3$): δ 202.4, 162.4, 149.0, 135.3, 129.0, 128.5, 128.2, 118.6, 114.2, 75.0, 64.0, 56.6, 48.1, 45.5, 42.8, 37.5, 36.9, 32.8, 30.4, 27.6, 22.6, 17.6 ppm.

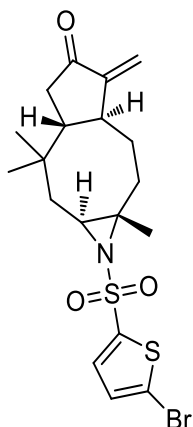
HRMS (ESI): m/z Calcd for $C_{22}H_{29}NNaO_4S$: 426.1715; Found : 426.1709.

1-((5-bromothiophen-2-yl)sulfonyl)-1a,7,7-trimethyl-4-methylenedecahydrocyclopenta[5,6]cycloocta[1,2-b]azirin-5(1aH)-one (53v)

Following the general procedure as described in section, the reaction was carried out with 30 mg of aziridinated zerumbone **52v** with 5 mol% indium triflate in DCM at room temperature for 3 hours and the corresponding product was isolated in 14 mg (yield 45 %).

R_f: 0.554 (ethyl acetate : hexane = 3:2); Colorless amorphous solid.

IR (neat) ν_{\max} : 3370, 2910, 2856, 1644, 1755, 1721, 1533 cm^{-1} .



¹H NMR (500 MHz, CDCl₃): δ 7.33 (d, *J* = 4 Hz, 1H), 7.03 (d, *J* = 4 Hz, 1H), 6.14 (d, *J* = 3 Hz, 1H), 5.27 (d, *J* = 2.5 Hz, 1H), 3.98-3.96 (m, 1H), 3.05 (d, *J* = 19 Hz, 1H), 3.00-2.97 (m, 1H), 2.54-2.48 (m, 1H), 2.21 (d, *J* = 19 Hz, 1H), 2.01-1.97 (m, 1H), 1.94-1.88 (m, 1H), 1.86-1.81 (m, 1H), 1.69-1.66 (m, 2H), 1.40-2.34 (m, 1H), 1.03 (s, 3H), 0.82 (d, *J* = 6.5 Hz, 3H), 0.60 (s, 3H) ppm.

¹³C NMR (125 MHz, CDCl₃): δ 201.5, 148.5, 144.8, 130.8, 129.9, 119.0, 118.4, 75.9, 63.6, 48.1, 45.5, 42.8, 37.0, 36.9, 30.9, 30.3, 27.6, 22.6, 17.5 ppm.

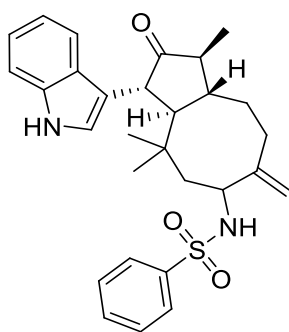
HRMS (ESI): *m/z* Calcd for C₁₉H₂₄BrNNaO₃S₂: 480.0278; Found: 480.02813 and 482.0259.

N-(3-(1H-indol-3-yl)-1,4,4-trimethyl-7-methylene-2-oxodecahydro-1H-cyclopenta[8]annulen-6-yl)benzenesulfonamide (55a)

Following the general procedure as described in section, the reaction was carried out with 30 mg of aziridinated zerumbone (as 1 equiv.) **52a** with 1 equiv. of corresponding indole and 5 mol% of indium triflate in DCM at room temperature for 6 hours and the corresponding products were isolated in 19 and 20 mg (yields 46 % and 48 %).

R_f: 0.458 (ethyl acetate : hexane = 3:2); Colorless amorphous solid.

IR (neat) ν_{max}: 3420, 2920, 1644, 1459, 1159, 1098cm⁻¹.



¹H NMR (500 MHz, CDCl₃): δ 8.05 (brs, 1H), 7.86-7.84 (m, 2H), 7.73 (d, *J* = 8 Hz, 1H), 7.57-7.55 (m, 1H), 7.51-7.48 (m, 2H), 7.32 (d, *J* = 8.5 Hz, 1H), 7.20-7.17 (m, 1H), 7.13-7.09 (m, 1H), 6.88 (d, *J* = 7 Hz, 1H), 5.11 (s, 1H), 5.04 (s, 1H), 4.82 (d, *J* = 9.5 Hz, 1H), 4.12-4.10 (m, 1H), 3.54 (d, *J* = 5 Hz, 1H), 2.77 (t, *J* = 6 Hz, 1H), 2.62-2.58 (m, 1H), 2.30-2.27 (m, 1H), 2.18-2.12 (m, 2H), 2.01-1.96 (m, 1H), 1.78-1.73 (m, 1H), 1.53-1.48 (m, 1H), 1.26-1.25 (m, 1H), 1.01 (d, *J* = 7 Hz, 3H), 0.90 (s, 3H), 0.78 (s, 3H) ppm.

¹³C NMR (125 MHz, CDCl₃): δ 216.6, 149.6, 140.9, 136.6, 132.6, 129.1, 129.0, 127.0, 126.2, 122.6, 121.2, 119.9, 119.8,

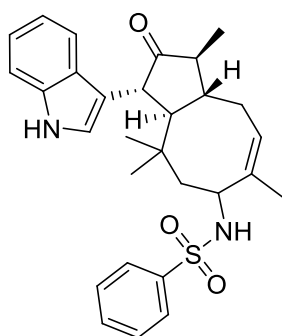
116.6, 111.9, 111.2, 110.0, 57.2, 51.1, 50.9, 48.9, 47.7, 42.8, 37.4, 37.2, 32.1, 30.0, 23.3, 12.7 ppm.

HRMS (ESI): m/z Calcd for $C_{29}H_{34}N_2NaO_3S$: 513.2187;
Found: 513.2207.

N-(3-(1H-indol-3-yl)-1,4,4,7-tetramethyl-2-oxo-2,3,3a,4,5,6,9,9a-octahydro-1H-cyclopenta[8]annulen-6-yl)benzenesulfonamide (56a)

R_f: 0.457 (ethyl acetate : hexane = 3:2); Colorless amorphous solid.

IR (neat) ν_{max} : 3277, 2921, 1737, 1597, 1457, 1329 cm^{-1} .



¹H NMR (500 MHz, $CDCl_3$): δ 8.08 (brs, 1H), 7.86-7.85 (m, 2H), 7.58-7.56 (m, 1H), 7.51-7.47 (m, 3H), 7.29-7.27 (m, 1H), 7.15-7.12 (m, 1H), 7.06-7.03 (m, 1H), 6.79 (d, $J = 2.5$ Hz, 1H), 5.48 (t, $J = 8.5$ Hz, 1H), 4.72 (d, $J = 8$ Hz, 1H), 4.54 (t, $J = 10$ Hz, 1H), 3.36 (d, $J = 11.5$ Hz, 1H), 2.54-2.45 (m, 2H), 2.26-2.16 (m, 2H), 1.70 (s, 4H), 1.51-1.46 (m, 1H), 1.19-1.16 (m, 1H), 1.11 (d, $J = 7$ Hz, 3H), 0.88 (s, 3H), 0.59 (s, 3H) ppm.

¹³C NMR (125 MHz, $CDCl_3$): δ 217.4, 140.8, 140.5, 136.6, 132.7, 129.0, 127.1, 126.3, 122.2, 122.1, 120.4, 119.5, 119.0, 116.2, 111.4, 62.8, 51.0, 49.2, 48.2, 47.9, 46.7, 36.2, 32.4, 25.7, 22.2, 18.0, 11.9 ppm.

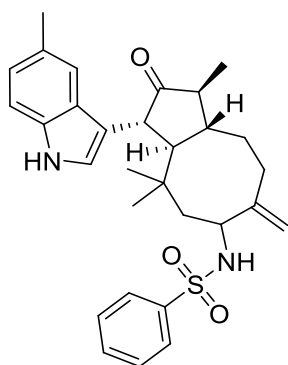
HRMS (ESI): m/z Calcd for $C_{29}H_{34}N_2NaO_3S$: 513.2187;
Found : 513.2201.

N-(1,4,4-trimethyl-3-(5-methyl-1H-indol-3-yl)-7-methylene-2-oxodecahydro-1H-cyclopenta[8]annulen-6-yl)benzenesulfonamide (55b)

Following the general procedure as described in section, the reaction was carried out with 30 mg of aziridinated zerumbone (as 1 equiv.) **52a** with 1 equiv. of corresponding indole and 5 mol% of indium triflate in DCM at room temperature for 6 hours and the corresponding products were isolated in 19 and 20 mg (yield 45 % and 47 %).

R_f : 0.486 (ethyl acetate : hexane = 3:2); colorless amorphous solid.

IR (neat) ν_{max} : 3397, 3062, 2926, 2867, 1731, 1641, 1446, 1322, 1159, 1094, 743 cm^{-1} .



¹H NMR (500 MHz, CD₃COCD₃): δ 9.82 (brs, 1H), 7.73-7.72 (m, 2H), 7.62-7.60 (m, 1H), 7.46-7.44 (m, 1H), 7.42-7.41 (m, 1H), 7.09-7.03 (m, 2H), 6.92 (d, *J* = 2.5 Hz, 1H), 6.78-6.77 (m, 1H), 6.41 (d, *J* = 9 Hz, 1H), 4.98 (s, 1H), 4.80 (s, 1H), 4.05-4.03 (brs, 1H), 3.35 (d, *J* = 6 Hz, 1H), 2.57 (t, *J* = 6.5 Hz, 1H), 2.44-2.40 (m, 1H), 2.24 (s, 3H), 2.02-1.91 (m, 3H), 1.74-1.73 (m, 1H), 1.65-1.61 (m, 1H), 1.56-1.52 (m, 1H), 1.19-1.15 (m, 1H), 0.83 (d, *J* = 6.5 Hz, 3H), 0.74 (s, 3H), 0.70 (s, 3H) ppm.

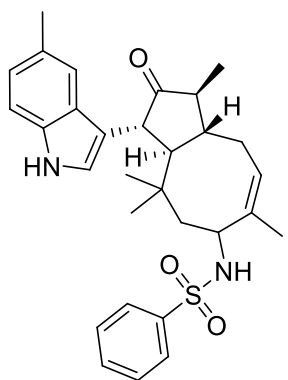
¹³C NMR (125 MHz, CD₃COCD₃): δ 215.6, 149.5, 142.3, 137.4, 135.3, 132.0, 130.6, 128.8, 127.7, 127.5, 126.9, 123.2, 122.3, 119.1, 115.7, 112.2, 111.0, 57.0, 52.5, 48.8, 47.7, 44.8, 42.4, 36.4, 35.9, 31.6, 30.1, 21.9, 20.9, 11.8 ppm.

HRMS (ESI): *m/z* Calcd for C₃₀H₃₆N₂NaO₃S: 527.2344; Found : 527.2357.

N-(1,4,4,7-tetramethyl-3-(5-methyl-1H-indol-3-yl)-2-oxo-2,3,3a,4,5,6,9,9a-octahydro-1H-cyclopenta[8]annulen-6-yl)benzenesulfonamide (56b)

R_f : 0.401 (ethyl acetate : hexane = 3:2); Colorless amorphous solid.

IR (neat) ν_{\max} : 3426, 2923, 2901, 1643, 1467, 1326, 1158, 1101, 1031, 746 cm⁻¹.



¹H NMR (500 MHz, CDCl₃): δ 7.96 (brs, 1H), 7.86-7.85 (m, 2H), 7.57-7.56 (m, 1H), 7.51-7.48 (m, 3H), 7.19-7.17 (m, 1H), 6.97-6.95 (m, 1H), 6.78 (d, *J* = 2 Hz, 1H), 5.49 (t, *J* = 8 Hz, 1H), 4.67 (d, *J* = 8.5 Hz, 1H), 4.48-4.44 (m, 1H), 3.32 (d, *J* = 11.5 Hz, 1H), 2.55-2.49 (m, 2H), 2.39 (s, 3H), 2.27-2.22 (m, 1H), 2.20-2.16 (m, 1H), 1.71 (s, 4H), 1.53-1.48 (m, 1H), 1.19-1.17 (m, 1H), 1.11 (d, *J* = 6.5 Hz, 3H), 0.88 (s, 3H), 0.60 (s, 3H) ppm.

¹³C NMR (125 MHz, CDCl₃): δ 217.0, 140.7, 140.6, 135.0, 132.6, 129.0, 128.7, 127.1, 126.5, 123.8, 122.2, 120.6, 118.8, 116.0, 111.0, 51.1, 51.0, 49.2, 47.9, 46.6, 35.2, 32.4, 25.7, 22.3, 21.6, 18.0, 11.9 ppm.

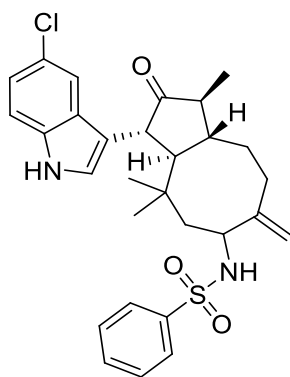
HRMS (ESI): m/z Calcd for $C_{30}H_{36}N_2NaO_3S$: 527.2344;
Found : 527.2358.

N-(3-(5-chloro-1H-indol-3-yl)-1,4,4-trimethyl-7-methylene-2-oxodecahydro-1H-cyclopenta[8]annulen-6-yl)benzenesulfonamide (55c)

Following the general procedure as described in section, the reaction was carried out with 30 mg of aziridinated zerumbone (as 1 equiv.) **52a** with 1 equiv. of corresponding indole and 5 mol% of indium triflate in DCM at room temperature for 6 hours and the corresponding products were isolated in 19 and 22mg (yield 41 % and 47 %).

R_f : 0.43 (ethyl acetate : hexane = 3:2); Colorless amorphous solid.

IR (neat) ν_{max} : 3313, 2917, 2849, 2366, 1977, 1642, 1366, 1271, 755 cm^{-1} .



1H NMR (500 MHz, $CDCl_3$): δ 8.07 (brs, 1H), 7.86-7.84 (m, 2H), 7.68-7.67 (m, 1H), 7.58-7.55 (m, 1H), 7.52-7.49 (m, 2H), 7.25-7.23 (m, 1H), 7.15-7.13 (m, 1H), 6.91 (d, $J = 2.5$ Hz, 1H), 5.10 (s, 1H), 5.06 (s, 1H), 4.74 (d, $J = 9$ Hz, 1H), 4.13-4.11 (m, 1H), 3.48-3.47 (d, $J = 5.5$ Hz, 1H), 2.77 (t, $J = 6$ Hz, 1H), 2.64-2.59 (m, 1H), 2.26-2.24 (m, 1H), 2.17-2.13 (m, 2H), 2.03-1.97 (m, 1H), 1.77-1.75 (m, 1H), 1.65-1.61 (m, 1H), 1.53-1.50 (m, 1H), 1.04 (d, $J = 7$ Hz, 3H), 0.87 (s, 3H), 0.80 (s, 3H) ppm.

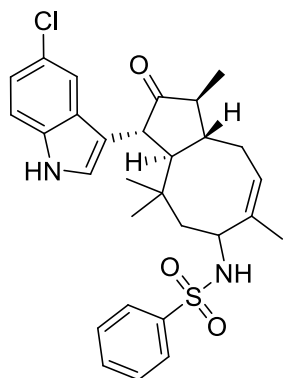
^{13}C NMR (125 MHz, $CDCl_3$): δ 217.1, 149.3, 140.8, 135.0, 132.6, 129.1, 129.0, 127.2, 127.0, 125.4, 123.0, 122.7, 119.2, 115.9, 112.3, 62.8, 57.1, 48.8, 48.3, 42.8, 37.0, 36.8, 31.9, 23.1, 21.1, 14.2, 12.9 ppm.

HRMS (ESI): m/z Calcd for $C_{29}H_{33}ClN_2NaO_3S$: 547.1798;
Found : 547.1809.

N-(3-(5-chloro-1H-indol-3-yl)-1,4,4,7-tetramethyl-2-oxo-2,3,3a,4,5,6,9,9a-octahydro-1H-cyclopenta[8]annulen-6-yl)benzenesulfonamide (56c)

R_f : 0.428 (ethyl acetate : hexane = 3:2); Colorless amorphous solid.

IR (neat) ν_{max} : 3274, 2919, 1734, 1641, 1458, 1327, 1158, 1098, 958 cm^{-1} .



^1H NMR (500 MHz, CDCl_3): δ 8.05 (brs, 1H), 7.79-7.78 (m, 2H), 7.52-7.49 (m, 1H), 7.45-7.42 (m, 2H), 7.37 (d, $J = 1$ Hz, 1H), 7.13-7.11 (m, 1H), 7.02-7.00 (m, 1H), 6.77 (d, $J = 2.5$ Hz, 1H), 5.43 (t, $J = 8.5$ Hz, 1H), 4.53 (d, $J = 8.5$ Hz, 1H), 4.42-4.38 (m, 1H), 3.24 (d, $J = 11.5$ Hz, 1H), 2.50-2.45 (m, 1H), 2.42-2.38 (m, 1H), 2.20-2.16 (m, 1H), 2.11-2.06 (m, 1H), 1.65 (s, 4H), 1.45-1.40 (m, 1H), 1.16-1.13 (m, 1H), 1.05 (d, $J = 7$ Hz, 3H), 0.83 (s, 3H), 0.52 (s, 3H) ppm.

^{13}C NMR (125 MHz, CDCl_3): δ 217.7, 141.0, 140.5, 134.9, 132.7, 129.0, 128.2, 127.2, 127.1, 125.1, 123.7, 122.2, 120.3, 118.4, 115.7, 112.6, 60.4, 51.1, 49.2, 48.0, 46.6, 36.1, 32.4, 25.6, 22.2, 17.9, 14.2, 11.9 ppm.

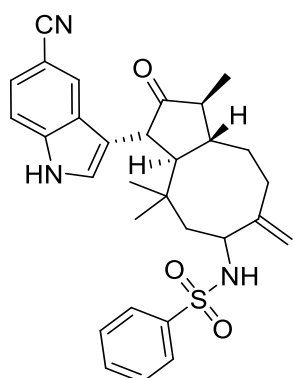
HRMS (ESI): m/z . Calcd for $\text{C}_{29}\text{H}_{33}\text{ClN}_2\text{NaO}_3\text{S}$: 547.1798; Found : 547.1805.

N-(3-(5-cyano-1H-indol-3-yl)-1,4,4-trimethyl-7-methylene-2-oxodecahydro-1H-cyclopenta[8]annulen-6-yl)benzenesulfonamide (**55d**)

Following the general procedure as described in section, the reaction was carried out with 30 mg of aziridinated zerumbone (as 1 equiv.) **52a** with 1 equiv. of corresponding indole and 5 mol% of indium triflate in DCM at room temperature for 6 hours and the corresponding products were isolated in 19 and 22 mg (yield 41 % and 46 %).

R_f : 0.389 (ethyl acetate : hexane = 3:2); Colorless amorphous solid.

IR (neat) ν_{max} : 3422, 2968, 2100, 1643, 1461, 1326, 1156, 1097 cm^{-1} .



^1H NMR (500 MHz, CD_3COCD_3) : δ 10.58 (brs, 1H), 8.03-8.02 (m, 1H), 7.73-7.72 (m, 2H), 7.47-7.45 (m, 1H), 7.44-7.39 (m, 3H), 7.27-7.25 (m, 1H), 7.21 (d, $J = 2$ Hz, 1H), 6.44 (d, $J = 9$ Hz, 1H), 4.99 (s, 1H), 4.82 (s, 1H), 4.07-4.03 (m, 1H), 3.50 (d, $J = 6.5$ Hz, 1H), 2.63 (t, $J = 7$ Hz, 1H), 2.47-2.43 (m, 1H), 2.18-2.5 (m, 1H), 2.05-1.95 (m, 3H), 1.78-1.74 (m, 1H), 1.70-1.61 (m, 2H), 0.86 (d, $J = 7$ Hz, 3H), 0.76 (s, 3H), 0.73 (s, 3H) ppm.

^{13}C NMR (125 MHz, CD_3COCD_3): δ 215.5, 149.5, 142.3, 138.6, 132.0, 128.8, 126.9, 126.5, 125.3, 124.9, 124.2, 120.3,

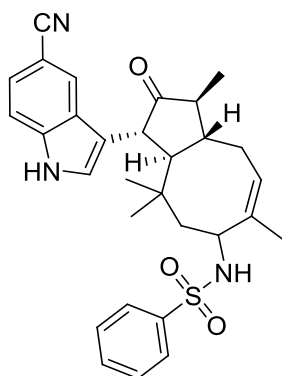
117.2, 112.6, 101.9 56.9, 52.6, 48.5, 48.1, 45.2, 42.4, 36.4, 35.5, 31.6, 30.3, 21.6, 11.8 ppm.

HRMS (ESI): m/z Calcd for $C_{30}H_{33}N_3NaO_3S$: 538.2140; Found : 538.2156.

N-(3-(5-cyano-1H-indol-3-yl)-1,4,4,7-tetramethyl-2-oxo-2,3,3a,4,5,6,9,9a-octahydro-1H-cyclopenta[8]annulen-6-yl)benzenesulfonamide (56d)

R_f: 0.387 (ethyl acetate : hexane = 3:2); Colorless amorphous solid.

IR (neat) ν_{max} : 3405, 2916, 2851, 2390, 2215, 1645, 1467, 1161, 1117 cm^{-1} .



¹H NMR (500 MHz, CD_3COCD_3): δ 10.62 (brs, 1H), 8.04 (s, 1H), 7.89-7.88 (m, 2H), 7.66-7.58 (m, 3H), 7.53-7.51 (m, 1H), 7.37-7.36 (m, 1H), 7.25 (d, $J = 2.5$ Hz, 1H), 6.61 (d, $J = 8$ Hz, 1H), 5.57-5.54 (m, 1H), 4.53-4.49 (m, 1H), 3.62 (d, $J = 11.5$ Hz, 1H), 2.64-2.58 (m, 1H), 2.52-2.48 (m, 1H), 2.30-2.23 (m, 2H), 1.85-1.81 (m, 1H), 1.79 (s, 3H), 1.62-1.57 (m, 1H), 1.21-1.18 (m, 1H), 1.06 (d, $J = 6.5$ Hz, 3H), 0.89 (s, 3H), 0.58 (s, 3H) ppm.

¹³C NMR (125 MHz, CD_3COCD_3): δ 220.3, 147.0, 146.9, 143.6, 137.4, 134.2, 132.6, 132.2, 130.7, 130.2, 127.6, 125.5, 125.0, 123.0, 121.8, 117.8, 107.0, 57.0, 55.9, 53.8, 53.4, 52.5, 51.9, 40.1, 37.2, 30.6, 26.7, 22.7, 16.4 ppm.

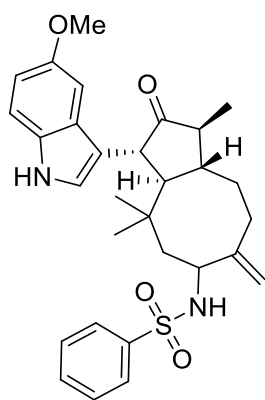
HRMS (ESI): m/z Calcd for $C_{30}H_{33}N_3NaO_3S$: 538.2140; Found : 538.2153.

N-(3-(5-methoxy-1H-indol-3-yl)-1,4,4-trimethyl-7-methylene-2-oxodecahydro-1H-cyclopenta[8]annulen-6-yl)benzenesulfonamide (55e)

Following the general procedure as described in section, the reaction was carried out with 30 mg of aziridinated zerumbone (as 1 equiv.) **52a** with 1 equiv. of corresponding indole and 5 mol% of indium triflate in DCM at room temperature for 6 hours and the corresponding products were isolated in 19 and 22 mg (yield 42 % and 47 %).

R_f: 0.321 (ethyl acetate : hexane = 3:2); Colorless amorphous solid.

IR (neat) ν_{max} : 3415, 2919, 2852, 2064, 1646, 1516 cm^{-1} .



¹H NMR (500 MHz, CDCl₃) : δ 8.03 (brs, 1H), 7.86-7.85 (m, 2H), 7.58-7.55 (m, 1H), 7.51-7.48 (m, 2H), 7.21-7.19 (m, 2H), 6.85-6.83 (m, 2H), 5.12 (s, 1H), 5.04 (s, 1H), 4.94 (d, *J* = 9 Hz, 1H), 4.10 (brs, 1H), 3.86 (s, 3H), 3.48 (d, *J* = 5 Hz, 1H), 2.73 (t, *J* = 5.5 Hz, 1H), 2.60-2.57 (m, 1H), 2.30-2.27 (m, 1H), 2.17-2.11 (m, 1H), 2.01-1.94 (m, 1H), 1.77-1.72 (m, 2H), 1.63-1.59 (m, 1H), 1.54-1.49 (m, 1H), 1.00 (d, *J* = 7 Hz, 3H), 0.92 (s, 3H), 0.77 (s, 3H) ppm.

¹³C NMR (125 MHz, CDCl₃): δ 216.6, 154.2, 149.7, 140.9, 132.6, 131.7, 129.0, 127.0, 126.7, 121.8, 116.1, 113.0, 111.9, 101.5, 57.3, 56.9, 50.6, 48.9, 47.5, 42.8, 37.6, 37.2, 32.2, 29.9, 29.7, 14.1, 12.5 ppm.

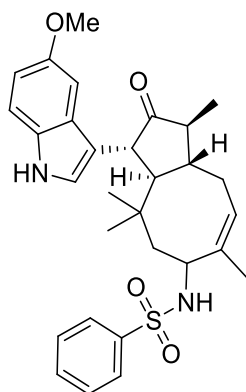
HRMS (ESI): *m/z* Calcd for C₃₀H₃₆N₂NaO₄S: 543.2293; Found: 543.2308.

N-(3-(5-methoxy-1H-indol-3-yl)-1,4,4,7-tetramethyl-2-oxo-2,3,3a,4,5,6,9,9a-octahydro-1H-cyclopenta[8]annulen-6-yl)benzenesulfonamide (56e)

R_f : 0.301 (ethyl acetate : hexane = 3:2); Colorless amorphous solid.

IR (neat) *ν*_{max}: 3650, 3645, 3427, 2351, 1652, 1161 cm⁻¹.

¹H NMR (500 MHz, CDCl₃): δ 8.00 (brs, 1H), 7.87-7.85 (m, 2H), 7.59-7.56 (m, 1H), 7.52-7.48 (m, 2H), 7.16 (d, *J* = 8.5 Hz, 1H), 6.94 (d, *J* = 2 Hz, 1H), 6.81-6.79 (m, 1H), 6.76 (d, *J* = 2.5 Hz, 1H), 5.46 (t, *J* = 8.5 Hz, 1H), 4.79 (d, *J* = 8.5 Hz, 1H), 4.48-4.44 (m, 1H), 3.81 (s, 3H), 3.32 (d, *J* = 11.5 Hz, 1H), 2.58-2.50 (m, 1H), 2.41 (t, *J* = 11.5 Hz, 1H), 2.26-2.21 (m, 1H), 2.18-2.13 (m, 2H), 1.74-1.72 (m, 1H), 1.70 (s, 3H), 1.53-1.48 (m, 1H), 1.11 (d, *J* = 6.5 Hz, 3H), 0.87 (s, 3H), 0.60 (s, 3H) ppm.



¹³C NMR (125 MHz, CDCl₃): δ 217.2, 154.0, 140.8, 140.5, 132.7, 131.8, 129.0, 127.1, 126.7, 122.7, 120.3, 116.2, 112.3, 112.0, 101.1, 55.8, 51.1, 50.9, 49.1, 48.2, 47.9, 46.6, 35.3, 32.4, 25.7, 22.2, 18.1, 11.9 ppm.

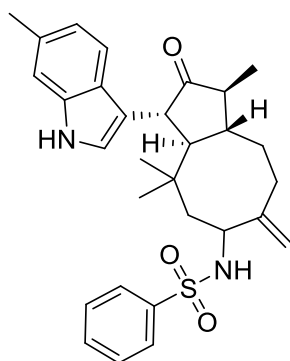
HRMS (ESI): *m/z* Calcd for C₃₀H₃₆N₂NaO₄S: 543.2293; Found : 543.2301.

N-(1,4,4-trimethyl-3-(6-methyl-1H-indol-3-yl)-7-methylene-2-oxodecahydro-1H-cyclopenta[8]annulen-6-yl)benzenesulfonamide (55f)

Following the general procedure as described in section, the reaction was carried out with 30 mg of aziridinated zerumbone (as 1 equiv.) **52a** with 1 equiv. of corresponding indole and 5 mol% of indium triflate in DCM at room temperature for 6 hours and the corresponding products were isolated in 19 and 22 mg (yield 41 % and 46 %).

R_f : 0.436 (ethyl acetate : hexane = 3:2); colorless amorphous solid.

IR (neat) ν_{max}: 3422, 2091, 1638, 1448, 1326, 1159 cm⁻¹.



¹H NMR (500 MHz, CD₃COCD₃): δ 9.96 (brs, 1H), 7.88-7.87 (m, 2H), 7.63-7.55 (m, 4H), 7.15 (s, 1H), 7.03 (d, *J* = 1 Hz, 1H), 6.86-6.85 (m, 1H), 6.58 (d, *J* = 9 Hz, 1H), 5.13 (s, 1H), 4.94 (s, 1H), 4.18 (brs, 1H), 3.49 (d, *J* = 6 Hz, 1H), 2.73-2.70 (m, 1H), 2.59-2.56 (m, 1H), 2.41-2.37 (m, 4H), 2.32-2.30 (m, 1H), 2.18-2.11 (m, 2H), 1.90-1.86 (m, 1H), 1.81-1.77 (m, 1H), 1.72-1.67 (m, 1H), 0.98 (d, *J* = 7 Hz, 3H), 0.89 (s, 3H), 0.85 (s, 3H) ppm.

¹³C NMR (125 MHz, CD₃COCD₃): δ 216.4, 150.4, 143.2, 138.3, 132.9, 131.8, 129.7, 127.8, 126.9, 125.5, 122.4, 121.4, 120.1, 116.9, 113.1, 112.0, 111.0, 57.9, 49.8, 48.6, 43.3, 37.3, 36.9, 32.5, 31.1, 22.7, 21.7, 12.6 ppm.

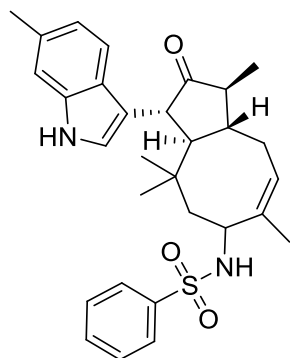
HRMS (ESI): *m/z* Calcd for C₃₀H₃₆N₂NaO₃S: 527.2344; Found : 527.2358.

N-(1,4,4,7-tetramethyl-3-(6-methyl-1H-indol-3-yl)-2-oxo-2,3,3a,4,5,6,9,9a-octahydro-1H-cyclopenta[8]annulen-6-yl)benzenesulfonamide (56f)

R_f : 0.434 (ethyl acetate : hexane = 3:2); Colorless amorphous solid.

IR (neat) ν_{max}: 3428, 2104, 1643, 1460, 1328, 1159 cm⁻¹.

¹H NMR (500 MHz, CDCl₃): δ 8.02 (brs, 1H), 7.86-7.84 (m, 2H), 7.57-7.54 (m, 1H), 7.50-7.47 (m, 2H), 7.34 (d, *J* = 8.5 Hz, 1H), 7.03 (brs, 1H), 6.86 (d, *J* = 8 Hz, 1H), 6.68 (d, *J* = 2.5 Hz, 1H), 5.46 (t, *J* = 8.5 Hz, 1H), 4.93 (d, *J* = 8 Hz, 1H), 4.45-4.41 (m, 1H), 3.32 (d, *J* = 11.5 Hz, 1H), 2.53-2.43 (m, 3H), 2.39 (s, 3H), 2.24-2.16 (m, 2H), 1.69 (s, 3H), 1.50-1.45 (m, 1H), 1.16-



1.13 (m, 1H), 1.10 (d, $J = 7$ Hz, 3H), 0.84 (s, 3H), 0.57 (s, 3H) ppm. ^{13}C NMR (125 MHz, CDCl_3): δ 217.4, 140.8, 140.5, 137.1, 132.7, 131.8, 129.0, 127.1, 124.1, 121.6, 121.2, 120.4, 118.7, 116.0, 111.4, 51.0, 50.9, 49.3, 48.1, 47.9, 46.7, 36.2, 32.4, 25.7, 22.2, 21.6, 18.0, 11.9 ppm.

HRMS (ESI): m/z Calcd for $\text{C}_{30}\text{H}_{36}\text{N}_2\text{NaO}_3\text{S}$: 527.2344;
Found : 527.2351.

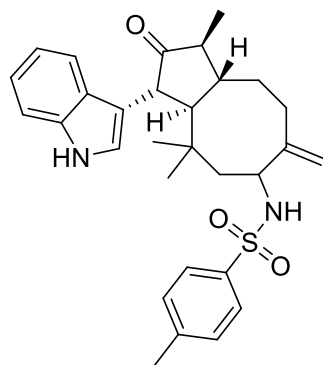
N-(3-(1H-indol-3-yl)-1,4,4-trimethyl-7-methylene-2-oxodecahydro-1H-cyclopenta[8]annulen-6-yl)-4-methylbenzenesulfonamide (55g)

Following the general procedure as described in section, the reaction was carried out with 30 mg of aziridinated zerumbone (as 1 equiv.) **52i** with 1 equiv. of corresponding indole and 5 mol% of indium triflate in DCM at room temperature for 6 hours and the corresponding products were isolated in 19 and 20 mg (yield 46 % and 47 %).

R_f : 0.462 (ethyl acetate : hexane = 3:2); Colorless amorphous solid.

IR (neat) ν_{max} : 3427, 2360, 2102, 1642, 1025, 784 cm^{-1} .

^1H NMR (500 MHz, CDCl_3): δ 8.10 (brs, 1H), 7.73-7.70 (m, 3H), 7.34-7.31 (m, 2H), 7.26-7.16 (m, 1H), 7.12-7.09 (m, 2H), 6.87-6.86 (m, 1H), 5.13 (s, 1H), 5.04 (s, 1H), 4.86 (d, $J = 9.5$ Hz, 1H), 4.06 (brs, 1H), 3.53 (d, $J = 5$ Hz, 1H), 2.76 (t, $J = 6$ Hz, 1H), 2.61-2.56 (m, 1H), 2.41 (s, 3H), 2.29-2.26 (m, 1H), 2.19-2.10 (m, 2H), 2.01-1.95 (m, 1H), 1.79-1.74 (m, 1H), 1.61-1.59 (m, 1H), 1.53-1.49 (m, 1H), 1.01 (d, $J = 7$ Hz, 3H), 0.89 (s, 3H), 0.78 (s, 3H) ppm.



^{13}C NMR (125 MHz, CDCl_3): δ 216.7, 149.6, 143.3, 137.9, 137.5, 136.7, 130.2, 129.6, 127.5, 127.1, 126.3, 122.5, 121.3, 119.8, 116.5, 112.1, 111.2, 57.2, 51.1, 48.9, 47.8, 43.0, 42.8, 37.3, 37.1, 32.1, 30.1, 23.2, 21.5, 12.6 ppm.

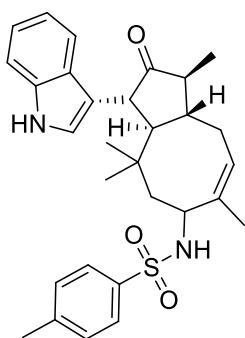
HRMS (ESI): m/z Calcd for $\text{C}_{30}\text{H}_{36}\text{N}_2\text{NaO}_3\text{S}$: 527.2344;
Found: 527.2350.

N-(3-(1H-indol-3-yl)-1,4,4,7-tetramethyl-2-oxo-2,3,3a,4,5,6,9,9a-octahydro-1H-cyclopenta[8]annulen-6-yl)-4-methylbenzenesulfonamide (56g)

R_f : 0.461 (ethyl acetate : hexane = 3:2); Colorless amorphous solid.

IR (neat) ν_{\max} : 3447, 2917, 2660, 2370, 1649, 1548, 1368, 733 cm^{-1} .

^1H NMR (500 MHz, CDCl_3): δ 8.14 (brs, 1H), 7.73-7.72 (m, 2H), 7.48-7.47 (d, $J = 8$ Hz, 1H), 7.28-7.25 (m, 3H), 7.13-7.10 (m, 1H), 7.05-7.02 (m, 1H), 6.75 (d, $J = 1$ Hz, 1H), 5.47 (t, $J = 8.5$ Hz, 1H), 4.81 (d, $J = 8$ Hz, 1H), 4.44-4.40 (m, 1H), 3.36 (d, $J = 11.5$ Hz, 1H), 2.51-2.44 (m, 2H), 2.42 (s, 3H), 2.25-2.16 (m, 2H), 1.70 (s, 4H), 1.49-1.44 (m, 1H), 1.18-1.16 (m, 1H), 1.11 (d, $J = 6.5$ Hz, 3H), 0.87 (s, 3H), 0.58 (s, 3H) ppm.



^{13}C NMR (125 MHz, CDCl_3): δ 217.3, 143.4, 140.9, 137.6, 136.6, 129.6, 127.1, 126.3, 122.2, 122.0, 120.3, 119.5, 119.0, 116.3, 111.4, 51.0, 49.2, 48.3, 47.9, 46.7, 36.2, 32.4, 25.7, 22.2, 21.5, 18.0, 11.9 ppm.

HRMS (ESI): m/z Calcd for $\text{C}_{30}\text{H}_{36}\text{N}_2\text{NaO}_3\text{S}$: 527.2344; Found: 527.2355.

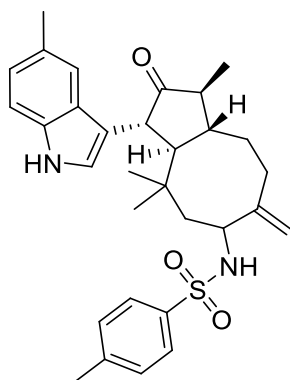
4-methyl-N-(1,4,4-trimethyl-3-(5-methyl-1H-indol-3-yl)-7-methylene-2-oxodecahydro-1H-cyclopenta[8]annulen-6-yl)benzenesulfonamide (55h)

Following the general procedure as described in section, the reaction was carried out with 30 mg of aziridinated zerumbone (as 1 equiv.) **52i** with 1 equiv. of corresponding indole and 5 mol% of indium triflate in DCM at room temperature for 6 hours and the corresponding products were isolated in 19 and 20 mg (yield 43 % and 45 %).

R_f : 0.542 (ethyl acetate : hexane = 3:2); colorless amorphous solid.

IR (neat) ν_{\max} : 2913, 2853, 1868, 1736, 1625, 1466, 1329, 1158, 746 cm^{-1} .

^1H NMR (500 MHz, CDCl_3): δ 7.99 (brs, 1H), 7.72 (d, $J = 8.5$ Hz, 2H), 7.51 (s, 1H), 7.27 (d, $J = 8$ Hz, 2H), 7.19 (d, $J = 8$ Hz, 1H), 7.01-6.99 (m, 1H), 6.83 (d, $J = 2$ Hz, 1H), 5.13 (s, 1H), 5.04 (s, 1H), 4.86 (d, $J = 9$ Hz, 1H), 4.07 (brs, 1H), 3.50 (d, $J = 5$ Hz, 1H), 2.76 (t, $J = 6$ Hz, 1H), 2.62-2.58 (m, 1H), 2.44 (s, 3H), 2.42 (s, 3H), 2.30-2.27 (m, 1H), 2.18-2.11 (m,



2H), 2.01-1.91 (m, 1H), 1.78-1.74 (m, 1H), 1.60-1.59 (m, 1H), 1.53-1.48 (m, 1H), 1.01 (d, $J = 7$ Hz, 3H), 0.89 (s, 3H), 0.78 (s, 3H) ppm.

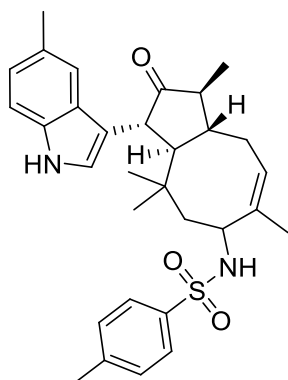
^{13}C NMR (125 MHz, CDCl_3): δ 217.0, 149.6, 143.2, 137.9, 137.5, 135.0, 130.2, 129.6, 129.0, 127.1, 126.5, 124.1, 121.5, 119.4, 115.9, 112.0, 110.9, 62.8, 57.1, 50.9, 48.9, 47.7, 42.8, 37.1, 32.1, 30.0, 23.3, 21.5, 12.7 ppm.

HRMS (ESI): m/z Calcd for $\text{C}_{31}\text{H}_{38}\text{N}_2\text{NaO}_3\text{S}$: 541.2500; Found : 541.2510.

4-methyl-N-(1,4,4,7-tetramethyl-3-(5-methyl-1H-indol-3-yl)-2-oxo-2,3,3a,4,5,6,9,9a-octahydro-1H-cyclopenta[8]annulen-6-yl)benzenesulfonamide (56h)

R_f : 0.514 (ethyl acetate : hexane = 3:2); Colorless amorphous solid.

IR (neat) ν_{max} : 2917, 2850, 1869, 1739, 1604, 1466, 1158, 740, 746 cm^{-1} .



^1H NMR (500 MHz, CDCl_3): δ 7.95 (brs, 1H), 7.73 (d, $J = 8.5$ Hz, 2H), 7.29-7.25 (m, 3H), 7.18 (d, $J = 8.5$ Hz, 1H), 6.97-6.95 (m, 1H), 6.79 (d, $J = 1.5$ Hz, 1H), 5.49 (t, $J = 8.5$ Hz, 1H), 4.57 (d, $J = 8.5$ Hz, 1H), 4.47-4.43 (m, 1H), 3.34 (d, $J = 11.5$ Hz, 1H), 2.54-2.49 (m, 2H), 2.42 (s, 3H), 2.40 (s, 3H), 2.26-2.17 (m, 3H), 1.72 (s, 3H), 1.53-1.48 (m, 1H), 1.21-1.18 (m, 1H), 1.11 (d, $J = 7$ Hz, 3H), 0.89 (s, 3H), 0.61 (s, 3H) ppm.

^{13}C NMR (125 MHz, CDCl_3): δ 217.2, 143.4, 140.8, 137.6, 135.0, 129.6, 128.6, 127.1, 126.5, 123.7, 122.2, 120.4, 118.8, 115.9, 111.0, 51.0, 49.2, 47.9, 46.6, 35.2, 32.4, 30.9, 25.7, 22.3, 21.6, 21.5, 18.0, 11.9 ppm.

HRMS (ESI): m/z Calcd for $\text{C}_{31}\text{H}_{38}\text{N}_2\text{NaO}_3\text{S}$: 541.2500; Found: 541.2513.

N-(3-(5-chloro-1H-indol-3-yl)-1,4,4-trimethyl-7-methylene-2-oxodecahydro-1H-cyclopenta[8]annulen-6-yl)-4-methylbenzenesulfonamide (55i)

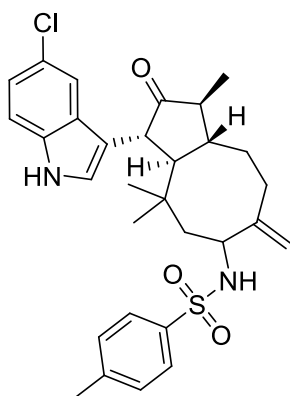
Following the general procedure as described in section, the reaction was carried out with 30 mg of aziridinated zerumbone (as 1 equiv.) **52i** with 1 equiv. of corresponding

indole and 5 mol% of indium triflate in DCM at room temperature for 6 hours and the corresponding products were isolated in 19 and 23 mg (yield 41 % and 47 %).

R_f: 0.342 (ethyl acetate : hexane = 3:2); Colorless amorphous solid

IR (neat) ν_{max} : 3277, 2920, 1736, 1642, 1461, 1327, 1156, 1098 cm^{-1} .

¹H NMR (500 MHz, CD_3COCD_3): δ 10.32 (brs, 1H), 7.76-7.73 (m, 3H), 7.38-7.36 (m, 3H), 7.21 (d, $J = 2.5$ Hz, 1H), 7.09-7.07 (m, 1H), 6.47 (d, $J = 9$ Hz, 1H), 5.15 (s, 1H), 4.97 (s, 1H), 4.16 (brs, 1H), 3.54 (d, $J = 6$ Hz, 1H), 2.75 (t, $J = 7$ Hz, 1H), 2.60-2.56 (m, 1H), 2.41 (s, 3H), 2.32-2.27 (m, 1H), 2.18-2.14 (m, 1H), 2.12-2.09 (m, 1H), 2.08-2.05 (m, 1H), 1.89-1.84 (m, 1H), 1.81-1.76 (m, 1H), 1.72-1.70 (m, 1H), 0.99 (d, $J = 6.5$ Hz, 3H), 0.90 (s, 3H), 0.87 (s, 3H) ppm.



¹³C NMR (125 MHz, CD_3COCD_3) : δ 215.6, 149.7, 142.6, 139.5, 129.3, 127.7, 126.9, 124.2, 124.0, 121.5, 118.9, 116.0, 112.7, 112.3, 56.9, 52.3, 48.6, 47.8, 44.8, 42.5, 36.4, 35.9, 31.6, 30.1, 21.8, 20.5, 11.7 ppm.

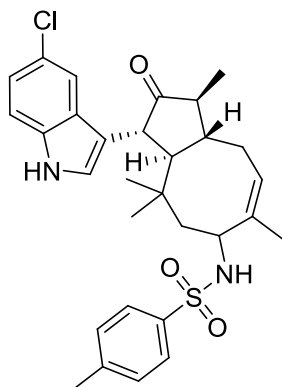
HRMS (ESI): m/z Calcd for $\text{C}_{30}\text{H}_{35}\text{ClN}_2\text{NaO}_3\text{S}$: 561.1954; Found: 561.1967.

N-(3-(5-chloro-1H-indol-3-yl)-1,4,4,7-tetramethyl-2-oxo-2,3,3a,4,5,6,9,9a-octahydro-1H-cyclopenta[8]annulen-6-yl)-4-methylbenzenesulfonamide (56i)

R_f: 0.314 (ethyl acetate : hexane = 3:2); Colorless amorphous solid.

IR (neat) ν_{max} : 3415, 2960, 2927, 1731, 1645, 1463, 1373, 1317, 1157, 1093 cm^{-1} .

¹H NMR (500 MHz, CD_3COCD_3): δ 10.12 (brs, 1H), 7.63 (d, $J = 8.5$ Hz, 2H), 7.44 (d, $J = 2$ Hz, 1H), 7.27 (d, $J = 7.5$ Hz, 2H), 7.21 (d, $J = 8.5$ Hz, 1H), 6.98 (d, $J = 2.5$ Hz, 1H), 6.92-6.90 (m, 1H), 6.37 (d, $J = 8$ Hz, 1H), 5.41 (t, $J = 8.5$ Hz, 1H), 4.37-4.34 (m, 1H), 3.38 (d, $J = 11.5$ Hz, 1H), 2.50-2.44 (m, 1H), 2.36-2.34 (m, 1H), 2.29 (s, 3H), 2.19-2.06 (m, 3H), 1.66



(s, 3H), 1.47-1.42 (m, 1H), 1.08-1.05 (m, 1H), 0.93 (d, $J = 6.5$ Hz, 3H), 0.76 (s, 3H), 0.46 (s, 3H) ppm.

^{13}C NMR (125 MHz, CD_3COCD_3): δ 216.4, 143.7, 142.7, 139.9, 136.2, 130.3, 129.0, 128.0, 125.1, 124.9, 122.2, 120.6, 119.4, 117.4, 113.6, 51.7, 51.6, 49.4, 49.3, 48.2, 47.6, 35.8, 32.9, 26.3, 22.5, 21.4, 18.5, 12.2 ppm.

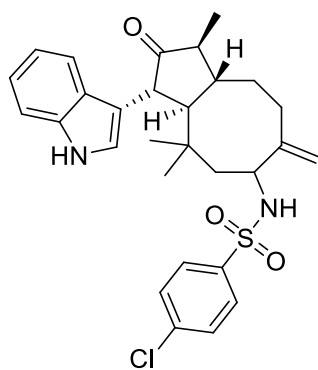
HRMS (ESI): m/z Calcd for $\text{C}_{30}\text{H}_{35}\text{ClN}_2\text{NaO}_3\text{S}$: 561.1954; Found : 561.1970.

N-(3-(1H-indol-3-yl)-1,4,4-trimethyl-7-methylene-2-oxodecahydro-1H-cyclopenta[8]annulen-6-yl)-4-chlorobenzenesulfonamide (55j)

Following the general procedure as described in section, the reaction was carried out with 30 mg of aziridinated zerumbone (as 1 equiv.) **52j** with 1 equiv. of corresponding indole and 5 mol% of indium triflate in DCM at room temperature for 6 hours and the corresponding products were isolated in 19 and 20 mg (yield 46 % and 49 %).

R_f: 0.462 (ethyl acetate : hexane = 3:2); Colorless amorphous solid.

IR (neat) ν_{max} : 3415, 2916, 2849, 2369, 1645, 1272, 1160, 755 cm^{-1} .



^1H NMR (500 MHz, CDCl_3): δ 8.12 (brs, 1H), 7.76-7.75 (m, 2H), 7.72-7.71 (m, 1H), 7.43-7.42 (m, 2H), 7.28-7.25 (m, 1H), 7.18-7.15 (m, 1H), 7.14-7.10 (m, 1H), 6.84 (s, 1H), 5.04-5.01 (m, 3H), 4.08 (brs, 1H), 3.52 (d, $J = 5.5$ Hz, 1H), 2.72 (t, $J = 6$ Hz, 1H), 2.56-2.54 (m, 1H), 2.29-2.26 (m, 1H), 2.16-2.11 (m, 2H), 1.99-1.94 (m, 1H), 1.79-1.71 (m, 1H), 1.62-1.54 (m, 2H), 1.01 (d, $J = 6.5$ Hz, 3H), 0.88 (s, 3H), 0.80 (s, 3H) ppm.

^{13}C NMR (125 MHz, CDCl_3): δ 216.8, 149.3, 139.4, 139.0, 137.5, 136.6, 130.3, 129.3, 129.1, 128.5, 128.2, 126.2, 122.5, 121.4, 119.8, 116.4, 111.2, 57.3, 51.2, 50.1, 48.9, 47.9, 42.7, 37.1, 32.0, 30.2, 23.2, 14.2, 12.7 ppm.

HRMS (ESI): m/z Calcd for $\text{C}_{29}\text{H}_{33}\text{ClN}_2\text{NaO}_3\text{S}$: 547.1798; Found : 547.1803.

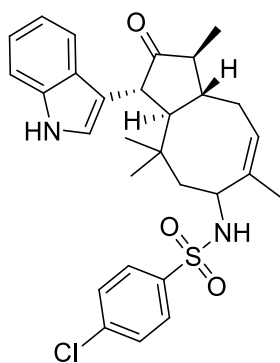
N-(3-(1H-indol-3-yl)-1,4,4,7-tetramethyl-2-oxo-2,3,3a,4,5,6,9,9a-octahydro-1H-cyclopenta[8]annulen-6-yl)-4-chlorobenzenesulfonamide (56j)

R_f : 0.414 (ethyl acetate : hexane = 3:2); Colorless amorphous solid.

IR (neat) ν_{\max} : 3447, 2916, 2849, 2366, 1646, 1271, 1160, 755 cm^{-1} .

^1H NMR (500 MHz, CDCl_3): δ 8.10 (brs, 1H), 7.76 (d, $J = 8$ Hz, 2H), 7.47-7.44 (m, 3H), 7.27-7.26 (m, 1H), 7.12 (t, $J = 7.5$ Hz, 1H), 7.05-7.02 (m, 1H), 6.75 (s, 1H), 5.49 (t, $J = 8.5$ Hz, 1H), 4.90 (d, $J = 8.5$ Hz, 1H), 4.49-4.45 (m, 1H), 3.37 (d, $J = 11.5$ Hz, 1H), 2.54-2.44 (m, 2H), 2.27-2.17 (m, 2H), 1.77-1.70 (m, 1H), 1.66 (s, 3H), 1.51-1.46 (m, 1H), 1.21-1.19 (m, 1H), 1.11 (d, $J = 6.5$ Hz, 3H), 0.93 (s, 3H), 0.60 (s, 3H) ppm.

^{13}C NMR (125 MHz, CDCl_3): δ 217.3, 140.5, 139.2, 139.1, 137.5, 136.6, 130.3, 129.3, 128.5, 126.2, 122.3, 122.1, 120.8, 119.5, 119.0, 116.2, 111.5, 51.2, 49.3, 48.2, 48.0, 46.7, 35.3, 32.5, 25.7, 22.3, 17.9, 14.2, 12.0 ppm.



HRMS (ESI): m/z Calcd for $\text{C}_{29}\text{H}_{33}\text{ClN}_2\text{NaO}_3\text{S}$: 547.1798; Found : 547.1801.

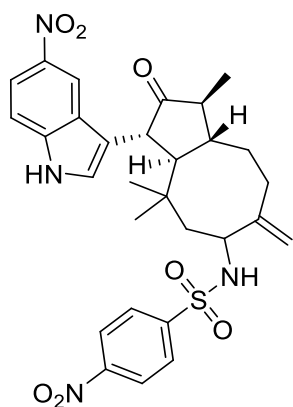
4-nitro-N-(1,4,4-trimethyl-7-methylene-3-(5-nitro-1H-indol-3-yl)-2-oxodecahydro-1H-cyclopenta[8]annulen-6-yl)benzenesulfonamide (55k)

Following the general procedure as described in section, the reaction was carried out with 30 mg of aziridinated zerumbone (as 1 equiv.) **52i** with 1 equiv. of corresponding indole and 5 mol% of indium triflate in DCM at room temperature for 6 hours and the corresponding products were isolated in 19 and 23 mg (yield 40 % and 49 %).

R_f : 0.286 (ethyl acetate : hexane = 3:2); Colorless amorphous solid.

IR (neat) ν_{\max} : 2918, 285, 1869, 1738, 1615, 1466 cm^{-1} .

^1H NMR (500 MHz, CD_3COCD_3): δ 10.82 (brs, 1H), 8.70 (d, $J = 2.5$ Hz, 1H), 8.42-8.40 (m, 2H), 8.12-8.10 (m, 2H), 8.03-8.01 (m, 1H), 7.54 (d, $J = 9$ Hz, 1H), 7.40 (d, $J = 2$ Hz, 1H), 6.99 (d, $J = 9.5$ Hz, 1H), 5.08 (s, 1H), 4.94 (s, 1H), 4.30 (brs, 1H), 3.71 (d, $J = 6.5$ Hz, 1H), 2.81-2.79 (m, 2H), 2.58-2.56



(m, 1H), 2.31-2.27 (m, 1H), 2.20-2.15 (m, 2H), 1.93-1.88 (m, 2H), 1.82-1.77 (m, 1H), 1.01 (d, $J = 7$ Hz, 3H), 0.96 (s, 3H), 0.92 (s, 3H) ppm.

^{13}C NMR (125 MHz, CD_3COCD_3): δ 215.4, 149.8, 149.1, 147.8, 141.4, 139.8, 128.3, 125.9, 124.1, 118.8, 116.9, 116.7, 112.7, 111.5, 57.4, 48.6, 48.3, 45.4, 42.4, 35.5, 31.3, 29.1, 21.6, 13.5, 11.8 ppm.

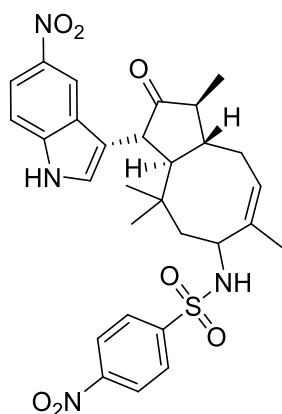
HRMS (ESI): m/z Calcd for $\text{C}_{29}\text{H}_{32}\text{N}_4\text{NaO}_7\text{S}$: 603.1889; Found : 603.1901.

4-nitro-N-(1,4,4,7-tetramethyl-3-(5-nitro-1H-indol-3-yl)-2-oxo-2,3,3a,4,5,6,9,9a-octahydro-1H-cyclopenta[8]annulen-6-yl)benzenesulfonamide (56k)

R_f : 0.257 (ethyl acetate : hexane = 3:2); Colorless amorphous solid.

IR (neat) ν_{max} : 2916, 2849, 1868, 1738, 1532, 1162 cm^{-1} .

^1H NMR (500 MHz, CD_3COCD_3): δ 10.64 (brs, 1H), 8.47 (d, $J = 1.5$ Hz, 1H), 8.33 (d, $J = 8.5$ Hz, 2H), 8.03 (d, $J = 8.5$ Hz, 2H), 7.88-7.86 (m, 1H), 7.39 (d, $J = 9$ Hz, 1H), 7.19 (d, $J = 2$ Hz, 1H), 6.94 (d, $J = 9$ Hz, 1H), 5.46 (t, $J = 8$ Hz, 1H), 4.53-4.49 (m, 1H), 3.59 (d, $J = 12$ Hz, 1H), 2.57-2.50 (m, 1H), 2.44-2.39 (m, 1H), 2.20-2.18 (m, 1H), 2.14-2.10 (m, 1H), 1.80-1.76 (m, 1H), 1.63 (s, 3H), 1.56-1.52 (m, 1H), 1.16-1.13 (m, 1H), 0.95 (d, $J = 6.5$ Hz, 3H), 0.88 (s, 3H), 0.51 (s, 3H) ppm.



^{13}C NMR (125 MHz, CD_3COCD_3): δ 215.4, 142.8, 141.6, 139.0, 135.7, 129.4, 128.2, 127.2, 124.2, 124.0, 121.3, 119.7, 118.6, 116.5, 112.8, 50.7, 48.4, 48.3, 47.3, 46.7, 34.9, 32.0, 25.4, 21.5, 20.5, 17.5, 11.2 ppm.

HRMS (ESI): m/z Calcd for $\text{C}_{29}\text{H}_{32}\text{N}_4\text{NaO}_7\text{S}$: 603.1889; Found : 603.1903.

N-(3-(1H-indol-3-yl)-1,4,4-trimethyl-7-methylene-2-oxodecahydro-1H-cyclopenta[8]annulen-6-yl)-4-methoxybenzenesulfonamide (55l)

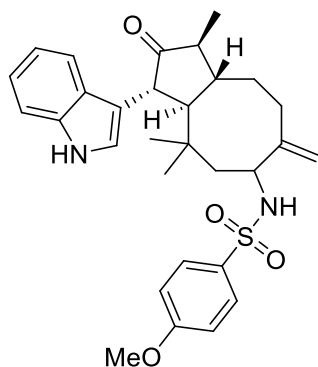
Following the general procedure as described in section, the reaction was carried out with 30 mg of aziridinated zerumbone (as 1 equiv.) **52o** with 1 equiv. of corresponding

indole and 5 mol% of indium triflate in DCM at room temperature for 6 hours and the corresponding products were isolated in 19 and 21 mg (yield 45 % and 48 %).

R_f : 0.413 (ethyl acetate : hexane = 3:2); colorless amorphous solid.

IR (neat) ν_{max}: 3275, 2921, 1731, 1596, 1490, 1262, 1100, 839, 745, 671 cm⁻¹.

¹H NMR (500 MHz, CDCl₃): δ 8.10 (brs, 1H), 7.84-7.73 (m, 3H), 7.32-7.30 (m, 1H), 7.18 (t, *J* = 7.5 Hz, 1H), 7.12-7.09 (m, 1H), 6.95-6.93 (m, 2H), 6.87 (brs, 1H), 5.13 (s, 1H), 5.04 (s, 1H), 4.87-4.85 (m, 1H), 4.05 (brs, 1H), 3.86 (s, 3H), 3.53 (d, *J* = 5 Hz, 1H), 2.76 (t, *J* = 5.5 Hz, 1H), 2.60-2.58 (m, 1H), 2.29-2.26 (m, 1H), 2.17-2.11 (m, 2H), 2.01-1.96 (m, 1H), 1.77-1.74 (m, 1H), 1.66-1.60 (m, 1H), 1.55-1.51 (m, 1H), 1.01 (d, *J* = 7 Hz, 3H), 0.90 (s, 3H), 0.79 (s, 3H) ppm.



¹³C NMR (125 MHz, CDCl₃): δ 216.8, 162.8, 149.7, 136.6, 132.4, 129.2, 128.6, 126.2, 122.5, 121.3, 119.9, 119.8, 116.5, 114.2, 114.1, 112.0, 111.2, 60.4, 57.1, 56.6, 50.9, 48.9, 47.8, 42.8, 37.2, 32.1, 30.1, 23.3, 14.2, 12.7 ppm.

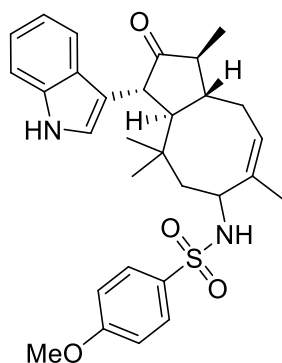
HRMS (ESI): *m/z* Calcd for C₃₀H₃₆N₂NaO₄S: 543.2293; Found: 543.2310.

N-(3-(1H-indol-3-yl)-1,4,4,7-tetramethyl-2-oxo-2,3,3a,4,5,6,9,9a-octahydro-1H-cyclopenta[8]annulen-6-yl)-4-methoxybenzenesulfonamide (56l)

R_f: 0.40 (ethyl acetate : hexane = 3:2); Colorless amorphous solid.

IR (neat) ν_{max}: 3399, 3066, 2921, 1730, 1644, 1597, 1498, 1461, 1330, 1261, 1153, 1100, 1028 cm⁻¹.

¹H NMR (500 MHz, CDCl₃): δ 8.16 (brs, 1H), 7.77 (d, *J* = 8 Hz, 2H), 7.47 (d, *J* = 8 Hz, 1H), 7.26-7.25 (m, 1H), 7.13-7.10 (m, 1H), 7.05-7.02 (m, 1H), 6.94 (d, *J* = 8 Hz, 2H), 6.74 (brs, 1H), 5.48-5.45 (m, 1H), 4.84-4.83 (m, 1H), 4.41 (t, *J* = 10 Hz, 1H), 3.85 (s, 3H), 3.36 (d, *J* = 11.5 Hz, 1H), 2.55-2.44 (m, 2H), 2.24-2.16 (m, 2H), 1.70 (s, 4H), 1.47 (t, *J* =



12.5 Hz, 1H), 1.19-1.15 (m, 1H), 1.11 (d, $J = 6.5$ Hz, 3H), 0.88 (s, 3H), 0.58 (s, 3H) ppm.

^{13}C NMR (125 MHz, CDCl_3): δ 217.4, 162.8, 141.0, 136.6, 132.2, 129.2, 126.3, 122.2, 122.0, 120.3, 119.4, 119.0, 116.2, 114.1, 111.4, 60.4, 56.6, 50.9, 49.2, 48.2, 47.9, 46.7, 35.2, 32.5, 25.7, 22.3, 18.0, 14.2, 11.9 ppm.

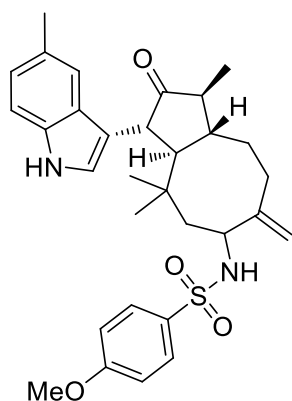
HRMS (ESI): m/z Calcd for $\text{C}_{30}\text{H}_{36}\text{N}_2\text{NaO}_4\text{S}$: 543.2293; Found: 543.2302.

4-methoxy-N-((1S,3R,3aR,9aR)-1,4,4-trimethyl-3-(5-methyl-1H-indol-3-yl)-7-methylene-2-oxodecahydro-1H-cyclopenta[8]annulen-6-yl)benzenesulfonamide (55m)

Following the general procedure as described in section, the reaction was carried out with 30 mg of aziridinated zerumbone (as 1 equiv.) **52o** with 1 equiv. of corresponding indole and 5 mol% of indium triflate in DCM at room temperature for 6 hours and the corresponding products were isolated in 19 and 21 mg (yield 42 % and 46 %).

R_f: 0.343 (ethyl acetate : hexane = 3:2); Colorless amorphous solid.

IR (neat) ν_{max} : 3425, 2921, 2863, 2089, 1643, 1155, 1101 cm^{-1} .



^1H NMR (500 MHz, CD_3COCD_3): δ 9.98 (brs, 1H), 7.83-7.79 (m, 2H), 7.49 (s, 1H), 7.23 (d, $J = 8$ Hz, 1H), 7.08-7.06 (m, 3H), 6.93 (d, $J = 7$ Hz, 1H), 6.39 (d, $J = 9$ Hz, 1H), 5.15 (s, 1H), 4.97 (s, 1H), 4.14 (brs, 1H), 3.88 (s, 3H), 3.51 (d, $J = 6$ Hz, 1H), 2.75-2.72 (m, 1H), 2.61-2.56 (m, 1H), 2.40 (s, 3H), 2.34-2.30 (m, 1H), 2.19-2.14 (m, 1H), 2.13-2.10 (m, 1H), 2.07-2.05 (m, 1H), 1.90-1.85 (m, 1H), 1.80-1.75 (m, 1H), 1.71-1.68 (m, 1H), 0.98 (d, $J = 7$ Hz, 3H), 0.90 (s, 3H), 0.86 (s, 3H) ppm.

^{13}C NMR (125 MHz, CD_3COCD_3): δ 215.6, 162.6, 149.7, 135.4, 134.1, 129.0, 128.1, 127.5, 126.9, 123.2, 122.3, 119.1, 115.8, 113.9, 113.8, 112.2, 110.9, 59.7, 56.8, 56.1, 48.8, 47.7, 42.4, 36.5, 31.7, 30.2, 21.9, 20.8, 19.9, 13.6, 11.7 ppm.

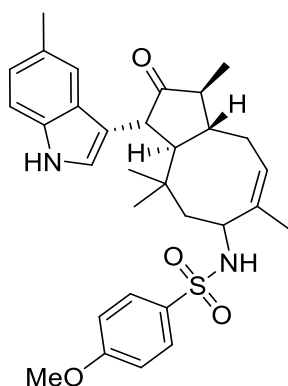
HRMS (ESI): m/z Calcd for $C_{31}H_{38}N_2NaO_4S$: 557.2450;
Found : 557.2461.

4-methoxy-N-(1,4,4,7-tetramethyl-3-(5-methyl-1H-indol-3-yl)-2-oxo-2,3,3a,4,5,6,9,9a-octahydro-1H-cyclopenta[8]annulen-6-yl)benzenesulfonamide (56m)

R_f : 0.344 (ethyl acetate : hexane = 3:2); Colorless amorphous solid.

IR (neat) ν_{max} : 3429, 2091, 1643, 1464, 1329, 1260, 1154, 1030, 1101 cm^{-1} .

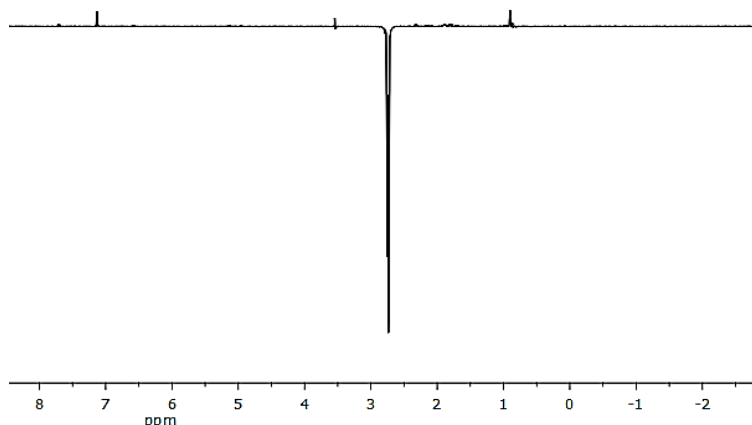
1H NMR (500 MHz, CD_3COCD_3): δ 9.78 (brs, 1H), 7.67 (d, $J = 9$ Hz, 2H), 7.19 (s, 1H), 7.08 (d, $J = 8$ Hz, 1H), 6.97 (d, $J = 9$ Hz, 2H), 6.83 (d, $J = 2.5$ Hz, 1H), 6.75 (d, $J = 8.5$ Hz, 1H), 6.32 (d, $J = 8$ Hz, 1H), 5.45-5.42 (m, 1H), 4.35-4.31 (m, 1H), 3.76 (s, 3H), 3.30 (d, $J = 11.5$ Hz, 1H), 2.46-2.42 (m, 2H), 2.27 (s, 3H), 2.17-2.09 (m, 2H), 1.66 (s, 3H), 1.63-1.61 (m, 1H), 1.44-1.38 (m, 1H), 1.08-1.02 (m, 1H), 0.93 (d, $J = 7$ Hz, 3H), 0.76 (s, 3H), 0.47 (s, 3H) ppm.



^{13}C NMR (125 MHz, CD_3COCD_3): δ 216.5, 163.6, 142.7, 135.9, 134.1, 130.0, 128.0, 127.9, 123.7, 123.6, 120.6, 119.6, 116.2, 114.9, 112.0, 56.0, 51.7, 49.6, 49.1, 48.2, 47.7, 35.8, 32.8, 26.4, 22.5, 21.6, 18.5, 12.2 ppm.

HRMS (ESI): m/z Calcd for $C_{31}H_{38}N_2NaO_4S$: 557.2450;
Found : 557.2461.

NOE spectra for ring junction protons of compound **55a**



6.8. References

1. (a) R. W. Huigens 3rd, K. C. Morrison, R. W. Hicklin, T. A. Flood Jr, M. F. Richter and P. J. Hergenrother, *Nat. Chem.*, **2013**, 5, 195-202. (b) J. Newman and G. M. Cragg, *J. Nat. Prod.*, **2016**, 79, 629-661.
2. (a) Y. Yamamoto, *J. Org. Chem.*, **2007**, 72, 7817-7831. (b) C. Avonto, O. Tagliatalata-Scafati, F. Pollastro, A. Minassi, V. Di Marzo, L. De Petrocellis and G. Appendino, *Angew. Chem. Int. Ed.*, **2011**, 50, 467-471.
3. (a) G. Gopalan, B. P. Dhanya, J. Saranya, T. R. Reshmitha, T. V. Baiju, M. T. Meenu, M. S. Nair, P. Nisha and K. V. Radhakrishnan, *Eur. J. Org. Chem.*, **2017**, 2017, 3072–3077. (b) B. P. Dhanya, G. Gopalan, P. Sasikumar, S. Neethu, M. T. Meenu, P. Sharathna, J. John, S. Varughese, M. Sabu, M. Dan and K. V. Radhakrishnan, *Asian J. Org. Chem.*, **2018**, 7, 471-476. (c) H. W. D. Matthes, B. Luu and G. Ourisson, *Tetrahedron*, **1982**, 38, 3129-3135.
4. S. Lakhdar, M. Westermaier, F. Terrier, Re'gis Goumont, T. Boubaker, A. R. Ofial, and H. Mayr, *J. Org. Chem.*, **2006**, 71, 9088-9095.
5. (a) M. Yamasaki, *J. Chem. Soc. Chem. Commun.*, **1972**, 0, 606-607. (b) M. Kaisin, J. C. Braekman, D. Dalozze and B. Tursch, *Tetrahedron*, **1985**, 41, 1067-1072. (c) R. C. Gadwood, R. M. Lett, J. E. Wissinger, *J. Am. Chem. Soc.*, **1986**, 108, 6343–6350. (d) P. A. Wender and L. Zhang, *Org. Lett.*, **2000**, 2, 2323-2326.
6. (a) O. F. Güner, *Curr. Top. Med. Chem.*, **2002**, 2, 1321-1332. (b) A. R. Voet, A. Kumar and K. Y. Zhang, *J. Comput. Aided Mol. Des.*, **2014**, 28(4), 363-373. (c) G. Jones, P. Willett and R. C. Glen, *J. Comput. Aided Mol. Des.*, **1995**, 9(6), 532-549. (d) V. Hähnke and G. Schneider, *J. Comput. Chem.*, **2011**, 32(8), 1635-1647.

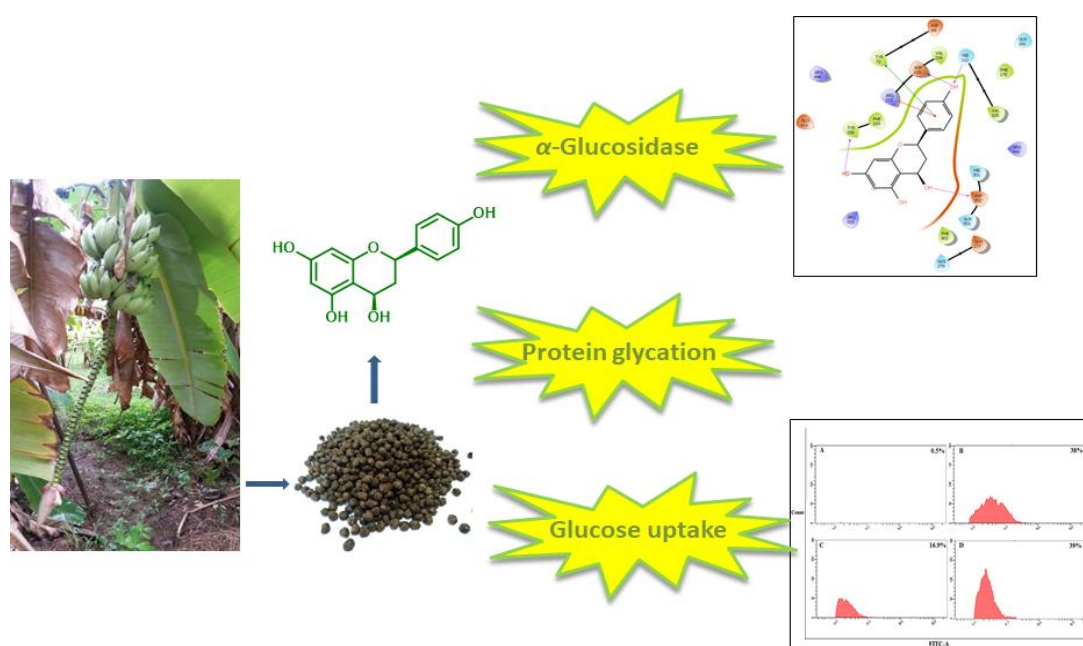
SUMMARY

The history of medicines date back nearly to the existence of human civilization. Before the 19th century, crude or semi-pure extracts of plants, microbes and animals represented the only medications available to treat different illness of man and domestic animals. Medicinal plants based traditional systems of medicines play an important role in providing health care to a large section of the population, especially in developing countries. India has a unique distinction of having six recognized systems of medicine in this category *viz* Ayurveda, Siddha, Unani, Yoga, Naturopathy and Homoeopathy. All the above systems in India are mainly based on herbal drugs. Many valuable medicinal plants of India are being lost at a shocking rate by the rapid depletion of forests, impairing the availability of raw drugs which leads to a critical phase in herbal medicines. In this context, our investigations involved the phytochemical investigations of some selected medicinal plants: *Musa balbisiana* from Musaceae, *Anethum graveolens* from Apiaceae, *Rotula aquatica* from Boraginaceae and, *Zingiber nimmonii* and *Zingiber zerumbet* from Zingiberaceae and diversity oriented synthesis of chemical libraries using an abundant phytomolecule, Zerumbone from *Zingiber zerumbet*.

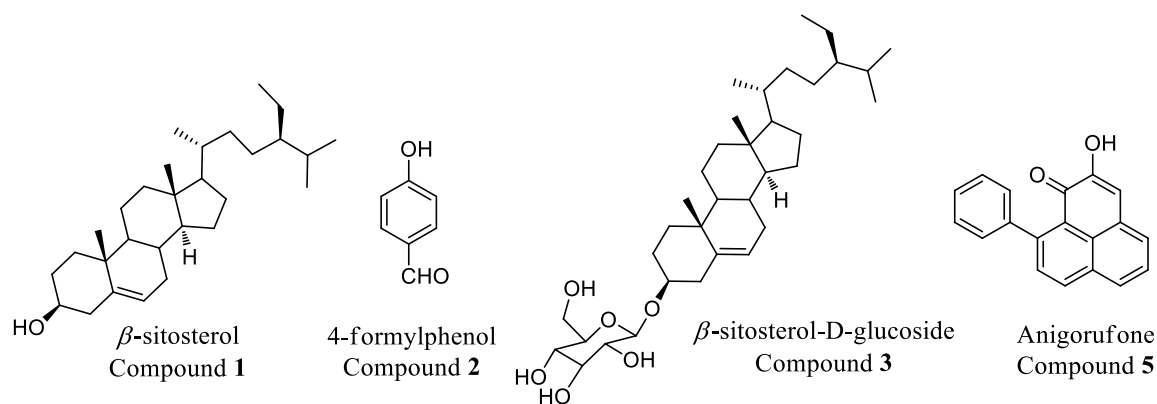
Chapter 1 gives an overview of natural products and its importance in drug discovery. Some of the important natural products and their derivatives, which are available in the current market for the treatment of various diseases are emphasized in this chapter.

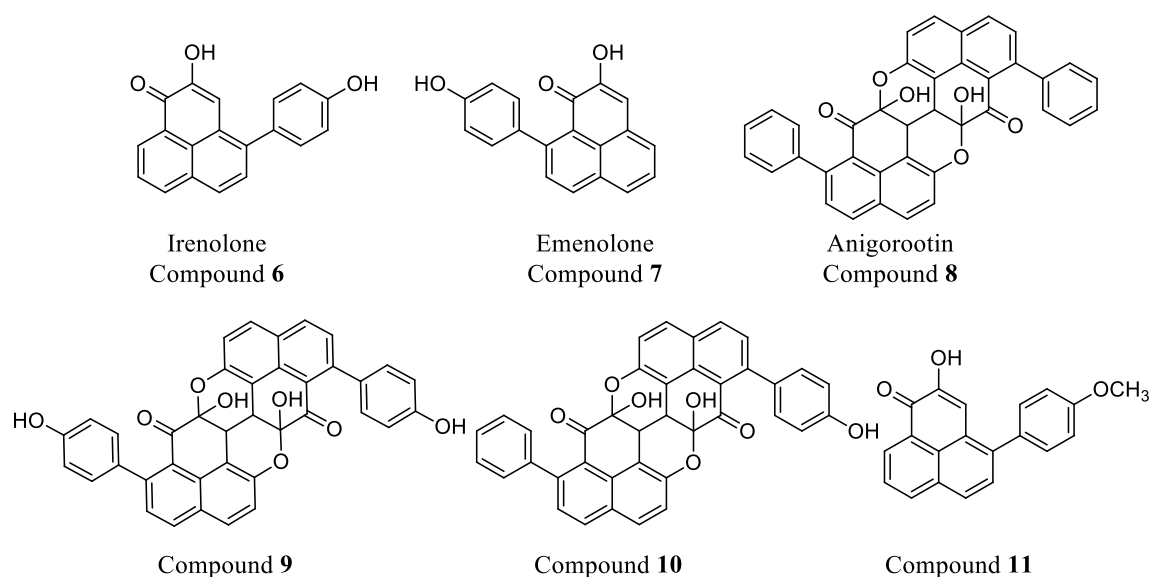
Being of great economic importance in tropical agriculture, the cultivated bananas have attracted a good deal of research in many countries over many years. The wild relatives, however, have attracted much less attention. India is well known for its vast genetic diversity of members of Musaceae comprising seeded wild species to seedless cultivars of various levels of ploidy. **Chapter 2** discusses our phytochemical investigations on *Musa balbisiana* from Musaceae or banana family, a wild seeded species. The first part of the chapter deals with the isolation and evaluation of antidiabetic properties of a phytomolecule, apiforol from the seeds of *Musa balbisiana* while the second part discusses the isolation and characterization of phytochemicals from the rhizome and fruit peels of *Musa balbisiana* (scheme 1 & 2). The acetone extract of the seeds *Musa balbisiana* demonstrated the highest inhibition of α -amylase and α -glucosidase enzyme with an IC₅₀

value of $36.67 \pm 0.367 \mu\text{g/mL}$ and $100.61 \pm 0.707 \mu\text{g/mL}$ respectively. The extract also exhibited significant glycation inhibition property with an IC_{50} value of 86.48 ± 0.751 . Furthermore, a major phytochemical, apiforol was isolated from the acetone extract for the first time, which demonstrated promising α -glucosidase inhibition ($\text{IC}_{50} = 48.25 \pm 0.255 \mu\text{M}$), antiglycation property ($\text{IC}_{50} = 114.23 \pm 0.567 \mu\text{M}$) and enhanced glucose uptake in L6 myoblasts. In the Molecular docking studies, apiforol efficiently bonded to the active sites of α -glucosidase enzyme, **3A4A**. Also, from the rhizome and fruit peels of *Musa balbisiana*, we could successfully isolate and characterize ten different compounds, among which, seven were phenylphenalenones in nature.



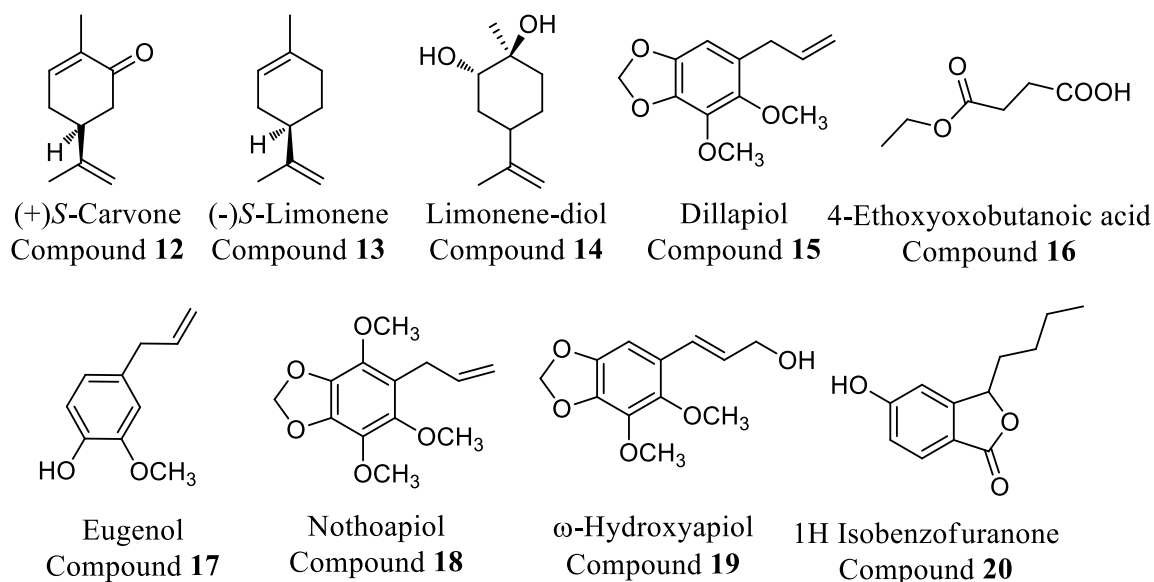
Scheme 1. Antidiabetic properties of Apiforol

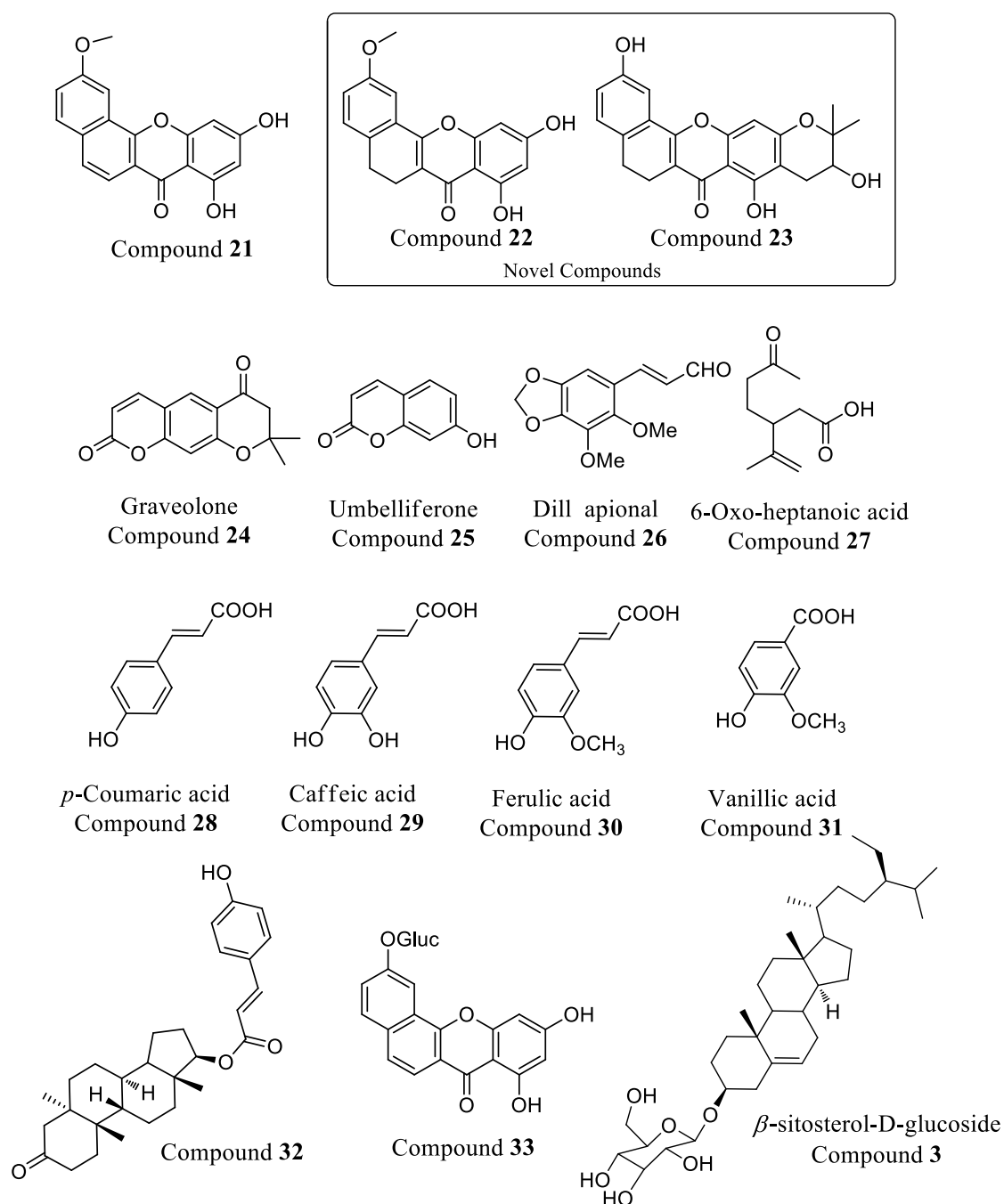




Scheme 2. Phytochemicals, isolated from the rhizome and fruit peels of *Musa balbisiana*

Chapter 3 focuses on the chemo-profiling of two important medicinal plants; *Anethum graveolens* and *Zingiber nimmonii*. *Anethum graveolens* is a species from Apiaceae family and is used in Ayurvedic medicines and as a herb. Owing to the great biological significance of *Anethum graveolens*, a detailed phytochemical investigation of seeds of this plant was carried out and this resulted in the isolation of twenty three compounds, including two novel molecules (scheme 3).

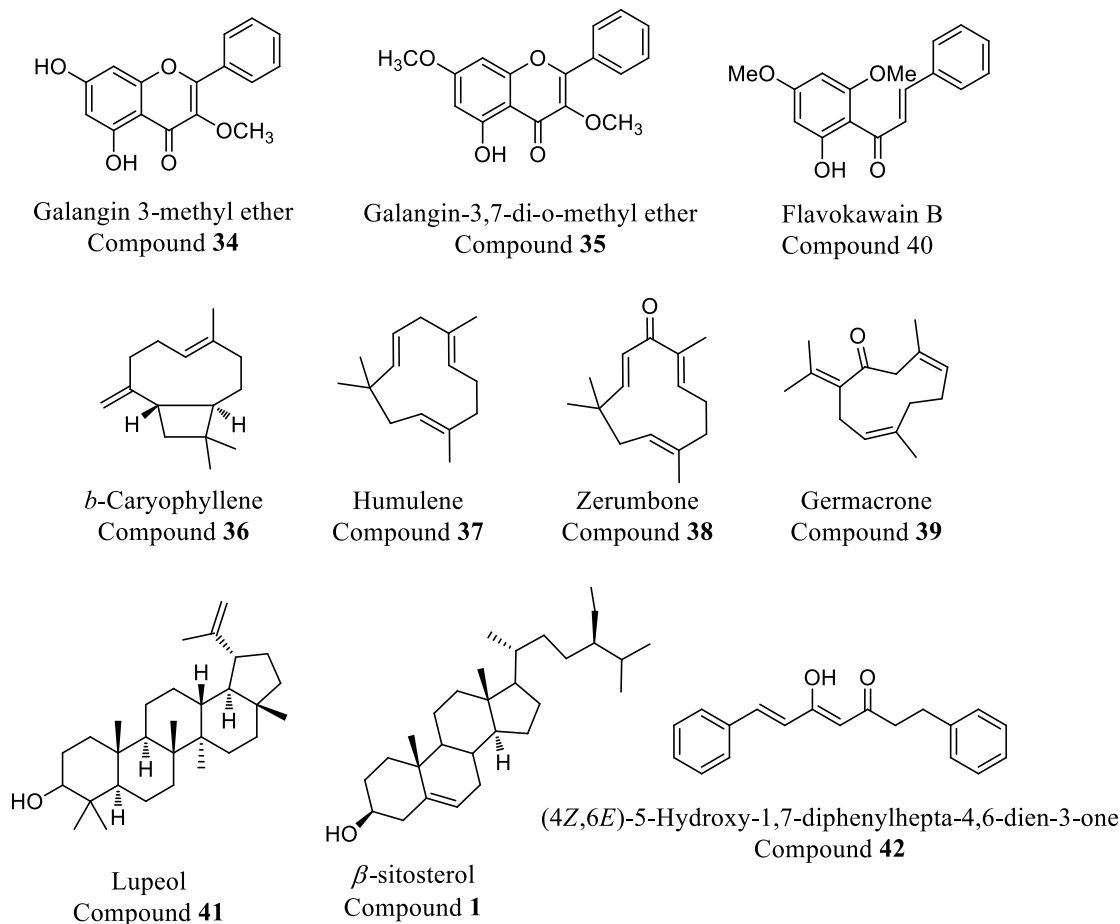




Scheme 3. Phytochemicals isolated from *Anethum graveolens*

After the successful isolation of these compounds, we carried out a detailed anti-oxidant study to explore the antioxidant properties of these molecules and most of them exhibited promising scavenging activity towards DPPH, ABTS and NO radicals. We also carried out a molecular docking studies of these isolated compounds with two enzymes, namely **3A4A** (antidiabetic) and 2ITW (anti-inflammatory and anticancer), in which the xanthone derivatives showed better binding scores. In the second part, the chemo-profiling of the rhizomes of the plant species *Zingiber nimmonii* is described. This is one of the

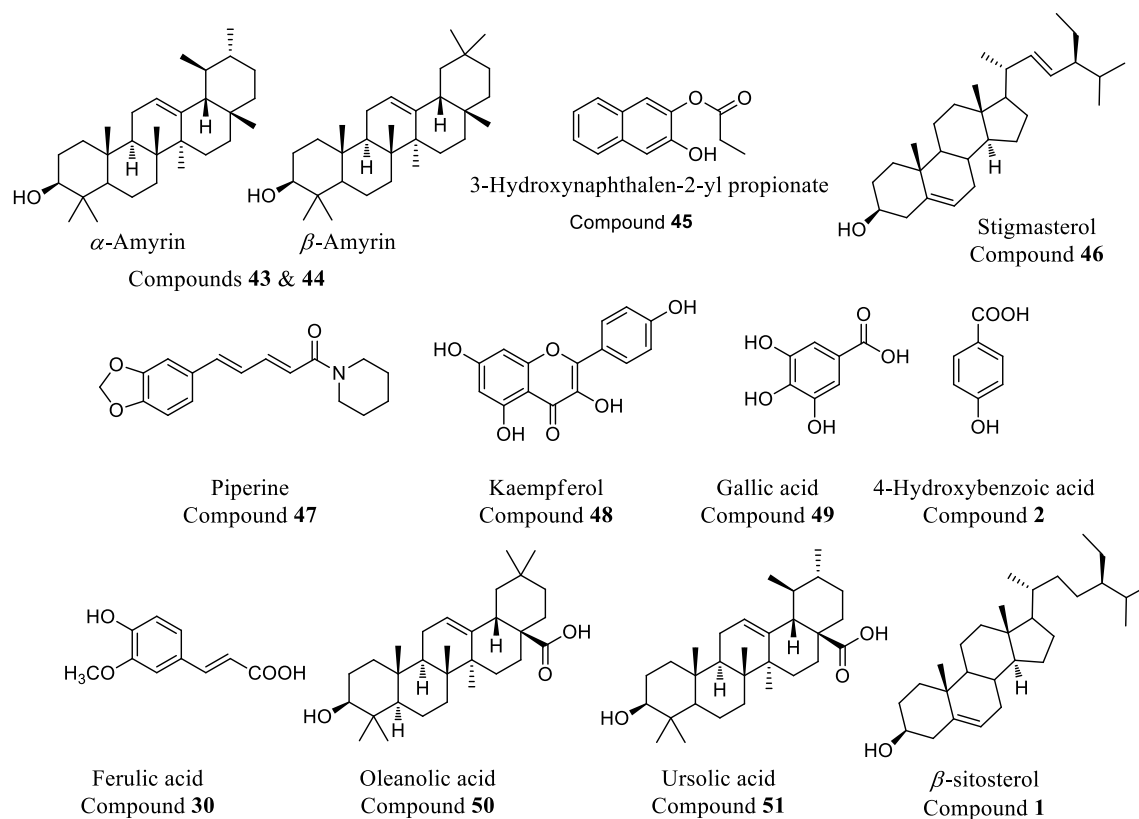
newly identified species which belongs to the family Zingiberaceae, and we could successfully isolate and characterize, ten different compounds from this species (scheme 4). We also explored the anti-oxidant and molecular Docking studies of the isolated compounds.



Scheme 4. Phytochemicals isolated from *Zingiber nimmonii*

Chapter 4 deals with the phytochemical evaluation of whole parts of *Rotula aquatica*, belonging to the family Boraginaceae. *R. aquatica* is one of the most extensively used medicinal plant in the Ayurvedic system to dissolve urinary calculi and kidney stones. Though, the plant is known for centuries there is no any systematic evaluation of phytochemicals that is present in it and this encouraged us to carry out a detailed chemo profiling of this plant. We could successfully isolate and characterize a number of molecules from different parts of this plant and the results are summarized in this chapter (scheme 5). We also explored the antiurolithiatic activities of the various extracts of *Rotula aquatica* roots and the results pointed out that, aqueous extract of this plant effectively dissolves the calcium phosphate stones rather than calcium oxalate. In the comparison studies with *Scoparia dulcis* and *Bryophyllum pinnatum*, in the case of calcium oxalate

stones, the ethanol and aqueous extracts of *S. dulcis* exhibited the highest dissolution (38.48 % and 40.28 %) followed by the aqueous extracts of *B. pinnatum* (31.21 %) and *R. aquatica* (30.56 %) respectively. Here the efficiency of the standard drug (37.33 %) was comparably lesser than *Scoparia dulcis*.



Scheme 5. Phytochemicals isolated from *Rotula aquatica*

Encouraged by the structure and abundance of zerumbone from *Zingiber zerumbet*, we undertook the conversions of easily available zerumbone to other derivatives of bioactive natural products through simple chemical methods. In the first part of **chapter five**, we discuss our efforts in the synthesis of zerumbone pendant derivatives, *via* base catalyzed reactions. The *in vitro* and *in silico*, antidiabetic and anti-proliferating properties zerumbone-sulfonamide and zerumbone-oxazolidinone derivatives were also investigated. The second part of this chapter deals with the aziridination of zerumbone under metal free conditions. This is the first report on the *trans* aziridination of zerumbone under one-pot metal-free strategy, and the reaction conditions are quite tolerable with a large number of sulfonamides (scheme 6). In order to explore the biological activity of these synthesized derivatives, we carried out a detailed *in silico* and *in vitro* studies. In the preliminary antidiabetic and antiproliferative studies, most of these derivatives exhibited promising

activities. We also carried out the pharmacophore modeling (figure 1) and QSAR studies of these derivatives and in our studies, the theoretical values of most of the derivatives were in good agreement with the experimental values.

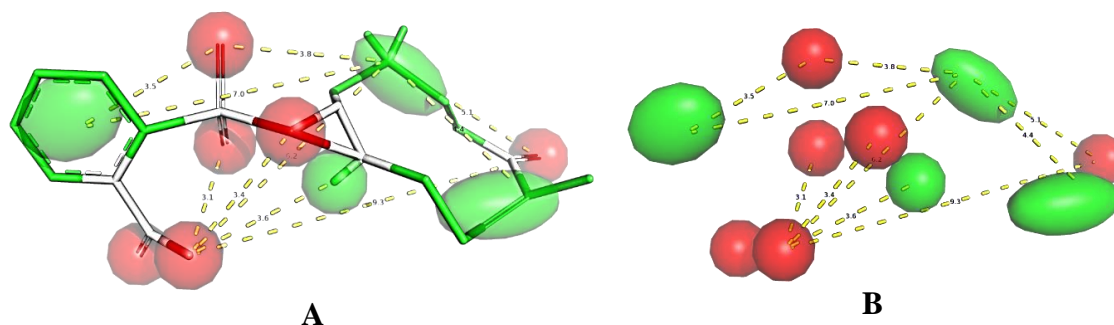
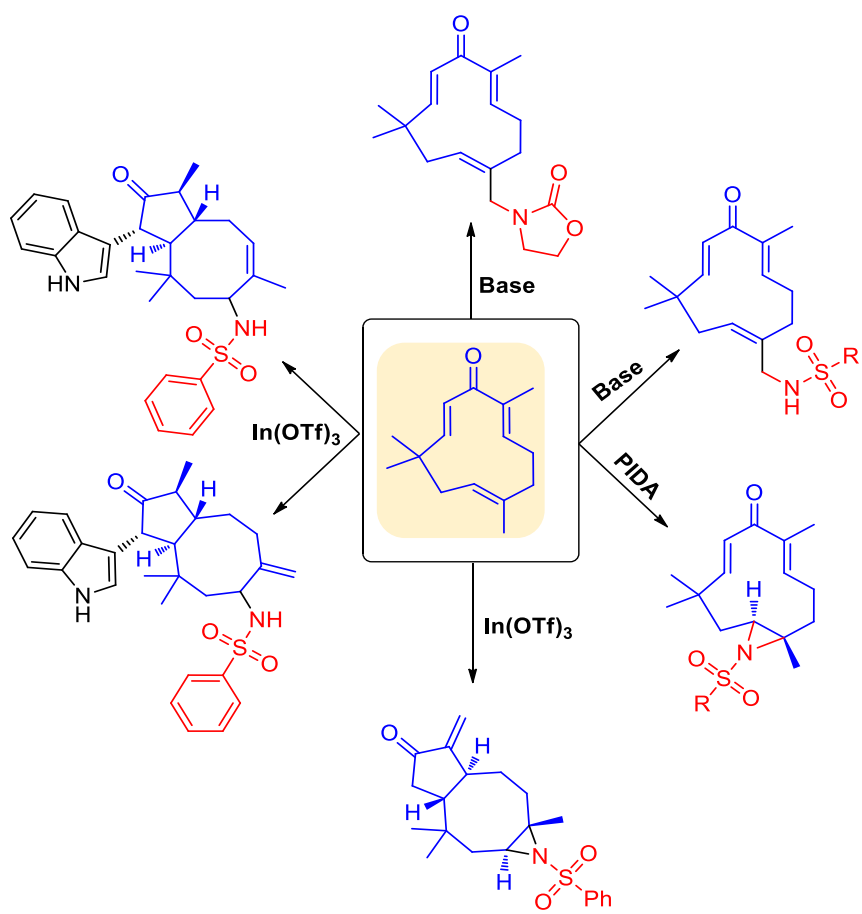


Figure 1. **A** Pharmacophore model with molecule; **B** Pharmacophore model without molecule display

In the final chapter (**chapter 6**) we focused on utilizing zerumbone and its derivatives in cyclization reactions and our efforts resulted in the synthesis of diverse sesquiterpenoid derivatives. Starting from zerumbone, we could efficiently design and execute a Lewis acid catalyzed annulation processes for the synthesis of [5.8.3] and [5.8] fused ring systems. It was demonstrated that by selectively functionalizing zerumbone and thereby controlling the conformation of the 11-membered ring, the ring-closing processes could be tuned to fused-ring systems of choice (Scheme 6). The synthesized derivatives have multiple points for functionalization, and can be used as an efficient scaffold in the total syntheses of many biologically relevant molecules. Also, most of these scaffolds are the core units of numerous biologically active molecules. Furthermore, this reaction strategy opens new opportunities for the development of structurally diverse natural product scaffolds that contain heterocyclic or carbocyclic appendages. In addition to these, the preferable binding modes of these derivatives were analyzed through molecular docking studies.

In conclusion, detailed phytochemical investigations of *Musa balbisiana*, *Anethum graveolens*, *Zingiber nimmonii* and *Rotula aquatica* were carried out. A total of fifty-one different compounds were isolated from these plants, and many of them were subjected to various biological studies, such as anti-oxidant, antidiabetic, anticancer and so on. In addition to these, we carried out a diversity oriented synthesis of chemical libraries, with promising biological activities, using an abundant phytomolecule, Zerumbone, from *Zingiber zerumbet*.



Scheme 6. Synthetic modifications of zerumbone

List of publications

1. Lewis Acid Catalyzed Regioselective Hydroheteroarylation of Pentafulvenes, S. Sarath Chand, **Greeshma Gopalan**, P. V. Santhini, P. Preethanuj, Jubi John, Dominique Harakat, Florian Jaroschik, and K. V. Radhakrishnan, *Org. Lett.*, **2016**, *18*, 964.
2. Metal-Free trans-Aziridination of Zerumbone: Synthesis and Biological Evaluation of Aziridine Derivatives of Zerumbone. **Greeshma Gopalan**, B. P. Dhanya, J. Saranya, T. R. Reshmitha, T. V. Baiju, M. T. Meenu, Mangalam S. Nair, P. Nisha and K. V. Radhakrishnan, *Eur. J. Org. Chem.*, **2017**, *2017*, 3072-3077.
3. Synthesis and *in vitro* Evaluation of Zerumbone Pendant Derivatives: potent candidates for anti-diabetic and anti-proliferative activities. B. P. Dhanya, **Greeshma Gopalan**, T. R. Reshmitha, J. Saranya, P. Sharathna, I. G. Shibi, P. Nisha and K. V. Radhakrishnan. *New J. Chem.*, **2017**, *41*, 6960-6964.
4. Effects of a New Synthetic Zerumbone Pendant Derivative (ZPD) on Apoptosis Induction and Anti-Migratory Effects in Human Cervical Cancer Cells. J. Saranya, B. P. Dhanya, **Gopalan Greeshma**, K. V. Radhakrishnan, S. Priya. *Chem. Biol. Interact.*, **2017**, *278*, 32-39
5. A Facile Access to trans-3-Styryl-4-hydrazinocyclopentenes via Palladium Catalyzed Ring Opening of Diazanorbornenes with (Z)- β -Bromostyrenes/2,3-Dibromohydrocinnamic Acids. S. Saranya, S. Sarath Chand, **Greeshma Gopalan**, V. Jijitha, K. V. Radhakrishnan. *Synthesis*, **2018**, *50*(1), 184-192.
6. Lewis Acid Catalysed Activation of Zerumbone towards Sesquiterpenoid Derivatives: Sustainable Utilisation of Abundant Natural Resources towards Chemically Diverse Architectures. Dhanya, B. P.†, **Greeshma Gopalan**†, Sasikumar Parameswaran, Neethu S, Meenu M T, Sharathna P, John, Jubi, Sunil Varughese, Sabu. M, Dan Mathew, Kokkuvayil Vasu Radhakrishnan. *Asian J Org Chem*, **2018**, *7*, 471–476. †equally contributed.
7. Lewis acid catalyzed Povarov reaction of pentafulvenes and spiro[2,4]-hepta-[4,6]-diene: An efficient access to cyclopentene fused quinolines" S. Saranya, T. V. Baiju, **Greeshma Gopalan**, K. V. Radhakrishnan. *Synthetic Communications*, **2018**, *48* (7), 816-829.

-
8. Rhodium(III)-Catalyzed C–H Activation/Alkylation of Diazabicyclic Olefins with Aryl Ketones: Facile Synthesis of Functionalized Cyclopentenes, P. V. santhini, **Greeshma Gopalan**, A. S. Smrithy and K. V. Radhakrishnan, *Synlett*, **2018**, 29(15), 2023-2026.
 9. Chloroform as a carbon monoxide source in palladium-catalyzed synthesis of 2-amidoimidazo [1,2-a]pyridines, Nitha P. R, Manu M. Joseph, **Greeshma Gopalan**, K. K. Maiti, K. V. Radhakrishnan and Parthasarathi Das. *Org. Biomol. Chem.*, **2018**, 16, 6430–6437.
 10. Screening of *Musa balbisiana Colla*. seeds for Antidiabetic Properties and Isolation of Apiforol, a Potential Lead, with Antidiabetic Activity **Greeshma Gopalan**, B. Prabha, Alfred Joe, T. R. Reshmitha, D. R. Sherin, M. Sabu, T. K. Manojkumar, K. V. Radhakrishnan, and P. Nisha, Under minor revision, *Journal of science of Food and Agriculture*.
 11. Phytochemical Investigation and Isolation of Novel xanthone Derivatives from *Anethum graveolens* Linn. **Geeshma Gopalan** and K. V. Radhakrishnan, Manuscript under preparation.
 12. Investigations on Phytochemical Constituents of *Zingiber nimmonii* (J. Graham) Dalzell. **Geeshma Gopalan** and K. V. Radhakrishnan, Manuscript under preparation.
 13. *Rotula aquatica* Lour- Phytochemistry and *in vitro* Antiurolithiatic Activity against Experimental Kidney Stones. **Greeshma Gopalan** and K. V. Radhakrishnan, Manuscript under preparation

Contributions to academic conferences

1. Synthesis of Isoquinolone Fused Azabicycles *via* Rhodium (III) Catalyzed C-H Activation of *N*-Pivaloyloxy Amides. **Greeshma Gopalan**, Praveen Prakash, E. Jijy, P. S. Aparna, and K. V. Radhakrishnan: *TFOC- 2014* at CSIR- NIIST, Thiruvananthapuram. 09-11 October, 2014. Best poster award.
2. Synthesis and Evaluation of Anti-diabetic Activity of Indole Functionalised Zerumbone Derivatives. **Greeshma Gopalan**, Dhanya B. P., Nisha P., K. V. Radhakrishnan: *International Symposium On Phytochemistry (ISP-2015) and Prof. Dr. A. Hisham Endowment Award Ceremony*: Kerala Academy of Sciences, Thiruvananthapuram. 25th April, 2015.

-
3. Unprecedented Regioselective Hydroheteroarylation of Pentafulvenes with Indole. **Greeshma Gopalan**, S. Sarath chand, K. V. Radhakrishnan: *Nascent Developments in Chemical Sciences: Opportunities for Academia-Industry Collaboration (NDCS-2015)*”, BITS Pilani, India. 16-18 October, 2015.
 4. Hydroindolysation of Pentafulvenes towards the Synthesis of Biologically Important Scaffolds. **Greeshma Gopalan**, S. Sarath chand , K. V. Radhakrishnan: *CTDDR-2016*, at CSIR-CDRI, Lucknow, Uttarpradesh. 25-28 February, 2016.
 5. Lewis Acid Catalyzed Regioselective Hydroindolysation of pentafulvenes. **Greeshma Gopalan**, S. Sarath chand , K. V. Radhakrishnan : *CRSI-2016* at NBU, Darjeeling, West Bengal. 14-16 July, 2016
 6. Lewis Acid Catalysed Indolysation of Pentafulvenes: A Facile Synthetic Route for Biologically Important Scaffolds. **Greeshma Gopalan**, S. Sarath Chand, K. V. Radhakrishnan, *53rd Annual Convention of Chemists* at GITAM University, Visakhapatnam. 27-29, December 2016.
 7. Phytochemical Investigation of Seeds, Rhizome and Peels of *Musa balbisiana*. **Greeshma Gopalan**, N. K. Linu, M. Sabu and K. V. Radhakrishnan. *2nd International Conference on “Nutraceuticals and Chronic Diseases”* September 1-3, 2017, Goa, India. 01-03 September 2017.
 8. Phytochemical investigation and *in vitro* antidiabetic potential of compounds from seeds, rhizome and peels of *Musa balbisiana*, **Greeshma Gopalan**, Prabha B., Sherin D. R., Sabu M., Nisha P. and Radhakrishnan K. V, *ISP-2018*, an International seminar on Phytochemistry organized by Kerala academy of Sciences & Jawaharlal Nehru Tropical Botanic Garden and Research Institute, Palode. 26-27 March, 2018. Best oral presentation award.